METRIC ASPECTS OF RECONNAISSANCE FRAME PHOTOGRAPHY

by

ISMAT MOHAMED ELHASSAN

B.Sc. (Civil Eng. (University of Khartoum))

A Thesis submitted for the degree of

Doctor of Philosophy in

Photogrammetry

to the

University of Glasgow

June, 1978

ACKNOWLEDGMENTS

The author acknowledges a great debt to his supervisor, Professor G. Petrie who suggested this research topic and for his continuous encouragement, supervision and useful comments throughout the period of the research, and without whom this work would not have come to stand as it does.

The author would also like to express his thanks to Mr. B.D.F. Methley for his useful comments and assistance with the analytical methods especially in the computer programing stage, and for revising some manuscripts of the thesis.

The author would also acknowledge the freedom granted by the two Heads of the Department of Geography, Professors Miller and Thompson, to make full use of all the facilities of the Department through the period of his stay.

Sincere thanks are also due to the following individuals and organisations:-

The Royal Aircraft Establishment (R.A.E.) at Farnborough for providing the F-126 photography to our specification and supplying the information on the lens used, etc. required to complete the analysis. In particular the very full collaboration made by Mr. G. Kirk of the Instruments and Testing Group is acknowledged.

The Ordnance Survey and, in particular, the Regional Officers concerned were very cooperative in allowing the author to carry out coordinate measurements for the test points from the original copies of the 1/1250 plans held in the Region Offices.

The Aeronautical and General Instruments Co. Ltd. (A.G.I.) at Croydon and the Vinten Co. Ltd. at Bury St. Edmond for arranging useful visits for the author to their companies and for supplying useful prints about their recently manufactured reconnaissance cameras.

Professor R. Welch of the University of Georgia who went to a great deal of trouble to provide the S-190B Skylab photography and the U.S.G.S. map sheets covering the test area.

Zeiss Oberkochen for supplying the author with the information required about the Zeiss Topogon lens used with the F-126 reconnaissance camera.

The Department of Civil Engineering at City University London and, in particular, Mr. Lindsay and Mr. Cooper, for allowing the author to carry out the photo-coordinate measurements on their stereocomparator.

The technicians, especially Mr. I. Gerrard and Mr. M. Shand, at the Department of Geography for their assistance and advice in drawing and photographing all the figures and diagrams in this thesis.

Mrs. Whyte at the Department of Medical Illustration for her careful typing of the thesis.

Special appreciation is expressed to the University of Khartoum for the financial support which allowed the author to carry out this research.

Sincere thanks are also due to the author's wife for her patient and continuous encouragement and to his parents and friends for their support.

I.M. ELHassan

June, 1978

CONTENTS

	Page
Introduction	1
1. History and Development of Aerial Reconnaissance Photography	5
1.1 Introduction	6
1.2 Early history of Aerial Photography	7
1.3 Photo Reconnaissance during the First World War	8
1.4 Development during the Inter-War period	11
1.5 Photo Reconnaissance during the Second World War	17
1.6 Developments Post-World War II.	21
2. Continuous Strip and Panoramic Cameras	31
2.1 Introduction	32
2.2 Image Movement Compensation	32
2.3 Continuous Strip Cameras	34
2.4 Panoramic Cameras	37
2.4.1 Rotary Lens-type of Panoramic Camera	41
2.4.2 Rotary-Prism Panoramic Camera	42
2.4.3 Rotating Optical-Bar Panoramic Camera	44
2.5 Use of Panoramic Photography	47
2.6 Comparison of Strip, Panoramic and Frame Cameras	50
3. The Aerial Reconnaissance Frame Camera	51
3.1 Introduction	52
3.2 Basic Design of the Aerial Frame Cameras	52
3.3 The Camera Body	53

	Page
3.4 The Film Magazine	54
3.5 The Lens Cone	56
3.6 Optical System	57
3.6.1 The Lens	57
3.6.2 Concentric mirror Optics	59
3.6.3 Lens Resolution	62
3.7 Format Size and Arrangement	68
3.8 Image Movement Compensation (IMC)	71
3.8.1 Camera movements	71
3.8.2 The Effects of Craft Speed, Flying Altitude and Exposure Time on Image Movement	72
3.8.3 Image Motion Compensation as a means of maintaining resolving power	73
3.8.4 IMC Systems	74
3.8.5 Accuracy of IMC	77
3.9 Shutters	78
3.9.1 The Intra-lens Shutter	78
3.9.2 The Focal Plane Shutter	80
3.9.3 Comparison of Shutters	83
3.10 Summary	85
4. Geometric Theory of Reconnaissance Frame Photography taken with Focal Plane Shutters	90

		Page
4.1	Introduction - Geometrical Distortions resulting from use of a Focal Plane Shutter	91
4.2	Operation of the Focal Plane Shutter	92
4.3	Introduction of Movement of the Camera Platform during Exposure	93
4.4	Rotary Focal Plane Shutter	98
4.5	Effect of Crab	101
4.6	The Effect of IMC on Image Geometry	102
4.6.1	The Effect of using Film Movement for IMC	102
4.6.2	Rotation of the Camera for IMC	104
4.6.3	Effect of Hilly or Mountainous Terrain on the Application of IMC	106
4.6.4	IMC for Oblique Photography	110
4.7	The Combined Effect of the Focal Plane Shutter and IMC	115
4.8	Effect on Relative Orientation	117
4.9	Model Deformations	117
4.10	Conclusions	126
5.	Analytical Techniques for use with Reconnaissance Frame Photography	128
5.1	Introduction - The Use of Analytical Techniques	129
5.2	Lack of Knowledge of Inner Orientation	129
5.3	Corrections to Image Coordinates	131
5.4	Tilt Variations during Shutter Transit Time	132

	Page
5.5 Possible Analytical Approaches	132
5.6 Space Resection/Space Intersection Method	134
5.6.1 Single Photographs - Basic Geometrical Relationships	134
5.6.2 Space Resection (Point-by-point)	138
5.6.3 Space Intersection	143
5.7 Space Resection with Additional Parameters	145
5.8 Conventional Analytical Relative and Absolute Orientation followed by a Polynomial Adjustment to correct Terrain Coordinates	149
5.9 Comparison between the Three Techniques	154
6. Experimental Tests - Procedures, Characteristics of the Photography and Provision of the Control points for the Test Fields	156
6.1 Introduction	157
6.1.1 Test Procedures	157
6.2 The S-190B Photography Test	158
6.2.1 Introduction	158
6.2.2 The S-190B Camera	160
6.2.3 Photography	164
6.2.4 Test Area and Ground Control	166
6.3 The F-126 Photography Test	167
6.3.1 The F-126 Camera	167
6.3.2 The Zeiss Oberkochen Topogon Lens	169

	Page
6.3.3 The Photography and the Test Area	174
6.3.4 Ground Control	178
6.4 Measurement of Photo-coordinates	179
7. The Computer Programs	183
7.1 Introduction	184
7.2 Program (A) - Image Coordinates Refinement	186
7.2.1 Function of the Program	186
7.2.2 Mathematical Basis	186
7.2.3. Flexibility and Limitations	188
7.3 Program (B) - Analytical Relative Orientation	189
7.4 Program (C) - Absolute Orientation and Polynomial Adjustment	190
7.4.1 Introduction	190
7.4.2 Mathematical Basis	190
7.4.3 Flexibility and Limitations	194
7.5 Program (D) - Space Resection/Intersection	195
7.5.1 Introduction	195
7.5.2 Mathematical Basis	195
7.5.3 Flexibility and Limitations	197
7.6 Program (E) - Plot of Discrepancies	199
7.6.1 Introduction	199
7.7 Program (F) - Transformation of Geographic Coordinates to Secant Plane Coordinate System	200

	Page
7.7.1 Introduction	200
7.7.2 Mathematical Basis	200
7.8 Program (G) - Transformation of Geographic Coordinates to U.T.M. Coordinates	203
7.8.1 Introduction	203
7.8.2 Mathematical Basis	204
7.9 Conclusions	205
8. <u>Results of the Experimental tests</u>	207
8.1 Introduction	208
8.2 S-190B Test Results	210
8.2.1 Results	211
8.3 Analysis of the S-190B test results	222
8.3.1 Planimetric Accuracy	222
8.3.2 Height Accuracy	228
8.4 The F-126 Test Results	233
8.4.1 Results	233
8.5 Analysis of the F-126 Test Results	239
8.5.1 Planimetric Accuracy	239
8.5.2 Height Accuracy	242
8.6 Conclusions	
9. <u>Conclusions and Recommendations for Future Work</u>	248
9.1 Some General Conclusions	249
9.2 Suggestions and Recommendations for Future Work	251

		Page
9.3	Epilogue	255
Bibliography		256
Appendix A	Coefficients of the linearised collinearity equations	264
Appendix B	Detailed Description of the Computer Programs	266
Appendix C	Vector Maps of the height and planimetric Residuals for the tested photography	377

INTRODUCTION

Aerial cameras can be classified according to their use, into two main categories. These are mapping cameras and reconnaissance cameras.

Mapping cameras are designed, constructed and calibrated to give an image of precisely known geometry. The interior orientation elements (i.e. the principal distance, the location of principal point and the lens distortion characteristics) of each individual camera are determined with very high accuracy by the camera calibration. An intra-lens shutter that allows simultaneous exposure of all image points is invariably used. Hence measurements made on photographs taken with such a camera can be used to recover accurately the position, height,size and shape of any ground object whose image has been recorded. In other words, such a camera satisfies completely the projective relations of photogrammetry. In addition to this requirement for high geometric fidelity, most mapping cameras and the photography taken with them are designed to provide a favourable base: height ratio for accurate height determination.

By contrast, reconnaissance frame cameras are designed on simpler lines and with very different objectives in mind. The elements of inner orientation are not precisely known or determined. Instead, the foremost requirements of a reconnaissance camera are reliability and excellent image quality. For this latter condition to be satisfied, the highest possible performance lenses and films are used to give high image resolution. Consideration of geometric fidelity of the image are secondary. With these objectives in mind, the simple design, the reliability and the wide range of possible exposure times make the focal plane shutter a favourite with the designers of the reconnaissance cameras. However, the sequential operation of the focal plane shutter introduces a marked distortion in the image geometry.

In spite of the geometric distortions inherent in reconnaissance photography, factors such as its wide availability and high image resolution have meant that, on occasions, it is necessary to make measurements and compile maps from such photographs, e.g. for thematic maps, measurement of change, map revision, etc. These occasions are becoming more numerous in the United Kingdom with the release of, and easy access to, the complete reconnaissance photography of the country taken by the R.A.F. For many areas and purposes, no other photography exists and users have no option but to attempt to use it for mapping purposes. However, the results are often poor, which is a matter of frustration to these users. One of the major difficulties is that the traditional analogue methods of photography do not provide means to correct for the geometric distortions present in reconnaissance-frame photography. It is only quite recently with the widespread availability of, and easy access to, electronic computers that it has been possible to consider the use of analytical methods to solve the geometric problems of this photography. With an analytical approach, the results are in digital form which is not too useful to some users. However, with the advent of the new digitally-based analytical plotters, computer-driven orthophotoscopes, etc. this situation will certainly change in future. Therefore a comprehensive study of the metric aspects of reconnaissance frame photography is timely and appropriate.

The alternative strip and panoramic types of reconnaissance camera have, in fact, already been analysed and photogrammetric techniques have been devised and applied to photography taken with them (Case, 1966; Konecny, 1970; Devenyi, 1971). However, to the author's knowledge, the metric problems associated with the reconnaissance frame photography have not been investigated.

It is the objective of this thesis to analyse the metric aspects of reconnaissance frame photography and to devise and test analytical techniques which allow them to be used for metric purposes, and, in particular, for mapping. This report on the work carried out is organised along the following lines. The development of the aerial reconnaissance camera since its first use in the First World War, through its intensive development during and after the Second World War to its use in this present age of space and satellites is outlined in Chapter I. Chapter II is devoted to a discussion of the two alternative types of reconnaissance cameras (strip and panoramic cameras) which are currently used for reconnaissance purposes. This review opens the way to a detailed discussion of the design, construction and operational characteristics of the reconnaissance frame camera itself in Chapter III. In particular, the quality of the image produced by reconnaissance frame cameras is analysed and compared to that obtained from metric cameras. The thesis then proceeds (in Chapter IV) to a detailed analysis of the geometry of the reconnaissance frame photography. The distortions resulting from the use of focal plane shutters and the combined effect of the focal plane shutter and image motion compensation on the image geometry are thoroughly investigated in this Chapter. The analytical techniques which have been devised or adapted by the author for use with single photographs and stereopairs of reconnaissance frame photographs are derived and explained in Chapter V. To test their validity, experimental work has been carried out on reconnaissance frame photography taken with different cameras under widely differing conditions. An account of the methods used and the preparation for these tests is given in Chapter VI. Computer programs have been developed specifically for the processing of the measured data. These are outlined in Chapter VII; more detailed accounts, flow diagrams, listings and samples of input and output data for the programs are given in Appendix B. The results of the two main programs of testing are given in Chapter VIII; further information, including vector diagrams of the planimetric and height residuals, is given in Appendix C. In this Chapter (VIII) the results are also analysed in detail, comparisons are made as to the effectiveness of the various methods used and with the results recently obtained by other authors; especially for the Skylab S-190B satellite photography which became available in the course of the present work. The closing chapter (IX) summarises the conclusions reached through this research work, and makes recommendations for future work.

CHAPTER I

History and Development of Aerial Reconnaissance Photography

CHAPTER I

HISTORY AND DEVELOPMENT OF AERIAL RECONNAISSANCE PHOTOGRAPHY

1.1. Introduction

A very important factor in planning military operations is a knowledge of what the enemy or potential enemy possesses in the way of man-power, weapons, material, fortifications and other resources and the manner and position in which they are deployed. The knowledge of what the enemy is doing beyond the range of eyesight is generally termed intelligence and the effort to obtain this information is usually known as reconnaissance. Such information may come from prisoners, spies, patrols, etc.; this type of source has been and is still employed extensively. However, with the growth of science and technology, instruments have been devised to allow the information to be gathered in other ways. The invention of the optical telescope in the sixteenth century allowed military commanders to extend this direct observation of enemy deployment in the battlefield areas. Since then, military needs have a strong influence on the development of certain types of optical instrument, these requirements always demanding improvements in the state-of the-art, backed often by substantial financial resources. In turn, these new instruments have become available to non-military users for peaceful purposes.

From the nineteenth century onwards, two major developments have extended military reconnaissance capabilities greatly. The first is the development of various types of air vehicle, starting with the balloon, and the second that of the photographic camera which allows a permanent and more complete record of a scene to be made, thus allowing interpretation by military personnel and others who have not been present at the scene itself. With the invention of the aeroplane in the first decade of the twentieth century, the extent of this capability has rapidly extended to country-wide and continent-wide observations. Since 1960, by employing spacecraft and modern photographic cameras, man has been able to observe the entire globe.

1.2 Early history of Aerial Photography

The first attempt to take an aerial photograph was made in 1858 by the French photographer, Gespard Nadar (Heiman 1972). Nadar used a camera to photograph Paris from a balloon at altitude of 80 metres. Balloon photography then extended to America where, for example, the city of Boston was photographed by J. Black in 1860 (Heiman 1972). The wet plates which were used during this period were replaced in 1871 by dry gelatin plates. One of the first aerial photographers to use this type of plate was the British photographer W.B.Woodbury who designed an almost automatic system of balloon photography in 1877 (Newhall 1969).

Another vehicle that was used to carry the camera in the early days of air photography was the kite. To raise the camera to greater heights, often more than one kite was used. In 1895, for example, the American metrologist William Eddy used six to nine kites to lift the camera to a height of 1000 ft (300 m). At that time, the German army attempted to use rocket photography. But the first successful flight of an aircraft was that by the Wright brothers which took place in America in 1903. The use of the aircraft as a camera platform has the great advantage over balloon, kites and rockets in that it can be flown with great accuracy at specific heights over any specific area. Moreover, the flight is relatively steady and it can be flown at a constant speed. The development of aerial photography in the twentieth century spurred on by two World Wars, numerous smaller wars and certain periods of "cold" war, has been quite phenomenal and it is now a primary method of reconnaissance with enormous data-gathering capabilities. A short review of this development is a necessary preliminary to set the work reported on in this thesis in a correct perspective.

1.3 Photo Reconnaissance during the First World War

The use of aircraft for reconnaissance started at the end of the first decade of the twentieth century. During the period 1909-1914, experimental aerial photographic flights were carried out in many countries. The British Royal Flying Corps (R.F.C.) for example, started their experiments in 1912 using commercially available cameras. In 1913, the first specially designed camera for the R.F.C. was built. This was the Watson Air Camera (Fig. 1) which had a f = 6 in. (15 cm) lens and used plates of 12.5 x 4 in (31 x 10 cm) (Laws 1959). In 1914, the Thornton-Pickard Manufacturing Co. Ltd. built the model "A" air camera (Fig. 2) for the R.F.C. (Newhall 1969). This camera comprised a brass-bound tapering wooden box, a focal plane, a focal plane shutter and a f = 9 7/18 in. (25 cm) Zeiss Tessar lens. It utilised 4 x 5 in (10 x 12.5 cm) plates enclosed in ingenious light-tight paper envelopes which were inserted into the camera one after the other by hand.

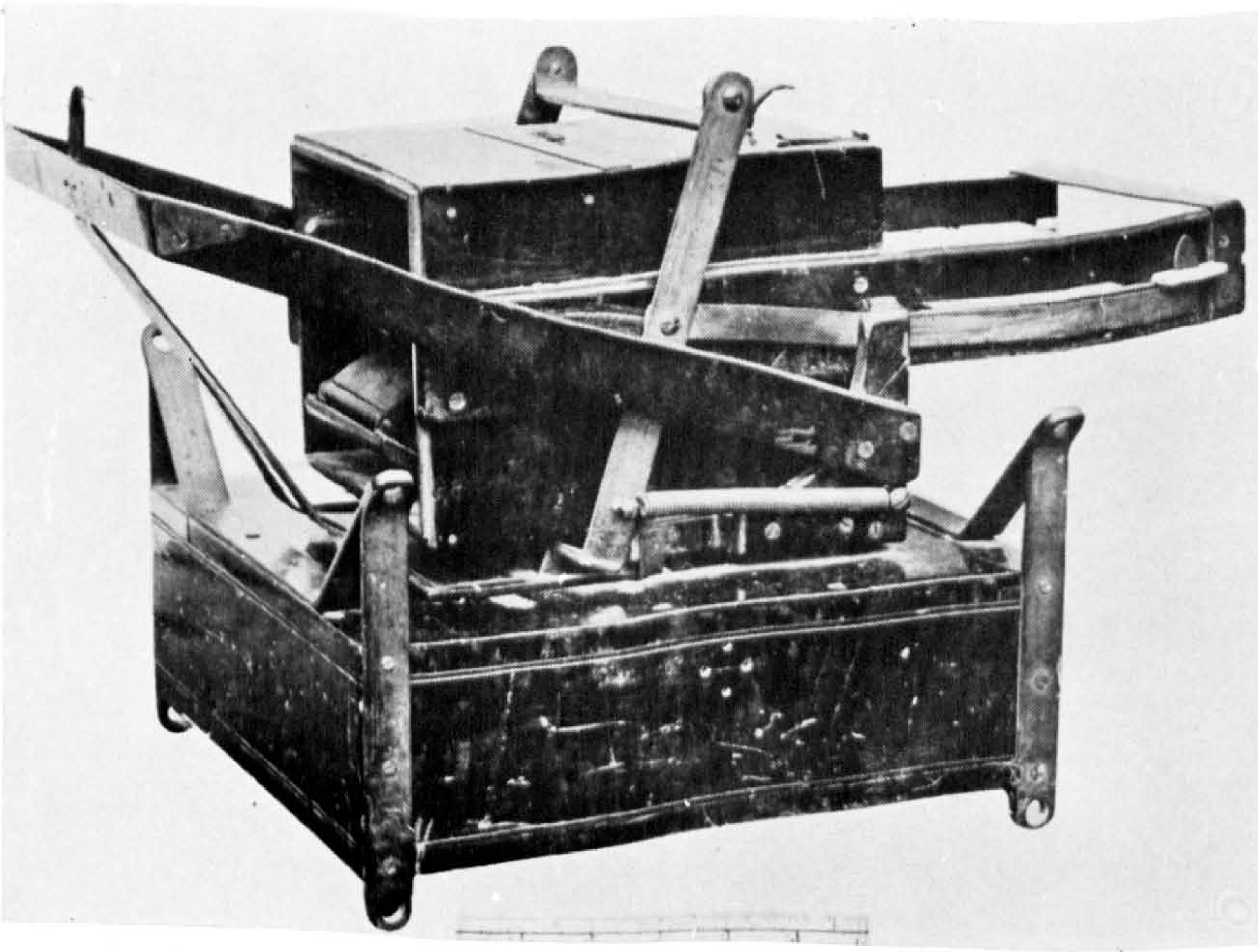

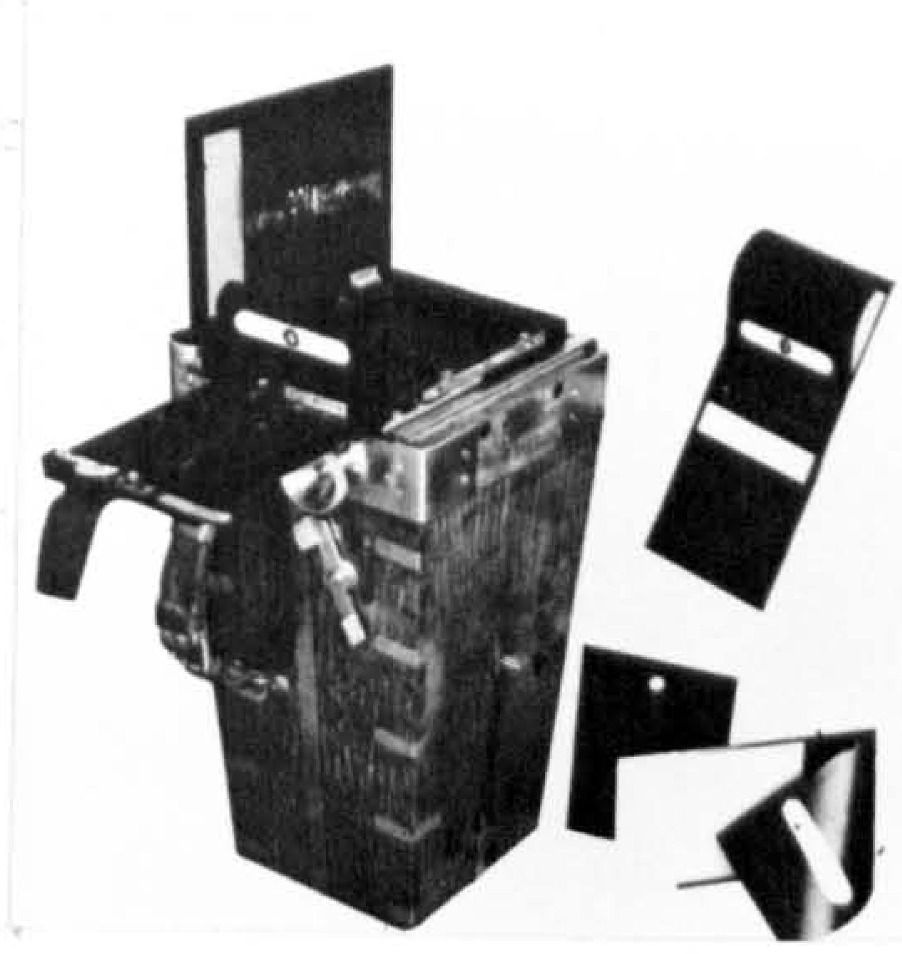

Fig. 2 Type "A" Camera

Fig. 1 Watson Air Camera

The importance of reconnaissance aerial photography rapidly increased during the First World War. The armies soon found that it was possible, by this new means, to obtain information on the enemy's man-power, disposition of troops, weapons and defence installations in a way that had previously been impossible. An enormous increase in the resources (aircraft, cameras, personnel, processing facilities, etc.) made available for aerial reconnaissance took place and a rapid development of equipment was undertaken. The first improvement to be made to the British Model "A" air camera was to add a magazine. A dozen fresh plates were stacked face down in a box directly over the focal plane. The plate was slid in a frame over a second box, into which it fell by gravity. The plates could be changed only when the camera was held vertically. This version was introduced as the Model "C" camera and was followed by the Model "E", which was of similar design but made of metal instead of wood (Newhall 1969). These two cameras were used by the R.F.C. throughout the First World War. Initially all of these cameras were hand-held and were operated manually over the side of the aircraft either obliquely or vertically.

To say this was a difficult operation is an understatement. Hence, the R.F.C. asked that the cameras be adapted or re-designed for remote operation from a position inside the aircraft with the camera axis pointing vertically downwards. F.C. Laws drew up specifications for a camera of this type (designated the Model "L" after its designer) which was equipped with a f = 6 in. (15 cm) lens and would use 4 x 5 in. (10 x 12.5 cm) plates.

Laws and Moore-Brabazon then designed the "L.B." Type Camera (Fig. 3) which initially was driven by an external propeller and later by an electric motor, and which could be equipped with alternative lenses of 5, 8, 14 and 20 in. (i.e. 12.5, 20, 35 and 50 cm) focal length. This became the standard equipment of the R.F.C. (later the R.A.F.) from 1916 to 1925 (Laws 1959).

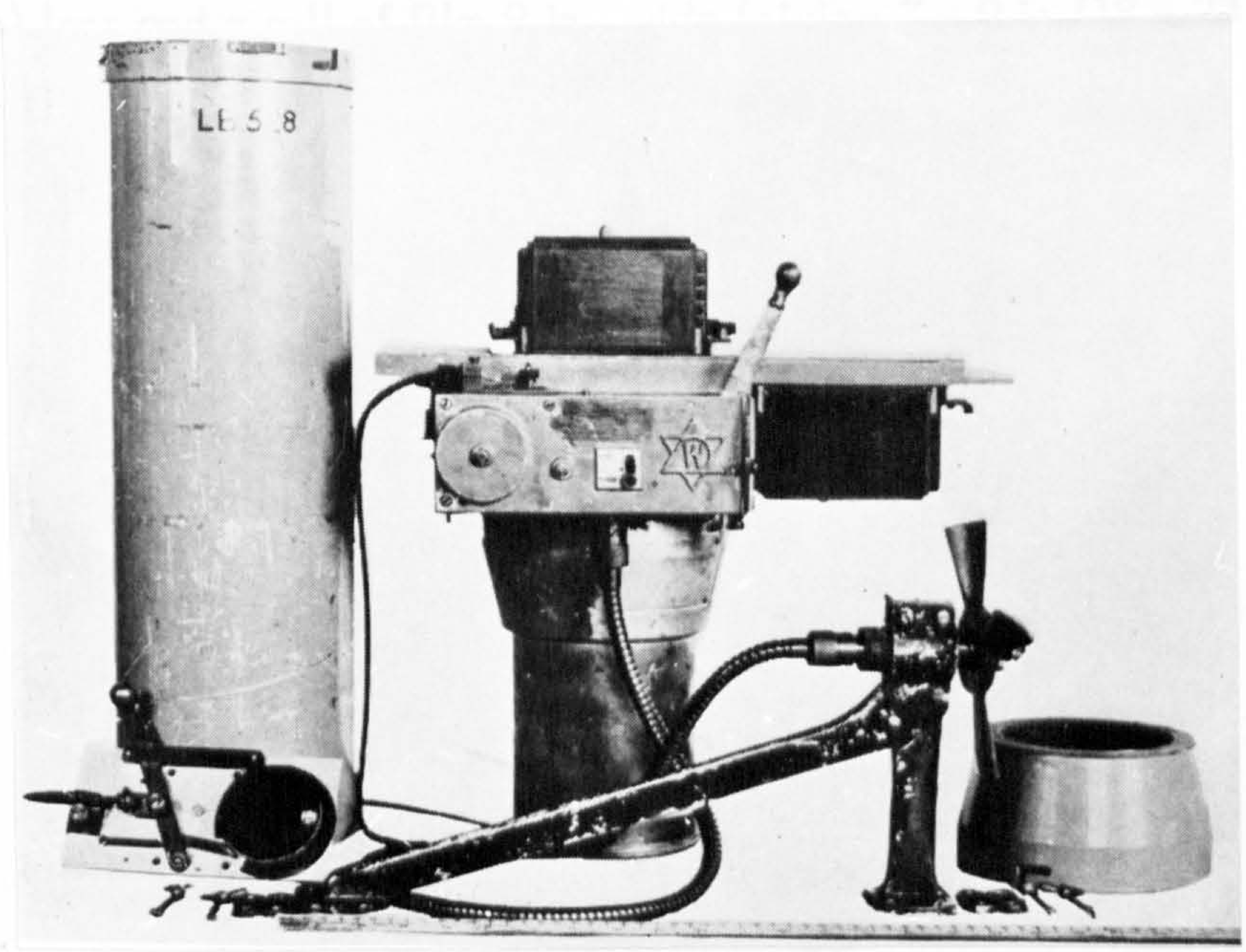

Fig. 3 L.B. camera

The Germans started the war with better preparation and equipment. Initially a 3.5 x 4.5 in. (9 x 12 cm) plate camera fitted with a f/4.5 Zeiss Tessar lens was used. However, in 1915, Oskar Messter, a motion-picture pioneer, designed and built a semi-automatic roll film camera, which is, in a general sense, the prototype of all modem aerial film cameras. A total of 250 negatives, each 4 x 4 in. (10 x 10 cm) could be taken on 100 ft (30 m) of film $4\frac{3}{4}$ in. (12 cm) wide. A single manual operation was used to cock the shutter and to bring fresh film into position for the next exposure. However, according to Williamson (1945), the Germans predominately used the manually-operated sliding-plate-changing box type of aerial camera throughout the war.

In the period up to 1916, the Americans used a Folmer-Schwing hand-held camera with 12 plates in the magazine to take 4 x 5 in. (10 x 12.5 cm) photographs. A view-finder with cross-hairs was used by the camera operator to take photographs of the prescribed area. Later on, when the Americans entered the war, a new K-1 camera (Fig. 4) went into production, which employed a f = 20 in. (50 cm) lens and a roll of film 9 in. wide (giving 7 x 9 in (18 x 23 cm) format), which allowed 75 photographs to be taken (Goddard 1969).

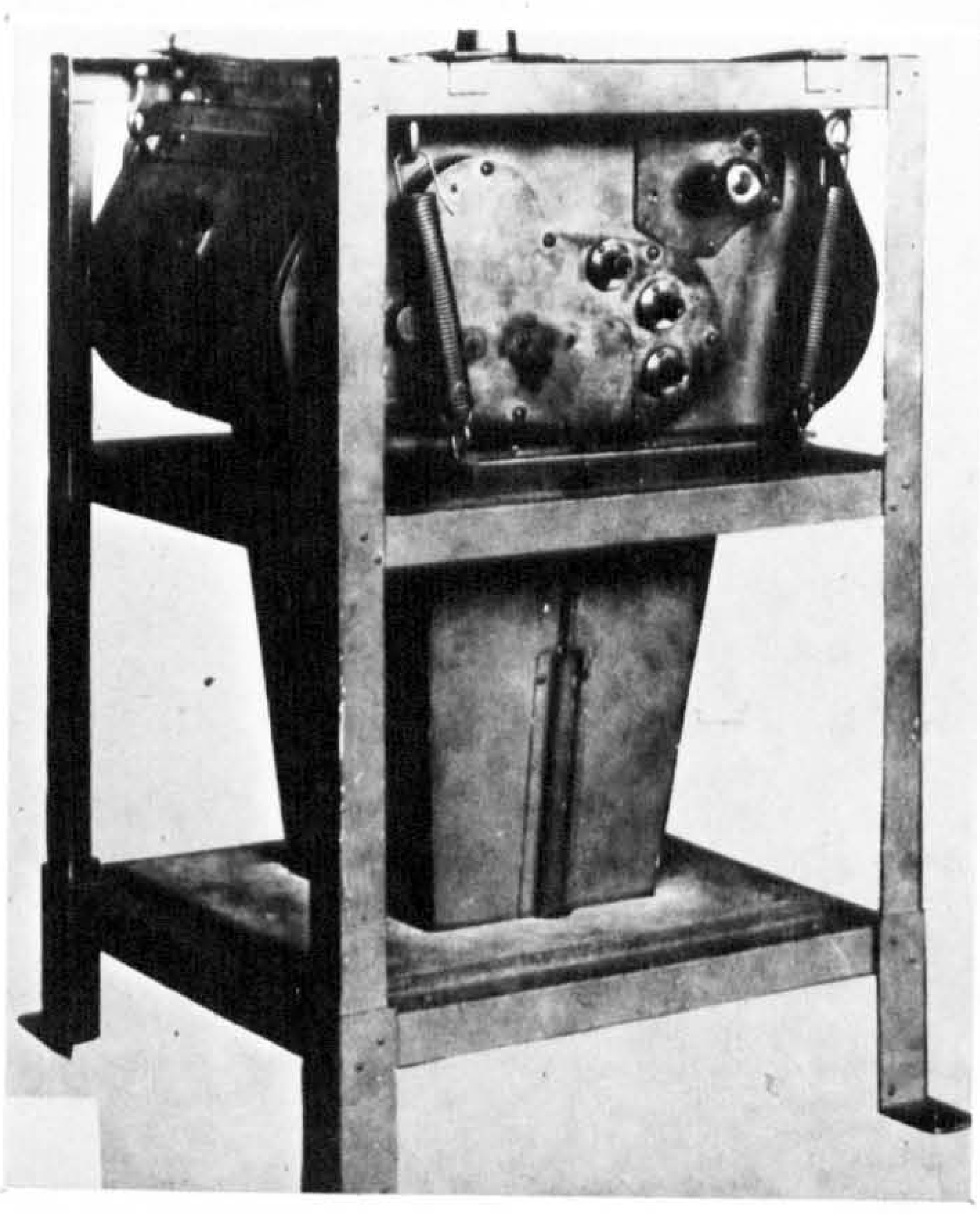

Fig. 4 K-1 Camera

1.4 Development during the Inter-War Period

At the end of the First World War, it became clear to the various air forces concerned that they should be re-equipped with new reconnaissance cameras and other ancilliary equipment based on the mass of experience gained during the war. However, the actual implementation of this policy proved difficult in the poor economic circumstances and depression period of the 1920's and early 1930's. Development took place slowly and painfully.

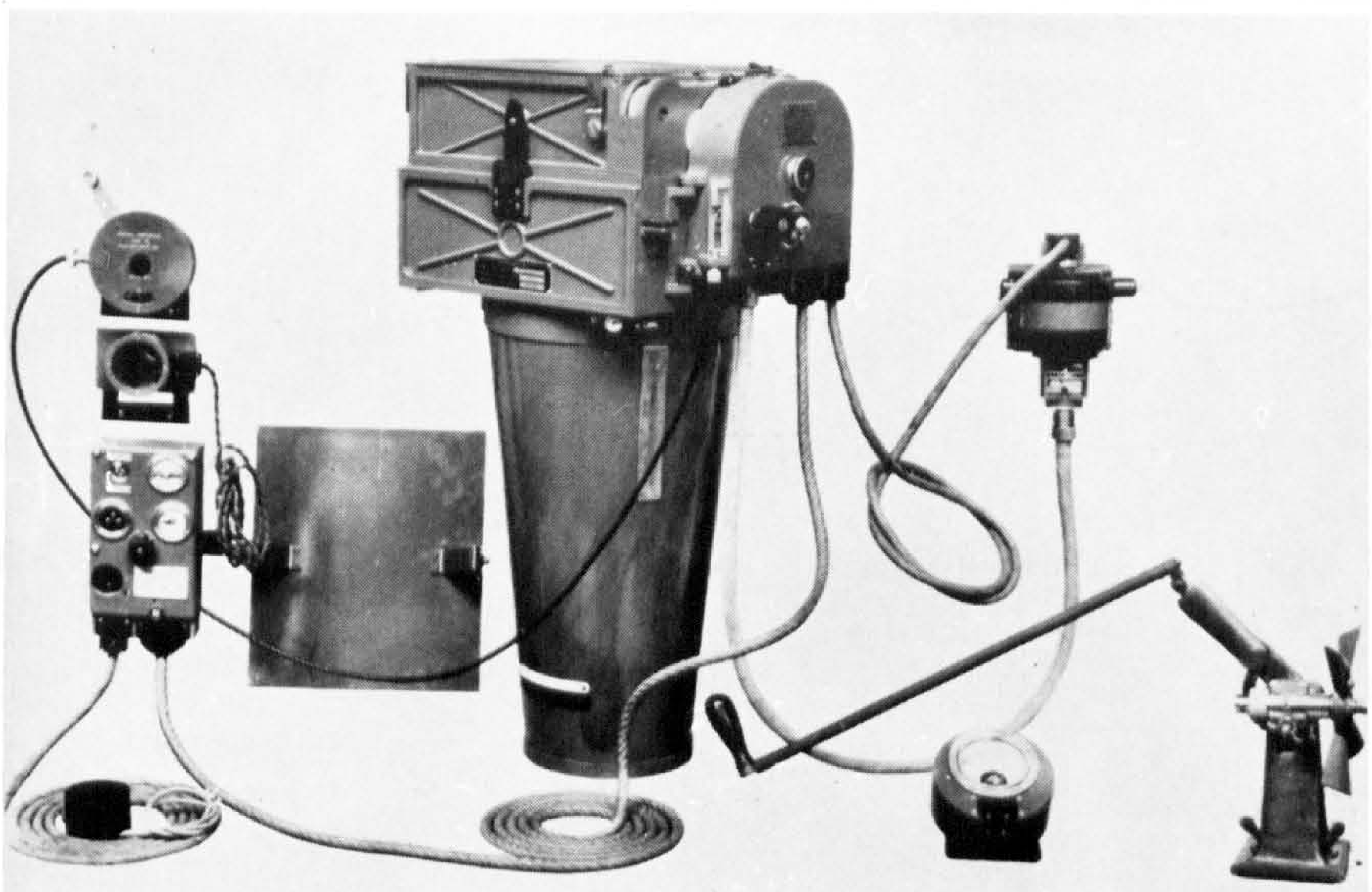

Fig. 5. F8 Camera

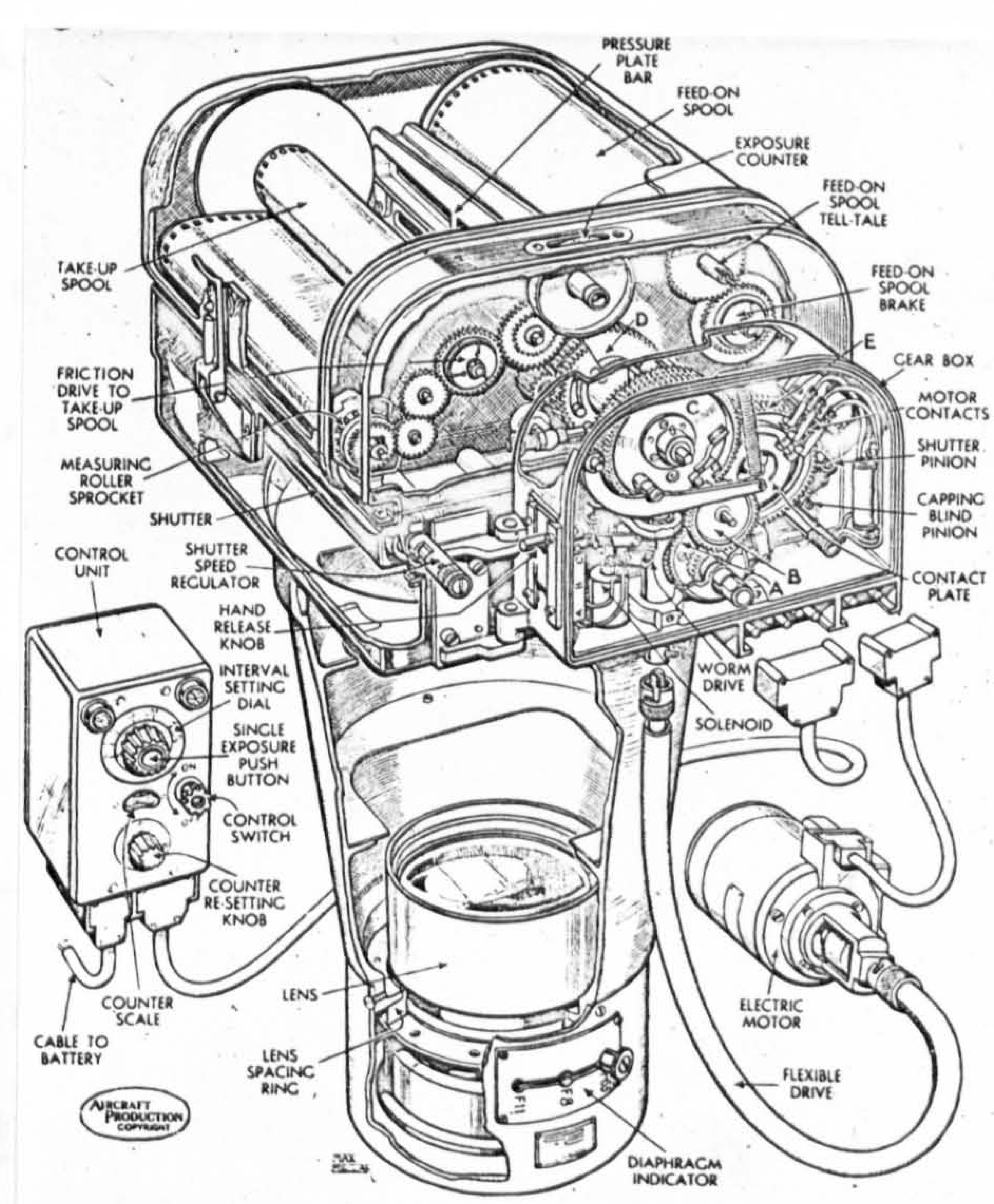

Fig. 6 F8 Camera diagram

In Britain, it was realised that a larger format than the standard 4 x 5 in. (10 x 12.5 cm) size used in all the cameras from the "A" to the "L.B." was required. Also that the glass plates should be replaced by film and that the camera should be completely automatic in operation. The result was the F8 camera (Fig. 5) designed originally by the Instrument Design Establishment at Biggin Hill, but finalised into a prototype by the Royal Aircraft Establishment (R.A.E.) at Famborough (Laws 1959). The F8 camera with its format size of 8¼ x 7 in.(20 x 17.5 cm) and a focal plane shutter (Fig. 6) was first produced in 1924. But not more than thirty (Laws 1959) or sixty (Laws 1946) of these cameras were delivered to the R.A.F. before the Air Ministry authorities decided that the F8 was too large, too heavy and too expensive. Instead, instructions were given for the design and construction of a camera with a smaller 5 x 5 in.(12.5 x 12.5 cm) format. The resulting F24 camera (Fig. 7) was designed along much the same lines as the F8 and, for the next twenty years, it was a standard piece of equipment fitted to numerous types of aircraft. Indeed it is still in use, .e.g. in the E.S.A. Skylark Earth Resources rocket experiments in Argentina, Sweden and Australia in 1972 and 1973 it was even used to obtain photography from space. The range of lenses which were developed for fitting to the F24 ranged from f = 3¼ in. (8.25 cm) through 6 in. (15 cm), 8 in. (20 cm), 14 in. (35 cm), 20 in. (50 cm) to 36 in. (90 cm) and 40 in. (100 cm) (Laws 1945; Williamson 1945).

Developments in the United States in this inter-war period took place along rather different lines, a colourful and non-technical account being given in Goddard's book (Goddard 1969). First, a modified version of the wartime Folmer-Schwing K-1 was produced as the K-2 in 1921. Two years later, the

Fig. 7 F-24 Camera

Fig. 8 K-3 Camera

completely new K-3 camera (Fig. 8) was completed, designed by Sherman Fairchild. This was an electrically-driven camera which featured the first intervalometer and a between the lens shutter. The K-3 camera became a standard aerial camera in the American Army and Navy Air services during the inter-war period, and was used both for mapping and reconnaissance.

Goddard and Albert Stevens alternated as Directors of Research and Development for Aerial Photography based on a small laboratory at Dayton, Ohio, throughout the inter-war period. Both of them placed a special emphasis on the development of very long focal length cameras, not initially for very high altitude operation (the ceilings of aircraft were then very limited), but for long range oblique photography.

Fig. 9
f = 60 in. Camera

There is a photograph of an experimental camera (Fig. 9) equipped with f = 60 in. (150 cm) dating from 1925 (see p.371 of Goddard's book) and in 1926, Goddard initiated a new design for a f = 35 in. (90 cm) camera which was built by Eastman Kodak. The loss of angular coverage was of course severe and, to recover this, the K-7 camera was built by Fairchild in 1926 using 9 in. (23 cm) film to give a 9 x 18 in. (23 x 46 cm) format, the camera being operated with its longer side cross-track to give wider coverage. In the early thirties, Stevens made many very high altitude flights both in aircraft and in balloons, which resulted in much development of pressurised cabins, oxygen supplies, long-range radio links, etc. His balloon flights, made in co-operation with the National Geographic Society, culminated in 1935 with a flight which reached 72,000 ft (22,000 m). A large number of long-range vertical and oblique photographs resulted from these flights, many taken with the black and white infra-red films first developed by Dr. Mees of Kodak specifically for these missions (Goddard 1969).

Goddard also pioneered the use of flash powder bombs and cartridges from 1925 onwards which, in conjunction with specially developed shutters triggered by photo-electric cells, allowed night reconnaissance photographs to be taken.

Developments in all these areas was hampered by lack of money throughout the period of the Depression but as prosperity began to recover and war approached, the financial stringency eased and a period of rapid development took place. For example, in 1935, the Kodachrome process first appeared and when this could not be adopted to aerial photography, Kodacolor Aero Reversal films were developed between 1936 and 1939. An alternative night illumination system utilising powerful electrical strobe lamps was developed by Dr. Edgerton of M.I.T. and work began on a shutterless strip camera which would overcome the difficulties in getting a sharp photograph from a low-flying fast aircraft. This was based on a shutterless race-track camera developed by Del Riccio in California, in which the film was synchronised electrically to travel at the same speed as the horses, moving across a 1/4,000 in. (0.006 mm) slit which acted as both shutter and lens. This idea was adapted for use in aircraft, though it was not until well into World War II that all the difficulties were solved and the strip camera and the twin-lens stereo strip camera were produced in quantity.

Fig. 10

K-17 Camera

In parallel with these developments came a whole series of new frame cameras. The K-17 (Fig. 10) was produced by Fairchild with several variants, A, B, C and D which could be used for mapping and for reconnaissance equipped with lenses, mostly from Bausch and Lamb, from the famous wide angle f = 6 in. (15 cm) Metrogon to a f = 40 in. (100 cm) model. The K-18 was a long focal length camera, the K-19 a special night reconnaissance camera, the K-20 a hand-held small-format (4 x 5 in., 10 x 12.5 cm) camera, etc. The contrast with the

British position could hardly have been greater. On the one hand, standardisation on the apparently well-proven small format F-24, available with a great number of lenses of different focal length; on the other a large number of newly developed, partly experimental cameras with a great variety of formats, often designed for specific roles and purposes.

1.5 Photo Reconnaissance during the Second World War

This topic is one which has had a great deal of coverage, especially in a series of popular books (e.g. Babington-Smith 1957; Heiman 1972; Goddard, 1969; Brookes 1975, etc.). However, the emphasis in these is on the aircraft and the personalities involved, the applications to the various battlefields and to strategic bombing and the related economic aspects, etc. Much less information is available on the technical aspects of cameras, lenses, emulsions, etc., both because of wartime security and the fact that it is not of interest to the general public and to the lay reader.

For the British the story opened disastrously and ended well. The period 1939-40 led to the discovery that the F-24 was unsatisfactory in many respects. It had been designed for operation from maximum altitudes between 12,000 and 20,000 ft (4,000 to 6,000 m) and as the altitudes of operational aircraft quickly rose, its small format exacted a penalty either in scale or resolution or in angular coverage. In March 1940, the situation was partially remedied by bringing back into service the F8 cameras, including fifteen hastily repatriated from India (Laws 1959). Steps were taken to put the F8 camera back into production (Oates 1943) and a parallel effort was made by the R.A.E. to produce a more modern camera capable of operation from high altitudes.

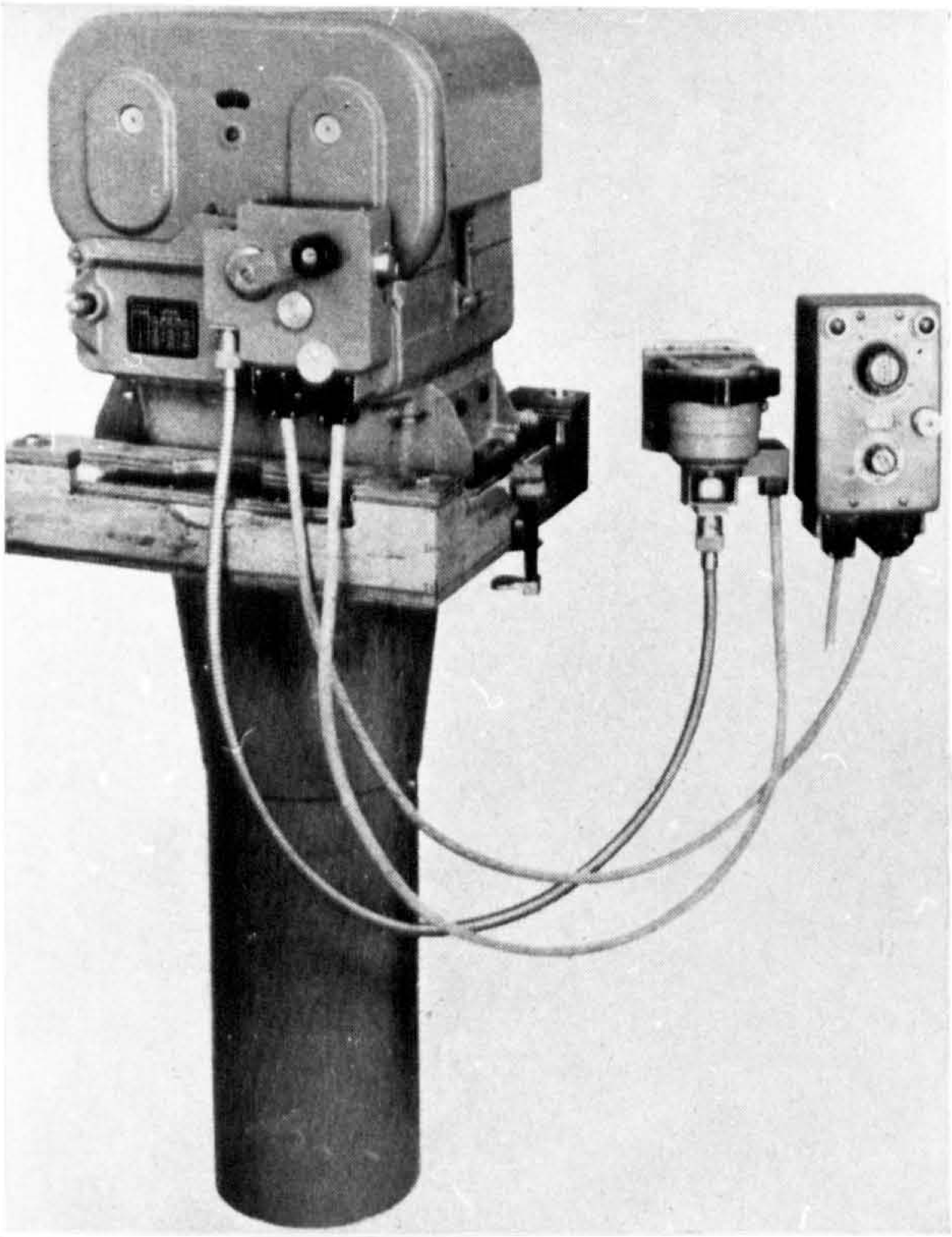

Fig. 11 F52 Camera

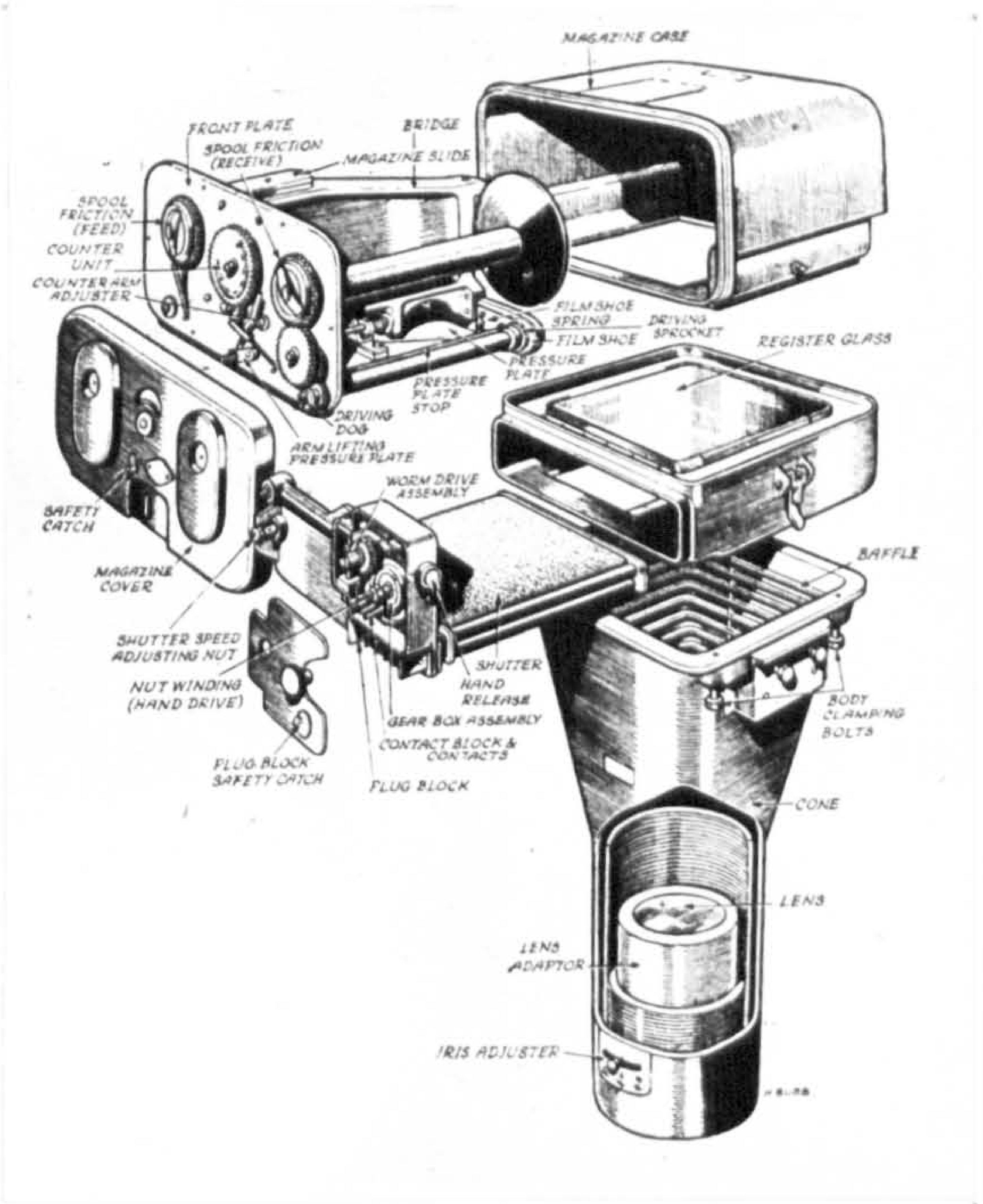

Fig. 12 F52 Camera Diagram

This was the F52 camera (Fig. 11) the prototype of which was produced in the quite remarkable time of 54 days (Laws 1945). It had a $8\frac{1}{4} \times 7$ in. (20×17.5 cm) format (Fig. 12) and was normally equipped with a f = 36 in. (90 cm) lens. Manufactured by Williamson, it was used especially from fast, specially developed high-altitude Spitfire and Mosquito aircraft which, by the end of the war, operated from altitudes in excess of 40,000 ft (12,000 m). The F24 camera continued to be used extensively e.g. from low altitudes and as a night camera on R.A.F. bomber aircraft. It was also mass-produced in the U.S.A. as the K-24 and supplied to all the Allied countries under the Lease-Lend programme. A survey and mapping camera, the F49, with a 9×9 in. (23×23 cm) format and a f = 6 in. (15 cm) with wide-angle lens was also developed along the same lines as the F52 and a hybrid, the F83, appeared which utilised the magazine, body and format of the F52 together with the Ross survey lens (an example of this camera is in the possession of the Department of Geography at the University of Glasgow).

In the United States, the new designs already being produced experimentally in the period prior to the War were rapidly developed and mass-produced in the typical American manner. The K-17, K-18, K-19, K-20 etc. were used widely. The K-22 was produced both by Fairchild and the Chicago Aerial Survey Co. as a standard day reconnaissance camera with a 9 x 9 in. (23 x 23 cm) format and a range of lenses from the f = 6 in. (15 cm) model to the f = 40 in. (100 cm) model giving a range of angular coverages from 93° to 9°.

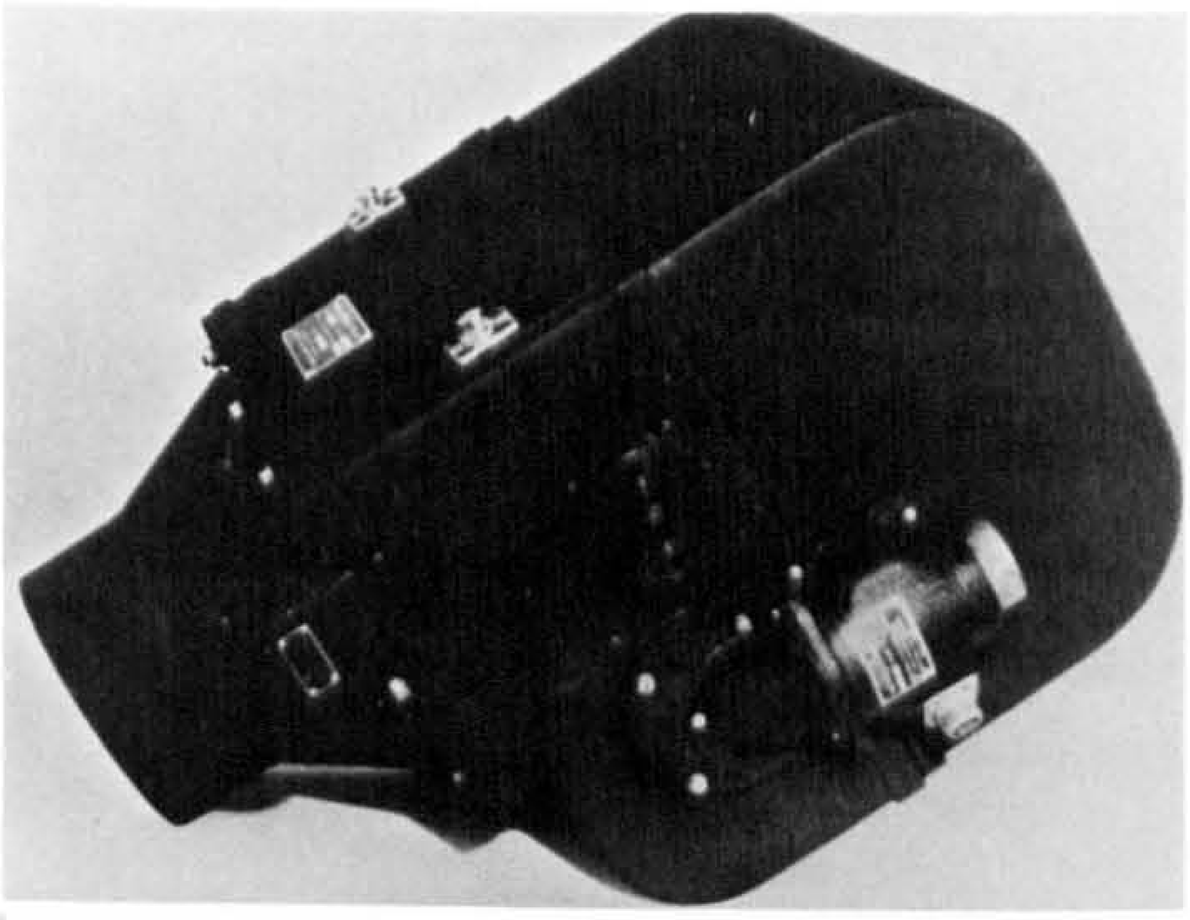

Fig. 13 Sonne S7 Camera

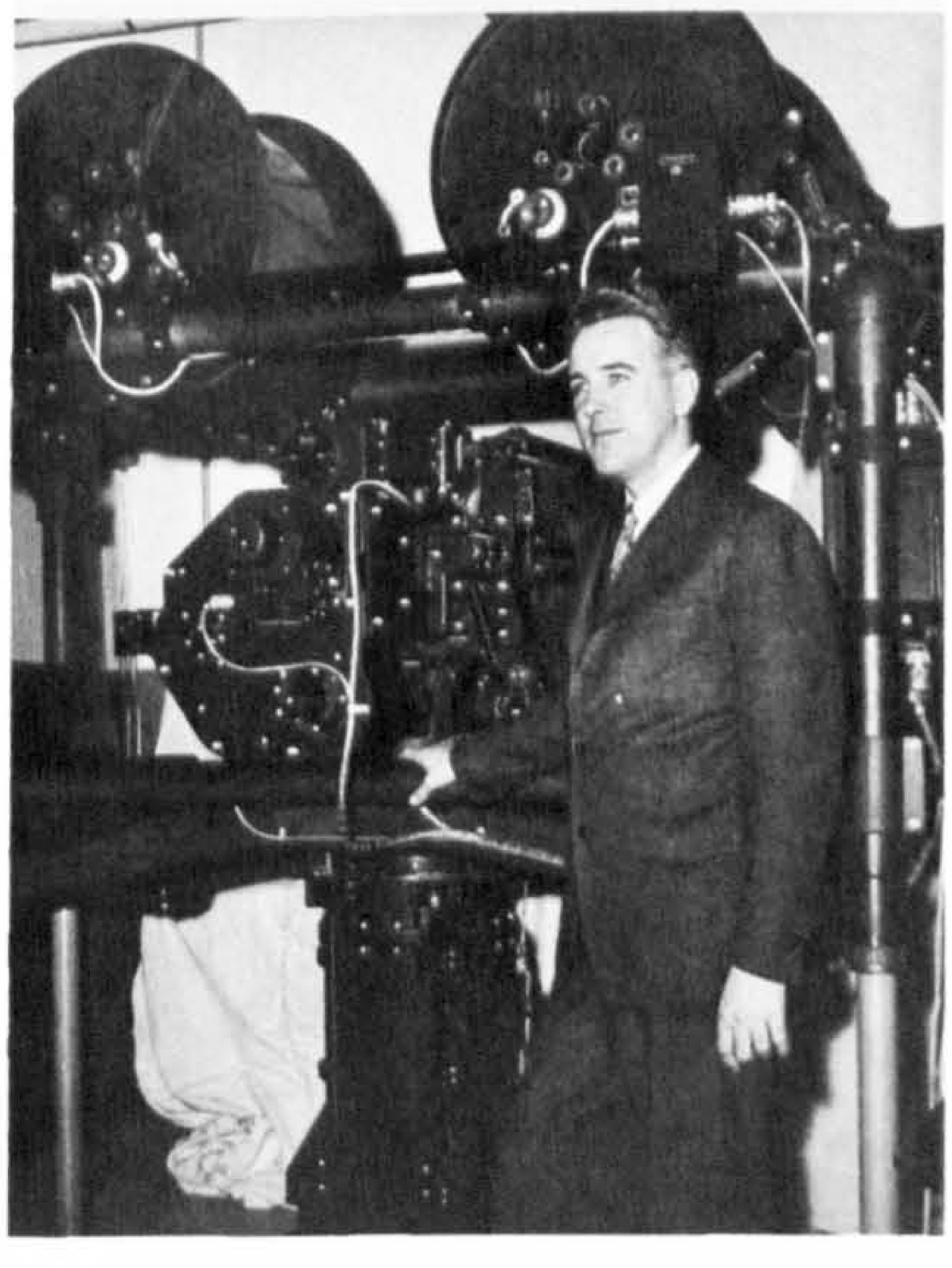

Fig. 14 Dr. Baker with high altitude Camera.

While these cameras were the principal ones used, for specialist low-level work, e.g. stereo-cover of invasion beach sites both in France and in the Pacific, the Sonne strip and stereo-strip cameras (Fig. 13) produced by the Chicago Aerial Survey Co. were employed, especially by the U.S. Navy. In

1940, a development was initiated which was to have far-reaching consequences for high-altitude reconnaissance work. This was the establishment, with the U.S. A.F. support, of the Optical Research Laboratory at Harvard University under Dr. James Baker, then a young astronomer. Work started on a series of advanced f = 40 in. (100 cm), 60 in. (150 cm) and 100 in. (250 cm) long focal length lenses with very high resolution (Fig. 14). The 40 in. lens was used in the K-22 camera, but the 60 in. lens was only made ready in 1944 and used in Western Europe in limited quantities (Goddard 1969). The lens was a folded design (in the form of a U) and was the first to provide automatic compensation for changes in air temperature and pressure. The 100 in. lens was only completed as the War ended.

On the German side, there was little use of high speed fighter aircraft for reconnaissance and twin-engined bomber aircraft were mostly used. These were quite suitable for the Russian front until late in the War, but since such aircraft were no match for the Allied Spitfire and Mustang fighters, it meant that little reconnaissance of Britain and other heavily defended areas took place. The Germans did convert a few Junkers 86 aircraft (Models P1 and P2) to high-flying operation (40,000 ft), but it appears in general that strategic reconnaissance was little practised (Brookes 1975). The main cameras used were the Zeiss RB series with 20, 50 and 75 cm focal lengths and the unusually large 30 x 30 in. format.

To summarise the situation at the end of World War II, one can say that, on the Allied side, high-performance reconnaissance frame cameras were the norm. While a range of lenses had been developed for a wide variety of possible uses, the emphasis was on photo-reconnaissance using the Spitfire, Mosquito, P-51 Mustang and F-5 Lightning which, by operating at altitudes of 40,000 ft (12,000 m), offered safety from enemy fighter aircraft and anti-aircraft fire. Hence long focal length, narrow-angled lenses were standard especially for strategic reconnaissance as distinct from tactical battlefield missions.

1.6 Developments Post-World War II

At first, developments in the immediate post-War period were slow, but with the onset of the Cold War and the sudden advent of the Korean War, development began apace. At first, American developments were concentrated on frame cameras with still longer focal length lenses. The K-30 camera utilised the Baker f = 100 in. (250 cm) lens with an aperture of f/10 (Fig. 15) and had a format size of 9 x 18 in. (22.5 x 45 cm).

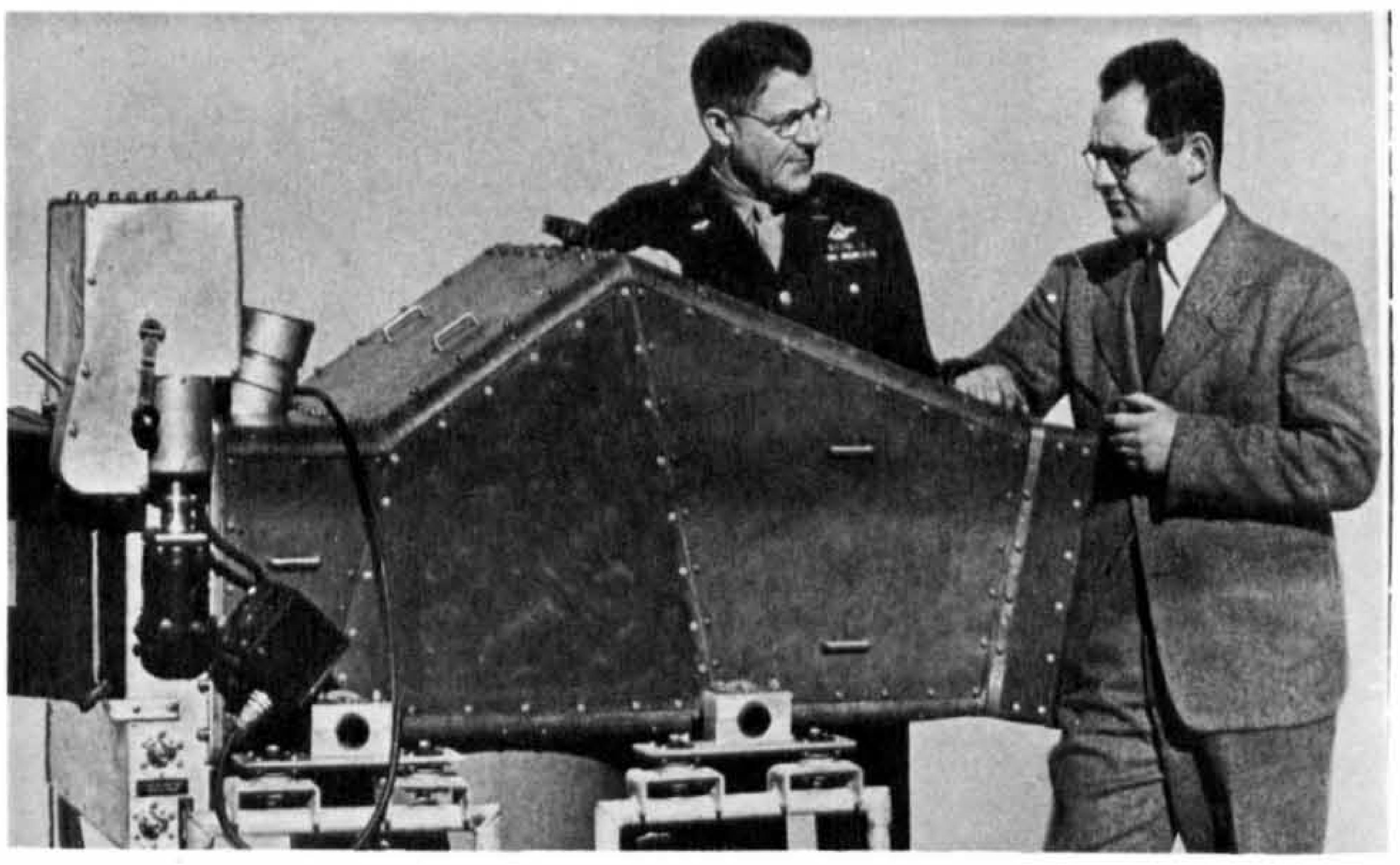

Fig. 15. The f = 100 in. (250 cm) lens camera.

When installed in an aircraft flying at an altitude of 50,000 ft (15,000 m) it provided a photo scale of 1/6000. The K-30 camera was equipped with a focal plane shutter with speeds varying from 1/100 to 1/1000 second. The relatively slow shutter speeds were inevitable with the restricted apertures common with these long focal lengths. Such cameras were physically quite enormous and very heavy (Fig. 14). This did not trouble the Americans with their giant B-29

Superfortress and B-36 high-altitude bomber aircraft. However, the trend was to change quite rapidly as jet aircraft e.g. the F-80 and F-86 fighters and the B-47 and B-52 bombers, began to be introduced in large numbers. These could operate at still greater altitudes and much higher speeds but, apart from the B-52, they were much smaller in size than their propeller-driven predecessors. New cameras to take care of these new operational parameters were developed. Supersonic aircraft were brought into service so that still newer designs were produced. Specialist photo-reconnaissance aircraft such as the RF-101 Voodoo and RF-4 Phantom were introduced. With the development of anti-aircraft missiles, operating ceilings increased on the one hand while, on the other, many reconnaissance missions were conducted at high speeds and at very low altitudes to avoid radar, gunfire and missiles.

The number and range of American reconnaissance cameras developed in the 1950's and 1960's is quite bewildering. Attempting to isolate a few main trends during this period , the first is the continued development of ultra-long focal length, high resolution reconnaissance cameras. In the forefront of this development was the Optical Research Laboratory, previously at Harvard University, but later transferred to Boston University under the direction of Dr. Duncan Macdonald. (Still later, when the USAF cut back its support for the laboratory, the famous Itek Corporation was formed to operate it as a commercial company.) The Baker f = 100 in. (250 cm) design was refined by the laboratory, so that a lighter weight version was produced, but focal lengths increased to f = 240 in. (610 cm), again on a large 9 x 18 in. (23 x 46 cm) rectangular format to combat lack of coverage but still using standard 9 in. (23 cm) film.

With advent of the Lockheed U-2 and the Martin B-57E Canberra ultra-high altitude (with ceilings in excess of 70,000 ft (21,000 m))strategic reconnaissance aircraft, ever-greater performance was required from cameras, lenses, shutters and films. The testimony of Dr. Alekseyevich, the Russian reconnaissance expert, given at the trial of Gary Powers, the pilot of the U-2 shot down near Sverdlovsk in 1960 (and recently analysed by Brock 1976), allows some insight into the performance achieved. This particular U-2 had a f = 36 in. (90 cm) camera (believed to have been built by Perkin-Elmer) which produced a scale of 1/22,000 from H = 70,000 ft (21,000 m). To give relatively wide-angle coverage with this lens, the camera utilised two rolls of standard 9½ in. (24 cm) film run side by side across the focal plane to give a format of 46 x 46 cm and a coverage of 28°. Seven parallel strips were taken by a rotating lens through seven glass windows in the body of the plane. This appears to indicate the use of a horizontally positioned camera axis with the lens and 45° mirror rotating as a unit. Thus the total lateral cover was 200 km. No less than 2,000 m of film was available in the camera magazine.

Goddard in his book also refers to the development of reflective mirror optics to cut down the size and weight of these large lenses and to give relatively wide apertures and acceptable exposure times at long focal lengths. This development was started at the California Institute of Technology during the Second World War under Dr. Milliken. The resulting cameras did not go into production during the War due to problems with the mirror tarnishing, especially in the tropics, and to problems with vibrations associated with propeller-driven aircraft. The development continued later at the Boston Optical Research Laboratory, and Baker was of course responsible for the optical design of the well-known Baker-Nunn satellite tracking cameras which were built in the early 1960's and utilise reflective mirror optics. One may assume that American cameras of this type exist for use in aircraft. Almost certainly, the USAF 240 in. camera was of the Cassagrain reflective mirror type. Itek mention that they had built a f = 240 in. (610 cm) f/20 system to this design in which the front mirror was located only 40 in. (100 cm) from the focal plane (Itek Laboratories 1961). The best-known of such cameras are, however, the range (TA-20 to TA-120) developed by the Oude Delft company in the Netherlands with focal lengths of up to 1.20 m (Fig. 16).

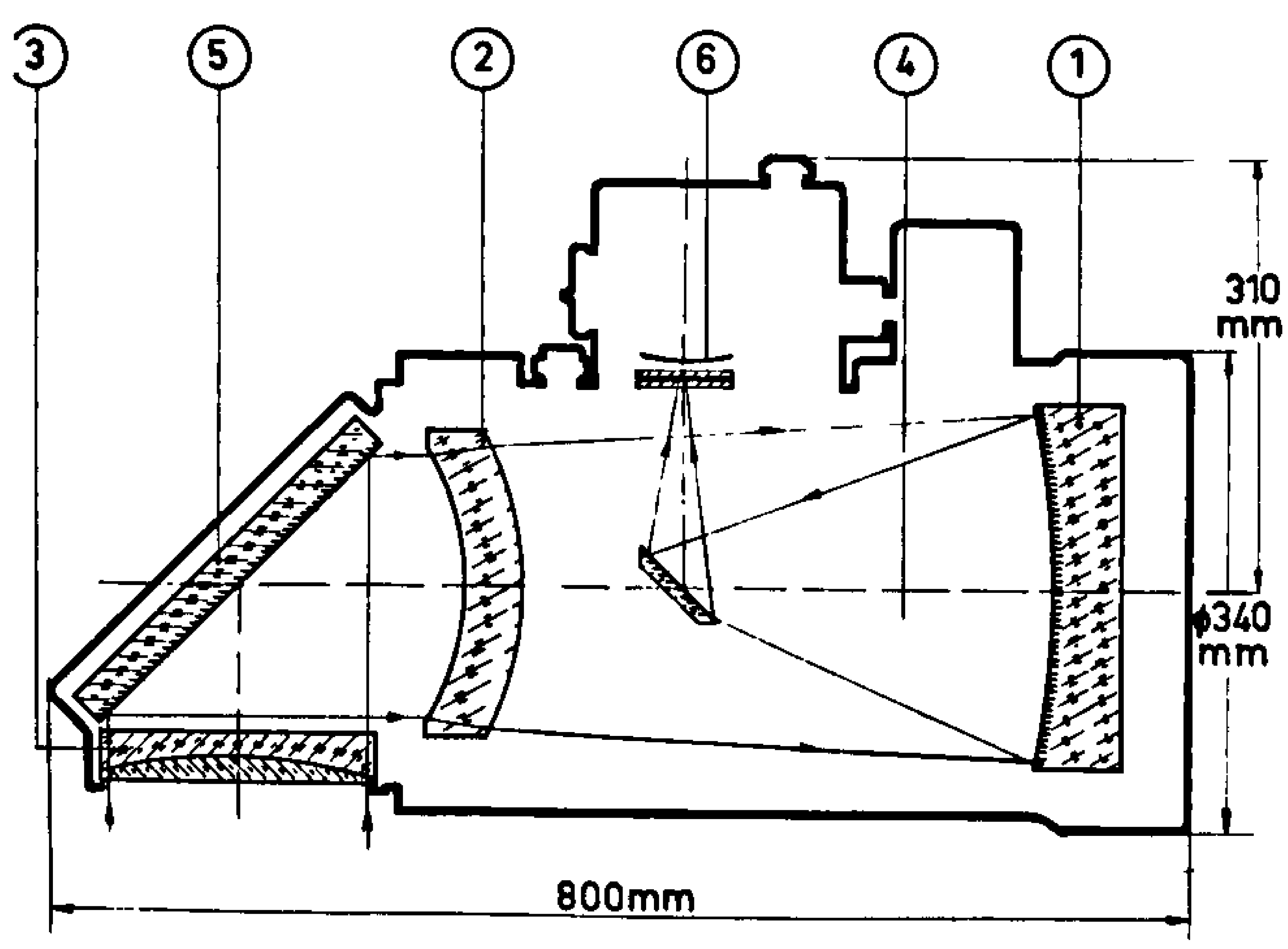

Fig. 16 Oude Delft TA- series Camera Diagram

Since 1960, operating altitudes of jet reconnaissance aircraft have grown still greater, the Lockheed SR-71 being capable of operating at H=100,000 to 120,000 ft (30,500 to 36,500 m). Furthermore, since 1962, Earth-orbiting satellites have been used for strategic photo-reconnaissance (Klass 1971a). With these, the speeds of the camera platforms have become still greater (29,000 k.p.h. v 3,000 k.p.h.) and operating altitudes still higher (180 km and upwards v 30 km). Thus the needs for longer focal lengths, ever shorter exposure times and higher film resolution (which are all contradictory) are, as ever, primary requirements for strategic reconnaissance. Reportedly, the current Lockheed Big Bird reconnaissance satellites use a Perkin-Elmer camera of f = 8 ft(2.5 m) which gives a scale of 1/65,000 from H = 180 km (Klass 1971b). There is little doubt that the cameras used so successfully and reliably in the various N.A.S.A. projects had been developed earlier for military reconnaissance purposes. Thus the film camera with radio-transmission used in 1966 and 1967 in the Lunar Orbiter series of exploratory satellites had already been developed for the Samos series of strategic reconnaissance satellites operated from 1962 onwards (Klass 1971a). Also, the film cameras used in the manned Apollo lunar missions were long focal length military reconnaissance cameras - the Hycon (later Actron) KA-74 frame camera (Fig. 17) and the Itek KA-80 panoramic camera (Fig. 18). Therefore the civilian N.A.S.A. flights, executed in the full glare of World press and television coverage, have helped greatly in lifting the curtain on various types of high performance reconnaissance cameras, which would otherwise be little known.

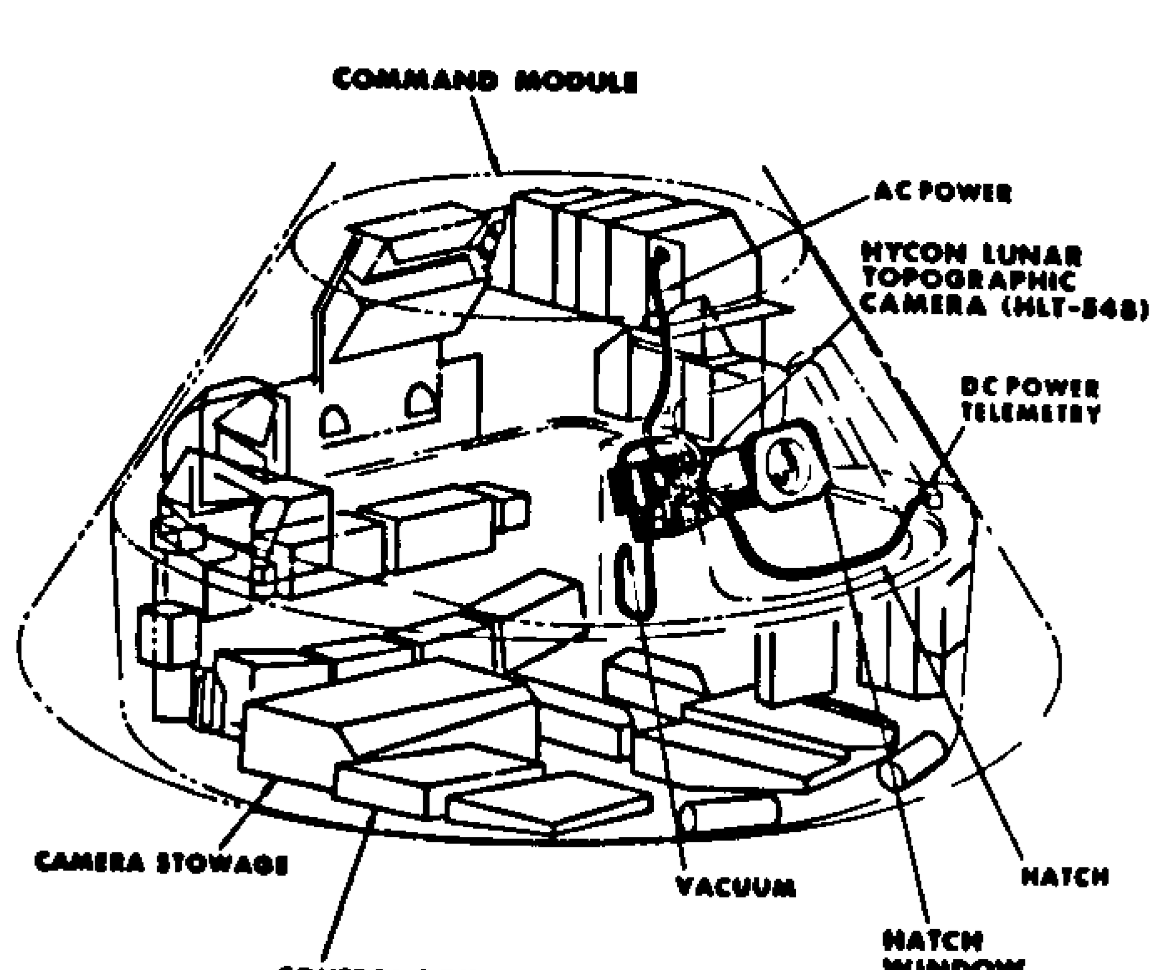

Fig. 17 KA-74 Camera in Apollo Spacecraft

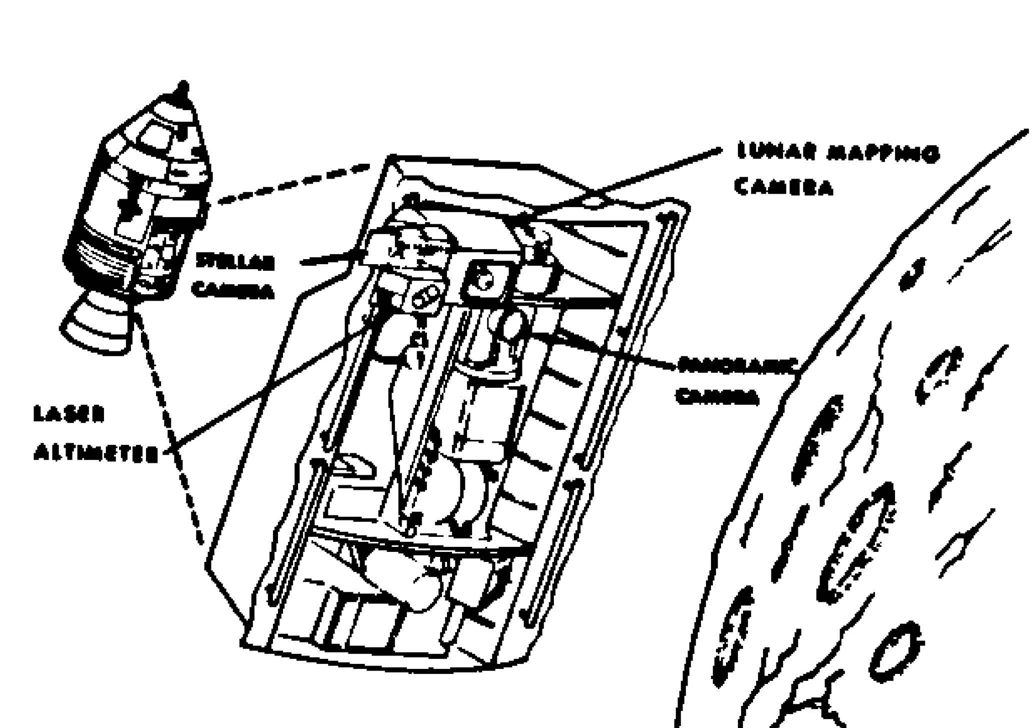

Fig. 18 Itek KA-80 Camera fitted to Apollo Spacecraft

Another main trend in the United States developments has been the widespread adoption of panoramic cameras. Goddard (p. 379) assigns their introduction to aerial reconnaissance work to Philbrick, a U.S.A.F. officer working at the Boston Optical Research Laboratory. He modified an S7 strip camera to give a 9 x 30 in. (23 x 75 cm) format and a coverage that, from a flying height of 30,000 ft (9,000 m) over New England, stretched from Portland Maise to New England. A panoramic camera was a solution to solve the age-old problem of obtaining large scale and high resolution with wide angular coverage. This it does achieve especially since the long focal length narrow-angle lens is used on-axis through the exposure. However, it is achieved at the cost of large scale changes and considerable geometrical distortion, especially towards the edges of each photograph.

A final point about American developments has been the introduction of small, remotely-controlled drones (or remote piloted vehicles (R.P.Vs) such as the Ryan Firebee since the Vietnam War. These generally have restrictions concerning the size and weight of the cameras which can be installed in them. A development closely associated with these drones has been that the photographs taken by cameras on board these vehicles can be developed, scanned electronically and transmitted back by radio to a receiving station, so that the information is not lost if the drone does not return to its base. Parallel developments have taken place on board "search and find" reconnaissance satellites with radio transmission to an Earth station (Klass 1971a) and, as mentioned above, the technology involved is known from the highly successful series of Lunar Orbiter satellites of N.A.S.A. (Figs. 19 and 20).

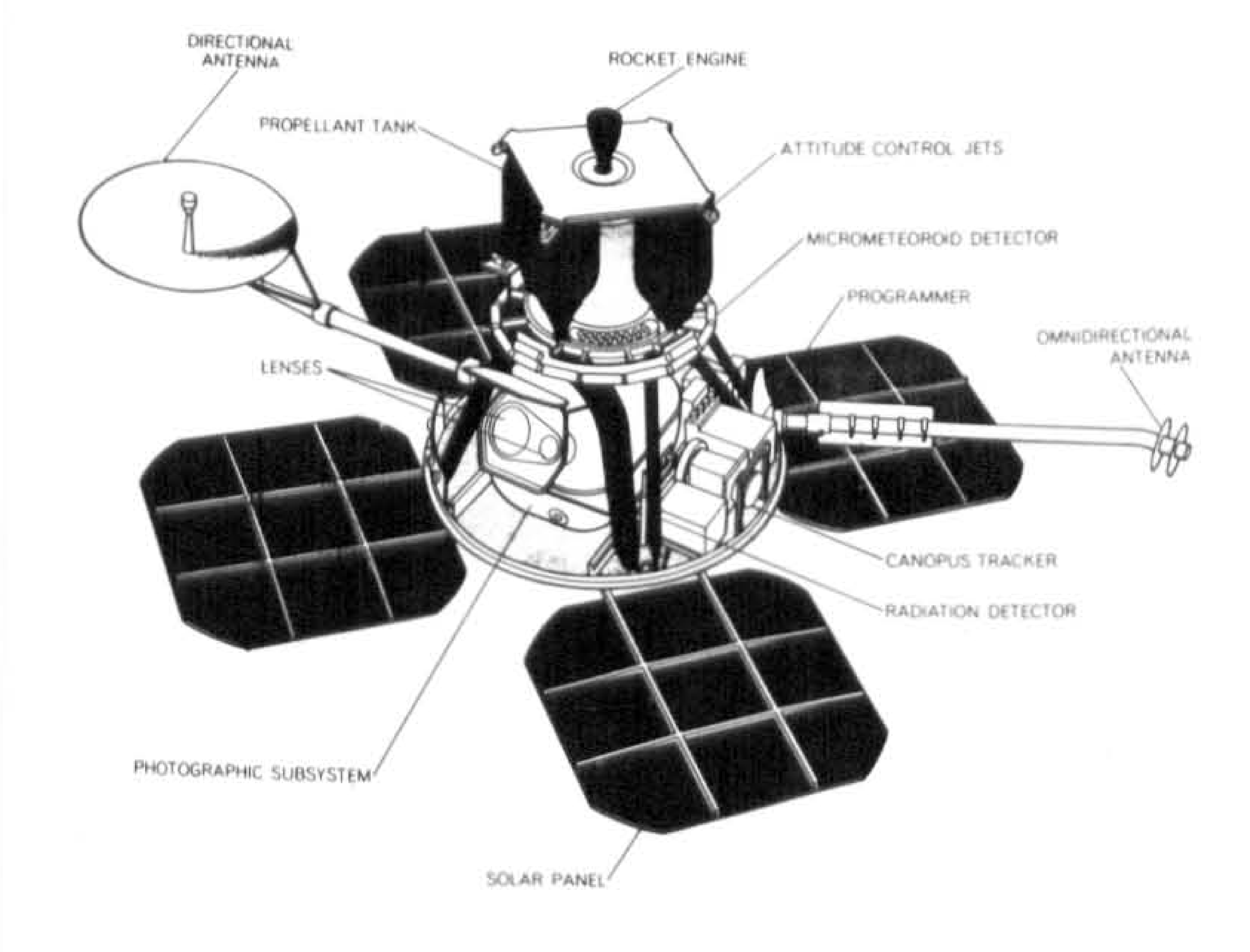

Fig. 19 Lunar Orbiter Spacecraft

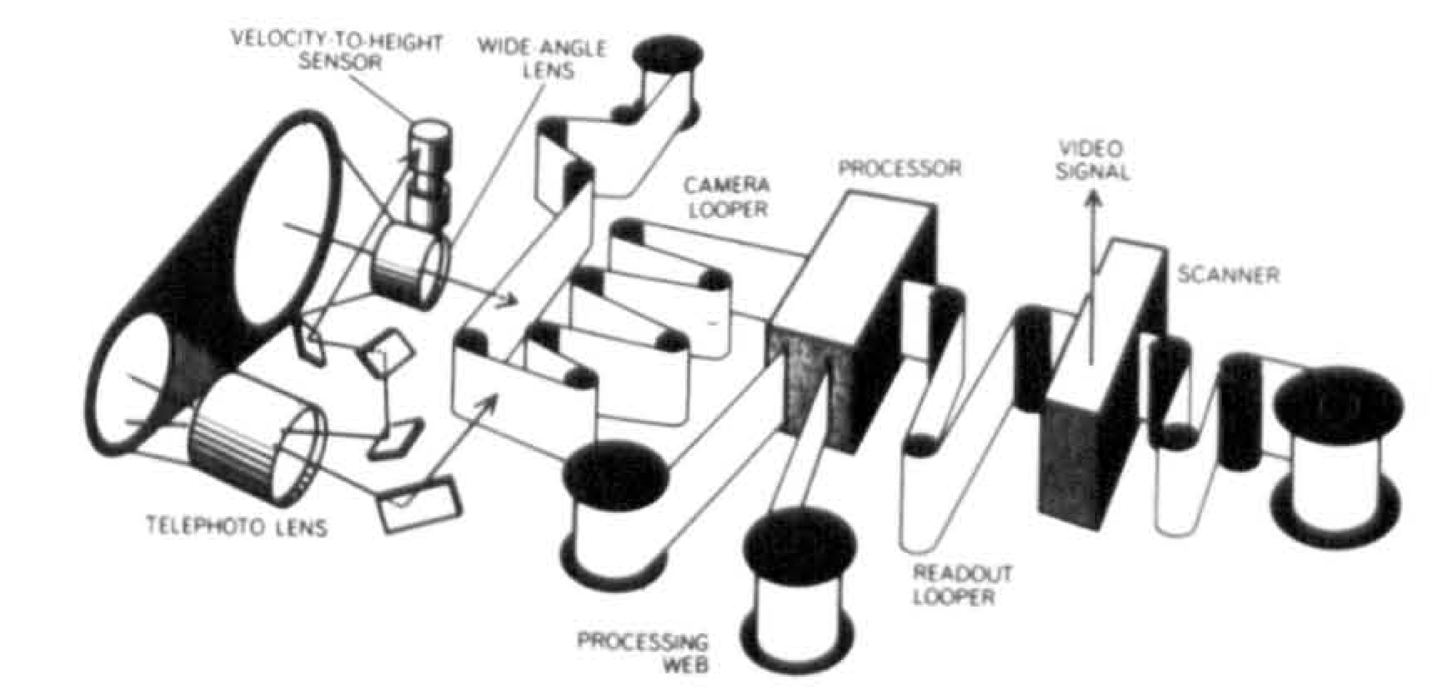

Fig. 20 Lunar Orbiter Camera System

Placing special emphasis on American work is justified, given the giant effort and great variety of reconnaissance camera development which has taken place in the United States. In the other Western European countries, development has been on an altogether more modest but still significant scale and has been remarkably successful though restricted to certain fields. In Britain, the traditional reconnaissance frame camera has remained the chief type and a series of cameras have been produced on the standard 70 mm, 5 in. (12.5 cm) and 9 in. (23 cm) film formats. The main producer of 70 mm cameras has been the firm of Vinten, especially with their F95 series (Fig. 21) though Williamson has also produced the F134 design. The 5 in. film cameras include the F117 of Williamson (Fig. 22), the type 690 of Vinten and the unusual F135 (Fig. 23) of A.G.I. which produces two side-by-side photographs looking forward and

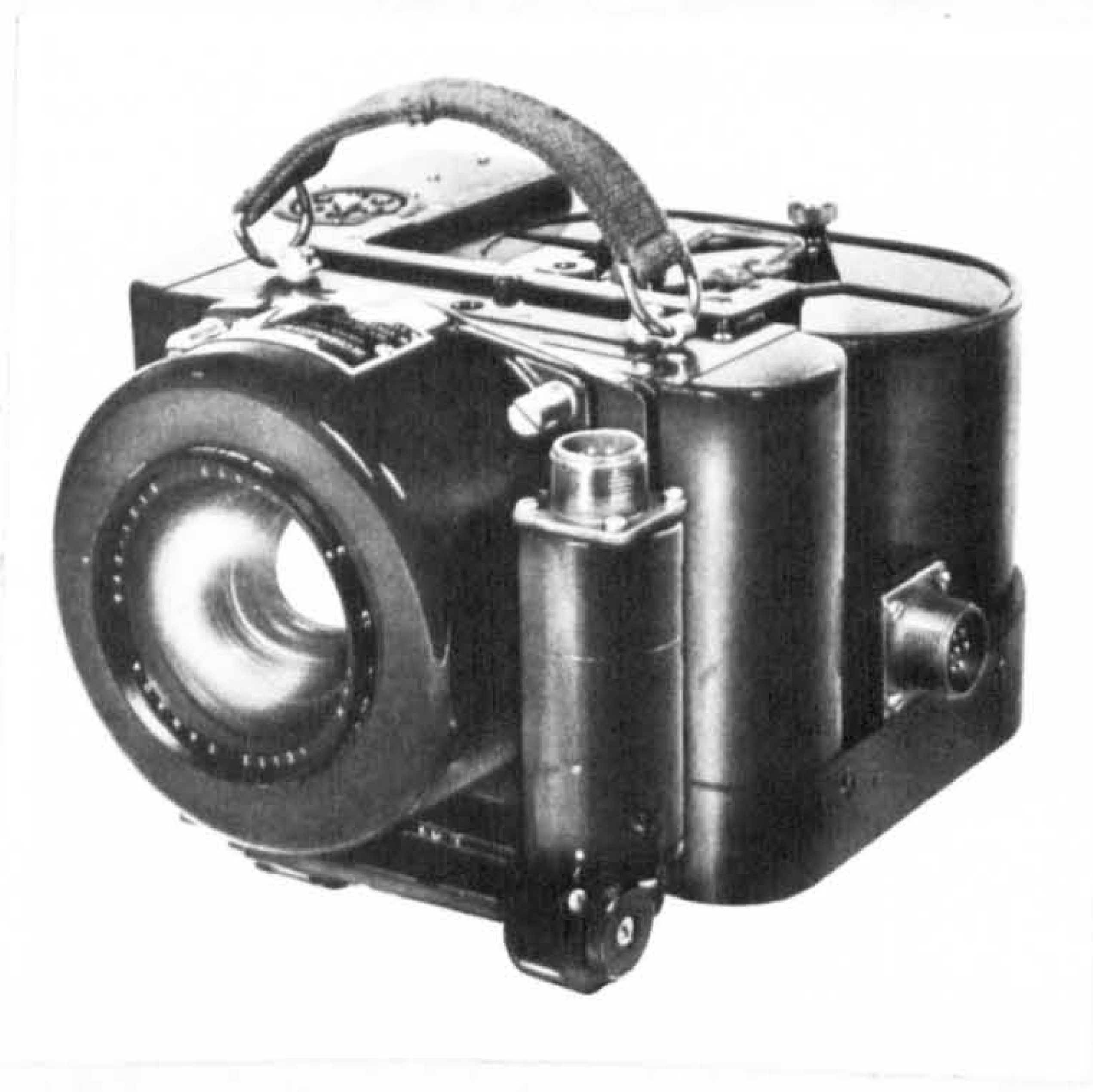

Fig. 21 Vinten 70 mm Camera

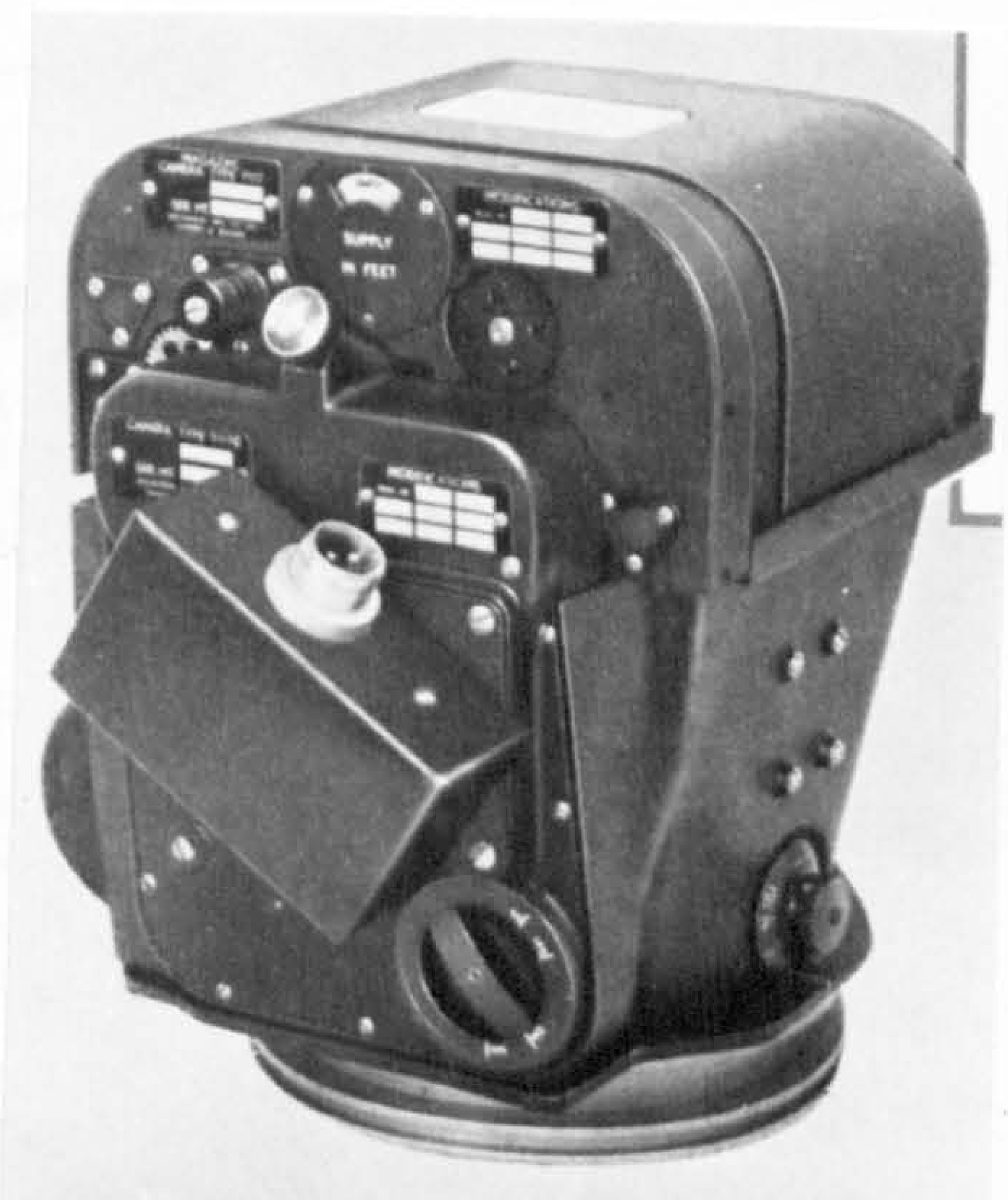

Fig. 22 Williamson F117 Camera

backward rather like a stereo-strip camera, but utilising a frame format. The ubiquitous F52 has been replaced first by the F96 camera and then by the A.G.I. F126 design with a range of lenses from f = 6 in. (15 cm) to 36 in. (90 cm). Experimental large-format panoramic cameras have been developed in the U.K., e.g. the Williamson F85 (Williamson 1954), but they do not appear to have entered service. However, this may change with the recent introduction of the type 750 camera by Vinten which may be regarded as a scaled-down version (using 70 mm film) of the Itek KA-80 rotating optical bar panoramic camera used in the Apollo lunar photographic missions.

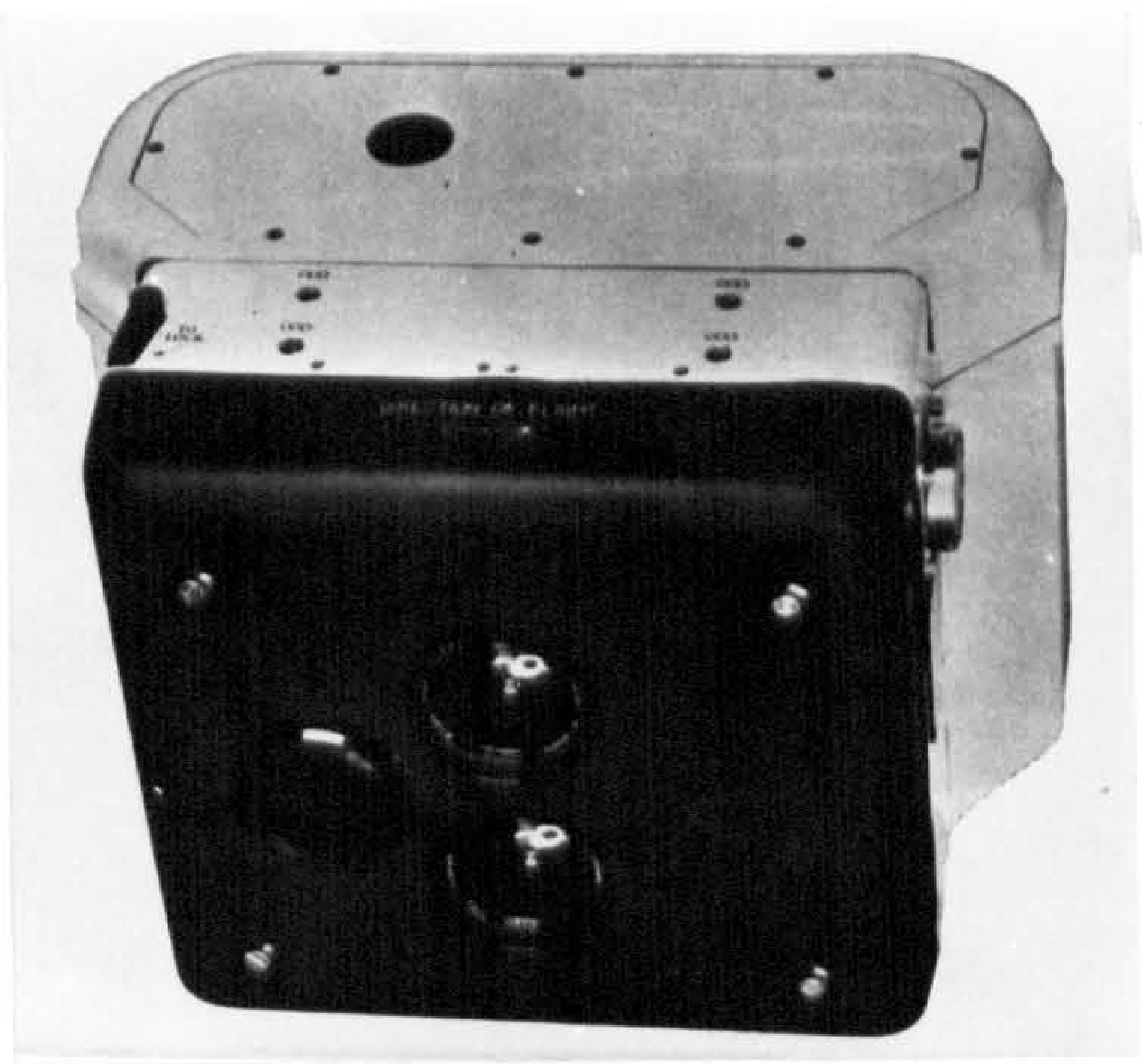

Fig. 23 A.G.I. F135 Camera

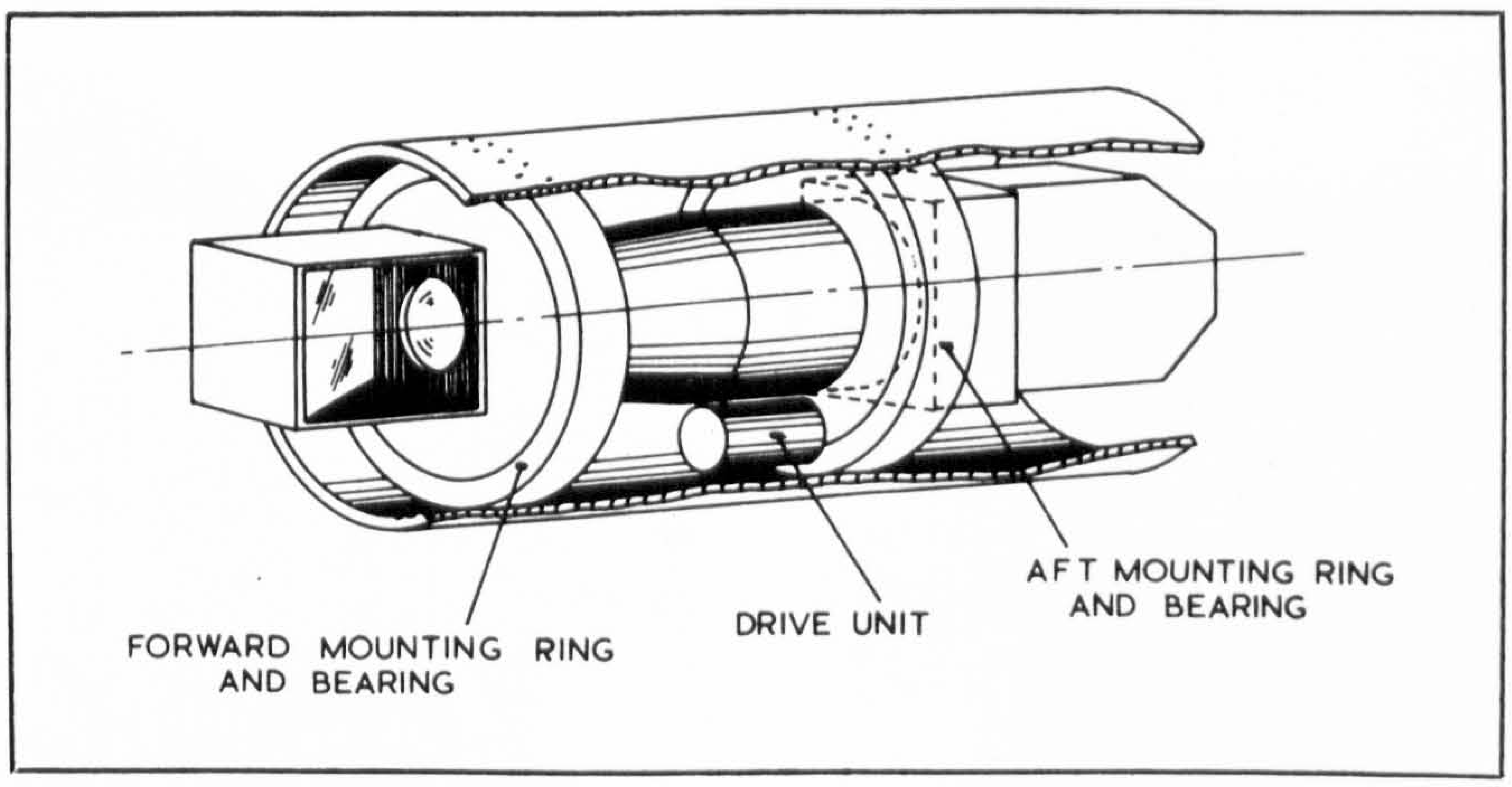

Fig. 24 Vinten LOROP design

The influence of American development (and of Brock who has returned to Vinten from Itek) may also be noted in the Vinten LOROP (long range oblique camera) (Fig. 24) proposal discussed in Flight International, 16 May 1974. This also bears a noticeable resemblance to the U-2 camera arrangement described by Alekseyevich, but again a small-size of camera (the type 690 with 5 in. (12.5 cm) film) is used, fitted with a Leitz f = 24 in. (60 cm) f/4 lens.

In the Netherlands, as already mentioned, the outstanding designs are the Oude Delft cameras equipped with reflective mirror optics which appear to have had widespread use in N.A.T.O. reconnaissance aircraft. But 70 mm film frame cameras employing lens optics, e.g. the TA-7 (Fig. 25) and TA-8 series, have also been developed by Oude Delft. French development appears to have followed much the same path as in the U.K. with a range of frame cameras utilising the standard 70 mm, 5 in. (12.5 cm) and 9 in. (23 cm) formats, e.g. the Omera series utilising Matra-S.F.O.M. lenses. In West Germany, the large format 23 x 23 cm Type HRb cameras (Fig. 26) produced by Zeiss Oberkochen appear to be adapted versions of the well-known RMK series of metric cameras.

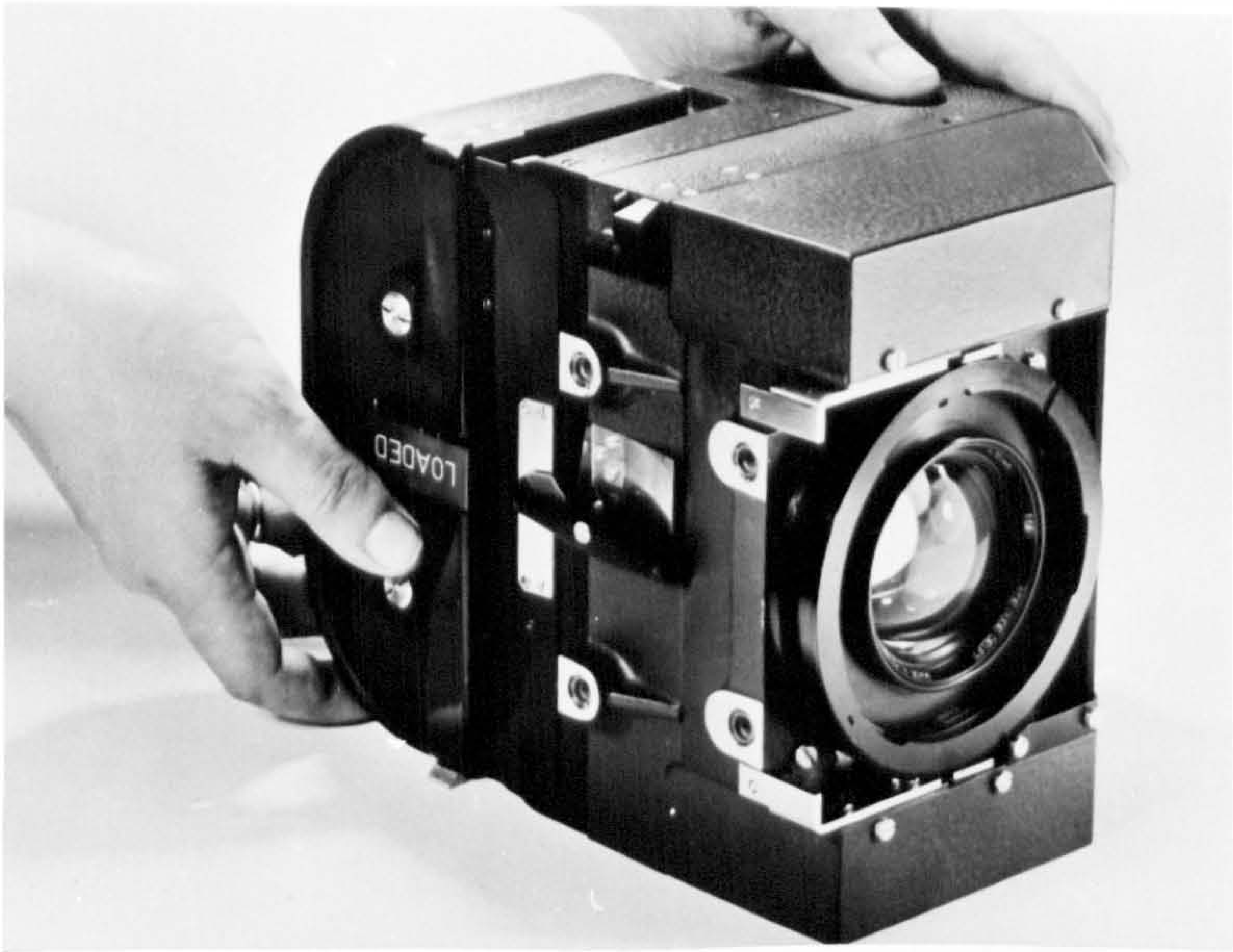

Fig. 25 Oude Delft TA-7 M 70 mm Camera

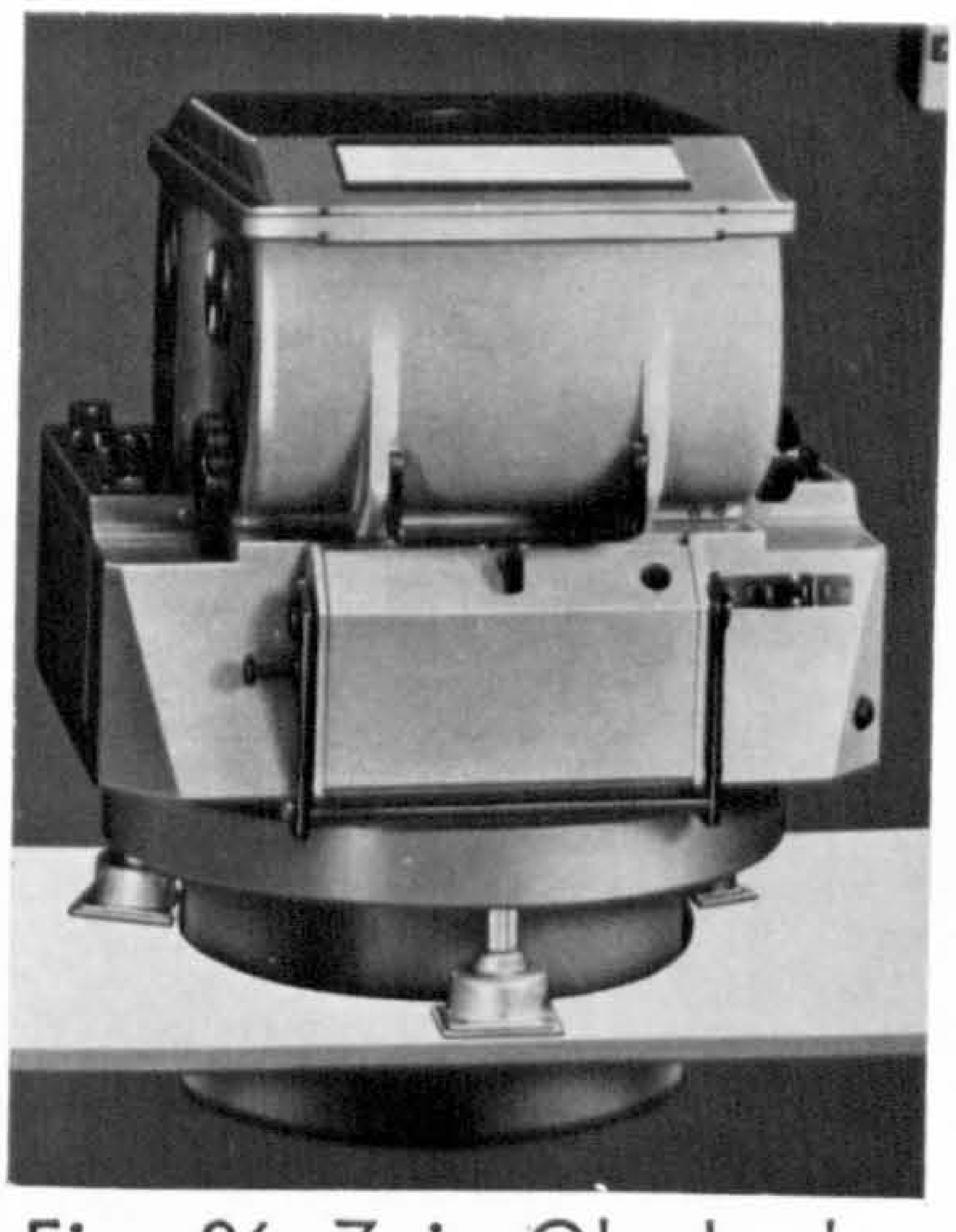

Fig. 26 Zeiss Oberkochen HRb reconnaissance frame Camera

Having quickly sketched the history and development of aerial reconnaissance cameras and photography, it is profitable to consider in more detail some of the most recent developments mentioned above, since several of these are of particular relevance to this dissertation.

CHAPTER II

Continuous strip and panoramic cameras

CHAPTER II

CONTINUOUS STRIP AND PANORAMIC CAMERAS

2.1 Introduction

Arising from the previous chapter, it can be seen that there are three types of reconnaissance camera:-

(i) the frame type

(ii) the continuous strip type and

(iii) the panoramic type.

In this chapter, the latter two types will be discussed in some detail. They have been developed more recently than the traditional type of frame camera - in the case of the continuous strip cameras from just before the Second World War; in the case of the panoramic cameras from the period of the late 1950's onwards. Although this thesis is concerned primarily with frame-type cameras, some consideration of these alternative solutions is justified both on the grounds of completeness and also so that the comparisons between these different types, made later on, can be better understood and placed in a correct context. In particular, it will be seen that, while the continuous strip and panoramic cameras are optimised for certain roles and missions, the traditional type of frame camera has been developed continuously and successfully and still offers considerable advantages in many situations, not least to the military and civilian users.

2.2 Image Movement Compensation

One of the major problems encountered when using conventional aerial cameras to obtain photography from aircraft flown at low-altitudes and at high speed is that the distance moved by the image on the focal plane during the exposure time results in a discernible image blur. This image movement is directly proportional to the craft speed and the exposure time, and inversely proportional to the flying height. However, even if a high speed of exposure can be employed, the image motion may still be significant when the camera is installed in an aircraft flying at supersonic speed and at low altitude.

For example, an aircraft flying at Mach 1 (280 m/sec) at a low altitude of 200 ft (60 m) - which is now frequently required in military air operations - and using a camera with a f = 38 mm lens, would certainly produce a blurred image irrespective of exposure speed, as the following diagram (Fig. 27) shows:

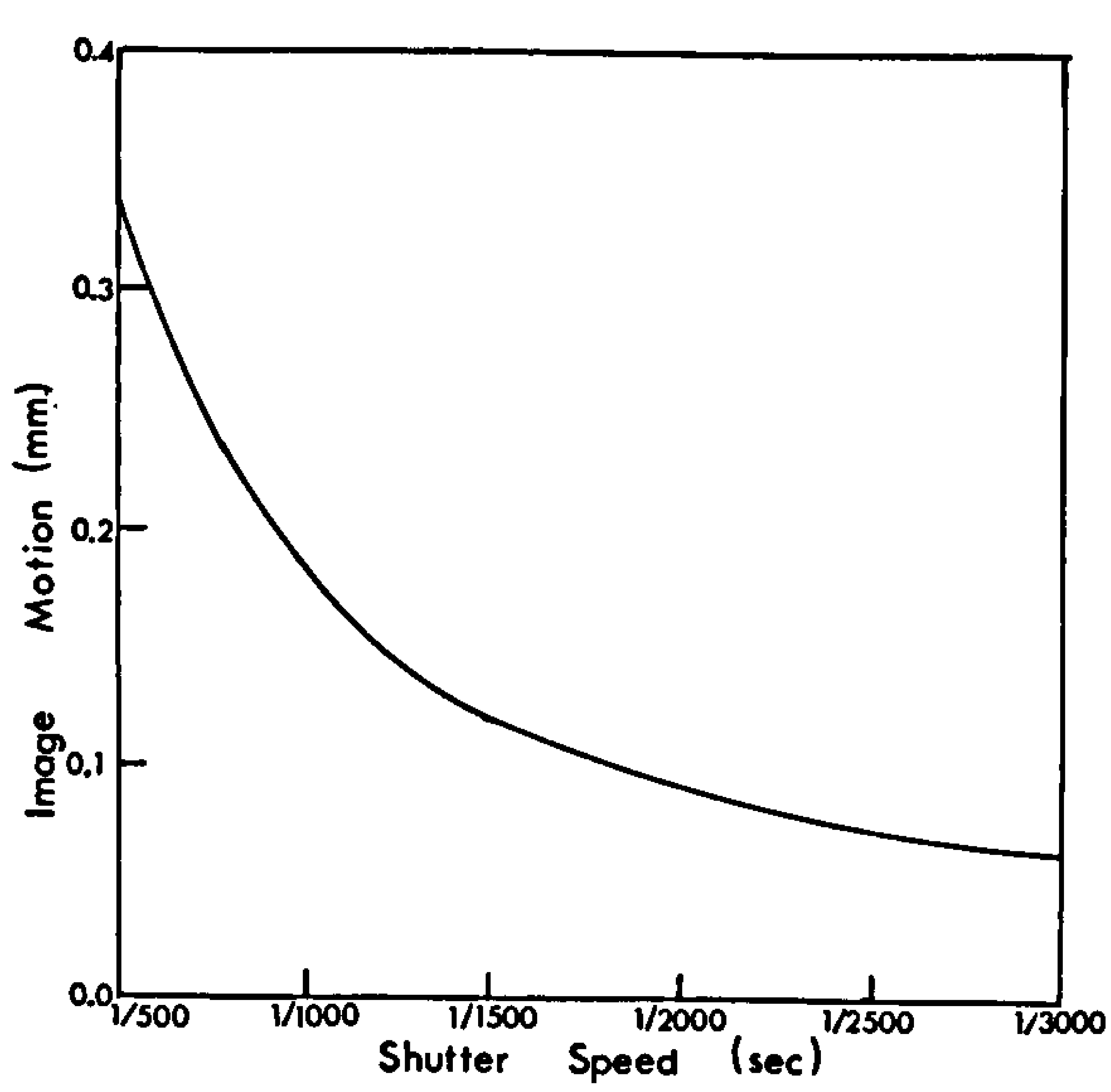

Fig. 27 Image motion at different shutter speeds

Although the amount of blur is dependent on the exposure time, it can be seen that no practical shutter speed would eliminate this image motion.

At first, high altitude photography was largely free from such troubles because of the smaller scale and lower resolution. But as camera lenses and films have improved in resolution and aircraft speeds have gone up (the SR-71 flies at 3000 k.p.h. - nearly 800 m/sec), image blur can be important even from high altitudes. With the advent of satellites orbiting at 29,000 k.p.h. 8 km/sec, and the use of high resolution cameras, the problem is still present. The result of these considerations is that image movement compensation (i.m.c.) is fitted to virtually all reconnaissance cameras no matter which principle they are based upon. In principle, this can be done by moving either the film or the lens, the other component remaining fixed: the former is usually the more practical method (though not in some types of panoramic camera). An alternative procedure is by continuous tilting of the camera during exposure so that the optical axis always points at a fixed position on the terrain; as will be seen later, this method is confined however to cameras with narrow-angled lenses.

2.3 Continuous Strip Cameras

Quite apart from the modifications to cameras and to procedures to combat image motion, special continuous strip and stereo strip cameras have been designed specifically for low altitude photography taken from a high-speed platform. In these cameras, the film is continuously in motion to compensate for image movement and so the photography taken with such cameras exhibits very unusual characteristics both for measurement and interpretation.

As already mentioned, the strip camera was first developed by Del Riccioin the United States at the request of Goddard and brought into service during World War II. In this type of camera, the film is moved continuously past a slit in the focal plane during exposure of the strip image (Fig. 28) The

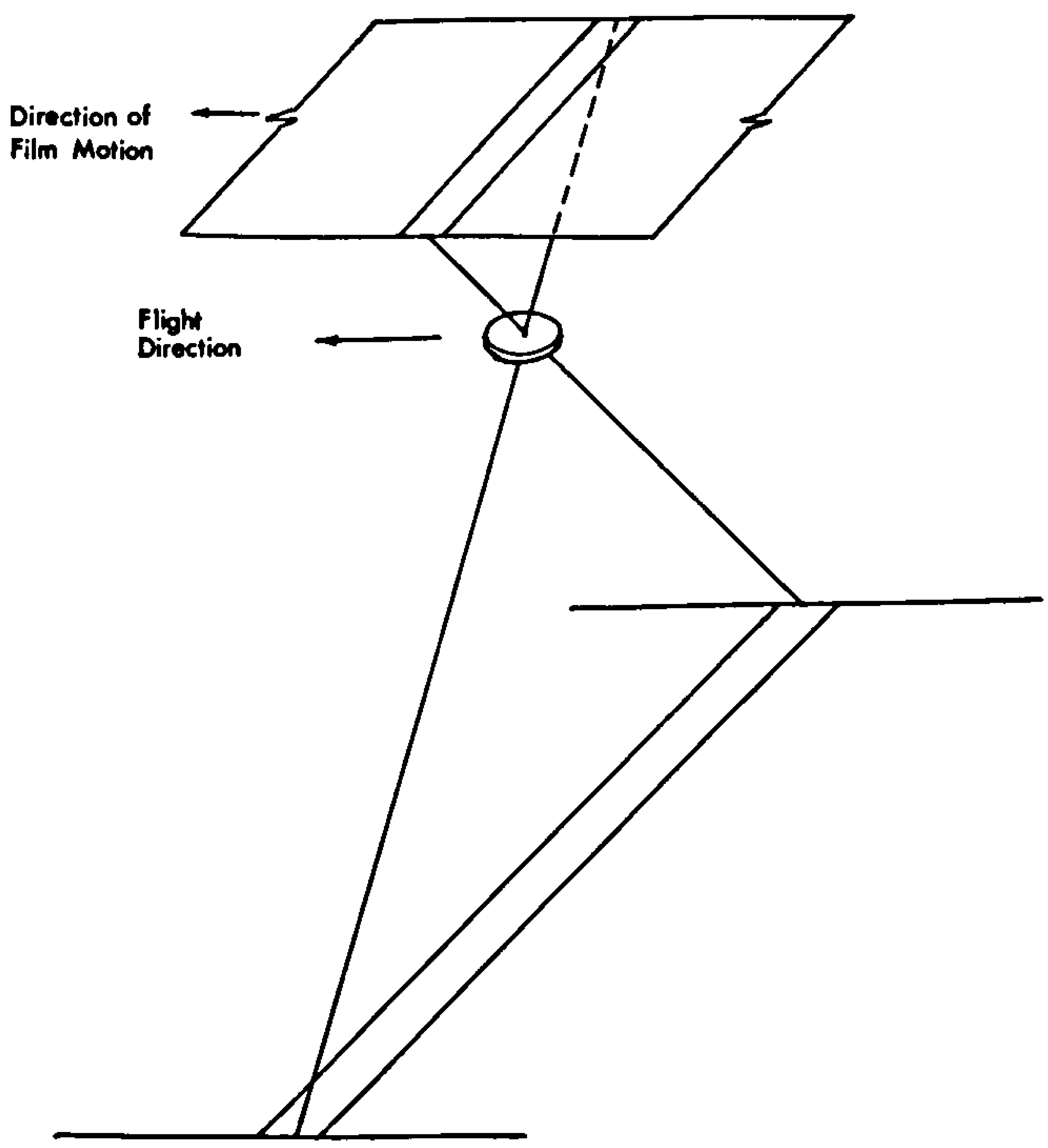

Fig. 28 Design Concept of the Continuous Strip Camera

speed of the film is proportional to and synchronised with the speed of the aircraft, which has to be measured and fed to the camera film advance mechanism. The slit is set perpendicular to the direction of flight and has a variable width according to the exposure time required. Since there is no relative image movement during exposure, short exposure times are not needed to stop image motion and hence a very narrow slit is not obligatory. Exposure may also be controlled by the iris diaphragm of the lens. However, camera stabilisation of some sort is usually applied to the strip camera, otherwise the rapid changes in tilts likely to be encountered in low altitude, high-speed flight would result in double imaging or gaps in coverage. From high altitudes, the effects of aircraft roll and pitch and aircraft vibration are magnified greatly and so strip cameras are seldom employed outside the low-level role. A twin-lens type of strip camera has also been produced which allows stereo-photographs to be taken and used. The desired stereobase is achieved by setting the lenses some distance apart on opposite sides of the slit as shown in Fig. 29.

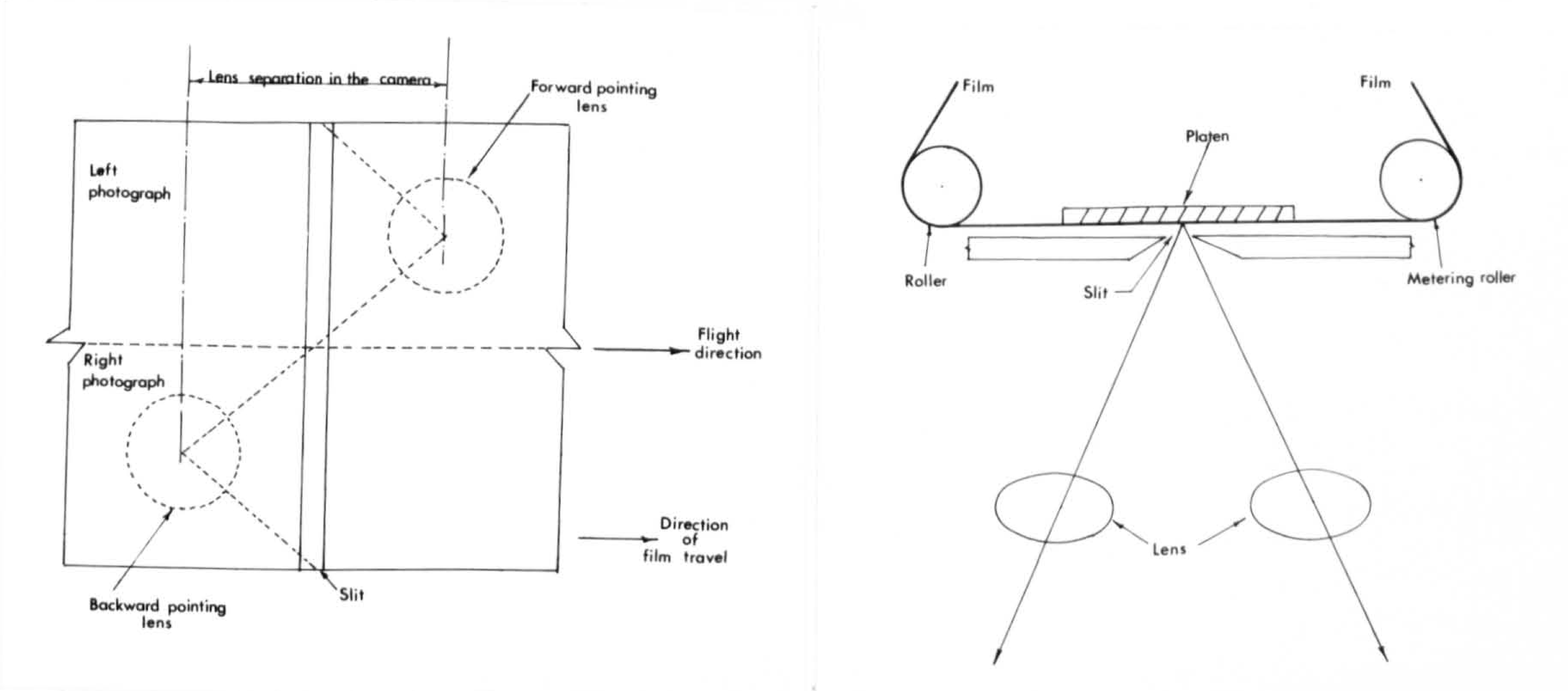

Fig. 29 Continuous Stereo Strip Camera Diagram

The Sonne S-7A was developed during World War II. It utilised standard 9 in. (23 cm) film and was available with a wide range of lenses from f = 3.5 in. (9 cm) to 20 in. (50 cm). The later S-11 camera was first used in 1950 during the Korean War, installed in the RF-80 jet aircraft. The KA-18A Continuous Strip Camera illustrated below (Fig. 30 and 31) dates from the 1960's.

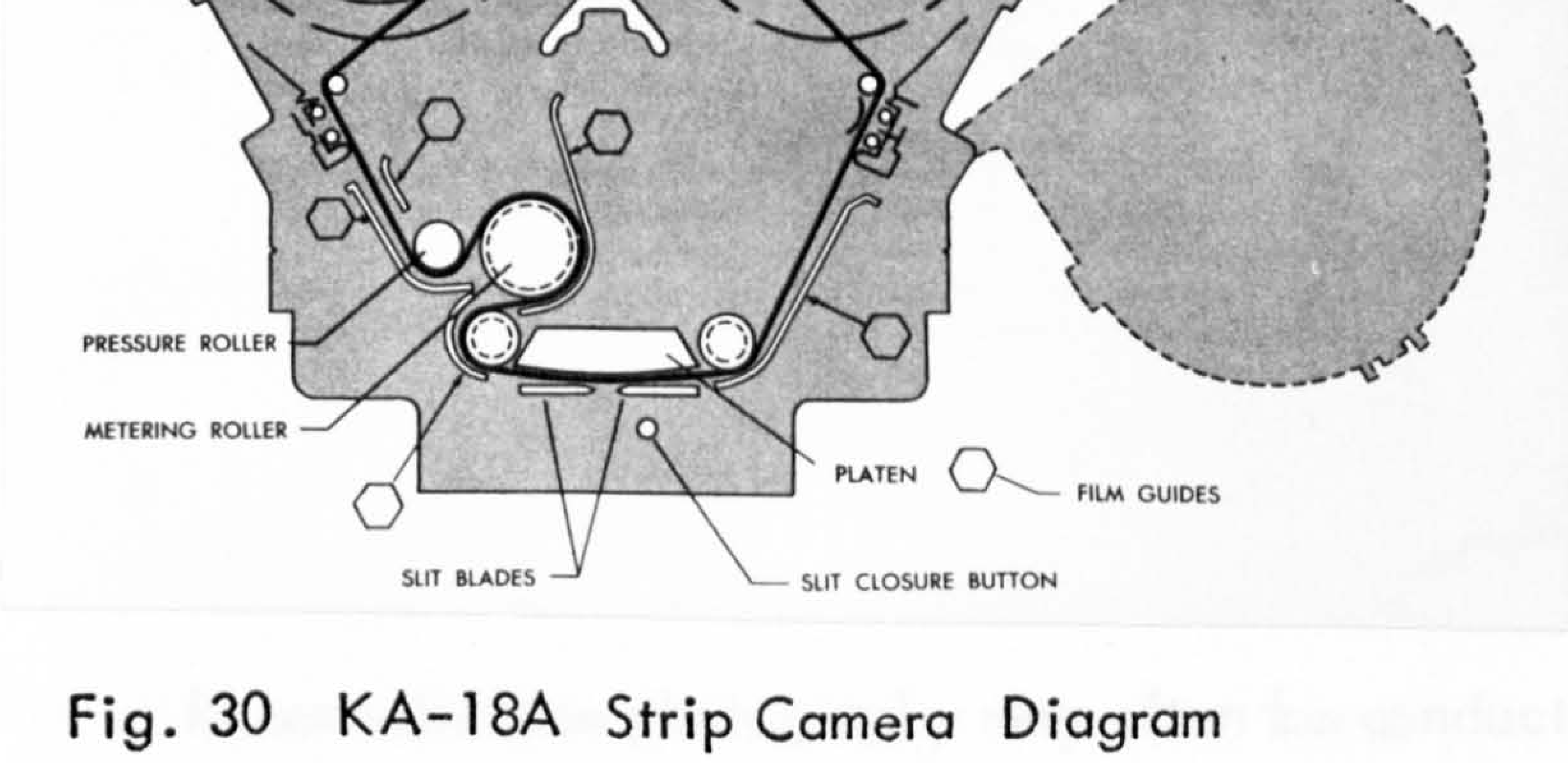

Fig. 30 KA-18A Strip Camera Diagram

Fig. 31 KA-18A Strip Camera

From the discussion above, it can be readily seen that the practical utilisation of strip and stereo-strip photography will involve the use of special instruments and procedures which are very different to those available and familiar to those practising photo-interpretation and photogrammetry on the traditional type of frame photography. Special offset stereo-viewers have been developed and measurements on strip photography can be made on comparators for later reduction by analytical methods. However, the restriction of the strip and the stereo strip cameras to low level, high speed missions has meant that the utilisation of the resultant photography remains a specialist activity restricted to a very small group of military users. Certainly, it is far less likely to be encountered than panoramic and frame type reconnaissance photography.

2.4 Panoramic Cameras

Reconnaissance photography may often be conducted from extremes of high and low altitude. For high altitude operation, cameras are equipped with long focal length lenses to give large-scale high resolution photography. In such cases, frame-type cameras have very small angles of view and restricted areal coverage. In order to overcome this difficulty, often several such cameras are installed in a fan configuration to give the widest possible view across the direction of flight. However, the installation of two or more such large cameras (since focal length may be from 24 in. to 36 in. (60 to 90 cm) with large format sizes) brings problems arising from their volume and weight and the available space in the aircraft. Furthermore, the problems of shutter synchronisation, the possibility of failure of one camera, the difficulty of handling and correlating several rolls of film and the difficulties of installation and maintenance all combine to make multiple camera installations undesirable.

The oblique camera axes and tilted photographs give also difficulties with both interpretation and mapping. However, for many years there was no alternative solution and much of the R.A.F. coverage of the U.K. has been carried out with fans of two, four or six long focal length cameras. For very low altitudes, the matter of wide angular coverage is also a problem even with shorter focus, wider angled cameras and again, the use of fans of cameras often carried in special reconnaissance pods slung below the aircraft is not uncommon, especially in current R.A.F. practice.

However, the panoramic camera offers an alternative to multiple frame camera installations and is now in quite widespread use, especially in American military reconnaissance aircraft. It is adaptable to high, medium or low altitude operation. In the high-altitude case, large scale and high resolution results from the use of a long focal length lens while wide angular coverage (which can be from horizon-to-horizon) is achieved by causing the lens to rotate and so scan the terrain on either side of the flight line. Usually the high altitude panoramic cameras, like their frame equivalents, utilise large width film and formats. Taken in conjunction with the long focal length lenses, they are comparatively large and heavy - though much less so than a corresponding multiple fan configuration. For low altitudes, focal lengths are shorter, smaller-width film is employed and formats are smaller. So low altitude panoramic cameras are much smaller in size and weight.

The basic principle of panoramic photography is shown in Fig. 32 below.

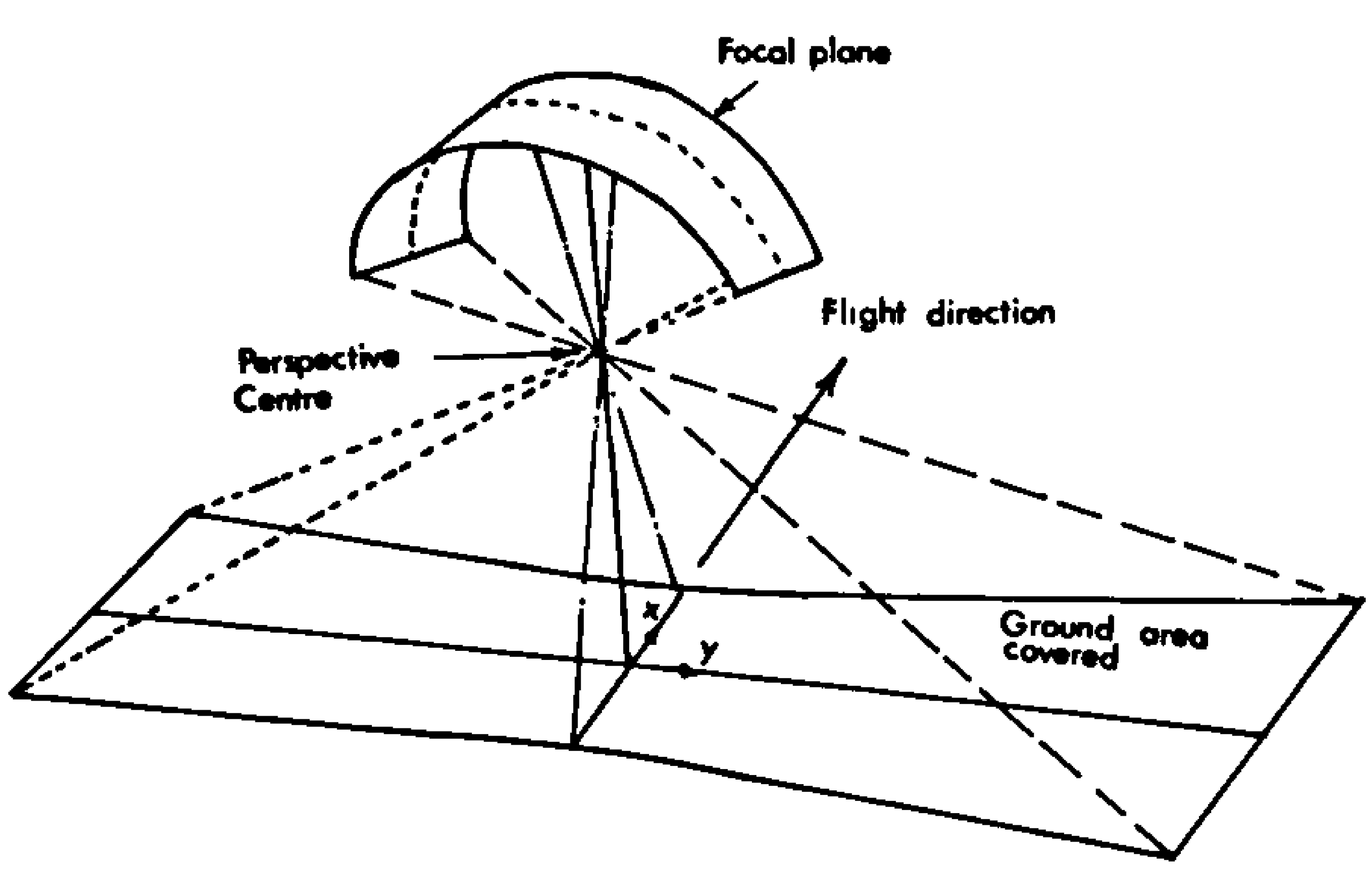

(a)

Fig. 32 Principle of Panoramic Photography

(b)

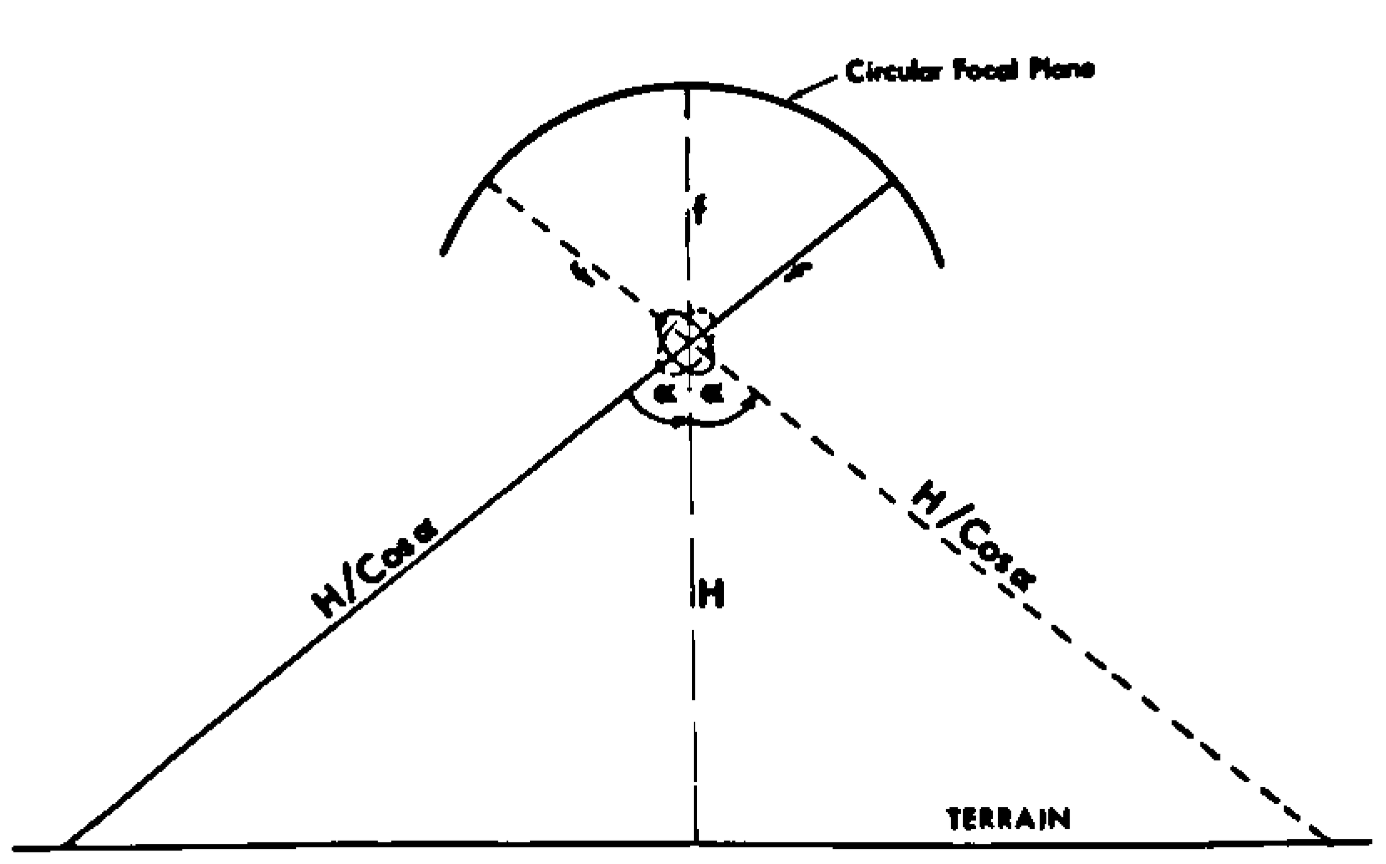

The focal plane is circular and the lens rotates around the perspective centre to give a wide angular coverage at right angles (i.e. cross track) to the flight direction.

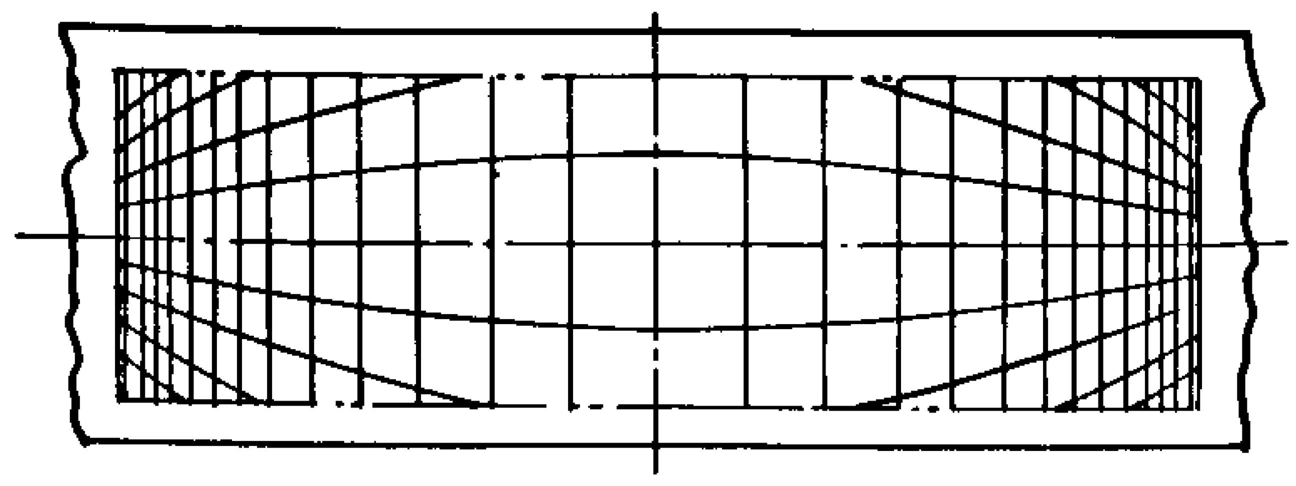

Fig. 33 Panoramic Distortion

Considering a grid of unit-sized squares laid out on flat terrain the resultant panoramic photograph will appear as in Fig. 33. This shows the so-called '<u>panoramic distortion</u>' which results from the cylindrical focal plane and the rotary sweep action of the lens.

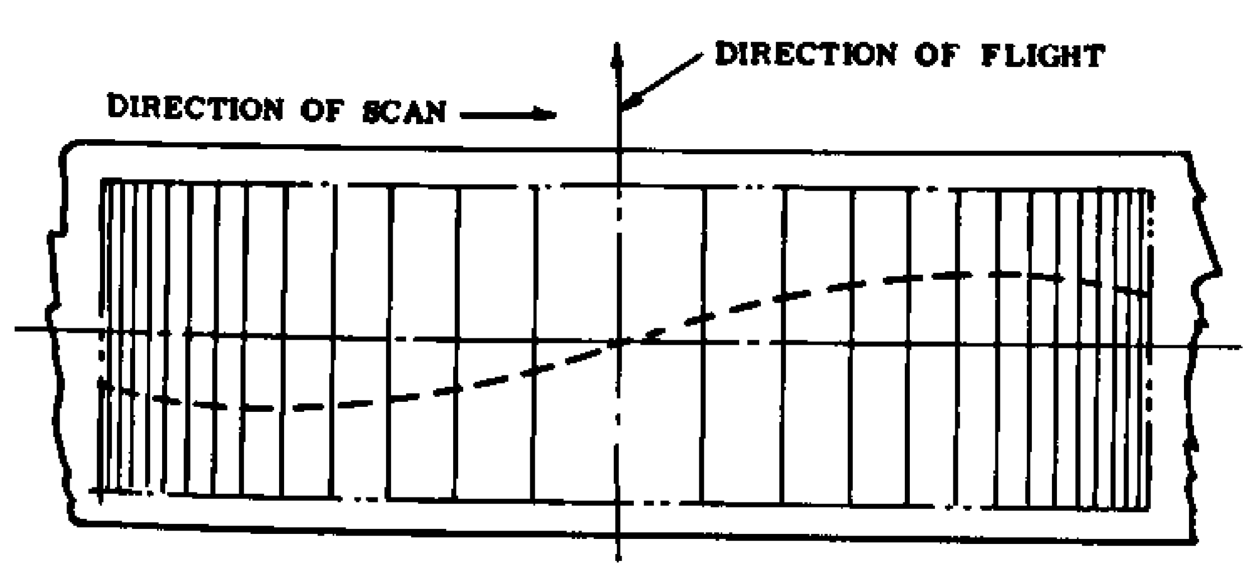

Fig. 34 Sweep Distortion

Since the panoramic camera is here being considered for aerial photography, the aircraft will have moved forward during the sweep time of the lens. This so-called '<u>sweep distortion</u>' (Fig. 34) modifies the positions given by the panoramic distortion.

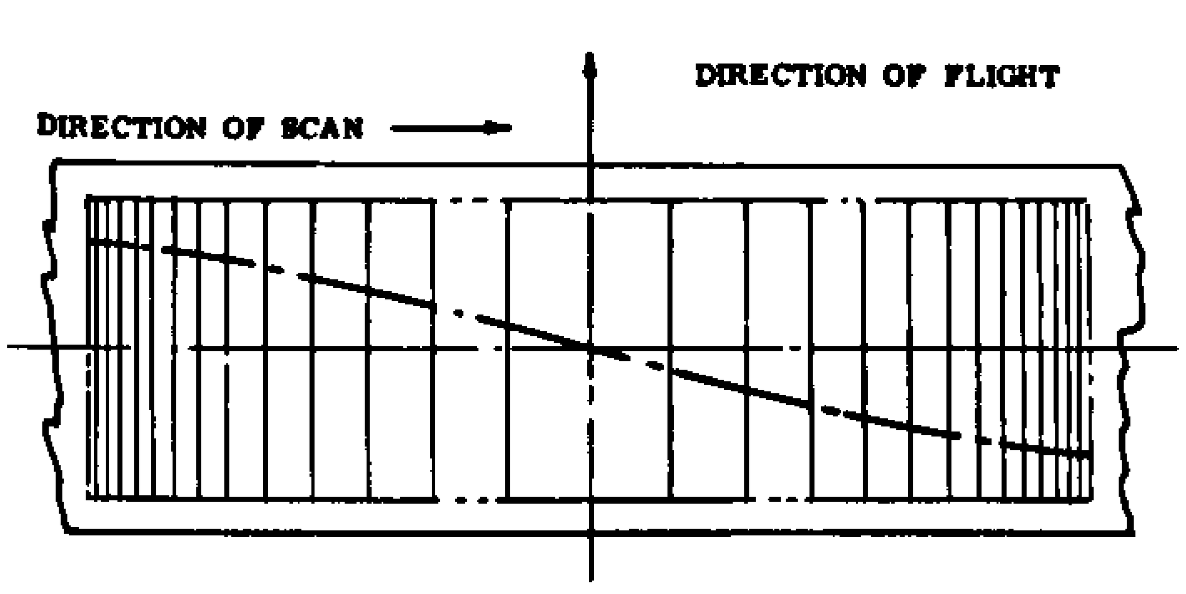

Fig. 35 I.M.C. Distortion

Still further, there will be an additional displacement of the positions of the imaged points due to the translation of the lens or the film in its own focal plane to compensate for image motion during the exposure time (Fig. 35). This is usually termed the "<u>IMC distortion</u>".

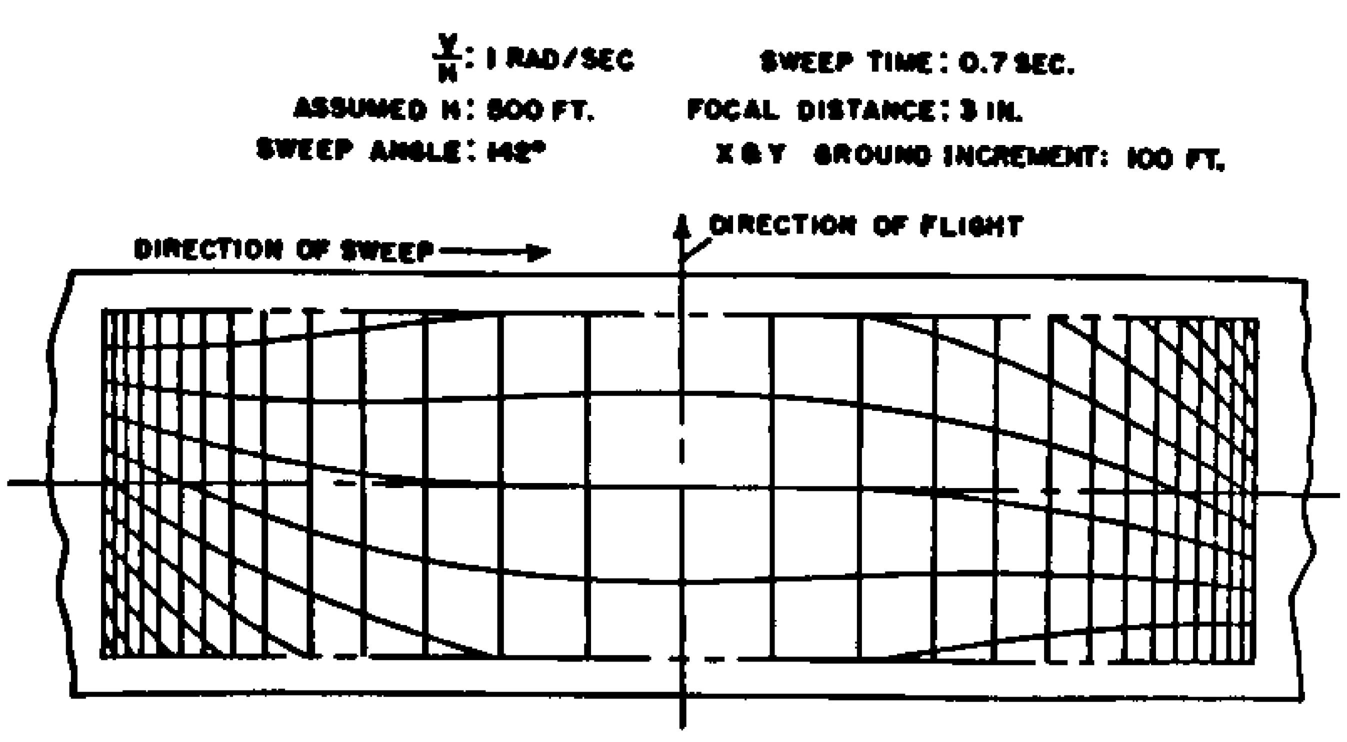

Fig. 36 Combined Effect of Panoramic, Sweep and I.M.C. Distortion

The combined effect of all three distortions is given in Fig. 36

Although, in principle, all panoramic cameras produce an image with a geometry and distortion pattern as shown in the diagrams (Fig. 32 to 36) given above, there are numerous approaches to actually realising the sweep action in the camera. In the late 1950's and early 1960's when American manufacturers were asked to submit designs for panoramic cameras, almost every one came up with a different design. A few representative examples will be outlined below.

2.4.1 Rotating Lens Type of Panoramic Camera

This design corresponds to the arrangement already described (Fig. 32) above. A cylindrical focal plane is used, the film being stationary during the scan (Fig. 37). The lens is rotated about its rear nodal point. Attached to it is a scanning arm at the end of which are small rollers for flattening the film and a slit through which the light from the terrain is admitted to expose an image on the photographic emulsion. The slit must of course cover the width of the film which is being exposed. The size of the slit in the direction of scan determines the length of exposure; the wider the slit, the longer the exposure. Obviously, the maximum scan which can be obtained by this design will be less than 180°, otherwise the lens will be pointing into the focal plane. This simple arrangement gives excellent resolution and, since there is no movement of the film (as in the other types to be discussed below), no synchronisation of lens and film is required. When used with long focal lengths it is a bulky and space-consuming design. However, because of its high resolution capability, it has been used for a large number of medium to high altitude panoramic cameras built by Itek (e.g. the <u>Hyac</u> design) and Fairchild (e.g. the <u>KA-81</u> and <u>KA-82</u> designs).

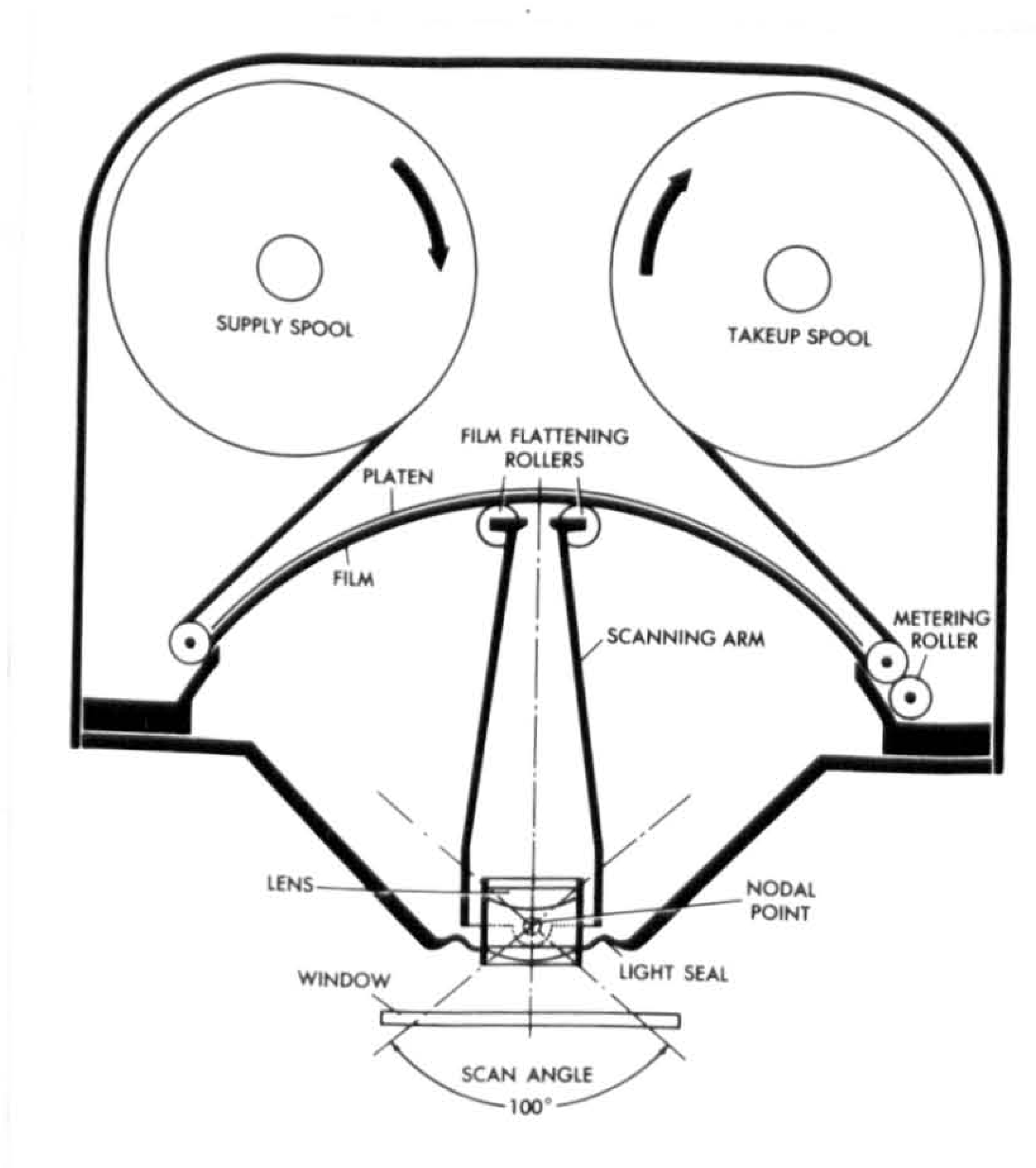

Fig. 37 Stationary Film, Rotating Lens Panoramic Camera

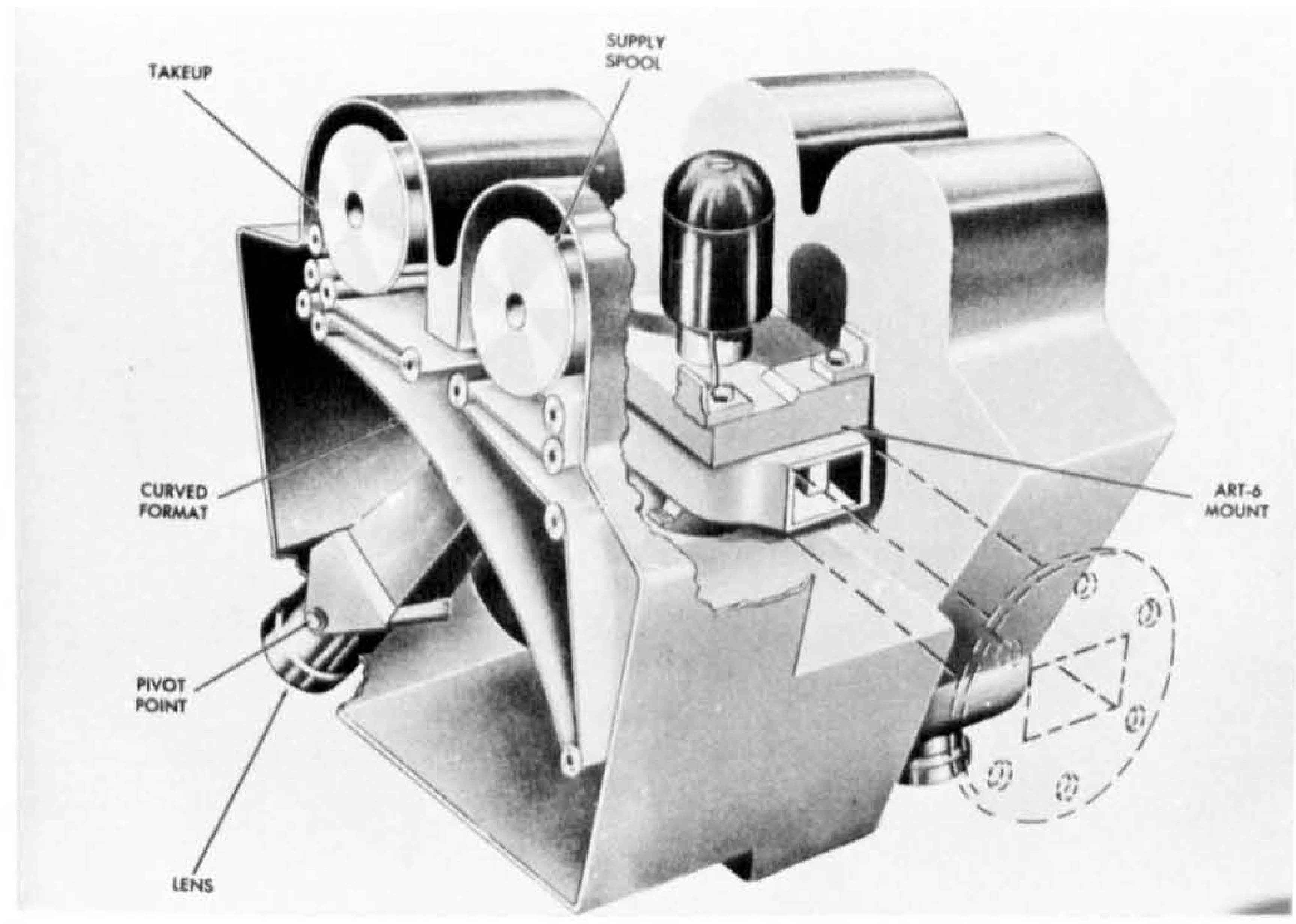

Fig. 38 Split Scan Rotating Lens Panoramic Camera

A variant of this design is the split-scan type (Fig. 38) in which two lenses are used, the one pointing to the left and the other to the right of the flight track. A common drive system ensures simultaneous left and right scans.

In both the single lens and split scan types, because of the impracticability of moving the curved film plane during exposure of the film, image movement compensation is normally carried out by moving the lens or lenses in the direction of flight. During the non-imaging part of the cycle, the lens or lenses return to their starting position (the slit being capped). While this is taking place, fresh film is transported into position for the next exposure to be made. Inevitably, this means that a rather slower minimum cycling speed results as compared with alternative designs.

2.4.2 Rotating Prism Panoramic Camera

This is a configuration by which a full 180-degree or greater scan can be achieved. As shown in Fig. 39, a double-dove prism whose diagonals are aluminised and cemented together is placed in front of the stationary lens with its vertical axis. This prism rotates at a uniform rate through 90 degrees for each 180-degree scan. The film passes around and is advanced by a rotating drum whose rotation must be accurately co-ordinated with that of the prism in order to achieve good image quality. To compensate for the image motion, the lens is translated longitudinally at a continuously varying rate during the picture-taking cycle. This arrangement has been used in the Fairchild KA-60C and KB-18A cameras designed for low-level reconnaissance photography. Both employ a f = 3 in. (75 mm) lens and a 70 mm film giving a 6 x 24 cm format.

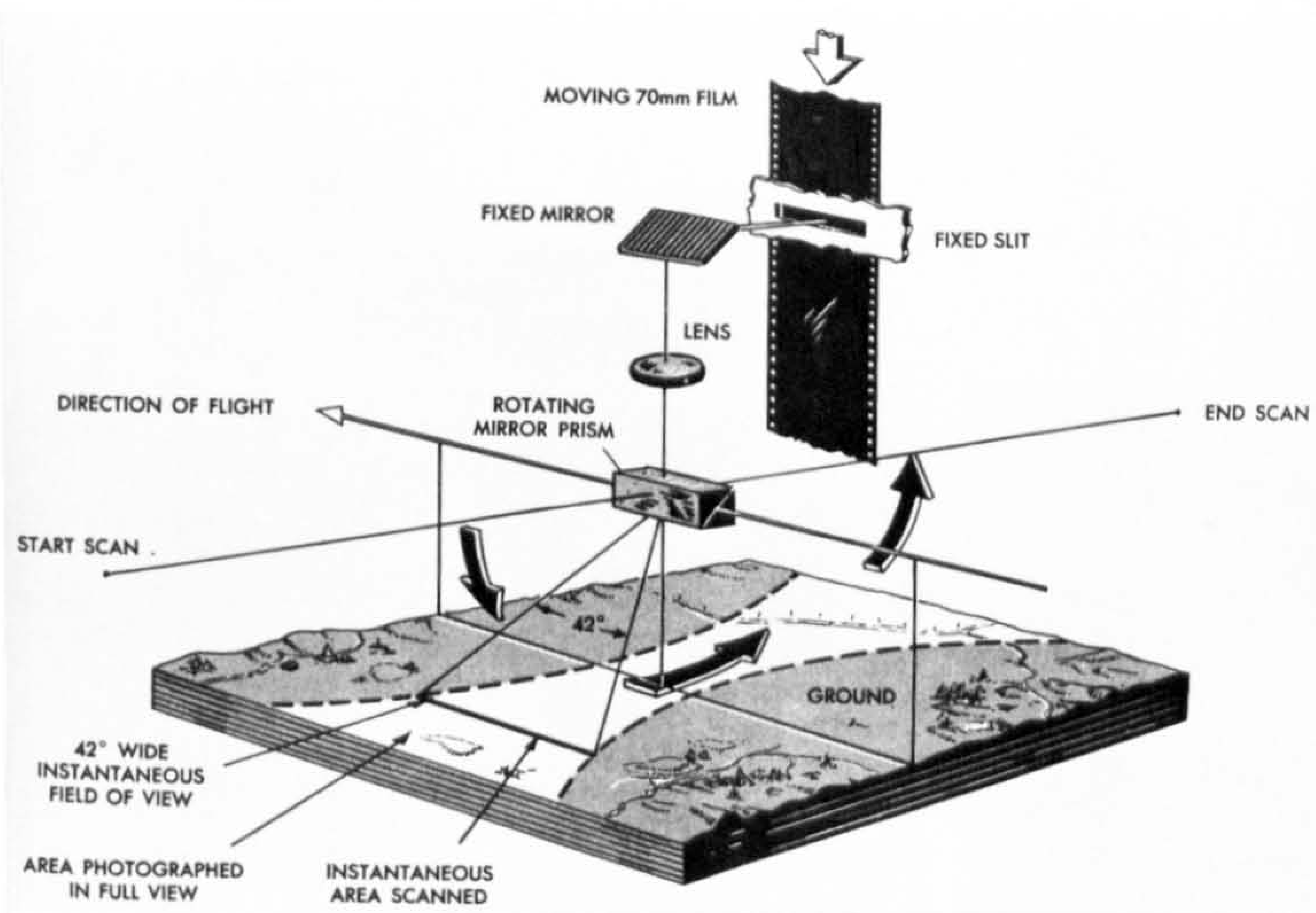

Fig. 39 Rotating Prism Panoramic Camera

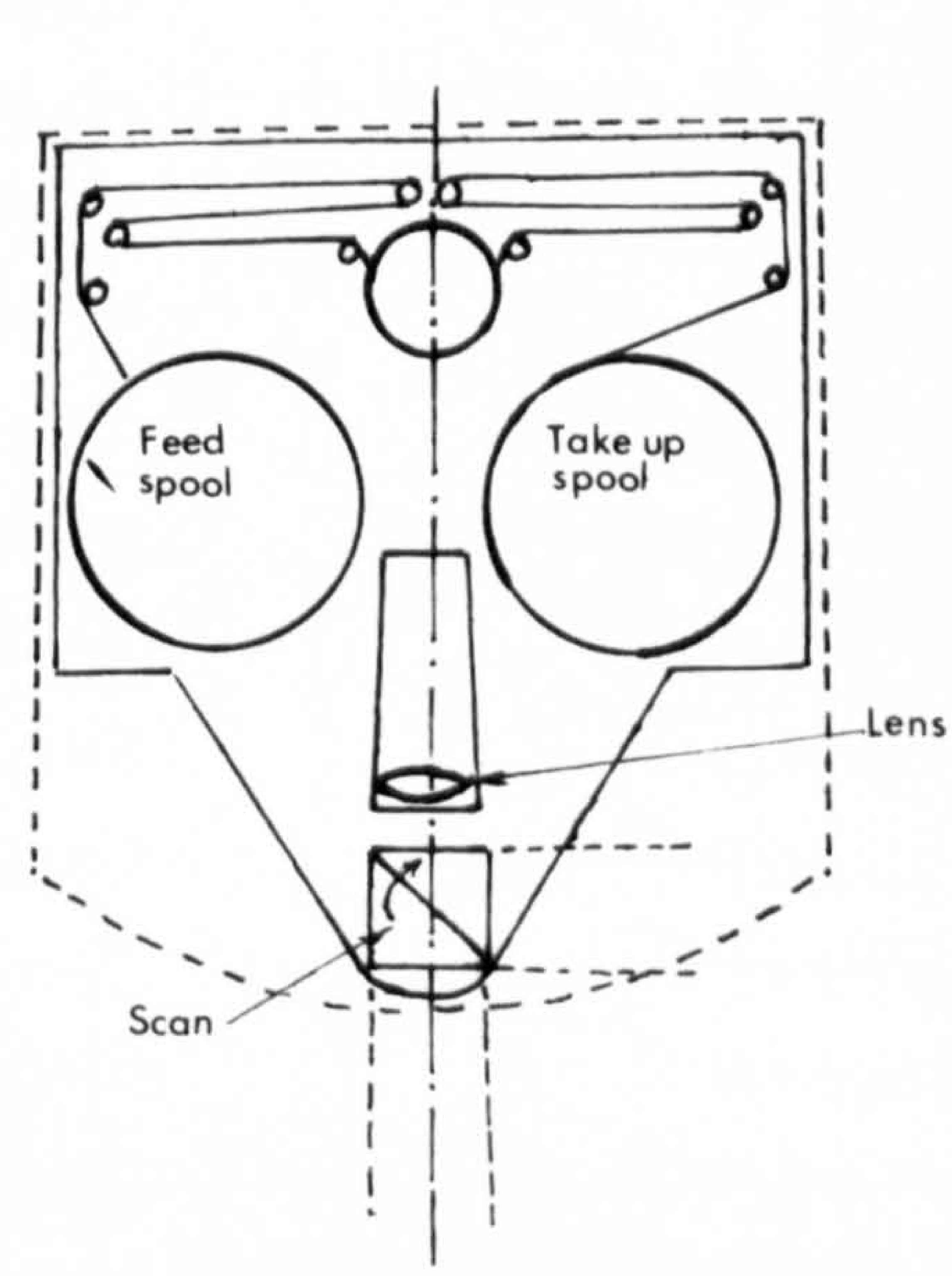

Fig. 40 Rotating Prism Panoramic Camera Perkin-Elmer

An alternative arrangement utilised in Perkin-Elmer design is that shown in Fig. 40 in which the optical axis is turned through a right angle and the film is moved in a plane past a fixed slit. As with the rotating lens type, so the rotating-prism type has also appeared in a split-scan version. An example is the Williamson F85 (Fig. 41), one of the very few British panoramic camera designs. This utilises two f = 36 in. (90 cm) lenses, each of which has a scanning mirror placed in front of it (Fig. 42). Again the film is advanced using a drum.

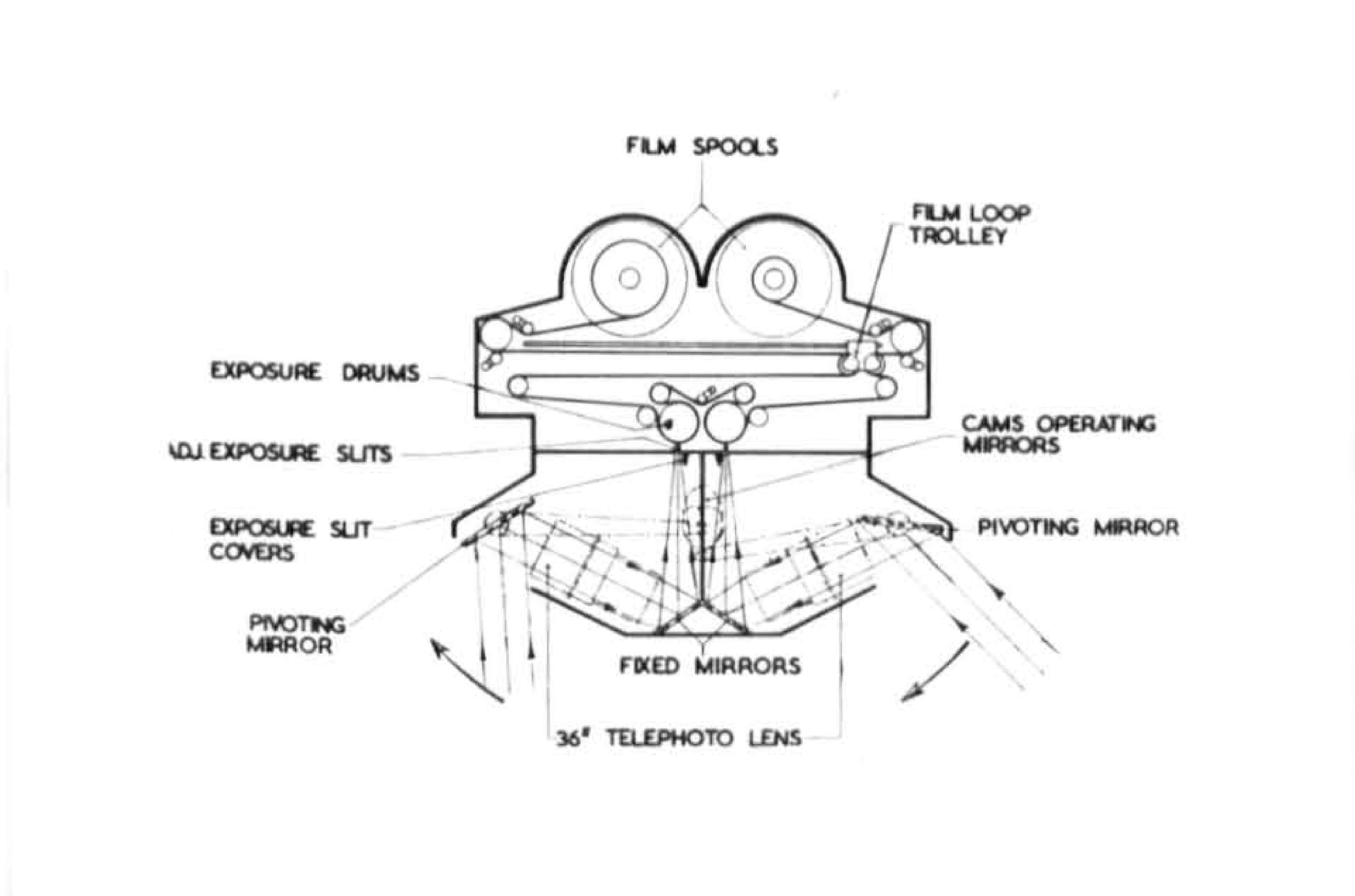

Fig. 41 Williamson F85 Panoramic Camera Design

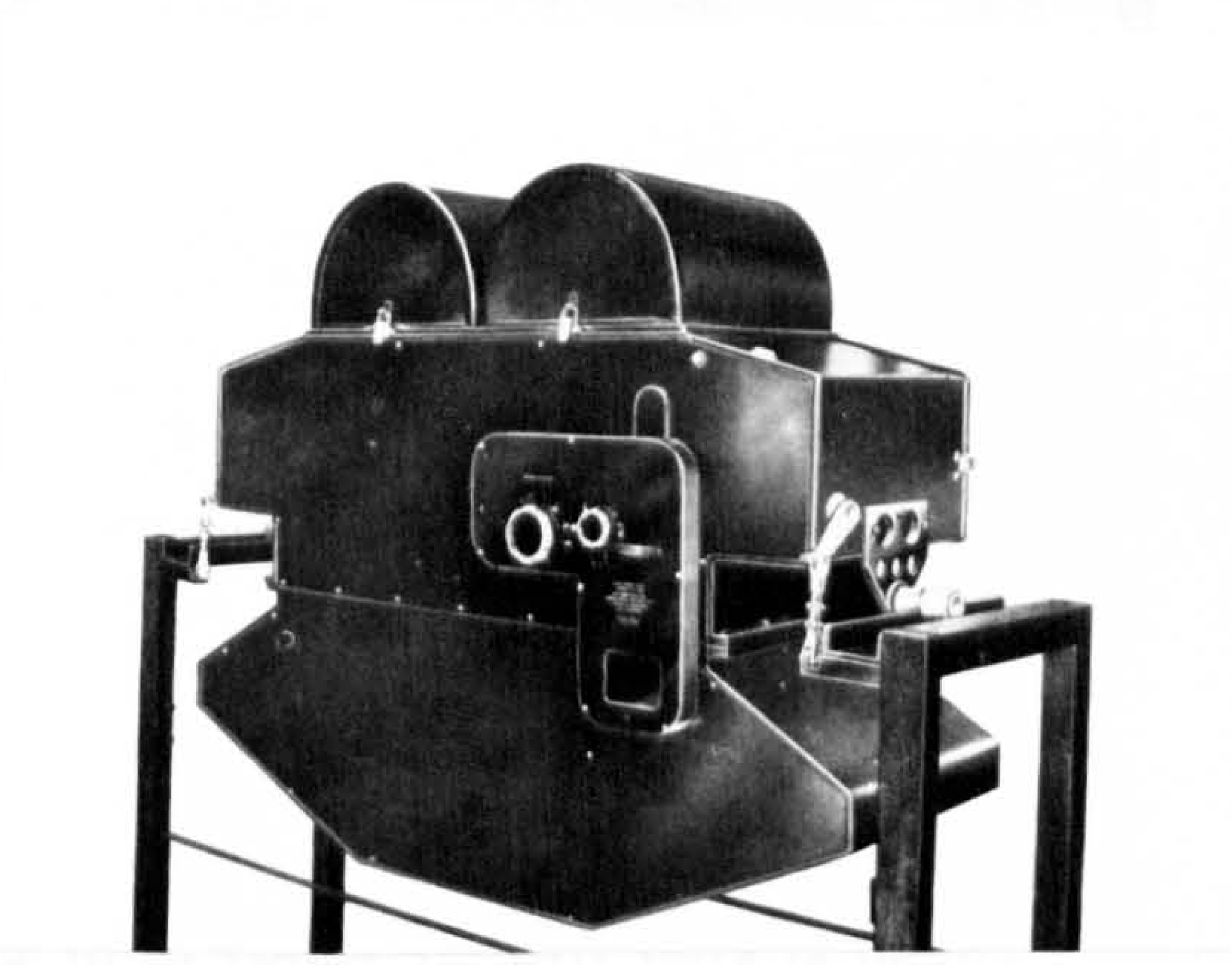

Fig. 42 Williamson F85 Panoramic Camera

The rotating-prism type of panoramic camera has the feature that it needs extremely accurate co-ordination and synchronisation of film movement and prism rotation to realise the highest resolution. So generally the design is not favoured for cameras where resolution is a top priority. On the other hand, it gives a more compact design than the rotating lens type and its continuously spinning prism allows a very rapid series of photographs to be taken which makes it particularly suitable for high-speed low-level operations where ultra-high resolution is not the highest priority.

2.4.3 <u>Rotating Optical-Bar Panoramic Camera</u>

This design (Fig. 43) attempts to combine the high resolution inherent in the scanning lens type with the need for rapid cycling speeds in high speed reconnaissance aircraft, which will occur especially when the angular coverage in the direction of flight is restricted.

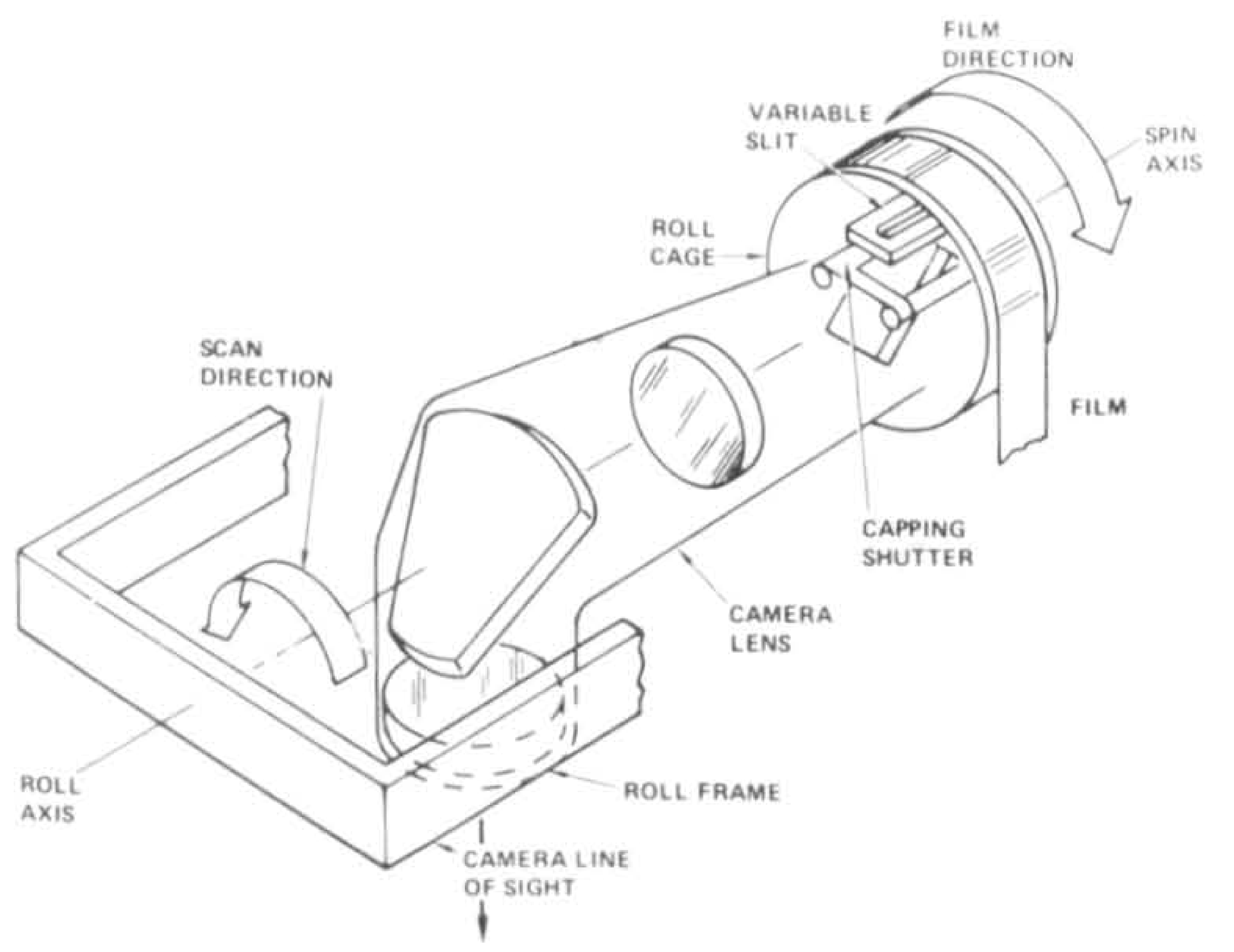

Fig. 43 Rotating Optical Bar Type of Panoramic Camera Diagram

Fig. 44 Itek KA-80 Panoramic Camera

The main part of the optical axis is placed horizontally, which is of course advantageous for installation in an aircraft, if a long focal length lens is used. Two mirrors are used, one of which turns the optical path through the objective lens itself, the other turning the path on to the film. The whole optical bar consisting of the lens and the two mirrors rotates continuously around the optical axis at a constant speed - which obviates the need to start and stop the rotating lens and allows high cycling speeds if required.

The film is placed on a cylindrical focal plane concentric with the optical axis. Although the film motion across the focal plane is intermittent, usually the film supply and take-up spools revolve continuously, supplying film to a series of sprung rollers which, in essence, produce a buffer store of film ready for use in the next exposure.

The design is obviously more complex than those described above. The continuous rotation characteristics of lens and film are favourable for operation with no need for deceleration, stopping and acceleration of lens and film and with minimum power requirement. On the other hand, the weight is unusually high since two large high quality mirrors are required. Nevertheless, this design has been produced as the Itek KA-80 (Fig. 44) with a f = 24 in. (60 cm) f/3.5 Petzval lens using 5 in. (12.5 cm) film. While it has been used in drones, it has attracted a great deal of attention through its use on certain of the Apollo lunar missions. By using a highly-corrected large-aperture lens working over a small angular field and a slow very high resolution film (Kodak 3404), the truly remarkable resolution of 135 line pairs/mm at low contrast has been achieved on-axis and 108 line pairs/mm at the edge of the field (Brock 1976).

The same philosophy and design has since been adopted by Vinten whose new Type 750 camera (Fig. 45) is essentially a scaled-down version of the KA-80 using 70 mm film and a f = 3 in. (75 mm) f/2.8 lens and so is designed specifically for low-level high-speed flights.

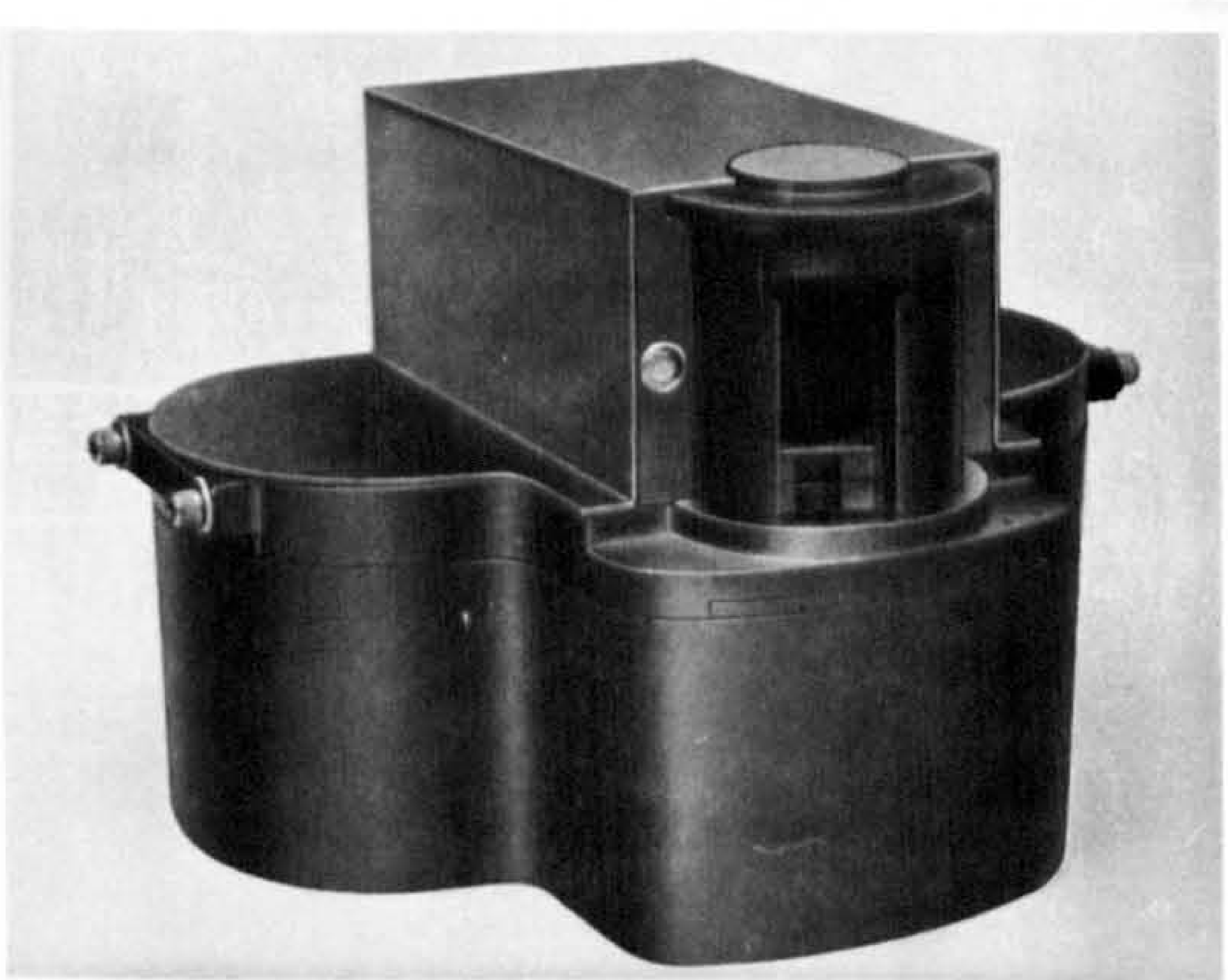

Fig. 45 Vinten 750 Panoramic Camera

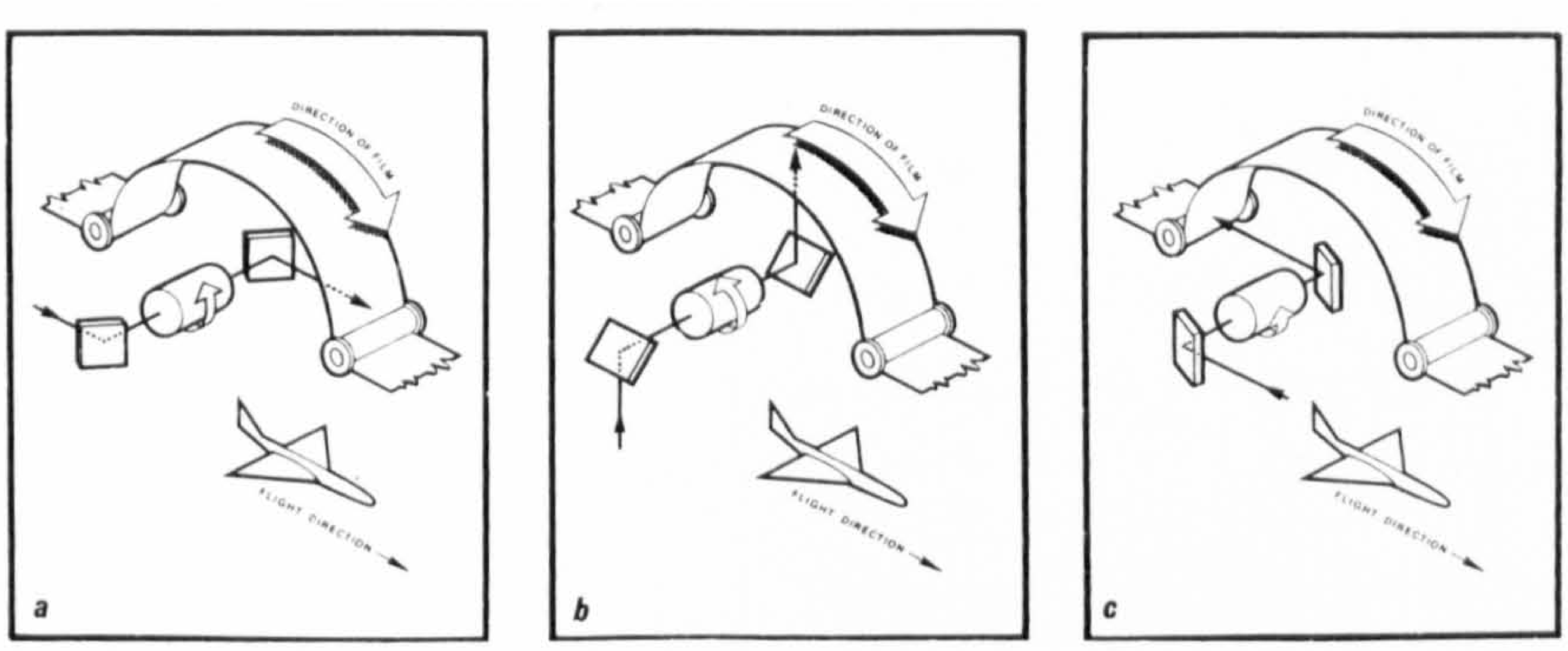

Fig. 46 Operation of Vinten Type 750 Panoramic Camera

Fig. 46 illustrates the operation of the camera. The magazine has a film capacity of 280 ft (85 m) which gives up to 335 photographs. The maximum framing rate is 7.4 photographs per second and, with a 10 percent overlap, the film capacity is sufficient for 8.7 miles (14 km) coverage at 200 ft (60 m) altitude and speed of 1100 km/hr.

2.5 Use of Panoramic Photography

While the advantages of panoramic photography - the high resolution large-scale photographs and the wide-angle cross-track coverage - have been stressed, there are also disadvantages, especially from the point of view of the users.

(i) Geometrical Distortions

The first difficulty is that of geometry. Unlike vertical frame photography, there are very large scale changes from the central part of each panoramic photograph out to the edges. Along with this comes the very distorted geometrical pattern of the plan detail and the considerable extent of the dead areas resulting from the ultra-wide-angle coverage. Transformation printers, e.g. by Itek, attempt to remove the scale changes and distorted geometry, but obviously the rectified photographs cannot have the same quality over the whole format. Also the need to rectify the photography incurs a considerable delay which is unacceptable in many military operations.

(ii) Stereo-viewing

The geometrical aspect also looms large with the very small base : height ratio which is inherent in normal panoramic photography. The along-track angular coverage of panoramic photography is very narrow so that numerous photographs have to be taken to ensure coverage and overlap. Even then, only a poor stereo-impression can be obtained. This is a major consideration for some types of photo-interpretation where stereoscopic viewing of objects in 3-D model is a requirement.

To improve the base : height ratio and thus to improve the geometrical accuracy and the stereo-impression, the Itek KA-80 camera was used in the Lunar Apollo mission in the convergent mode (Fig. 47), by tilting the camera to point alternately 12.5° fore and aft.

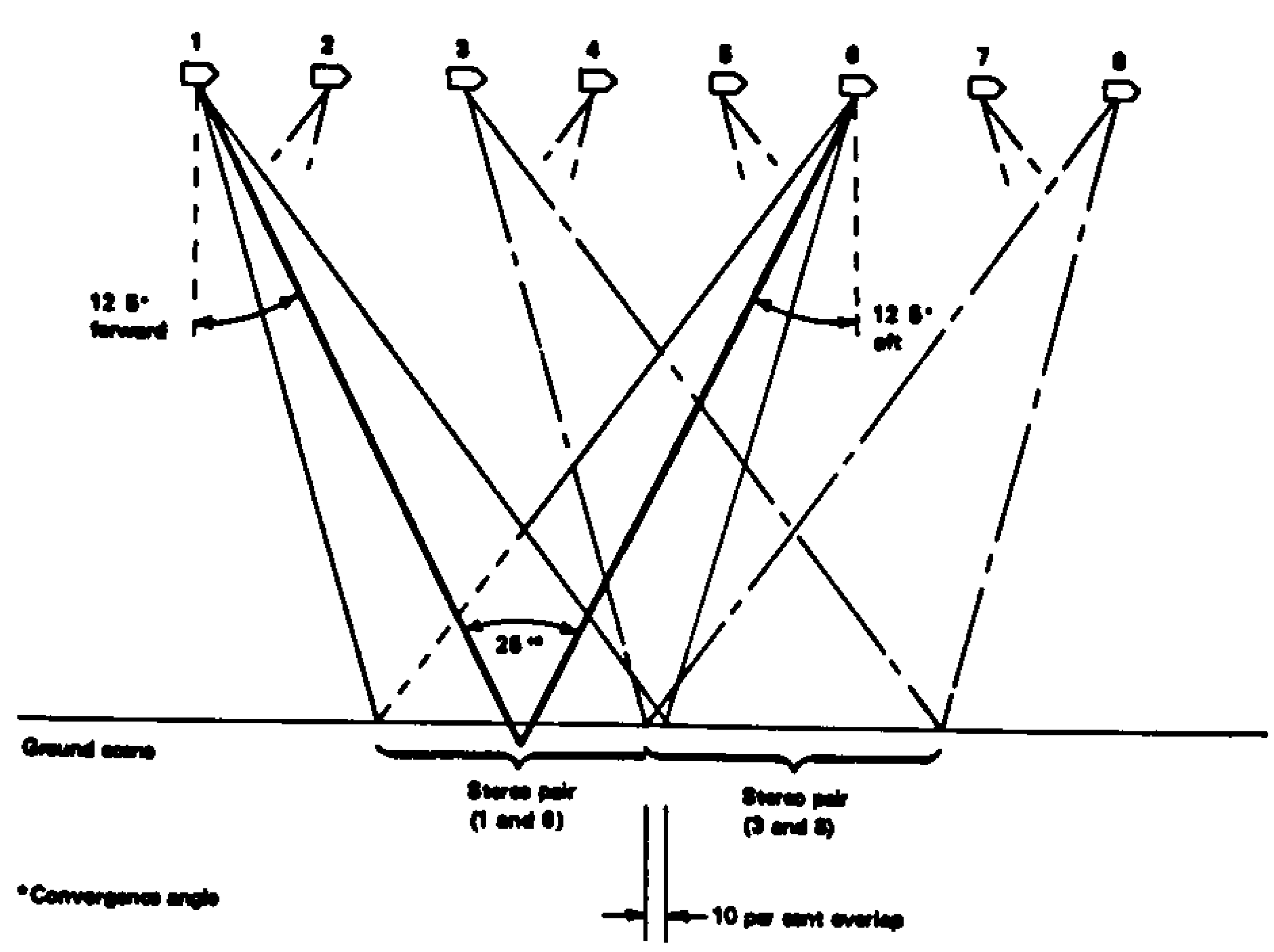

Fig. 47 Convergent mode for operation of KA-80 Camera in Apollo

This imposes an additional set of large tilt displacements to superimpose on the already complicated and distorted geometry of panoramic photography (Fig. 48).

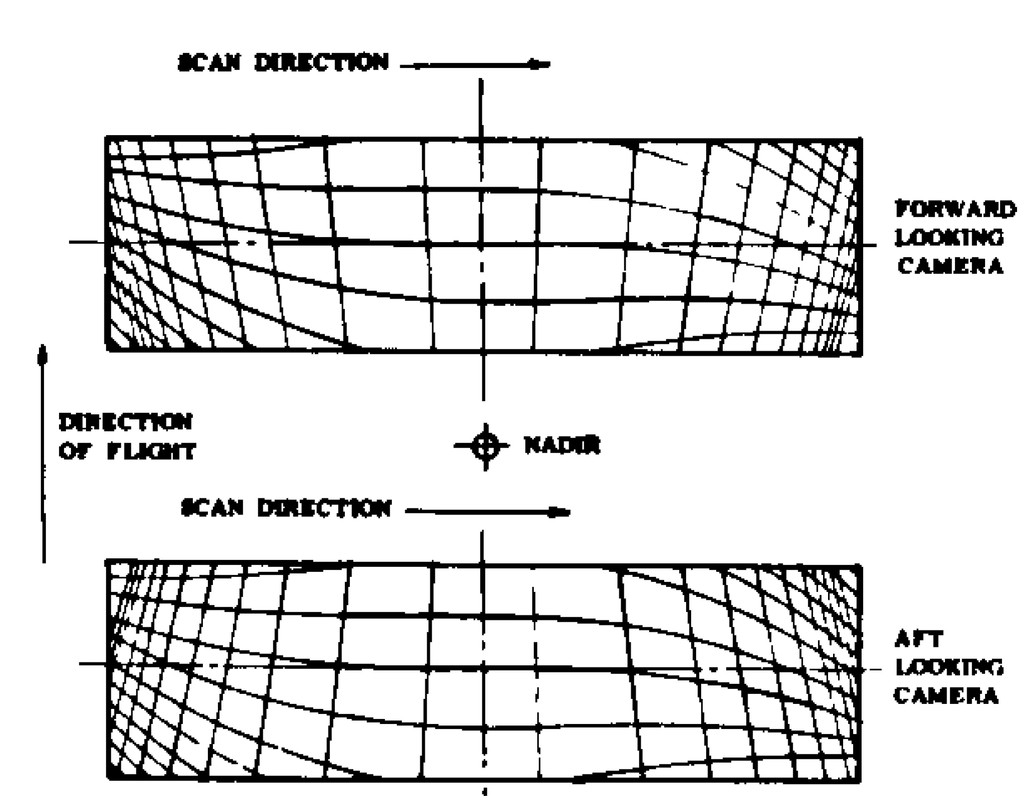

Fig. 48 Diagram showing Forward and Backward obliques - Effect on unit-sized grid squares.

The resulting photographs require special, complex stereo-viewing devices which incorporate separate pancratic systems to allow the images from the two photographs to be presented to the observer's eyes at equal scale. Obviously, it is also necessary to provide Dove prisms for image rotation so that the images can also be presented to the observer with epipolar lines parallel to the observer's eye-base. The operation of such complex stereo-viewing devices needs not inconsiderable training and skills on the part of the interpreter.

(iii) Mensuration

In view of the foregoing discussion, it is obvious that measurement of distances, areas and positions on panoramic photography, even to a low degree of accuracy, is a task of considerable complexity, not readily performed by the majority of users. At the low accuracy end of the spectrum, special monocular panoramic mensuration viewers have been built, e.g. by Itek, which incorporate purpose-built analogue computers which compensate for the main components of the geometrical displacements inherent in panoramic photography. Such devices are complex and expensive and yet, since they are monocular, they cannot be used to give measurements of height.

For more accurate planimetric measurements and for the determination of heights even to a limited accuracy, resort has to be made to complex and enormously expensive analytical plotters such as the OMI-Bendix AS-11 series. These machines can accommodate the long focal lengths often used and can be programmed to deal with the complex geometrical characteristics of panoramic photographs. Also, they have zoom pancratic systems and Dove prisms available to cope, under computer control, with the difficult stereo-viewing of panoramic photographs. However, only a very few of the AS-11 B series of analytical plotters have been built with all these characteristics and these are located almost entirely in the Aerospace and Topographic Centres of the U.S. Defence Mapping Agency. The photogrammetric solutions used by this agency for measurements of panoramic photography have been outlined by Mahoney (1963) and by Case (1967).

2.6 Comparison of Strip, Panoramic and Frame Cameras

From the discussion above, it can be seen that, while strip photography and panoramic photography have definite and undisputed roles to play in reconnaissance photography, they are not useful in all situations and circumstances, nor are they acceptable to all users. The traditional type of reconnaissance frame camera is still widely used, even by the American military services who have been the major force behind the development of strip and panoramic cameras and photography. For many tasks the frame camera has great advantages both from the operational and the user's points of view. It is, however, a curious feature that the metric aspects of reconnaissance frame photography have received little attention, and, as far as the present writer is aware, no thorough analysis of this subject has taken place or, if it has, it has not been published - perhaps for reasons of military security. The succeeding chapters will analyse the mechanical and optical characteristics of reconnaissance frame cameras, provide a theory for the geometrical aspects of these cameras and give the results of a series of tests and experiments to confirm the results of these theoretical investigations.

CHAPTER III

The Aerial Reconnaissance

Frame Camera

CHAPTER III

THE AERIAL RECONNAISSANCE FRAME CAMERA

3.1 Introduction

In this chapter, the basic construction of the aerial reconnaissance frame camera will be outlined. The characteristics and components that play a major role in the image quality and geometry of photographs taken with such a camera will be discussed in more detail.

3.2 Basic Design of the Aerial Frame Cameras

Fig. 49 shows the general configuration of an aerial frame camera

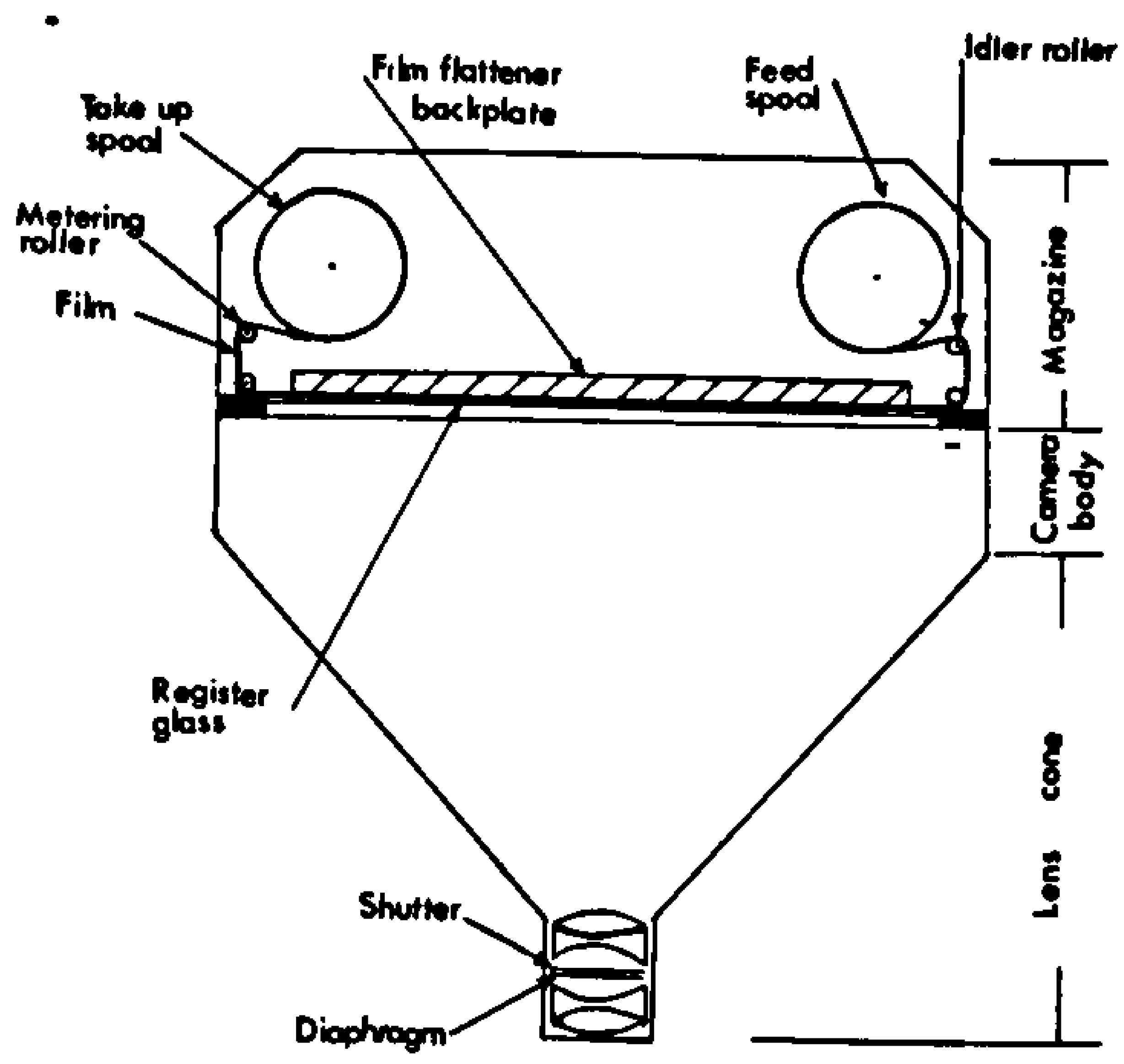

Fig. 49 Schematic Diagram of an aerial frame camera

The following are the main components of such a camera:-

(a) Camera body including the camera drive mechanism and electrical supply,

(b) Film magazine,

(c) Lens cone,

(d) Lens (or mirror optical system),

(e) Image motion compensation system,

(f) Shutter.

Although the basic construction of all aerial frame cameras is similar, those designed for reconnaissance purposes are optimised for resolution and for image quality, whereas those built for mapping applications have an emphasis on stable and calibrated geometrical characteristics. In turn, this leads to very different characteristics for some of the components given above, in particular the lens, shutter and image movement compensation system.

3.3 The Camera Body

This part usually houses the camera drive motor and mechanisms, electrical power supply and connections, the focal plane and the image motion compensation system. The film magazine fits on top of the focal plane and the lens cone, shutter and the lens itself are attached to the underside of the camera body. When an aerial camera is operated, a means to wind the shutter and to advance the film for the next exposure is required. An electric motor is the power source for the entire camera. The electric motor receives current from the aircraft power supply, and, in turn, moves the cams, gears and shafts so that power is transmitted to the camera shutter and to the film magazine.

Another part of the camera body is the focal plane which may have a register glass plate to support the film and to ensure that it lies flat in the focal plane. The register glass is located in the camera body with its surface perpendicular to the central axis of the lens.

3.4 The Film Magazine

For most aerial cameras, the film magazine acts as a light-tight container for the film.

The alternative glass plate type of camera has a (limited) use in photogrammetric work where very high precision is required. However, it finds no place in reconnaissance operations, where there are no requirements for high metric accuracy and where the weight and bulk of the plates and the slow cycling speed are unfavourable characteristics. Glass plates also require much delicate handling and do not lend themselves to fast continuous processing as can be carried out on films for reconnaissance work.

The detachable type of magazine is that mostly used in reconnaissance cameras. It can be taken as a unit to a darkroom for loading and unloading the supply and take-up spools which actually carry the film. Since the magazine cannot be changed in most reconnaissance flights (unlike mapping operations), the capacity of an individual magazine is often very large. The film length depends on the base thickness but with the advent of very thin-based polyester films, lengths of several hundred metres are not unknown for large format cameras – the extreme of 2,000 metres for the U-2 camera has already been mentioned.

An alternative arrangement is to use film cassettes e.g. as in the standard RAF large format camera, the A.G.I. F-126. These are light-tight units enclosing the supply and take-up spools which are quickly detachable from the main camera body which, in this case, contains the film transport mechanism and film-flattening mechanism. The cassettes are light-weight, easy to handle and to change.

A third possibility which has been tried experimentally in reconnaissance cameras is to use cut-films (Williamson 1957). In this case, individual sheets of 70 mm film are used instead of a roll film, giving a format size of $2\frac{1}{4} \times 2\frac{1}{4}$ in. (57 x 57 mm). This makes it easier to keep the films perfectly flat and free from curl. It also has the advantage that the selection and abstraction of any individual photograph is much more rapid (random access) than having to use a spool-winder (serial or sequential access). No problem of accelerating and decelerating two heavy spools at each cycle is encountered, and, since only a single piece of film is moved, this causes a considerable saving in motor power in automatic cameras. Moreover, the stress by tension and the resultant differential film distortion encountered during the processing of a roll of film is eliminated. The lack of development of this apparently attractive idea makes one speculate on the possible reasons. It seems probable that the minimum cycling speed is quite high, since a mechanism not too dissimilar to that required to change glass plates is involved. Fast continuous processing machines cannot be used readily either. These two reasons may have played a part in the idea not being pursued further for reconnaissance work.

The film magazine also contains a means for holding the film flat in the focal plane during the exposure. Various arrangements are encountered - vacuum flattening, mechanical flattening by pressure plate, etc. The vacuum flattening method is widely used, especially with metric cameras; for example, the Wild and Zeiss Oberkochen mapping cameras. The U.S. Air Force usually employs vacuum film flattening with its large format 9 x 9 in (23 x 23 cm) reconnaissance cameras. As is well-known, British mapping cameras (e.g. the Williamson F-49 and Watts FX-105) use the alternative arrangement of mechanical flattening using a pressure plate and register glass. The same system is employed in large format British reconnaissance cameras. In the F-126 camera, the film is clamped between an optically flat register plate and a spring-loaded backplate just before exposure. Certain American small-format (5 in. or 70 mm film) cameras use a similar arrangement. The register glass (which then forms part of the camera body) can be engraved with a reseau which is, of course, of considerable advantage when metric aspects of reconnaissance photography are being considered.

In the case of many small format (70 mm) cameras, e.g. the British A.G.I. F-135 camera, the narrow film is held flat by simply being tensioned across a spring loaded backplate. As in vacuum flattening cameras, no reseau will be possible. Since image movement compensation systems are common in reconnaissance cameras, the magazine will often contain a special motor which allows it to wind the film during each exposure. In the F-126 camera, the back pressure plate, the film and the register glass move as a unit for image movement compensation purposes.

3.5 The Lens Cone

The purpose of the lens cone is to exclude light from striking the film or plate and to support the lens, keeping it at a predetermined distance from the focal plane. In the case of metric cameras, the relationship between the lens and the focal plane (inner orientation) is accurately determined during the process of camera calibration. The position of the principal point is defined by the stationary fiducial marks in the supporting frame, and images of these fiducial marks are formed on the photograph at the time of exposure. In most reconnaissance cameras, however, the image frame is a part of the detachable film magazine, and hence no fiducial mark images are available on the photograph to locate the position of the principal point. Some cameras are designed with interchangeable lens cones to suit different photographic missions. This is applied to both reconnaissance and mapping cameras. For example, the A.G.I. F-126 reconnaissance camera can be fitted with f = 150 mm (6 in.), 300 mm (12 in.), 600 mm (24 in.) or 900 mm (36 in.) lenses in interchangeable lens cones, while the Wild RC-10 mapping camera has three interchangeable lens cones to accommodate lenses of f = 88 mm ($3\frac{1}{2}$ in.), 152 mm (6 in.) and 305 mm (12 in.) focal lengths.

3.6 Optical System

3.6.1. The Lens

The function of the lens is, of course, to gather the bundle of light rays for each of an infinite number of points on the terrain and to bring each bundle to focus as a point on the focal plane. When a lens designer is undertaking the design of a lens for a modern aerial camera, he must consider all the various aberrations - spherical aberration, coma, astigmatism, curvature of field and chromatic aberration - which can occur in any lens.

However, an individual lens can only be corrected for certain aberrations. If these are removed or minimised, the other aberrations will still be present. Normally, lens designers have to use a number of lenses or lens elements to ensure that certain aberrations are corrected to the degree that may be required for a particular application. In this respect, the advent of electronic computers has allowed lens designers to consider far more alternatives and to make modifications much more readily than before. Even then, some sort of balance or compromise has to be reached regarding these lens aberrations. Sometimes the aberrations can be kept small at the cost of introducing large geometrical distortions. If this results in an improvement in performance in terms of resolution, illumination and image quality, then this will be preferred since the metric aspects are unimportant. In most reconnaissance camera lenses, geometric lens distortion can be expected to be large in amount and sometimes irregular in distribution.

The lenses used in reconnaissance cameras, besides exhibiting comparatively large radial distortions (Fig. 50 a) often exhibit asymmetric radial distortions, e.g. quite different distortion patterns may occur along different radial paths from the centre of the photograph (Fig 50 b). The main reason for this phenomenon is the lack of precise centering of the lens elements when assembling the lens. Usually this is also accompanied by tangential distortions (i.e. geometrical distortions which occur tangentially to the normal radial distortion) (Fig. 50 c).

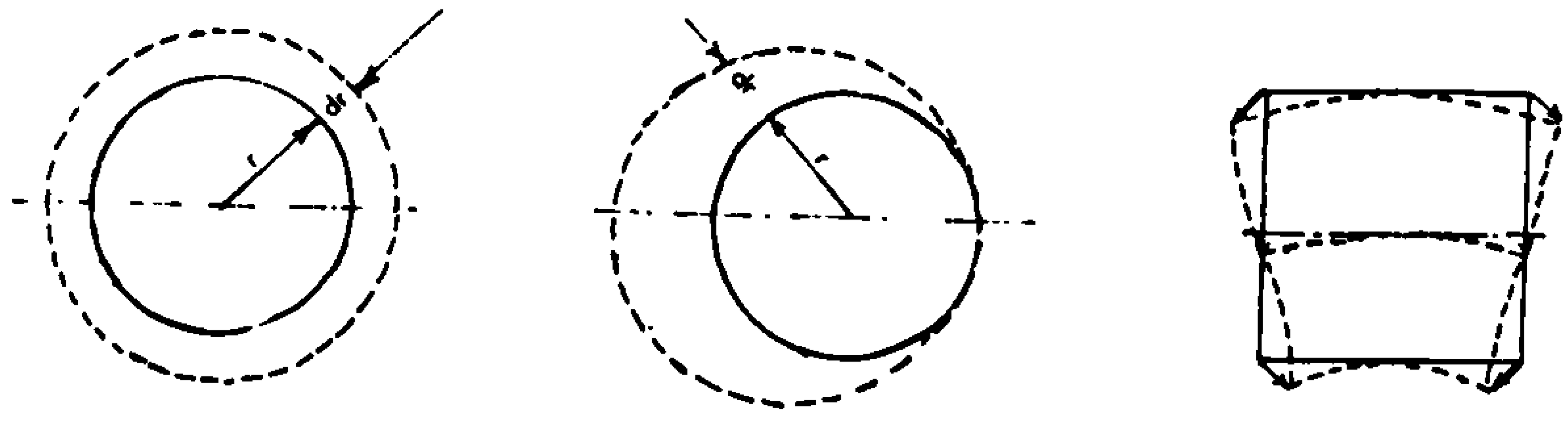

(a) Symmetric distortion (b) Asymmetric distortion (c) Tangential distortion

Fig. 50 Geometric lens distortions

From discussions with the British manufacturers of reconnaissance cameras (Williamson, A.G.I. and Vinten) it appears that since there are no special requirements for geometrical fidelity of the image and no stringent specifications to be met in this respect, thus the task of centering the lens elements is undertaken using the procedures and tolerances for "normal" photographic lenses. On the other hand, when Professor Petrie raised the matter with Zeiss Oberkochen, the reply was that Zeiss assemble the lenses for their reconnaissance cameras on the same jigs and using the same procedures as for their metric cameras - so, in this case, asymmetric and tangential distortions are low.

It is obvious that such considerations play a most important part when trying to consider the metric potential of reconnaissance cameras. Only a systematic programme of calibrating reconnaissance cameras will elucidate fully the extent of the problems. In the case of the particular lenses used in the experimental part of the present investigation, by good fortune, these exhibited symmetric distortions only. Their characteristics will be discussed in some detail later in Chapter VI.

3.6.2 Concentric mirror optics

The alternative to a lens producing an image of the terrain in the focal plane is to use concentric mirror optics. As mentioned in Chapter I, these appear to have been used in various reconnaissance frame cameras. Information is not easily found (nor is it complete) on American designs. However, much fuller information has been made available to the present writer by the Oude Delft company in the Netherlands, which has produced a series of reconnaissance frame cameras based on concentric mirror optics since 1957. The design is based on the concentric mirror arrangement of Bouwers. In this, all the mirror surfaces are spherical and have a common centre of curvature located in the centre of the entrance pupil (Fig. 51). Any line passing through this common centre may be considered as an optical axis.

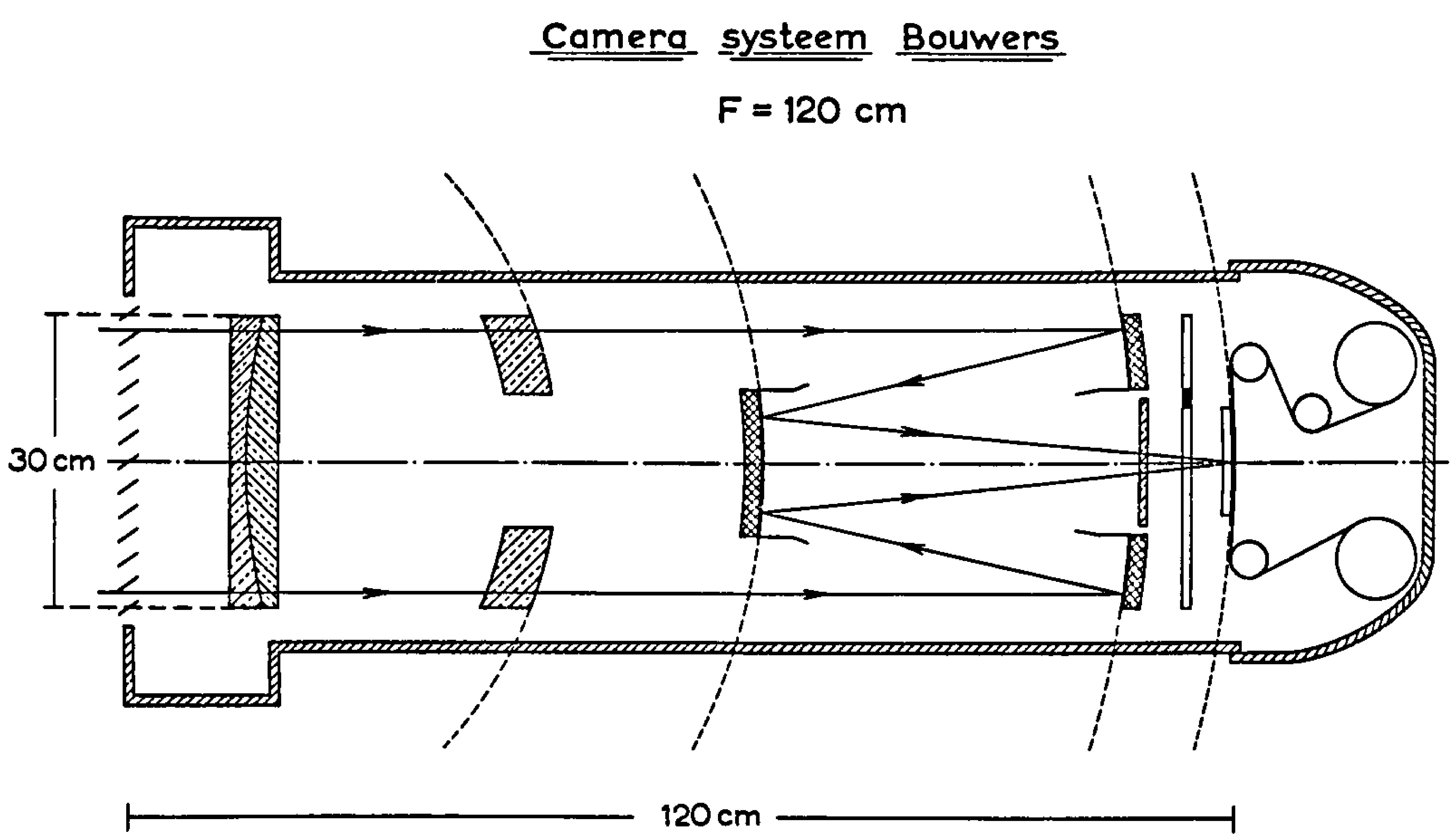

Fig. 51 Bouwers Concentric Mirror System applied to an aerial camera

Consequently, the aberrations are reduced, and the image quality should be high and the same over the entire field. However, the focal plane is also curved so that the film is forced to assume a spherical shape during the exposure. Even if implemented perfectly, this has, of course, considerable implications for the geometry of the negative when placed flat for actual use in a viewing/measuring instrument. In practice, one might expect that this difficult requirement for flattening film to a spherical shape might not be fulfilled exactly, in which case some additional and unpredictable film distortions may result. Due to the spherical shape of the focal plane and the possible film flattening difficulties, the Oude Delft cameras all use narrow width (70 mm or 5 in.) film. Also, rather remarkably, focal plane shutters are used which, with a spherical focal plane, must give considerable design and operational problems. Speeds are high (up to 1/1,000 sec) which, in conjunction with the very wide apertures, will reduce image blur and increase resolution to a high level.

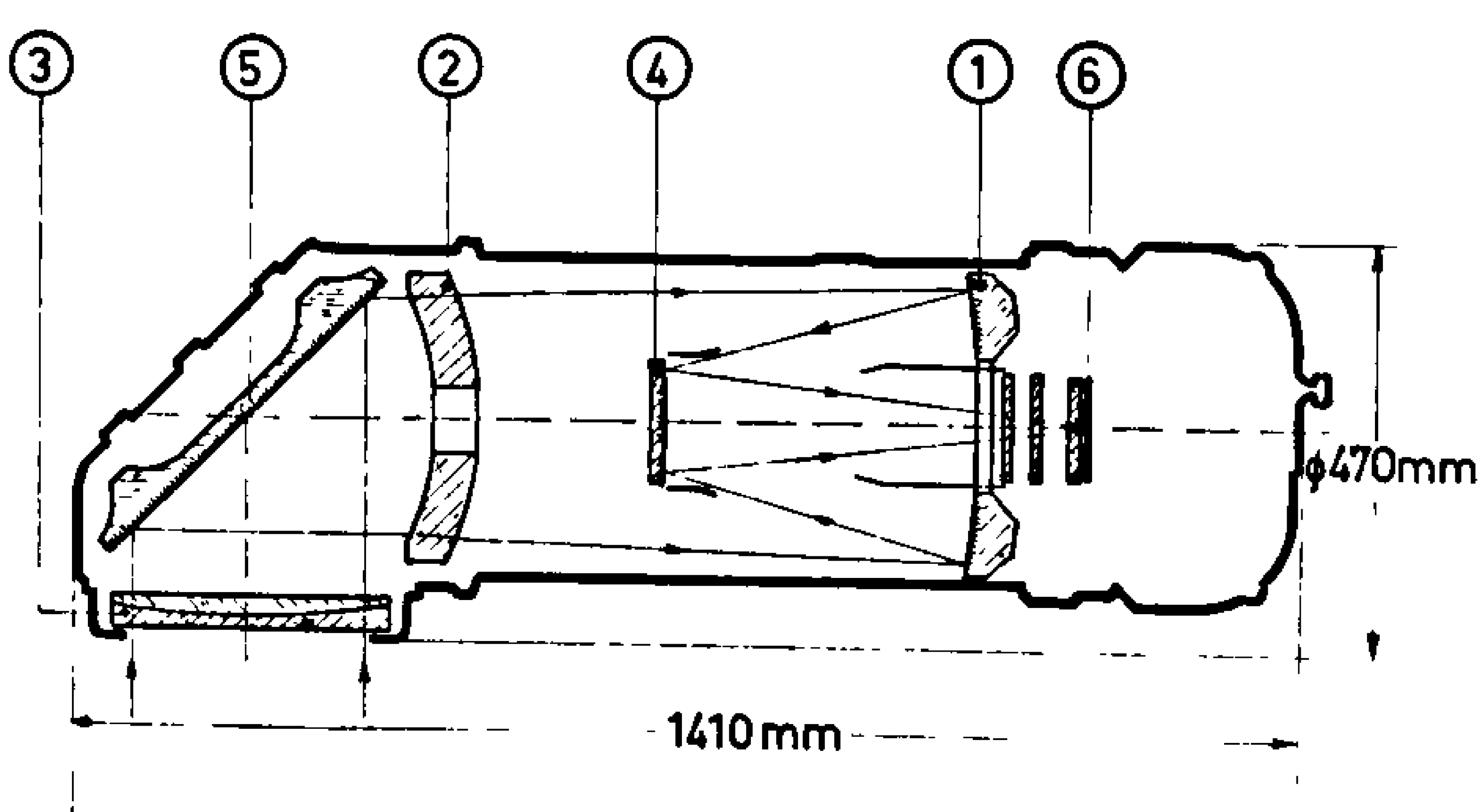

Fig. 52 Optical arrangement of long-focus Oude Delft Camera equipped with concentric optics and right angled prism.

As can be seen from Fig. 52, the concentric mirror system consists of:

(1) a spherical concave mirror,

(2) a negative meniscus lens,

(3) a doubling colour correcting plate,

(4) a vertical plane mirror,

(5) a 45 degree plane mirror for the right-angle models and

(6) the image plane having a slight spherical shape.

As mentioned above, very wide apertures are possible.

In the Oude Delft series these range from f/0.8 in the shortest (but still long) focal length (20 cm) to f/3.9 in the longest focal length (1.20 m). These permit the use of fine-grain films to achieve high resolution or the taking of photographs at very short exposure times which is of great advantage in reducing image blur at high flying speeds.

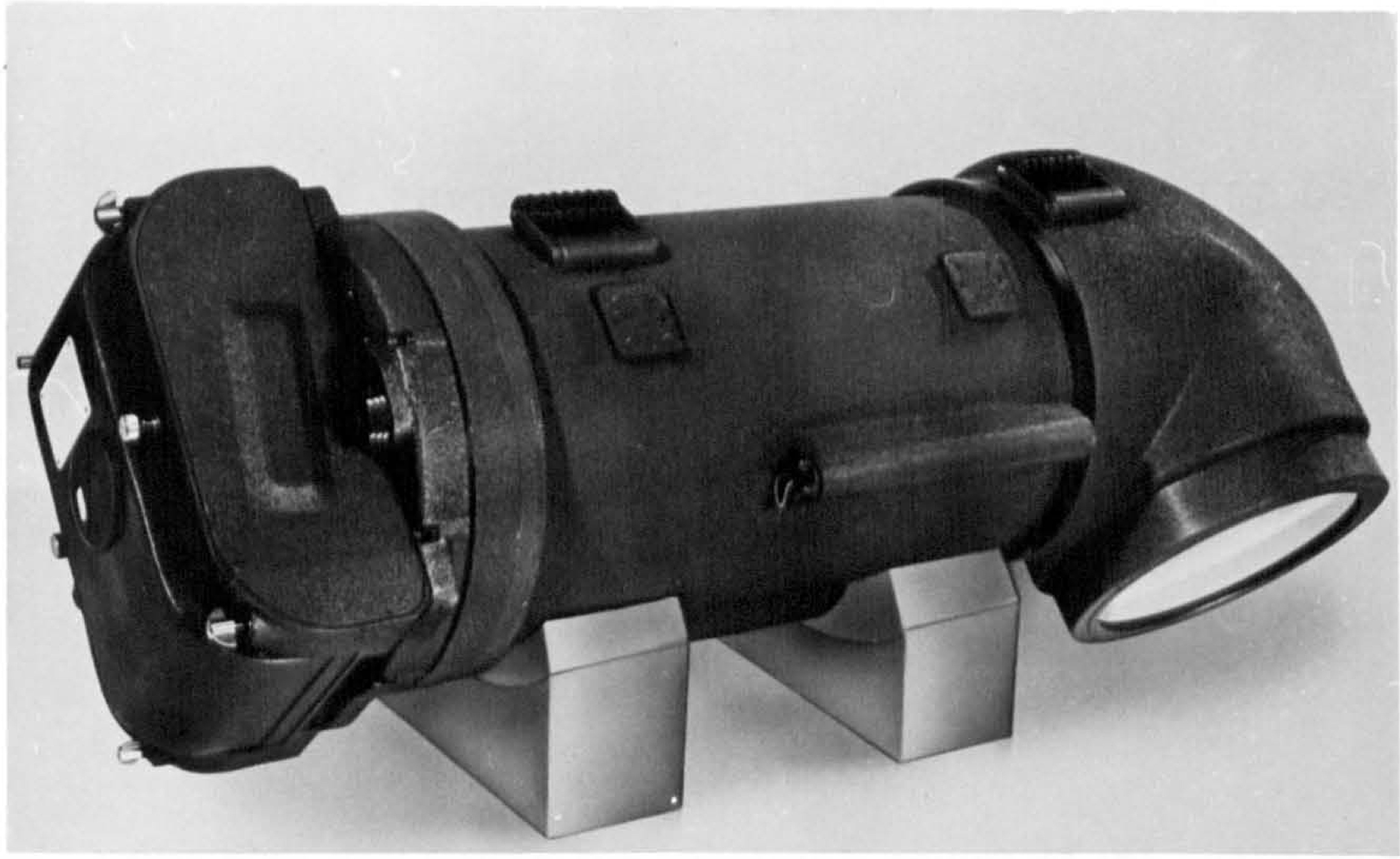

Fig. 53 Oude Delft TA-120 Camera

The Oude Delft series are designed mainly for medium and high altitude operations and thus are equipped with mirror systems having equivalent focal lengths of 20, 30, 60, 90 and 120 cm (The TA-20, TA-30, TA-60, TA-90 and TA-120 respectively). The TA-120 air camera (Fig. 53) is equipped with 250 ft (80 m) of 5 in. (12.5 cm) unperforated film to produce an image size of 4.5 x 4.5 in. (11.5 x 11.5 cm). Right-angle models have been produced (Fig. 52 and 53) incorporating an additional 45° plane mirror, which permits a horizontal position of the rather long focal length camera in the aircraft.

3.6.3. Lens Resolution

The ability of an image-forming system to reproduce detail is determined by its resolving power, which may be expressed as the number of the smallest elements per unit area or per unit length that can be resolved in the photograph. The lens aberrations which have already been mentioned cannot be eliminated entirely and they impose several limitations on the lens performance and its resolving power.

Even with an ideal aberration-free and distortion-free lens, which is also free of all the imperfections resulting from its manufacture, an infinitely great resolving power is impossible because of the diffraction phenomena. Real lenses always have finite openings and, therefore, they always produce diffraction effects.

Airy (1834) found that the image of a point produced by an ideal lens is a bright disc of a measurable dimension, surrounded by an infinite number of rings. The size of this disc and hence the resolving power of the lens was found to be dependent on the wavelength of the light used and the aperture of the lens. This is expressed by the diffraction limiting formula (Shershen, 1958):

$$r = \frac{M\lambda}{\pi} \cdot \frac{f}{d} \quad \dots\dots\dots\dots \quad (1)$$

where r is the radius of the Airy disc, or simply the minimum distance between the images of the points or lines that may be distinguished separately;

λ is the wavelength of the light;

M is a coefficient to indicate the amount of contrast;

d is the diameter of the entrance pupil of the lens;

and f is the focal length of the lens. (f/d is the aperture of the lens).

This formula is correct only for an ideal aberration free lens. The reciprocal of r in the equation gives the number of line pairs (lp) resolved per millimetre (resolving power) Fig. 54 shows graphically the resolution in line pairs per millimetre obtainable with an ideal lens of variable aperture.

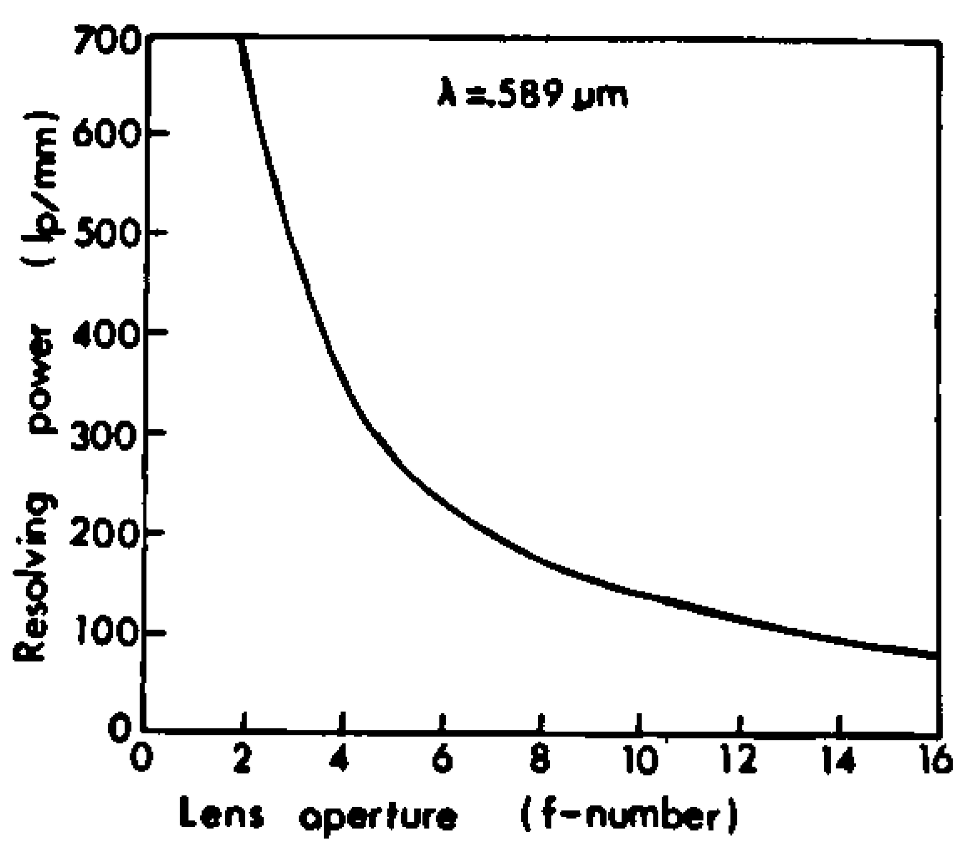

Fig. 54

Variation of resolving power with the lens aperture for an ideal lens.

It is clear that, as the ideal lens is stopped down, its resolving power drops rapidly. For example, aberration-free f/4 lens has a theoretical resolution of 350 lp/mm, whereas stopped down to f/16 its resolving power would drop to 85 lp/mm. This explains why wide-aperture lenses are usually preferred in the case of reconnaissance photography.

The point is reinforced by the fact that wide-aperture lenses also allow shorter exposure times, thereby minimising loss of resolution caused by image motion resulting from the movement of the camera-carrying platform (aircraft, satellite, etc.). However, it is far from easy to manufacture and assemble large aperture lenses for the very large focal lengths used in high-altitude reconnaissance work. For example, to achieve an aperture of f /2 for a lens of f = 24 in (610 mm) means that the diameter of the lens elements is 12 in (305 mm). This means that the lens elements will be very large and heavy and will be much more difficult to manufacture, handle and assemble. In turn, they will also be much more expensive than narrower-aperture lenses.

The highest figures for resolution are obtainable on-axis, i.e. around the central area of the format. However, there may be a drastic reduction in resolution towards the corners of the photograph. This fall-off in resolution is very much more significant with the super-wide-angle and wide-angle lenses which are favoured, for geometrical reasons, in metric cameras. In normal-angle lenses, however, it is much less of a problem.

To determine the resolution of a system containing several components, such as lens, film, image motion, the following empirical formula (Shershen 1958; American Society of Photogrammetry, 1966) is often used:

$$1/R_s = 1/R_1 + 1/R_2 + 1/R_3 + \quad \ldots\ldots\ldots\ldots\ldots\ldots \quad (2)$$

where R_s is the resolution of the system and

R_1, R_2 etc. are the limiting resolutions of the components. However, the resolving power of the lens cannot simply be determined as such since, inevitably, resolution measurements also involve a target and an emulsion. Thus the resolving power quoted will (or should) specify the target used e.g. high or low contrast and the type of film used.

However, even these resolution values do not readily point out the factors responsible for favourable or unfavourable system performance. Thus, an alternative statement of image quality; the Modulation Transfer Function (MTF) is now preferred. The MTF or sinewave response is a curve indicating the degree to which image contrast is reduced as spatial frequency is increased. The MTF's of the well-known Wild Aviogon mapping lens and the Skylab S-190B reconnaissance camera lens are given in Figs. 55a and b. respectively.

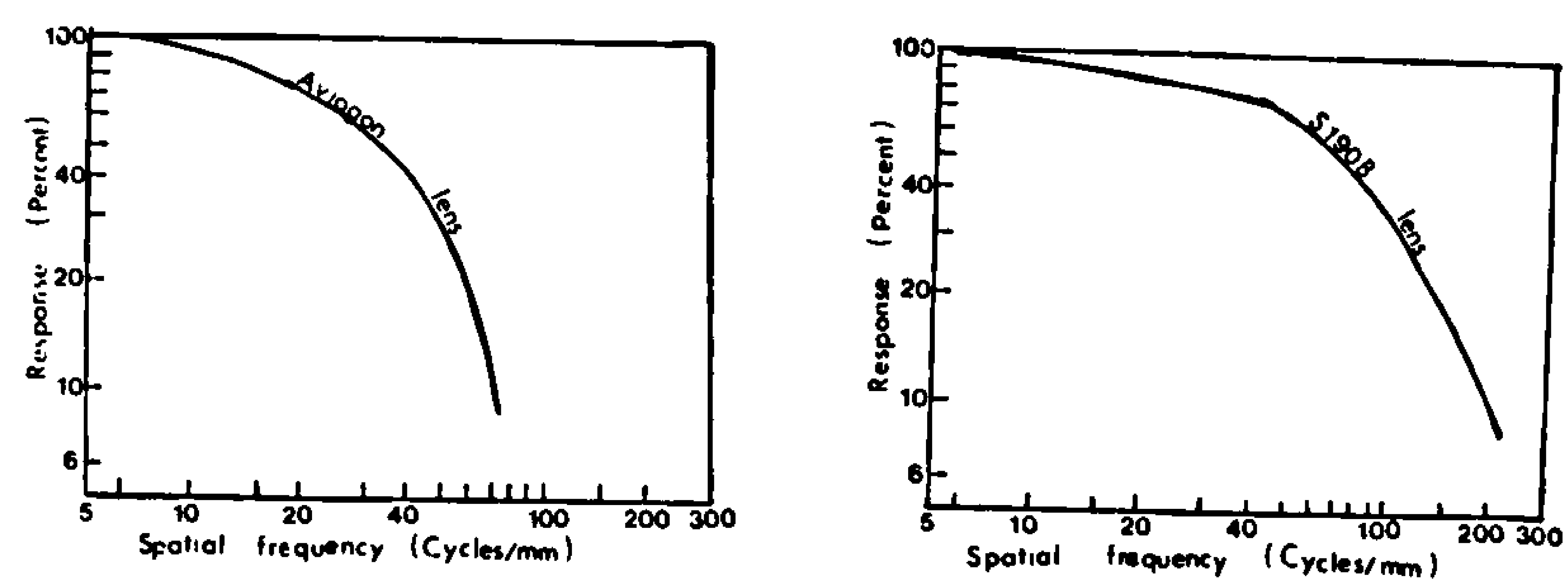

Fig. 55 (a) MTF for the Aviogon Lens (Welander 1968, Welch 1971) (b) MTF for the S-190B Lens (Gimlett 1975, Welch, 1976).

From the above, it can be seen that the S-190B lens has higher MTF values at higher spatial frequencies than the mapping Aviogon lens. For example, at the modulation of 40 percent, the Aviogon lens has a spatial frequency of 45 cycles/mm while the S-190B lens has a spatial frequency of 90 cycles/mm. Again starting from spatial frequency of 30 cycles/mm, the MTF curve from the Aviogon lens drops rapidly when compared with that of the ETC lens. This is one example to show the superiority of reconnaissance lenses over metric lenses in terms of lens quality.

Individual MTF curves can be produced for lens, film, image motion and other relevant variables in the camera system and a single MTF value for the camera system could be obtained by multiplying the responses of the appropriate lens, film and other curves, frequency by frequency. This process of combining the individual MTF curves is known as cascading.

This process can be illustrated by Fig. 56. The former (Fig. 56a) shows the individual MTF curves for the Wild Aviogon lens, the Kodak 3400 film and 10 μm of image motion and also the product of these three MTF's which is the system MTF (Welch 1970) The latter (Fig. 56b) shows the MTF curves for the S-190B lens, the 3434 and 2430 Eastman Kodak films employed to record and duplicate S-190B photographs. The predicted MTF's obtained by cascading the lens MTF with the MTF's for the original (3414) and (2430) duplicating films are shown in Fig. 56c (Welch 1976). It can be noticed from these figures that while the MTF value of 40 percent for the S-190B photograph corresponds to a spatial frequency of 60 cycles/mm, at the same MTF value for the Aviogon system, the spatial frequency is only 25 cycles/mm. This example further emphasizes the point that final MTF value of the total system in reconnaissance photography is significantly higher than that produced by what most photogrammetrists and photo-interpreters would regard as high-quality mapping or metric photography.

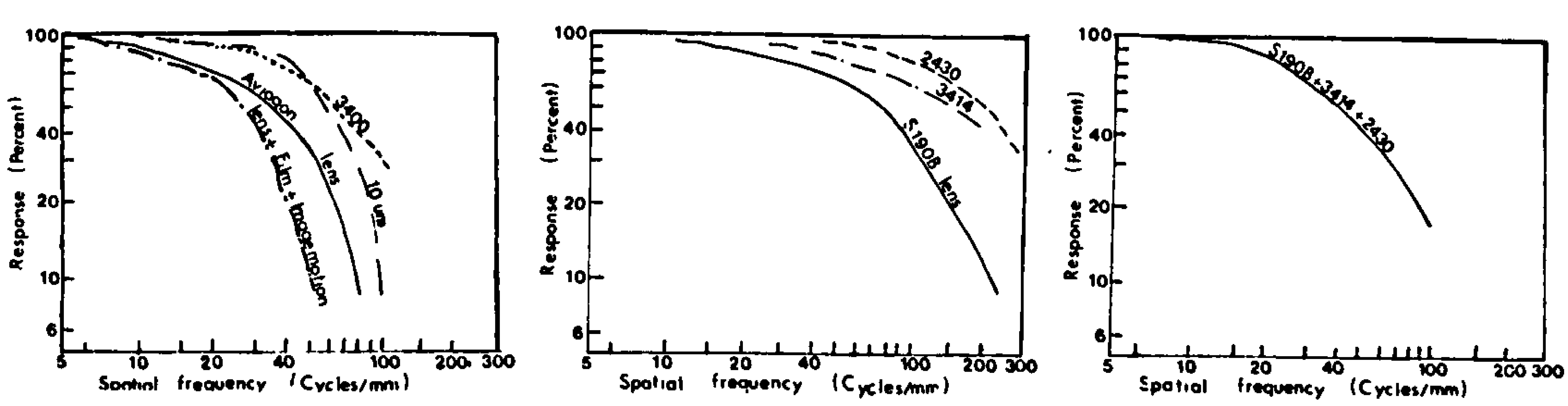

(a) (b) (c)

Fig. 56
(a) MTF's for a Wild Aviogon lens; Kodak 3400 film; 10 µm of image motion, and the total MTF of the system (Welch 1971)

(b) MTF's for the S-190B lens; the Eastman Kodak 3414 and 2430 films (Welch 1976)

(c) Total MTF for second generation S-190B photographs (Welch 1976).

The <u>actual resolution</u> of the photographic system (which is a concept more readily understood by most users) can be predicted by intersecting the MTF curve of the system, excluding the film, with a Threshold Modulation (TM) curve which is a graphical plot of visually determined film resolution for targets of several contrasts. This is illustrated by Figs. 57 a and b in which resolution values for the photographic systems have been determined for each of the examples given above. Again, the predicted resolution for the S-190B reconnaissance system exceeds that of the Aviogon metric system (cf. 60-70 lpr/mm for 1.6 : 1 target contrast v. 46 lpr/mm for 2 : 1 target contrast).

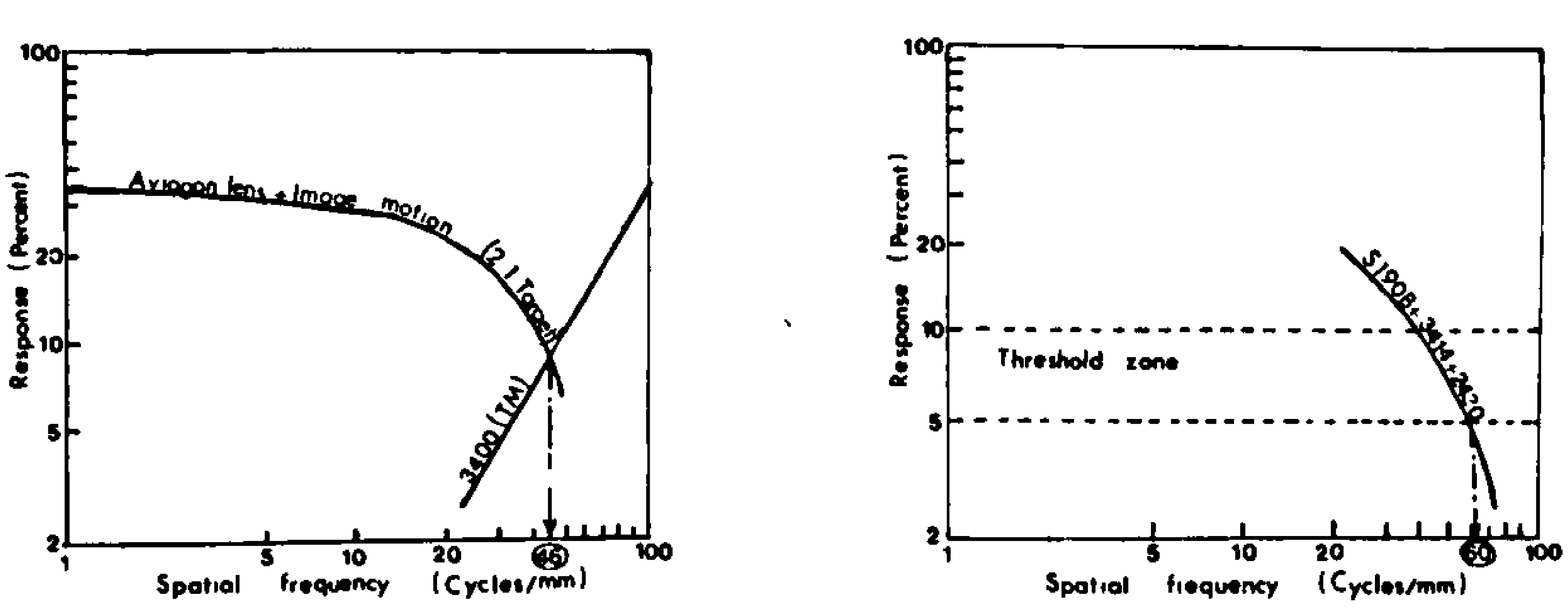

(a) (b)

Fig. 57 a. Estimated resolution at a target contrast of 2 : 1 for the Aviogon system (Welch 1971).

b. Estimated resolution at a target contrast of 1.6 : 1 for the S-190B system (Welch 1976).

3.7 <u>Format Size and Arrangement</u>

As already mentioned, within the N.A.T.O. countries the film widths have become standardised at 70 mm , 5 in. (12.5 cm) and 9 in (23 cm). In general, the 70 mm width is used for low altitude reconnaissance photography where demands for resolution are lower and the small bulk of the camera allows several cameras to be used in a fan arrangement which is frequently a requirement to achieve angular coverage. The wide width (23 cm) film is employed mostly at high and medium altitudes where high resolution is a priority and the intermediate 5 in. (12.5 cm) width is employed at both low altitudes (to give better resolution if required) and at high altitudes where it is more economical of film and allows more exposures, though at the cost of angular coverage.

Normally, the formats used with these films are square, e.g. 6 x 6 cm, 11.5 x 11.5 cm and 23 x 23 cm, but there are some interesting departures from this. American practice with many high altitude reconnaissance frame cameras equipped with long focal length narrow angle lenses has been to recover angular coverage by using rectangular formats, usually 9 x 18 in. (23 x 46 cm) with the long side normally sat across the flight direction.

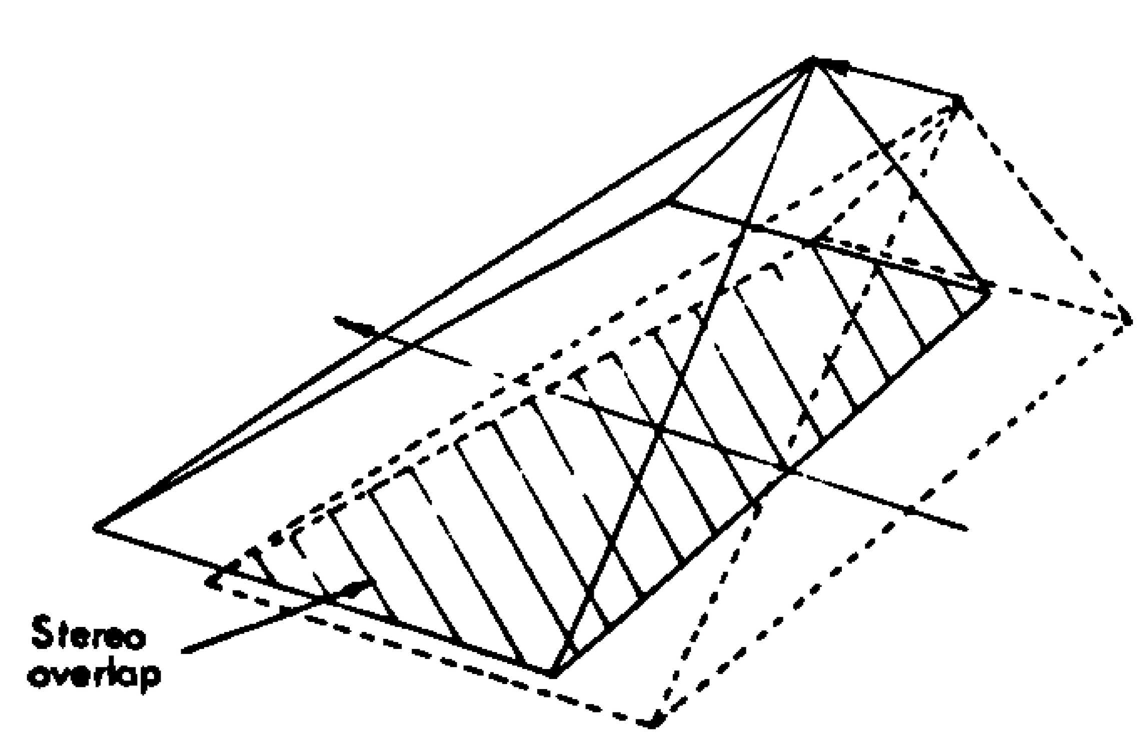

Fig. 58 Rectangular Format Camera operated cross-track.

This format was first used in the K-7 camera of 1926, but it is also used in the following recently manufactured cameras:-

Focal length / Camera	12 in. (30 cm)	24 in.(60 cm)	36 in.(90 cm)	48 in.(1.20m)
KA-1	✓	✓	✓	-
KA-13	✓	✓	✓	✓
KA-21	–	–	–	✓
KA-38	✓	✓	✓	-
K-50	–	✓	✓	✓

The result is a very poor base/height ratio caused by the small longitudinal or forward overlap and the very narrow forward angular coverage, which gives a poor stereoscopic impression of the terrain.

However, it is also possible to set the long side of the format parallel to the flight line, in which case the base/height ratio will be increased, albeit at the cost of limited lateral coverage. There is reason to believe that this is in fact being done increasingly to achieve good stereoscopic viewing from high altitude aircraft and Earth-orbiting spacecraft. As a pointer to this, the Itek Company announced in 1974 that it would build the so-called Metritek camera. This will be available with a 9 x 18 in. (23 x 46 cm) format and with alternative focal lengths of f= 12 in. (30 cm) and 18 in. (46 cm). This is to be mounted in a four-engined, ultra-high altitude version of the Learjet, capable of flying at altitudes greater than 60,000 ft (20,000 m). The same camera is also proposed for the Geosat satellite and the trial flight will take place in one of N.A.S.A's Shuttle proving flights in 1980. In all cases, the camera, which is thought to be a metric version of a military reconnaissance camera, is to be operated with its long side parallel to the flight line.

3.8 Image Movement Compensation (IMC)

An important factor that may well determine the resolution of the photograph is image movement. Any movement by the camera system during the exposure of the photographic material may cause a degradation of the image. This image degradation depends upon several factors including the following:

1. Time of exposure.
2. Type and speed of movement.
3. Ground resolution of the camera system.

3.8.1. Camera movements

The camera system movements may be classified in two groups: angular movement and linear movement. An angular movement is a tilt of small order resulting from aircraft vibrations and aerodynamic forces acting on the aircraft. A linear movement is the forward, backward or sideways movement of the image. The main item is the rapid forward movement of the aircraft, but smaller linear movements are produced by aerodynamic forces.

At the low altitudes at which many reconnaissance aircraft fly, the extent of the former (angular) movement can be quite discernible. But in such cases, the photo scale is large, so while resolution may be degraded a little, it takes place without any serious results for the users. However, the latter (linear) movement can be much greater in overall amount with more serious consequences for the user.

3.8.2 The Effects of Craft Speed, Flying Altitude and Exposure Time on Image Movement

With a forward motion of the aircraft at speed V, the exposed image will move on the focal plane at a speed $v = \frac{f}{H} . V$. During the exposure time t_e the image displacement (dx) on the focal plane will be

$$dx = \frac{f}{H} . V . t_e \qquad \dots\dots\dots\dots\dots\dots \qquad (3)$$

Expressing the image displacement dx in millimetres, the craft speed V in km/h, the exposure time t_e in seconds, the camera focal length in millimetres and the flying height H in metres, the above formula can be written as:

$$dx = 0.278 . \frac{f}{H} . V . t_e \qquad \dots\dots\dots\dots\dots\dots \qquad (4)$$

Assuming a camera focal length of 12 in. (300 mm) and an exposure time of 1/500 second, the image displacements for various flying altitudes (H) and craft speeds (V) are shown in Fig. 59

Fig. 59 Variation of image motion with craft speed and flying height.

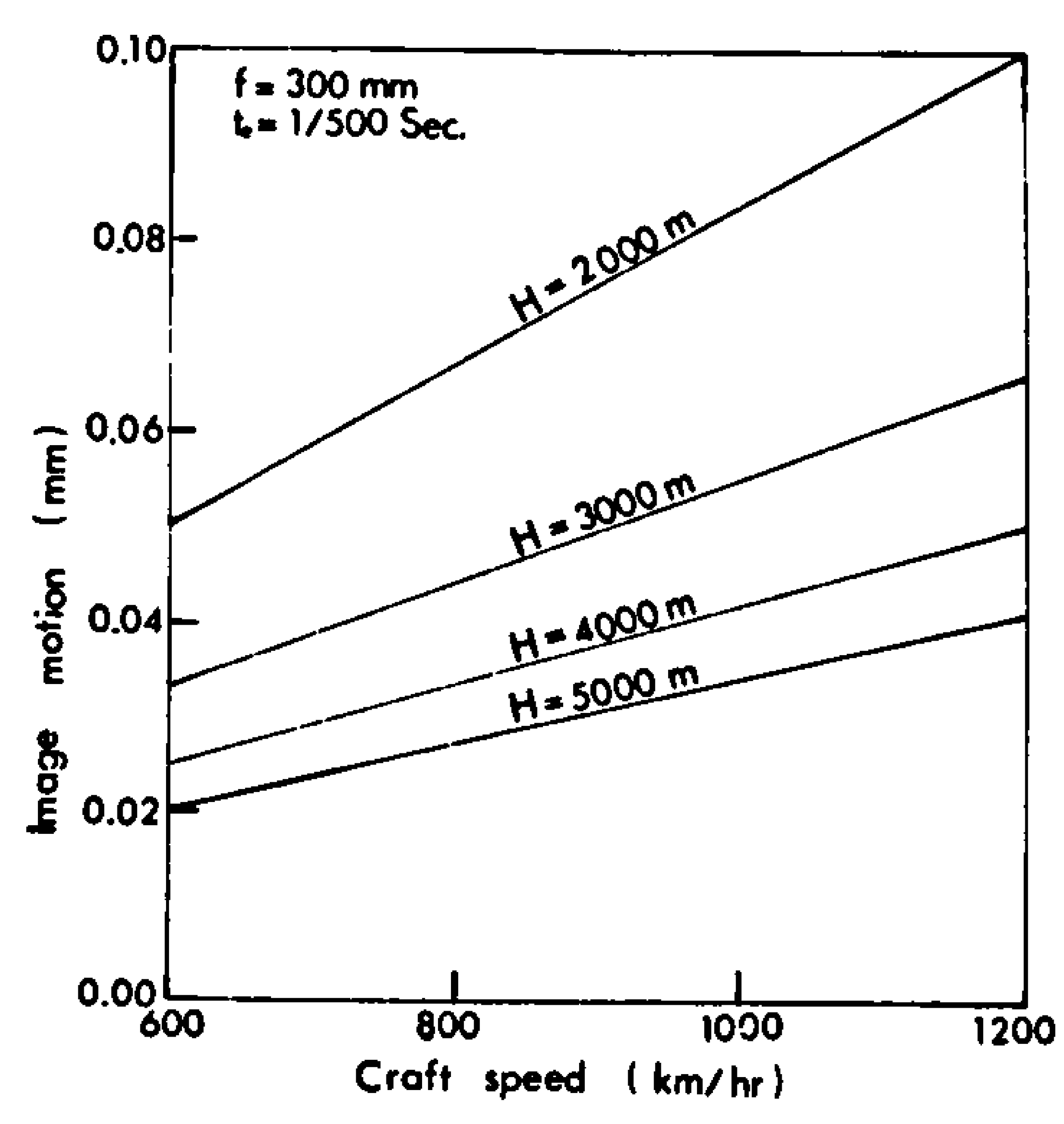

It is clear from the above diagram that the image displacement is directly proportional to the craft speed and inversely proportional to the flying height.

For example, for a flying height of 2,000 m, and a craft speed of 1,200 km/h, the image displacement will be 0.10 mm which is a considerable image blur. But such a craft speed at even lower altitudes is often met in reconnaissance conditions.

However, if the image scale (f/H) is being kept constant, the exposure time should be varied inversely as the speed of the aircraft, in order to minimise the image motion. This is illustrated by Fig. 60, which shows obviously that the shorter the exposure time, the less the image motion. This is of course, only possible if the lens aperture can be widened to give the correct exposure. But even then, at the high speeds of modern reconnaissance aircraft and of Earth-orbiting satellites, the image motion can be considerable and other solutions have to be found.

Fig. 60 Variation of image motion with craft speed and exposure time.

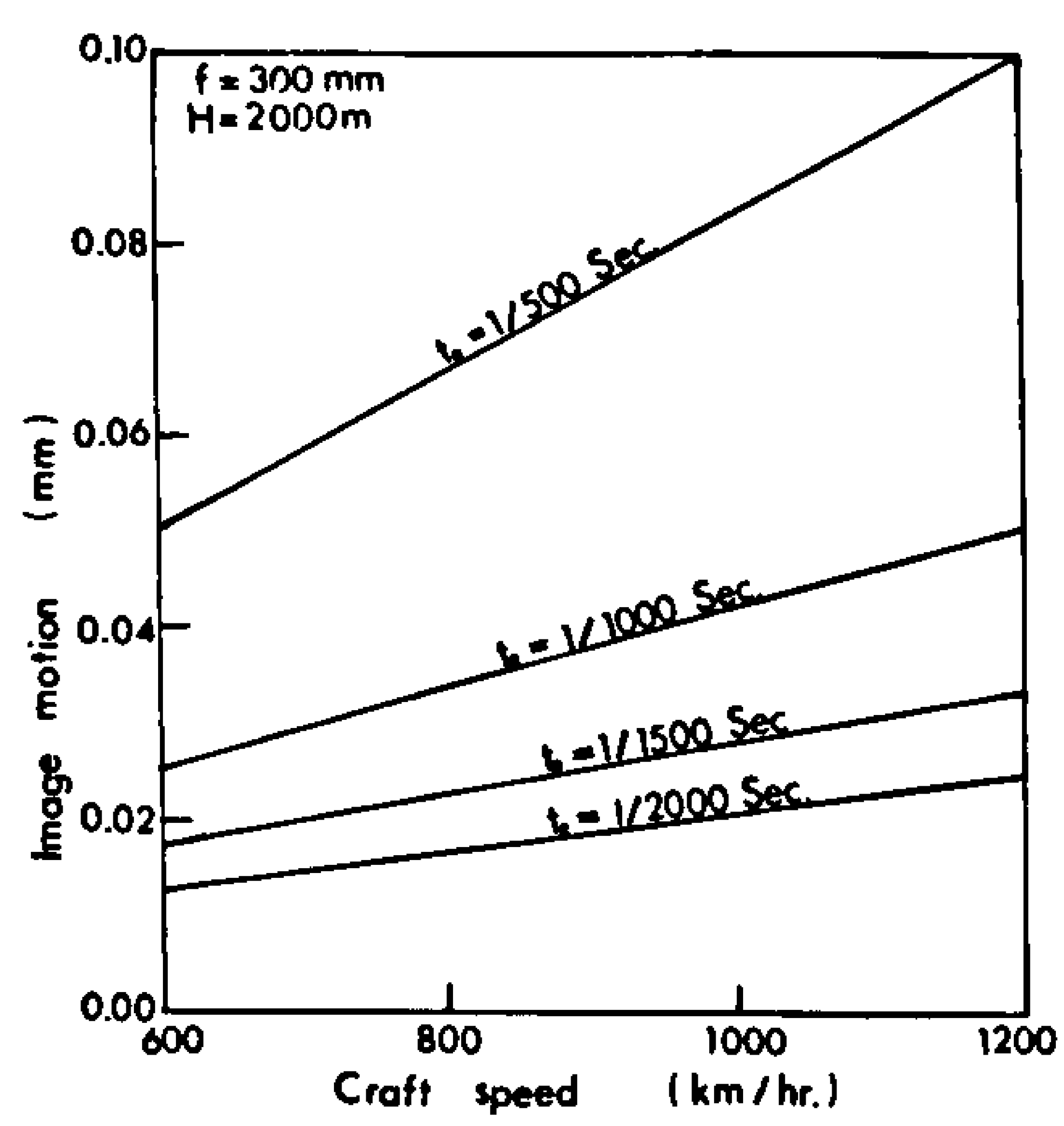

3.8.3 Image Motion Compensation (IMC) as a means of maintaining resolving power.

Many modern films possess high speed (in exposure terms) but, if so, this characteristic is achieved at the cost of lower resolution than can be got from fine grained slower films. When image motion is an important factor as in reconnaissance work, then using a high-speed film in conjunction with a faster shutter speed often produces better resolution than would be obtainable on a fine grain film and a slow shutter speed. The needs for high shutter speeds to stop image movement and the needs for fine-grained film to give the high resolution necessary in reconnaissance work are contradictory. For the first of these two requirements, the solution has been to incorporate Image Movement Compensation (IMC) in the camera. IMC was first used shortly after the Second World War when cameras had to be installed in the new jet-aircraft that flew at very high speed and low altitudes.

3.8.4. IMC Systems

There are two main IMC systems which are in current use with reconnaissance cameras.

(a) Moving the film during the exposure.

Experience has shown this to be the more convenient method of IMC and it is that commonly used in most reconnaissance cameras.

Fig. 61 IMC by moving the film in the flight direction.

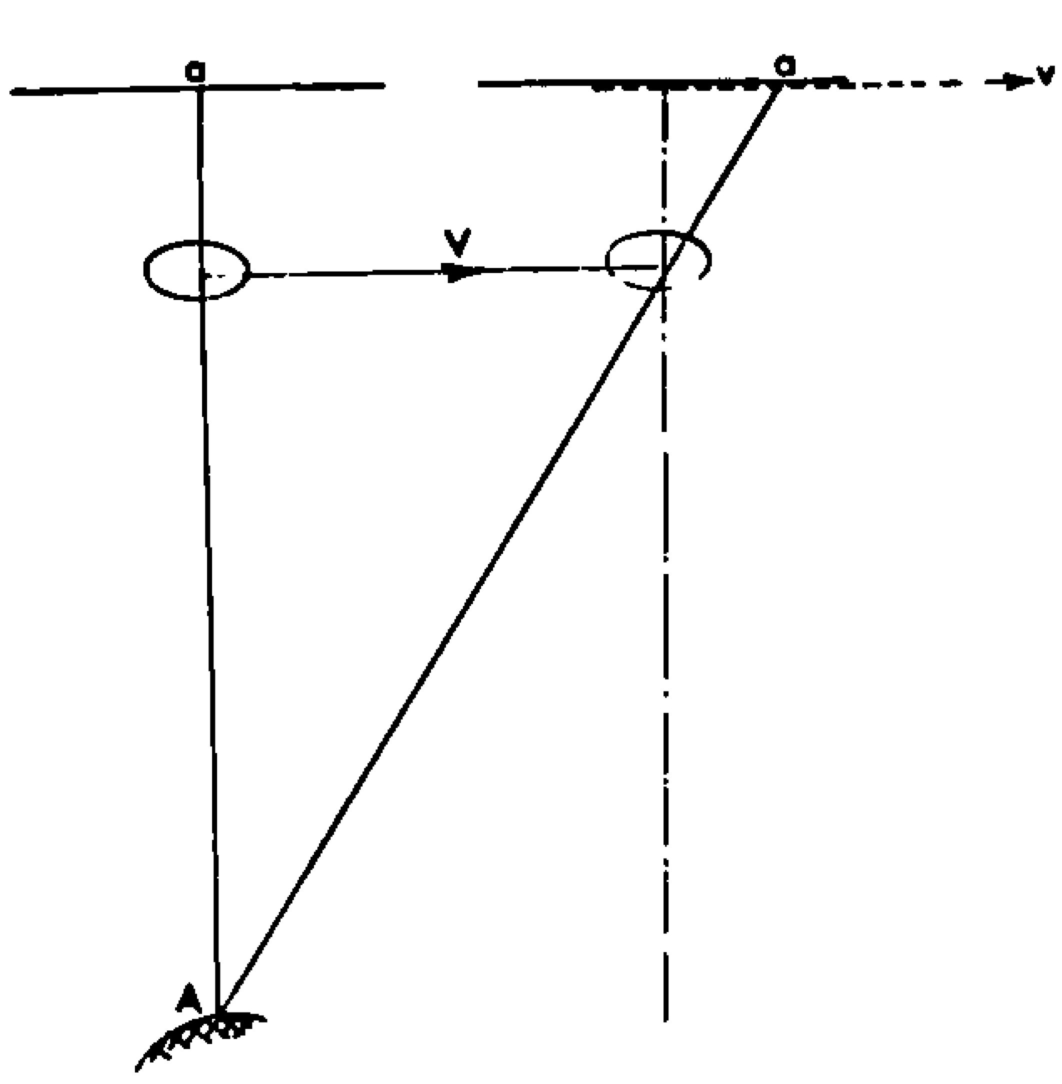

The technique is to move the film in the focal plane in the direction of flight with speed $v = V\frac{f}{H}$ to achieve zero image motion (see Fig. 61). In cameras equipped with a register glass plate and a pressure plate, e.g. the F-126 camera, the film is clamped between the two and all are driven by the IMC motor. The pressure plate is lifted immediately after exposure and returns together with the register glass to their starting positions while the film is rapidly wound on (Fig. 62).

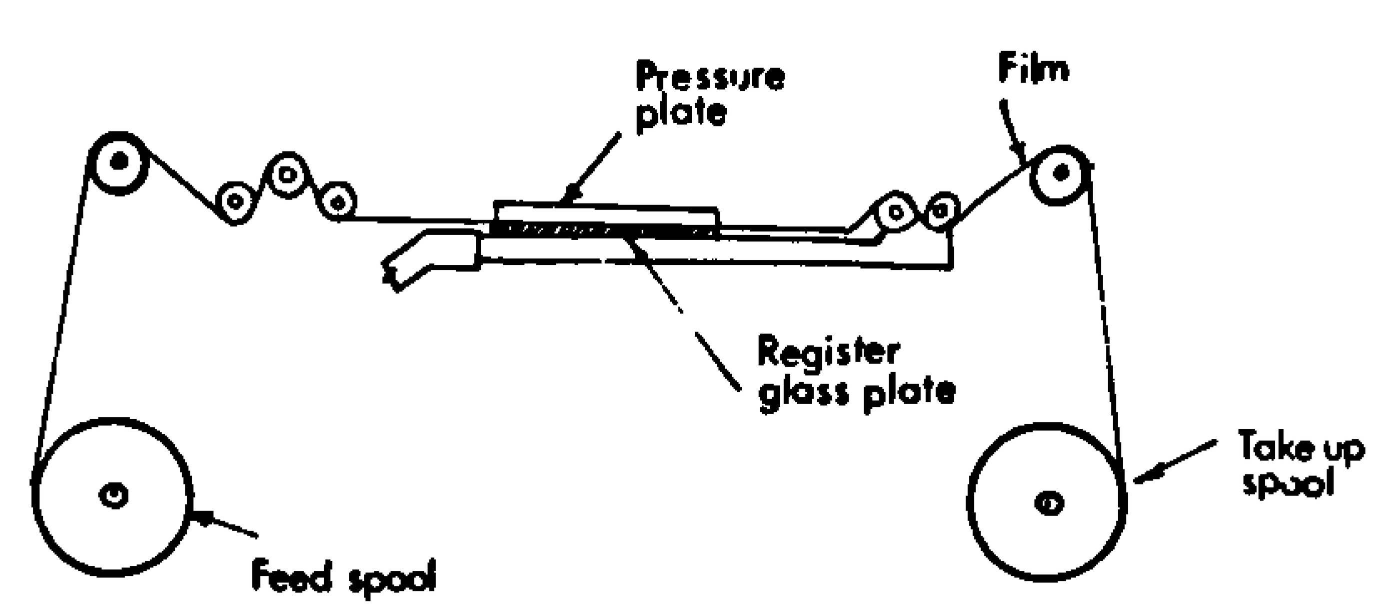

Fig. 62 Moving glass plate and pressure plate to achieve IMC.

An alternative to this is to displace the lens in a direction opposite to the flight direction, again at a speed of $v = V.\frac{f}{H}$. However, the movement of the lens is perhaps more difficult to achieve; therefore it is not in common use in reconnaissance frame cameras. As noted previously, the method is used in many panoramic cameras where moving the film in a curved focal plane is a still more difficult procedure.

(b) Rotating the camera:

In this method, the optical axis points towards the same ground point throughout the duration of the exposure. This is done by tilting the camera in the direction shown by the curved arrow in Fig. 63. In this case, the image compensation is not equal over the whole format. While the compensation

Fig. 63 IMC by tilting the camera.

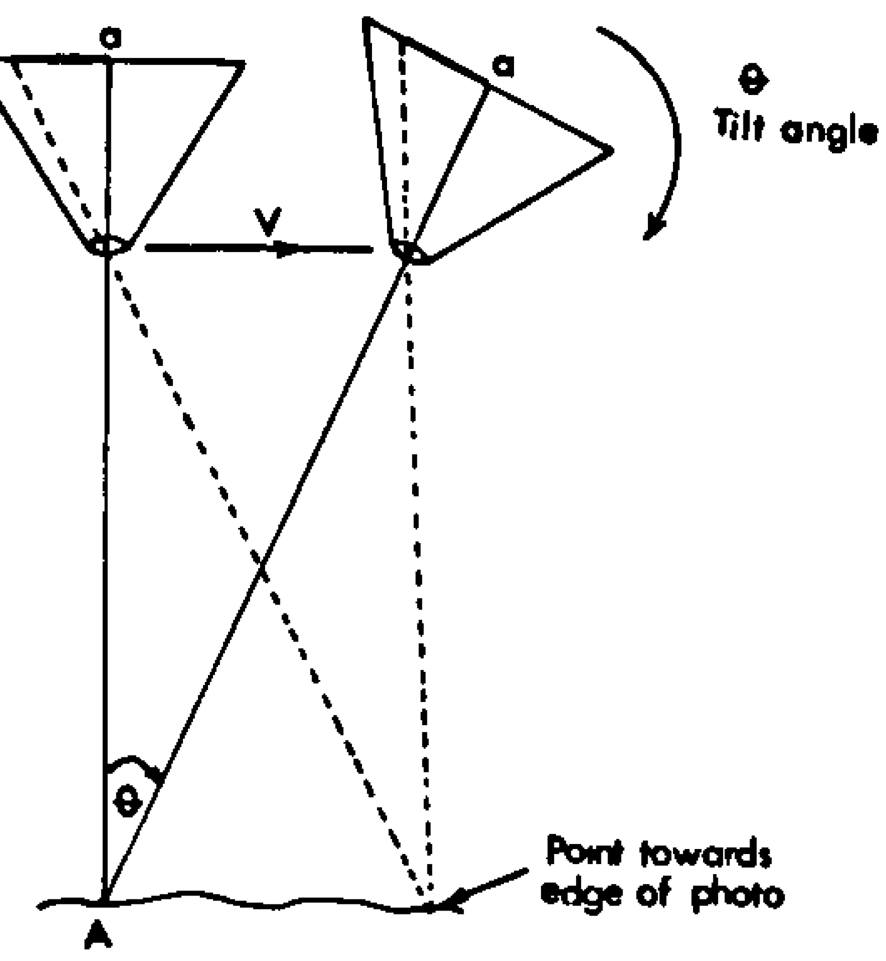

is effective around the point A, it will not be so effective towards the edges of the field and leads to a residual image blur which will be discussed in more detail in the next chapter. However, it is the only method of implementing IMC for cameras which are not equipped with moving film capability.

The use of the rotating camera system is however limited by certain factors:

(i) It is impracticable to use this system with a wide-angle camera since the lack of image compensation at the edges of the format would impair the image quality. This technique, therefore, is only applied to cameras with long focal lengths, narrow-angles and small format size such as the S-190B camera (f = 460 mm, 14° angular coverage and format size = 115 x 115 mm) used in the Skylab spacecraft.

(ii) The camera rotation has to be synchronised exactly with the camera shutter in some way. Furthermore, when rotating the camera in its mount, a smooth-acting mechanism is needed which will produce the continuous change in tilt needed throughout the exposure. If this is not achieved, the effect is similar to that of a camera vibration. Obviously the provision of this mechanism adds weight and requires more space in the aircraft or spacecraft.

An alternative method of achieving IMC which has been tried experimentally is to rotate a spherically configured element mounted in front of the main camera lens (Shershen 1958), see Fig. 64.

Fig. 64 Rotation of the projection rays by means of an accessory optical device.

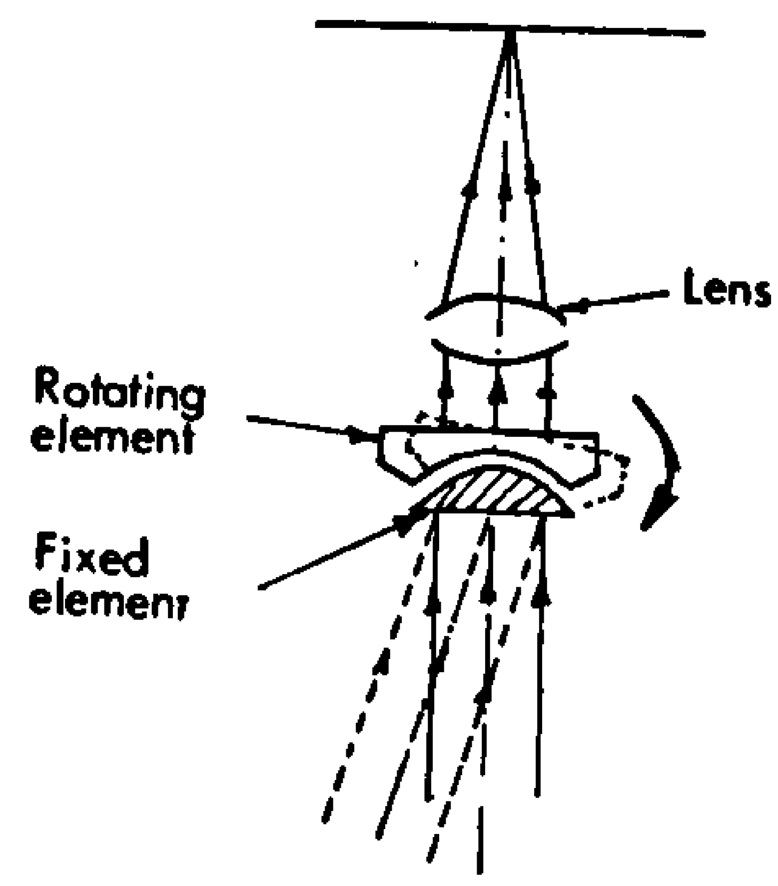

This consists of two elements, a fixed element and a rotating one. Again, it is impossible to produce a complete displacement over the whole format by this method. Moreover, the manufacture and assembly of these extra elements is complex and their effect on the resolution and other qualities of the main camera lens may be to lower the overall performance, so it is not used in current aerial cameras.

3.8.5 Accuracy of IMC

Quite apart from the mechanical aspects of ensuring accurate IMC, it is quite essential that the flying height (H) and the speed (V) of the platform carrying the camera be measured accurately. In practice these are provided by the standard aircraft instruments; the height by means of the aircraft (barometric) altimeter and the ground speed by pressure-sensing devices. In the F-126 camera, the speed of the "IMC motor" is controlled by a closed-loop electronic device which is locked to the V/H signals from the aircraft navigational system. The accuracy of IMC employed in this camera is claimed to be within 2 percent.

3.9 Shutters

The aerial camera shutter is one of the main components of the aerial photographic camera. It plays the role of preventing light from striking the film emulsion except during the time of exposure.

Two types of shutter are used in modern frame cameras. These are (1) the intra-lens shutters, and (2) the focal plane shutters.

3.9.1 The Intra-lens Shutter

The intra-lens or between-the-lens shutter, as its name indicates, is located in the air space between the elements of the lens. This type of shutter is commonly used in mapping cameras and in certain reconnaissance frame cameras. The common types of the intra-lens shutter are the leaf or blade type; the rotating disc type, and the louvre shutter.

Fig. 65 Leaf-type shutter

(a) Half open position

(b) Closed position.

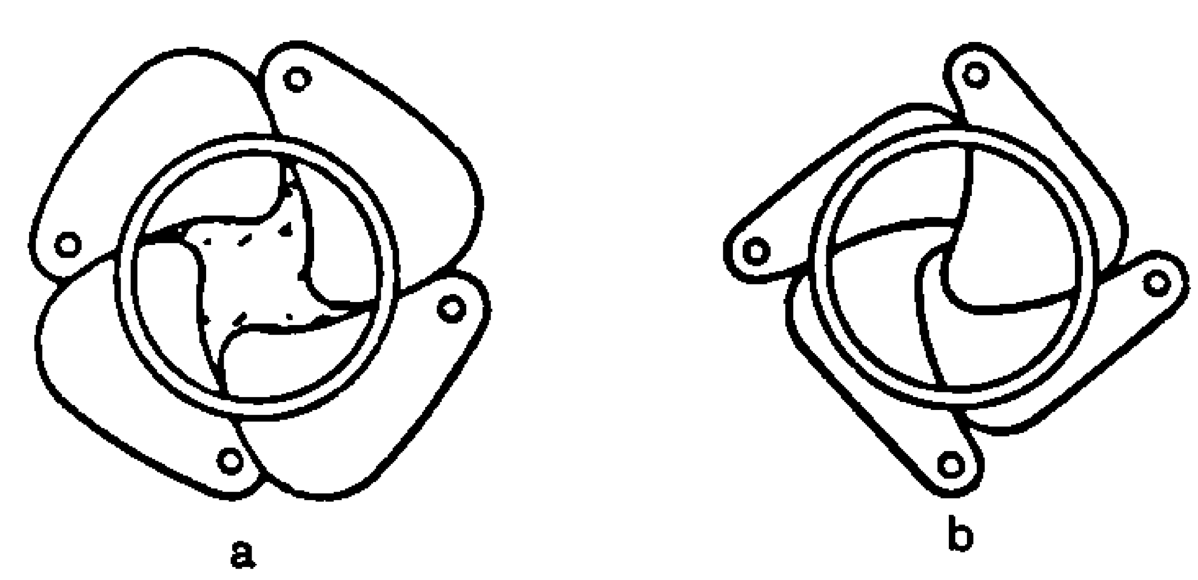

The leaf-type shutter (Fig. 65) is composed of four or more leaves mounted on pivots and spaced around the periphery of the diaphragm. When the shutter is tripped, the leaves rotate about their pivots to the open position, remain open for the required exposure time and then close up. This type of shutter is used in some American reconnaissance frame cameras (e.g. KA-3A Fairchild camera).

Fig. 66

Rotating-disc

type shutter.

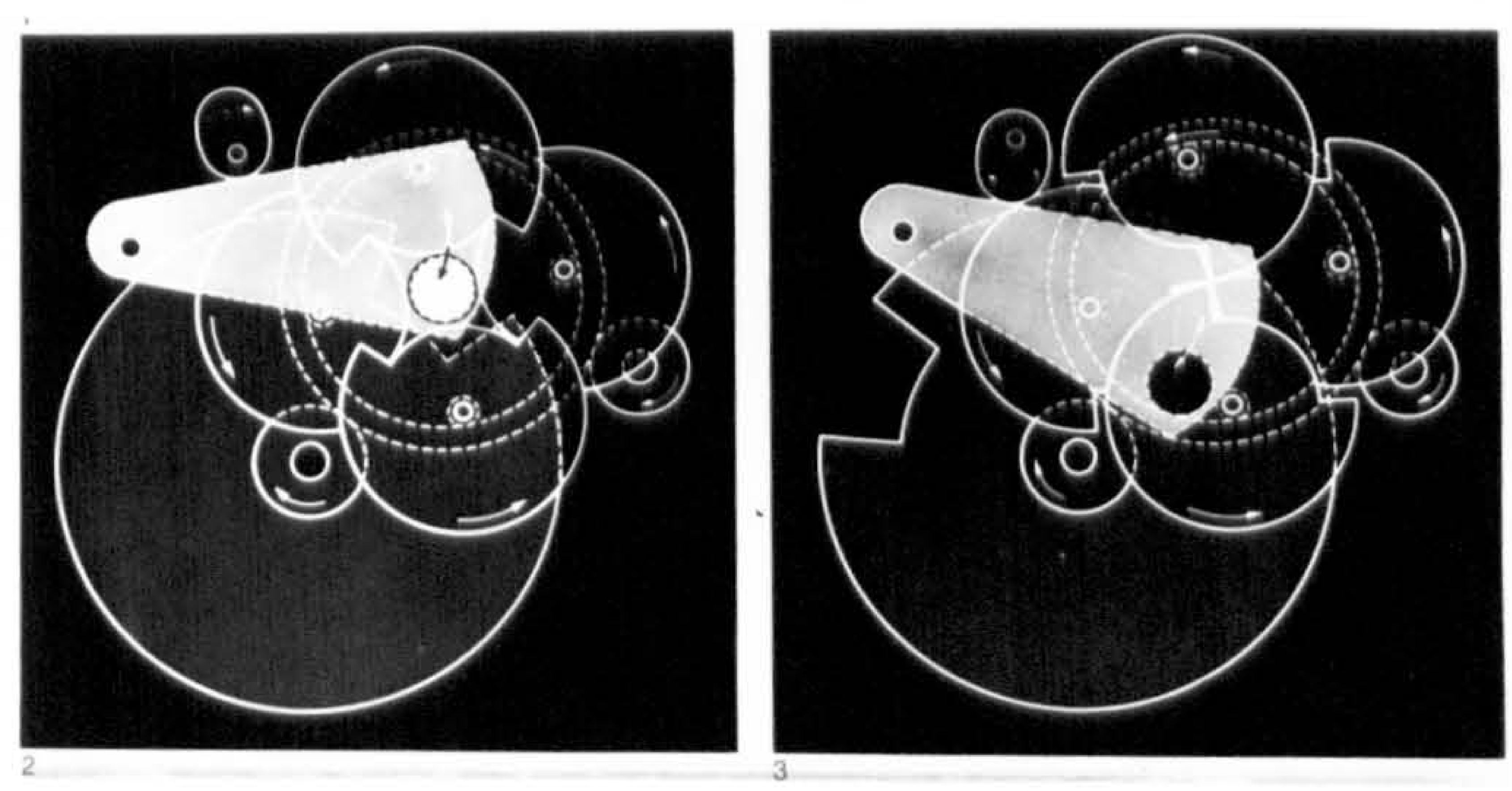

The <u>rotating disc type</u> shutter (Fig. 66) consists of a series of continuously rotating discs. Each disc has a cutaway section. When these cutaways mesh, they form an open aperture which allows the exposure to be made. The speed of rotation of the disc can be controlled such that the desired exposure times and intervals between exposures are obtained. This type of shutter is very efficient (up to 90 per cent efficiency) since no stopping or starting of the parts is required as with the other types. Certain reconnaissance cameras such as the Zeiss HRb and some American cameras (e.g. the HR-233 camera) are equipped with this type of shutter.

The <u>louvre type</u> shutter consists of a row of thin overlapping blades (Fig. 67) made of steel or a light alloy.

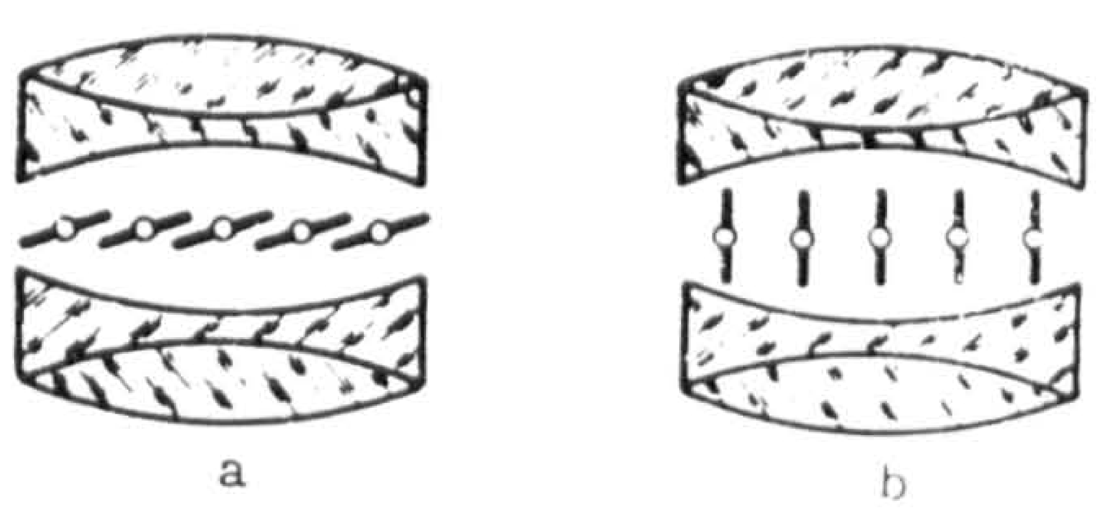

Fig. 67 Louvre-type shutter. (a) Closed position

(b) Open position.

The blades rotate about their axes by about 180 degrees during the exposure. When the blades come to the vertical position the light is allowed to pass through the lens, thereby causing an exposure to be made. In principle, the louvre-type of shutter may be located anywhere in the optical system, but to keep down the physical size of the shutter it is usually located close to the camera lens. In certain older British reconnaissance cameras, the shutter was mounted behind the rear lens element, while in the large German and Russian cameras, it is mounted between the elements of the lens.

Obviously, there must be a considerable number of blades to cover the entire lens aperture. When all the blades are in the vertical position, their thickness forms an area which substantially reduces the light-gathering area of the lens aperture. Therefore, the <u>light efficiency</u> of this shutter only approaches 45 to 47 percent (Shershen 1958). Another disadvantage of the louvre-type shutter is that it adversely affects the <u>distribution of illumination</u> over the image field, since when the blades are in a vertical position they tend to obstruct the oblique rays which have entered the lens from reaching the focal plane. Therefore, in practice the louvre-type shutter is only used with normal-angle lens reconnaissance cameras. From the geometrical point of view, it can be considered together with the other intra-lens shutters detailed above.

3.9.2 <u>The Focal Plane Shutter</u>

It is thus named because it operates close to the focal plane of the camera. In the most common form of the focal plane shutter, the main component is a <u>light-tight curtain</u> in which there is a <u>slit</u> which is moved rapidly across the focal plane to allow an exposure to be made. The curtain is usually composed of a piece of rubberised cloth, wider than the focal plane and a little longer than twice the frame size. The curtain is attached to rollers, one at each end of the negative area (Fig. 68).

Fig. 68 The curtain-type focal plane shutter.

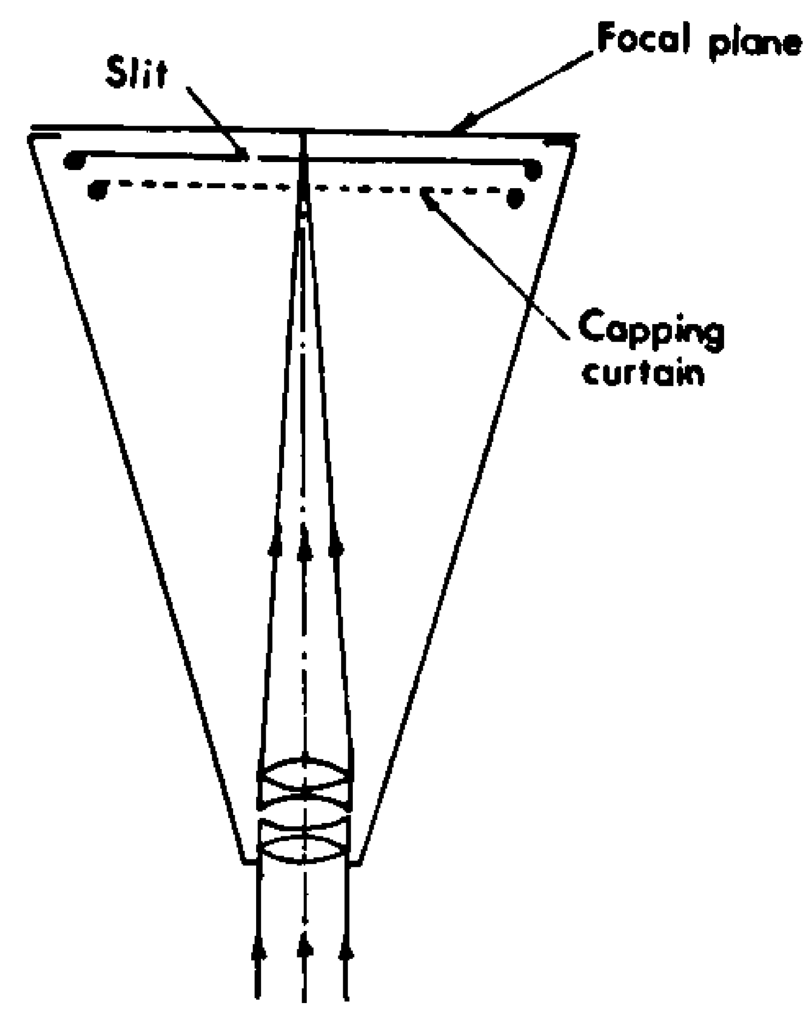

A tensioned spring is used to wind the curtain back until the slit is clear of the frame opening. When the shutter is tripped, the slit moves across the focal plane towards the opposite side of the frame. Hence light is admitted through the slit and an image is formed on the film. To prevent light from striking the film while the curtain is being wound back to the starting position, another capping curtain is located in front of the shutter curtain. The capping curtain has a large opening to prevent capping of the lens during the exposure time. Most of the older large-format British reconnaissance cameras, e.g. F-8 and F-52, are equipped with this type of shutter.

In newer designs of the focal plane shutter, the necessity for a capping curtain during rewinding has been removed by making the curtain travel in opposite directions for alternate exposures. This bi-directional design also allows room for the blind to decelerate, its inertia and that of the roller being taken up and stored in springs, which are used to accelerate it at the beginning of the next exposure. The exposure duration is controlled by changing the initial tension of the spring or by changing the width of the slit itself. A typical example is the focal plane shutter used with the F-126 reconnaissance camera.

An alternative design which has only recently been developed is the rotary focal plane shutter which has a circular disc with a slit across its centre that sweeps the focal plane admitting light to pass to the film during the time of exposure (Fig. 69).

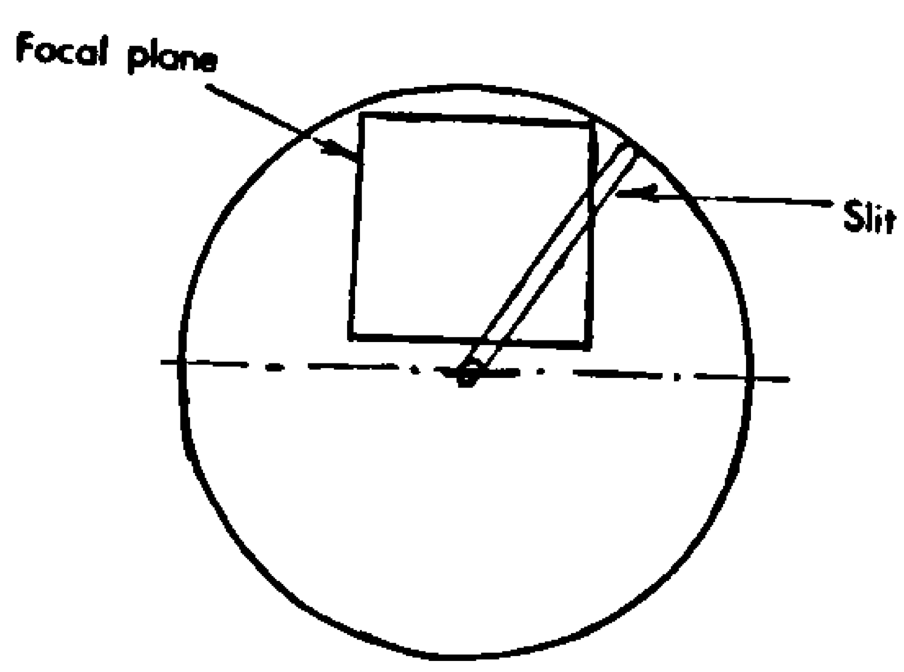

Fig. 69 Rotary focal plane shutter

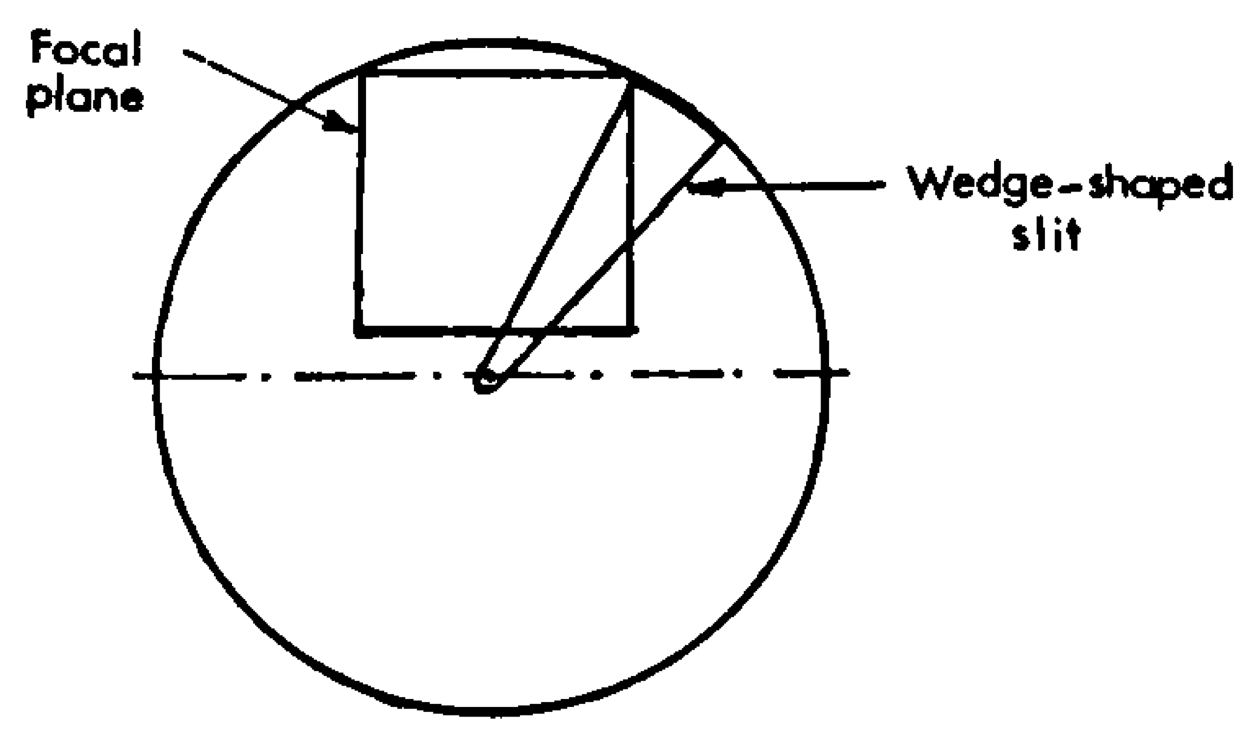

Fig. 70 Wedge-shaped slit for even exposure

However, if the slit width was kept constant, the exposure time would vary from one part of the photograph to another, due to the quite different speed of the slit at different radial distances from its centre of rotation. Thus there would be a longer exposure at short radial distances. To overcome this difficulty, the slit is made as a wedge (Fig. 70) thus ensuring an even exposure.

This most interesting design has the great advantage that it can, if necessary, be run continuously so that there is no starting and stopping, no acceleration or deceleration, no change of direction etc. This means in turn that power requirements are lessened, that very high cycling speeds are possible and ultra-short exposure times can be used. In the case of the Oude Delft TA-7 camera, the speed can be as high as 1/9,000 or 1/15,000 sec. Even with a low-level high speed aircraft this reduces image blur to a minimum, e.g. at 1,000 km/hr (280 m/sec), an exposure time of 1/9,000 sec corresponds to a movement over the ground of 3 cm. IMC will certainly not be necessary in this case.

The disadvantage of this shutter is that the diameter of the disc must exceed the format size by a factor of more than two as a complete minimum. This effectively limits the use of the shutter to very small formats or the circular disc will become impossibly large. Thus its main application is to small format cameras using 70 mm film, e.g. the Oude Delft TA-7, Williamson F-134 and A.G.I. F-139 Agiflite cameras.

Another interesting point is that it will produce a quite different type of geometrical distortion pattern compared with that of the usual type of focal plane shutter with the slit set parallel to the format edges.

3.9.3 Comparison of Shutters

From the design point of view, the louvre-type of shutter is the simplest of the intra-lens type. But, as already mentioned, the efficiency is low and the illumination is reduced towards the edges of the field. Hence its use with reconnaissance cameras is limited. The efficiency of the blade and rotating disc is very much higher (general light efficiency ranges from 80 to 85 percent) and the illumination limitation does not occur.

Also from the geometrical point of view, the intra-lens shutters are the most accurate type of shutters, since they expose all image points simultaneously. Therefore, this type of shutter is the standard for all metric cameras and they are used with certain, mainly American and German, reconnaissance cameras derived from metric cameras. However, their use with long focal length lenses is limited. For a lens with a large effective aperture, the overall dimensions of the aperture increase and so the shutter size and the mass of the blades increase to an extent that makes them impractical to manufacture and operate. For example, the leaf- or blade-type of between-the-lens shutter would require great spring forces for their operation. In order to operate such a shutter across a lens aperture of approximately 130 mm to obtain an exposure of 1/000 second, an operating spring force of the order of 208 kg would be required.

In general, the <u>focal plane type</u> of shutter is the most simple and effective for reconnaissance work, both in principle and in practice. A relatively small force is needed to operate its springs. A wide range of exposure times (up to 1/3000 second) can be achieved, the very short exposure times being especially appropriate to reconnaissance operations carried out at low altitudes and high speeds. The light efficiency coefficient is also high and, with a small aperture, can easily exceed 90 percent. The simplicity and robustness of the shutter also make it extremely reliable with a high time between failures (HTBF) even in the very demanding conditions under which many reconnaissance cameras are operated. These various advantages make the focal plane shutter the most favoured type when designing and building reconnaissance frame cameras. Furthermore, as mentioned above, with the long focal length lenses used in high altitude operation, if a wide aperture is used (as is desirable to achieve short exposure times and high resolution), it becomes impracticable to use an intra-lens shutter, which would become large, heavy, very expensive and (possibly) inefficient. The focal plane shutter is independent of aperture size, so that this difficulty does not arise.

However, the fundamental principle of operation of focal plane shutters causes significant geometrical distortions of the aerial photographic image from the ideal perspective projection on which most photogrammetric theory, methods and instruments are based - though this was not appreciated for some time. For this reason, the focal plane shutter is not used with current mapping cameras. These geometric effects have been a limitation in the use of photography taken with reconnaissance cameras in that distances, areas, positions, heights, etc. can only be obtained from them to a limited degree of accuracy. They are also of a nature which is very difficult to overcome with analogue-type measuring equipment or devices. It is only with the advent of analytical and numerical methods and, in particular, the more convenient computing devices that have become available in the last few years, that practical methods of overcoming these difficulties can be envisaged.

3.10 Summary

From the discussion in this chapter so far, it can be seen that reconnaissance frame cameras are designed on as simple a basis as possible, with the main aims of producing cameras able to operate in every testing conditions both in the air and on the field, yet with a high degree of reliability. At the same time, the photography must be of the highest image quality and resolution. The lenses used are therefore designed and built so that they produce images of this type without regard to any lens distortions which may result. Again, this demand for high resolution images meant that the IMC technique is employed almost invariably to compensate for the image motion caused by the forward craft motion. Another important factor that helps in producing the high quality image is the use of the focal plane shutter which has given high efficiency, excellent reliability and very short exposure times, again at the cost of the geometrical qualities of the photograph.

The matter of the geometrical disturbances of photographs taken by reconnaissance cameras will be investigated thoroughly in this thesis both from the point of view of the geometrical theory and the alternative strategies and methods that can be used to overcome the difficulties that occur. Also a series of experimental tests have been conducted to prove the effectivenes of the methods proposed. However, before reporting on these, it is perhaps appropriate to conclude this chapter on reconnaissance frame cameras by including three summary tables which give the main characteristics of representative reconnaissance cameras which are in current use. These three tables cover the three standard film widths used in N.A.T.O. reconnaissance cameras, but show cameras which are designed for quite different flying heights (low, high and orbital altitudes); for operation from different types of platform (aircraft v. satellite); and which use different IMC arrangements (film movement v. camera rotation).

Table 1

70 mm Reconnaissance Frame Aerial Cameras

Camera	F-139	Type 360 (F-95)	KA-72	P-220	TA-7M
Manufacturer	A.G.I.	Vinten	Fairchild	J.A.Maurer Inc.	N.V. Optische Industrie Delft
Primary use	High speed, low altitude reconnaissance	High speed, low altitude reconnaissance	High speed, low altitude reconnaissance	High speed, low altitude reconnaissance	High speed, low altitude reconnaissance
Format (cm)	5.7 x 5.7	5.7 x 5.7	5.7 x 5.7	5.7 x 5.7	5.7 x 5.7
Cycle time (sec)	Up to 2 frame/sec.	4 & 8 frame/sec	1.0, 2.0, 4.0	0.2	1.5, 2.5, 4, 6, 9, 15 frame/sec.
Film length (m)	7.5	33	5	15	33
FMC type	-	-	moving platen	-	moving film
Angular coverage	(i) 32° (ii) 11°	(i) 65°30' (ii) 41° (iii) 33° (iv) 32° (v) 21° (vi) 11°	(i) 74° (ii) 41°	11°	(i) 74° (ii) 56° (iii) 48° (iv) 41° (v) 32°
Shutter type	focal plane rotary blade	focal plane endless shutter blind	intra-lens	focal plane	focal plane rotary blade
Shutter speed (sec)		1/1000 and 1/2000	1/1000	1/500, 1/1000 1/2000	1/900, 1/9000 1/15000 upon request.
Lens (focal length)	(i) 100mm (ii) 300mm	(i) 43mm (ii) 75mm (iii) 98mm (iv) 100mm (v) 150mm (vi) 300mm	(i) 38mm (ii) 76mm	300 mm	(i) 35mm (ii) 50mm (iii) 62mm (iv) 75mm (v) 100mm

Table 2

13 cm Reconnaissance Frame Aerial Cameras

Camera	F-117	S-190B	KA-50A	TA-120	KS-25
Manufacturer	Williamson	Actron	Chicago Aerial Industry	N.V. Optische Industrie, Delft.	Fairchild
Primary use	Reconnaissance	Satellite	Reconnaissance	Reconnaissance	Reconnaissance
Format (cm)	11.5 x 11.5	11.5 x 11.5	11.5 x 11.5	11.5 x 11.5	11.5 x 11.5
Cycle time (sec)	0.8	2.4 max.	0.17 autos	-	1.0
Film length (m)	16.5	60	30, 76	83	76
FMC type	-	rocking camera	moving film	-	-
Angular coverage	41° 6'	14° 8'	104° 20'	5°	10°
Shutter type	Twin blade intra-lens	focal plane bidirectional	focal plane	focal plane	focal plane
Shutter speed (sec)	1/60, 1/125, 1/250, 1/400	1/100, 1/140 1/200	1/60 to 1/3000	1/125 to 1/1000	1/25 to 1/1000
Lens (focal length)	150mm	460mm	45mm	120mm	600mm

Table 3

24 cm Reconnaissance Frame Aerial Cameras

Camera	F-126	KA-88A	KA-63A	HRb
Manufacturer	A.G.I.	Hycon	Chicago Aerial Industry	Zeiss Oberkochen
Primary use	Medium/high altitude reconnaissance	High altitude reconnaissance	Day reconnaissance	Day reconnaissance
Format (cm)	23 x 23	23 x 23	11 x 24	23 x 23
Cycle time (sec)	1.0 max	1.5 - 3.1	0.33 max	2.0
Film length(m)	76	460	55	120 - 150
FMC type	moving platen	rocking camera	moving platen	-
Angular coverage	(i) 74° (ii) 41°	12° 30'	57°	(i) 74° (ii) 41° (iii) 12° 30'
Shutter type	focal plane bidirectional	focal plane monodirectional	focal plane	intra-lens (rotary disc)
Shutter speed (sec)	1/250,1/500 1/1000	1/500 to 1/2000	1/500,1/1000 1/2000	1/300 to 1/3000
Lens (focal length)	(i) 152mm (ii) 305mm	610mm	1-55 mm vertical 2-80 mm oblique	(i) 152mm (ii) 300mm (iii) 600mm

CHAPTER IV

Geometric Theory of Reconnaissance Frame Photography taken with Focal Plane Shutters

CHAPTER IV

GEOMETRIC THEORY OF RECONNAISSANCE FRAME PHOTOGRAPHY TAKEN WITH FOCAL PLANE SHUTTERS

4.1 Introduction - Geometrical distortions resulting from the use of a focal plane shutter

From the discussion in Chapter 3, it can be seen that, due to its simple design, reliability of operation, wide range of exposure speeds and high efficiency, the focal plane shutter has proven to be the most suitable shutter for use in reconnaissance frame cameras. However, the intra-lens shutter is still the type invariably employed in mapping cameras. The reason for this is that, on opening, the intra-lens shutter admits light to all parts of the negative at one instant and similarly it cuts off the light from the whole negative at the moment when the exposure is completed. This mode of operation allows the image points on the negative to have a precisely defined relationship with all the object points photographed. This is the well-known perspective projection relationship which is the basis for all normal photogrammetric operations.

By contrast, the operation of the focal plane shutter causes a change in the simple perspective geometry of the photographic image, since it does not allow the exposure of the whole format simultaneously. However, this statement does require a little qualification. If the camera is stationary relative to the object during exposure, no difference in the normal geometrical relationships between image points, perspective centre and ground points will result from the use of the focal plane shutter. These will be identical to those produced by the normal between-the-lens shutter. But as soon as the camera platform is moving relative to the object (as in photography taken from an aircraft or spacecraft) then considerable departures from the normal perspective geometry occur when a focal plane shutter is used, due to its sequential mode of operation.

4.2 Operation of the Focal Plane Shutter

This will be considered for the usual type of slit which is set parallel to two sides of the image format and operated with a parallel motion. Its sequential operation is illustrated by Fig. 71 which gives a cross-section through the lens, the shutter and the image plane. The corresponding plan view of the image plane (Fig. 72) gives the sequence of events for the exposure of a particular point

(i) the slit approaches the object;

(ii) the position of the slit just before the opening phase;

(iii) end of the opening phase;

(iv) end of the wide-open phase and start of the closing phase;

(v) end of closing phase.

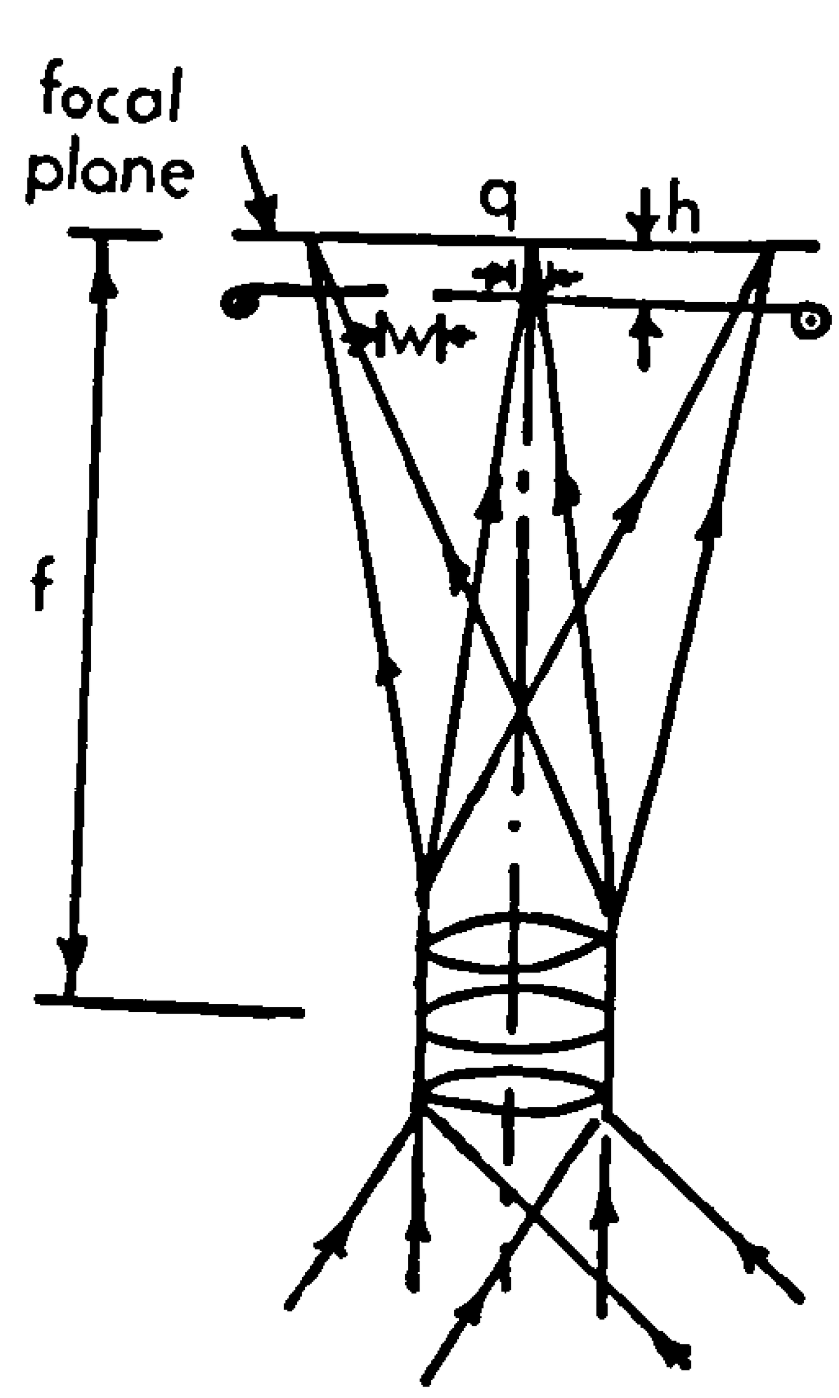

Fig. 71 Operation of the Focal Plane Shutter

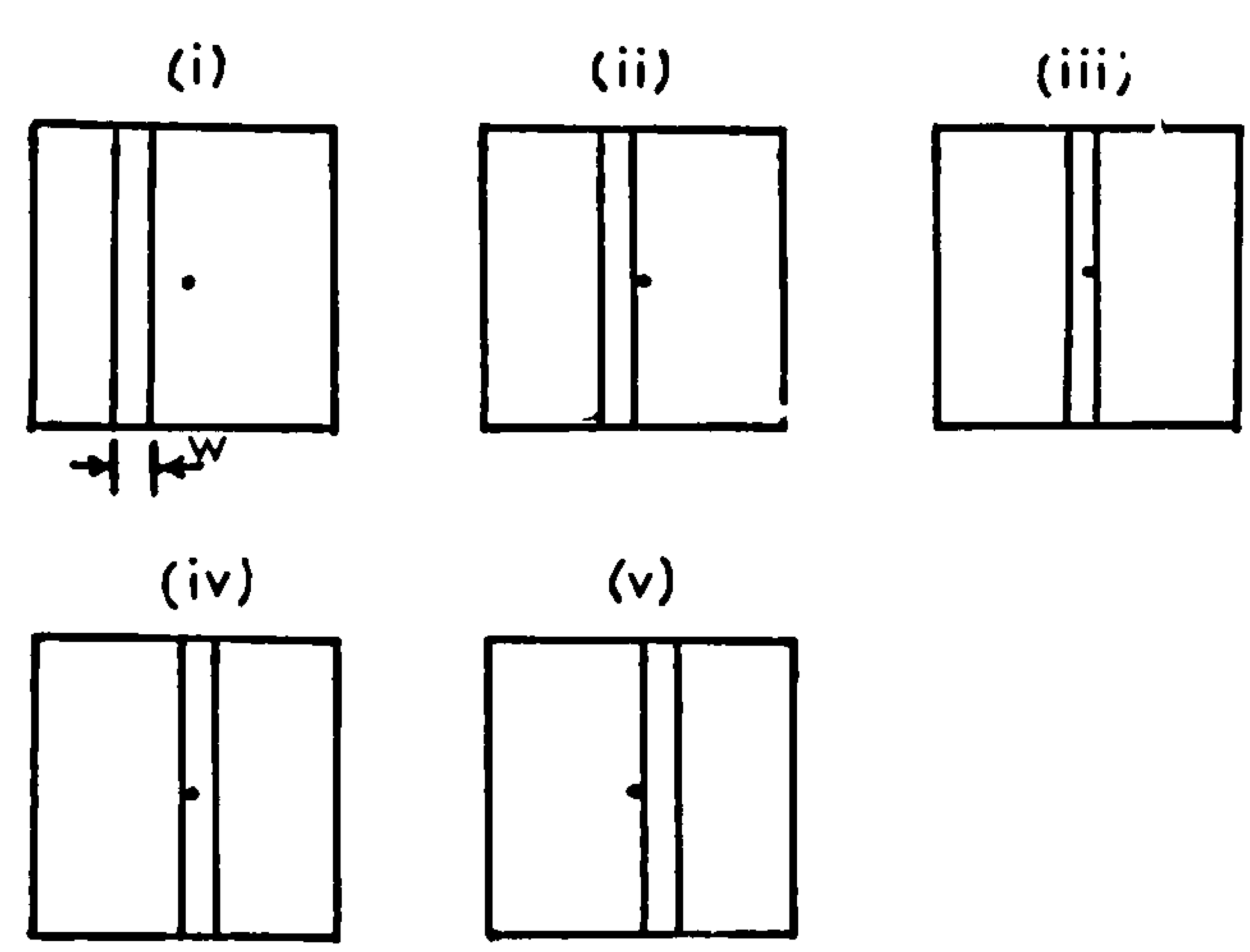

Fig. 72 Sequence of events for the exposure of a particular point.

From this, the exposure time (te) can be expressed as:

$$te = \frac{W + q}{U_s} \quad \ldots\ldots\ldots\ldots\ldots\ldots\ldots\ldots \quad (5)$$

where W = width of the slit, q = the width of the light cone intersected by the shutter blind; U_s = slit speed at the time of exposure.

Therefore, the effective exposure time is directly proportional to the width of the slit and is inversely proportional to the slit speed. In other words, the exposure time can be shortened either by using a slit of smaller width or by increasing the speed of movement of the slit.

4.3 Introduction of Movement of the camera platform during exposure

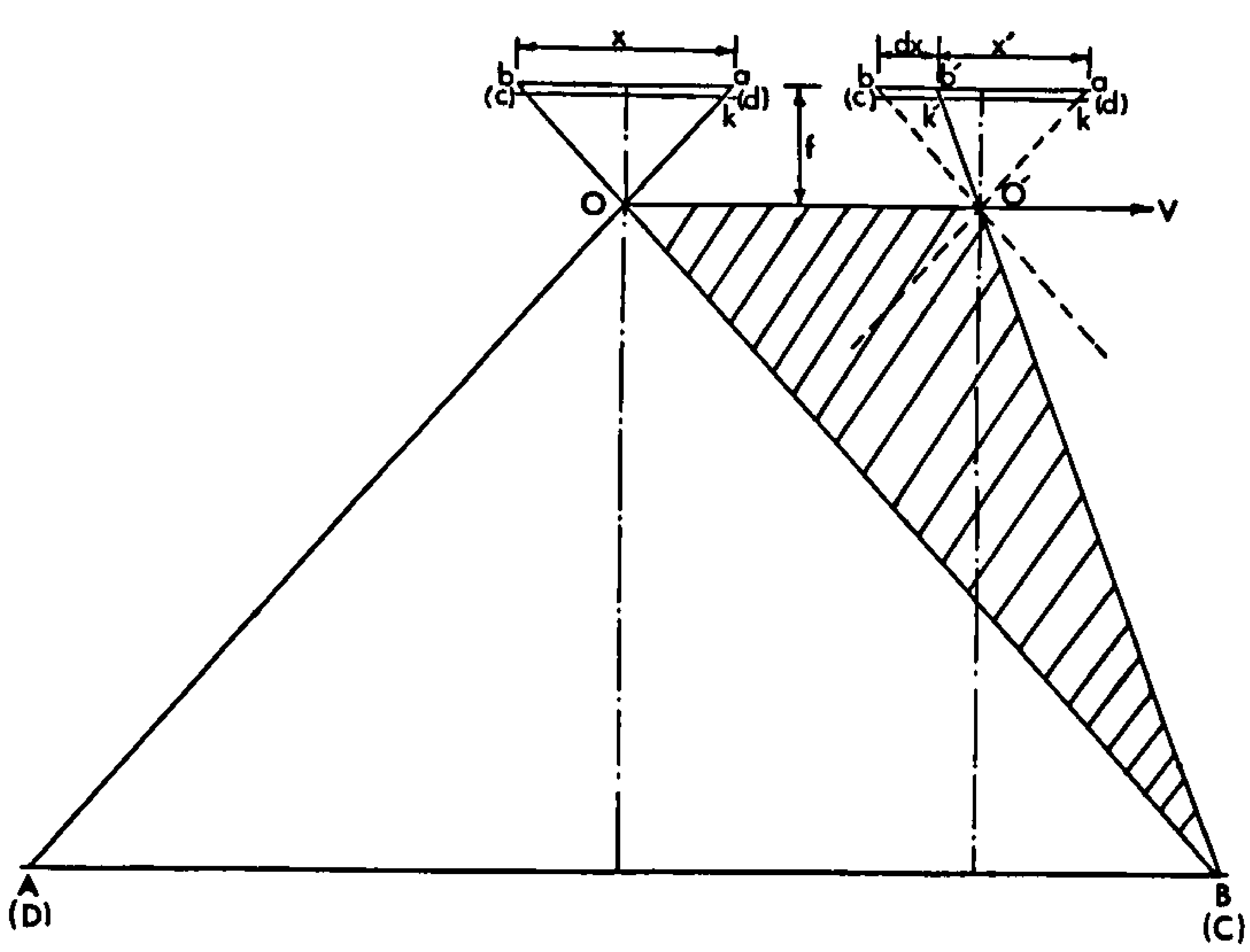

Fig. 73 Image displacement caused by craft motion 00' due to the focal plane shutter operation.

If the whole format is exposed while the camera is at station 0 (as with an intra-lens shutter), then the perspective geometry of the image will not be disturbed (the terrain points A and B would be imaged at positions a and b respectively in the focal plane). In the case of the focal plane shutter (Fig. 73) the slit starts from the position where the image point a is recorded. By the time the slit has reached the position k', at which point B will be imaged, the craft will have moved to station 0'. If the time required to move the slit from position k to position k' is equal to t_i (the shutter transit time), then the ground distance 00' moved by the craft is equal to Vt_i, where V is the craft speed. Due to this motion of the craft, the image point will now be recorded at point b'. From similar triangles, 0'bb' and B00' it can be seen that the resulting image displacement (dx) is bb' $= \frac{1}{s} \cdot 00'$ where s is the scale number. This leads to the following relationship

$$dx_{fp} = \frac{V}{s} \cdot t_i \quad \text{..............................} \quad (6)$$

Assuming that the slit speed U_s is constant then

$$t_i = \frac{kk'}{U_s} \quad \text{..............................} \quad (7)$$

Substituting for U_s from equation (5) into equation (7), we get

$$t_i = \frac{kk'}{W + \varphi} \cdot t_e \quad \text{.........................} \quad (8)$$

In practice, however, the shutter curtain is placed so near to the focal plane that the value of φ can be considered to be negligible and that kk' = x'. Hence equation (8) can be written as:

$$t_i = \frac{x'}{W} \cdot t_e \quad \text{.........................} \quad (9)$$

Substituting in equation (6) we get

$$dx_{fp} = \frac{V}{s} \cdot \frac{x'}{W} \cdot t_e \quad \text{.....................} \quad (10)$$

This means, in simple terms, that the image has been compressed along the direction of flight for the case described in Fig. 73 - as compared with the normal perspective geometry. No displacement takes place in the y-direction.

However, the camera can be mounted in the aircraft such that the slit may move in any one of <u>four directions</u> relative to the flight direction. An appropriate photo-coordinate system, in which the x-coordinate axis is the direction of the shutter slit movement and the y-coordinate axis is set 90 degrees counter-clockwise, is chosen for each case to illustrate the resulting displacement (Fig. 74).

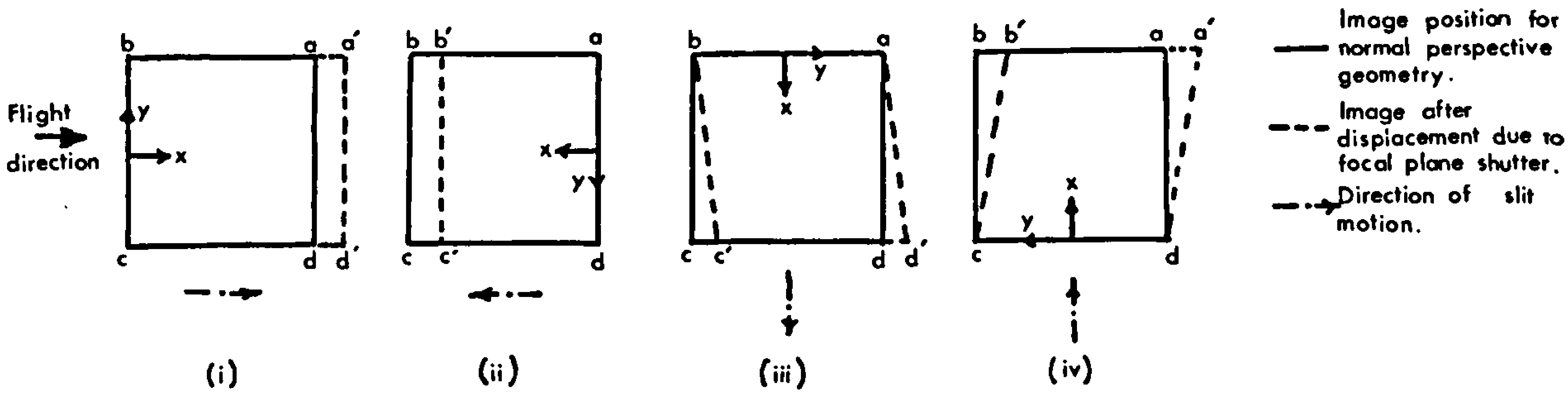

Fig. 74 Displacement due to the focal plane shutter

If the shutter is moving in the flight direction (case (i)), it introduces <u>image enlargement or elongation</u> in this direction. Thus, in each case when the shutter is moving parallel to the flight direction, a uniform change in scale in the x-direction is produced.

In the two cases, (iii) and (iv), where the shutter moves <u>across the flight direction</u>, the image will be twisted about the x-axis of the photo-coordinate system (see Fig. 76). It can also be noticed that in all cases the y-photocoordinates are not affected and the correct scale is maintained in the y-direction.

In order to simplify analysis, let the distortion be expressed as a function of the image position relative to the geometric centre of the photograph. Fig. 75 below shows this situation when this geometric centre point p (which acts as the origin of the photo-coordinate system) is being exposed for case (i) above. The elongation of the image to a' and b' instead of a and b can also be seen.

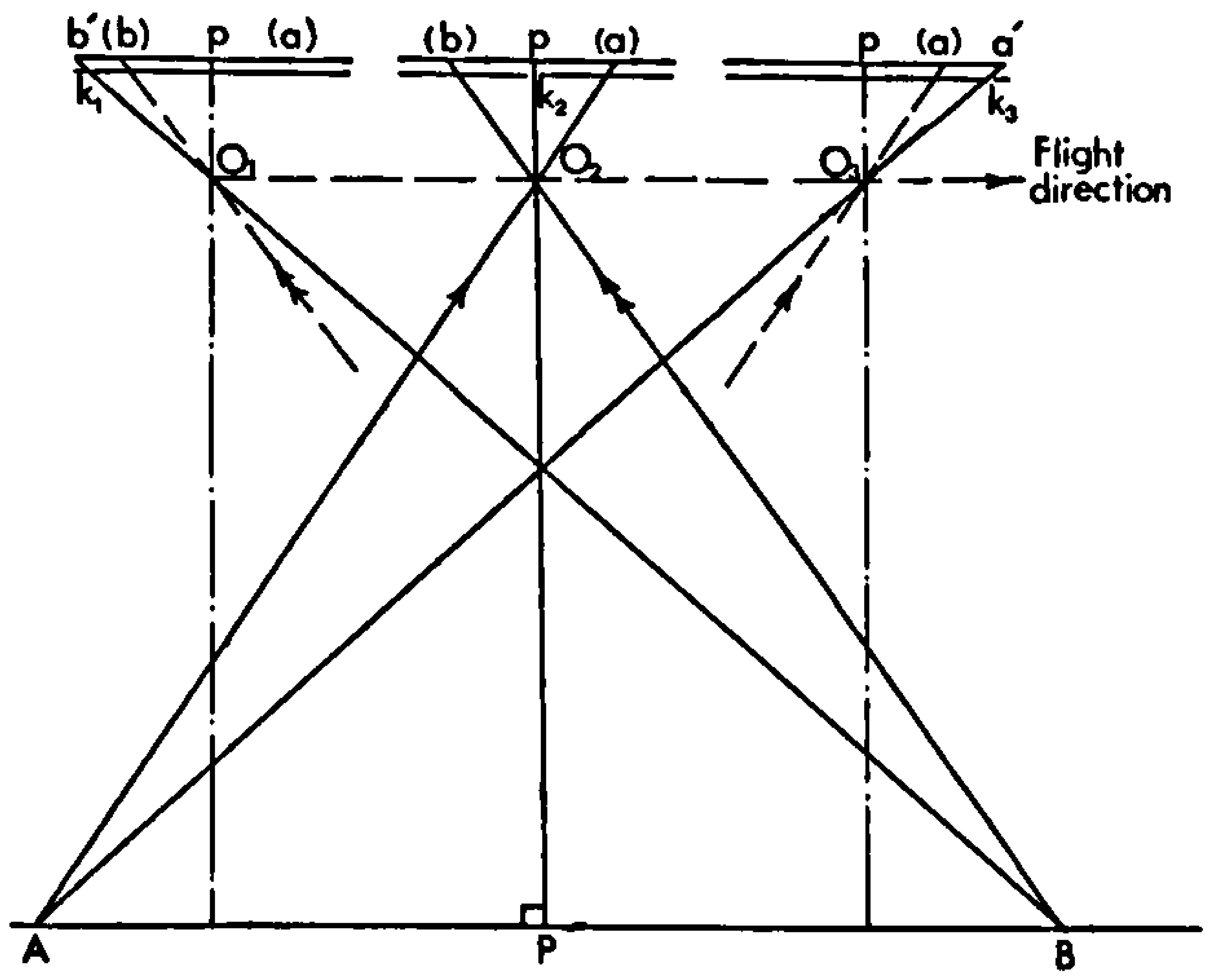

Fig. 75

Exposure of the

geometric centre (p)

The four cases (i) to (iv) considered above can now be replotted to produce the following diagrams (Fig. 76).

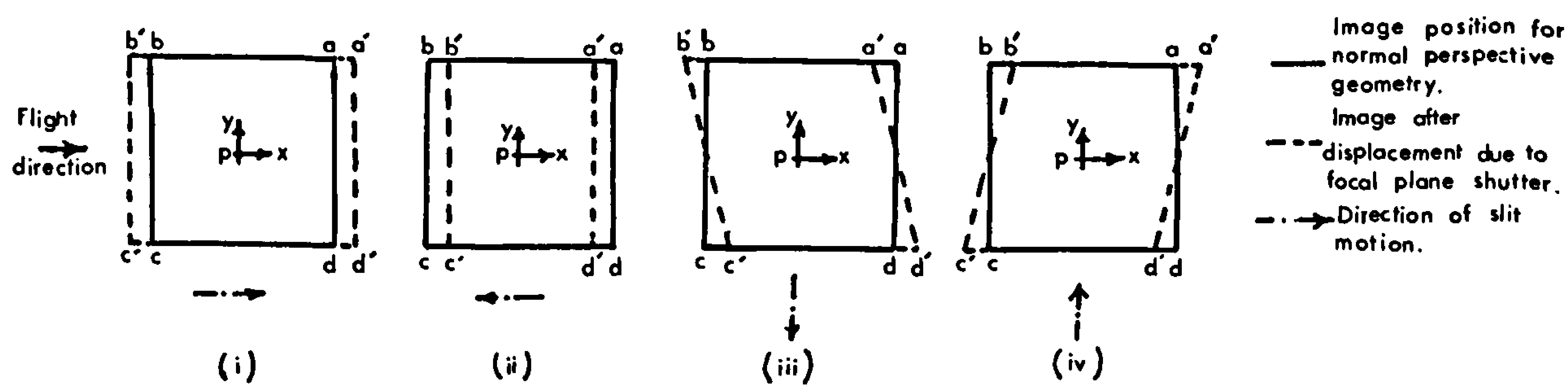

Fig. 76 Displacement of image due to focal plane shutter (measured from the geometric centre of the photograph).

For the case where the shutter is moving along the flight direction, the image distortion can be expressed as:

$$dx_{fp} = \frac{V}{s} \cdot \frac{t_e}{W} \cdot x'_i \quad \ldots\ldots\ldots\ldots\ldots\ldots\ldots\ldots \quad (11)$$

x'_i being the x-photo-coordinate of the image.

Whereas $$dx_{fp} = \frac{V}{s} \cdot \frac{t_e}{W} \cdot y_i \quad \ldots\ldots\ldots\ldots\ldots\ldots\ldots \quad (12)$$

represents the distortion when the shutter is moving across the flight direction.

If the craft is assumed to be moving with a <u>constant velocity</u> during the time required to expose the whole format, then the term $\frac{V}{s} \cdot \frac{t_e}{W}$ can be considered as a constant (k) for each photograph. Hence the formula for the distortion can be written as:

$$dx_{fp} = k\ x'_i \quad \ldots\ldots\ldots\ldots\ldots\ldots\ldots\ldots\ldots\ldots\ldots \quad (13)$$

(if the shutter is moving along the flight direction) or

$$dx_{fp} = ky_i \quad \ldots\ldots\ldots\ldots\ldots\ldots\ldots\ldots\ldots\ldots\ldots\ldots \quad (14)$$

(when the shutter is moving across the flight direction).

However, if the value of the constant (k) is known for the photograph, then the image coordinate can be corrected and the whole photograph will then be reduced to the situation which would occur when the whole photograph is exposed simultaneously (see Fig. 75).

The above relations hold for flat terrain. In the case of <u>mountainous terrain</u>, however, the photo scale will vary with the height ($\pm$ dh) of the point considered relative to the average terrain height. In this case, the scale is given as: $\frac{1}{s} = \frac{f}{H \pm dh}$.

Hence the image displacement due to the focal plane shutter in hilly terrain is:

$$dx_{fp} = \frac{Vf}{H \pm dh} \cdot \frac{t_e}{W} x' \quad \ldots\ldots\ldots\ldots\ldots\ldots\ldots \quad (15)$$

for the shutter moving along the flight direction, or

$$dx_{fp} = \frac{Vf}{H \pm dh} \cdot \frac{t_e}{W} y \quad \ldots\ldots\ldots\ldots\ldots\ldots\ldots \quad (16)$$

for the shutter moving across the flight direction.

4.4 Rotary Focal Plane Shutter

In this type of shutter (which is only used with small-format cameras) the slit performs a circular motion. In this case, the slit speed U_s at any point (i) along the slit at radial distance r_i from the centre of motion (Fig. 77) is given by:

$$U_s = \omega r_i \quad \ldots\ldots\ldots\ldots\ldots\ldots\ldots\ldots \quad (17)$$

where ω = the angular speed of the slit in radians per second. The exposure time (t_e) is given as:

$$t_e = \frac{W}{U_s} = \frac{W}{\omega r_i} \quad \ldots\ldots\ldots\ldots\ldots\ldots \quad (18)$$

Hence the exposure time (t_e) is inversely proportional to the radial distance (r) and is directly proportional to the width of the slit (W).

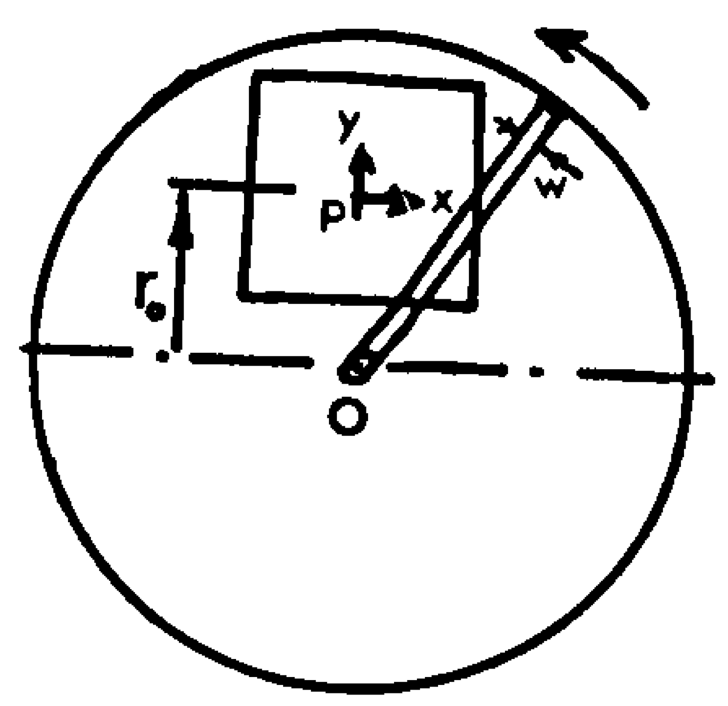

Fig. 77 Rotary focal plane shutter

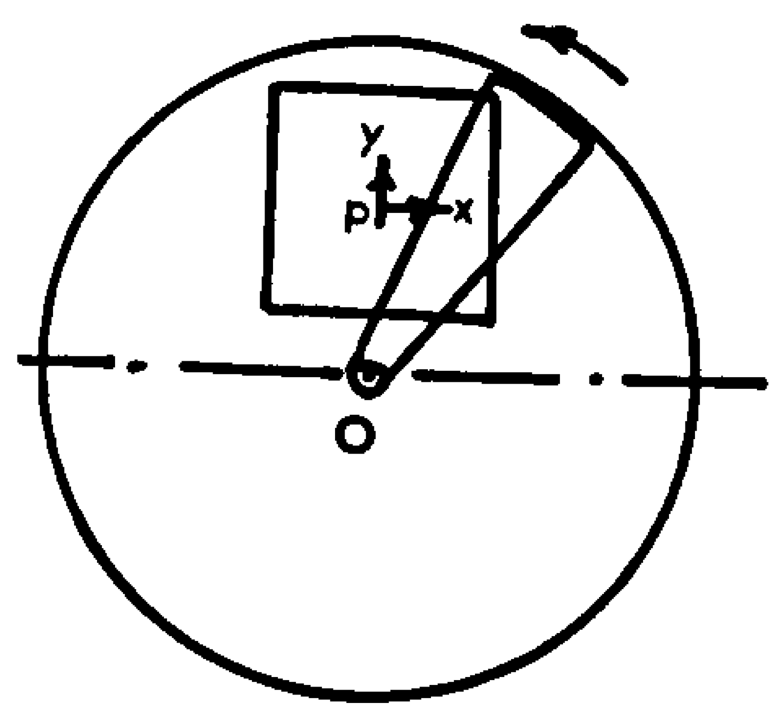

Fig. 78 Wedge-shaped slit

Therefore for a constant slit width, the exposure time for points along the slit will depend on the radial distance (r) of the point from the centre of rotation 0. The exposure time could be constant if the ratio $\frac{W}{r_i}$ is kept constant (i.e. increasing the width of the slit (W) as the radial distance (r) is increased). This leads to the use of a <u>wedge-shaped slit</u> as in the A.G.I. F-139 camera (Fig. 78).

Again, as in the parallel motion type focal plane shutter, the image displacement due to the shutter operation is given by

$$dx_{fp} = -\frac{V}{s} \cdot t_i$$

But in this case the slit speed is not constant and the <u>shutter transit time</u> (t_i) is given by

$$t_i = \frac{x'_i}{W} t_e = \frac{x'_i}{\omega r_i} \quad \ldots\ldots\ldots\ldots\ldots\ldots \text{(19)}$$

Hence $$dx_{fp} = -\frac{V}{s} \cdot \frac{x'_i}{\omega r_i} \quad \ldots\ldots\ldots\ldots\ldots\ldots\ldots\ldots \text{(20)}$$

The minus sign indicates contraction of the image.

From the Fig. 77, if the radial distance of the geometric centre (p) from the centre of rotation of the slit 0 is r_o, then the value of r_i for any point on the photo is given by

$$r_i = \sqrt{x_i'^2 + (y'_i + r_o)^2}$$

Substituting for r_i in equation(20) results in

$$dx_{fp} = -\frac{V}{s} \cdot \frac{x'_i}{\omega \sqrt{x_i'^2 + (y'_i + r_o)^2}} \quad \ldots \text{(21)}$$

In practice, however, the slit motion is mono-directional and the format can be positioned in either of the four positions shown in Fig. 79.

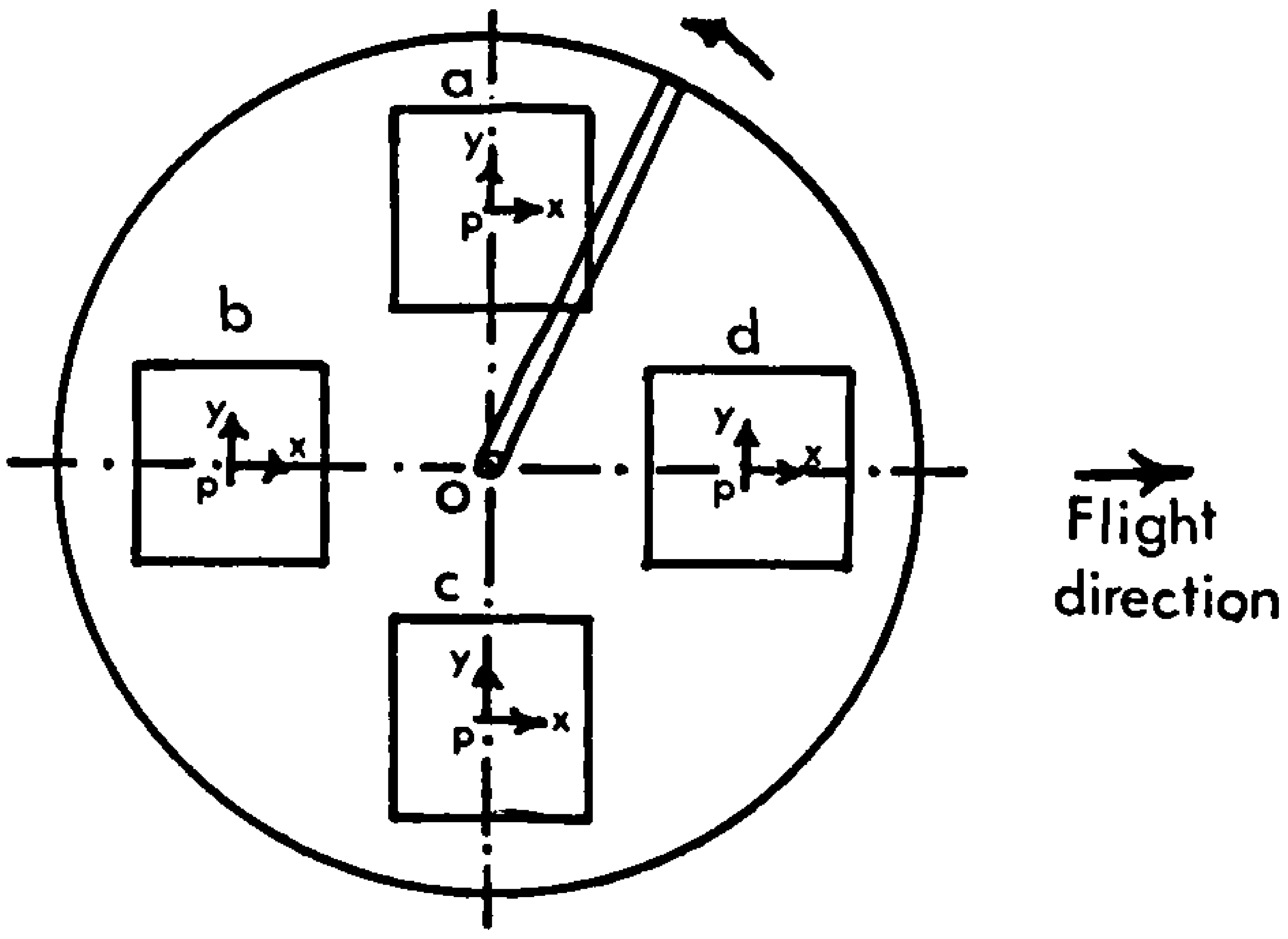

Fig. 79 The four possible positions of the rotary focal plane shutter.

Using a similar derivation, the image displacement for each of the other three cases can be expressed as follows:

case (b) $$dx_{fp} = -\frac{V}{s} \cdot \frac{y_i}{\omega\sqrt{y_i^2 + (r_o - x'_i)^2}} \quad \ldots\ldots \quad (22)$$

case (c) $$dx_{fp} = +\frac{V}{s} \cdot \frac{x'_i}{\omega\sqrt{x'^2_i + (r_o - y'_i)^2}} \quad \ldots\ldots \quad (23)$$

case (d) $$dx_{fp} = +\frac{V}{s} \quad \frac{y_i}{\omega\sqrt{y_i^2 + (r_o + x'_i)^2}} \quad \ldots\ldots \quad (24)$$

This will be similar to the distortion caused by the parallel motion focal plane shutter, derived before, if the values of x'_i and y'_i are negligible when compared with the value of r_o (i.e. if r_o is infinitely large with respect to x'_i and y'_i). In this case the displacement will be

$$dx_{fp} = \pm \frac{V}{s} \cdot \frac{x'_i}{\omega r_o} \quad \ldots\ldots\ldots\ldots\ldots\ldots \quad (25)$$

$$\text{or} \quad dx_{fp} = \pm \frac{V}{s} \cdot \frac{y'_i}{\omega r_o} \quad \dots\dots\dots\dots\dots\dots\dots \quad (26)$$

depending on the position of the format.

4.5 Effect of Crab

In practice, some cases will arise where, due to side winds, if the craft is heading from A to B (Fig. 80 a) it actually travels along AC. If the camera remains aligned with the longitudinal axis of the craft (i.e. it is not corrected), then the format sides are no longer parallel to the base line. The angle between the format sides and the base line is known as the angle of crab.

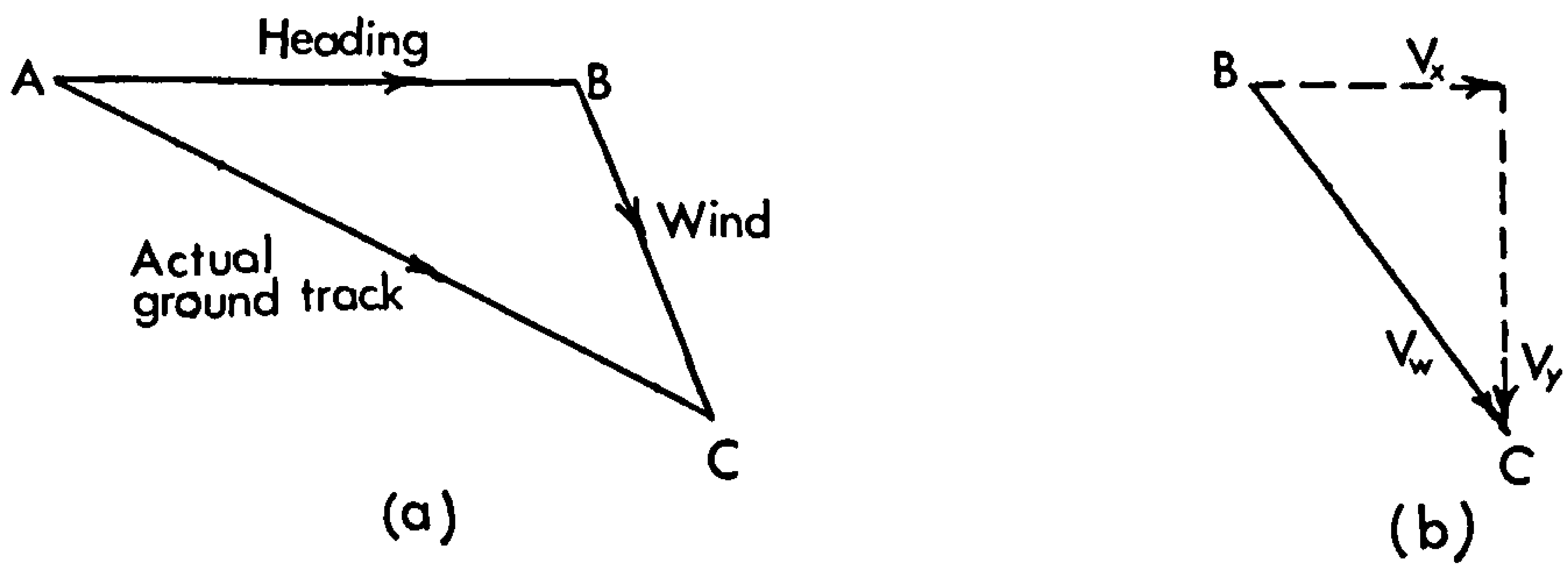

Fig. 80 Crab

If the camera is equipped with a parallel motion focal plane shutter, the effect of the crab is to add a displacement to the y-photo-coordinate, additional to the distortion in the x-photo-coordinate introduced by the focal plane shutter. If the wind speed V_w is resolved into two directions, V_x parallel to the heading direction and V_y perpendicular to it (Fig. 80b), then the image displacements are given by:

$$dx = \frac{V}{s} t_i + \frac{V_x}{s} t_i \quad \dots\dots\dots\dots\dots\dots\dots \quad (27)$$

$$dy = \frac{V_y}{s} t_i \quad \ldots\ldots\ldots\ldots\ldots\ldots\ldots\ldots\ldots \quad (28)$$

Figure 81 shows the displacement for all the possible directions of the shutter motion relative to the ground track.

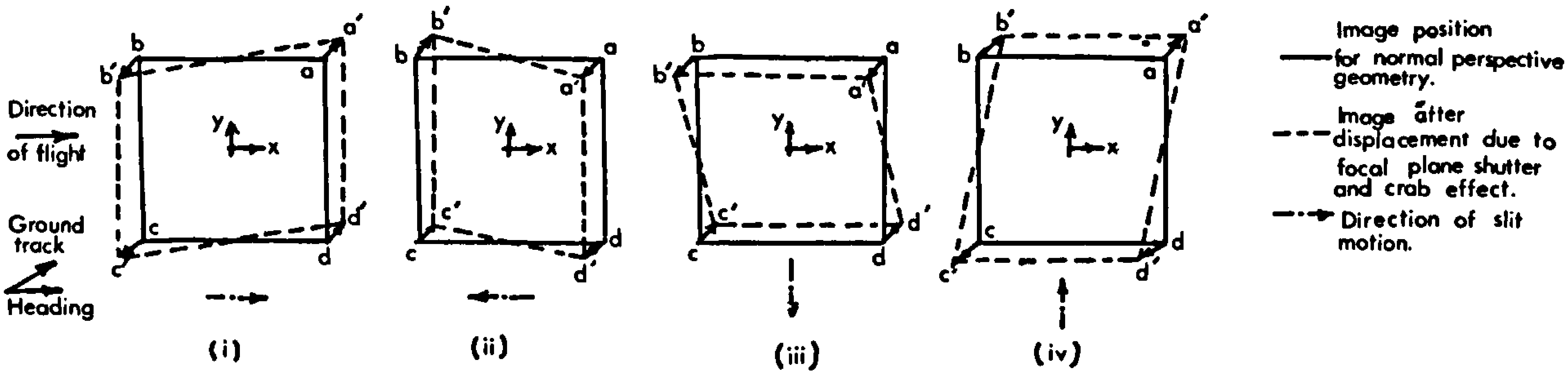

Fig. 81. Displacement of image due to focal plane shutter with additional effect of crab being taken into account.

However, the reconnaissance camera is often mounted on an aircraft with a very high flight speed, in which case the effect of crab is negligible and the component of the displacement in the y-direction is insignificant.

4.6 The Effect of Image Motion Compensation (IMC) on Image Geometry:

As previously discussed in Chapter III, the forward motion of the aircraft causes an image motion, given by the relationship:

$$dx_i = \frac{f}{H} V t_e \quad \text{or} \quad \frac{V}{s} \cdot t_e \quad \ldots\ldots\ldots\ldots \quad (29)$$

It has also been shown that two different methods can be employed to compensate for the image motion which takes place during the exposure time. The effects of these methods will be discussed below.

4.6.1 The Effect of using Film Movement for IMC

If the film is moved with speed V_f in the flight direction, then the value of the geometric blur will be

$$dx_i = \left(\frac{fV}{H} - V_f\right) t_e \quad \ldots\ldots\ldots\ldots \quad (30)$$

which is uniform over the entire aerial film for flat terrain, vertical photograph and constant flying height and speed. If the film speed is equal in magnitude and direction to the image speed, $\frac{f}{H}V$, during the exposure, then the image motion would be completely eliminated and $dx_i = 0$. In this case, the image a_2 will coincide with the image a_1, and object A will have a sharp non-distorted image (Fig. 82).

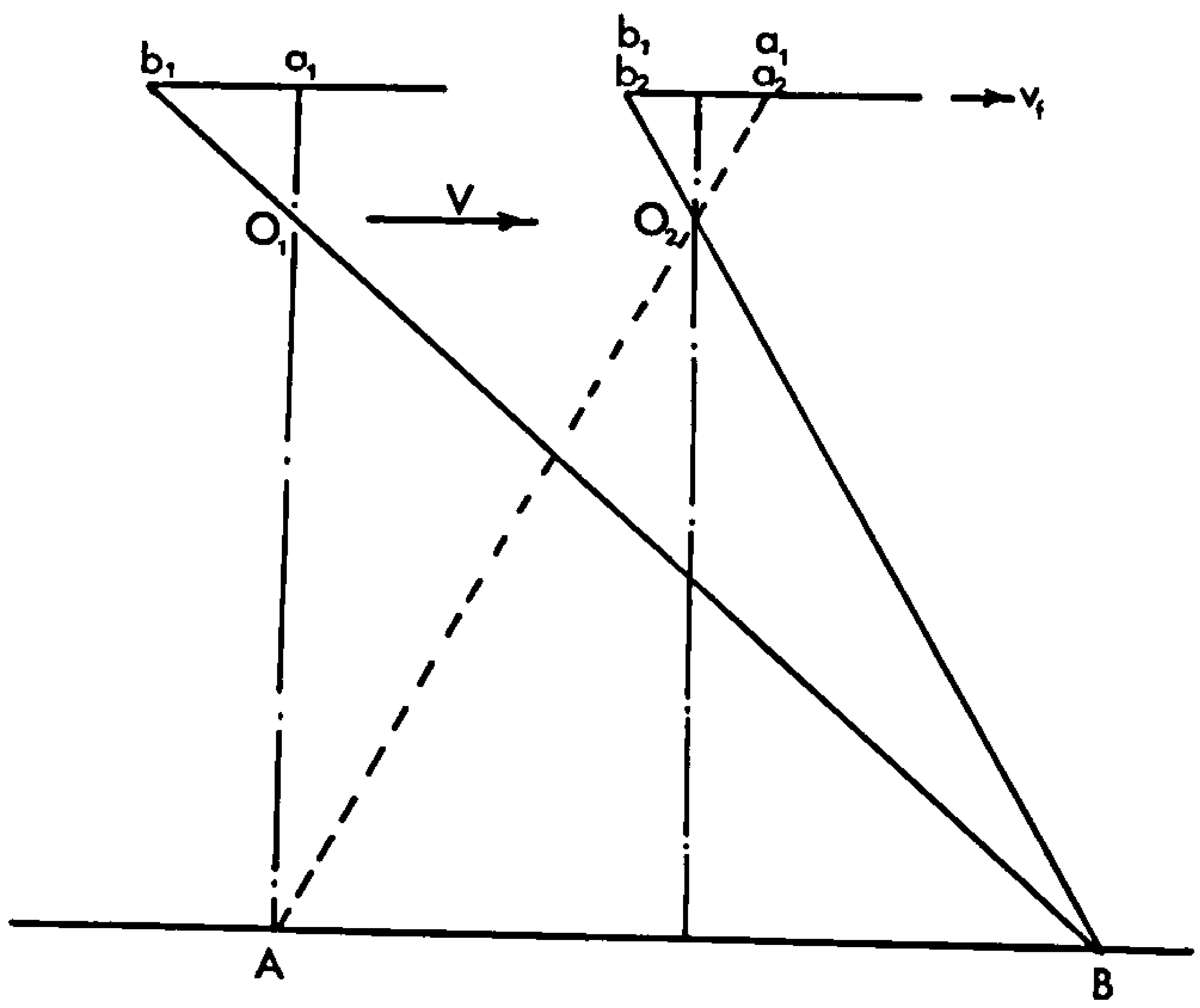

Fig. 82 IMC by moving the film in the flight direction

If the geometric centre of the photograph is taken as the origin of the photo-coordinate system, then there will be no image distortion, provided the IMC is perfect. The only effect will be a mislocation of the principal point. However, this can be taken as the position at the mid-point of the exposure.

4.6.2 Rotation of the Camera for IMC

The second method which is based on a rotation of the bundle of projection rays can be accomplished by rocking the entire camera about an axis transverse to the flight direction (Fig. 83). The basic formula relating the image position, x_i, on the photograph and the angular field 2β is given by

$$x_i = f \tan \beta_i \quad \dots\dots\dots\dots\dots\dots \quad (31)$$

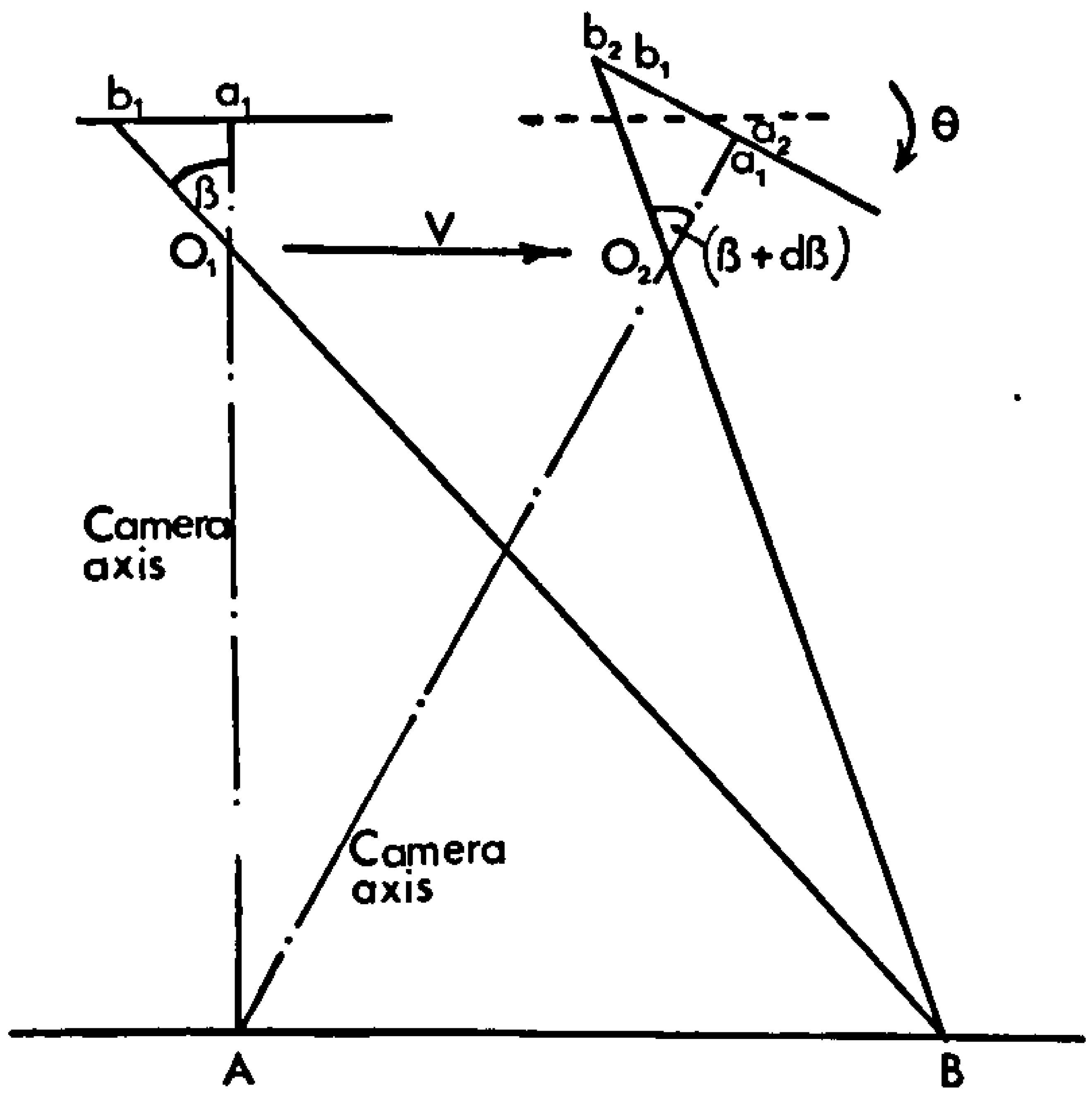

Fig. 83 IMC by rocking the entire camera

If the camera is tilted through an angle θ, the angular field β_i will be changed by an amount $d\beta_i$. Differentiating the basic formula (31) one gets

$$dx_i = \frac{f}{\cos^2 \beta_i} \, d\beta_i \quad \dots\dots\dots\dots\dots\dots \quad (32)$$

It is clear from the differential formula that dx_i is not a linear function of β_i and hence the image motion introduced by rocking the camera is not uniform throughout the entire field of view. Therefore it will be impossible to compensate for the uniform image motion over the entire field of view by this technique.

From Fig. 83 it can be concluded that, if the image motion is compensated for at the centre of the photograph, there will still be residual image motion towards the edges.

Referring to Fig. 84, the camera is tilted such that the geometric centre, p, of the photograph is compensated for image motion throughout the exposure time. Point a is used to determine the residual image movement after applying the IMC.

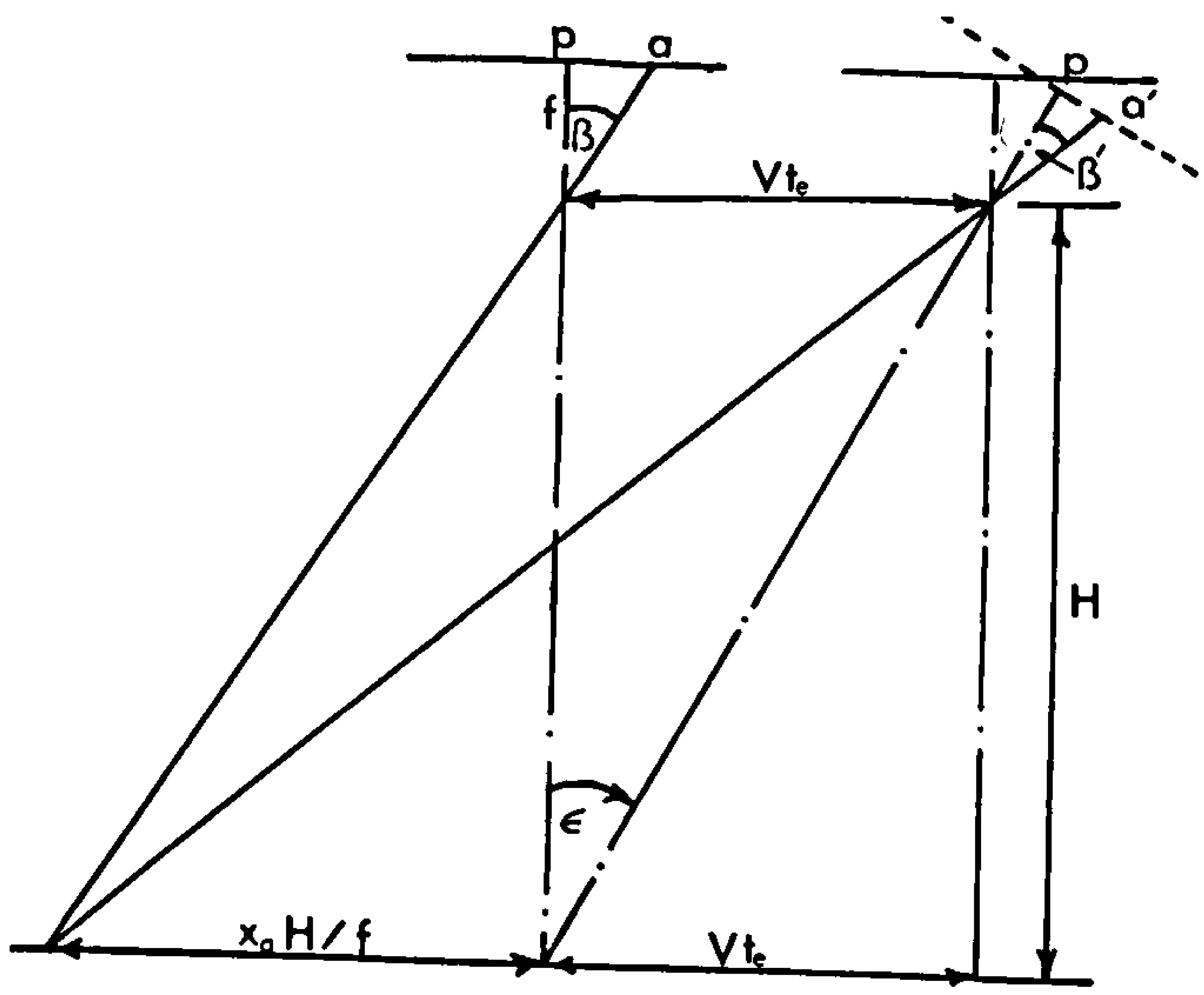

Fig. 84 Applying IMC for the geometric centre throughout the exposure.

From the above Fig. 84,

$$\tan(\epsilon + \beta') = \frac{Vt_e + x_a H/f}{H} \quad \ldots\ldots\ldots\ldots\ldots \quad (33)$$

$$\tan(\epsilon + \beta') = \frac{Vt_e}{H} + \frac{x_a}{f}$$

$$\tan(\epsilon + \beta') = \tan\epsilon + \tan\beta \quad \ldots\ldots\ldots\ldots\ldots\ldots \quad (34)$$

But $$\tan(\epsilon + \beta') = \frac{\tan\epsilon + \tan\beta'}{1 - \tan\epsilon \tan\beta} \quad \ldots\ldots\ldots\ldots\ldots\ldots \quad (35)$$

Substituting (35) in(34), results in the expression

$$\frac{\tan\epsilon + \tan\beta'}{1 - \tan\epsilon \tan\beta} = \tan\epsilon + \tan\beta \quad \ldots\ldots\ldots\ldots\ldots \quad (36)$$

Substituting the values $\tan \epsilon = \frac{Vt_e}{H}$, $\tan\beta = \frac{x_a}{f}$ and $\tan \beta' = \frac{x'_a}{f}$ in equation (36) and rearranging the resulting formula results in

$$dx_a = \frac{Vt_e}{H}\left[\frac{x_a}{f} - \frac{Vt_e}{H}\right] x_a \quad \ldots\ldots\ldots\ldots \quad (37)$$

For cameras with long focal length the term $\left(\frac{x_a}{f} - \frac{Vt_e}{H}\right) x_a$ in equation (37) is very small, so that the residual displacement is insignificant. This can be illustrated by a numerical example applied to the S190B camera (which has a 14° angular coverage). In this case, a focal plane shutter is used and the exposure time (t_e) in formula (37) will be replaced by the shutter transit time (t_i) using the relation given in equation (9). The following data can be used: $f = 460$ mm; $H = 435$ km; $V = 8$ km/sec; $t_e = 1/100$ sec; $W = 10$ mm; and $x_a = 55$ mm (edge of format). Substituting in equation (37) the residual distortion will be 6 μm. For shorter focal lengths e.g. 300 mm and 150 mm (i.e. angular coverage of 20° and 36°) the residual distortion will be 10 μm and 20 μm respectively.

This is why this technique is only used in long-focal length aerial cameras where the angular field of view does not exceed 25 degrees.

4.6.3 Effect of Hilly or Mountainous Terrain on the Application of IMC

The analysis of the effect of IMC given above was based on the flat terrain case. Now, the case of hilly or mountainous terrain is to be considered.

(i) Moving Film Technique

The first case to be considered is when the film is moved in the flight direction to compensate for the image motion. If point A is of height dh above the average terrain height, and the film is moved to compensate motion at the geometric centre p of the photograph, then the case will be illustrated by Fig. 85 below.

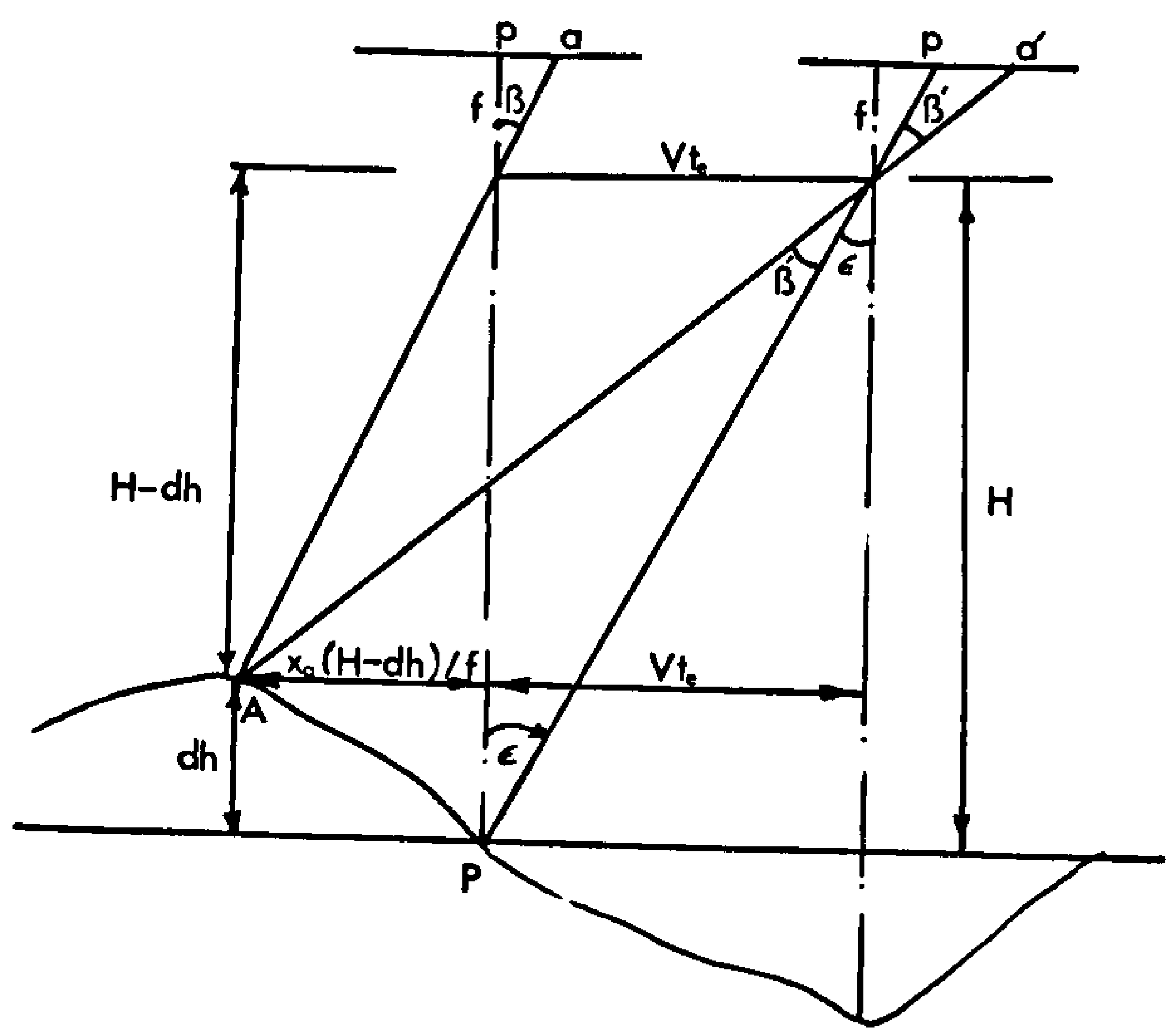

Fig. 85 Moving film technique and mountainous terrain

Angles β , β' and ϵ are as shown in Fig. 85 . From Fig. 85

$$\tan(\beta' + \epsilon) = \frac{Vt_e + x_a(H - dh)/f}{(H - dh)} \quad \ldots\ldots\ldots\ldots \quad (38)$$

$$= \frac{Vt_e}{(H - dh)} + \frac{x_a}{f}$$

But $$\tan(\beta' + \epsilon) = \frac{\tan\beta' + \tan\epsilon}{1 - \tan\beta' \tan\epsilon} \quad \ldots\ldots\ldots\ldots\ldots\ldots \quad (39)$$

Substituting (39) in(38)

$$\frac{\tan\beta' + \tan\epsilon}{1 - \tan\beta' \tan\epsilon} = \frac{Vt_e}{H - dh} + \frac{x_a}{f} \quad \ldots\ldots\ldots\ldots \quad (40)$$

Neglecting higher than second-order terms, results in

$$\tan\beta' + \tan\epsilon = \frac{Vt_e}{H - dh} + \frac{x_a}{f}$$

But $\tan \beta' = \dfrac{x'_a}{f}$

and $\tan \epsilon = \dfrac{Vt_e}{H}$

$$\text{Hence} \quad \frac{x'_a}{f} + \frac{Vt_e}{H} = \frac{Vt_e}{H - dh} + \frac{x_a}{f} \quad \ldots\ldots\ldots\ldots\ldots \quad (41)$$

Rearranging terms, gives the relationship

$$x'_a - x_a = dx_a = \frac{fVt_e}{H} \left(\frac{dh}{H - dh}\right) \quad \ldots\ldots\ldots\ldots \quad (42)$$

Similarly, if another point B is at elevation - dh (lower than the average terrain height) the image displacement after compensating the motion at the geometric centre p will be

$$dx_b = \frac{fVt_e}{H} \left(\frac{-dh}{H + dh}\right) \quad \ldots\ldots\ldots\ldots\ldots\ldots\ldots \quad (43)$$

Example: In practice, however, this effect is not significant as can be illustrated by the following example: If the craft is flying at a speed of 300 m/sec (Mach 1) at a height of 3000 metres, and if the variation in the terrain height is $\pm$ 600 metres (i.e. 20% of the flying height which is considered as mountainous terrain), then for a camera with focal length of 300 mm mounted vertically and for the average terrain level the image speed (v) on the focal plane would be

$$v = f\frac{V}{H} = \frac{300 \times 300}{3000} = 30 \text{ mm/sec.}$$

If the exposure time is 1/1000 second then the image movement is $x_{im} = Vt_e = 30\,\mu m$. If a $\pm$ 600 m variation in terrain height is considered, then the residual image motion will be

$$dx = \frac{fVt_e}{H} \left(\frac{\pm\, dh}{H \mp dh}\right)$$

$$= 30 \left(\frac{\pm 600}{3000 \mp 600}\right)$$

= $-5\,\mu m$ for the point below the average terrain height.

or = $+7.5\,\mu m$ for the point above the average terrain height.

(ii) Rotation of the Camera

The other case to be considered is the effect of mountainous terrain when rocking the camera to achieve IMC. Fig. 86 shows the effect for a point A of height dh above the average terrain height. Again, the geometric centre of the photo, p, is compensated for image motion throughout the exposure time.

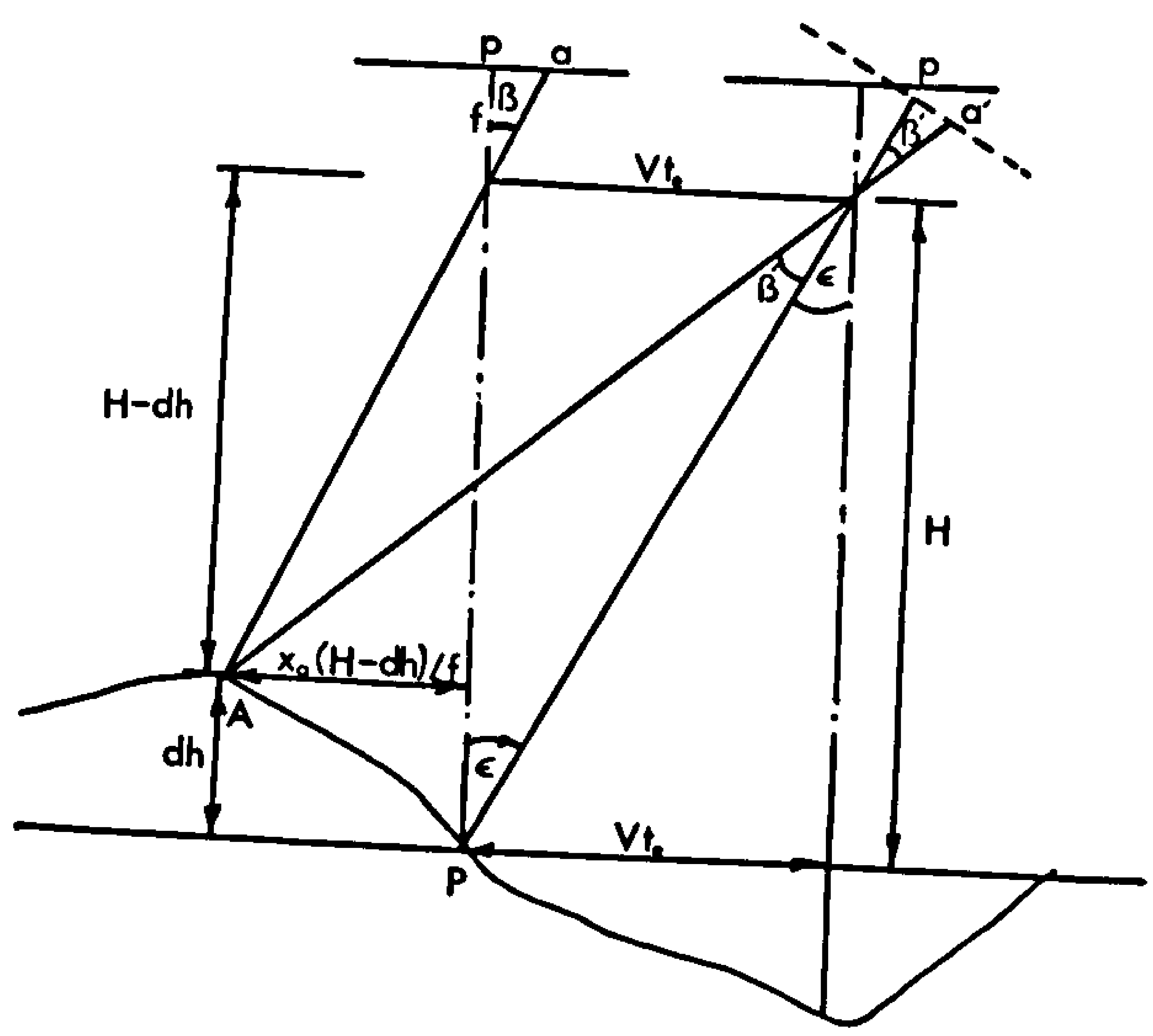

Fig. 86 Rotation of the camera and mountainous terrain

From the above Fig. 86

$$\tan(\beta' + \epsilon) = \frac{Vt_e + \frac{x_a}{f}(H - dh)}{H - dh}$$

$$= \frac{Vt_e}{H - dh} + \frac{x_a}{f} \qquad \ldots\ldots\ldots\ldots\ldots\ldots \quad (44)$$

But $\tan(\beta' + \epsilon) = \dfrac{\tan\beta' + \tan\epsilon}{1 - \tan\beta' \tan\epsilon}$ .... (45)

Therefore, $\dfrac{\tan\beta' + \tan\epsilon}{1 - \tan\beta' \tan\epsilon} = \dfrac{Vt_e}{H - dh} + \dfrac{x_a}{f}$ ...... (46)

Neglecting terms of second and higher degree, results in the expression

$$\tan\beta' + \tan\epsilon = \frac{Vt_e}{H - dh} + \frac{x_a}{f} \quad \text{......................} \quad (47)$$

Substituting for $\tan\beta' = \dfrac{x'_a}{f}$

and $\tan\epsilon = \dfrac{Vt_e}{H}$

then $\dfrac{x'_a}{f} + \dfrac{Vt_e}{H} = \dfrac{Vt_e}{H - dh} + \dfrac{x_a}{f}$ .... (48)

From this equation the image displacement will be expressed as:

$$dx = x'_a - x_a = \frac{fVt_e}{H - dh} - \frac{fVt_e}{H}$$

$$dx = \frac{fVt_e}{H}\left(\frac{dh}{H - dh}\right) \quad \text{................} \quad (49)$$

It can be similarly derived that for a point of height $-dh$ (i.e. below the average terrain height) the displacement will be:

$$dx = \frac{fVt_e}{H}\left(\frac{-dh}{H + dh}\right) \quad \text{..................} \quad (50)$$

It is clear from these equations that points below the average terrain height will have smaller displacements than those above the average terrain height.

4.6.4 IMC for Oblique Photography

Reconnaissance frame cameras are often mounted in multiple in a fan configuration so as to cover a wider angle of field. Normally one of the cameras is mounted in a vertical position and the others would be oblique.

(a) In the base of lateral (side) oblique photography, the optical axis is tilted about the axis of flight and hence the image will no longer have a uniform motion on the focal plane (Fig. 87).

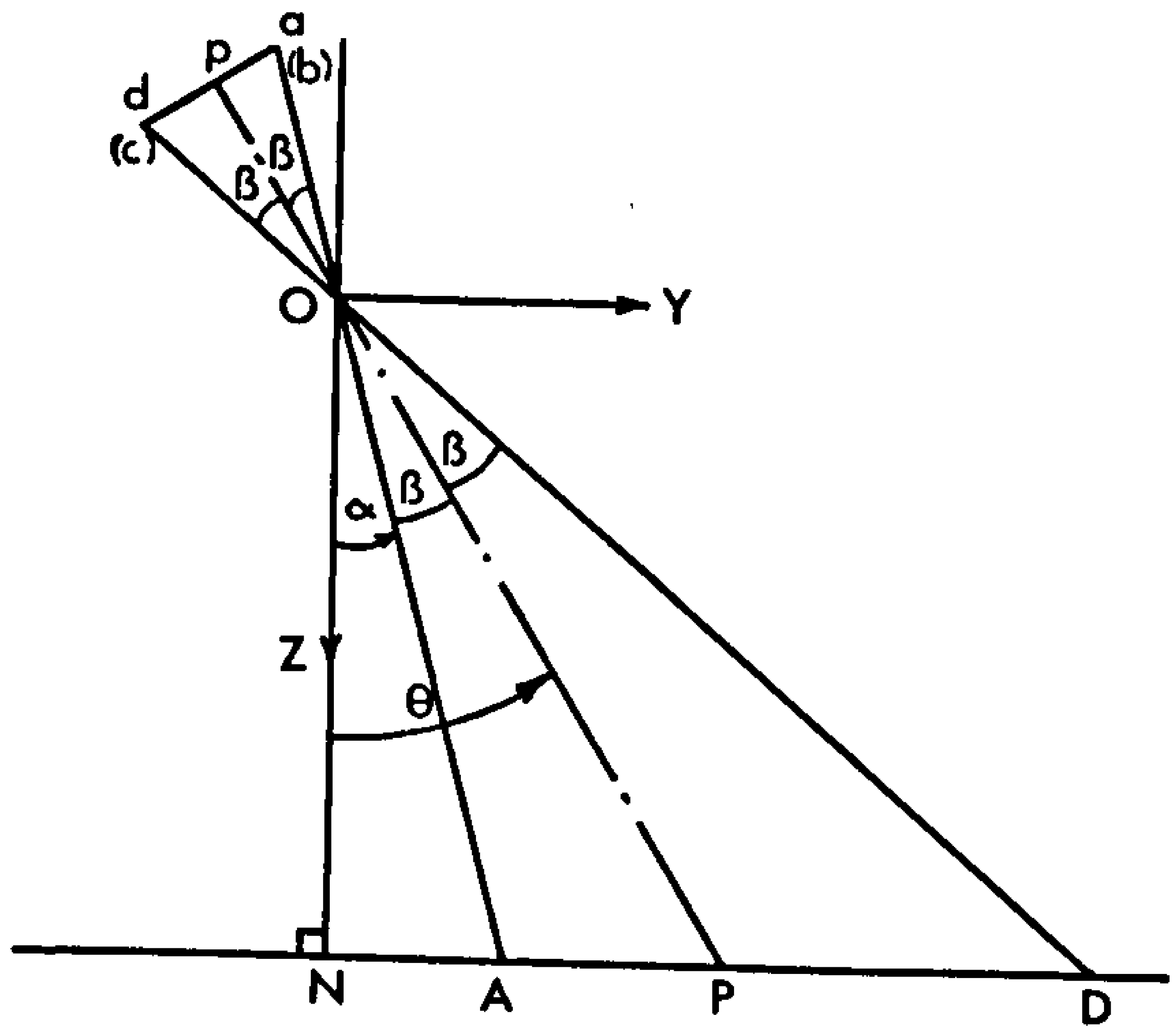

Fig. 87 The case of lateral oblique photography

The image speed, v, at any point on the focal plane is given by Vx scale at the point, where V is the craft speed.

From Fig. 87, the image speeds at points a,b (situated at the format edges) and at p (the geometric centre of the photograph) are given by:

$$v_a = \frac{aO}{Oa} . V = \frac{fV}{H} \frac{\cos \alpha}{\cos \beta} \quad \dots\dots\dots\dots\dots \quad (51)$$

$$v_p = \frac{pO}{Op} . V = \frac{fV}{H} \cos(\alpha + \beta) \quad \dots\dots\dots \quad (52)$$

$$v_b = \frac{dO}{Od} . V = \frac{fV}{H} \frac{\cos(\alpha + 2\beta)}{\cos \beta} \quad \dots\dots\dots \quad (53)$$

The conclusion from this is that a uniform image motion on the focal plane and therefore a complete IMC over the whole field of view will be impossible.

However, the film can be moved by an amount v_p and hence motion at the central point of the format can be completely compensated. In this case, other points on the focal plane would have residual image motion which can be derived as follows:

(i) The residual image motion at point a is given as

$$dx_a = dv_a \cdot t_e = (v_a - v_p)\, t_e \quad \ldots\ldots\ldots\ldots \quad (54)$$

Substituting for V_a and V_p from equation (51) and (52), then

$$dx_a = \frac{fV}{H} t_e \left(\frac{\cos\alpha}{\cos\beta} - \cos(\alpha+\beta)\right) \quad \ldots\ldots\ldots \quad (55)$$

$$= \frac{fV}{H} t_e \frac{(\cos\alpha - \cos\alpha\cos^2\beta + \sin\alpha\sin\beta\cos\beta)}{\cos\beta}$$

$$= \frac{fV}{H} t_e \frac{(\cos\alpha(1-\cos^2\beta) + \sin\alpha\sin\beta\cos\beta)}{\cos\beta}$$

$$= \frac{fV}{H} t_e (\cos\alpha\sin^2\beta + \sin\alpha\sin\beta\cos\beta)/\cos\beta$$

$$= \frac{fV}{H} t_e \left(\frac{\sin\beta}{\cos\beta}\right)(\cos\alpha\sin\beta + \sin\alpha\cos\beta)$$

Hence $dx_a = \frac{fV}{H} t_e \cdot \tan\beta \cdot \sin(\alpha+\beta)$

Since $\tan\beta = \frac{y_a}{f}$ and $\alpha + \beta = \theta$

then $$dx_a = \frac{V}{H} t_e \, Y_a \sin\theta \quad \ldots\ldots\ldots\ldots\ldots\ldots \quad (56)$$

(ii) or if we consider the residual image motion at point d

$$dx_d = (v_p - v_d)\, t_e \quad \ldots\ldots\ldots\ldots\ldots\ldots \quad (57)$$

and substituting for v_p and v_d from equations (52) and (53) respectively we get

$$dx_d = \frac{fV}{H} t_e \left(\cos(\alpha+\beta) - \frac{\cos(\alpha+2\beta)}{\cos\beta}\right) \quad \ldots\ldots (58)$$

$$= \frac{fV}{H}\ te\ \left[\cos\beta(\cos\alpha\cos\beta - \sin\alpha\sin\beta) - \cos\alpha\cos 2\beta + \sin\alpha\sin 2\beta\right] / \cos\beta$$

$$= \frac{fV}{H}\ t_e\ \left[\cos^2\beta\cos\alpha - \sin\alpha\sin\beta\cos\beta - \cos\alpha(2\cos^2\beta - 1) + 2\sin\alpha\sin\beta\cos\beta\right] / \cos\beta$$

$$= \frac{fV}{H}\ t_e\ \left[-\cos^2\beta\cos\alpha + \cos\alpha + \sin\alpha\sin\beta\cos\beta\right] / \cos\beta$$

$$= \frac{fV}{H}\ t_e\ \left[-\cos\alpha + \cos\alpha\sin^2\beta + \cos\alpha + \sin\alpha\sin\beta\cos\beta\right] / \cos\beta$$

$$= \frac{fV}{H}\ t_e\ \left(\frac{\sin\beta}{\cos\beta}\right)\left[\cos\alpha\sin\beta + \sin\alpha\cos\beta\right]$$

$$= \frac{fV}{H}\ te\ \tan\beta\sin(\alpha + \beta)$$

In this case $\tan\beta = \dfrac{y_d}{f}$

Hence $dx_d = \dfrac{V}{H}\ t_e\ y_d\ \sin\theta$ .... (59)

Hence a general expression for the residual image motion at any point i is given by

$$dx_i = \frac{V}{H} t_e\ y_i\ \sin\theta \qquad \text{.............................. (60)}$$

For each point, the sign of the displacement depends on the sign of the y -photo-coordinate.

(b) Another case to be considered is the longitudinal (forward) oblique in which case the optical axis is tilted about the Y-axis (Fig. 88).

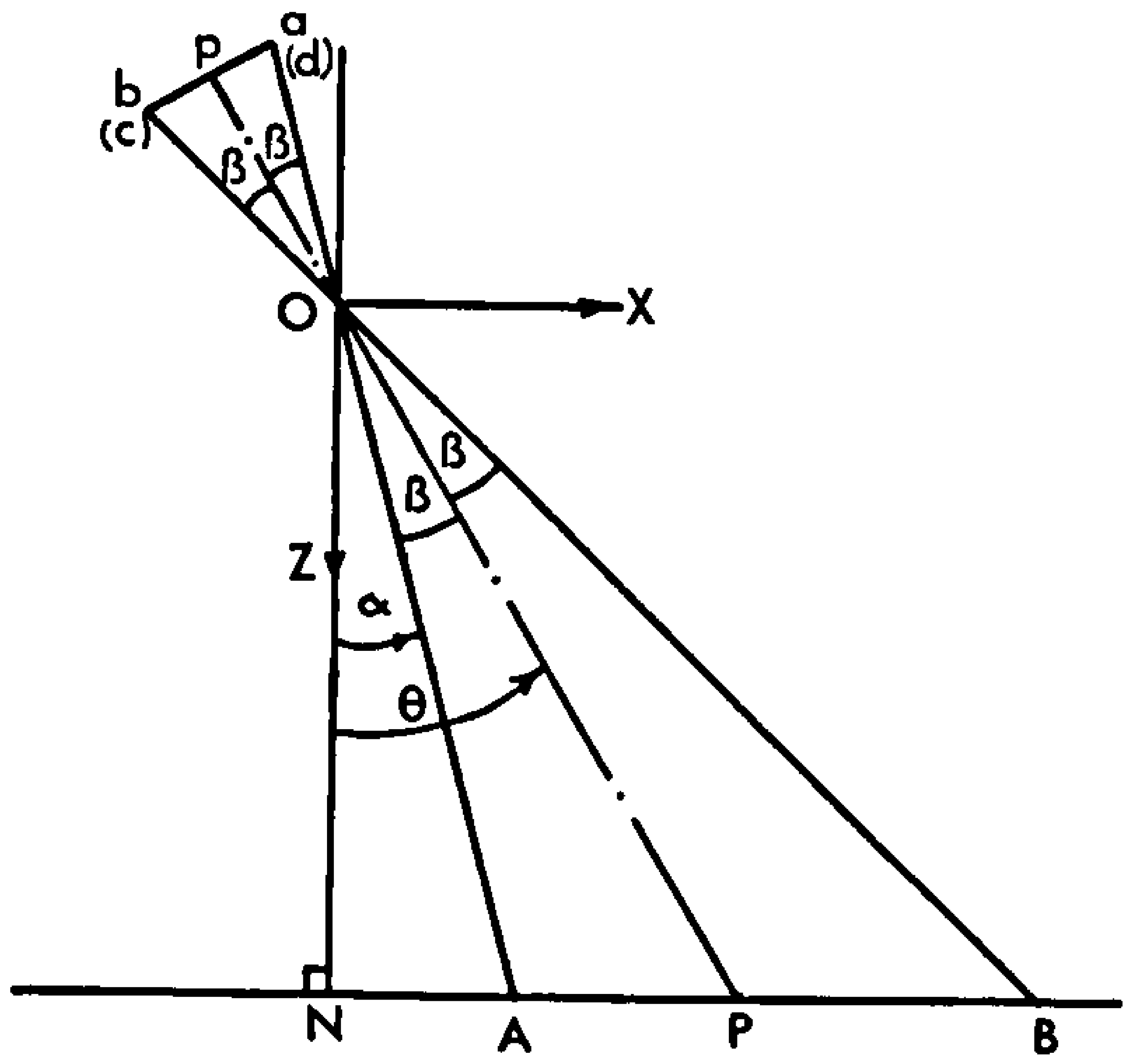

Fig. 88 The case of longitudinal (forward) oblique photography.

Considering the image point, a, the image motion is given by

$$v_a = \frac{fV}{H} \cdot \frac{\cos\alpha}{\cos\beta} \quad \ldots\ldots\ldots\ldots\ldots\ldots\ldots\ldots \quad (61)$$

$$= \frac{fV}{H} \quad \frac{\cos(\theta - \beta)}{\cos\beta}$$

$$= \frac{fV}{H} \left[\cos\theta \cos\beta + \sin\theta \sin\beta\right] / \cos\beta$$

$$= \frac{fV}{H} \left[\cos\theta + \tan\beta \sin\theta\right] \quad \ldots\ldots\ldots\ldots\ldots \quad (62)$$

But in this case $\tan\beta = \frac{x}{f}$

$$\text{Hence } v_a = \frac{fV}{H} \left[\cos\theta + \frac{x}{f}\sin\theta\right] \quad \ldots\ldots\ldots\ldots\ldots \quad (63)$$

Again at p, the geometric centre of the photograph, the image speed will be $v_p = \frac{fV}{H} \cos\theta$ since $x = 0$. Therefore, if the film is moved at speed $f\frac{V}{H}\cos\theta$ the residual image motion at any point on the photograph will be

$$dx_i = \frac{fV}{H} \; t_e \; \frac{x_i}{f} \; \sin\theta \quad \ldots\ldots\ldots\ldots\ldots\ldots \quad (64)$$

$$dx_i = \frac{Vt_e}{H} \; x_i \; \sin\theta \quad \ldots\ldots\ldots\ldots\ldots\ldots \quad (65)$$

<u>Example</u>: A numerical example will illustrate the accuracy of IMC at the edges of the format when applied to compensate for the image motion at the centre of the photograph (p in Fig.87). A camera of 30 cm (12 in.) focal length and of format size 23 x 23 cm (9 x 9 in.) and exposure time 1/500 sec installed in a craft flying at an altitude of 3000 m with a speed of 300m/sec would have residual image motion of at the edges of the format ($x = y = 115$ mm) for the corresponding angle of tilt, θ, as shown in the Table 4 below.

Table 4 Residual image motion for oblique photography

Tilt angle θ^o	Residual image motion dx_i (μm)
20	7.8
30	11.5
40	14.7

However, in practice at such flying speed the shutter speed used is usually not less than 1/1000 sec and the residual image motion will therefore be less than half the values given in this table.

4.7 <u>The Combined Effect of the Focal Plane Shutter and IMC</u>

For the case of a vertical frame camera with <u>intra-lens shutter</u>, the image displacement due to the linear motion of the aircraft during exposure is given by

$$dx_i = \frac{V}{s} . t_e$$

This displacement is opposite to the direction of flight. However, when the IMC is applied perfectly, the image is moved by the same displacement in the direction of flight, hence

$$dx_{IMC} = \frac{V}{s} t_e$$

If the frame camera is equipped with a parallel-motion focal plane shutter, the displacement introduced by the IMC to compensate for the image motion is given by

$$dx_{IMC} = \frac{V}{s} t_i$$

where t_i is the shutter transit time as defined before.

When discussing the geometric effect of the focal plane shutter, it was deduced that the image distortion due to the focal plane shutter is:

$dx_{fp} = k\,x'_i$ if the shutter is moving parallel to the flight direction,

or $dx_{fp} = k\,y'_i$ if the shutter is moving across the flight direction.

Normally the film can be moved such that $\frac{V}{s} t_i = k\,x'_i$ or $\frac{V}{s} t_i = k\,y'_i$ and, in this case, the distortion due to the focal plane shutter would be completely eliminated and the residual distortion Δx_i will be zero. If the IMC is not perfect, then the residual distortion is

$$\Delta x_i = dx_{fp} - dx_{IMC} \quad \ldots\ldots\ldots\ldots\ldots\ldots\ldots\ldots \quad (66)$$

This is illustrated by Fig. 89 for the case that

$$dx_{IMC} > dx_{fp}$$

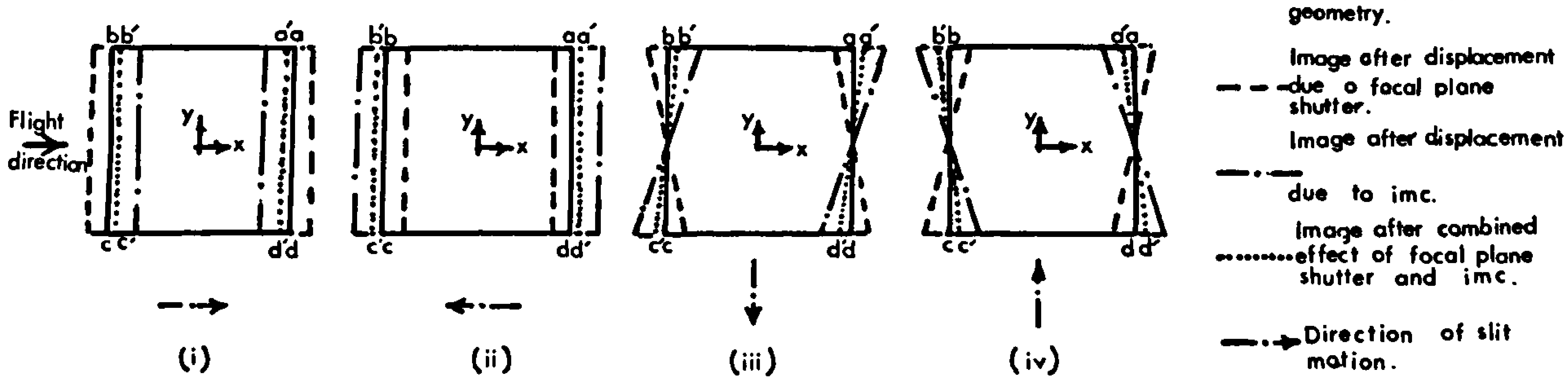

Fig. 89 Combined effect of the focal plane shutter and IMC on image geometry

4.8 Effect on Relative Orientation

From the above discussion, it can be seen that the image displacement caused by the parallel-motion focal plane shutter (and imperfect IMC) is a change in scale in the x-direction only i.e. only x-parallax is introduced. This means that the relative orientation procedures (empirical, numerical or analytical) which are used for metric photography can also be applied to reconnaissance frame photography.

This x-parallax, however, will cause some deformations in the model coordinates. Discussion of the model deformations will follow.

4.9 Model Deformations

Reconnaissance frame photography is usually taken with longitudinal overlap of up to 60 per cent to allow stereoscopic viewing by users. Since this thesis is concerned with metric aspects of such photography, the stereo-model will be analysed to see if it actually represents the terrain as an exact geometrical model and, if not, whether and to what extent it departs significantly from this model.

The departures or deformations of the model will be considered for the two cases, where

(a) the camera is equipped with a parallel-motion focal plane shutter and no IMC is used;

(b) there is residual image distortion due to the combined effect of the parallel-motion focal plane shutter and IMC.

Flat terrain will be considered since, as was shown in the previous analysis, the variations in terrain height have no significant effect. The crab effect will also be neglected for the same reason.

As already explained, the focal plane shutter can move in any one of four different directions relative to the direction of flight. Each of these four cases will be considered.

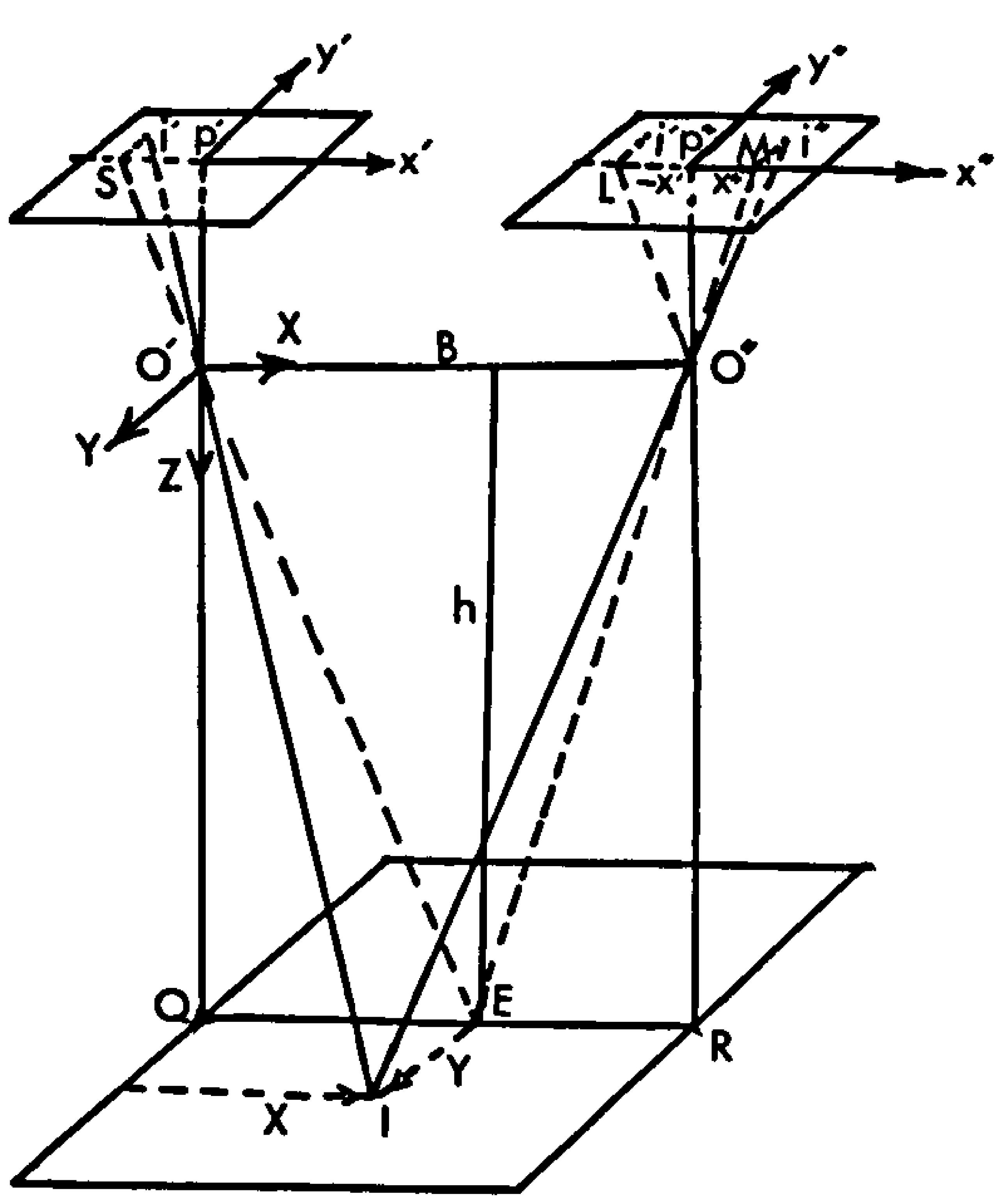

Fig. 90 Model coordinates system

Considering a right-handed coordinate system in which the origin is located at the left-hand perspective centre (Fig. 90), the departures dX, dY and dZ in the model coordinates due to shifts dx' and dx" in the x-photo-coordinates (x' and x") can be derived. By definition, the parallax p is given by

$$p = x'' - x' \quad \ldots\ldots\ldots\ldots\ldots\ldots\ldots\ldots \quad (67)$$

The residual parallax dp due to the shifts dx' and dx" is

$$dp = dx'' - dx' \quad \ldots\ldots\ldots\ldots\ldots\ldots\ldots\ldots \quad (68)$$

Referring to Fig. 90, from similar triangles LMO" and O'O"B,

$$Z = \frac{Bf}{p} \quad \ldots\ldots\ldots\ldots\ldots\ldots\ldots\ldots \quad (69)$$

Differentiating this equation gives

$$dZ = \frac{-Bf}{p^2} \; dp \quad \ldots\ldots\ldots\ldots\ldots\ldots\ldots\ldots \quad (70)$$

Substituting for Z = B f/p in equation (70) results in

$$dZ = \frac{-Z}{p} \, dp \quad \ldots\ldots\ldots\ldots\ldots\ldots\ldots\ldots \quad (71)$$

Expressing this at the photo scale gives

$$dZ = -\frac{f}{p} \; dp \quad .$$

$$\text{or} \quad dZ = \frac{f}{p} \, (dx' - dx'') \quad \ldots\ldots\ldots\ldots\ldots\ldots \quad (72)$$

Again, from similar triangles SP'O' and EQO',

$$X = x' \frac{Z}{f} \quad \ldots\ldots\ldots\ldots\ldots\ldots\ldots\ldots \quad (73)$$

The differential form of this equation is

$$dX = \frac{x'}{f} \, dZ + \frac{Z}{f} \, dx' \quad \ldots\ldots\ldots\ldots\ldots \quad (74)$$

Substituting for dZ from equation (71) and expressing the results at the photo scale, one gets

$$dX = \frac{x'}{p} \, (dx' - dx'') + dx' \quad \ldots\ldots\ldots\ldots \quad (75)$$

Similarly, $Y = y' \frac{Z}{f}$ .... (76)

the derivative of which is

$$dY = y' \frac{dZ}{f} + \frac{Z}{f} dy' \quad \text{...............} \quad (77)$$

For $y' = y'' = y$ (i.e. $dy' = 0$), substituting for dZ from equation (71) and expressing the result at the photo scale, gives

$$dY = \frac{y'}{p} (dx' - dx'') \quad \text{....................} \quad (78)$$

The model deformations resulting from the displacements in x-photo-coordinate, caused by the parallel-motion focal plane shutter, will be determined by substituting the appropriate values in equations (72), (75) and (78). It should be noticed that the value of x' will have a minus sign as seen in Fig. 90. In this case, $p = x'' - (-x') = x'' + x'$.

(i) Mono-Directional Focal Plane Shutter moving in the Direction of Flight:

The first case to be considered is the one where the shutter moves in the same direction of flight in each of the two consecutive exposures. In this case, the image will be elongated in each of the two overlapping photographs. Substituting for $dx' = -kx'$ and $dx'' = kx''$ in equations (75), (78) and (72) we get:

$$dX = 0 \quad \text{..........................} \quad (79)$$

$$dY = -ky \quad \text{..........................} \quad (80)$$

$$dZ = -kf \quad \text{..........................} \quad (81)$$

Fig. 91 illustrates the model deformations for this case.

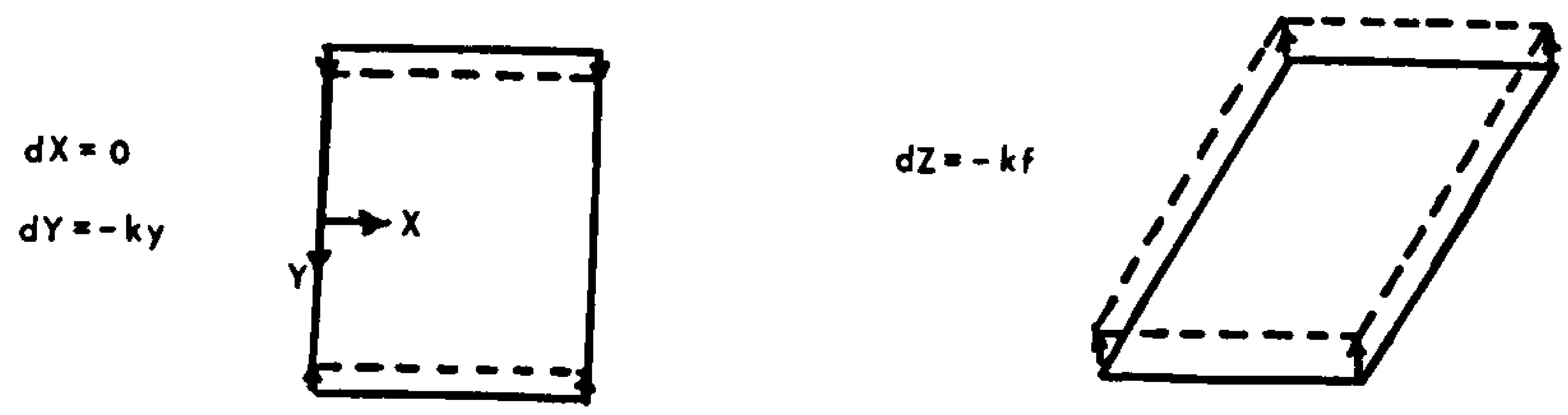

Fig. 91 Model deformations for case (i)

(ii) Mono-Directional Focal Plane Shutter moving against the Direction of Flight

In this case, both exposures are made with the shutter moving against the direction of flight, i.e. the image will be compressed in each photograph. The resulting image displacements are $dx' = kx'$ and $dx'' = -kx''$. Substituting these values in the equations expressing the model deformations, we get:

$$dX = 0 \quad \ldots\ldots\ldots\ldots\ldots\ldots \quad (82)$$

$$dY = ky \quad \ldots\ldots\ldots\ldots\ldots\ldots \quad (83)$$

$$dZ = kf \quad \ldots\ldots\ldots\ldots\ldots\ldots \quad (84)$$

(See Fig. 92).

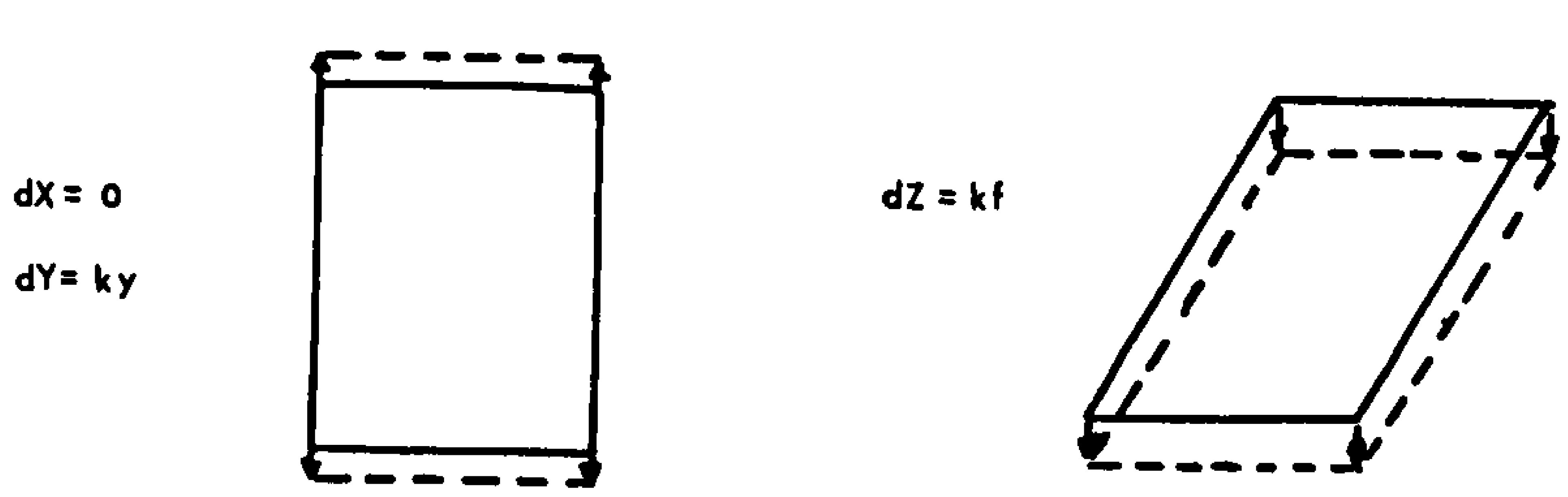

Fig. 92 Model deformations for case (ii).

(iii) Bi-Directional Shutter

In this case, the shutter moves along the flight direction for one photograph and opposite to the flight direction for the alternate exposure. Hence, the image would be elongated in the first photograph and compressed in the second overlapping photograph. In this case $dx' = -kx'$ and $dx'' = -kx''$ is substituted in the formulae for the model deformation. After rearranging the formulae, they reduce to

$$dX = -2kx' + \frac{2kx'^2}{p} \quad \ldots\ldots\ldots\ldots\ldots\ldots\ldots\ldots \quad (85)$$

$$dY = ky - \frac{2kx'y}{p} \quad \ldots\ldots\ldots\ldots\ldots\ldots\ldots\ldots \quad (86)$$

$$dZ = kf - \frac{2kfx'}{p} \quad \ldots\ldots\ldots\ldots\ldots\ldots\ldots\ldots \quad (87)$$

The model deformation is illustrated by Fig. 93.

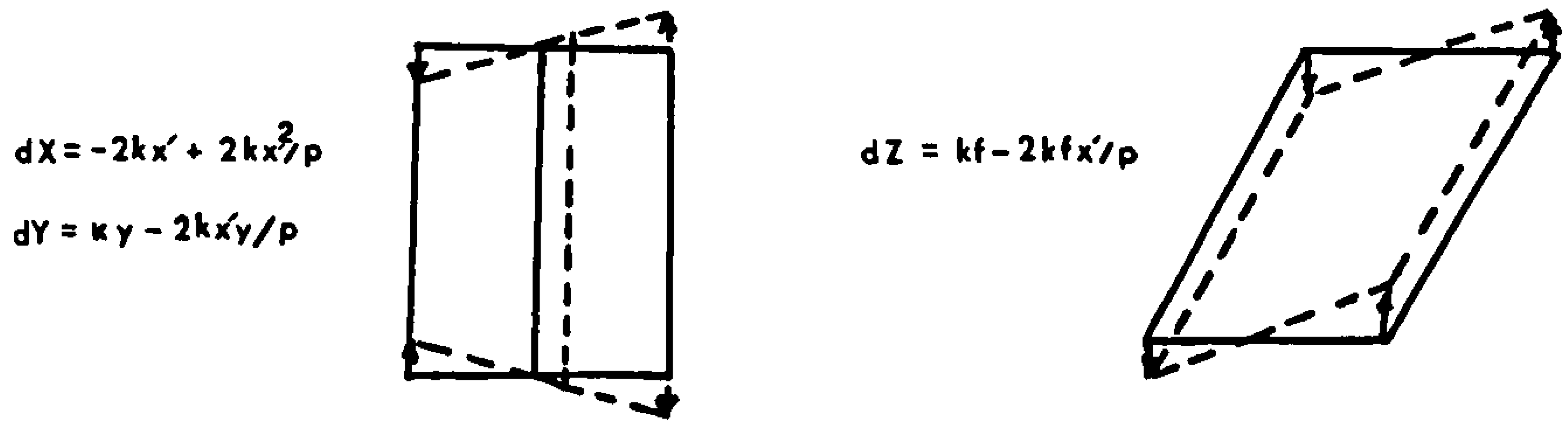

Fig. 93 Model deformations for case (iii)

(iv) Mono-Directional Focal Plane Shutter moving across the Direction of Flight

The shutter moves across the flight direction without reversing its direction for the consecutive exposure. In this case, $dx' = ky$ and $dx'' = ky$. The model deformations, therefore, are given as:

$$dX = ky \quad \ldots\ldots\ldots\ldots\ldots\ldots\ldots\ldots \quad (88)$$

$$dY = 0 \quad \ldots\ldots\ldots\ldots\ldots\ldots\ldots\ldots \quad (89)$$

$$dZ = 0 \quad \ldots\ldots\ldots\ldots\ldots\ldots\ldots\ldots \quad (90)$$

Fig. 94 illustrates the model deformations for this case.

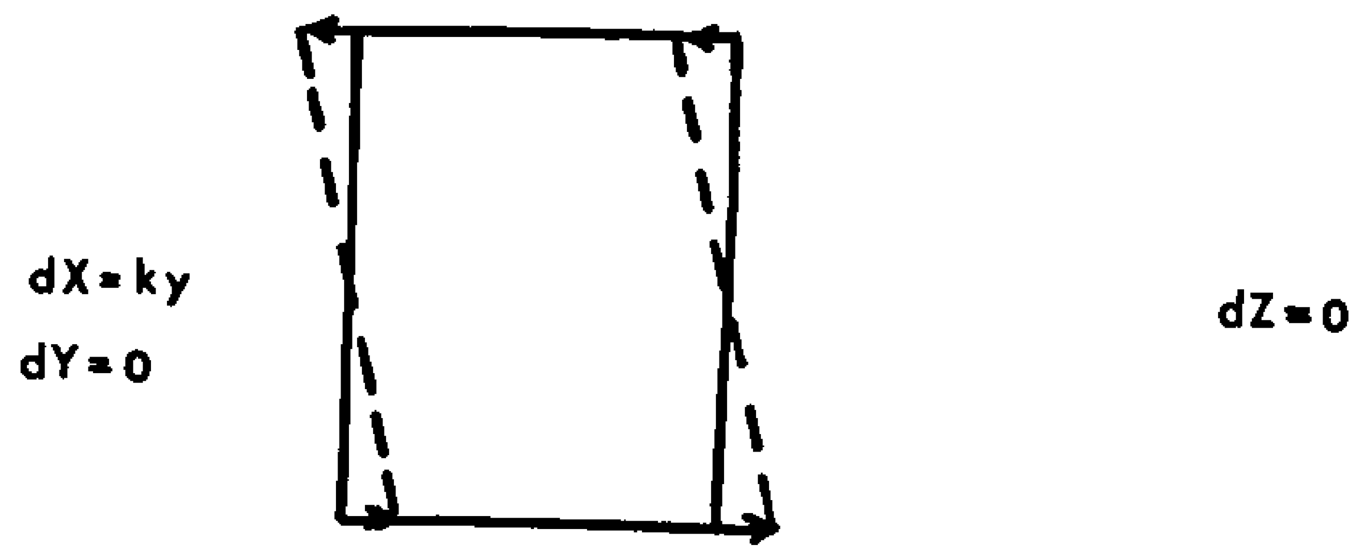

Fig. 94 Model deformations for case (iv)

(v) <u>Bi-Directional Focal Plane Shutter moving across the Direction of Flight</u>

The shutter moves across the flight direction, reversing its direction for the alternate exposure. Now, one can substitute for $dx' = ky$ and $dx'' = -ky$. The resulting model deformations are:

$$dX = ky - \frac{2kx'y}{p} \quad \ldots\ldots\ldots\ldots\ldots\ldots\ldots\ldots \quad (91)$$

$$dY = \frac{2ky^2}{p} \quad \ldots\ldots\ldots\ldots\ldots\ldots\ldots\ldots \quad (92)$$

$$dZ = \frac{2fky}{p} \quad \ldots\ldots\ldots\ldots\ldots\ldots\ldots\ldots \quad (93)$$

The model deformations for this case are shown in Fig. 95.

Fig. 95 Model deformations for case (v)

Examples:

A numerical example will give some idea of the magnitude of the errors in the model coordinates arising from the effect of the parallel-motion focal plane shutter (a) when used without IMC and (b) when the IMC is not absolutely exact.

(a) No IMC employed

As a numerical example, consider a camera of 150 mm focal length equipped with a focal plane shutter of speed 1/1000 sec, with the width of slit (W) equal to 10 mm. If the camera is carried by a craft flying at a speed of 300m/sec, and at an altitude of 6000 metres then the factor k is given by

$$k = \frac{V}{s} \cdot \frac{t_e}{W}$$

$$= \frac{300}{40{,}000} \times \frac{1000}{1000 \times 10} = \frac{3}{4000}$$

Assuming the format size of the camera to be 230 mm x 230 mm (9 x 9 in.) and that a longitudinal overlap of 60% is employed then the values of the discrepancies at the model coordinates due to the effect of the focal plane shutter, computed at a point of image coordinates $x = 115$ mm, $y = 115$ mm (i.e. where the effect is maximum) are given in Table 5, both at image scale and at ground scale.

Table 5. Numerical values of model deformations caused by the focal plane shutter

Case Number	Discrepancies at image scale (μm)			Discrepancies at ground scale (m)		
	dx	dy	dz	dX	dY	dZ
(i)	-	-86	-112	-	-3.44	-4.48
(ii)	-	86	112	-	3.44	4.48
(iii)	43	-129	-168	1.72	-5.16	-6.72
(iv)	86	-	-	3.44	-	-
(v)	-129	215	281	-5.16	8.60	11.24

(b) Effect due to incorrect IMC:

If an IMC system is used, with an error of 5% the above discrepancies would reduce to the values given in Table 6.

Table 6. Numerical values of model deformations for an IMC with 5% inaccuracy.

Case Number	Discrepancies at image scale (μm)			Discrepancies at ground scale (m)		
	dx	dy	dz	dX	dY	dZ
(i)	-	-4.30	-5.60	-	-0.17	-0.22
(ii)	-	4.30	5.60	-	0.17	0.22
(iii)	2.10	-6.45	-8.40	0.08	-0.26	-0.34
(iv)	4.30	-	-	0.17	-	-
(v)	-6.45	10.75	14.05	-0.26	0.43	0.56

It can be concluded from the above tables that the effect of the parallel-motion focal plane shutter on the geometry of the model is quite significant specially in the Y-direction and in height. The most serious case, however, is case (v) when the shutter moves across the flight direction and reverses its direction for the alternate exposure. When IMC is employed, the magnitude of the errors would fall to insignificant values even if there is 5% inaccuracy.

The values of f, p and k in equations (79) to (93) can be considered as constants for any model, hence the deformations which have been derived can be summarised in the following formulae:

$$dx_i = a_o + a_1 x_i y_i + a_2 x_i + a_3 y_i + a_4 x_i^2 \quad \ldots\ldots \quad (94)$$

$$dy_i = b_o + b_1 x_i y_i + b_2 y_i + b_3 y_i^2 \quad \ldots\ldots\ldots\ldots \quad (95)$$

$$dz_i = c_o + c_1 x_i + c_2 y_i \quad \ldots\ldots\ldots\ldots\ldots\ldots\ldots\ldots \quad (96)$$

After a conventional relative orientation, the model deformations can be corrected using the above formulae.

4.10 Conclusions

The reconnaissance frame camera, when equipped with a parallel-motion focal plane shutter, produces an image distorted in the x-photo axis only. The only situation where this will not apply will occur when the effect of crab is significant - which is usually not the case in reconnaissance photography.

If the IMC technique of translating the film in the flight direction is applied to a vertical reconnaissance frame camera when exposing over flat terrain, the image motion due to the linear craft movement during exposure can be completely eliminated. Theoretical investigations showed that oblique photography and mountainous terrain have insignificant effects on the accuracy of IMC system.

However, even if the camera is equipped with focal plane shutter and no IMC is applied, the image distortions resulting from the use of focal plane shutters can be computed. Analytical techniques to correct for this distortion which can be employed in utilising reconnaissance frame photography for photogrammetric purposes will be devised and discussed in the next chapter.

CHAPTER V

Analytical Techniques for Use with Reconnaissance Frame Photography

CHAPTER V

ANALYTICAL TECHNIQUES FOR USE WITH RECONNAISSANCE FRAME PHOTOGRAPHY

5.1 Introduction - The Use of Analytical Techniques

In this chapter, various possible approaches which would allow relative orientation and the formation of corrected model and terrain coordinates are examined. It is obvious from the discussion in the previous chapter, that these operations cannot be carried out in a conventional analogue type of stereo-plotting machine, since these instruments are not equipped with devices which can compensate for the type of displacements produced by focal plane shutters. An analytical approach to the problem is therefore obligatory. Thus the basic input for all of the operations mentioned above will be the photo or image coordinates as measured in a mono-comparator or stereo-comparator. The techniques which have been devised and are described below are, of course, equally suitable for use with an analytical plotter.

5.2 Lack of Knowledge of Inner Orientation

In order to reconstruct the bundle of rays between the object and the lens during exposure using the image points, the main elements of inner orientation (i.e. the principal distance and the position of the principal point) must be known. As has already been mentioned, the principal point of the reconnaissance frame camera cannot be precisely located since there are no fiducial marks or reseau crosses. On the other hand, the geometric centre of the photograph can be defined by joining the opposite corners of the format.

The effects of lack of knowledge or deviation (dx_p and dy_p) of the geometric centre from the principal point and an error in the principal distance (df) on the model coordinates have been investigated by Hadem (1968), and the following relations were derived:

$$dZ = \frac{Z}{Bf}\left[(X - B)(df_1 - df_2) + B\,df_1 - Z(dx_{p_1} - dx_{p_2})\right] +$$

$$\frac{Z^2 + (X - B)^2}{B}\,d\Phi_2 - \frac{Y(X - B)}{B}\,d\omega_2 - \frac{YZ}{B}\,d\varkappa_2$$

$$- \frac{X - B}{B}\,dZo_2 \quad \ldots\ldots\ldots\ldots\ldots\ldots\ldots\ldots\ldots\ldots \quad (97)$$

$$dX = \frac{X}{Z}\,dZ - \frac{x}{f}\,df_1 + \frac{Z}{f}\,dx_{p_1} \quad \ldots\ldots\ldots\ldots\ldots\ldots\ldots\ldots \quad (98)$$

$$dY = \frac{Y}{Z}\,dZ - \frac{Y}{f}\,df_1 + \frac{Z}{f}\,dy_{p_1} -$$

$$S\left[-\frac{(X - B)Y}{Z}\,d\Phi_2 + \frac{Z^2 + Y^2}{Z}\,d\omega_2\right.$$

$$\left.- (X - B)\,d\varkappa_2 - dYo_2 + \frac{Y}{Z}\,dZo_2\right] \ldots\ldots\ldots\ldots\ldots\ldots \quad (99)$$

where dX, dY, dZ are displacements in the model coordinates X, Y and Z respectively, due to errors in the inner orientation elements; $d\omega_2$, $d\Phi_2$, $d\varkappa_2$, dYo_2, dZo_2 are errors in outer orientation elements of the right-hand projector caused by errors in the inner orientation elements; B is the model base; f is the principal distance; the terms with suffix 1 or 2 are related to the left hand photograph and the right hand photograph respectively; S is the ratio of the distance from the left projection to the observed point in relation to the distance between the two projections.

For vertical photographs and flat terrain, these effects will be insignificant and can be compensated by performing relative and absolute orientations (Helava, 1963). In practice, one can expect to encounter tilted photographs and hilly terrain in which case consideration has to be given to these effects. They will, of course, be still more significant for the case of mountainous terrain and convergent photography.

The new analytical technique of self calibration, using additional parameters, (Brown, 1976) which will be discussed in this chapter will take account of these errors.

5.3 <u>Corrections to Image Coordinates</u>

Before carrying out any analytical relative orientation and absolute orientation, usually the image coordinates are corrected for distortions resulting from lens distortion, Earth's curvature, atmospheric refraction and film deformation. In the situation being considered here (that of a parallel-motion focal plane shutter with no IMC) a similar procedure can be followed. The displacements induced by the focal plane shutter can be computed using equations (13) or (14) depending on the direction of the shutter motion relative to the flight direction. So when the factor $K = \frac{V}{s} \cdot \frac{t_e}{W}$ is computed for the photograph, the image coordinates of any point on the photograph can be corrected. After correcting the image coordinates by this technique, a conventional method of relative orientation can be employed followed by the normal absolute orientation.

The advantage of this technique is that it is very simple and follows the same procedures as are used with metric photography. Also the number of ground control points needed is the same as is required to solve a conventional model. The additional information required however, is to know the <u>direction</u>

of the shutter motion relative to the flight direction for each photograph being measured. Unfortunately this information is seldom, if ever, available.

5.4 Tilt Variations during Shutter Transit Times

In conventional photogrammetric work using metric photography, the tilts present during exposure and derived by standard orientation techniques are assumed to be fixed. Such an assumption is justified with metric photographs taken using an intra-lens shutter - the exposure time is commonly 1/300 to 1/500 th second and any tilt variation in this short time period will be negligible. With a focal plane shutter, while the exposure time (t_e) for any individual image point will be the same, the transit time (t_i) of the shutter across the focal plane will be quite different - perhaps 20 to 100 times longer. It is then much more difficult to assume that the tilt values remain constant, in which case a quite different situation is encountered to that familiar to photogrammetrists from their use of standard metric photography. One has instead a type of dynamic imaging system - the term introduced by Case (1967) in his analysis of strip and panoramic photography. In this situation, the exposure station position and the camera attitude are both changing while the shutter is in motion exposing the whole of the focal plane. Therefore the elements of exterior orientation should be considered as varying with time.

5.5 Possible Analytical Approaches

With regard to the analytical methods which might be applied to photography taken with a focal plane shutter with no IMC, two basic approaches appear to be possible:-

(a) Space Resection/Space Intersection Method

The first is to resect each photograph individually, so that the coordinates of the perspective centre and the tilts present at exposure may be derived. This so-called space resection technique is then followed by a space intersection in which the measured image coordinates, the now known coordinates of the perspective centre and the elements of orientation from the two photographs are combined to give model-coordinates or, when an appropriate number of control points with known ground coordinates has been used, terrain coordinates. An advantage of this approach is that it more readily allows the derivation of the time-varying orientation parameters discussed above.

(b) Analytical Relative and Absolute Orientation

The second approach is to carry out a conventional analytical relative and absolute orientation as used with normal metric photography. Since this will produce model or terrain coordinates which are displaced or deformed compared with what they should be (due to the uncorrected image coordinates), corrections must then be applied to the model or terrain coordinates. This approach has the advantage of using well-understood and well-known computational methods (and readily-available and existing computer programs (e.g. Methley,1972)). The deviations of the transformed ground coordinates from the given values can be used to model the deformations and these can be used to derive correction parameters (e.g. using polynomials) suitable for the correction of any other points for which coordinates are required.

5.6 Space Resection/Space Intersection Method

The problem of resection in photogrammetry is defined as the determination of the three angular and three linear positions of a single photograph (American Society of Photogrammetry, 1966), based on the known positions and elevations of at least three non-linear objects. This problem has been treated by different authors (e.g. Church, 1945; Anderson, 1949; Schmid, 1953).

The solution adopted here is the one by Schmid (1953, 1955, 1959) which is based on the principle of collinearity. The principle of collinearity states that every object, its photographic image and the camera exposure station must lie on a common straight line. This method allows the application of least squares when redundant data is available to minimise the random observational discrepancies, and is easily programmed for an electronic computer. Moreover, the time factor can be introduced to determine the exterior orientation elements of the exposure station corresponding to any point on the photograph.

Nowadays, space resection is only used as a phase preceding the bundle adjustment in analytical aerotriangulation as e.g. in the National Ocean Survey's (NOS) block adjustment procedure to provide initial approximations for the exterior orientation elements of each photograph.

5.6.1 Single Photographs - Basic Geometrical Relationships

For the normal perspective photograph taken with a metric camera, the relationship between the object and image in space can be expressed by the following projective relations:

$$\begin{bmatrix} X_i \\ Y_i \\ Z_i \end{bmatrix} = \lambda_i A \begin{bmatrix} x_i \\ y_i \\ -f \end{bmatrix} + \begin{bmatrix} X_o \\ Y_o \\ Z_o \end{bmatrix} \quad \ldots\ldots\ldots\ldots\ldots \quad (100)$$

where X_i, Y_i, Z_i = coordinates of the object point in a fixed exterior Cartesian coordinate system;

x_i, y_i = coordinates of the image point in the photo-coordinate system with the principal point as origin (for reconnaissance cameras, the geometric centre determined by reference to the frame corners can be adopted as origin without much effect);

f = camera focal length;

A = orthogonal orientation matrix which relates the photo system to the exterior coordinate system with its elements formed by the three rotational angles ω, ϕ and κ.

X_o, Y_o, Z_o = coordinates of the exposure station in the exterior coordinate system.

However, the projective relationship given in equation (100) is also applicable to photography taken with focal plane shutters. In this case, however, the focal plane is replaced by a focal line of width defined by the slit width.

As has been mentioned above, for a single photograph the shutter moves either parallel to or transverse to the flight direction. Thus, a photo-coordinate system will be considered which has the x- and y-axis normal to and along the slit line respectively (Fig. 96).

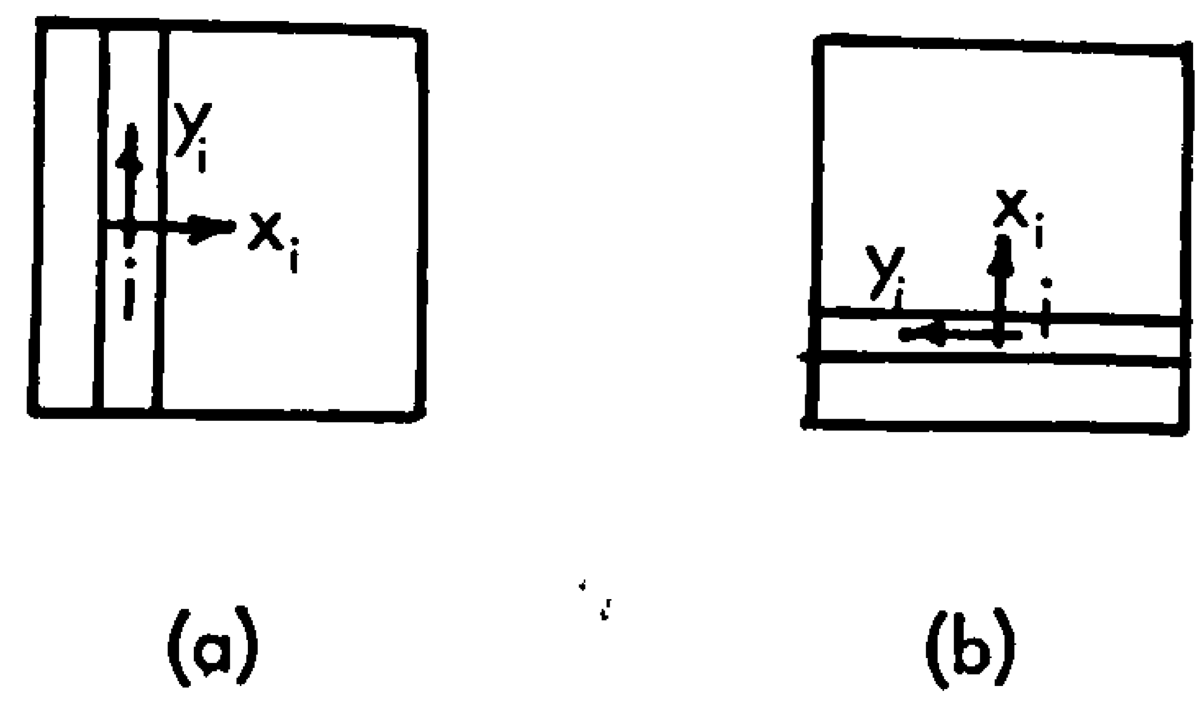

Fig. 96 Photo-coordinate system with origin at the centre point of the focal line.

(i) The origin for this system will be the <u>centre point</u> (i) <u>of the focal line</u>, which can be defined as the mid-point of the slit at a given instant of time. The projective relations would be given as follows (Konecny, 1975):

$$\begin{bmatrix} X_i \\ Y_i \\ Z_i \end{bmatrix} = \lambda_i \begin{bmatrix} \cos\theta_i & 0 & \sin\theta_i \\ 0 & 1 & 0 \\ -\sin\theta_i & 0 & \cos\theta_i \end{bmatrix} . A . \begin{bmatrix} 0 \\ y_i \\ -f/\cos\theta_i \end{bmatrix} + \begin{bmatrix} Xo_i \\ Yo_i \\ Zo_i \end{bmatrix} \quad ..(101)$$

x_i is always 0 for any individual focal line being considered.

where θ_i = the angle formed at the perspective centre by points p and i, due to the movement of the slit from the geometric centre of the photograph (p) to the point (i) (Fig. 97);

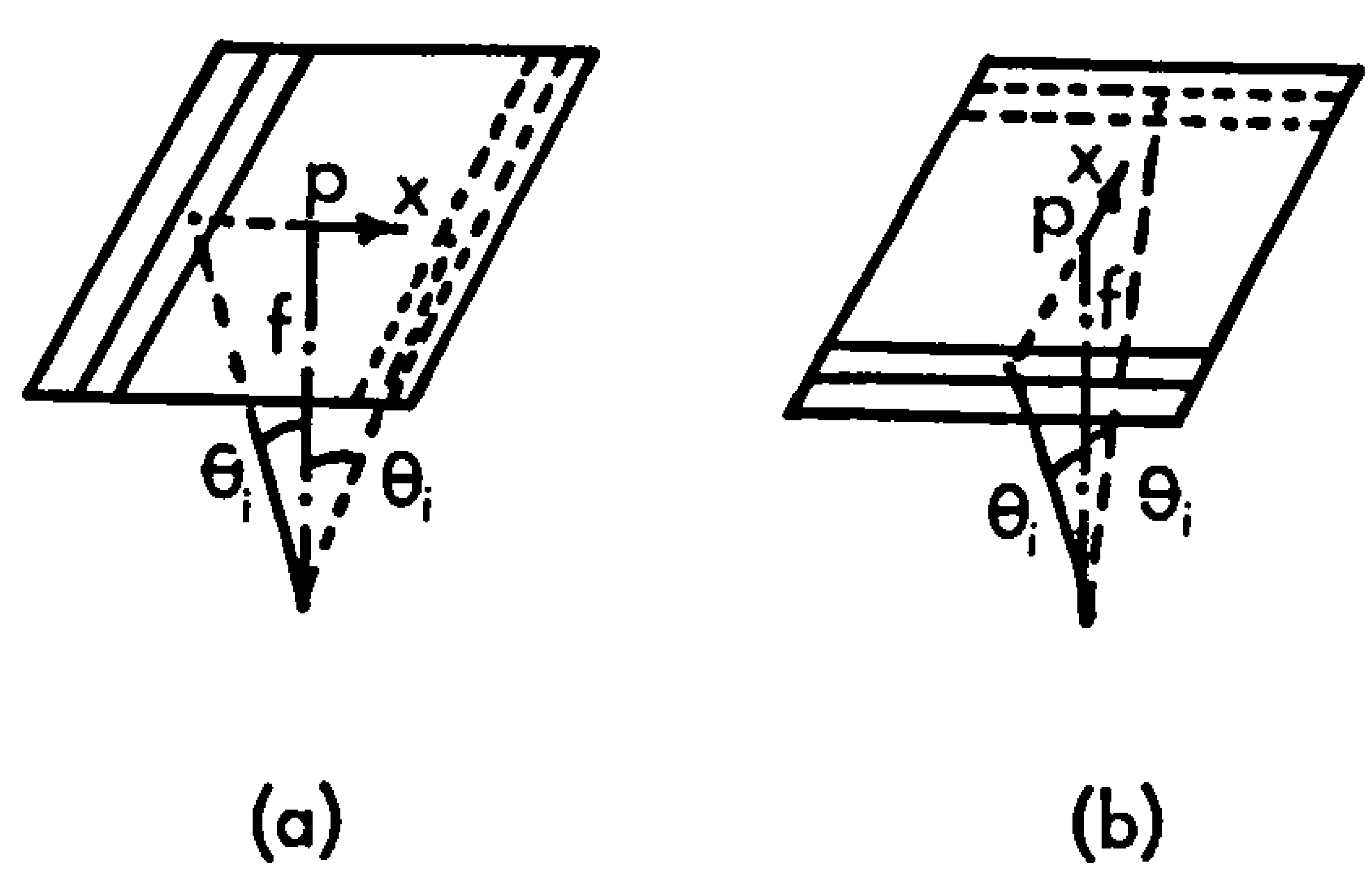

Fig. 97 Angle θ_i

Xo_i, Yo_i, Zo_i are the coordinates of the perspective centre in the exterior orientation system at the instant at which the image point i is exposed; and

A_i is the orthogonal transformation matrix, composed of the rotation elements ω_i, Φ_i and κ_i present at the moment of exposure of point i and referred to the instantaneous projection centre (Xo_i, Yo_i, Zo_i), and relating the photo system to the ground system.

(2) Therefore if the origin of the previous photo-coordinate system is taken to be the geometric centre of the photograph (p) (Fig. 98), equation (101) will reduce to the form:

$$\begin{bmatrix} X_i \\ Y_i \\ Z_i \end{bmatrix} = \lambda_i A_i \begin{bmatrix} x_i \\ y_i \\ -f \end{bmatrix} + \begin{bmatrix} Xo_i \\ Yo_i \\ Zo_i \end{bmatrix} \qquad (102)$$

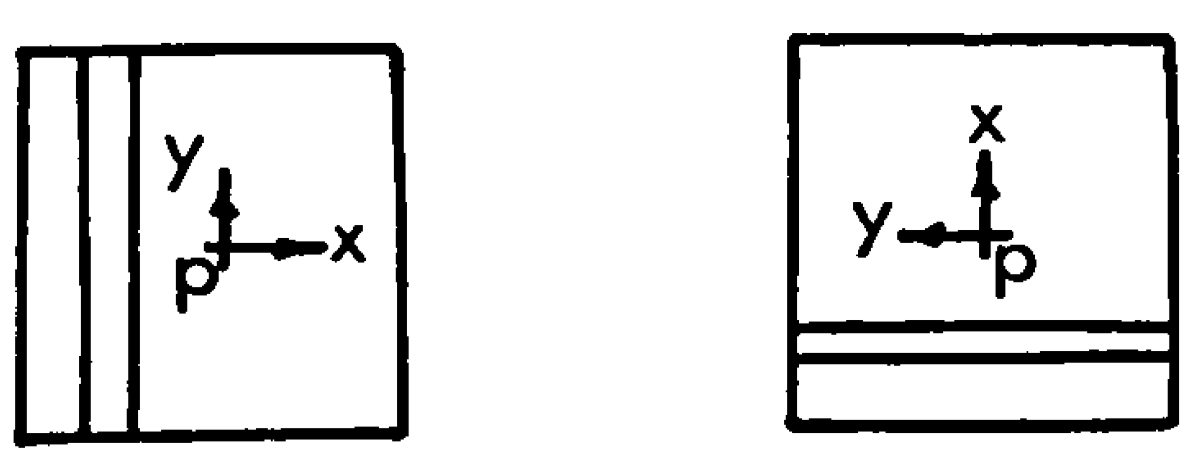

(a) (b)

Fig. 98 Photo-coordinate system with origin at the geometric centre of the photograph.

The corresponding inverse form for this relation will be:

$$\begin{bmatrix} x_i \\ y_i \\ -f \end{bmatrix} = \frac{1}{\lambda_i} A_i^T \begin{bmatrix} X_i - Xo_i \\ Y_i - Yo_i \\ Z_i - Zo_i \end{bmatrix} \qquad \text{...........} \qquad (103)$$

In the Space Resection phase, the position and attitude of the exposure station for each photograph will be determined. If these elements are determined for the two overlapping photographs and are substituted in equation (102), the scale factors (λ) can be determined as will be shown later. The exterior orientation elements, the scale factor and the measured image coordinates will be used in the Space Intersection phase to determine the ground object coordinates $\begin{bmatrix} X \\ Y \\ Z \end{bmatrix}$.

5.6.2 Space Resection (point-by-point)

Due to the operation of the focal plane shutter, the exposure station is changing its position and attitude while the negative is being exposed. Therefore, the image points would be treated individually (i.e. for each point on the photo the corresponding exposure station position and camera attitude is to be determined).

From equation (100), the following collinearity equations can be derived:

$$x_i = -f \; \frac{a_{11_i}(X_i - Xo_i) + a_{12_i}(Y_i - Yo_i) + a_{13_i}(Z_i - Zo_i)}{a_{31_i}(X_i - Xo_i) + a_{32_i}(Y_i - Yo_i) + a_{33_i}(Zi - Zo_i)}$$

$$y_i = -f \; \frac{a_{21_i}(X_i - Xo_i) + a_{22_i}(Yi - Yo_i) + a_{23_i}(Z_i - Zo_i)}{a_{31_i}(X_i - Xo_i) + a_{32_i}(Y_i - Yo_i) + a_{33_i}(Z_i - Zo_i)} \qquad \ldots\ldots\ (104)$$

where a_{11_i}, a_{12_i}, etc. are the elements of the orthogonal matrix A_i.

These equations can be linearised by Taylor's series and can be written in the form:

$$V_{x_i} = \left(\frac{\partial x_i}{\partial \omega_i}\right) d\omega_i + \left(\frac{\partial x_i}{\partial \phi_i}\right) d\Phi_i + \left(\frac{\partial x_i}{\partial \kappa_i}\right) d\kappa_i + \left(\frac{\partial x_i}{\partial Xo_i}\right) dXo_i + \left(\frac{\partial x_i}{\partial Yo_i}\right) dYo_i + \left(\frac{\partial x_i}{\partial Zo_i}\right) dZo_i - J_i$$

$$V_{y_i} = \left(\frac{\partial y_i}{\partial \omega i}\right) d\omega_i + \left(\frac{\partial y_i}{\partial \phi i}\right) d\Phi_i + \left(\frac{\partial y_i}{\partial \kappa i}\right) d\kappa_i + \left(\frac{\partial y_i}{\partial Xo_i}\right) dXo_i + \left(\frac{\partial y_i}{\partial Yo_i}\right) dYo_i + \left(\frac{\partial y_i}{Zo_i}\right) dZo_i - K_i$$

where V_{x_i}, V_{y_i} are corrections to the measured photo-coordinates;

J_i, K_i are the discrepancies of the measured photo-coordinates from the values computed using approximate exterior orientation elements experienced at the moment of exposure of the point centre; the partial derivatives of x_i and y_i with respect to the unknown orientation elements are also evaluated at the approximate values of the exterior orientation elements.

Now, if the approximate values of the exterior orientation elements corresponding to the exposure of the central point of the photograph (p) are given by ωp, ϕ_p, χ_p, Xo_p, Yo_p, Zo_p then the approximate exterior orientation elements ω_i, ϕ_i, χ_i, Xo_i, Yo_i, and Zo_i corresponding to the exposure of the point i on the photograph will be given by:

$$\begin{bmatrix} \omega i \\ \phi i \\ \chi i \\ Xo_i \\ Yo_i \\ Zo_i \end{bmatrix} = \begin{bmatrix} \omega p \\ \phi p \\ \chi p \\ Xo_p \\ Yo_p \\ Zo_p \end{bmatrix} + \begin{bmatrix} d\omega_i \\ d\phi_i \\ d\chi_i \\ dXo_i \\ dYo_i \\ dZo_i \end{bmatrix} \quad \ldots\ldots\ldots (106)$$

where $d\omega_i$, $d\phi_i$, $d\chi_i$, dXo_i, dYo_i and dZo_i are the changes in the exterior orientation elements from their position at which point (i) is exposed. However, these changes are functions of the craft speed, V, (with components $\dot{X}o_i$, $\dot{Y}o_i$, $\dot{Z}o_i$) and the roll ($\dot{\omega}_i$), yaw ($\dot{\phi}_i$) and pitch ($\dot{\chi}_i$), and can be expressed as follows:

$$\begin{bmatrix} d\omega_i \\ d\Phi_i \\ d\dot{\varkappa}_i \\ dXo_i \\ dYo_i \\ dZo_i \end{bmatrix} = t_i \begin{bmatrix} \dot{\omega}_i \\ \dot{\Phi}_i \\ \dot{\varkappa}_i \\ \dot{X}o_i \\ \dot{Y}o_i \\ \dot{Z}o_i \end{bmatrix} \quad \ldots\ldots\ldots\ldots \quad (107)$$

If the slit velocity is given by U_s, assumed to be constant, then the time, t_i, for photo point i, measured from the instant at which the central point of the photograph (p) is exposed will be:

$$t_i = \frac{x_i}{U_s} \quad \ldots\ldots\ldots\ldots\ldots\ldots\ldots\ldots \quad (108)$$

If point i is exposed before the central point of the photograph the corresponding value of t_i will be negative.

From equation (108) it is clear that t_i can be considered as a linear function of x_i. Thus equation (107) can be written in the following form:

$$\begin{aligned} d\omega_i &= a_o + a_1 x_i \\ d\Phi_i &= b_o + b_1 x_i \\ d\varkappa_i &= c_o + c_1 x_i \\ dXo_i &= d_o + d_1 x_i \\ dYo_i &= e_o + e_1 x_i \\ dZo_i &= f_o + f_1 x_i \end{aligned} \quad \ldots\ldots\ldots\ldots\ldots\ldots \quad (109)$$

The constants a_o, b_o ... f_o are to correct for the approximate values of the exterior orientation elements corresponding to the exposure of the central point of the photograph. The correction values of equation (109) are then substituted in equation (105) to give:

$$V_{x_i} = \left(\frac{\partial x_i}{\partial \omega_i}\right) a_o + \left(\frac{\partial x_i}{\partial \omega_i}\right) a_1 x_i + \left(\frac{\partial x_i}{\partial \Phi_i}\right) b_o + \left(\frac{\partial x_i}{\partial \Phi_i}\right) b_1 x_i + \left(\frac{\partial x_i}{\partial \chi_i}\right) c_o +$$
$$\left(\frac{\partial x_i}{\partial \chi_i}\right) c_1 x_i + \left(\frac{\partial x_i}{\partial Xo_i}\right) d_o + \left(\frac{\partial x_i}{\partial Xo_i}\right) d_1 x_i + \left(\frac{\partial x_i}{\partial Yo_i}\right) e_o + \left(\frac{\partial x_i}{\partial Yo_i}\right) e_1 x_i +$$
$$\left(\frac{\partial x_i}{\partial Zo_i}\right) f_o + \left(\frac{\partial x_i}{\partial Zo_i}\right) f_1 x_i - J_i \qquad \ldots\ldots\ldots\ldots\ldots\ldots\ldots (110)$$

$$V_{y_i} = \left(\frac{\partial y_i}{\partial \omega_i}\right) a_o + \left(\frac{\partial y_i}{\partial \omega_i}\right) a_1 x_i + \left(\frac{\partial y_i}{\partial \Phi_i}\right) b_o + \left(\frac{\partial y_i}{\partial \Phi_i}\right) b_1 x_i + \left(\frac{\partial y_i}{\partial \chi_i}\right) c_o +$$
$$\left(\frac{\partial y_i}{\partial \chi_i}\right) c_1 x_i + \left(\frac{\partial y_i}{\partial Xo_i}\right) d_o + \left(\frac{\partial y_i}{\partial Xo_i}\right) d_1 x_i + \left(\frac{\partial y_i}{\partial Yo_i}\right) e_o + \left(\frac{\partial y_i}{\partial Yo_i}\right) e_1 x_i +$$
$$\left(\frac{\partial y_i}{\partial Zo_i}\right) f_o + \left(\frac{\partial y_i}{\partial Zo_i}\right) f_1 x_i - K_i$$

Equation (110) contains 12 unknown orientation parameters (a_o to f_1); two for each orientation element. Since each observed point gives a set of two equations of the form (110) then for a single photo, a minimum number of six full control points (known in X, Y and Z), distributed as shown in Fig. 99, are needed to determine the unknown parameters. For two overlapping photographs, the number

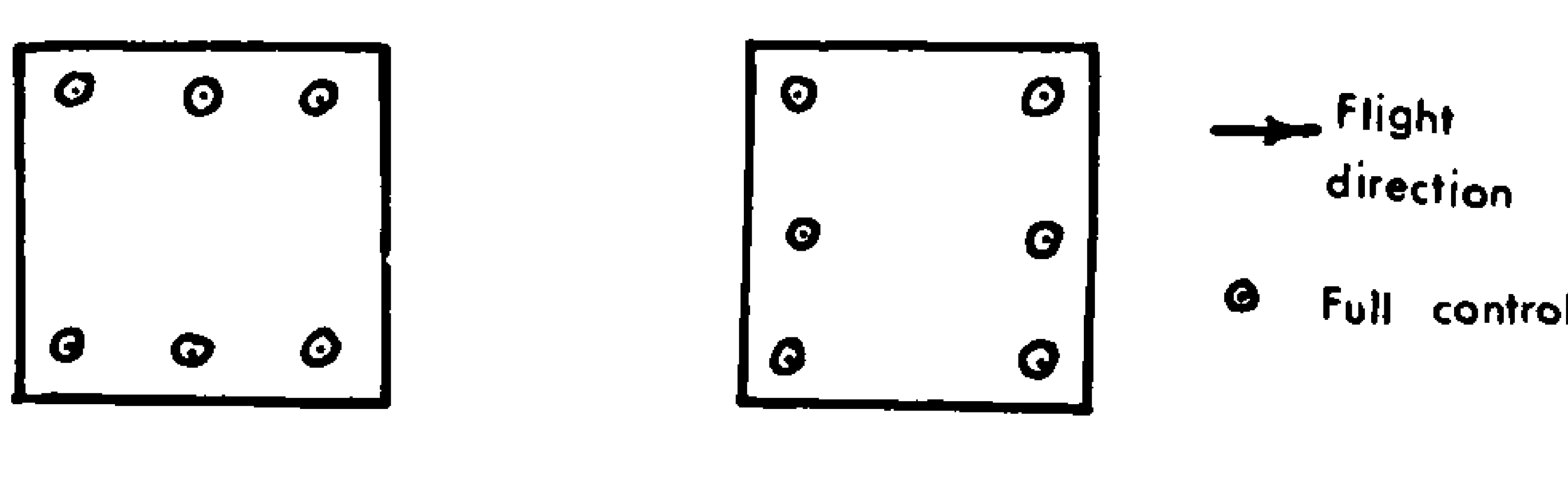

Fig. 99 Ground control required for a single photograph.

(a) shutter moving parallel to the flight direction

(b) shutter moving across the flight direction.

of unknown parameters will be 24, but the number of control points required will be reduced due to the fact that either six (case a) or four (case b) of the control points will be common to the two photos. Hence for case (a) the number of control points required for the two overlapping photographs will be 8 (known in X, Y and Z) while for case (b), 12 control points (known in X, Y and Z) will be required (Fig. 100). In case (b), for each photograph, there will be three redundant control points which would allow the use of the least square method

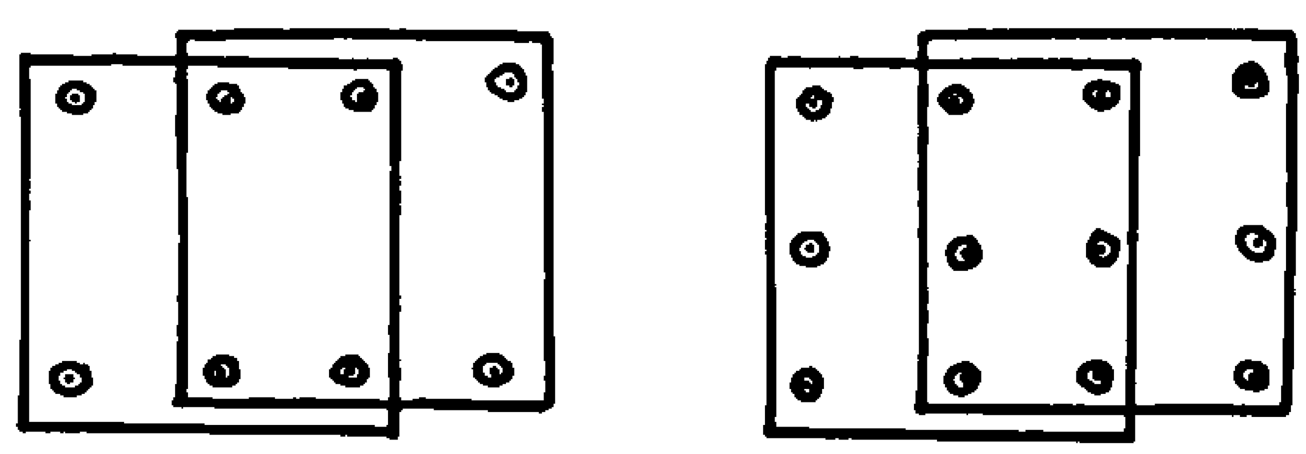

(a) (b)

Fig. 100 Ground control required for a pair of overlapping photographs.

of adjustment. Values of the computed parameters would be used to determine new correction values from equation (109). The new values for changes in orientation elements are then used in equation (105), to determine new approximate values for the orientation elements and the procedure is repeated. Hence an iterative solution will finally lead to the exact exterior orientation elements for each point on the photograph, determined by parameters a_o, b_o .... to f_1.

The previous discussion considered the cases where the direction of the shutter motion is known. In many cases, the direction of the shutter motion will be unknown and hence a method must be devised which takes account of this.

In this case, we will adopt the photo-coordinate system used for case (a) in the previous discussion. First, let us assume that the shutter is moving parallel to the flight direction. The time, t_i, will be a linear function of the x-photo-coordinate. The corrections to the exterior orientation elements would be expressed as in equation (109). The same iterative procedure will be used to determine the 12 unknown parameters and hence the values of the exterior orientation elements. These values for the parameters could be close to zero if the slit movement was in the y-direction or values which are more substantial if the slit movement was in the x-direction. Whatever the values, however, they represent the starting point (the initial approximation) for the solution based on the assumption that slit movement was in the y-direction. Now, the corrections to the exterior orientation elements would be given as linear functions of the y-photo-coordinate and the same procedure would again be used to determine new values for the exterior orientation elements. In this case, the same number and distribution of control points shown in Fig. 100 (b) will be required.

5.6.3. Space Intersection

Given the image coordinates in the photo system and the orientation elements being derived by the space resection solution, the projective relationship given in equation (102) can be used to solve the ground coordinates (X, Y and Z) of the object. This is done by space intersection where measurements made on the two overlapping photographs of the stereomodel and the exterior orientation elements determined by the space resection method are used to solve the scale factor.

The projective equations relating the object on the ground and its corresponding images on the two photographs would be given by:

$$\begin{bmatrix} X_i - Xo_i' \\ Y_i - Yo_i' \\ Z_i = Zo_i' \end{bmatrix} = \lambda_i' \; A_i' \begin{bmatrix} x_i' \\ y_i' \\ -f \end{bmatrix} \quad \ldots\ldots\ldots\ldots \quad (111)$$

and

$$\begin{bmatrix} X_i - Xo_i'' \\ Y_i - Yo_i'' \\ Z_i - Zo_i'' \end{bmatrix} = \lambda_i'' \; A_i'' \begin{bmatrix} x_i'' \\ y_i'' \\ -f \end{bmatrix} \quad \ldots\ldots\ldots\ldots \quad (112)$$

where the terms with a single prime correspond to one photograph (say the <u>left-hand photograph</u>) and the terms with double prime correspond to the other (<u>right-hand photograph</u>).

From these equations, the <u>scale factor</u> will be given (Konecny, 1975):

$$\lambda_i' = \frac{(Xo_i'' - Xo_i')\; W_i'' - (Zo_i'' - Zo_i')\; U_i''}{U_i'\; W_i'' - U_i''\; W_i'} \quad \ldots\ldots\ldots\ldots \quad (113)$$

and

$$\lambda_i'' = \frac{(Zo_i'' - Zo_i')\; U_i' - (Xo_i'' - Xo_i')\; W_i''}{U_i'\; W_i'' - U_i''\; W_i'} \quad \ldots\ldots\ldots\ldots \quad (114)$$

where

$$\begin{bmatrix} U_i' \\ Y_i' \\ W_i' \end{bmatrix} = A_i' \begin{bmatrix} x_i' \\ y_i' \\ -f \end{bmatrix} \quad \ldots\ldots\ldots\ldots \quad (115)$$

and

$$\begin{bmatrix} U_i'' \\ Y_i'' \\ W_i'' \end{bmatrix} = A_i'' \begin{bmatrix} x_i'' \\ y_i'' \\ -f \end{bmatrix} \quad \ldots\ldots\ldots\ldots \quad (116)$$

.

Substituting for the scale factor, and the given values of the image coordinates and the orientation elements in equation (111) or equation (112), the ground coordinates $\begin{bmatrix} X \\ Y \\ Z \end{bmatrix}$ of the object in question can be determined.

5.7 Space Resection with Additional Parameters

One of the main problems which is currently under investigation by photogrammetrists is the detection and elimination of systematic errors of photogrammetric image or model coordinates. The most direct method to determine and eliminate systematic errors is to carry out comprehensive system calibrations and then subsequently correct the image and model coordinates.

In general, the calibration of the photogrammetric system can be achieved by use of a test field in which signalised ground control points are used. The test field calibration is only used for metric cameras where accurate determination of the systematic errors in the photogrammetric data is required. In this method, however, additional flights and measuring effort is required.

More recently another approach has been adopted - that of self-calibration in which no prior system calibration is carried out, the calibration being achieved by suitable procedures while forming the model itself. This has been applied particularly to aerial triangulation using the bundle method, especially by Brown (1976) and by Bauer and Muller (1972). The principle of the self-calibration method is to add corrections to the measured image coordinates so that the projective relations defined in equation (100) are adhered to. The correction parameters are selected such that they model and correct for the appropriate distortions in the photography. The technique has in fact been used successfully even when a prior calibration has been carried out, as the method shows up systematic errors whose existence had previously been unsuspected or overlooked during the calibration stage.

Since photography taken with reconnaissance cameras equipped with focal plane shutters is taken with a totally uncalibrated system and one which has dynamic imaging characteristics, the additional parameter method appeared to be an obvious one to experiment with in the context of this photography.

The solution for the additional parameters is carried out during the space resection phase, in other words, they are solved simultaneously with the camera exterior orientation elements. The space intersection phase is then carried out using the corrected image coordinates.

The following error model has been chosen (Brown, 1976, Ebner, 1976) to be applied as a solution for reconnaissance frame photography.

$$\Delta x = a_1 x + a_2 y + b_1 xy + b_2 xy^2 + b_3 x^2 y + c_1 xr^2 + c_2 xr^5 + d_1 \quad \ldots . (117)$$

$$\Delta y = -a_1 y + a_2 x + b_4 xy + b_5 xy^2 + b_6 x^2 y + c_1 yr^2 + c_2 yr^5 + d_2$$

These equations are based on systematic errors due to film deformation and radial distortion of the image caused by earth curvature, atmospheric refraction or lens distortion.

e.g. the term a_1 corrects for change in image scale,

the term a_2 corrects for rotation of the photograph ,

the b-terms are to correct for film deformation,

the c-terms are to correct for radial distortion,

the d-terms are to correct the position of the principal point.

It can be seen that the a-terms correct for displacements similar to those caused by the focal plane shutter derived in chapter IV. The term a_1 corrects for the distortion (elongation or compression) caused by the focal plane shutter when it is moving parallel to the direction of flight, and for the scale change caused by a lack of knowledge of the principal distance (f). The term a_2 corrects for the distortion induced by the focal plane shutter when it is moving across the direction of flight. Again, since there are no fiducial marks or reseau crosses on the reconnaissance photograph, the addition of the b-terms to the error model will be the only means to correct for film deformation. Also, since the principal point cannot be exactly located, corrections for lens distortion would be referred to an erroneous principal point (the geometric centre of the photograph), hence additional parameters (the c-terms) for radial distortion are needed; and the addition of constant terms (the d-terms) to correct for the position of the principal point will be essential.

The first group contains only two terms (a_1 and a_2) and since each control point (known in X, Y and Z) will give two equations of the form (117), then only one full control point (known in X, Y and Z) in addition to the three full control points that are needed to solve for the six exterior orientation elements of the camera, should be available for each single photo (Fig. 101). In this case there will be two redundant control points when the stereomodel is considered (Fig. 101 c).

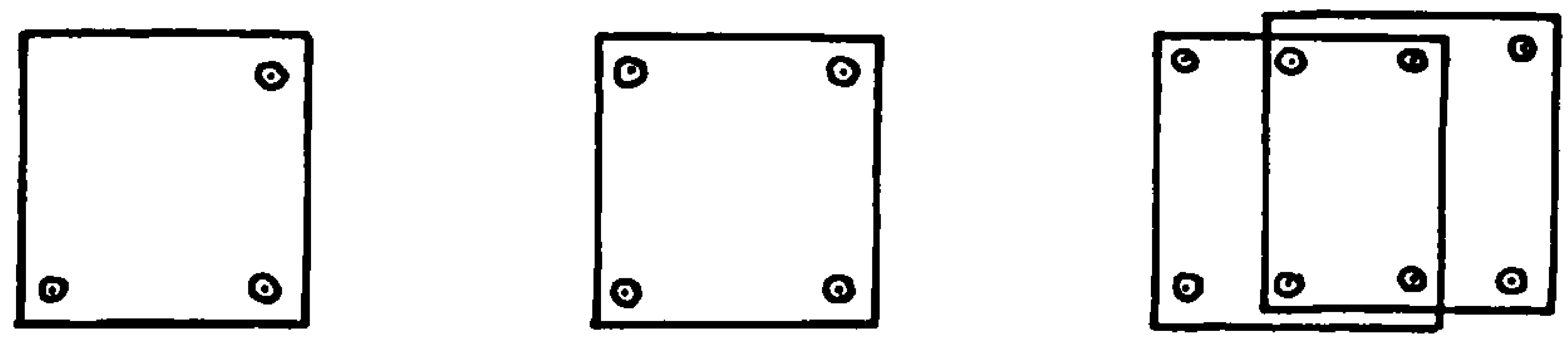

(a) (b) (c)

Fig. 101 Ground control required for the first group.

(a) Single photo - ground control to solve for the six exterior orientation elements.

(b) Single photo - ground control to solve for the six exterior orientation elements and the a-terms.

(c) Two overlapping photographs.

When group two (the b-terms) is added to the error model, the number of ground control points required for a single photo will be seven, known in X, Y and Z. Considering a stereo model, only two full control points are to be added (Fig. 102), and one redundant control point per single photo will be available.

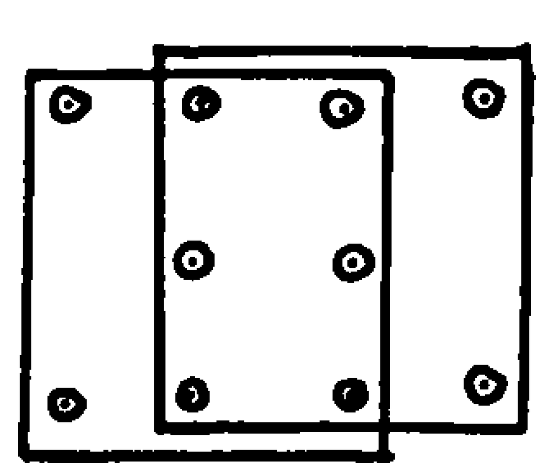

Fig. 102 Ground control required for the first three groups

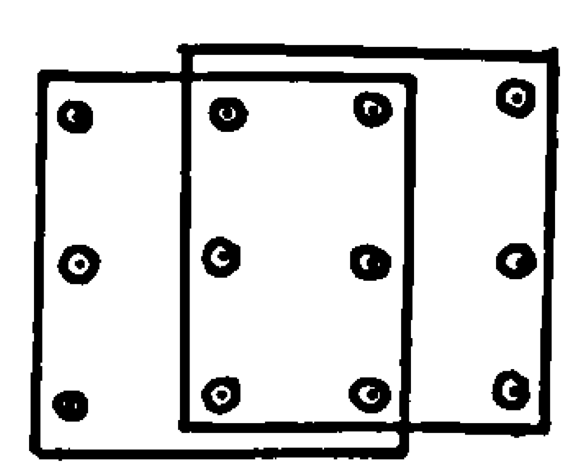

Fig. 103 Ground control required for the four groups

The addition of group three (the c-terms) to the error model will raise the number of unknown parameters to sixteen (including the six exterior orientation elements) and hence eight control points as those given in Fig. 102 will be sufficient for the solution. Now, when the fourth group (the d-terms) is added to the error model, one more control point (known in X, Y and Z) for each single photo will be required, making the total number of control points required per single photo as nine, or twelve for the two overlapping photos (Fig. 103).

Very high correlation between the parameters is a serious problem and would probably lead to an unstable solution. To avoid this correlation, it can be tested by the correlation matrix generated from the covariance matrix. The most ineffective parameters, having high correlations with others, could then be excluded from the error model.

5.8 Conventional Analytical Relative and Absolute Orientation followed by a Polynomial Adjustment to correct Terrain Coordinates

This alternative approach has been mentioned in the Introduction to this Chapter. Unlike the previous methods, no attempt is made to introduce corrections to the measured image coordinates. Instead, these are simply accepted and the normal procedure of analytical relative and absolute orientation is carried out.

In computing the relative orientation and forming the model coordinates, different procedures may be used depending on the mathematical approach. The method used here is based on the principle that when two photographs are in correct relative orientation, rays from corresponding image points intersect; the two corresponding image points and the two projection centres lie on these intersecting rays and must lie in one plane. The method is explained in detail by Methley (1972). This method is chosen mainly because a computer program developed by Methley (1972) is available for use.

The model coordinates formed after relative orientation are then transferred to terrain coordinates after solving for the seven orientation elements Ω, Φ, K, λ, X_o, Y_o, Z_o. A detailed description of the solution of this problem will be given later in Chapter VII when describing the computer program.

The deviations of the computed terrain coordinates from the given coordinates of the control points will then be reduced by means of polynomials.

Taking a ground coordinate system with the X- and Y-axis along and across the flight direction respectively, the displacements of the terrain coordinates are given by the following differential equations (Hallert, 1960) which are well known in photogrammetry:

$$dX = dX_o - \frac{X}{H} dZ_o - \frac{XY}{H} d\omega_o + \left(\frac{X^2}{H} + H\right) d\phi_o - Yd\kappa_o + \left[(dx_{imc} - dX_{fp}) \frac{H}{f}\right] \quad \ldots\ldots\ldots\ldots \quad (118)$$

$$dY = dY_o - \frac{Y}{H} dZ_o + \left(H + \frac{Y^2}{H}\right) d\omega_o + \frac{XY}{H} d\phi_o - X d\kappa \ldots\ldots \quad (119)$$

$$dZ = \frac{H}{B} dX_o - \frac{X}{B} dZ_o - \frac{XY}{B} d\omega_o + \left(\frac{X^2}{B} + \frac{H^2}{B}\right) d\phi_o - \frac{YY}{B} d\kappa_o \left[(dx_{imc} - dx_{fp}) \frac{H^2}{Bf}\right] \quad \ldots\ldots\ldots\ldots \quad (120)$$

where the terms between large brackets are added due to the effect of parallel motion focal plane shutter and IMC (Konecny, 1975), this term will be zero for perfect IMC,

dX = displacement along the flight direction,

dY = displacement transverse to the flight direction,

dZ = displacement in height,

H = flying height above ground,

B = base of photography

and $d\omega_o$, $d\Phi_o$, $d\chi_o$, dX_o, dY_o, dZ_o are the changes in the exterior orientation elements. For this type of photography, these changes are functions of the craft speed V and change in speed dV (with components $\dot{X}_o$, $\dot{Y}_o$, $\dot{Z}_o$ and $\ddot{X}_o$, $\ddot{Y}_o$, $\ddot{Z}_o$ respectively) and the roll ($\dot{\omega}_o$), yaw ($\dot{\Phi}_o$) and pitch ($\dot{\chi}_o$) and changes in roll ($\ddot{\omega}_o$), yaw ($\ddot{\Phi}_o$) and pitch ($\ddot{\chi}_o$). These can be expressed as follows:

$$
\begin{aligned}
dX_o &= t_i\dot{X}_o + \tfrac{1}{2}t_i^2\,\ddot{X}_o \\
dY_o &= t_i\dot{Y}_o + \tfrac{1}{2}t_i^2\,\ddot{Y}_o \\
dZ_o &= t_i\dot{Z}_o + \tfrac{1}{2}t_i^2\,\ddot{Z}_o \\
d\omega_o &= t_i\dot{\omega}_o + \tfrac{1}{2}t_i^2\,\ddot{\omega}_o \\
d\Phi_o &= t_i\dot{\Phi}_o + \tfrac{1}{2}t_i^2\,\ddot{\Phi}_o \\
d\chi_o &= t_i\dot{\chi}_o + \tfrac{1}{2}t_i^2\,\ddot{\chi}_o
\end{aligned}
\qquad \ldots\ldots\ldots\ldots\ldots \quad (121)
$$

Assuming the slit velocity to be constant, the time (t_i) will be a linear function of the x-photo-coordinate when the shutter is moving parallel to the flight direction. Hence the above relations can be expressed as follows:

$$
\begin{aligned}
dX_o &= a_o + a_1 X + a_2 X^2 \\
dY_o &= b_o + b_1 X + b_2 X^2 \\
dZ_o &= c_o + c_1 X + c_2 X^2
\end{aligned}
\qquad \ldots\ldots\ldots\ldots \quad (122)
$$

Cont'd)

$$d\omega_o = d_o + d_1 X + d_2 X^2 \quad \ldots\ldots\ldots\ldots\ldots \quad (122)$$

$$d\Phi_o = e_o + e_1 X + e_2 X^2$$

$$d\kappa_0 = f_o + f_1 X + f_2 X^2$$

in which the terms a_o - f_o refer to corrections to the orientation elements at the time of exposing the central point of the photograph, the terms a_1 - f_1 refer to the craft speed, roll, yaw and pitch, and the terms a_2 - f_2 refer to changes in the craft speed, roll, yaw and pitch.

Substituting equation system (122) into equations (118), (119) and (120) produces the displacements dX in the flight direction, dY transverse to the flight direction and dZ in height respectively:

$$dX = A_o + A_1 X + A_2 X^2 + B_o Y + B_1 XY + B_2 X^2 Y \quad \ldots\ldots \quad (123)$$

$$dY = C_o + C_1 X + C_2 X^2 + D_o Y + D_1 XY + D_2 X^2 Y$$
$$+ E_o Y^2 + E_1 XY^2 + E_2 X^2 Y^2 \quad \ldots\ldots\ldots\ldots \quad (124)$$

$$dZ = A_3 + A_4 X + A_5 X^2 + B_3 Y + B_4 XY + B_5 X^2 Y \quad \ldots\ldots \quad (125)$$

where the A-terms represent the effect of changes in $d\Phi_o$, dX_o and dZ_o, and the combined effect of the focal plane shutter and IMC on the image coordinates; the B-terms represent the effects of changes in $d\omega_o$ and $d\kappa_o$; the C-terms represent the effect of changes in dY_o, $d\omega_o$ and $d\kappa_o$; the D-terms represent the effect of changes in dZ_o and $d\Phi_o$ while the E-terms represent the effect of changes in $d\omega_o$ separately.

Equations (123), (124) and (125) can be rearranged and written in the following forms:

$$dX = a_o + a_1X + a_2Y + a_3XY + a_4X^2 + a_5X^2Y \quad \ldots\ldots\ldots \quad (126)$$

$$dY = b_o + b_1X + b_2Y + b_3XY + b_4X^2 + b_5X^2Y$$
$$+ b_6Y^2 + b_7Y^2X + b_8X^2Y^2 \quad \ldots\ldots \quad (127)$$

$$dZ = c_o + c_1X + c_2Y + c_3XY + c_4X^2 + c_5X^2Y \quad \ldots\ldots\ldots \quad (128)$$

It should be noticed that the polynomial coefficients used in these equations are not those used in equation system (117).

It is clear that six control points known in X-direction, nine in the Y-direction and six in height (Z) should be available within the model area to solve the equations.

If the shutter is moving across the flight direction the changes in the exterior orientation elements would similarly be expressed as functions of the Y-ground coordinates and the same analysis would result in the following equations:

$$dX = A_o + A_1X + A_2Y + A_3XY + A_4X^2 + A_5X^2Y$$
$$+ A_6Y^2 + A_7XY^2 + A_8X^2Y^2 \quad \ldots\ldots\ldots\ldots\ldots \quad (129)$$

$$dY = B_o + B_1X + B_2Y + B_3XY + B_4Y^2 + B_5Y^2X \quad \ldots\ldots\ldots \quad (130)$$

$$dZ = C_o + C_1X + C_2Y + C_3XY + C_4X^2 + C_5X^2Y$$
$$+ C_6Y^2 + C_7XY^2 + C_8X^2Y^2 \quad \ldots\ldots\ldots\ldots\ldots\ldots \quad (131)$$

A combination of the two cases would lead to a general solution expressed by the following equations:

$$dX = A_o + A_1X + A_2Y + A_3XY + A_4X^2 + A_5X^2Y$$
$$+ A_6Y^2 + A_7XY^2 + A_8X^2Y^2 \quad \ldots\ldots\ldots\ldots\ldots \quad (132)$$

$$dY = B_o + B_1X + B_2Y + B_3XY + B_4X^2 + B_5X^2Y + B_6Y^2 + B_7XY^2 + B_8X^2Y^2 \quad \ldots\ldots\ldots\ldots\ldots\ldots \quad (133)$$

$$dZ = C_o + C_1X + C_2Y + C_3XY + C_4X^2 + C_5X^2Y + C_6Y^2 + C_7XY^2 + C_8X^2Y^2 \quad \ldots\ldots\ldots\ldots\ldots\ldots \quad (134)$$

A solution of the general case equations requires a minimum of nine ground control points known in X, Y and Z.

5.9 Comparison between the Three Techniques

After describing the three different approaches (Space Resection/Space Intersection; Space Resection with Additional Parameters; Polynomial Adjustment of Derived terrain coordinates) which are suggested to treat the metric problem of the reconnaissance frame photography, a comparison between the different techniques will follow.

The polynomial adjustment technique seems to be the simplest to implement since it involves direct conventional relative and absolute orientation methods followed by an adjustment that can easily be programmed. Hence it can be easily utilised by most photogrammetrists and they would not encounter computational problems which are novel or unfamiliar to them.

The other two methods are very much alike from point of view of mathematical formulation. In the first (Space Resection/Space Intersection) method, parameters involving a time factor are added to the observation equations derived from the collinearity equations. In the other (Space Resection with Additional Parameters) an error model is also added to the observation equations. Therefore, the mathematical formulation is similar for the two methods and a single program can be developed to apply the two techniques. As has already been mentioned, a problem to be encountered when using the Additional Parameters is that of high correlation between the parameters which may give an unstable solution.

To apply each technique fully, the number of ground control points required for a single pair of photographs is given in Table 7 below.

Method	Space Resection/ Space Intersection	Space Resection with Additional Parameters	Polynomial Adjustment of derived terrain coordinates
No. of ground controls (known in X,Y,Z) for a pair of overlapping photographs	8 - 12	12	9

Table 7 Ground control required for the different techniques.

If the direction of the shutter motion is known, then the Space Resection/Space Intersection solution will require only 8 control points (known in X, Y and Z) and that would be the minimum required. If a general case is to be used then the Polynomial Adjustment method would require 9 control points (known in X, Y and Z) and that will be the minimum required.

These techniques, however, should be tested using practical data in order to evaluate their effects. The work associated with these tests will be discussed in the chapters which follow.

CHAPTER VI

Experimental Tests - Procedures, Characteristics of the Photography and Provision of the Control points for the Test Fields

CHAPTER VI

EXPERIMENTAL TESTS - PROCEDURES, CHARACTERISTICS OF THE PHOTOGRAPHY AND PROVISION OF THE CONTROL POINTS FOR THE TEST FIELDS

6.1 Introduction

The quality of the high resolution photography produced by the reconnaissance frame camera was discussed in Chapter III. The theoretical investigations in Chapters IV and V showed that this type of photography can be corrected analytically in various ways to allow useful metric measurements to be made. However, the validity of these analytical techniques must be established by suitably designed experimental tests.

6.1.1 Test procedures

The procedures used in this case are to make measurements on different types of reconnaissance frame photography taken over test fields with numerous suitably positioned ground points whose coordinates are already known. Using certain of these as control points for absolute orientation, the analytical techniques are then applied to the measured photo-coordinates to produce the terrain coordinates for all the points in the test field. The next step is to compare the photogrammetrically-derived coordinates with the known coordinates of these points and to compute the discrepancies between the two sets of coordinates. Finally, an analysis of the residual errors is conducted to establish the extent and nature (i.e. whether systematic, random, etc.) of these errors and to make comparisons of the various procedures which have been applied, with a view to establishing which are the most satisfactory for use with reconnaissance frame photography.

The tests have been carried out with two quite different cameras with totally different operational characteristics - the one, A.G.I. F-126 camera equipped with a wide-angle lens and having a format of 23 x 23 cm, the other the Actron KA-74 camera in its S-190B modified space-hardened form with a narrow-angle lens and a format of 11.5 x 11.5 cm. The two cameras have also been used with quite different IMC characteristics, the F-126 with the moving film technique, the S-190B camera by rocking the camera during exposure. Furthermore, the photography taken with these cameras has been taken at opposite ends of the operational spectrum. The F-126 photography was produced at comparatively large scales (1/20,000 and 1/40,000 scale) from an aircraft; the S-190B photographs are ultra small scale (1/950,000 scale) taken from a fast moving Earth-orbiting satellite. By utilising such very different parameters in the two sets of test photographs, it should be possible to indicate the range of application of the techniques which have been devised in Chapter V for use with reconnaissance frame photography.

6.2 The S-190B Photography Test

6.2.1 Introduction

The manned Skylab project was planned and implemented by the U.S. National Aeronautical and Space Administration (NASA), the satellite or space station being launched into a circular orbit of 435 km above the Earth on May 14, 1973. Six optical and electronic remote sensing systems or devices were mounted in the satellite for the Skylab Earth observational programme. These systems formed the Earth Resources Experiment Package (EREP) and comprised the following:-

(i) Multispectral photographic camera (S-190A)

(ii) Earth Terrain Camera (S-190B)

(iii) Infrared Spectrometer (S-191)

(iv) Multispectral Scanner (S-192)

(v) Microwave Radiometer (Scatterometer and Altimeter, S-193)

(vi) L-Band Radiometer (S-194).

The photographic components of EREP are the first two items listed. The objective of these two cameras was to photograph various parts of the Earth's surface (exhibiting very different terrain characteristics) over the whole spectral range for which photographic emulsions are available, i.e. from the blue end of the visible part of the spectrum to the near-infrared. High resolution photography with sufficient spectral definition was required to simplify the work of specialists in interpreting and analysing the photography.

The first item is the S-190A multispectral photographic system. It consists of six Itek 70 mm film cameras each with its optical system, shutter and film transport assembly, but sharing a common mount or platform and synchronised so that all six shutters are operated simultaneously. The focal length of each camera is 6 in. (152 mm), giving a negative scale of 1 : 2,850,000. The image format is 57 x 57 mm so that the ground coverage produced by a single frame is 163 km square. The second part of the photographic system is the S-190B Earth Terrain Camera (ETC) used in the test work in this project.

6.2.2 The S-190B Camera

The S-190B camera (Fig. 104) was built by Actron Industries, Inc., under contract to NASA (McLaurin, 1972). The body of the camera is a modified Hycon KA-74 reconnaissance camera equipped with a bi-directional focal plane shutter and vacuum film flattening. IMC is achieved by rocking the entire camera in its mount during the exposure. This allows the use of quite long shutter speeds (1/100, 1/140, 1/200 sec) which allows finer grained, higher resolution film to be used than might be expected from a fast-moving satellite. This IMC system can be set to operate within a range of 0 to 25 mrad/sec (in the case of Skylab, the actual angular rotation rate used was 18 mrad/sec). The camera was equipped with a lens having a focal length of 18 in (460 mm), a maximum aperture of f/4 and a maximum radial distortion of $\pm$ 10 μm. The format size of 11.5 x 11.5 cm. at the Skylab altitude (H = 435 km) covers a terrain area of 109 x 109 km at the scale of 1/945,600.

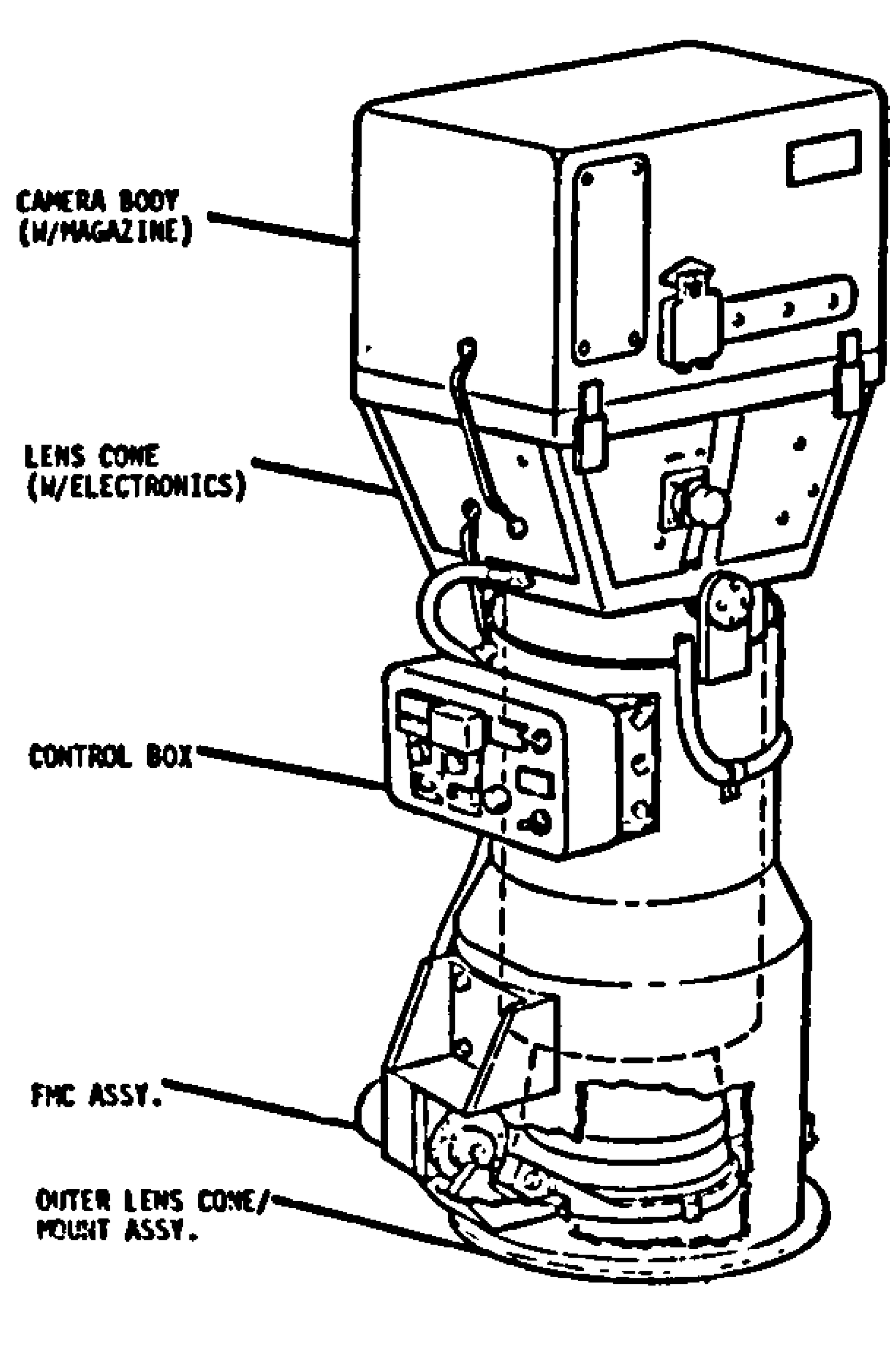

Fig. 104 The S-190B Skylab Camera

The S-190B camera was to provide high resolution colour, colour infrared or monochrome photography within the field of view of the smaller scale, lower resolution S-190A cameras. The three Kodak films used with the S-190B camera are given in Table 8 below.

Type	Description	Wavelength (μm)
SO-242	High resolution colour	0.4 to 0.7
EK 3414	High resolution Panchromatic	0.5 to 0.7
EK 3443	Colour infrared (i.e. false colour)	0.5 to 0.88

Table 8. Films used with the S-190B camera

Estimates of the ground resolutions obtainable by each of these films were made by Actron using computer simulations which modelled the IMC system, the altitude error rates of the spacecraft, the lens characteristics, the shutter speed and the film and filter characteristics. These resolution values are shown in Table 9, for each of the three possible shutter speeds.

Case	Film	Shutter speed (sec)	Ground resolution (High contrast 1000:1) (m/lp)	Ground resolution (Low contrast 2:1) (m/lp)	Equivalent Negative Resolution (lp/mm)
1	3443	1/100	21	39	24
2	3443	1/200	21	38	25
3	3443	1/500	21	38	25
4	3414	1/100	8	15	63
5	3414	1/200	6	11	86
6	3414	1/500	5	10	94
7	SO-242	1/100	12	22	43
8	SO-242	1/200	11	20	47
9	SO-242	1/500	11	20	47

Table 9. Predicted on-axis ETC resolution (McLaurin, 1972)

This table shows that the expected low contrast ground resolution from the S-190B camera would lie in the range from 10 to 39 metres per optical line pair. As would be expected, the highest resolution would be from the black and white 3414 film and the lowest from the false colour 3443 emulsion. It should be noted that a new colour infrared (i.e. false colour) SO-131 film with greatly improved image structure properties was actually used instead of the type 3443 originally planned and used in the predictions given above.

Welch (1976) determined the MTF's for second generation S-190B photographs by cascading the lens MTF with the appropriate MTF's for the original and duplicating films (Fig. 105). The duplicating films used to make the copies were type 2430 for the black and white photographs and type 2447 for the colour and false-colour photographs. Resolution figures were then determined at 1.6 : 1 contrast ratio from the intersection of the MTF's within the threshold modulation range of 5 to 10 percent (Welch, 1976). The on-axis resolution values are shown in Fig. 106 and Table 10.

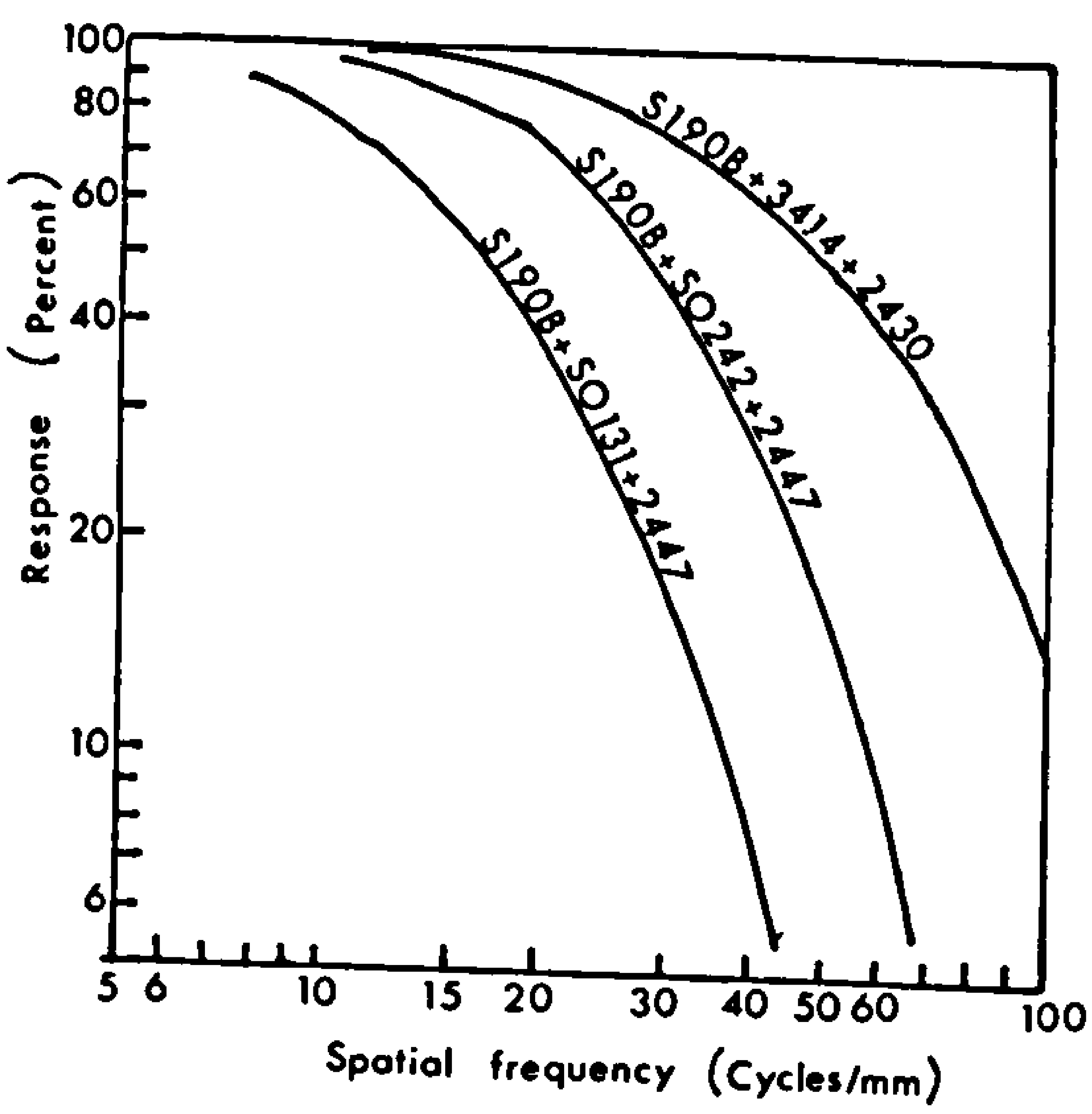

Fig. 105 Predicted MTF's for second-generation S-190B photographs obtained by cascading the lens MTF with the appropriate MTF's for the original and duplicating films (Welch, 1976).

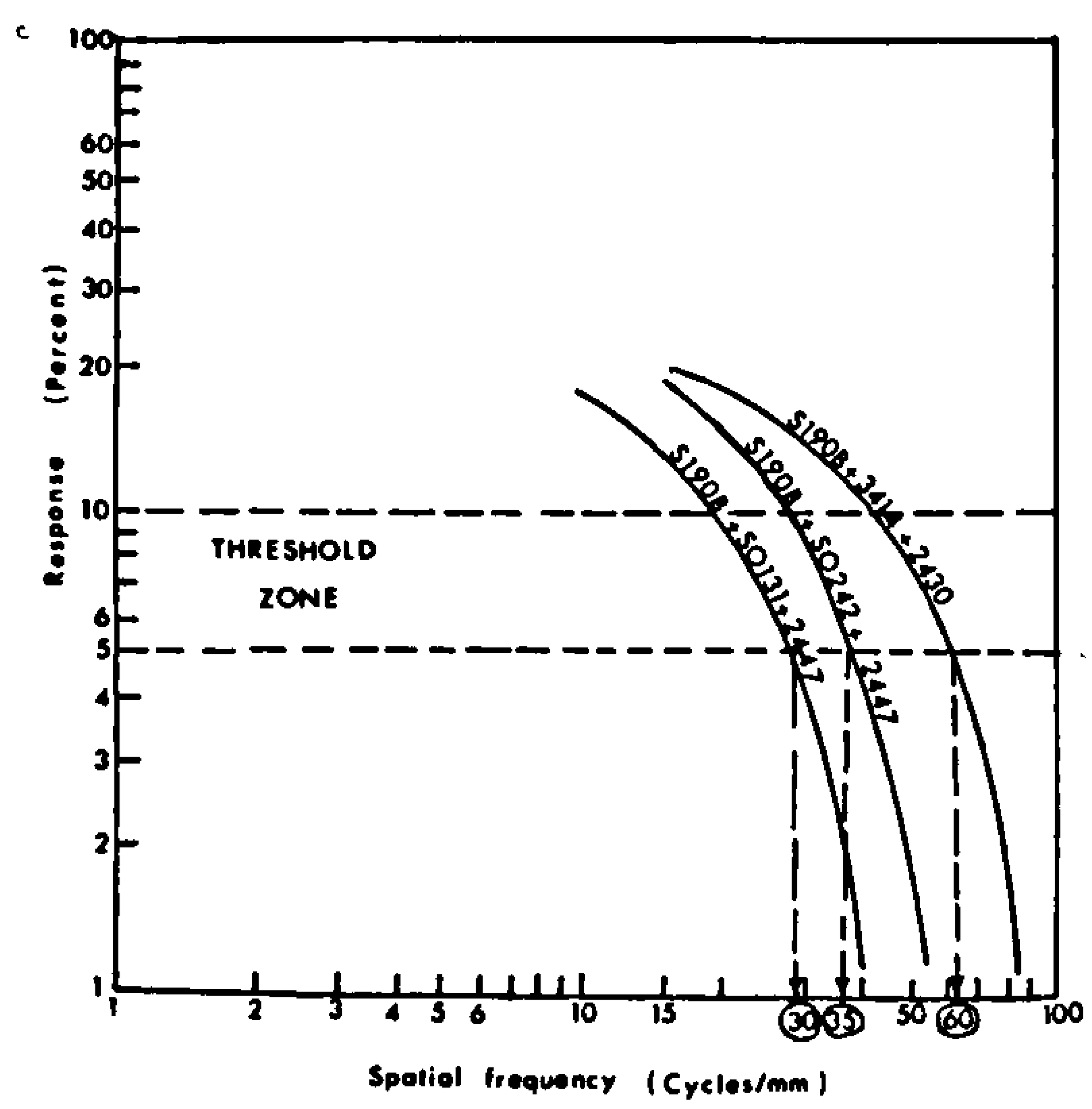

Fig. 106 Resolution estimate for low-contrast (1.6 : 1) targets (Welch, 1976).

Film/Duplicating film	Resolution estimates (lpr/mm) for 1.6 : 1 target contrast	Ground resolution (m)
3414/2430	60 - 70	15
SO-242/2447	35	25
SO-131/2447	30	30

Table 10. Resolution estimates for second-generation S-190B photographs (Welch, 1976)

It can be seen from this table and Table 9 that the ground resolution values of the the S-190B photographs agree well with the predicted resolution values (e.g. the predicted ground resolution for the SO-242 true colour film ranges from 20 to 22 metres, and the ground resolution for the second generation photos is found to be 25 metres). The small difference however, may be due to the fact that duplicating films were not used when predicting the resolution in the first case.

Turning to the metric aspects of the S-190B camera McLaurin, in his paper (1972), described the design of the S-190B camera as follows:- "The design of the S-190B will limit its applications. First, the S-190B is not a metric camera in the photogrammetric sense. Because the image frame is a part of the removable film magazine and because of the use of the focal plane shutter, the geometric quality of the photograph is limited. The principal point cannot be precisely located, and therefore analytical applications will be limited. The S-190B has a limited field of view, 14 degrees. When the camera is operated for 60 percent overlap, the base-height ratio is only 0.10; thus the use of the S-190B for stereoscopic height determination will be especially limited." All of these points shall of course be tested in the course of the experimental work carried out with the S-190B photographs. As will be seen later, there are, in fact, metric possibilities with this type of camera and photographs.

6.2.3 Photography

The photography used in the tests consisted of a strip of three photographs exposed on the SO-242 high resolution colour film. Second generation film transparencies made from the original film were used in the actual test. These, together with the small scale maps covering the area, were very kindly made available by Professor R. Welch of the University of Georgia, U.S.A. (who is a Glasgow graduate). The three photographs used - nos. 01334/5/6 - formed two stereomodels with a 60 percent longitudinal overlap. Fig. 107 shows the ground coverage of the central photograph (01335). The photographs have good illumination and high resolution throughout the format. No clouds were present nor was there an excessive amount of haze so that the observation conditions were good.

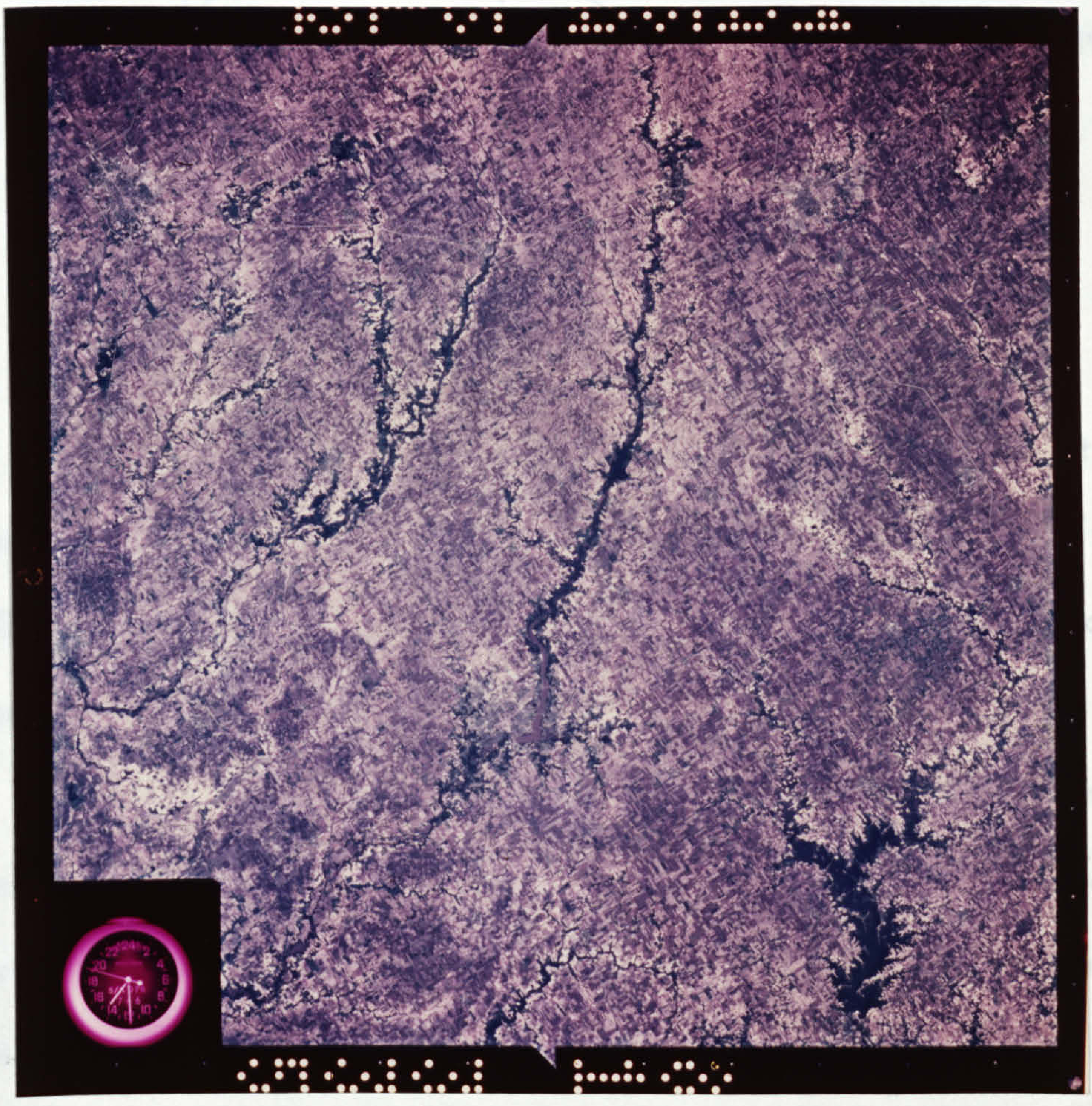

Fig. 107 Photo No. 01335

6.2.4 Test Area and Ground Control

The area covered by the photography was the central part of the State of Illinois in the U.S.A. This area extends from 39°30' N to 40°45'N in latitude and from 88°15'W to 90°0'W in longitude as shown in Fig. 108

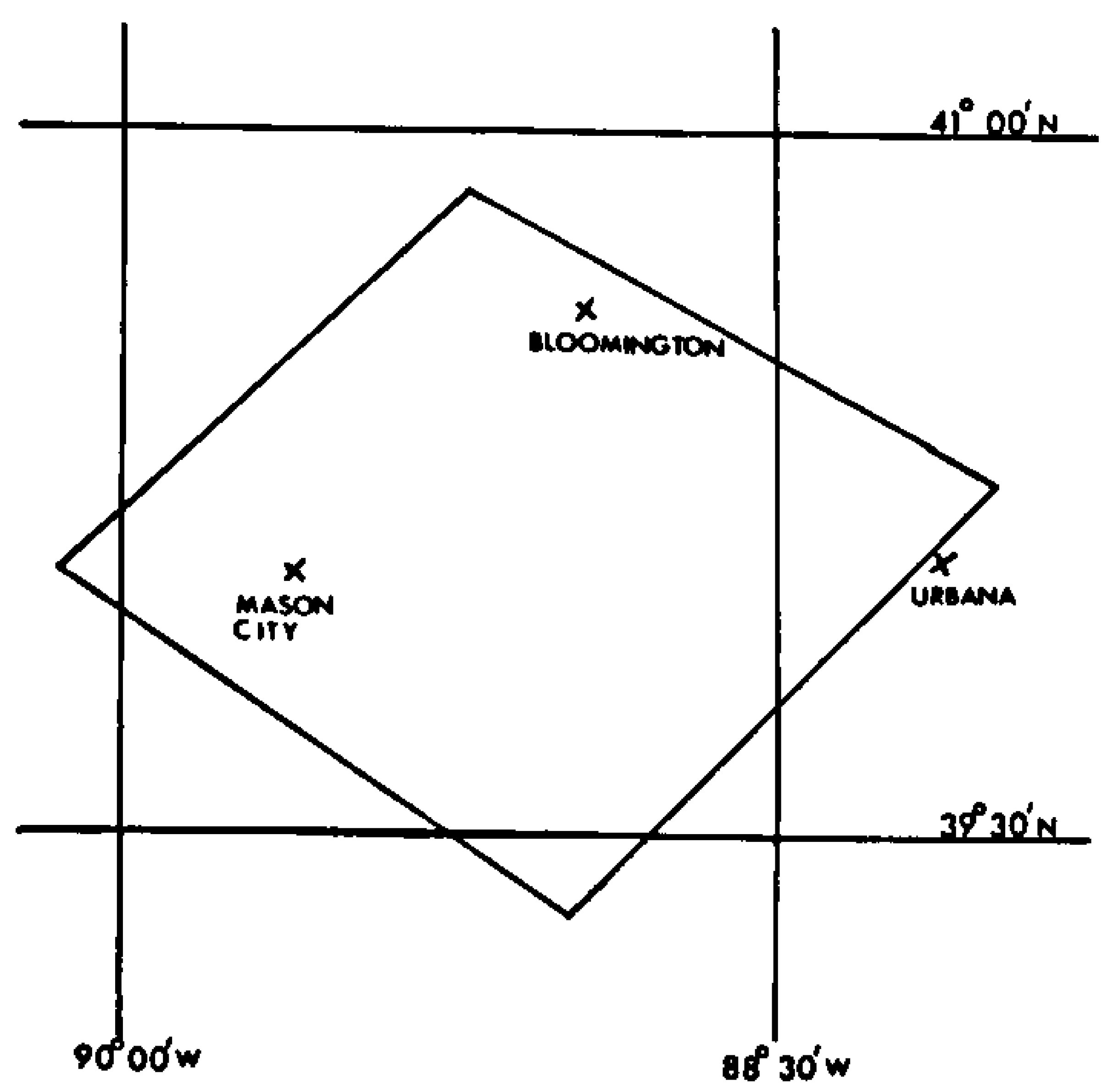

Fig. 108 Geographical boundaries of the S-190B test area

The small-scale map coverage for the area comprised 33 maps at 1/24,000 scale and 25 1/62,500 scale. All these maps had been produced by the U.S. Geological Survey (U.S.G.S.), being plotted on a Polyconic projection and compiled to U.S. National Map Accuracy Standards.

Mirror stereoscopes were used to select and identify suitable control and check points on the Skylab photography which could also be accurately located on these maps. Road intersections were found to be the most suitable points and a series of these were selected to give a set of control and check points which were fairly evenly distributed over the stereomodel. A careful sketch was made for each point so that it could be identified easily when measuring its photo-coordinates. A Hoag streit coordinatograph of 0.1 mm scaling resolution was used to measure the positions of 98 ground control points (of which 14 points were in the common area between the two models). The measurement of position was performed three times for each point. The mean measured rectangular coordinates (in mm) were then transformed to geographical coordinates by direct linear interpolation between the ticks at 2'30" intervals of latitude and longitude on the 1/24,000 scale maps or 5'0" intervals on the 1/62,500 scale maps.

According to the U.S. National Map Accuracy Standards, the accuracy of these points is ± 0.3 mm on the map scale. Therefore, points measured on the 1/24,000 scale maps will have an accuracy of ± 7.2 metres on the ground, and points measured on the 1/62,500 scale maps will have an accuracy of ± 18.75 metres on the ground.

For model 01334/5, 10 points were measured on the 1/24,000 scale maps and 50 points were measured on the 1/62,500 scale maps. For model 01335/6, 22 points were measured on the 1/24,000 scale maps and 30 points were measured on the 1/62,500 scale maps. The elevations of the points used were the spot height values on the printed map sheets given to the nearest foot (0.3 m).

6.3 The F-126 Photography Test

The second practical test was carried out using photography produced by A.G.I. F-126 reconnaissance camera. The photography was flown specifically for the purposes of the test: the cooperation of the Royal Aircraft Establishment (R.A.E.) in providing the material is gratefully acknowledged.

6.3.1 The F-126 Camera

As mentioned previously, the F-126 camera (Fig. 109) is the standard R.A.F.

medium to high-level reconnaissance frame camera. Like the S-190B, the F-126 camera is equipped with a bi-directional focal plane shutter for fast cycling. The slit has variable width to provide speeds of 1/250, 1/500, and 1/1000 second. IMC is achieved by moving the film, the glass register plate and the pressure plate as a single unit in the flight direction. The accuracy of the IMC system is estimated by the manufacturers to be ± 2 percent of the V/H signal from the aircraft navigational system.

Fig.109 The F-126 Camera

Four lenses of different focal lengths are available: 6 in. (150 mm), Zeiss Oberkochen Topogon lens; 12 in. (300 mm), 24 in. (600 mm) and 36 in. (900 mm). Wray lenses. The actual photography used in the test was taken using a wide angle Topogon f/5.6 lens of 150 mm focal length.

6.3.2 The Zeiss Oberkochen Topogon Lens

The Topogon wide angle lens was designed by Richter and has been developed steadily from the first version which appeared in the Zeiss P-10 aerial camera in 1934. It has been used in various cameras since then and has also been adopted for use in various instruments such as rectifiers, stereo-plotting machines, etc. The lens is of a symmetric design with two identical lens components on either side of the diaphragm (Fig. 110).

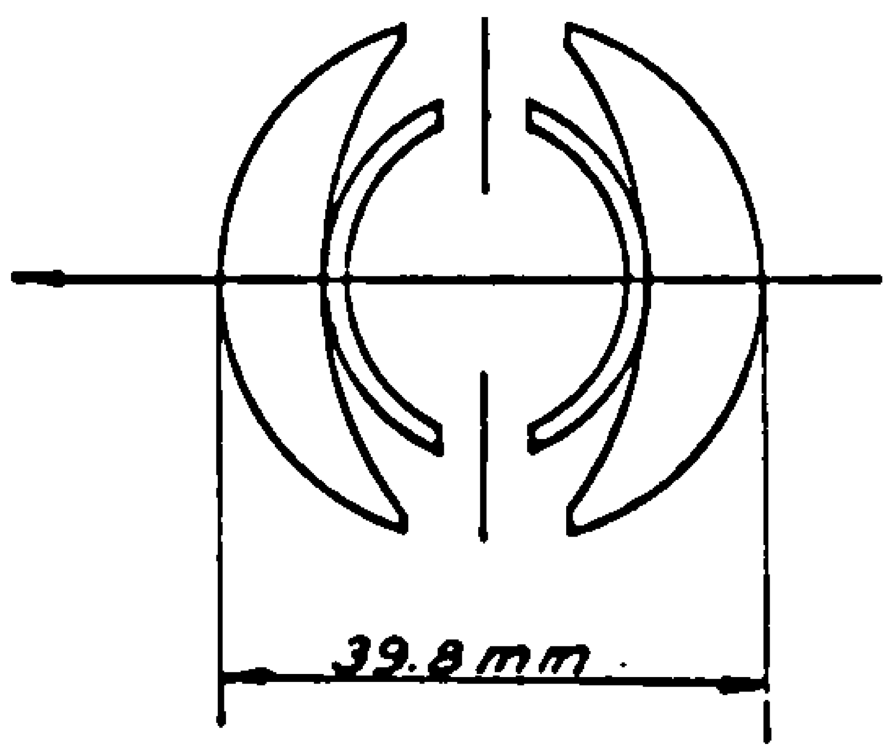

Fig. 110 Topogon lens

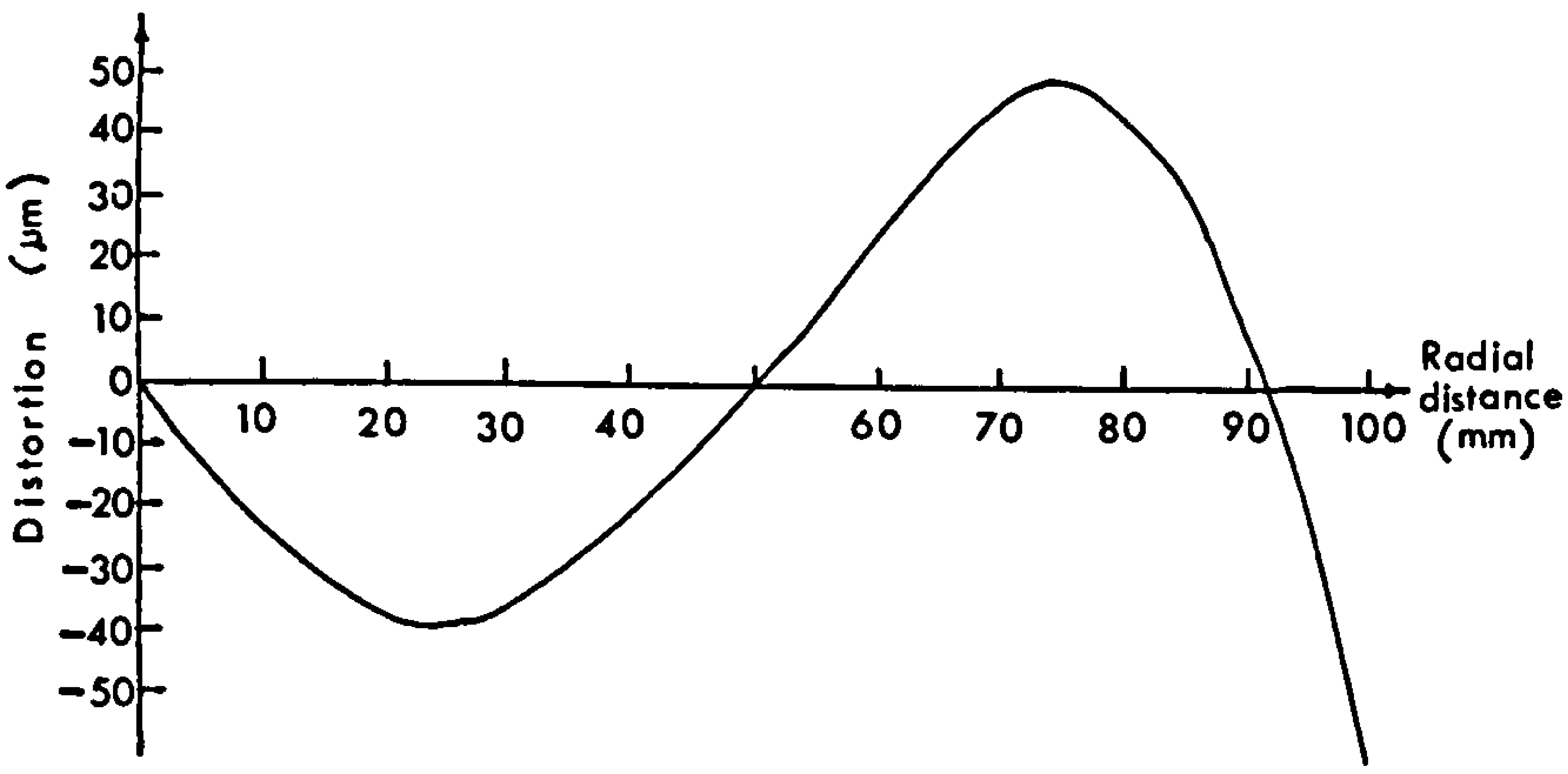

Fig. 111 Topogon f/6.3 Radial Distortion (Hallert, 1960)

As is well known, it has very marked and distinctive radial distortion pattern, e.g. that of the f/6.3 camera version is shown in Fig. 111.

The lens has been used both in metric and reconnaissance cameras. Its heavy distortion pattern needs elimination when photogrammetric measurements are to be made. Initially, this was done in analogue stereo-plotting machines by one of several methods: (i) using a lens of identical characteristics in each of the plotting cameras (i.e. the Porro-Koppe principle) e.g. as used in the Stereoplanigraph; (ii) by eliminating the distortion during production of the diapositives, e.g. in a projection printer for Multiplex work; or (iii) by the use of compensating plates, or cams in the stereo-plotter, e.g. as in the Wild and Galileo mechanical projection machines.

The four-element Topogen shown above was designed for objects located at infinity e.g. for aerial cameras. Thus it was not directly usable with rectifiers. So a modified version of the Topogon lens was developed for such purposes which has a thick plane parallel plate added on either side of the lens. This is the original f/6.3 Topogon V design (Fig. 112a).

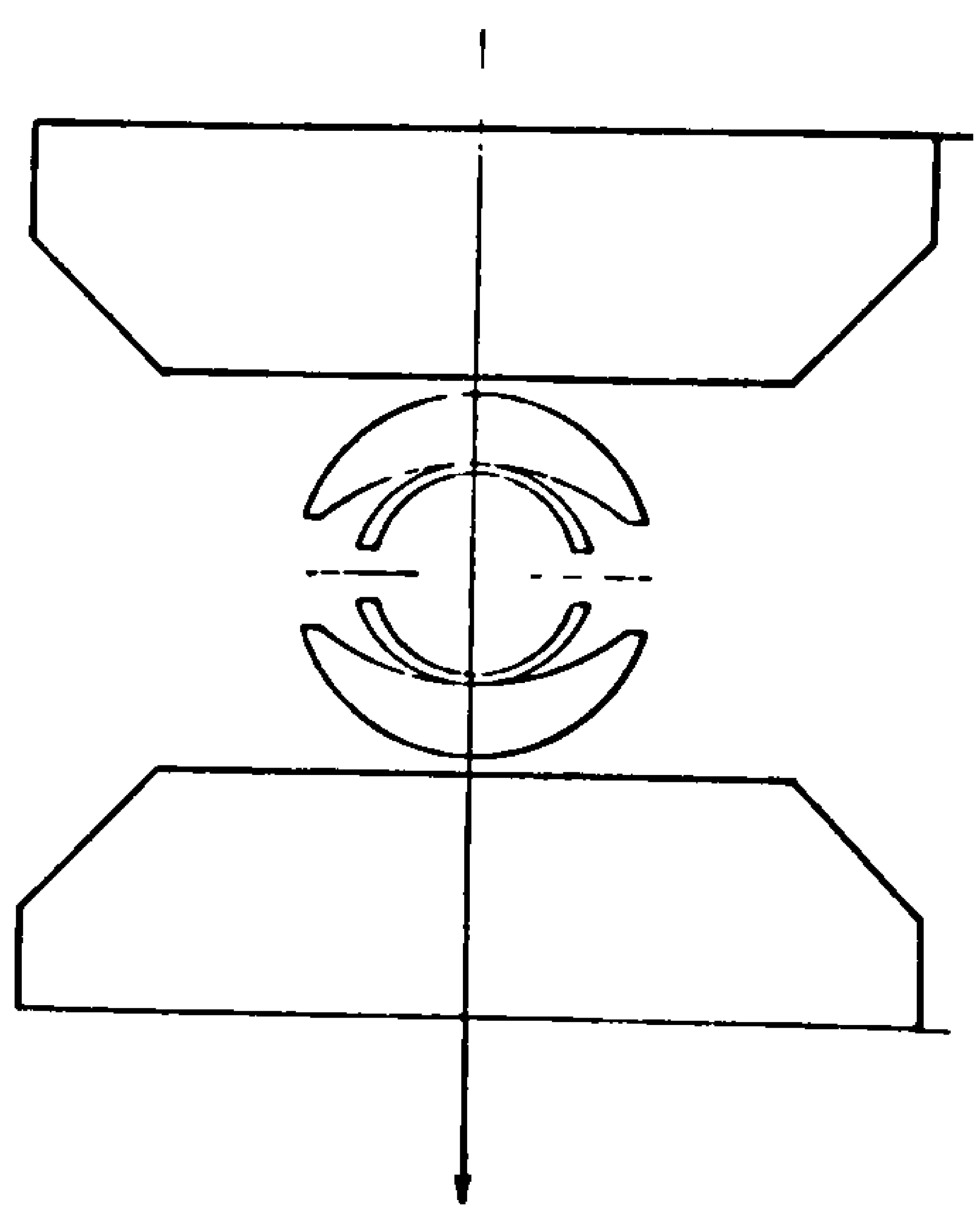

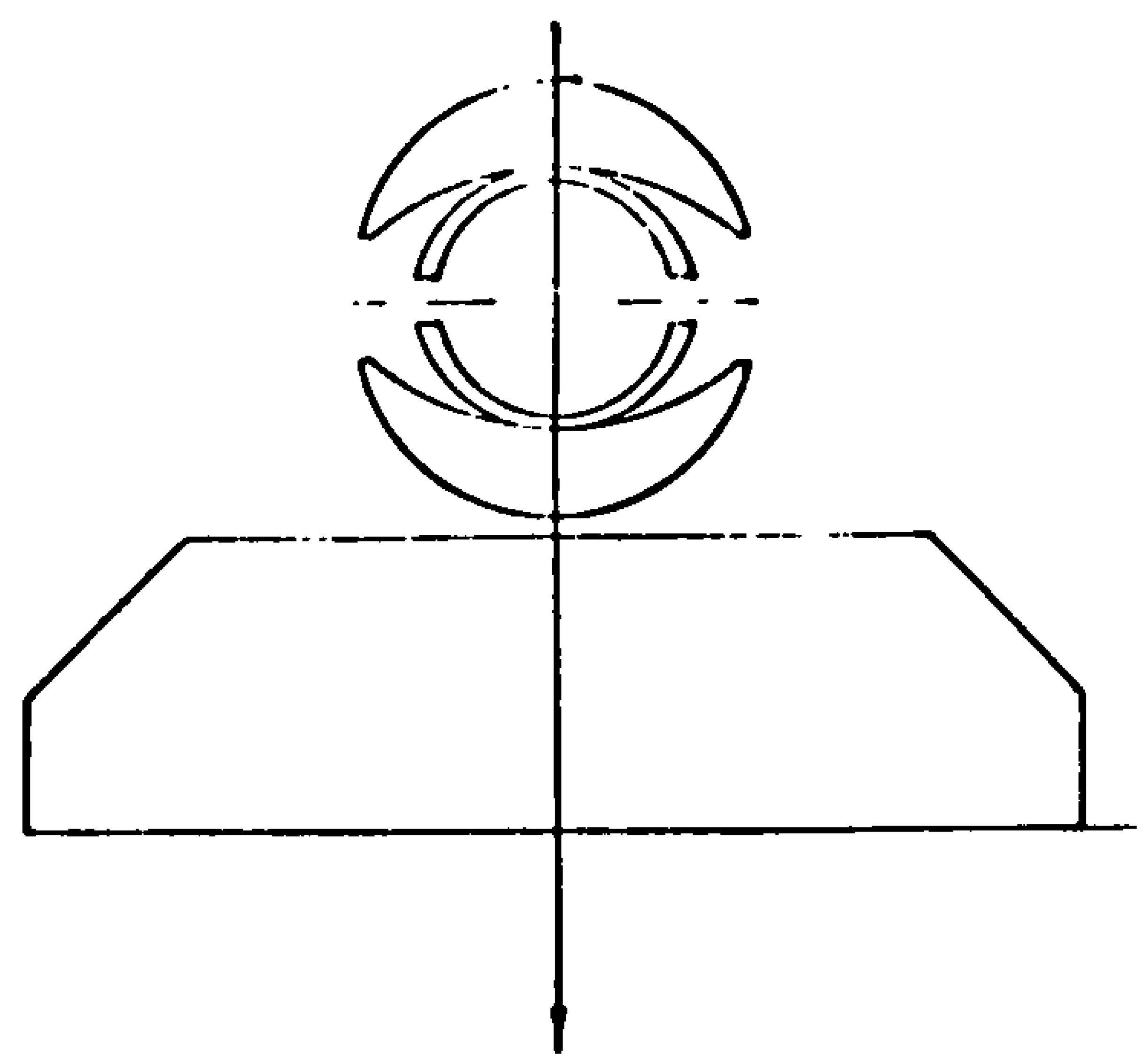

Fig. 112 (b) Topogon V f/6.3 lens

Fig. 112 (a) Topogon V f/6.3 lens

When this improved lens was later adapted for use with aerial cameras in the 1950's, only the glass plate between the lens and film was retained (Fig. 112 b). This special Topogon V mapping lens had a very small radial distortion – $\pm 6\,\mu m$ at focal length of 100 mm (See Fig. 113).(Richter, 1956).

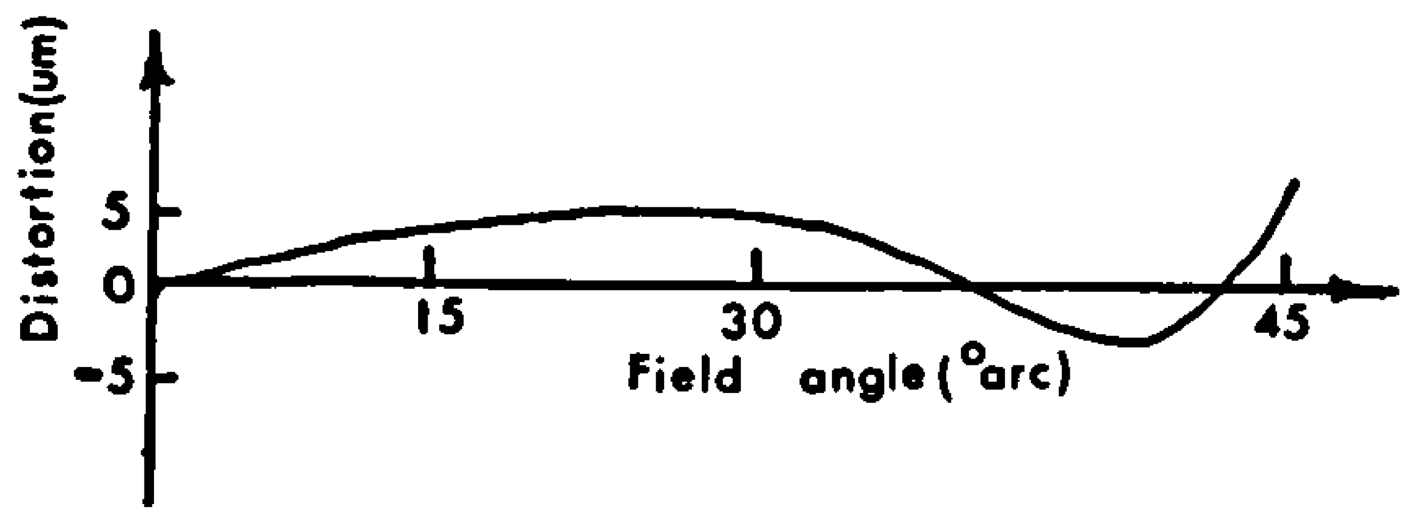

Fig. 113 Radial distortion for the Topogon V f/6.3 (Richter, 1956)

The Topogon lens used with the F-126 camera, however, is a new model modified from the standard Topogon. Its characteristics have been specified by R.A.E. to be optimised for reconnaissance purposes and so it has been redesigned accordingly. A computer print-out of the radial distortion curve of this lens has been provided by Zeiss Oberkochen (Fig. 114). This curve has been replotted on the basis of providing symmetrical distortion curve. This was achieved by selecting a focal length value such that the maximum positive distortion value is equal in magnitude to the maximum negative distortion value (Fig. 115). It can be seen from this, that the geometric radial distortion of this lens is very significant (up to $\pm$ 134 um) and far from distortion-free.

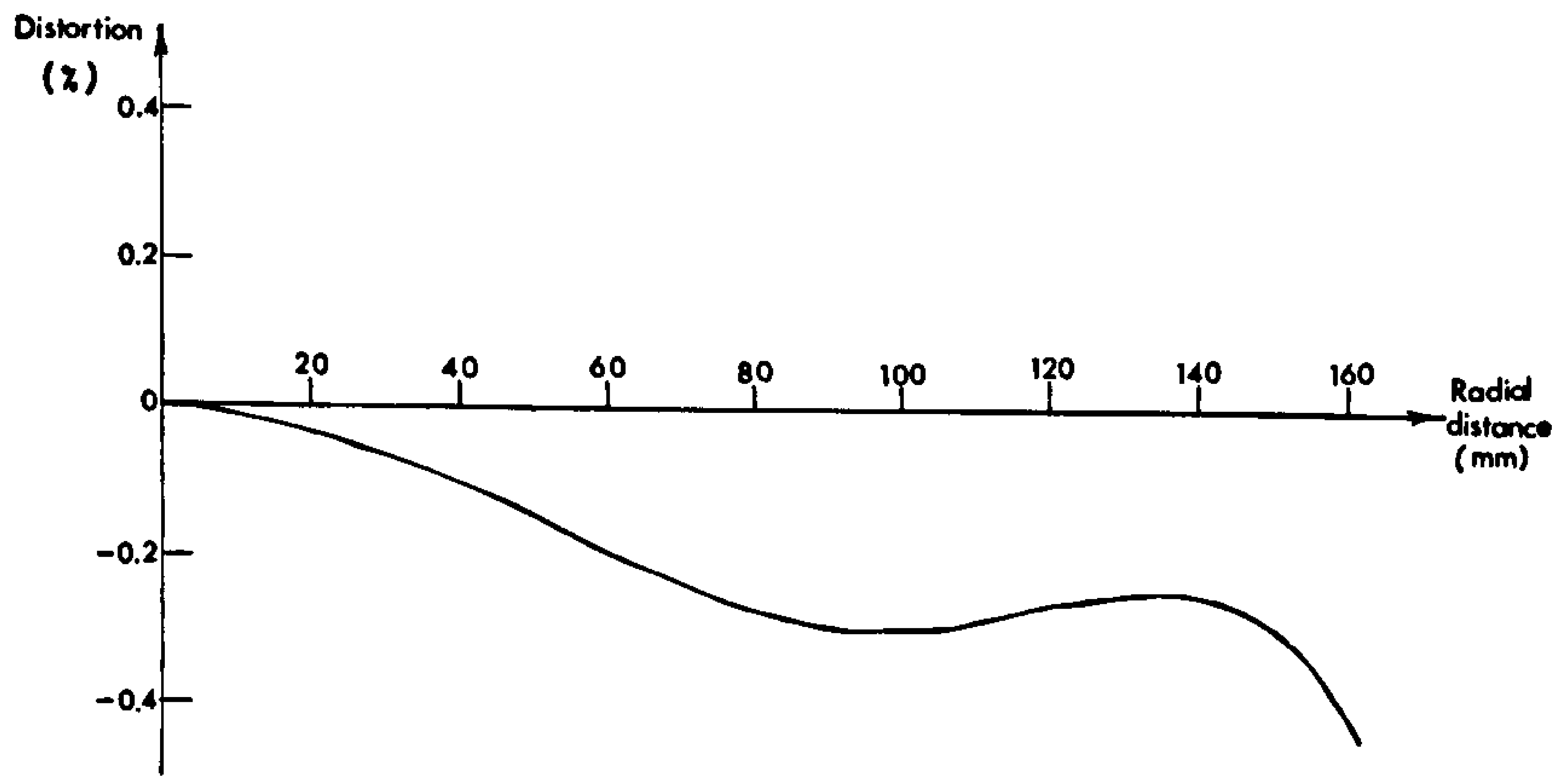

Fig. 114 Radial distortion curve of the F-126 Topogon 6 in. (150 mm) lens supplied by Zeiss.

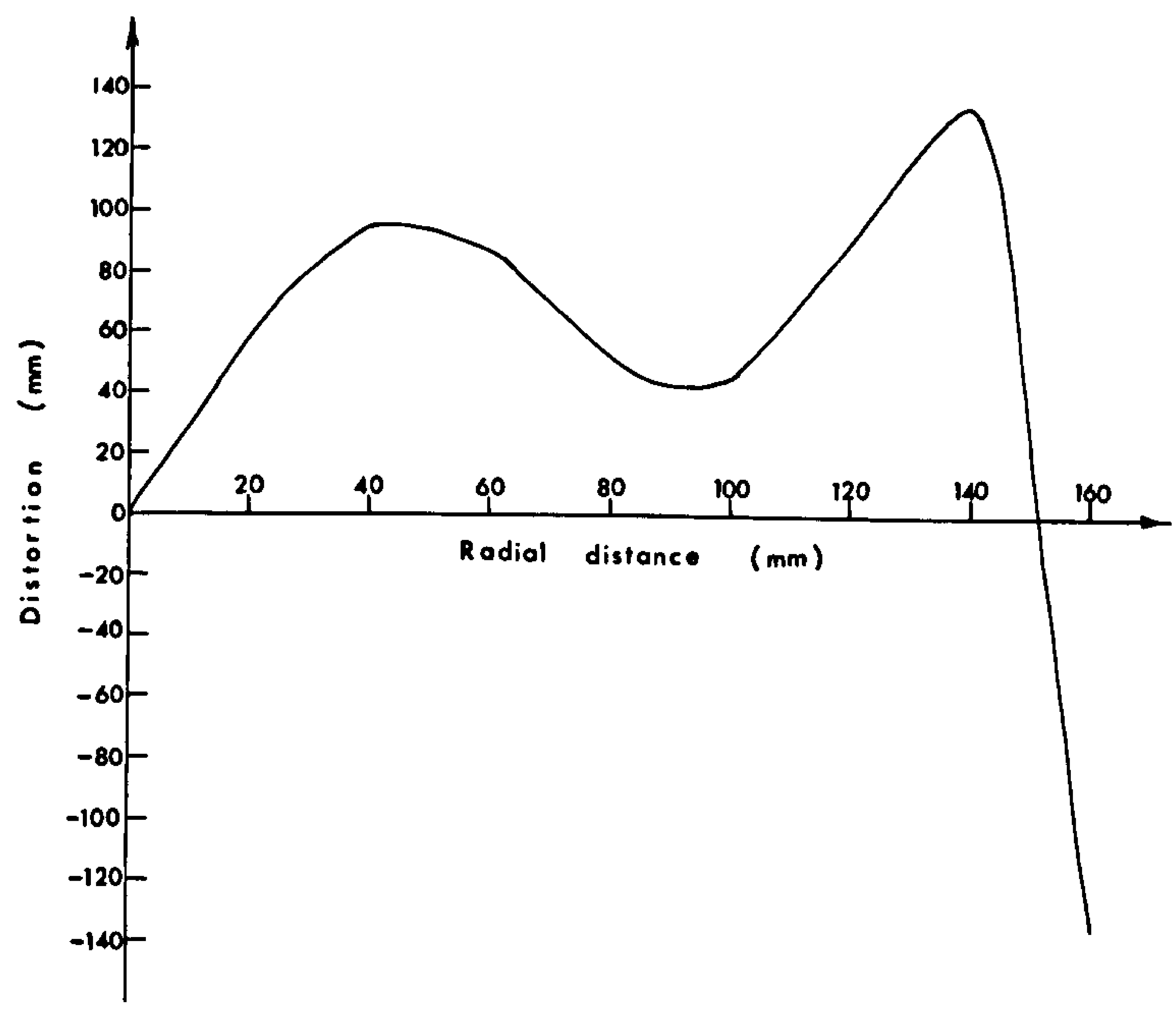

Fig. 115 Symmetrical Distortion curve of the F-126 Topogon 6 in. (150 mm) lens.

Figs. 116 and 117 show the tangential and radial MTF values of the Topogon lens for spatial frequencies of 5 cycles/mm, 10 cycles/mm and 20 cycles/mm as a function of the field angle, as provided by Zeiss Oberkochen. For all frequencies, the radial and tangential MTF values on-axis are greater than 0.7. However, degradation of the MTF with growing field angle can be noticed.

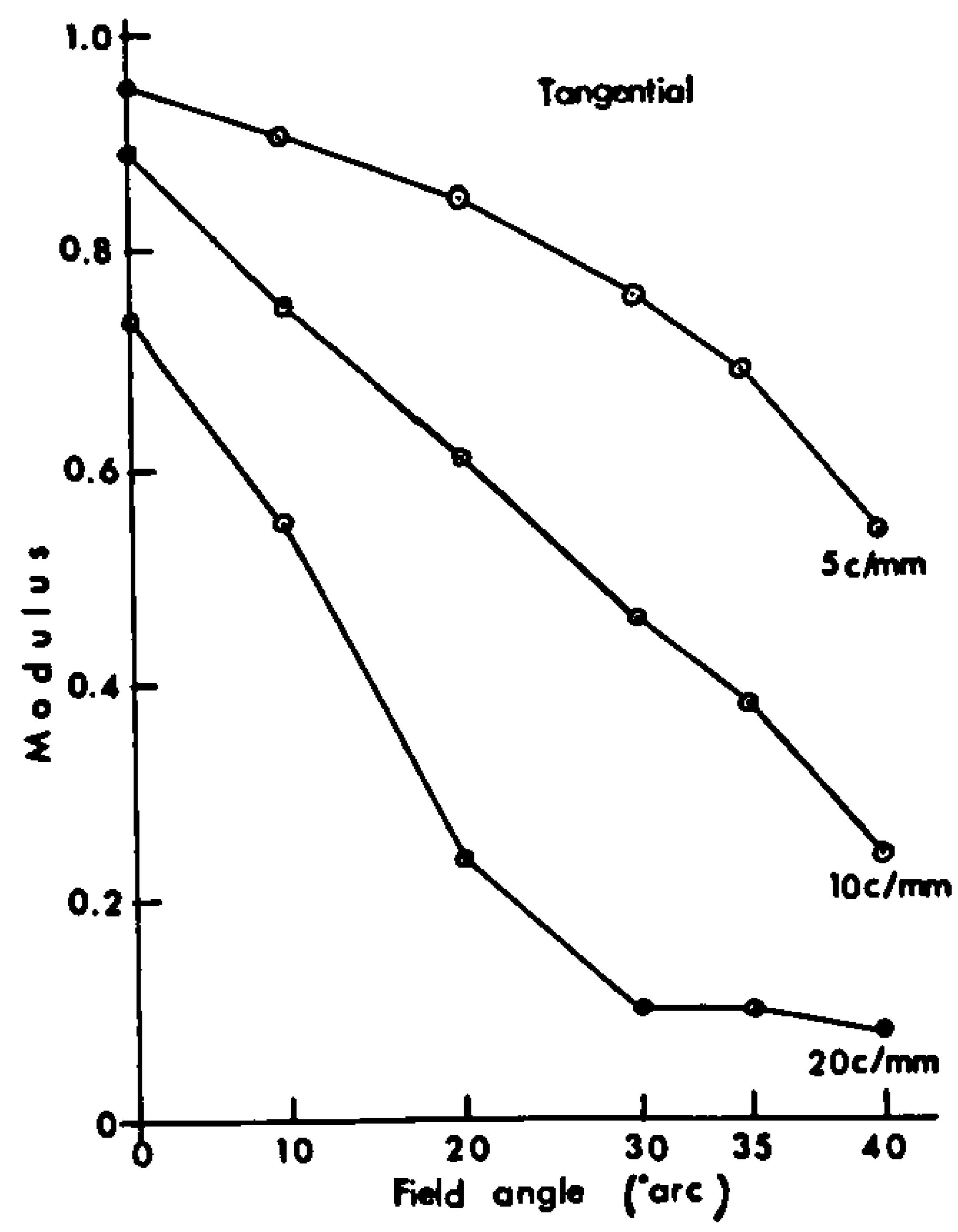

Fig. 116 Tangential MTF for the F-126 Topogon lens.

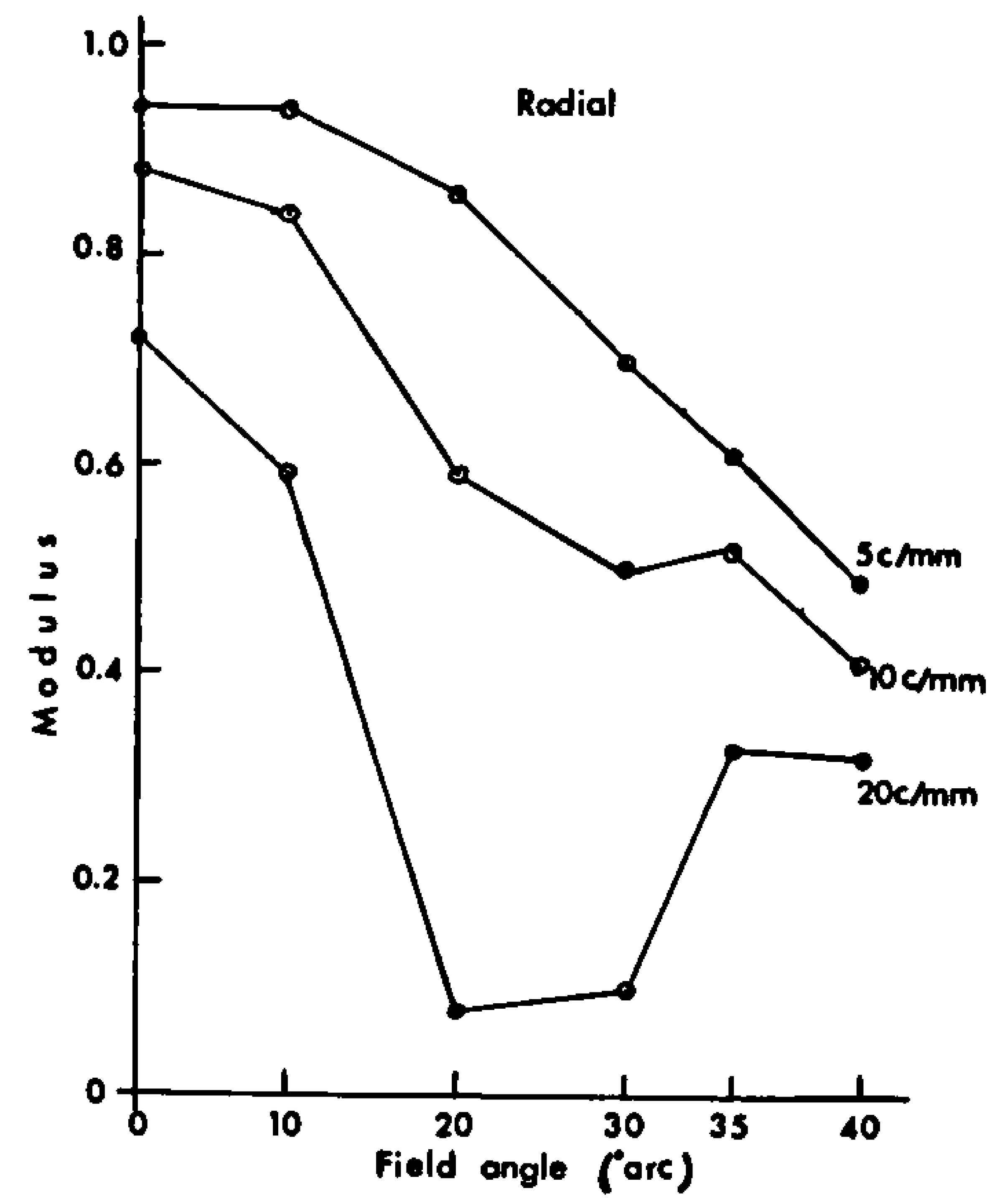

Fig. 117 Radial MTF for the F-126 Topogon lens.

The R.A.E. also provided the on-axis MTF of the Zeiss Topogon lens and the Threshold Modulation of the film test (Ilford 5-M). These were plotted on a log-log graph paper (Fig. 118) with the MTF of the Zeiss lens being translated to a response of 33 percent (which is equivalent to a contrast ratio of 2:1) and to 23 percent (equivalent to 1.6:1 contrast). The intersections of the MTF curves with the TM curve give the on-axis estimated resolution of the F-126 photographic system as 32 lp/mm and 25 lp/mm respectively.

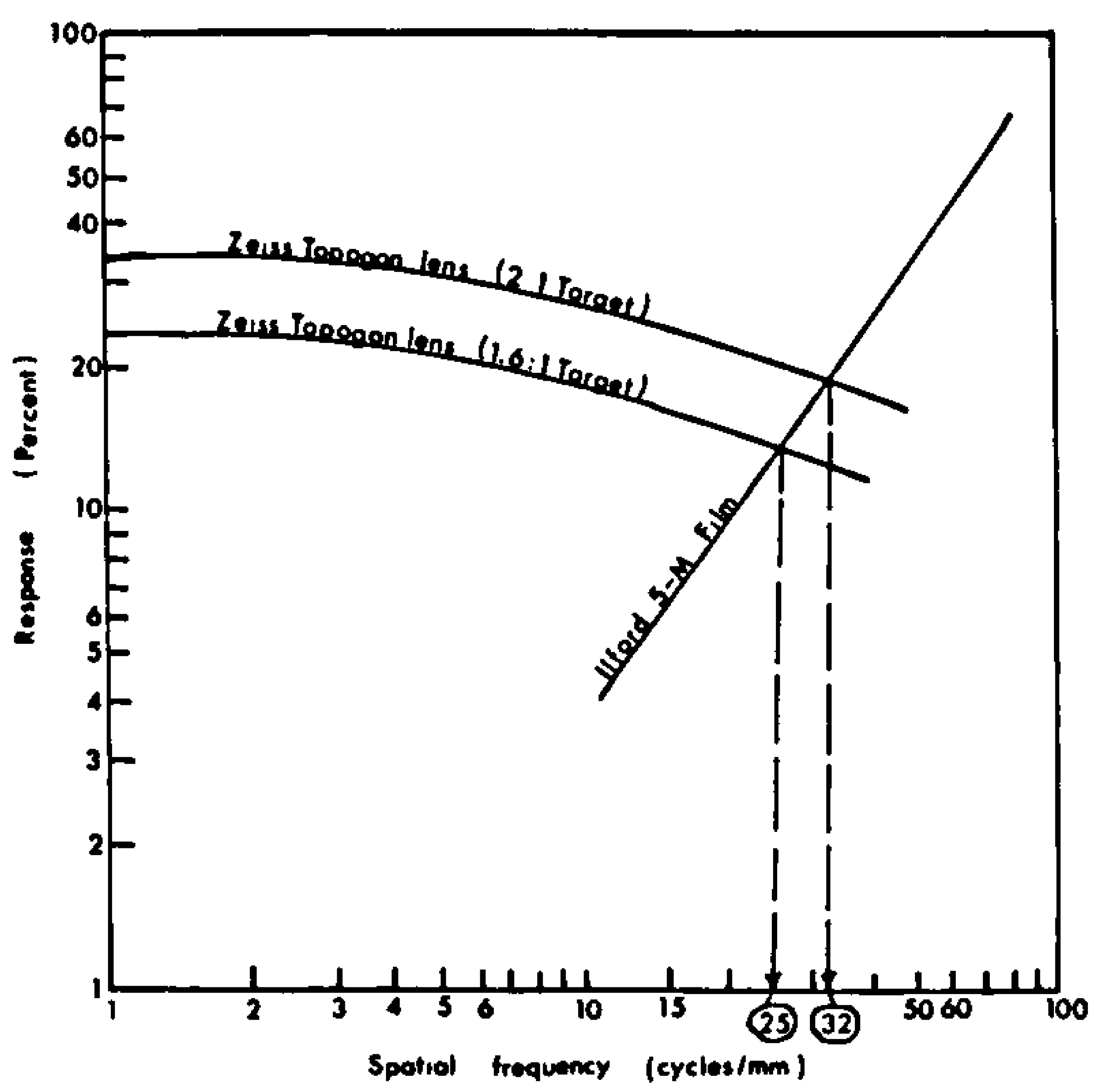

Fig. 118 Estimated on-axis resolution of the F-126 photographic system.

The estimated on-axis ground resolution at 1/20,000 and 1/40,000 scale is given in Table 11.

Photo scale	Ground resolution (2: 1 contrast) M	Ground resolution (1.6: 1 contrast) M
1/20,000	0.625	0.800
1/40,000	1.250	1.600

Table 11. Estimated on-axis Ground Resolutions

6.3.3 The Photography and the Test Area

The photographs were taken on Ilford black and white panchromatic film, the original negative film being supplied by the R.A.E. to the Department of Geography, University of Glasgow whose photographers produced film diapositives on stable polyster film. The photography was taken over two different areas located along the South coast of England.

(i) One strip was flown over Worthing at an altitude of 10,000 ft (3,000 m) to give a scale of 1/20,000. (ii) The other strip was flown over Southampton at an altitude of 20,000 ft (6,000 m) providing a scale of 1/40,000. Originally it was intended to fly both areas at the latter scale but, due to the weather conditions prevailing at the time of flight, this was not possible. The photographs were taken on 19th May, 1977 over Southampton and on 20th May, 1977 for the Worthing area.

Two models, one from each area, were selected for the purposes of the test (Figs. 119 and 120). The models were chosen such that the area under test would be covered by 1/1,250 Ordnance Survey (O.S.) plans to provide ground control of a sufficient accuracy for test purposes. The geographical boundaries of the chosen models were as follows: Worthing model: 0° 21.5' W to 0° 24.5' W and 50° 48.5' N to 50° 51.5'N; Southampton model: 1° 23' W to 1° 30' W and 50° 53' N to 50° 57' N. Their location is shown in Fig. 121 and Fig. 122.

The photographs used in the test were of good quality overall with good contrast and high resolution, especially in the centre of the format. However, although the illumination was good at the centre of the photographs, it was poor towards the edges with a marked fall off in the corners.

Fig. 119 F-126 (1/20,000 scale) photograph showing Worthing model

Fig. 120 F-126 (1/40,000 scale) photograph showing Southampton model

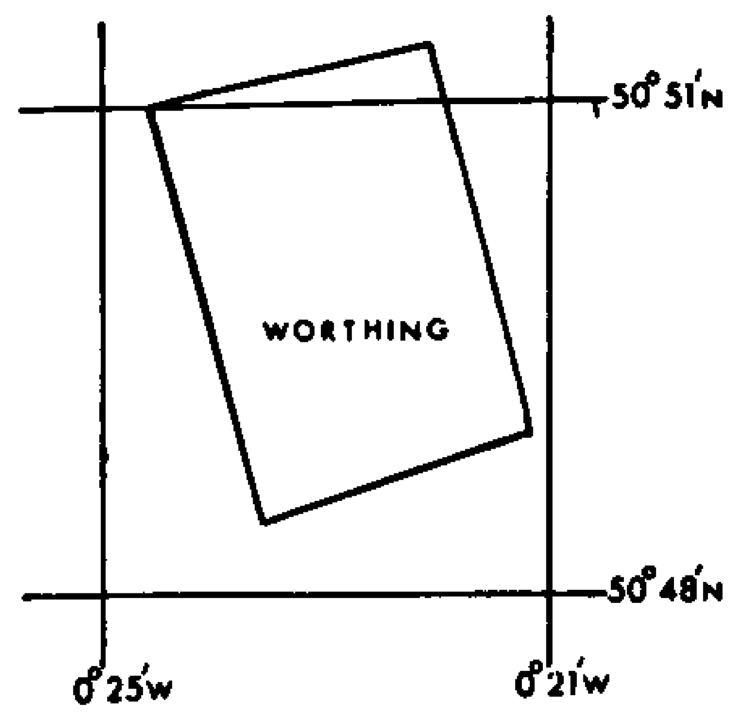

Fig. 121 Geographical boundaries of Worthing model

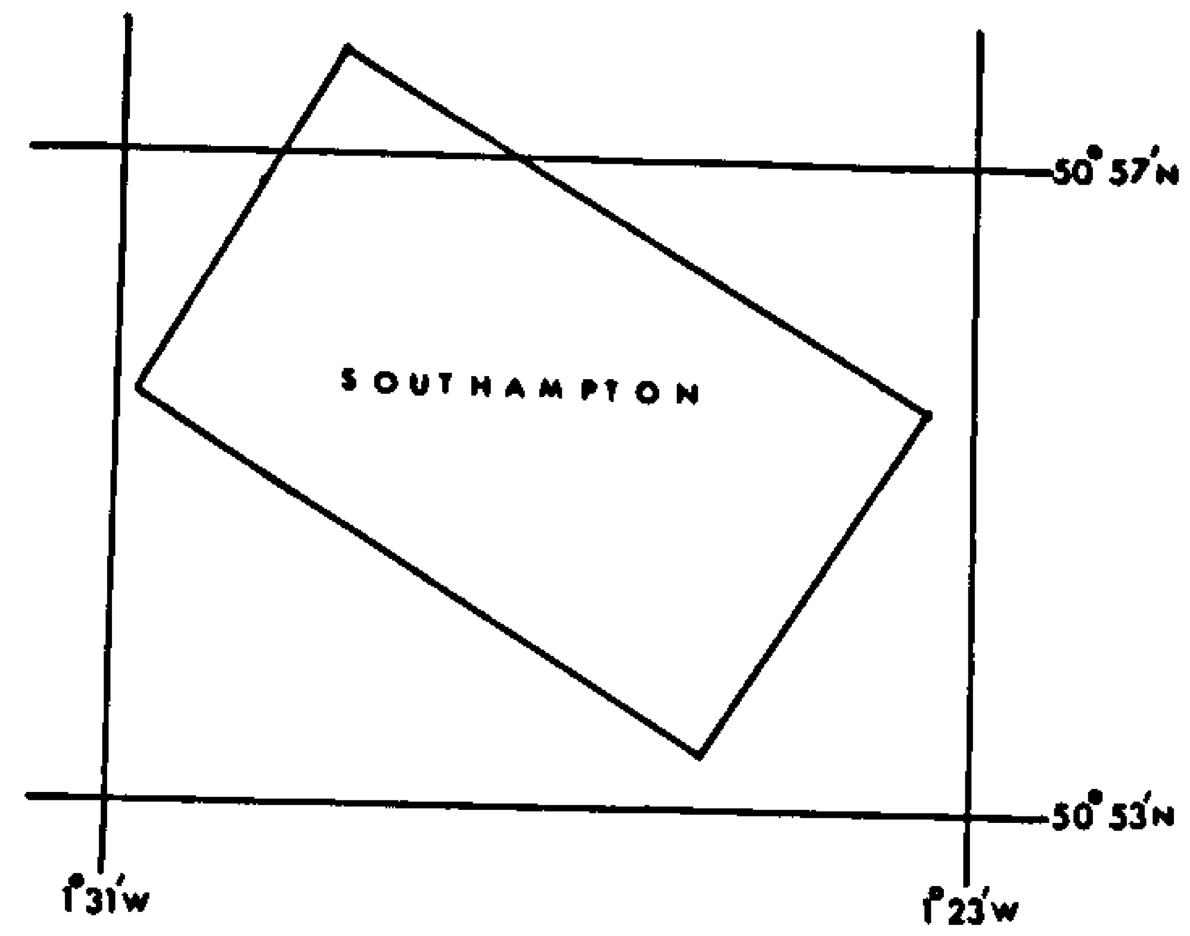

Fig. 122 Geographical boundaries of Southampton model.

6.3.4 Ground Control

When the experiment was being designed, the intention was to use O.S. traverse and revision points (which were available at the local Ordnance Survey Office) as control and check points. The estimated accuracy of these points is 0.01 m. Unfortunately, many of these points were found to be located at positions which were either difficult to observe on the photos due to poor illumination or shadow, or else considerable changes had taken place in the area which meant that the points had either been destroyed or could not be identified. Hence it was decided to select points on the photos and to measure their National Grid coordinates from the O.S. 1/1,250 plans covering the test areas. The procedures used for this task were similar to those used for provision of test points for the S-190B photographs. However, it was not possible to find points that could be used as full control points, hence the points used are divided into separate planimetric and height control points.

For planimetry, the points of intersection of fences or walls or the corners of fields which appeared to be well defined on the photographs which could be measured reliably on the plan were selected. The positions of these points were measured with reference to the nearest National Grid intersections given on the sheet. A glass measuring magnifier that allows measurement to an accuracy of 0.1 mm was used. Each point was measured several times and the mean of these measurements was adopted. This work was out on stable base materials at the O.S. local offices (at Worthing and at Southampton); the excellent cooperation of the O.S. personnel is gratefully acknowledged.

The accuracy (standard deviation) of the planimetry shown on O.S. 1/1,250 scale plan is $\pm$ 0.4 metre (Harley, 1975). This represents 20 μm at the photo scale of 1/20,000 (Worthing model) and 10 μm at the photo scale of 1/40,000 (Southampton model).

6.4 Measurement of Photo-coordinates

Since the highest possible accuracy in the measured photo-coordinates was required for the analytical procedures being employed, a high precision stereo comparator was used for the measurements. Since the Department of Geography at Glasgow does not possess such a device, the measurements were made on the new Zeiss Jena Stecometer stereo-comparator belonging to the Department of Civil Engineering of the City University of London.

The Stecometer measures the x-coordinate of the left hand photograph (x') and the y-coordinate of the right hand photograph (y") together with the parallaxes in x and y i.e. px and py (see Fig. 123).

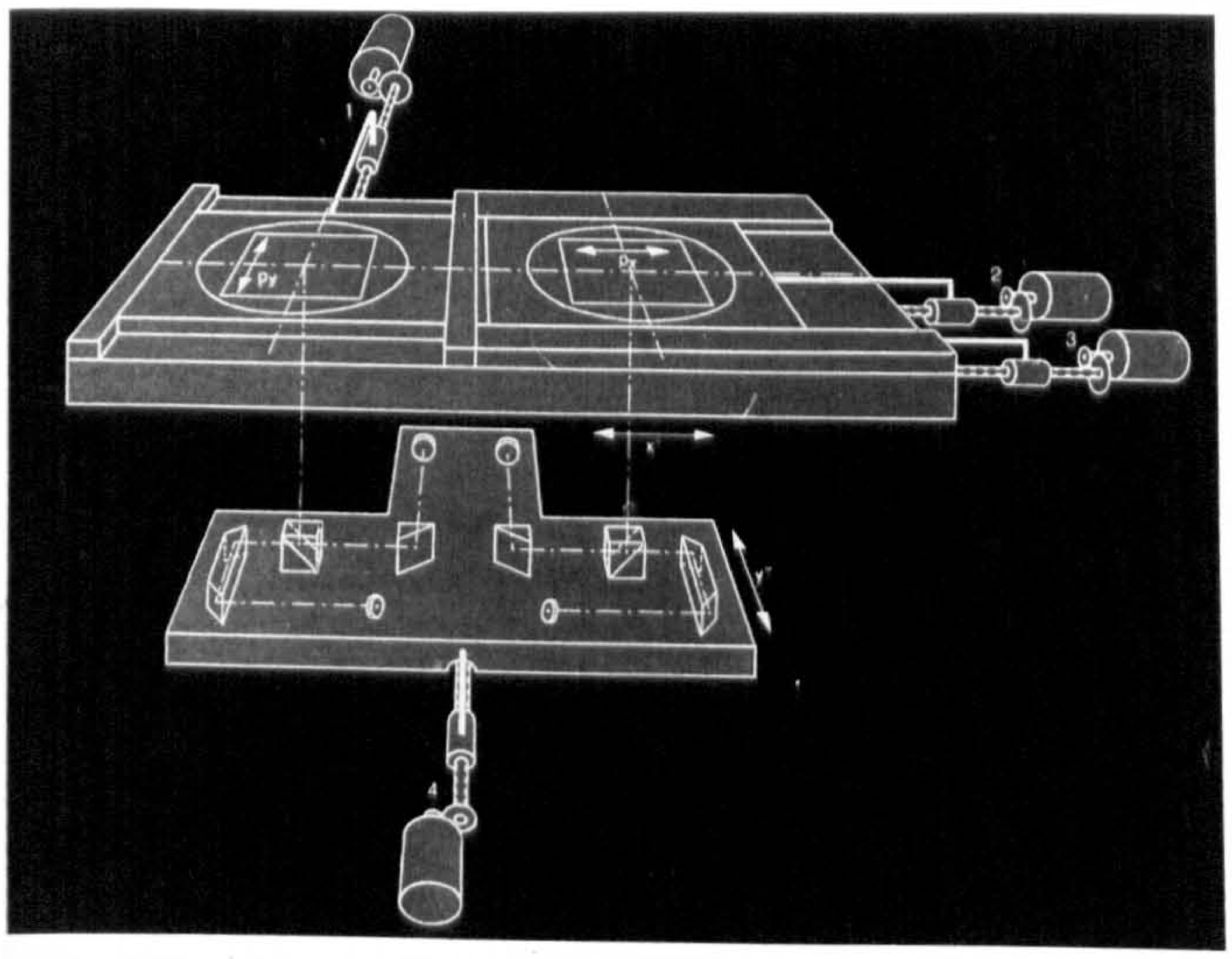

Fig. 123 Stecometer measuring system

Since the measuring ranges in the x' and y" directions are 0 to 280 mm, the two different formats of the test photographs were easily accommodated. The film transparencies were clamped to the holders by means of swivel brackets. Glass cover plates were used to ensure the flatness of the transparencies and to keep them from sliding about. The values of x', y", px and py were measured with a resolution of 2 µm using rotary shaft encoders attached to the lead screws which are used as driving agents. The measured values were automatically recorded in digital form on punched paper tape using a Facit 4070 punch and in printed form using a teleprinter.

In metric mapping cameras, the fiducial marks defining the principal point are located (i) in the corners of the camera focal plane, (ii) at the midpoints of the sides of the focal plane or (iii) the principal points are marked directly on the register glass (in the case of reseau cameras). The marks are normally a part of the focal plane and thus remain in a fixed position relative to the camera lens. This is not, however, the situation with the reconnaissance cameras used which were never designed with metric applications in mind.

In the case of the S-190B camera the image frame is a part of the removable film magazine and hence even this is not in a fixed position relative to the camera lens. However, the S-190B camera has a series of holes drilled around the perimeter of the image frame. These holes created photographic images having an approximate diameter of 330 µm. Four holes situated at the four corners of the frame were selected to serve as fiducial marks (Fig. 124). The measuring mark was centred in each of the circular holes. The photo-coordinates for each of the fiducial holes were then recorded to determine the coordinates of the geometric centre. Thus the S-190B data was made available for processing and analysis.

Because of the very small scale of the photos (1/945,600), attempts were made to use the highest possible magnification in the comparator (14 ×), but it proved difficult to observe due to poor resolution of the measured points at this setting. The magnification was therefore reduced to 9.6 × which gave an acceptable compromise between resolution and magnification. No special

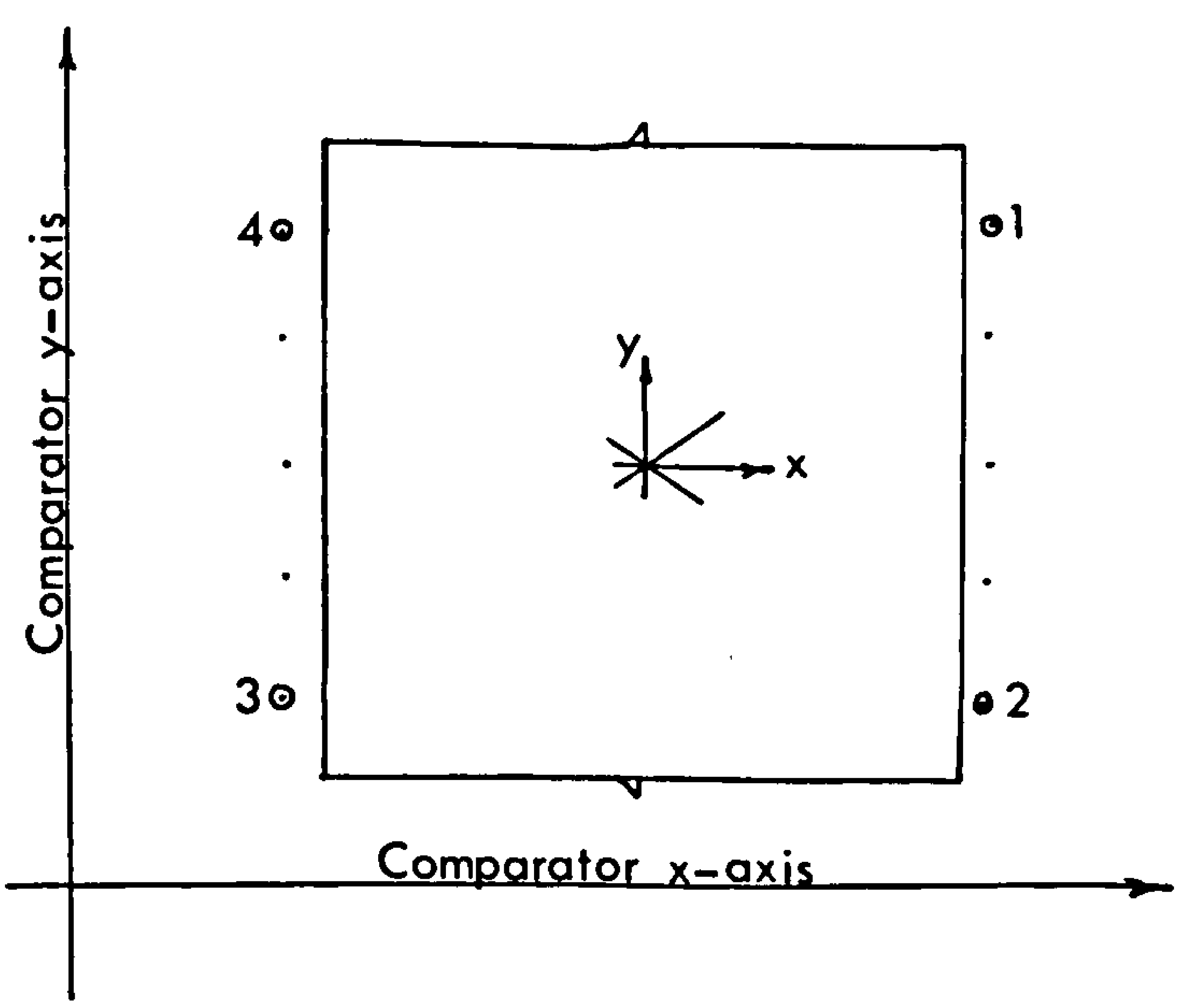

Fig. 124 The Photo-coordinate system and the Fiducial holes

difficulty arose in measuring the photo-coordinates of the control and check points since they were well defined and the sketch describing each point was clear. Two sets of observations were performed for each point and the mean was taken.

In the case of the F-126 photography, the only means of determining the geometric centre was by joining the opposite corners of the format. Although the corners themselves were not well defined due to poor illumination in the corners, they were treated as being fiducial marks and the intersection of their diagonals gave the geometric centre. The coordinates of this centre were set to zero during measurements and coordinates for all test points were referred to this as origin. The measurements were performed twice for each point. No special problems arose during the measurement of points lying in the central part of the model; however, the poor illumination towards the edges of the format led to difficulties in observing some points. Again the magnification used was 9.6 x which was high enough to allow optimum identification and observation of the control points on this photography.

To apply the analytical techniques developed in Chapter V, the processing of the data measured on the stereo-comparator will involve much computation. The most favourable approach obviously is the use of the electronic computer; indeed, without its use, the new procedures would be impracticable to implement. The computer programs developed to test the measured data will be discussed and described in the chapter which follows (i.e. Chapter VII). The results of the tests and the analysis of results will be given in Chapter VIII.

CHAPTER VII

The Computer Programs

CHAPTER VII

THE COMPUTER PROGRAMS

7.1. Introduction

The invention and development of the electronic computer over the last three decades has made it possible to solve complex problems in a fraction of a second, which would otherwise need days for a manual solution. This has led to the great expansion of analytical methods in photogrammetry and, in the particular context of this thesis, allows practical implementation of the techniques and procedures described in Chapter V. The following computer programs have been developed by the author for this purpose:

(i) Program (A): to correct the image coordinates for lens distortion, atmospheric refraction, Earth curvature and the effect of focal plane shutter and IMC;

(ii) Program (C): to transform model coordinates to ground coordinates using conventional absolute orientation and polynomial adjustment;

(iii) Program (D): to determine the exterior orientation elements of the camera either by: conventional resection in space, or by using additional parameters; or by point-by-point resection, and to determine the object coordinates by intersection;

(iv) Programs (F) and (G): to transform geographic coordinates to a local rectangular Secant Plane System and Universal Transverse Mercator System respectively;

(v) Program (E): to plot the residual discrepancies in plan and height in the form of vector diagrams;

(vi) Program B: is a program for analytical relative orientation already developed by Mr. B.D.F. Methley.

These various programs have been employed in the sequence illustrated by the flow diagram shown below.

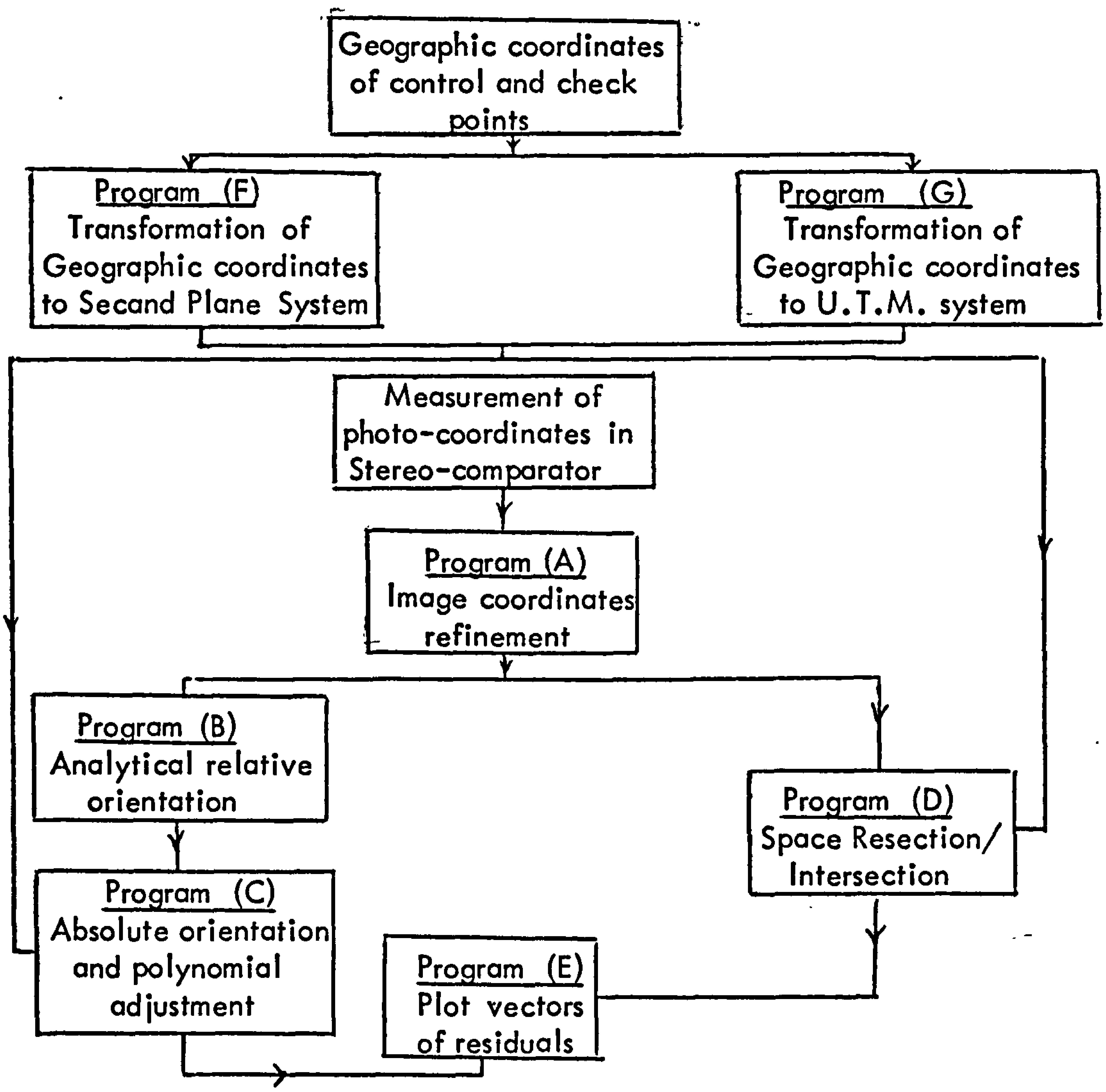

The basic characteristics of each of these programs are given in this chapter. For detailed descriptions and listings of each program see Appendix B. As will be seen, all of the programs are written in Algol 60, which is the language which has been used for all large photogrammetric programs (digital terrain models, aerial triangulation block adjustment, parallax heighting, etc.) developed in the Department of Geography over the last decade.

7.2 Program (A) - Image Coordinates Refinement

7.2.1 Function of the program:

The function of this program is to correct the image coordinates observed on a stereo-comparator, for the following effects:

(i) radial lens distortion;

(ii) atmospheric refraction;

(iii) Earth curvature; and

(iv) focal plane shutter and IMC.

7.2.2 Mathematical Basis

The corrections for lens distortion, atmospheric refraction and Earth curvature have been dealt with elsewhere in photogrammetry. However, the particular methods of correction used in this program are given below for reference purposes.

In all cases, the radial distance, r, of the image point from the geometric centre is given by

$$r^2 = x^2 + y^2 \quad \ldots\ldots\ldots\ldots\ldots\ldots\ldots\ldots \quad (135)$$

where x and y are the image coordinates with reference to the geometric centre as origin. If the radial distortion is dr, then the corrected image coordinates are given by:

$$x_c = x(1 - dr/r) \quad \ldots\ldots\ldots\ldots\ldots\ldots\ldots \quad (136)$$

$$y_c = y(1 - dr/r) \quad \ldots\ldots\ldots\ldots\ldots\ldots\ldots \quad (137)$$

(i) Radial lens distortion

The method used in this program for the lens distortion correction is to fit a polynomial to the distortion curve. The method is especially well suited for analytical photogrammetric calculations using a computer (Wolf, 1974). The polynomial is specified by the following equation

$$dr = k_0 r + k_1 r^3 + k_2 r^5 + k_3 r^7 \quad \ldots\ldots\ldots\ldots \quad (138)$$

where the four coefficients $k_o - k_3$ define the shape of the curve. They are determined through a least squares curve-fitting computation which matches a curve to known radial distortions at varying radial distances as determined through camera calibration. Once the k values have been determined, the radial lens distortion for any value of r may be calculated by substituting into equation (138). The corrected image coordinates can be determined by substituting the corresponding radial distortion in equations (136) and (137).

(ii) Atmospheric refraction

The correction for this radial distortion is given in the 1966 edition of the American Manual of Photogrammetry as:

$$dr = K_a \ (r + r^3/f^2) \quad \ldots\ldots\ldots\ldots\ldots\ldots\ldots\ldots\ldots \quad (139)$$

K_a, the constant for atmospheric refraction, is given by:

$$K_a = \left[\frac{2410\,H}{H^2 - 6H + 250} - \frac{2410\,h}{h^2 - 6h + 250}\left(\frac{h}{H}\right)\right] \times 10^{-6} \quad \ldots \quad (140)$$

where H is the absolute flying height in km and h is terrain height in km.

The formula was originally derived by Bertram (1965) who based it on the 1959 ARDC model atmosphere.

Again the substitution of dr in equations (136) and (137) gives the corrected image coordinates.

(iii) Earth curvature

The radial displacement due to Earth curvature is given by:

$$dr = \frac{Hr^3}{2Rf^2} \qquad \ldots\ldots\ldots\ldots\ldots\ldots\ldots\ldots \qquad (141)$$

in which R is the radius of the Earth in km,

H is the flying height above ground in km,

f is the focal length in mm and

r is the radial distance to the image point from the principal point (in mm).

The formula is based on the assumption that the photography is vertical.

(iv) Focal plane shutter and IMC

The mathematical basis for these corrections is given in Chapter IV (section 4.3) and the combined effect of both corrections is given in the same Chapter (section 4.7).

7.2.3 Flexibility and Limitations

The program can correct the coordinates of any number of image points, the only limiting factor being the storage capacity of the computer used. In fact, the ICL 2980 computer has a very large store capacity compared to the requirements of the comparatively small programs developed for the current work.

The image coordinates measured on each of the pair of overlapping photographs are used as input data, so that the output data can be used directly to form a model, either through relative orientation, or by the space resection and intersection technique.

The corrections to the image coordinates, which are mentioned above, may be applied either separately, or in any of the possible combinations. Hence, the program may be used not only to correct data from reconnaissance photography, but also to correct more conventional photogrammetric data, where the effect of focal plane shutter and IMC is not present.

7.3 Program (B) - Analytical Relative Orientation

This program establishes the relative orientation of a pair of overlapping photographs which have been observed in a stereocomparator and calculates the model coordinates of all the measured image points. This forms a very important phase of the polynomial adjustment solution. Output from the program (model coordinates) is used directly as input data for the absolute orientation and polynomial adjustment program (C).

The program was originally developed and fully described by Mr. B.D.F. Methley, Department of Geography at the University of Glasgow (1972). The program was slightly modified by the present author in the course of being transferred from the ICL 1906A computer of the University of Nottingham to the ICL 2980 computer of the Regional Computing Centre in Edinburgh.

7.4 Program (C) - Absolute Orientation and Polynomial Adjustment

7.4.1. Introduction

This program carries out two functions. Firstly, it transforms the model coordinates to ground coordinates through an analytical absolute orientation procedure. Then it applies a polynomial adjustment to the computed ground coordinates in order to fit them to known values. Finally, the results are analysed by a comparison of the photogrammetrically derived coordinates with the known terrain coordinates of the check points and the determination of the root mean square errors of the discrepancies between these two sets of coordinates.

7.4.2 Mathematical Basis

(a) Absolute Orientation

The relation between a model coordinate system and a ground coordinate system is given by the following set of equations.

$$\begin{bmatrix} X_i \\ Y_i \\ Z_i \end{bmatrix} = \lambda A \begin{bmatrix} x_i \\ y_i \\ z_i \end{bmatrix} + \begin{bmatrix} X_o \\ Y_o \\ Z_o \end{bmatrix} \quad \ldots\ldots\ldots\ldots \quad (142)$$

in which X_i, Y_i, Z_i are the ground coordinates of point i,

x_i, y_i, z_i are the model coordinates of point i,

λ is the scale factor,

X_o, Y_o, Z_o are the shifts to the origin of the model system,

A is the orthogonal matrix containing three rotations Ω, Φ and K.

These are non-linear equations, including seven unknown independent orientation parameters namely: λ, Ω, Φ, K, X_o, Y_o and Z_o. Since the equations are non-linear, the solution for the seven orientation parameters is based on a set of initial approximations which are corrected iteratively until the corrections are of insignificant value.

The corrections $d\Omega$, $d\Phi$, dK, $d\lambda$, dX_o, dY_o and dZ_o to the approximate values Ω_a, Φ_a, K_a, λ_a, X_{o_a}, Y_{o_a} and Z_{o_a} are obtained by solving the following set of observation equations derived from equations (142) (Tewinkel, 1962);

$$\begin{bmatrix} V_x \\ V_y \\ V_z \end{bmatrix} = \begin{bmatrix} 0 & -Z_a & Y_a & E_1 & 1 & 0 & 0 \\ Z_a & 0 & -X_a & E_2 & 0 & 1 & 0 \\ -Y_a & X_a & 0 & E_3 & 0 & 0 & 1 \end{bmatrix} \begin{bmatrix} d\Omega \\ d\Phi \\ dK \\ d\lambda \\ dX_o \\ dY_o \\ dZ_o \end{bmatrix} \quad \ldots (143)$$

In this set of equations, V_x, V_x, V_z are the corrections to the transformed coordinates. Terms with suffix a are approximate values, and the values of E_1, E_2, E_3 are given by:

$$\begin{bmatrix} E_1 \\ E_2 \\ E_3 \end{bmatrix} = A_a \begin{bmatrix} x \\ y \\ z \end{bmatrix} \quad \ldots\ldots\ldots\ldots\ldots\ldots\ldots (144)$$

The initial approximations by which the iterations start are given as follows:

$$\Omega_a = 0; \quad \Phi_a = 0$$

$$\kappa_a = \arctan\left((y_2 - y_1) / (x_2 - x_1) \right) - \arctan\left((Y_2 - Y_1) / (X_2 - X_1) \right)$$

$$\lambda_a = \left[\frac{(X_2 - X_1)^2 + (Y_2 - Y_1)^2}{(x_2 - x_1)^2 + (y_2 - y_1)^2} \right]^{\frac{1}{2}} \quad \ldots\ldots\ldots\ldots\ldots\ldots \quad (145)$$

where (X_1, Y_1) and (X_2, Y_2) are the ground coordinates of two plan control points selected to give the best approximation for κ, and λ; and (x_1, y_1) and (x_2, y_2) are their model coordinates. If the number of observation equations used to solve the set of equations (143) exceeds seven, then a least squares solution is necessary. In this case, a matrix of coefficients is formed. This contains seven columns and $(2m + n)$ rows, where m is the number of plan control points and n is the number of height control points. If this matrix is D, the normal equation matrix N can be obtained by multiplying D by its transpose, D^T. If the vector of corrections to the transformed coordinates is denoted by P, then the vector X of the unknown corrections to the orientation elements is given by:

$$X = N^{-1} D^T P \quad \ldots\ldots\ldots\ldots\ldots\ldots\ldots\ldots \quad (146)$$

These corrections are then used to find new values for the orientation elements as follows:

$$\begin{bmatrix} X_{o_N} \\ Y_{o_N} \\ Z_{o_N} \end{bmatrix} = \begin{bmatrix} dX_o \\ dY_o \\ dZ_o \end{bmatrix} + \begin{bmatrix} X_{o_a} \\ Y_{o_a} \\ Z_{o_a} \end{bmatrix}$$

$$\lambda_N = d\lambda + \lambda_a \qquad \ldots\ldots\ldots\ldots\ldots\ldots\ldots \quad (147)$$

$$A_N = dA \cdot A_a$$

where terms with suffix N are the new orientation elements and dA is given as:

$$dA = \begin{bmatrix} 1 & d\kappa & -d\Phi \\ -d\kappa & 1 & d\Omega \\ d\Phi & -d\Omega & 1 \end{bmatrix}$$

And so the iteration is continued until the corrections become insignificant.

(b) Polynomial Adjustment

The first step in the polynomial adjustment phase is to determine the discrepancies between the photogrammetrically-derived ground coordinates and the known ground coordinates of the control points. These discrepancies are used to determine the polynomial coefficients in the series of equations (132), (133) and (134), given in Chapter V. When these polynomial parameters are determined, corrections based on them can be applied to all other points measured in the model. In each of the equations mentioned, there are nine unknown parameters. These can be determined if nine plan control points and nine height control points are available. Any redundant control point would allow the use of a least squares solution.

(c) Accuracy of Results

The root mean square errors of the residuals in X, Y and Z can be determined by the following known equation.

$$m = \sqrt{\frac{\Sigma VV}{(n - u)}} \qquad (148)$$

where m = root mean square error

u = residual discrepancy

n = number of points being tested

u = the minimum number required to obtain a solution.

The accuracy of height in photo scale is determined by computing the corresponding residual parallax from the relation:

$$dp = \frac{B \cdot f}{H^2} m_h \quad \ldots\ldots\ldots\ldots\ldots\ldots\ldots\ldots \quad (149)$$

where B is the air base,

H is the flying height, and

f is the camera principal distance.

7.4.3. Flexibility and Limitations

If the polynomial adjustment is not required, the program may be stopped directly after transforming the model coordinates to the ground coordinates. In this case, the results after the absolute orientation would be printed out, together with the root mean square errors of the discrepancies.

A least squares method is used in both: the transformation and the polynomial adjustment phases, hence the number of ground control points is only limited by the computer's storage capacity.

If the number of ground control points available is not sufficient to solve for all the polynomial parameters, then some of the parameters may be omitted, so that a limited adjustment can be applied with the available control. Again, if the effects of the individual parameters on the adjustment are to be compared, the parameters may be reduced one by one with each successive adjustment.

A numbering system is designed to suit the different types of points in the model. This numbering system should be followed and used carefully.

The first two plan control points in the input data should be selected as those which would give good approximations for κ and λ, the azimuth and scale parameters respectively.

7.5 Program (D) - Space Resection/Intersection

7.5.1 Introduction

The first function of this program is to determine the exterior orientation elements of the camera. This is then followed by a determination of the ground coordinates of objects within the model, by means of an intersection of rays.

7.5.2 Mathematical Basis

As already outlined in Chapter V, the basic theory of the general resection problem is based on the collinearity principle specifying that each image, its object and the perspective centre of the camera lie on a common straight line.

(i) Conventional Space Resection

For the conventional case, the linearised collinearity equations are given by equations (105) in Chapter V. These equations can be rewritten in matrix form as follows:

$$V = D_1 X_1 - L \qquad \text{.....................} \quad (150)$$

in which

$$V = \begin{bmatrix} v_x \\ v_y \end{bmatrix} \; ; \quad L = \begin{bmatrix} J \\ K \end{bmatrix} \; ;$$

$$X_1^T = \begin{bmatrix} d\omega & d\phi & d\kappa & dX_o & dY_o & dZ_o \end{bmatrix} \; ;$$

and

$$D_1^T = \begin{bmatrix} P_{12} & P_{22} \\ P_{13} & P_{23} \\ P_{14} & P_{24} \\ P_{15} & P_{25} \\ P_{16} & P_{26} \\ P_{17} & P_{27} \end{bmatrix} \qquad \text{.................} \quad (151)$$

where the p-terms are coefficients derived from the partial derivatives. These coefficients are defined in Appendix A. All other terms are defined in Chapter V (section 5.6.1).

Equations (150) can be solved, using least squares, to give the unknown corrections for the orientation elements:

$$X = (D_1^T D_1)^{-1} D_1^T L \quad \dots\dots\dots\dots\dots\dots\dots\dots \quad (152)$$

(ii) Additional parameters

When the error model given by equation (117) is added to the observation equations, they can be written as:

$$V = D_1 X_1 + D_2 X_2 - L \quad \dots\dots\dots\dots\dots\dots \quad (153)$$

or

$$V = DX - L \quad \dots\dots\dots\dots\dots\dots\dots\dots\dots \quad (154)$$

in which D_2X_2 is the error model such that:

$$D_2 = \begin{bmatrix} x & y & xy & x^2y & xy^2 & 0 & 0 & 0 & xr^2 & xr^5 & 1.0 & 0 \\ -y & x & 0 & 0 & 0 & xy & x^2y & xy^2 & yr^2 & yr^5 & 0 & 1.0 \end{bmatrix}$$

$$\text{and} \quad X_2^T = \begin{bmatrix} a_1 & a_2 & b_1 & b_2 & b_3 & b_4 & b_5 & b_6 & c_1 & c_2 & d_1 & d_2 \end{bmatrix} \quad \dots\dots \quad (155)$$

Again, using least squares, the solution is given by

$$X = (D^T D)^{-1} . D^T L \quad \dots\dots\dots\dots\dots\dots\dots\dots \quad (156)$$

(iii) Point by point Space Resection

The exterior orientation elements corresponding to each point in the photograph are expressed as functions of the photo-coordinates of the point as given in equation (109). The observation equations for this case are given by equations (110).

These can also be written in the following matrix form:

$$V = D_1 X_1 + D_3 X_3 - L \quad \ldots\ldots\ldots\ldots\ldots\ldots \quad (157)$$

or

$$V = DX - L \quad \ldots\ldots\ldots\ldots\ldots\ldots\ldots\ldots\ldots\ldots \quad (158)$$

In this equation, D_1 is given in equation (151) and $D_2 = x_i D_1$ (see Chapter V, section 5.6.2). The least squares solution for equation (158) would give

$$X = (D^T D)^{-1} D^T L \quad \ldots\ldots\ldots\ldots\ldots\ldots\ldots\ldots \quad (159)$$

(iv) Space Intersection

Having determined the exterior orientation elements of the camera, from either of the above equations, it becomes necessary to consider the scale factor appropriate for two overlapping photographs. This scale factor may be determined using either equation (113) or (114). The ground coordinates X, Y and Z of any object can thus be determined by substituting the exterior orientation elements of the camera, the scale factor and the image coordinates of the object in equation (111) or equation (112).

(v) Accuracy of the Results

The formula for the root mean square errors of the discrepancies given in equation (148) is used to analyse the results in this program. Equation (149) is also used to compute the residual x-parallax corresponding to the residual of the computed height.

7.5.3 Flexibility and Limitations

The least squares method is used in solving the observation equations, hence the number of ground control points is only limited by the computer's storage capacity. The minimum number of ground control points is, however, determined by the type of resection solution; in other words, the number of unknown parameters involved in the computations.

The number of models which may be tested is also limited only by the computer storage available.

If ground coordinates of points outside the model area are given, and these points are measured monocularly they can be used in the resection phase to give a better determination of the exterior orientation elements of the camera since the ground control will cover a larger area in this case.

A conventional resection solution can be handled by the program, hence a conventional photogrammetric model could be formed and tested. In this case, the camera's relative orientation parameters determined by this solution are printed as output and could be used as preliminary values in a bundle block adjustment program.

To apply any of the space resection solutions (conventional space resection, additional parameters or point-by-point space resection), it is only required to input the appropriate tag and the number of unknown parameters.

In the case of space resection with additional parameters, the parameters are divided into four groups, added one by one to the observation equations. This is done by choosing the appropriate value of X, the number of unknown parameters in each case.

The point-by-point space resection can be applied in either x- or y-direction depending on the direction of the shutter motion, if it is known. Otherwise a general case can be applied. Again, this is achieved by indicating the appropriate tag.

Although it is not common that the two overlapping exposures are taken by quite different cameras, if this did occur, it could be coped with by the program since the resections are determined quite separately for each photograph.

Since the program would normally only be used for test purposes, the ground coordinates should be given for all test points.

The maximum number of iterations needed is left to the user's choice. However, if the corrections to each of the camera rotation elements and to the camera translation elements are less than 0.00001 radian and 0.00001 metre respectively, then these will be suitable criteria to stop the computation.

7.6 Program (E) - Plot of Discrepancies

7.6.1 Introduction

The function of this program is to plot the discrepancies in plan and height of all the test points.

Subroutines provided by the GHOST Graphical Output System are used to generate the graphical output using the CIL (Computer Instrumentation Limited) Model 6011 plotter. A short program, written in Delft Algol for use on the IBM 370/158 computer at the Edinburgh Regional Computing Centre, is used to call these routines. The scales at which the plots have been generated are 1/580,000 for the Skylab models, and 1/58,000 and 1/26,300 for the Southampton and Worthing models of the F-126 photography respectively.

7.7 Program (F) - Transformation of Geographic Coordinates to Secant Plane Coordinate System

7.7.1 Introduction

In order to apply analytical photogrammetric techniques, it is necessary to transform the geographical ground coordinates of the test points, extracted from the available maps, to a three-dimensional orthogonal system. The function of this program is to transform the geographic coordinates of the test points measured on the 1/24,000 and 1/62,500 scale maps for the Skylab test to a local rectangular secant plane coordinate system.

7.7.2 Mathematical Basis

The secant plane coordinate system is a local three-dimensional Cartesian coordinate system. In this system, the X and Y are comparable to horizontal grid coordinates and the Z is equivalent to the combination of elevation and Earth curvature in which case the image coordinates need not be corrected for Earth curvature (Harris *et al.*, 1962).

The first step of the transformation is to transform the geographic positions and elevations of the test points to a geocentric coordinate system (Fig. 125) as follows:

$$X_G = (N + h) \cos\phi \sin\lambda \qquad \dots\dots\dots\dots\dots \quad (160)$$

$$Y_G = (N + h) \cos\phi \cos\lambda \qquad \dots\dots\dots\dots\dots \quad (161)$$

$$Z_G = \left[N(1 - e^2) + h\right] \sin\phi \qquad \dots\dots\dots\dots\dots \quad (162)$$

in which

ϕ and λ are the latitude and longitude of the point, respectively;

e is the ellipsoid eccentricity;

h is the elevation of the point above the ellipsoid, and

N is the radius of curvature of the ellipsoid at right angles to the meridian (or the length of the ellipsoid normal through ϕ and λ, terminating at the minor axis).

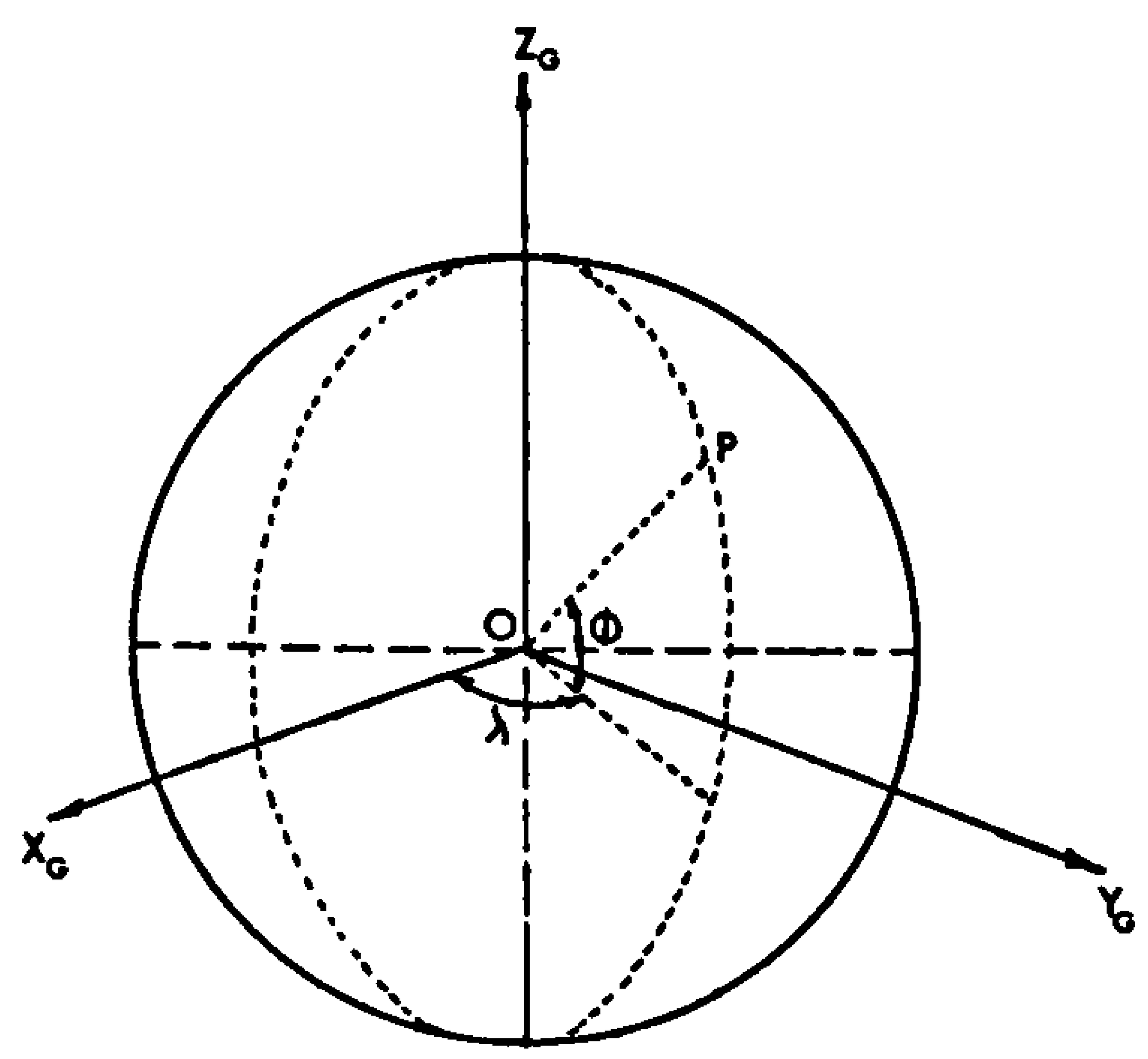

Fig. 125 $X_G\ Y_G\ Z_G$

Geocentric System

To rotate the geocentric system about the intersection of the polar axis and the normal of the ellipsoid through the secant plane origin, the X-Y plane is translated to this point by adding ($N_o\ e^2 \sin\ \phi_o$) to the Z_G coordinate (see Fig. 126), where N_o is the length of the normal through the secant plane origin:

$$Z_G' = \left[N\,(1 - e^2) + h\right]\ \sin\phi\ +\ N_o\ e^2 \sin\ \phi_o \quad \ldots\ldots\ldots\ldots \quad (163)$$

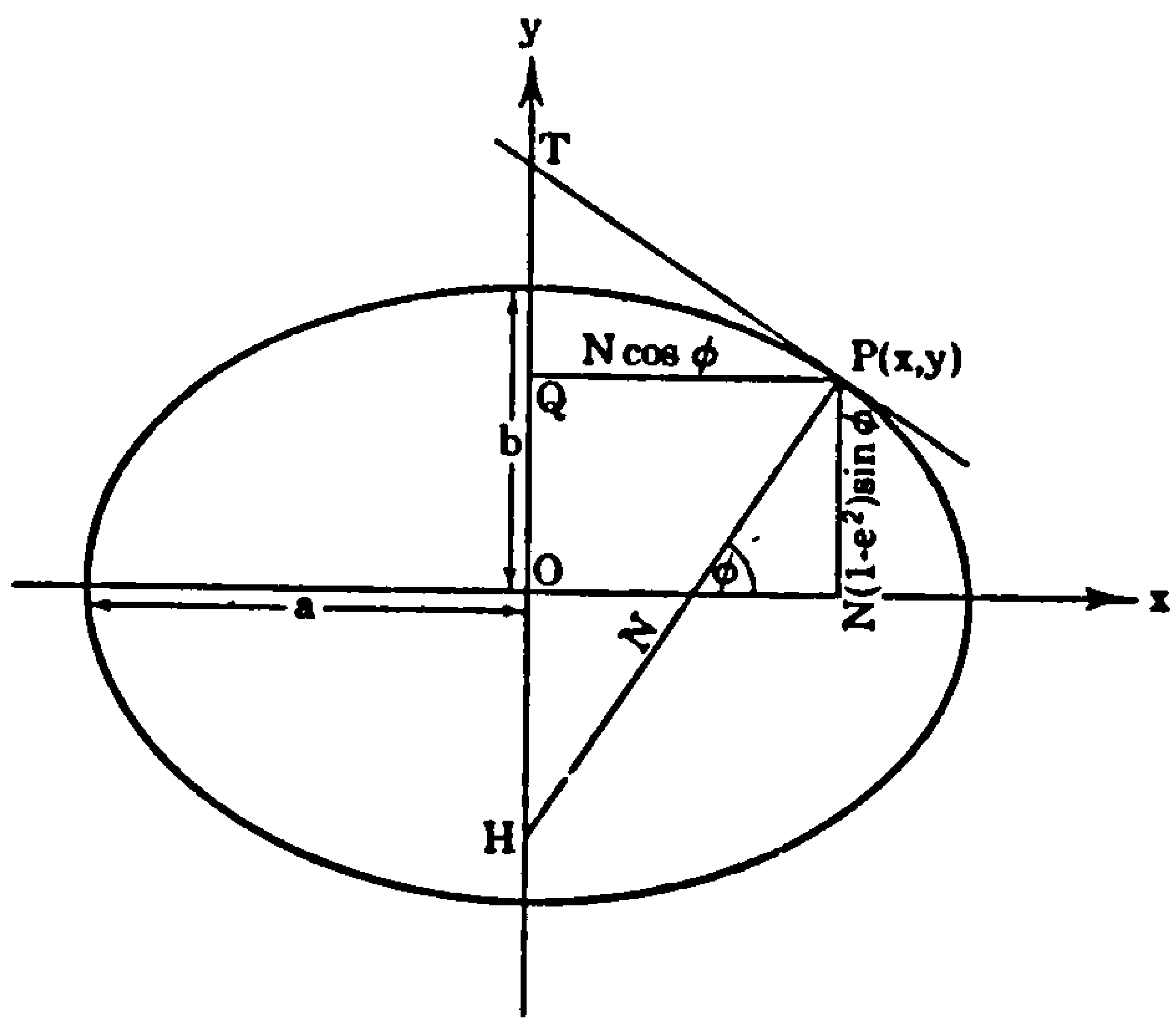

Fig. 126 Geometric elements used in the secant plane transformation

The modified geocentric system is then rotated to make the Z-axis coincide with the origin normal, with the Y-axis indicating north, and the X-axis indicating east:

$$\begin{bmatrix} X \\ Y \\ Z \end{bmatrix} = \begin{bmatrix} \cos\lambda_o & -\sin\lambda_o & 0 \\ \sin\phi_o \sin\lambda_o & -\sin\phi_o \cos\lambda_o & \cos\phi_o \\ \cos\phi_o \sin\lambda_o & \cos\phi_o \cos\lambda_o & \sin\phi_o \end{bmatrix} \begin{bmatrix} X_G \\ Y_G \\ Z'_G \end{bmatrix} \tag{164}$$

Since the Z-coordinate will be too large for practical computations, the X-Y plane of the rotated system is then translated along the Z-axis to a "secant position". The magnitude of the translation is arbitrarily chosen as the length of the origin normal reduced down to the nearest 10,000 metres. After this translation, the coordinates are in the secant plane system to be used in photogrammetric computations.

In order to check the validity of this transformation, the inverse transform of the secant plane system must be considered. This starts by translating the X-Y plane back to the intersection of the ellipsoid normal and the polar axis, followed by the rotation back into the modified geocentric system:

$$\begin{bmatrix} X_G \\ Y_G \\ Z_G \end{bmatrix} = \begin{bmatrix} \cos\lambda_o & -\sin\phi_o \sin\lambda_o & \cos\phi_o \sin\lambda_o \\ -\sin\lambda_o & -\sin\phi_o \cos\lambda_o & \cos\phi_o \cos\lambda_o \\ 0 & \cos\phi_o & \sin\phi_o \end{bmatrix} \begin{bmatrix} X \\ Y \\ Z \end{bmatrix} \qquad (165)$$

The longitude is computed from equations (160) and (161):

$$\lambda = \tan^{-1} (X_G/Y_G) \quad \ldots\ldots\ldots\ldots\ldots\ldots\ldots \quad (166)$$

and also $\phi = \tan^{-1} Z_G/(X_G^2 + Y_G^2)^{\frac{1}{2}}$ .... (167)

Using an iterative procedure to solve equations (163) and (167) for the latitude of the point, a number of two or three iterations would be quite sufficient. After computing the latitude of the point the elevation, h, may be computed from equation (160) or equation (161):

$$h = (X_G/\cos\phi \ \sin\lambda) - N$$

or

$$h = (Y_G/\cos\phi \ \cos\lambda) - N \quad \ldots\ldots\ldots\ldots\ldots\ldots \quad (168)$$

7.8 Program (G) - Transformation of Geographic coordinates to U.T.M. Coordinates

7.8.1. Introduction

A commonly-used alternative rectangular coordinate system , used in conjunction with analytical photogrammetric techniques, is the U.T.M. system. The function of program (G) is to transform geographic coordinates of the test points used for the Skylab test to the U.T.M. system. The objective is to compare the results obtained when using this system and the secant plane rectangular system, explained above, especially with regard to the effect of Earth curvature.

7.8.2 Mathematical Basis

The equations of the transformation of geographic positions to U.T.M. coordinates are given as follows (Department of the Army, 1958):

$$N = (I) + (II)p^2 + (III)p^4 + A_6 \quad \ldots\ldots\ldots\ldots\ldots \quad (169)$$

$$E = (IV)p + (V)p^3 + B_5 + FE \quad \ldots\ldots\ldots\ldots\ldots\ldots \quad (170)$$

in which

$$p = 0.0001 \Delta\lambda \text{ from central meridian} \quad \ldots\ldots\ldots\ldots\ldots\ldots\ldots \quad (171)$$

$$\text{central meridian} = 6 \times (\text{Zone number}) - 183$$

$$v = a/(1 - e^2 \sin^2 \phi)^{\frac{1}{2}}$$

$$I = 6367399.689 \text{ scale } \left\{ \phi_{\text{radians}} - \sin\phi \cos\phi \; 10^{-6} \left[5104.57388 - \cos^2\phi \,(21.73607 - 0.11422 \cos^2\phi) \right] \right\} \quad (172)$$

$$II = \frac{v \sin\phi \cos\phi \sin^2 1''}{2} \text{ scale } 10^8 \quad \ldots\ldots\ldots\ldots\ldots\ldots\ldots \quad (173)$$

$$III = \frac{\sin^4 1'' \, v \sin\phi \cos^3\phi}{24} (5 - \tan^2\phi + 9 e'^2 \cos^2\phi + 4e'^4 \cos^4\phi) \text{ scale } 10^{16} \quad \ldots\ldots\ldots\ldots \quad (174)$$

$$IV = v \cos\phi \sin 1'' \text{ scale } 10^4 \quad \ldots\ldots\ldots\ldots\ldots\ldots\ldots\ldots\ldots \quad (175)$$

$$V = \frac{\sin^3 1'' \, v \cos^3\phi}{6} (1 - \tan^2\phi + e'^2 \cos^2\phi) \text{ scale } 10^{12} \quad \ldots\ldots \quad (176)$$

$$A_6 = p^6 \frac{(\sin^6 1'' \cos^5\phi \sin\phi)}{720} (61 - 58 \tan^2\phi + \tan^4\phi + 270e'^2 \cos^2\phi - 330 e'^2 \sin^2\phi) \text{ scale } 10^{24} \quad \ldots\ldots \quad (177)$$

$$B_5 = p^5 \frac{(\sin^5 1'' \, v \cos^5\phi)}{120} (5 - 18 \tan^2\phi + \tan^4\phi + 14e'^2 \cos^2\phi - 58e'^2 \sin^2\phi) \text{ scale } 10^{20} \quad \ldots\ldots\ldots \quad (178)$$

In the above equations:

N = grid Northing coordinate

E = grid Easting coordinate

FE = False Easting = 500,000 metres

scale = 0.9996

a = semi-major axis

b = semi-minor axis

e = ellipsoid eccentricity

$$e' = \left(\frac{a^2 - b^2}{b^2}\right)^{\frac{1}{2}} = \left(\frac{e^2}{1 - e^2}\right)^{\frac{1}{2}}$$

The constants in these equations are based on the parameters of the Clarke Spheroid 1866.

7.9 Conclusions

It is obvious that the test work carried out would have been impossible without the availability of a computer. Therefore, considerable effort and time were expanded in developing and preparing the computer programs described in this Chapter. Nevertheless, much experience has been gained in a field which was previously unfamiliar to the author. The present programs were satisfactory for the purposes of the author's experimental work but no doubt could be made more efficient and quicker in operation. However, this would mean the expenditure of much more effort and time than was available during the present work.

Efforts were made to check the programs by using suitable data and results available from other projects and publications. Thus the absolute orientation program (C) was checked using data from the Durban test models provided by

Mr. B.D.F. Methley. Data extracted from Keller's report on Skylab photography (Keller, 1975) were used to check the Space Resection program (D). The inverse version of program (F) was used to check the transformation of geographic coordinates to rectangular plane coordinates. Program (G) was checked by data from the Clarke Spheroid (1866) Tables.

The results of the actual tests on the measured S-190B and F-126 reconnaissance frame photography are given and analysed in the next Chapter.

CHAPTER VIII

Results of the Experimental Tests

CHAPTER VIII

RESULTS OF THE EXPERIMENTAL TESTS

8.1 Introduction

The flow diagram shown on page 185 in Chapter VII shows two different procedures for the data processing. In each case, however, the image coordinates were first corrected for the various image distortions (lens distortion, Earth curvature and atmospheric refraction), where applicable, using program A. The Addendum to LEC/ASD Technical Memo No. TM73-002 issued on July 11, 1974, indicated that the S-190B camera lens distortion to be insignificant (maximum radial distortion = $\pm$ 10 um) (Keller, 1975), so no correction was made for the S-190B photography. In the case of the F-126 photography, the lens distortion curve shown in Fig. 115 was used to correct the image coordinates of the F-126 photography. Also the distortion due to atmospheric refraction at camera altitudes above 40 miles (64 km) is relatively negligible, hence no attempt was made to correct this for the S-190B photography (flying altitude 435 km). The output from program A will then go through the following processes.

I. Corrected image coordinates were used as input to the <u>analytical relative orientation program</u> developed by Mr. B.D.F. Methley (program B), to form the model coordinates which were then transformed to ground coordinates using the (i) <u>analytical absolute orientation</u> and (ii) the <u>polynomial adjustment program</u> (program C).

II. The same corrected image coordinates were also used as input data for the <u>Space resection/space intersection program</u> (program D), in which the exterior orientation elements were determined. These elements were determined using either (i) conventional space resection, (ii) the additional parameters method or (iii) the point-by-point space resection technique. Ground coordinates were then determined by intersection in space.

In all these tests, the ground coordinates were obtained by measurements on existing maps, and in the case of the S-190B photography were then transformed to rectangular coordinates (either UTM, or secant plane coordinates). Discrepancies between computed ground coordinates and their known values were determined. These were then used to determine the root mean square errors (RMSE's) of the residuals at the check points and were also plotted as vectors to analyse the results and see if any residual systematic errors could be identified.

For simple identification purposes the different techniques were given appropriate symbols as shown in Table 12.

Table 12

Technique	Symbol
Group I	
(i) Conventional absolute orientation uncorrected terrain coordinates	I(i)
(ii) Polynomial adjustment of terrain coordinates using 6 polynomial parameters	I(6)
" 7 " "	I(7)
" 8 " "	I(8)
" 9 " "	I(9)

Table 12 (continued)

Technique	Symbol
Group II	
(i) Conventional single photo resection followed by space intersection	II(i)
(ii) Space resection with additional parameters:	
using 2 parameters (a-terms)	II(2)
" 8 " (a- and b-terms)	II(8)
" 10 " (a-, b- and c-terms)	II(10)
" 12 " (a-, b-, c- and d-terms)	II(12)
(iii) Point by point space resection/space intersection	II(iii)

8.2 S-190B Test Results

As has already been mentioned, two models (01334/5 and 01335/6) were available for test.

In all the tests the ground coordinates of the test points, measured from 1/24,000 or 1/62,500 maps were used as known values. With the exception of one test, all ground coordinates are given in the secant plane coordinate system. Whenever such a coordinate system is used, the correction to image coordinates for Earth curvature is unnecessary, since the transformation accounts for the curvature of the Earth (Harris _et al_., 1962).

All the ground control points are full control (given in X, Y and Z coordinates). The root mean square errors (RMSE's) of the residuals of the computed ground coordinates from the known values were determined.

3.2.1 Results

The tests performed were divided into two groups according to the technique used. This will make it easy to compare the effects of the different techniques.

Group I (i)

Conventional absolute orientation was carried out for models 01334/5 and 01335/6 (4 and 6) as follows:

(a) using four control points at the corners of each model,

(b) using twenty control points evenly distributed throughout each model,

(c) using twenty control points (same as case (b)) with the ground coordinates given in UTM system,

(d) using all the test points as control.

The RMSE's were determined from the residuals at the check points only (at all the test points for case (d)) and are shown in Table 13,

where m_x = RMSE of residuals in X,

m_y = RMSE of residuals in Y,

m_{pl} = RMSE of residuals in plan $\left(=\sqrt{m_x^2 + m_y^2}\right)$

m_z = RMSE of residuals in height,

H = Flying height.

Table 13

	Model No. 01334/5						Model No. 01335/6					
	No. of control points	No. of check points	m_x (m) (μm)	m_y (m) (μm)	m_{pl} (m) (μm)	m_z (m) (‰H)	No. of control points	No. of check points	m_x (m) (μm)	m_y (m) (μm)	m_{pl} (m) (μm)	m_z (m) (‰H)
(a)	4	56	16.1	26.5	31.0	102.7	4	48	26.3	14.5	30.0	95.6
			17	28	33	0.24			28	15	32	0.22
(b)	20	40	16.5	17.4	24.0	90.4	20	32	20.8	13.3	24.7	60.9
			17	18	25	0.21			22	14	26	0.14
(c)	20	40	16.9	17.4	24.3	98.6	20	32	21.0	16.8	26.9	63.9
			18	18	26	0.23			22	18	28	0.15
(d)	60	60	15.9	18.1	24.1	79.2	52	52	18.4	14.7	23.6	57.2
			17	19	25	0.18			19	15	25	0.13

Model 01334/5

The results from the use of 4 control points (case (a)) gave the errors m_x, m_y and m_z to be $\pm$ 16.1, $\pm$ 26.5 and $\pm$ 102.7 m respectively. The use of additional control points, 20 in all (case (b)) resulted in no improvement in m_x but a considerable improvement in m_y and m_z. The m_y figure improved from $\pm$ 26.5m to $\pm$ 17.4 metres (a 30% improvement) and the m_z from $\pm$ 102.7m to $\pm$ 90.4m (a 12% improvement). In case (d) where all the available terrain points were used as control, there was no further improvement in the y coordinates ($m_y = \pm$ 18.1m) but there was a further improvement in the z of 12% ($m_z = \pm$ 79.2m).

Model 01335/6

With this model, the results were rather different. With 4 control points (case (a)), the errors m_x, m_y and m_z were $\pm$ 26.3m, $\pm$ 14.5m and 95.6m respectively. Thus the errors in x and in y were interchanged. When 20 points were used as control (case (b)) the m_x improved 25% to $\pm$ 20.8m and the m_y improved hardly at all to $\pm$ 13.3m. The heights showed a dramatic improvement $m_z = \pm$ 60.9m (a 35% improvement). In case (d) when all the available points were used as control, there were only small improvements in the figures for m_x, m_y and m_z.

It is very difficult to account for the initial discrepancies between the two models when only four controls were used. One may suggest that errors in only one control point in either model may be the reason for when 20 controls were used, the figures for each model immediately showed a closer agreement in x and y.

	m_x	m_y	m_z
<u>Case (b)</u> model 01334/5	16.5	17.4	90.4
model 01335/6	20.8	13.3	60.9

When all points were used (d), the agreement in x and y stayed much the same but the z improved in both models.

<u>Case (d)</u> model 01334/5	15.9	18.1	79.2
model 01335/6	18.4	14.7	57.2

Taking the average for the two models gives:-

Case (a) (4 points)	21.2	20.5	99.2
Case (b) (20 points)	18.7	15.3	75.6
Case (d) (All points)	17.2	16.8	68.2

From the <u>vector diagram of position errors</u>, shown in Appendix C it can be seen that, for both models, the patterns of the errors show a systematic tendency for each group of points whose ground coordinates were measured from the same map. In this context, it must be remembered that the final residuals obtained will be dependent on the accuracy of the control used. This may account for the fact that the results obtained for model 01335/6 in which only 61% of the test points were measured from the smaller scale 1/62,500 maps, are better than those obtained for model 01334/5 with 83% of its test points measured from the1/62,500 scale maps. As can be seen from inspection of the other vector diagrams, this tendency for a systematic pattern of errors in groups occurs for all the tests made. The size and pattern of these errors are, however, not so large as to invalidate the results of the tests.

When the vector diagrams of the height errors were examined (see Appendix C) the errors were noticed to be systematic along the axis transverse to the flight direction (Y-axis). It was initially suspected that these systematic errors were associated with Earth curvature. For this reason, the test was re-run using U.T.M. coordinate values, with the image coordinates being corrected for Earth curvature effect. Results of this test are given in the above Table 13(c). The results are virtually the same as those obtained using secant plane coordinates for the model 01334/5 and a little worse for the model 01335/6, the small deterioration being due possibly to the assumption that the photography was truely vertical, as far as correction for Earth curvature is concerned. The outcome of the investigation was that no source for the small systematic errors in height could be identified. Again they are not of such a magnitude that they are significant for the results of the tests.

Summarising the results of the tests of Group I(i), one can say that the use of increasing numbers of control points gave, as might be expected, better results. Especially, the increase from 4 to 20 points gave markedly improved results both in planimetry but more especially in height. All the remaining tests which follow have been carried out using 20 control points in each model, with 40 and 32 check points available respectively in the two models. Thus the same data in respect of measured plate coordinates, control points and test points has been input for all the other techniques investigated in this study.

Group I (ii)

16, 17, 18, 19 - Conventional absolute orientation followed by polynomial adjustment of six, seven, eight and nine parameters respectively was carried out for the two models using the twenty control points. The RMSE's were determined from the residuals at the check points only and are shown in Table 14.

Table 14

Technique	Model No. 01334/5 No. of check points 40				Model No. 01335/6 No. of check points=32			
	m_x (m) (µm)	m_y (m) (µm)	m_{pl} (m) (µm)	m_z (m) (‰H)	m_x (m) (µm)	m_y (m) (µm)	m_{pl} (m) (µm)	m_z (m) (‰H)
16	16.4 17	16.7 18	23.4 25	85.9 0.20	15.6 16	12.6 13	20.0 21	55.9 0.13
17	15.3 16	17.2 18	23.0 24	90.4 0.21	14.1 15	12.6 13	18.9 20	58.6 0.13
18	15.9 17	17.4 18	23.6 25	85.9 0.20	14.1 15	13.3 14	19.4 21	58.0 0.13
19	17.5 18	15.8 17	23.6 25	91.2 0.21	14.4 15	13.6 14	19.8 21	57.8 0.13

The general trend of the results is that the use of the six polynomial terms $(1, x, y, xy, x^2, y^2)$ is a fairly effective method of acheiving a good fit to the control. The figures for the two models:-

	m_x	m_y	m_z
model 01334/5	16.4	16.7	85.9
model 01335/6	15.6	12.6	55.9
mean	16.0	14.6	70.9

are of the same general order as (but slightly improved on) those achieved using 20 control points without a polynomial correction (Group I(i) case (d)). The tendency for the m_y and m_z figures to be much better in the second model than the first continues to be present.

When higher order polynomials are used, there is no discernible improvement in the results which points to the affectiveness of the six originally selected parameters. This also means that the use of and need for additional control points does not bring about any worthwhile improvement in results.

The vector diagrams show the same tendency for the groups of points associated with the same map sheet to exhibit the slightly systematic pattern of error first noted in the Group I (i) tests.

Conventional absolute orientation followed by polynomial adjustment was also carried out for the two models using all the test points as control points. The RMSE's were determined from the residuals at the test points and are shown in Table 15.

Table 15

Technique	Model No. 01334/5 No. of test points = 60				Model No. 01335/6 No. of test points = 52			
	m_x (m) (μm)	m_y (m) (μm)	m_{pl} (m) (μm)	m_z (m) (‰H)	m_x (m) (μm)	m_y (m) (μm)	m_{pl} (m) (μm)	m_z (m) (‰H)
16	15.2	16.9	22.7	92.3	15.6	14.5	21.3	59.4
	16	18	24	0.21	16	15	23	0.14
19	15.8	18.0	23.9	92.4	14.4	14.7	20.6	61.3
	17	19	25	0.21	15	16	22	0.14

This also does not show any improvement in results than when only the 20 points were used.

Group II

The second group of tests comprise those which use the space resection/space intersection procedure as the basis for converting the measured image coordinates to the final terrain coordinates.

II (i) Conventional space resection/space intersection was carried out for the two models using, as in the previous case, twenty control points. The RMSE's were determined from the residuals at the check points only and are shown in Table 16.

Table 16

Model No. 01334/5 No. of check points = 40				Model No. 01335/6 No. of check points = 32			
m_x (m) (μm)	m_y (m) (μm)	m_{pl} (m) (μm)	m_z (m) (‰H)	m_x (m) (μm)	m_y (m) (μm)	m_{pl} (m) (μm)	m_z (m) (‰H)
17.5	20.2	26.7	158.0	20.1	20.1	28.4	130.3
18	21	28	0.36	21	21	30	0.30

Corrections were made to the plate coordinates only. In all respects the results were markedly poorer with this method compared with any other. This may be explained by the fact that the space resection of each individual photograph was carried out with control only in the overlap area, resulting in a weak determination of the orientation parameters. Control points located across the full extent of the photograph would have provided a better solution. Another possible reason for the poor results was that a single perspective centre, corresponding to the geometric centre of the photograph, was assumed for the whole of each photograph. The intersections to give terrain coordinates of the test points were then calculated on this assumption. However, strictly speaking this is not true since the camera is equipped with a focal plane shutter where the perspective centre changes in position during the exposure. This may be a significant point given the high speed of a satellite (ca. 8 km/second) over the terrain. Thus for a single exposure during a typical shutter transit time of 1/10 sec, the satellite (and the perspective centre) will move through a distance of 800 metres or 400 metres on either side of the geometric centre of the photograph.

The next two methods in which the space resection/intersection method is modified to use (i) additional parameters and (ii) the point-by-point computational method have been devised to overcome this particular difficulty (as well as others).

Group II (ii) - Space resection with additional parameters was carried out for the two models using the same twenty control points. The RMSE's were determined from the residuals at the check points only and are given in Table 17.

Table 17

Technique	Model No. 01334/5 No. of check points = 40				Model No. 01335/6 No. of check points = 32			
	m_x (m) (μm)	m_y (m) (μm)	m_{pl} (m) (μm)	m_z (m) (‰H)	m_x (m) (μm)	m_y (m) (μm)	m_{pl} (m) (μm)	m_z (m) (‰H)
II (2)	15.3	16.1	22.2	93.8	16.1	11.9	20.0	65.8
	16	17	23	0.22	17	13	21	0.15
II (8)	17.1	16.3	23.6	99.1	15.0	11.8	19.1	87.0
	18	17	25	0.23	16	13	20	0.20
II (10)	16.6	16.2	23.2	106.2	14.9	13.1	19.8	69.8
	17	17	25	0.24	16	14	21	0.16
II (12)	18.5	16.8	24.9	66.9	19.6	12.8	23.4	49.0
	20	18	26	0.15	21	14	25	0.11

The improvement in the results with the use of first two additional parameters (the a-terms) is quite dramatic, especially in height. The a-terms represent principally the change in the image scale caused by the use of an incorrect or unknown principal distance. They also model the affine change in scale produced by the focal plane shutter. In the light of the analysis previously conducted in Chapter IV, this is less likely to be the source of error.

The use of further additional parameters in the form of the b-terms (8 parameters) and the c-terms (10 parameters) does not cause any significant change in the figures for m_x and m_y, but they do cause the errors in height to grow significantly larger. This may well be due to correlation between these parameters, or that they are insignificant, in which case they will change the accuracy of the model, a problem already raised by Ebner (1976).

However, when the d-terms which model the position of the principal point are used a quite emphatic improvement takes place in the heights with $m_z = \pm 66.9$ m and ± 49.0m in the two models. Again there is a slight deterioration in the results for m_x and m_y.

The effect of the error (dx_p) in the position of the principal point on the height is given as (Hadem, 1968):

$$dZ = \frac{H^2}{Bf}(dx_{p_2} - dx_{p_1})$$

where dZ = error in height caused by errors dx_{p_1} and dx_{p_2} in positions of left hand and right hand principal points,

H = flying height above terrain

f = principal distance and

B = air base.

Thus for narrow angle photography where the B/H ratio is small (0.10 for the S-190B photography), the height error caused by the error in the position of the principal point will be significantly large as compared with the super-wide-angle photography and its larger B/H ratio (1.0). This is illustrated by these two cases shown in Fig. 127 (a) and (b). For the same flying height and principal distance, the error in height caused by error in principal point for case (b) is 10 times larger than that for case (a).

Fig. 127

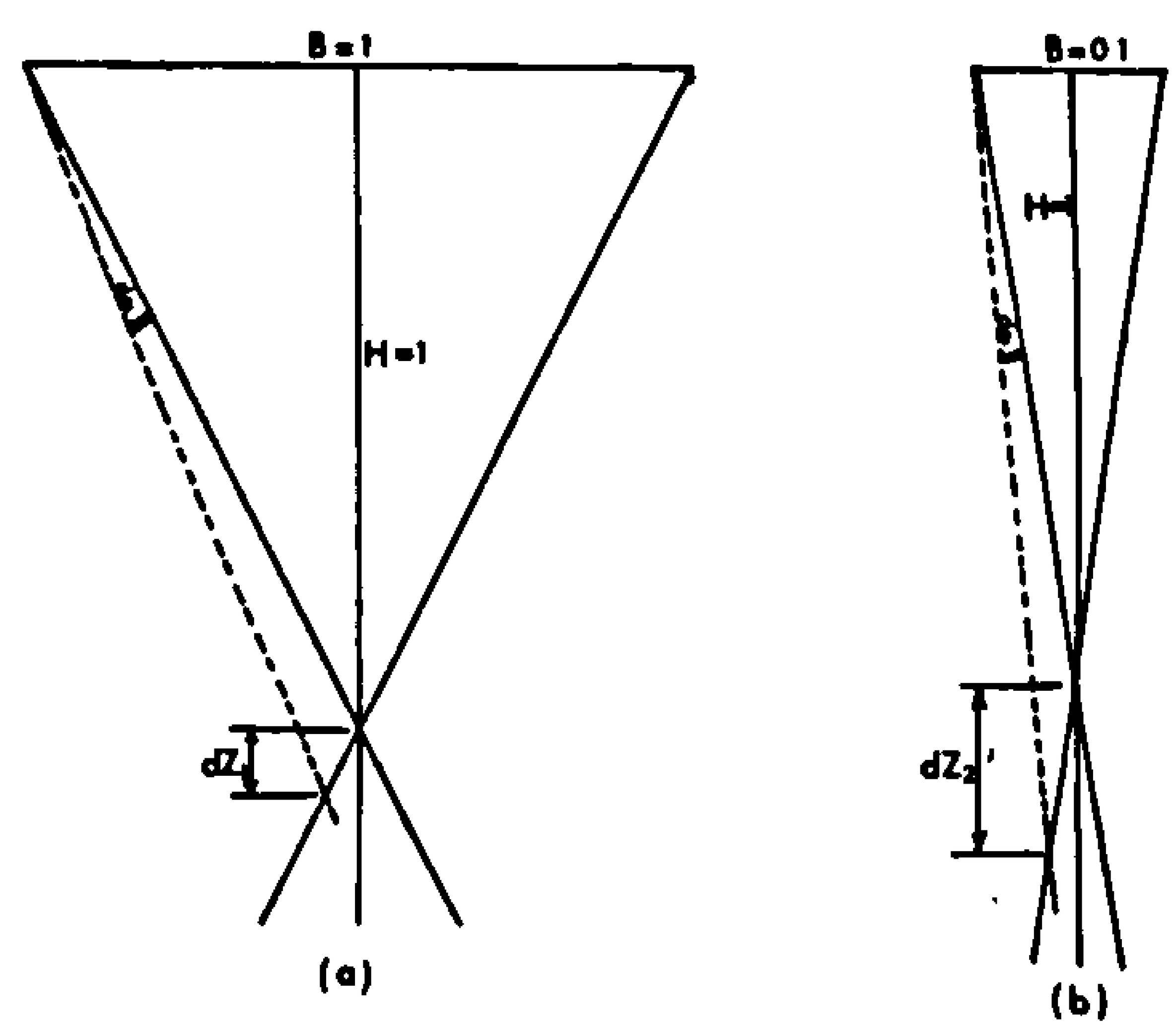

Group II (iii) Point-by-point space resection/space intersection was carried out for the two models using the twenty control points. The RMSE's were determined from the residuals at the check points only and are given in Table 18.

Table 18

Model No. 01334/5 No. of check points = 40				Model No. 01335/6 No. of check points = 32			
m_x (m) (μm)	m_y (m) (μm)	m_{pl} (m) (μm)	m_z (m) (‰H)	m_x (m) (μm)	m_y (m) (μm)	m_{pl} (m) (μm)	m_z (m) (‰H)
14.7	15.2	21.2	66.2	20.8	15.9	26.2	83.4
16	16	22	0.15	22	17	28	0.19

The results from this method are quite peculiar and disturbing in that model No. 01334/5 gave better results than model No. 01335/6 which is quite the opposite to the results obtained from all the other methods and tests given above. Results for model No. 01334/5 were significantly improved from that when the conventional resection method was used. (m_x from ± 17.5m to ± 14.7m, m_y from ± 20.2m to ± 15.2m and m_z from ± 158.0m to ± 66.2m). The improvement in results for model no. 01335/6 is only noticeable for m_y and m_z (m_y from ± 20.1m to ± 15.9m and m_z from ± 130.3m to ± 83m).

A considerable time has been spent on checking the input data, the programs etc. and in re-running the programs to try and locate any error which could have occurred which could cause the results for the second model (01335/6) to be much poorer than the first (01334/5) - but unfortunately without change in the results. Certainly one would expect this methdd of point-by-point space resection/space intersection to be an effective method of dealing with the time-varying parameters such as the camera rotations which are inherent in the operation of a camera equipped with a focal plane shutter. In fact the results from the first model show the method is just as effective as the use of additional parameters (Group II (ii)) and more effective than the use of polynomials (Group I (ii)) to warp out the terrain coordinates. It is frustrating not to have this confirmed by the second model and to be unable to find any reason for the anomalous results of this model.

8.3 Analysis of the S-190B Test Results

Before discussing the results shown above, it should be mentioned here, again, that the scale of this photography is 1/945,600 and the B/H ratio is 0.10. The accuracy of the ground control is between 10-20μm at the photo scale and the estimated ground resolution is 30 metres.

8.3.1 Planimetric Accuracy

Attempting an overall assessment of the planimetric results, one notices immediately that the special techniques devised in this study to treat this type of photography all improved the accuracy of the planimetric coordinates significantly. Figs. 128 and 129 enable a graphical comparison of the results using the different techniques to be made. The polynomial adjustment method (I6, I7, I8 and I9) and the additional parameters technique (II2, II8, II10 and II12) gave a planimetric accuracy (m_{pl}) between $\pm$ 20 — 25 μm at the photo scale for both models. The same result was also achieved with the point-by-point resection intersection method (II (iii)) but for the first model only. Hence all of these techniques are effective in improving the accuracy of the planimetric accuracy, significantly.

Comparing the effects of the different polynomials, it is clear that the first

TEST RESULTS - S-190B Photography

Planimetry

Fig. 128 Planimetric accuracy
Model No. 01334/5

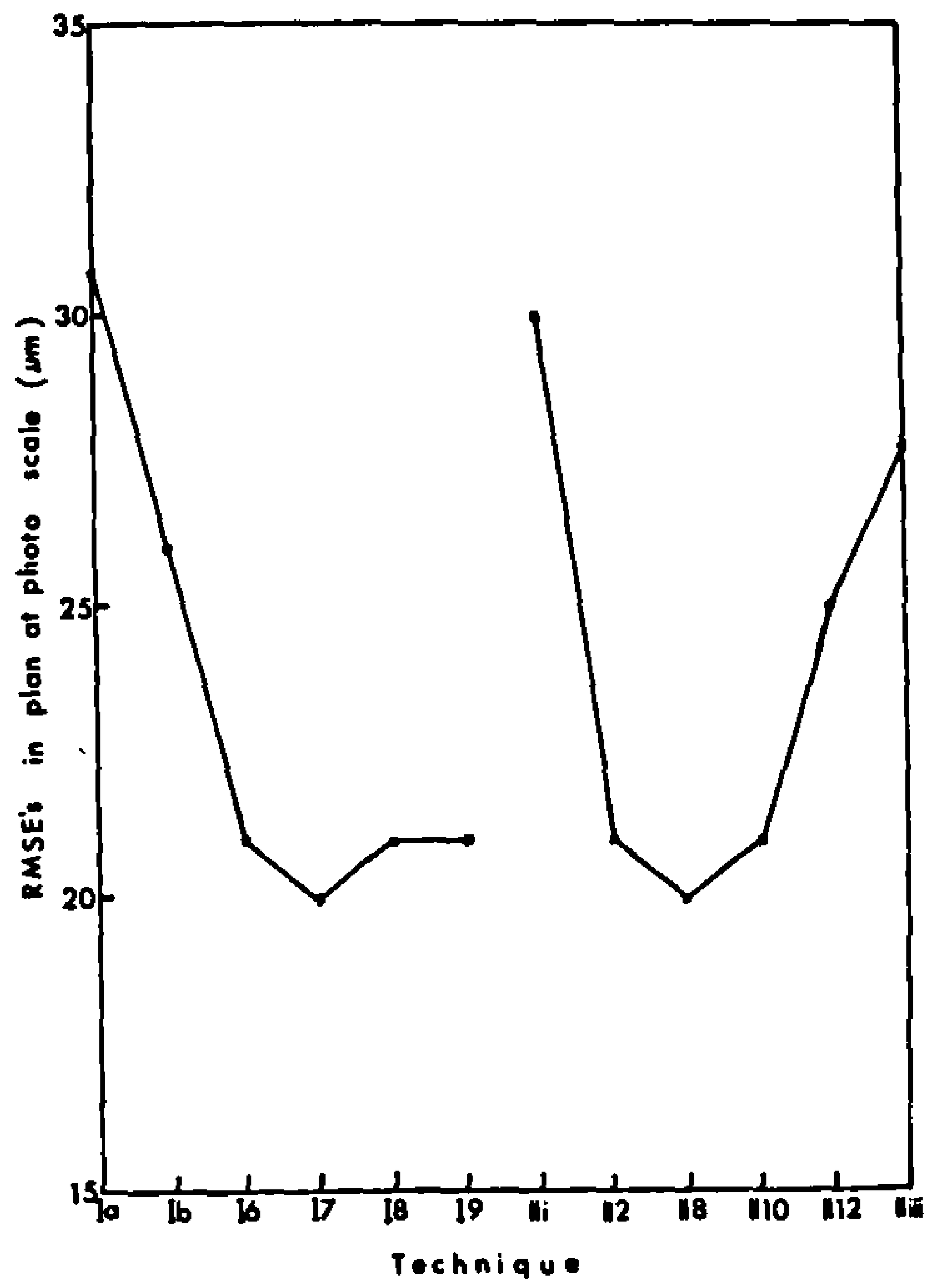

Fig. 129 Planimetric accuracy
Model No. 01335/6

Height

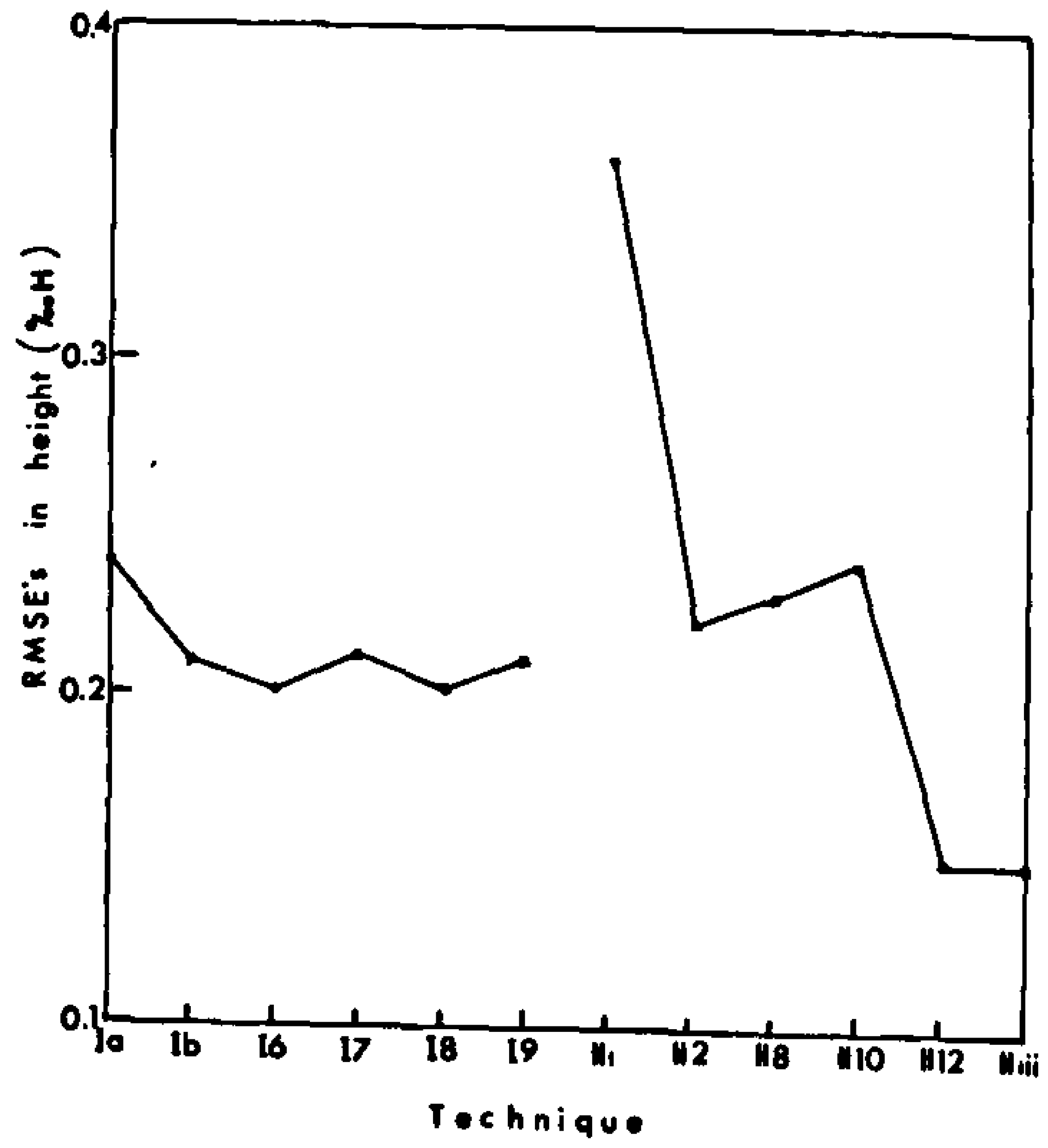

Fig. 130 Height accuracy
Model No. 01334/5

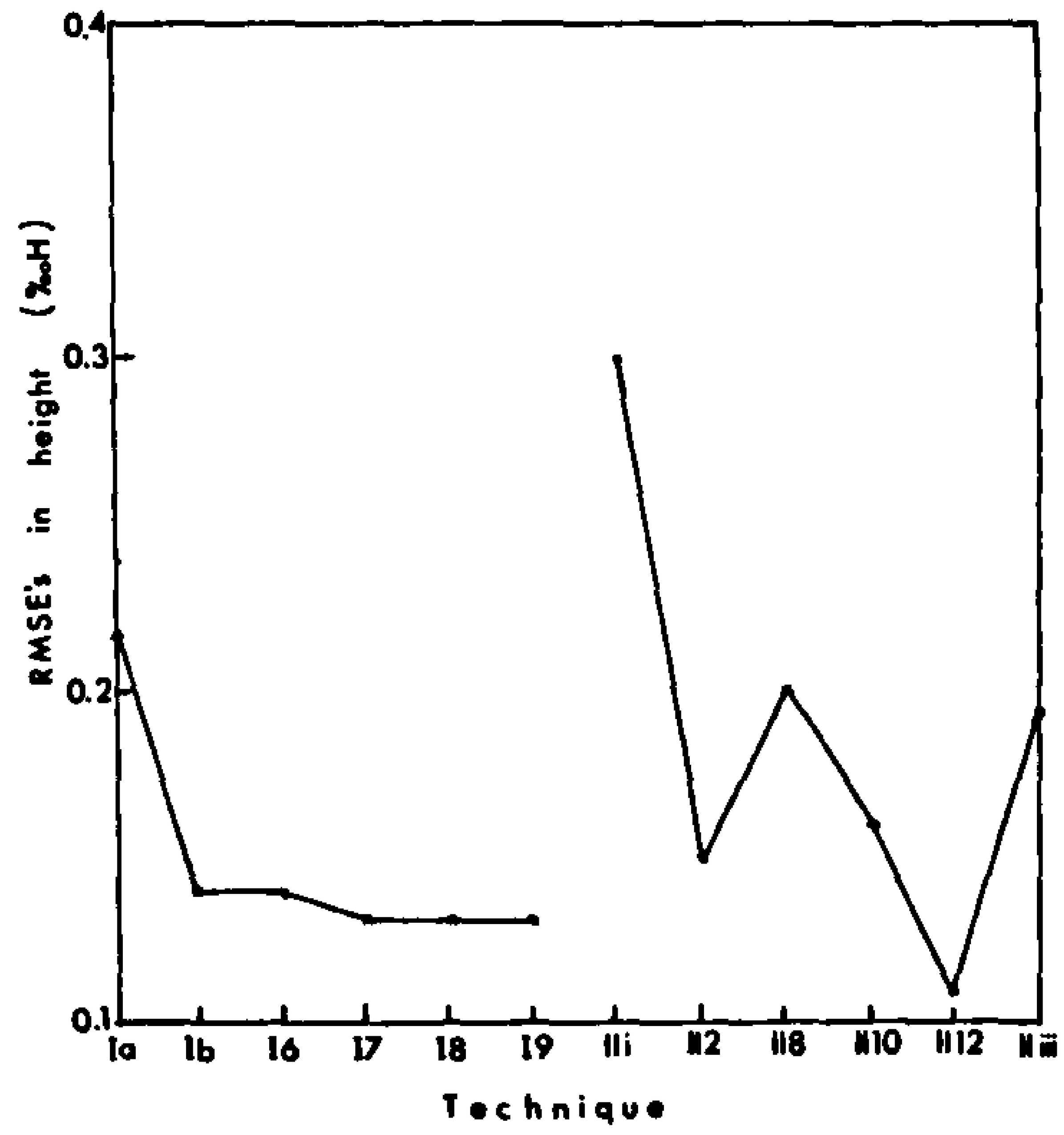

Fig. 131 Height accuracy
Model No. 01335/6

six parameters (I6) (see equations 132 and 133) are the most effective on the two models; the difference using higher-order polynomials (I7, I8 and I9) did not exceed 1 um at the photo scale, which is totally insignificant.

As far as the additional parameters method is concerned, the first group using the a-terms in equation 117 are the most effective when testing model No. 01334/5. These are the terms that correct for the scale change of the photography, most usually caused by inaccuracy in the principal distance. The addition of the second group (II8) which corrects for the film deformation (the b-terms in equation 117) did not improve the accuracy obtained by the first group to any significant extent. The same remarks can be made regarding the addition of the third group (II10) which corrects for radial distortion. The addition of the fourth group (the d-terms in equation 117) in fact makes the planimetric accuracy slightly worse (ca. 3µm), again relative to the accuracy obtained by the first group.

Comparison with other tests from Skylab photography

The planimetric results obtained here can be compared directly with those obtained by Keller (1976) when he applied an aerotriangulation test, using the N.O.S. least squares bundle adjustment method on a strip of the S-190B photography taken over North Carolina, U.S.A. and measured with a stereocomparator. Keller utilised as control and check points positions extracted from 1/24,000 scale maps, and obtained a planimetry accuracy (m_{pl}) of $\pm$16µm at the photo scale. These results are a little better than the 20 to 22µm obtained in the present series of tests. It is difficult to account for these differences. However, the N.O.S. method is a particularly rigorous method of adjustment, starting with the refinement of images and followed by a three-photo orientation phase in which a geometric fitting of the adjacent photographs is carried out, and any points exhibiting excessively large discrepancies are discarded and re-measured. This is then followed by a polynomial adjustment of the strip to provide provisional terrain coordinates and finally by the bundle adjustment itself, which gives a simultaneous solution of the absolute orientation of all the photographs and the final object coordinates. Obviously it proved in this case to be very effective method in detecting blunders, refining image coordinates and in compensating for systematic errors.

The only other published results (Stewart, 1975) from the Skylab flights utilised the 70mm format S-190A multi-spectral photography. Although the S-190A camera has shorter focal length (f = 152 mm), - hence producing smaller scale (1/2,850,000) photography - it is a metric camera and was equipped with an intra-lens shutter. The base:height ratio is 0.19. Stewart used the Stuttgart Adjustment Program PAT-M (which is a method based on the use of independent models) to adjust the model coordinates to the ground control points. The ground control for this Canadian test was extracted from 1/50,000 scale maps. A summary of the results is given in um in the plane of the negative for the purposes of comparison with the S-190B tests. In all cases, only 4 control points have been used, but with a large number of check points (58 to 87).

	No. of Check points	m_x µm	m_y µm	m_{pl} µm
(i) Two Black and White Models :				
1st model	58	16	30	34
2nd model	85	15	28	30
(ii) Two Colour Models:				
1st model	64	31	30	42
2nd model	87	20	24	31

It has already been mentioned that the S-190A camera is a metric camera where an intra-lens shutter that allows simultaneous exposure is used and no problem of positioning the principal point is encountered. Thus it can be concluded that the results obtained by Stewart from the S-190A photography (30 - 40μm) are markedly inferior to those obtained from the S-190B photography both in the current research and by Keller (1975).

Overall it may be assumed that the results obtained for planimetry in the present test are reasonably satisfactory. The figures of 20 to 25 m (corresponding to 20 - 25 μm) must be considered in the context of the circumstances prevailing in the test. The ground resolution of the S-190B colour photography is estimated at 30 m and the accuracy of the untargeted test points is estimated to be between 7 μm and 20 μm at the photo scale. Also the radial lens distortion ($\pm$ 10 μm maximum) has not been corrected. Thus the results obtained (while not quite as good as those of Keller) appear to be reliable and acceptable and would not indicate any other significant source of errors. This tends to support strongly the conclusion reached after the geometric analysis in Chapter IV that, with accurate IMC, the effect of the focal plane shutter is insignificant, at least as far as planimetric accuracy is concerned.

Possible Mapping Scales

Another special point for discussion is the question of the mapping scale which might be attempted from this type of photography. The NATO standard specifications for topographic maps at 1/600,000 and larger stipulate a standard error of $m_{pl} = \pm$ 0.3 mm (Petrie, 1974). On this basis, the planimetric detail accuracy has been plotted for different map scales between 1/50,000 and 1/250,000 (Fig. 132).

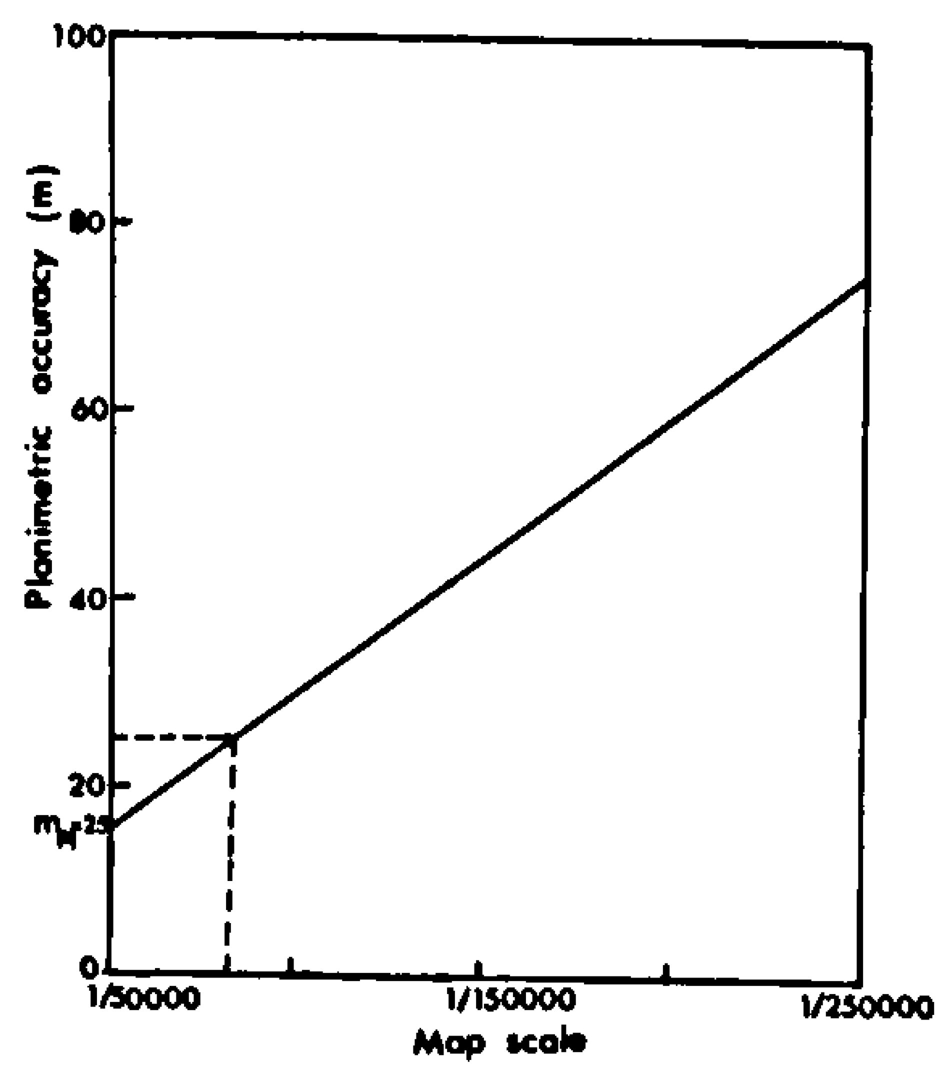

Fig. 132. Planimetric Detail Accuracy at different scales

From Fig. 132 it can be seen that the planimetric accuracy obtained from the S-190B photography in the tests conducted above would allow its use for purely planimetric mapping at 1/100,000 scale and smaller quite satisfactorily. The main difficulty would stem not from the accuracy stand point but from the question as to whether the resolution figures of 30 m would allow the detection and identification of some of the detail normally included in a topographic map at this scale. Thus the present series of tests have an importance as pointers to the possible performance of the two metric cameras - the Itek LFC and the Zeiss RMK 30/23, both equipped with f = 30 cm lenses - which will be orbited by NASA and ESA respectively using the Space Shuttle in 1980/81. In the case of the LFC camera, the scale will be 1/1,000,000 (H = 300 km) and for the Zeiss the scale will be 1/1,000,000 (H = 300 km). So the scales are of the same order as those of the S-190B; albeit the base: height ratios will be greater due to the use of larger-format cameras.

8.3.2 Height Accuracy

One of the major factors affecting the height accuracy will be the B/H ratio. While variations of angular field would not significantly affect the planimetric errors (Stark, 1976), the errors in height increase with decreasing angular field. One method of predicting the height accuracy to be expected from a particular series of tests is to use the general parallax-height formula:

$$dh = \frac{H}{f . B/H} . dp$$

where dh = error in height

dp = residual parallax

B = air base

H = flying height.

If one estimates the precision of the parallax measurements (dp) to be 5 μm (which could result from observational errors, uncompensated radial lens distortion and film deformation and errors in ground control), the corresponding height error (m_z) on the ground for the S-190B photography (B/H = 0.10, H = 435 km, f = 460 mm) would be ± 48 metres or ± 0.11 ‰H.

Another method of predicting height accuracy is the theoretical model devised by Stark (1976):

$$m_z^2 = \frac{1}{b^2} . 2f^2 . m_k^2$$

where m_z = height accuracy

b = photo base,

f = principal distance

m_k = standard deviation of image coordinates, assumed as 5 μm.

Stark based his more sophisticated theoretical model on the angular coverage of the camera and the B/H ratio. Fig. 133 shows the height accuracy prediction as obtained by Stark (1976), for a format size of 23 x 23 cm and f = 70 mm to f = 305 mm. This has been extended to f = 460 mm, where the expected height error (m_h) is found to be ± 35.4 μm (± 33 metres), or 0.08‰H.

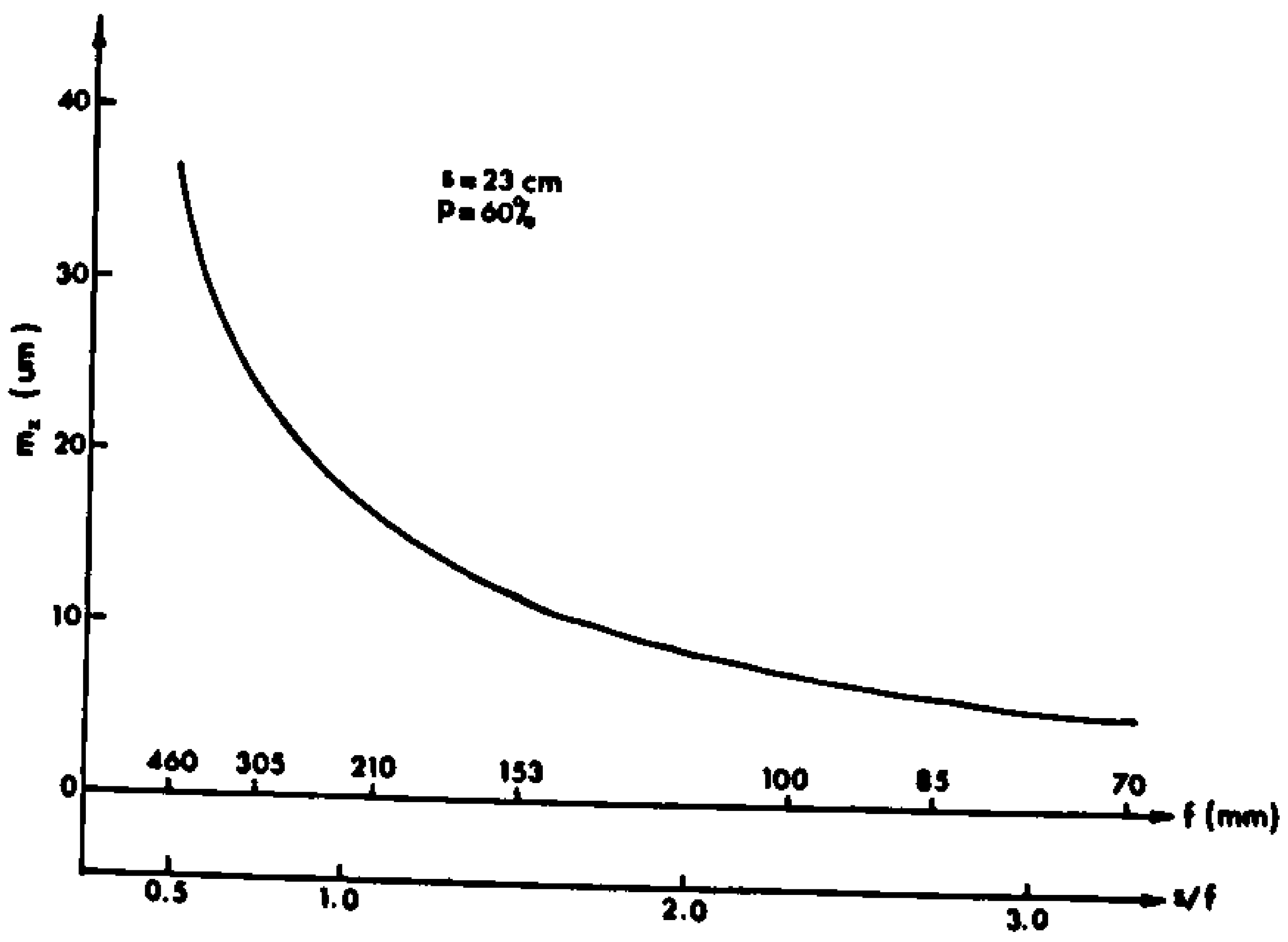

Fig. 133 Theoretical height accuracy m_z (Stark, 1976) extended to include f = 460 mm.

If the format size is reduced to 115 x 115 mm as in the case of the S-190B photography, the expected height error will be ± 66 metres (or 0.15‰H).

The results of the present series of tests show extremely favourable results in heights. Taking the mean (m_z) for both models gives the following results:

Test	m_z (metres)
Group I	
Conventional Abs. Orientation case (a) 4 control points	± 99.2
" " " case (b) 20 control points	± 75.6
" " " case (d) all control points	± 68.2

Test	m_z (metres)
Group I (i)	
Conventional Abs. Orientation, polynomial adj. (16) 6 terms	± 70.9
" " " " " (17) 7 terms	± 74.5
" " " " " (18) 8 terms	± 72.0
" " " " " (19) 9 terms	± 74.5
Group II (ii)	
Space Res./Space Inters., Add. parameters (II(2)) a-terms	± 79.8
" " " " " " (II(8)) a+b terms	± 93.0
" " " " " " (II(10)) a+b+c terms	± 88.0
" " " " " " (II(12)) a+b+c+d terms	± 58.0
Group II (iii)	
Point-by-point Space Res./Space Intersection	± 74.8

Obviously all the methods were effective in reducing the height errors to those predicted for the S-190B photography. The use of 20 control points does, of course, have the effect of ensuring that none of the check points lie too far away from control, so allowing the polynomial method and the additional parameters method to be used in an effective way.

The major difficulty in coming to a definite conclusion as to which approach is to be preferred lies in the significantly different results between the two models tested, the first model having the much larger errors in each case, except in the point-by-point space resection/intersection method.

Comparison with other tests from Skylab photography

Again only a few practical tests have been carried out on the Skylab photography that could show its height accuracy. Mott (1975) adjusted a strip of S-190B photography on a total of 20 points, achieving a RMSE of ±111 metres (0.25 ‰H). Unfortunately, when attempting to contour a single model gross discrepancies of up to 2000 metres were found. Although believing that this discrepancy is due to the distortion caused by the focal plane shutter, Mott makes no attempt to provide an explanation. From the results obtained by Keller (1975) when testing a strip of S-190B photography, the RMSE of discrepancies in height at check points (14 check points) is ± 114.39 metres (0.25‰H) which is similar to that of Mott. The results from the various methods utilised in the present series of tests are a significant improvement on those of Mott and Keller. Of course, both of these were carried out on a strip of aerial triangulation which, however well adjusted, cannot be expected to produce the results achieved from individual models with large numbers of control points.

Turning to the S-190A multi-spectral photography, Mott adjusted a strip on to 16 height control points obtaining a RMSE of ± 117 metres in height (0.25‰H). The RMSE in height, determined by Stewart (1975) when testing the S-190A photography, was ± 72 metres (0.16‰H). Again all these results (except the single model tested by Mott) show that height accuracy between 0.15‰H to 0.25‰H could be obtained from the two very different types of Skylab photography.

One must also mention the work by Welch and Lo (1977) who have tested S-190B photography using parallax heighting methods and a specially constructed zoom height finder (resolution 1 μm) for the measurements. They extracted the ground coordinates of the test points from the 1/24,000 and 1/62,500 maps and used the method of Methley (1970) for the adjustment of the crude heights. A polynomial adjustment using 5 to 9 control points was used to obtain RMSE's of ± 500 metres to ± 675 metres (1.03‰H to 1.55‰H). Even allowing for the limitations of the parallax method, this appears to be an unexpectedly poor result. Welch and Lo concluded that the reason was the weak B/H ratio (0.10) and the effect of the focal plane shutter. However, this is thrown into question by whole series of results quoted above. Certainly the theoretical analysis of the effects of the shutter carried out in Chapter IV, supported by the practical tests whose results are given in this Chapter (0.22‰H to 0.24‰H, using conventional absolute orientation with 4 ground control points) do not offer a great deal of support to their suggestion.

There is little doubt however that, unlike the planimetry, the heights as measured on the S-190B are in no way useful to even the smallest scale topographic mapping. As Petrie (1974) has pointed out contour intervals of 20 to 25 metres are not uncommon even in small-scale series and there is no hope of reaching such figures with photography of the S-190B type. A more definite answer as to the possibilities of heighting and contouring from metric space photography will come from the NASA-LFC and ESA-Zeiss RMK flights made with the space Shuttle in 1980 and 1981. These have the more favourable base/height ratios required for the task, but even then it is doubtful if the required accuracies can be reached.

8.4 The F-126 Test Results

The tests performed on the Southampton model (model 5), which is formed by a pair of photographs at 1/40,000 scale, and on the Worthing model (model 7), which is formed by a pair of photographs at 1/20,000 scale, are also divided into groups according to the technique applied.

The symbols that differentiated one solution from another in the S-190B test (given in Table 12) have also been used here. In all the tests, the ground coordinates of the test points, measured from 1/1,250 O.S. plans, were used as known values.

8.4.1 Results:

Group I

I (i) Conventional absolute orientation was carried out for models (5) and (7) as follows:

Model (5) (1/40,000 scale)

(a) using four plan control points and six height control points

(b) using ten planimetric control points and fourteen height control points

Model (7) (1/20,000 scale)

(c) using four plan control points and four height control points,

(d) using fourteen plan control points and fourteen height control points.

The RMSE's were determined from the residuals at the check points only and are shown in Table 19.

Table 19

Model No.		No. of control points plan	height	No. of check points plan	height	m_x (m) (μm)	m_y (m) (μm)	m_{pl} (m) (μm)	m_z (m) (‰H)
5	a)	4	6	13	23	1.073	1.030	1.487	2.510
						27	26	37	0.411
	b)	10	14	7	15	1.071	0.969	1.446	2.238
						27	24	36	0.367
7	c)	4	4	25	24	0.688	0.854	1.097	1.009
						34	43	55	0.331
	d)	15	14	14	14	0.695	0.783	1.046	0.666
						35	39	52	0.219

Model (5)

The results from the use of 4 plan control points and 6 height control points gave the errors m_x, m_y and m_z to be $\pm$ 1.073, $\pm$ 1.030 and $\pm$ 2.510m respectively. The use of additional control points, 10 in plan and 14 in height, resulted in no significant improvement in plan or height.

Model (7)

Using 4 plan and 4 height control points, the errors m_x, m_y and m_z were $\pm$ 0.688, $\pm$ 0.854 and $\pm$ 1009m respectively. When the number of control points was increased to 14 in plan and 14 in height, the errors for m_x, m_y and m_z were $\pm$ 0.695, $\pm$ 0.783 and $\pm$ 0.666m respectively. This shows no improvement in m_x, but considerable improvement in m_y and m_z are noticeable (12% in y and 11% in z).

Looking at both sets of results, one notices immediately the difference between the two models. Reduced to micrometres (μm) in the negative, the 1/40,000 scale model has the noticeably lower planimetric errors. This could be the result of errors in the coordinates of the test points used (estimated at m_{pl}=

± 0.6 m) which would be felt more strongly on the larger scale (1/20,000 scale) photography. On the other hand, the height errors reduced to ‰H for purposes of comparison are much lower for the larger scale photography. It is, however, difficult to give any good reason for this result.

Group I(ii)

16, 17, 18, 19 -- Conventional absolute orientation followed by polynomial adjustment was carried out for the two models. The RMSE's were determined from residuals at the check points only and are shown in Table 20.

Table 20

Technique	Model No. 5 No.of control points: plan = 10, height = 14 No. of check points: plan = 7, height = 15				Model No. 7 No.of control points: plan = 15, height = 14 No.of check points: plan = 14, height = 14			
	m_x (m) (μm)	m_y (m) (μm)	m_{pl} (m) (μm)	m_z (m) (‰H)	m_x (m) (μm)	m_y (m) (μm)	m_{pl} (m) (μm)	m_z (m) (‰H)
16	0.558 14	0.574 14	0.800 20	1.789 0.293	0.484 24	0.572 29	0.749 37	0.589 0.194
17	0.591 15	0.678 17	0.899 23	1.677 0.275	0.469 23	0.572 29	0.739 37	0.578 0.190
18	1.192 30	1.056 26	1.592 39	1.542 0.253	0.471 24	0.577 2929	0.745 37	0.572 0.188
19	0.953 24	0.899 22	1.310 33	1.537 0.252	0.486 24	0.578 29	0.755 37	0.680 0.224

As with the S-190B the first six polynomial terms ($1, x, y, xy, x^2, y^2$) are the most effective terms in adjusting the models to the ground control points. The errors in the check points for the two models are:

	m_x	m_y	m_z
Model (5)	0.558	0.574	1.789
Model (7)	0.484	0.572	0.589

They are very much improved on those achieved using the same number of control points and applying an absolute orientation without polynomial adjustment. The tendency for the planimetric errors to be smaller in terms of μm in the negative on the smaller-scale photography was still quite marked at this stage.

The use of higher order polynomials gave slightly better results in height (z) and no improvement in m_x and m_y. In fact for the smaller-scale model, the errors m_x and m_y were even larger when further polynomials were added to the first six.

Overall the results of the test show the effectiveness of introducing polynomials to correct for both planimetric and height errors. In the very broadest terms, they tend to confirm the results of the S-190B tests.

Group II

It has already been mentioned that no full control points (with x, y and z coordinates) were available in either of the two models. This would, of course, be needed to solve the space resection problem and hence to test techniques based on this solution. However, use was made of the ground coordinates of the test points determined by the polynomial adjustment in the first group to carry out the tests in Group II. Since the larger scale Worthing model (model 7) is the one in which sufficient tests points were available, it was used to carry out tests in this group.

II (i) Conventional Space Resection/Space intersection was carried out for model (7) as follows:

(a) Using 27 full control points with their heights taken from the 1/1,250 plans and their planimetric coordinates as derived from the polynomial adjustment technique in the previous group. In this case, the points whose planimetric positions were measured from the 1/1,250 O.S. plans (29 points) were used as check points.

(b) using 29 full control points with their planimetric coordinates measured on the 1/1,250 plans and their heights as derived from the polynomial adjustment technique. The points whose heights were taken from the 1/1,250 plans (27 points) were used as check points.

The RMSE's of the residuals at the check points are shown in Table 21.

Table 21

No. of full control points	No. of check points		m_x (m) (μm)	m_y (m) (μm)	m_{pl} (m) (μm)	m_z (m) (‰H)
	plan	height				
27	29	-	0.646 32	0.776 39	1.01 50	-
29	-	27	-	-	-	1.087 0.358

Applying the conventional space resection technique, the results in x and y are not very different from those using conventional absolute orientation without polynomial correction (Group I) but m_z is rather less accurate ($m_z = \pm 1.087$m) Again, this could be due to the fact that a common perspective centre corresponding to the geometric centre of the photograph was assumed, while it is actually changing position during the exposure time. Also the fact that the height values of the check points were not derived from ground measurement must have some significance.

II (ii) Space Resection with additional parameters was again carried out for model (7), only using the same control and check points as in Group II (i) (a) and (b). The results are shown in Table 22 below.

Table 22

Technique	(a) No. of full control points = 27 No. of plan check points = 29			(b) No. of full control points = 29 No. of height check points = 27
	m_x (m) (μm)	m_y (m) (μm)	m_{pl} (m) (μm)	m_z (m) (‰H)
II (2)	0.597 30	0.677 34	0.903 45	0.841 0.277
II (8)	0.682 34	0.631 31	0.929 46	0.806 0.265
II (10)	0.551 27	0.784 39	0.958 48	0.828 0.272
II (12)	0.570 29	0.806 40	0.987 49	0.744 0.248

It is noticed that the results were improved than when conventional space resection was applied. The improvement was quite small in planimetry, but very considerable in height. The first group of the additional parameters (the a-terms) which corrects for the change in image scale gave the best results in x and y ($m_x = \pm\, 0.597$m, $m_y = \pm\, 0.677$m). The use of the other additional parameters resulted in very slightly worse results. In height a steady improvement was, in general, observed as the additional groups were included (giving $m_z = \pm\, 0{,}744$m).

II (iii) Point-by-point space resection/space intersection was carried out for model (7) using the same control and check points for cases II (i) (a) and II (i) (b).

The RMSE's of the discrepancies at the check points were determined and are shown in Table 23.

Table 23

No. of full control points	No. of check points		m_x (m) (μm)	m_y (m) (μm)	m_{pl} (m) (μm)	m_z (m) (‰H)
	plan	height				
27	29	-	0.636 31	0.781 39	1.01 50	
29	-	27	-	-	-	0.713 0.234

Compared with the conventional space resection/space intersection method, the results of this test show no improvement in x and y, while a considerable improvement in z is noticeable (from $m_z = \pm 1.087$ to $m_z = \pm 0.713$m).

These results are shown in graphical form (Figs. 134 to 137) to allow comparison between the different techniques. The residuals for I (a) and I (9) tests in planimetry and height are shown in vector forms in Appendix C.

8.5 Analysis of the F-126 Test Results

As has already been mentioned, the accuracy (m_{pl}) of the test points used is $\pm$ 0.6 metre on the ground. The photo scale of the Worthing model (model 7) is 1/20,000 and the scale of the Southampton model (model 5) is 1/40,000. The B/H ratio for both models is 0.47. The estimated on-axis resolution of the F-126 photographic system is 25 - 32 lp/mm at 1.6: 1 and 2: 1 contrast.

8.5.1 Planimetric Accuracy

The conventional absolute orientation solution, using four planimetric control points (plus four height control points for model (7) and six height control points for model (5)) gave RMSE of 37 μm for the small scale model (5) and 55 μm for the larger scale model (7) as shown in Table 19. This again is within the expected accuracy taking into account the accuracy of the control used, the estimated resolution and the erroneous position of the principal point (taken as the geometric centre) with considerable radial lens distortion (up to $\pm$ 135 μm) to be corrected.

When the number of control points was increased and a least squares method was used in solving the absolute orientation problem, not much improvement was acquired (RMSE at check points was improved to 36 μm for model (5) and to 52 μm for model (7)).

However, when the polynomial adjustment was applied, a considerable improvement was achieved. The RMSE of the check points was reduced to 20 μm for model (5) and to 37 μm for model (7). This means an improvement of 33% and 45% in the planimetric accuracy was obtained for the two models. The most effective of the polynomial parameters are the first six parameters (see equations 132 and 133).

It is from the point of view of the type of ground control required that the polynomial adjustment technique can be considered to be more useful than the other techniques based on a space resection solution. This is because full control points (known in X, Y and Z) are required to implement the resection techniques. Hence the tests in GroupII (i,ii,iii) were carried out with control points whose planimetric coordinates in one case, and height coordinates in the other, were given by the polynomial adjustment solution. These tests were applied to model (7) to compare the effects of the techniques themselves. In all cases, the planimetric accuracy (RMSE) is between 45 - 50 μm at the photo scale. Most effective is the

TEST RESULTS - F-126 Photography

Planimetry

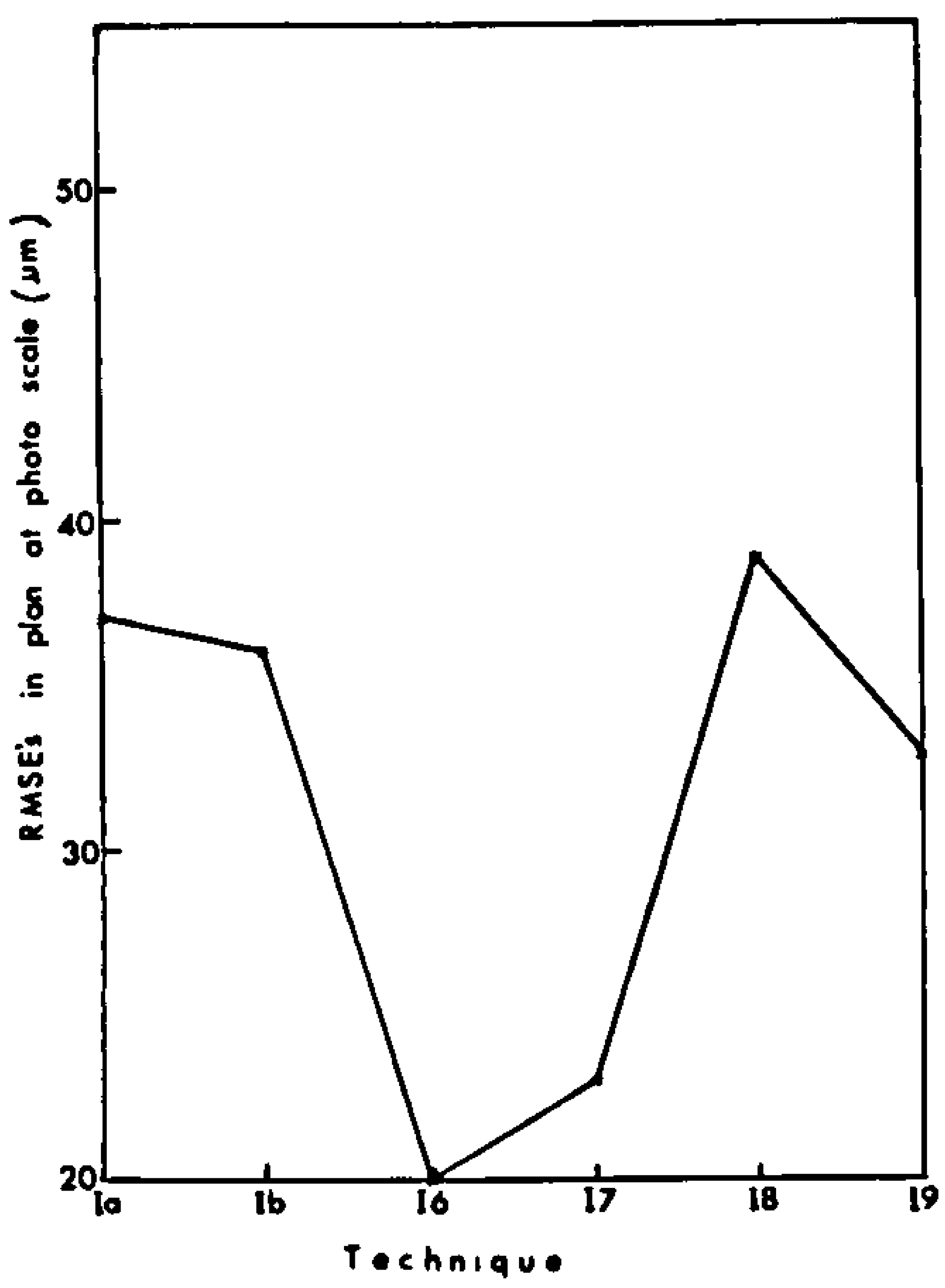

Fig. 134 Planimetric accuracy
Model (5)

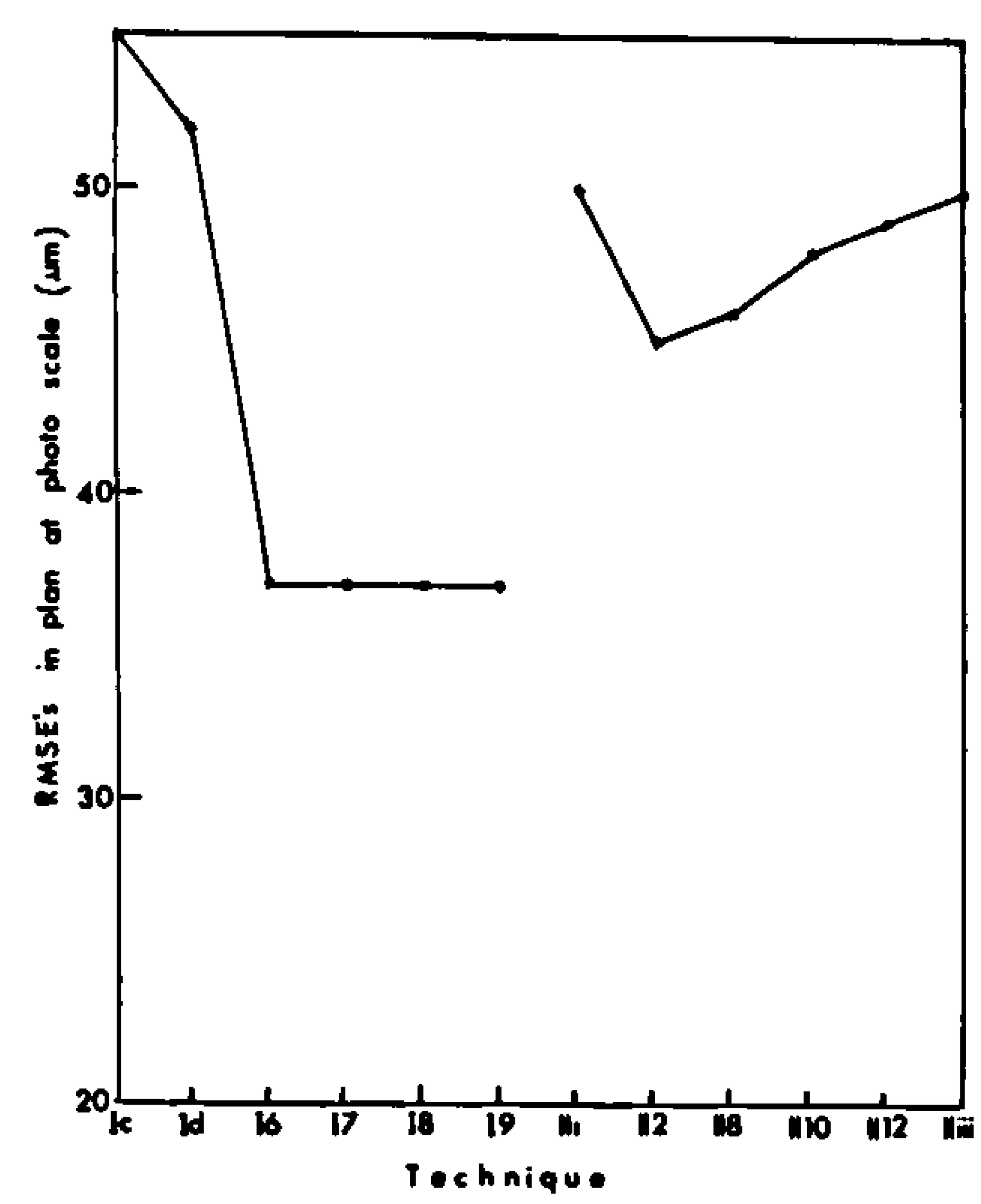

Fig. 135 Planimetric accuracy
Model (7)

Height

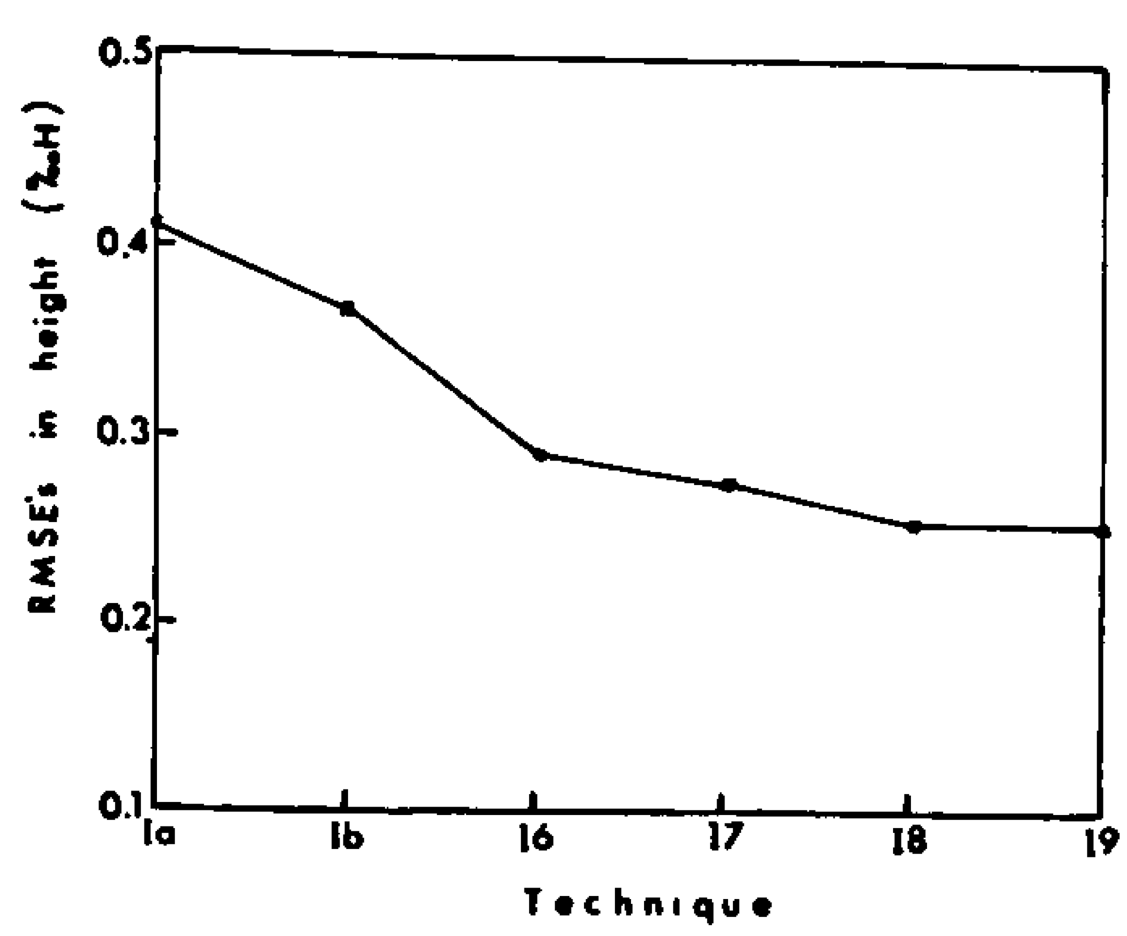

Fig. 136 Height accuracy
Model (5)

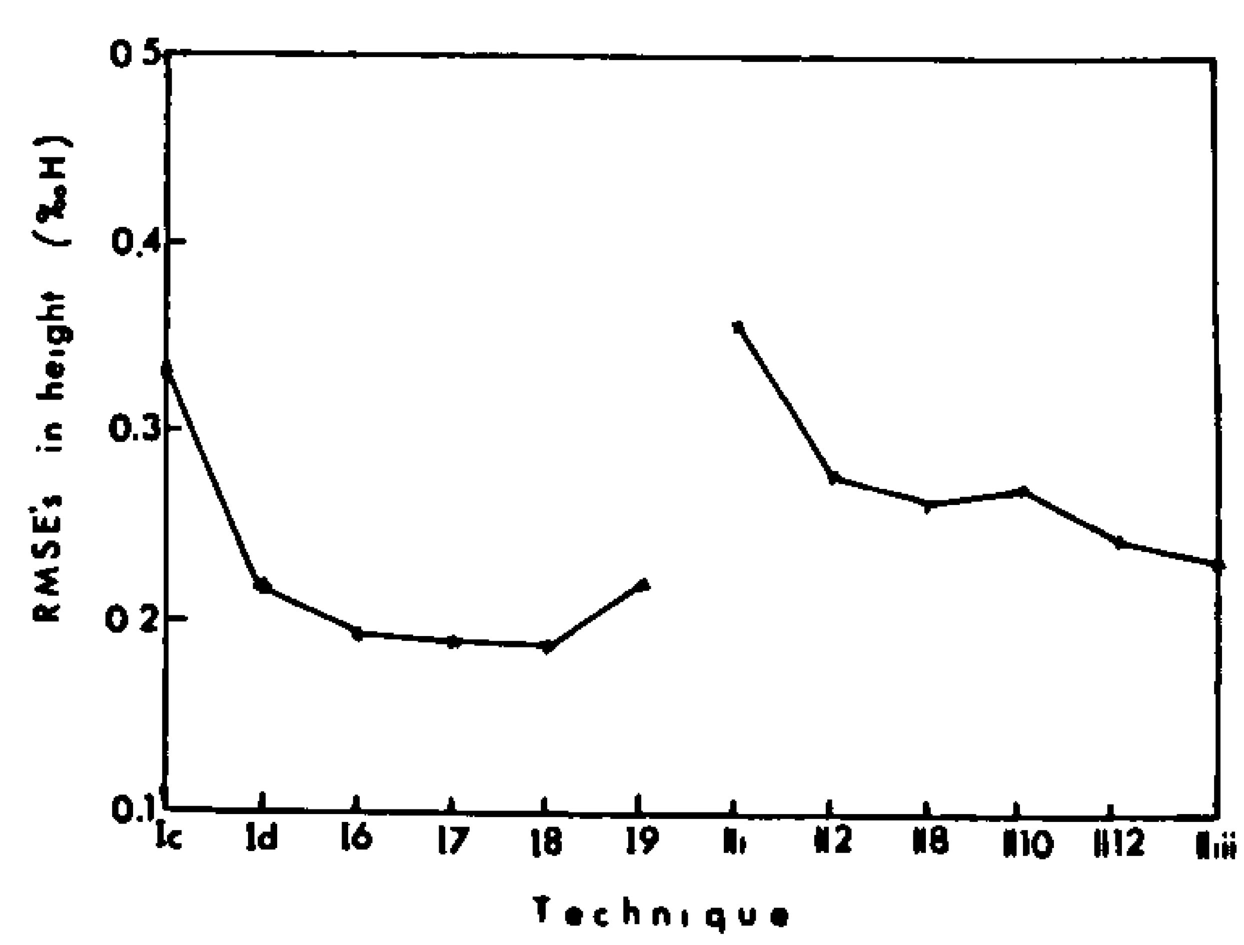

Fig. 137 Height accuracy
Model (7)

first group of the additional parameters that corrects for the affine scale change.

8.5.2 Height Accuracy

It has already been stated that the B/H ratio is the most important factor affecting the height accuracy. As shown in Table 19 a conventional absolute orientation gave RMSE's of 1.009 metres and 2.51 metres for models (7) and (5) respectively. These correspond to residual parallax of 23 μm for model (7) and 29 μm for model (5) which is again an acceptable accuracy when considering the inexact positioning of the principal point and the observational errors of untargeted points.

When the polynomial adjustment was applied the height accuracy was improved to 0.25‰H (18 μm residual parallax for model (5)) and to 0.19‰H (13 μm residual parallax for model (7)).

Again, the objective of the tests carried out in Group II (i, ii, iii) is to compare the capabilities of the space resection/intersection techniques. This comparison is clearly illustrated by Fig. 135. From this figure it can be seen that the point by point space resection/intersection techniques is the most effective (RMSE = 0.234‰H) followed by the additional parameters when the terms of group four (II 12) which correct for the position of the principal point, were added to the error model (RMSE = 0.248 ‰H).

The vector maps of height errors were plotted and are shown in Appendix C. From these maps, it can be seen that systematic height residuals, parabolic in Y, are shown. These systematic height deformations are broadly similar to those that arose when testing the S-190B photography. These are shown in Fig. 138 and 139 for the different pattern of control.

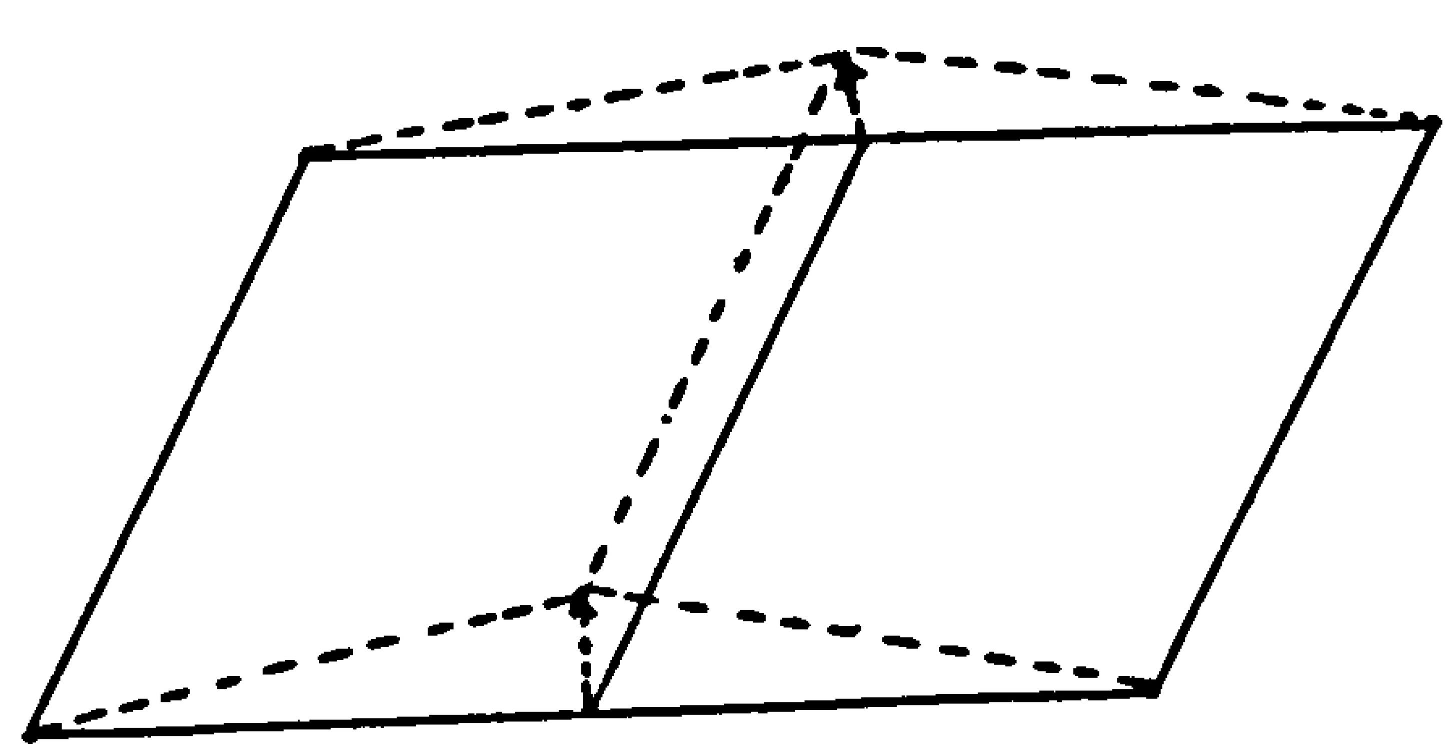

Fig. 138 Height errors using four control points at the corners of the model.

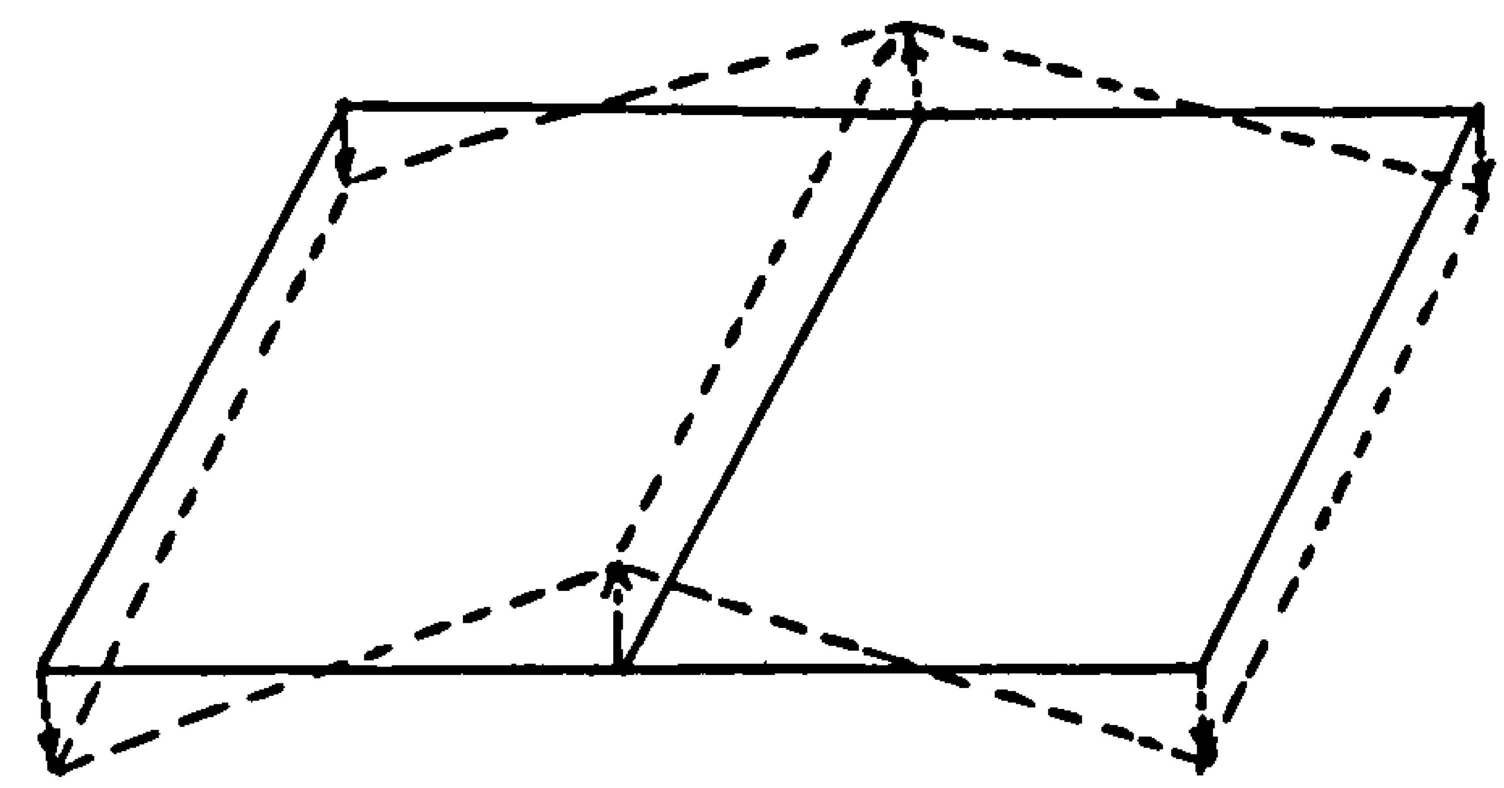

Fig. 139 Height errors using 14 control points distributed throughout the model

Investigations showed that these systematic errors in height were not caused by the focal plane shutter, since the height errors resulting from the effects of the focal plane shutter have a quite different pattern as shown in Chapter IV. It is striking that the same model deformations were obtained by Wiser, Liege and Ackermann (1976) when testing conventional wide-angle and super-wide angle photography flown over Oberschwaben in West Germany. These, shown in Figs. 140 and 141, were obtained when using the maximum control in the block adjustment.

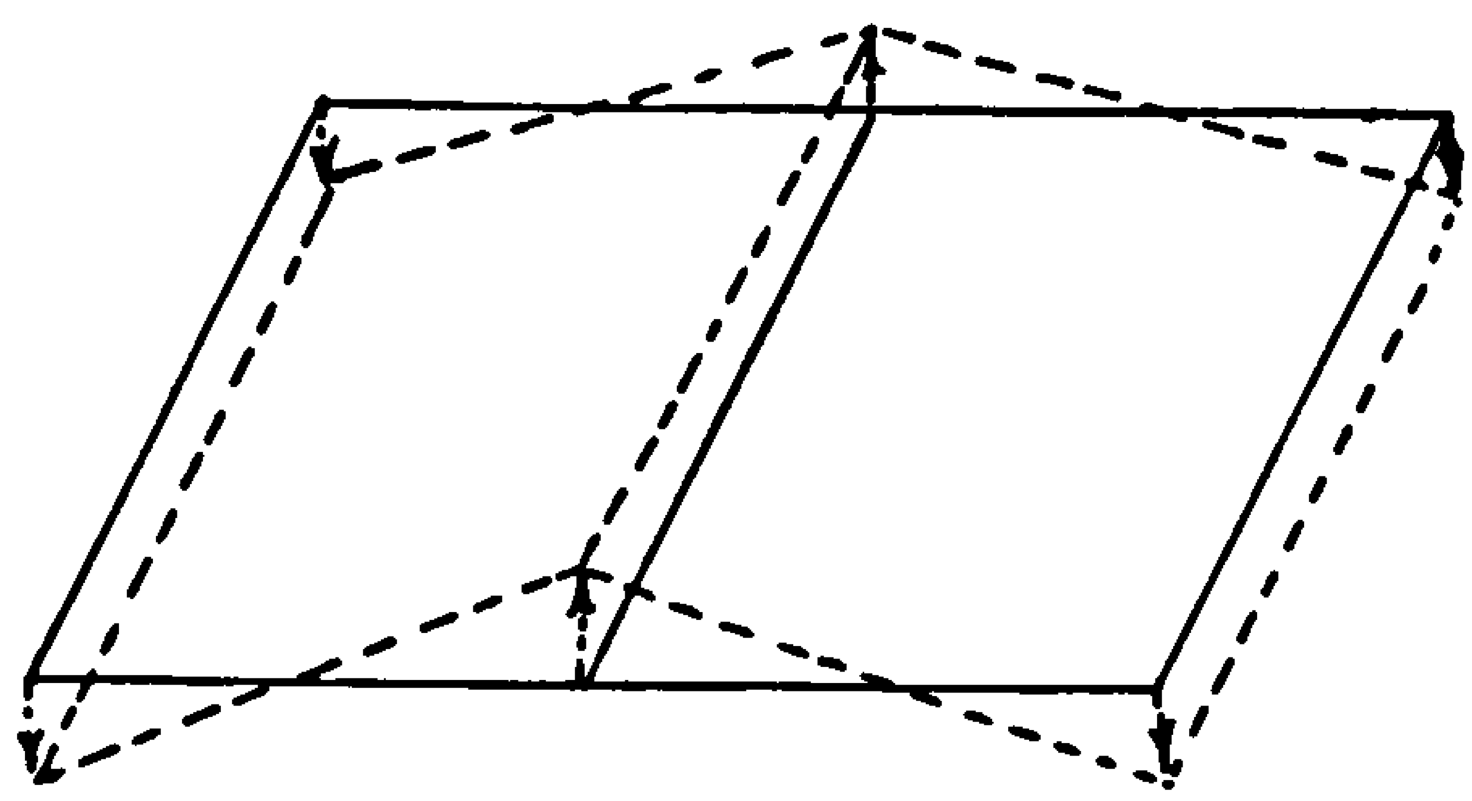

Fig. 140 Height errors for wide-angle photography (Wiser et al., 1976)

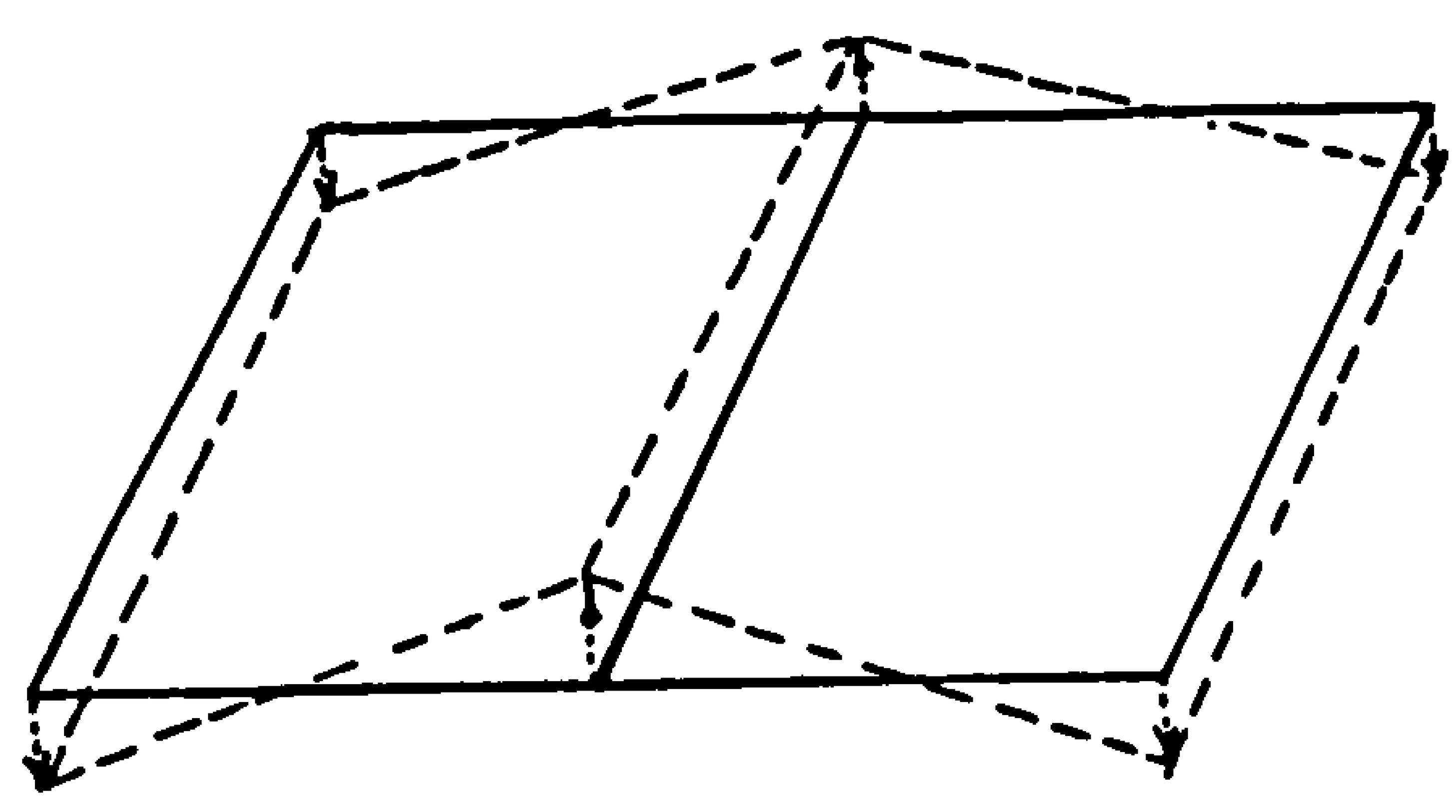

Fig. 141 Height errors for super wide angle photography (Wiser et al., 1976)

The conclusion reached by Wiser et al. was that these systematic height errors were caused by the camera/flight system since they go clearly with the flight direction.

Summarising the F-126 tests, they demonstrate (within certain limitations) the effectiveness of the techniques used in this study, but the results achieved do not approach those which might be expected with a wide-angle metric camera of similar characteristics. A limitation to the whole series of F-126 tests has been the quality and pattern of ground control available in the two test areas. The planimetric accuracy of the ground and check control points was estimated to be $\pm$ 0.6 metres and this figure was approached in most of the tests carried out. The lack of points with full ground control (X, Y and Z coordinates) resulted in limitations in testing the effectiveness of the point-by-point space resection/space intersection methods of Group II.

However, even within all these limitations, the results obtained are not unpromising. Unlike the Skylab photography, no other results with aircraft-borne reconnaissance cameras equipped with focal plane shutters, have been published which can be used for comparison. Obviously, further tests are required using photography taken with varying parameters of flying height, focal length, B/H ratio, etc. and over test areas of higher quality than used in the present series. But even the present results show that measurements and mapping data of a very useful kind can be obtained from aircraft reconnaissance photography - which is very widely available. With the increasing use of analytical methods based on computer solutions, this is certainly of interest to military organisations and to field scientists who may not require the highest accuracies demanded by government and private mapping agencies.

8.6 Conclusions

From the results of the two tests, carried out on the S-190B Skylab photography and the F-126 reconnaissance photography, it can be seen that the results of the former are very much more satisfactory than the latter, both in planimetry and height. This may be explained by the fact that the satellite which carried the S-190B camera is a much more stable camera platform than the aircraft that carried the F-126. None of the atmospheric turbulence experienced with aircraft at low and medium altitudes is present in space. Thus the time-varying tilts which can be expected to be encountered with a focal-plane shutter will be a minimum with the satellite-borne camera and a maximum with the aircraft-borne camera.

It can also be concluded that the satellite-borne S-190B photography, with the effects of its focal plane shutter effectively compensated by IMC, can be treated in the same way as conventional photography. Applying a conventional absolute orientation, using only four control points, the planimetric accuracy achieved (RMSE at check points) would be around $\pm$ 30 metres at the ground scale. This corresponds to $\pm$ 0.3 mm residual error on the map of 1/100,000 scale. Hence the S-190B photography, treated as conventional photography, could be used to plot planimetric detail at the saale of 1/100,000 with just sufficient accuracy to meet mapping specifications and at smaller scales, such as 1/250,000 and 1/500,000 with more than adequate accuracy.

If, however, more control points were available, then using the techniques tested in this study it is possible to obtain an accuracy of $\pm$ 20 metres in planimetry (which is below the resolution figures), and hence planimetric mapping (e.g. orthophotomapping) at 1/100,000 scale could be conducted with more than sufficient accuracy ($\pm$ 0.2 mm at the map).

The height accuracy of the S-190B photography is largely limited by the small B/H ratio (0.10). Again, analytical techniques could improve the RMSE at the check points from about $\pm$ 100 metres (0.23‰H) to an accuracy of $\pm$ 50 - 60 metres. However, this indicates likely contour intervals of 150 to 200 metres ($3 \times m_z$) which come nowhere near satisfying the needs of small-scale topographic series (20 to 50 metres). Obviously, one must await the advent of the satellite photography of the Space Shuttle scheduled for the early 1980's before a definite opinion can be given as to the usefulness of heighting and contouring from space photography.

On the other hand, the F-126 photography gave planimetric accuracies of $\pm$ 1.03 metres and $\pm$ 0.85 metres for the photo scales of 1/40,000 and 1/20,000 respectively, when conventional absolute orientation was applied without further adjustment. Applying the polynomial adjustment techniques, these results could be improved to $\pm$ 0.80 metres (1/40,000 scale photography) and $\pm$ 0.74 metres (1/20,000 scale photography), corresponding to 0.08mm at 1/10,000 scale. Thus these photos could be used to plot details for 1/10,000 scale maps, or for mapping at 1/5,000 scale still with acceptable results (0.15 - 0.16 mm at the map scale). Obviously no one is going to advocate using a reconnaissance camera for mapping purposes in place of a metric camera, but the situation certainly does arise when reconnaissance photography is the only type available. The possibility of using such reconnaissance photography for map revision purposes is an obvious application to the mapping field and the production of planimetric maps and orthophotographs, for field scientists is another. On the basis of the present limited series of tests, the results should be quite acceptable.

Turning to the matter of heights and contours, the RMSE's are improved from $\pm$ 1.009 metre (0.33‰H) to $\pm$ 0.572 metre (0.188‰H) for the large scale photography (model 7) and from $\pm$ 2.510 metre (0.411 ‰H) to $\pm$ 1.537 metre (0.252‰H) for the smaller scale photography (model 5). Adopting the usual yardstick that the minimum contour interval possible is from 3.3 to 5 x the spot heighting accuracy, the 1/20,000 scale reconnaissance photography could be used to plot contours at 2 to 2.5 metres interval with sufficient accuracy; and the 1/40,000 scale reconnaissance photography would allow contouring at 5 to 7.5 metres contour interval. For many purposes, such intervals would provide topographic information which is of a satisfactory and adequate nature to many users.

CHAPTER IX

Conclusions and Recommendations for Future Work

CHAPTER IX

CONCLUSIONS AND RECOMMENDATIONS FOR FUTURE WORK

9.1 Some General Conclusions

Since a detailed discussion of the results of the experimental tests has been conducted in the previous chapter, it is not necessary to repeat these or summarise them here. However, it is appropriate in this final chapter to try and correlate some conclusions of a general nature in the light of the work carried out for this thesis.

(i) The first is that to confirm the view that the quality of much reconnaissance photography is of a high-order and therefore of especial interest to those photogrammetrists and cartographers engaged in the production of very small-scale base maps e.g. from earth-orbiting satellites or very high flying aircraft.

(ii) It is possible to extract metric information of a sufficient standard of accuracy to be useful to a wide spectrum of users from military users through earth-scientists to topographic mapping agencies. The information may be produced in the form of a graphic line map of the traditional type; in digital form; in orthophotographic form, etc. However, it is necessary that the initial measurements be made digitally to allow analytical techniques of the type devised and tested in this present work to be used successfully. From the analysis conducted in this thesis, analogue methods appear to have very little promise for the generation of topographic information from reconnaissance photography. It is only with the increasing use of and present and future possibilities of implementing digital, numerical and analytical techniques via computers that reconnaissance frame photography can now be seriously considered for the production of such information.

(iii) The analysis of the effects of the focal plane shutter has shown that these can be modelled mathematically in a convenient way which allows practical methods of eliminating them to be devised. Three promising methods are those of polynomial corrections to model coordinates, the use of the additional parameters method with plate or photo-coordinates and the point-by-point space resection/space intersection method.

(iv) Of special importance in the context of reconaaissance frame photography is the advent of image movement compensation (I.M.C.) which is now widely used in reconnaissance cameras. This has the effect, in principle, of compensating for the effects of focal plane shutters. In practice, this compensation is not perfect due to the time varying orientation parameters and small errors in applying I.M.C. However, even then, the large magnitude displacements induced by the operation of the shutter are reduced to quite small amounts.

(v) The results of the tests show that satisfactory results can be achieved with reconnaissance frame photography using the analytical techniques and that these would provide useful metric and topographic information to a wide spectrum of users. It should be recognised however, that in terms of accuracy measured in the negative plane, the results from aircraft mounted camers will be less satisfactory than those mounted on satellites, which provide an inherently more stable platform. The latter has a special importance with a camera equipped with a shutter having a sequential mode of operation and a a shutter transit time considerably in excess of the exposure time.

(vi) The results from the satellite photography show that satisfactory results can be achieved in planimetry at least in terms of accuracy, if not always in content, for very small scale topographic maps. The results in heighting are not promising, even allowing for the poor geometrical arrangement of the photography used in the tests conducted here.

9.2 Suggestions and Recommendations for Future Work

The various possible approaches which have been used successfully in tests can be utilised according to which is the most appropriate to the particular situation regarding available control and the intended application. However, it is also apparent that further work should be carried out on reconnaissance frame photography at different focal lengths, B/H ratios etc. to define more exactly the limits of the methods used. The present tests are those that can be carried out by a single research student. If a large mapping or intelligence-gathering agency could be involved in further tests, some of the present limitations and uncertainties could be removed. For example (i) The use of a large test field of suitable signalised points of a high accuracy could remove some of the doubts which arose from the use of natural points with coordinates scaled from maps that had to be used in the present tests.

(ii) The use of test points with full control in plan and height could overcome the limitations of the present tests using the point-by-point space resection/space intersection method. Obviously this promising method was limited in the case of the F-126 photography by the non-availability of such control.

(iii) The comparison of the different groups of the additional parameters was not easy, because each group contains two or more parameters. Although the correlation matrix would show the correlation between the different parameters, the elimination or addition of each parameter separately is a difficult task for programming. However, more investigation of this point is required since, in general, the technique showed a very promising result.

(iv) Further tests are needed with cameras equipped with focal plane shutters but without I.M.C. Photography of this type taken with older cameras is commonly available here in the U.K. and the application to studies of movement, for example, dunes, spits, bars, etc, in a coastal situation would be dependent on measurements made on such photographs.

(v) Another obvious line of research and development is aerial triangulation. The results from Keller's limited test of S-190B photography showed how powerful modern block adjustment techniques are in removing systematic errors and the bundle method of block adjustment with additional parameters (Bauer and Muller, 1972; Brown, 1976) is an obvious and available tool for such studies.

(vi) A study in depth should be undertaken for reconnaissance frame cameras equipped with rotary focal plane shutters along the same lines as has been undertaken in this present study for parallel-motion focal plane shutters. These shutters are inevitably restricted by reason of their construction to small-format cameras, which is the reason that comparatively little emphasis was placed on them in this thesis. Nevertheless, they allow such high shutter speeds that their use must become more widespread.

(vii) Many specialist users would prefer to have output in accurate metric form while retaining the original photographic image i.e. in the form of orthophotographs. The necessary rectification can now be achieved in the computer-controlled optical transfer type of orthophotoprinter such as the Wild OR-1 Avioplan and the OMI-Nistri OP-2 devices introduced in prototype form at the I.S.P. Congress at Helsinki in 1976.

Suggestions such as these above that further research is needed can be looked on as the inevitable conclusion of any piece of research, thus ensuring (hopefully) an unending series of research projects to the person making the suggestions! Nevertheless, it must also be understood that this whole matter of the metric aspects of reconnaissance photography is only now being explored for the first time and, as this thesis has shown, it has many ramifications and possibilities that could be explored by a single research student in the course of the work required for a Ph.D. thesis. Only the advent of freely available high-speed computers, which could handle the large amount of computation inherent in the analytical methods which must be used, has made it possible to contemplate the methods which have been undertaken. Since computer power and availability will continue to grow and, with it, the understanding of analytical methods in photogrammetry, the extension of research along the lines outlined above would seem to be appropriate, if not inevitable,

Another possible line of enquiry and action is to investigate further the characteristics of reconnaissance frame cameras themselves. For example, to what extent are the lens distortions really assymmetric and how large are the tangential distortions in practice? Would some quite small attention to the assembly of the lens elements results in removal of these effects? The experience with the

Zeiss Topogon lenses points to such a result. Therefore suggestions along this line might include the following:-

(i) A programme of camera calibration of the lenses of reconnaissance frame cameras would give valuable information.

(ii) It might be recommended to the designers of reconnaissance frame cameras that fiducial marks be incorporated to define the geometric centre of the format. The difficulties encountered by the present author with both the S-190B and F-126 photographs should not be allowed to recur.

(iii) Following the same line of thought, it would be very easy and useful to incorporate a grid of reseau crosses on cameras such as the main large-format British reconnaissance frame cameras, e.g. the F-126, which are already equipped with a register glass plate on which the negative film is flattened. This reseau could easily be calibrated and would then form an invaluable reference for metric purposes.

(iv) For the application of the first technique used in the author's tests i.e. correcting the image coördinates for the effect of the focal plane shutter, before carrying out the exterior orientation, full information should be made available about the direction of the shutter motion, the exact width of the slit. Again if a means could be provided to mark the photos during exposure, to indicate the direction of motion of the slit, this would be invaluable.

Most of these suggestions made above move in the direction of adding some metric characteristics to reconnaissance frame cameras. It is not suggested that the reconnaissance camera be re-designed to become a metric one - obviously the designer must continue to emphasize reliability and resolution as prime objectives in reconnaissance cameras and photography and if these results for example in large lens distortions there can be no complaint. However, the changes or modifications to reconnaissance frame cameras suggested above are comparatively trivial and would not affect the camera's performance, while adding valuable metric properties to the photography. If some of the suggestions made above are adapted in practice, it would make this high-performance frame photography more readily measured,analysed and processed than is possible at the present time.

9.3 Epilogue

Ending this thesis on a personal note, the author has greatly benefited from undertaking this work in various ways. For example, before starting the project, the author had done no basic work in computing science. Nevertheless, he has been able to make full use of the facilities available in the computing service and succeeded in developing several computer programs. Although these programs are smaller in size than some other programs used in photogrammetry such as those on block adjustment, the methods of devising a suitable algorithm and developing a computer program have become a familiar task. The photogrammetric measurements on the stereocomparator were another new field of experience for the author as were the provision of test data; the identification of test points; the problems of photo interpretation especially on the small-scale satellite photography, etc.

Thus, quite apart from the theoretical studies, the practical work carried out during this research has been invaluable to the author from the point of view of training and experience gained in photogrammetry and computing. This will be of the greatest value in his future professional work.

BIBLIOGRAPHY

Aeronautical and General Instruments Ltd., (1974). The F-126 and F-135 Aerial Reconnaissance Cameras. Croydon.

Aeronautical and General Instruments Ltd., (1977). F-139 and Agiflite Cameras. Croydon.

Aldred, A.H., (1968). Distortion by Focal Plane Shutters. Photogrammetric Engineering, 34 (7): 688-689.

American Society of Photogrammetry, (1945). Manual of Photogrammetry, Second Edition.

American Society of Photogrammetry, (1966). Manual of Photogrammetry, Third Edition.

American Society of Photogrammetry, (1968). Manual of Colour Aerial Photography. First Edition.

Bauer, H. and Muller, J., (1972). Height accuracy of Blocks and Bundle Adjustment with Additional Parameters. Presented Paper, Commission III, 12th Congress of International Society of Photogrammetry, Ottawa.

Brown, E.B., (1965). V/H Image Motion in Aerial Cameras. Photogrammetric Engineering, 31 (2): 308-323.

Brown, D.C., (1976). The Bundle Adjustment - Progress and Prospects. Invited Paper, Commission III, 13th Congress of International Society of Photogrammetry, Helsinki.

Brock, G.C., (1959). The Quality of the Photographic Image. Photogrammetria, 26 (3): 131-157.

Brock, G.C.,(1970). Image Evaluation for Aerial Photography. The Focal Press, London and New York.

Brock, G.C.,(1976). The Possibilities for Higher Resolution in Air Survey Photography. Photogrammetric Record, 8 (47): 589-609.

Case, J.B.,(1967). The Analytical Reduction of Panoramic and Strip Photography. Photogrammetria, 22 (4): 124-141.

Chismon, H.J. and Mott, P.G.,(1975). The Use of Satellite Imagery for Very Small Scale Mapping. Photogrammetric Record, 8 (46): 458-475.

Cowin, H.,(1973). Treetop Photo-reconnaissance. Flight International, 14 June, p. 924.

Department of the Army, U.S.,(1958). Universal Transverse Mercator Grid. Technical Manual TM 5-241-8.

Derenyi, E.E.,(1971). Exploratory Investigation concerning the Relative Orientation of Continuous Strip Imagery. U.N.B. Technical Report No. 8, University of New Brunswick, Canada; 144 pp.

Derenyi, E.E.,(1974). Planimetric Accuracy of Infrared Line Scan Imagery. The Canadian Surveyor, 28 (3): 247-254.

Derenyi, E.E.,(1974). SLAR Geometric Test. Photogrammetric Engineering, 40 (5): 597-603.

Ebner, H.,(1976). A Mathematical Model for Digital Rectification of Remote Sensing data. Presented Paper, Commission III, 13th Congress of International Society of Photogrammetry, Helsinki.

Etrog, U. and Shmutter, B.,(1974). Analysis of Panoramic Photographs. Photogrammetric Engineering, 40 (4): 489-492.

Finsterwalder, R.,(1964). Plotting from Aerial Photographs with Arbitrary Principal Distances. Information relative to Cartography and Geodesy. Series II: German Contributions in Foreign Languages, No. 19

Goddard, G.W.,(1951). New Developments for Aerial Reconnaissance. Photogrammetric Engineering, 17 (5): 673-686.

Goddard, G.W.,(1969). Overview. Doublely and Co. Inc., Garden City, New York.

Hadem, I.,(1968). The Influence of Height Differences on the Accuracy of the Stereomodel. Presented Paper, Commission III, 11th Congress of the International Society of Photogrammetry, Lausanne.

Hallert, B.,(1957). Quality Problems in Photogrammetry. Report of Working Group on Fundamental Problems. Commission II, International Society of Photogrammetry.

Hallert, B.,(1960). Photogrammetry. McGraw-Hill Book Co. Ltd., New York.

Harley, J. B.,(1975). Ordnance Survey Maps. Southampton, Ordnance Survey.

Harris, W.D., Tewinkel, G.C. and Whitten, C.A.,(1962). Analytical Aerotriangulation, Photogrammetric Engineering, 28 (1): 44-69.

Heiman, G.,(1972). Aerial Photography. The Macmillan Co., New York.

Helava, U.V.,(1963). New Significance of Errors of Inner Orientation. Photogrammetric Engineering, 29 (1): 126-129.

Hogg, J.,(1974). Recent Developments in use of 70 mm Aerial Photography in Geographical Research in Australia. Working Paper 69. Department of Geography, University of Leeds.

Hovey, S.T., (1965). Panoramic Possibilities and Problems. Photogrammetric Engineering, 31 (4): 727-734.

Itek Laboratories, (1961). Panoramic Progress, 1. Photogrammetric Engineering, 27 (5): 747-754.

Itek Laboratories, (1962). Panoramic Progress, 2. Photogrammetric Engineering, 28 (1): 99-107.

Katz, A.H., (1949). Camera Shutters. Journal of Optical Society of America, 39 (1): 1-21.

Keller, M. and Tewinkel, G.C., (1965). Aerotriangulation: Image Coordinate Refinement. Coast and Geodetic Survey Technical Bulletin No. 25.

Keller, M. and Tewinkel, G.C., (1966). Space Resection in Photogrammetry. Coast and Geodetic Survey Technical Bulletin No. 32.

Keller, M., (1975, 1976). Analytical Aerotriangulation Utilising Skylab Earth Terrain Camera (S-190B) Photography. Final Report submitted by NOAA National Ocean Survey, Maryland. Also published in Photogrammetric Engineering, 42 (11): 1375-1383.

Klass, P.J., (1971a), Secret Sentries in Space. Random House, New York.

Konecny, G., (1970). Metric Problems in Remote Sensing. Presented Paper, Commission IV, International Society of Photogrammetry, Delft. Also published in ITC Publications, Series A, no. 50, p. 152-177.

Konecny, G., (1972). Geometric Aspects of Remote Sensing. Invited Paper, Commission IV, International Congress of Photogrammetry, Ottawa.

Konecny, G.,(1975). Analytical Relations for the Restitution of Dynamic Remote Sensing Imagery. Report submitted to E.R.D. - E.T.L. Conference, University of Glasgow.

Konecny, G.,(1976). Mathematical Models and Procedures for the Geometric Restitution of Remote Sensing Imagery. Invited Paper, Commission III, 13th Congress of International Society for Photogrammetry, Helsinki.

Kubik, K.,(1971). The Effects of Systematic Image Errors in Block Triangulation. ITC Publication, A 49, 1-143.

Kubik, K.,(1973). Systematic Image Errors in Aerial Triangulation. Photogrammetria, 29 : 113-131.

Laws, F.C.V.,(1942). Photography in the R.A.F. Popular Photography, 66-79.

Laws, F.C.V.,(1945). Photography's part in Air Operations. The Photographic Journal, Section A, 84-89.

Laws, F.C.V.,(1958). Looking Back. The Photogrammetric Record, 3 (13): 24-41.

Mahoney, W.,(1963). Operational use of the AP-2 at ACIC. The Canadian Surveyor, June: 189-205.

Masry, S.E.,(1969). Analytical treatment of Stereostrip Photos. Photogrammetric Engineering, 35 (12): 1255-1262.

McLaurin, J.D.,(1972). The Skylab S-190B Earth Terrain Camera. Presented Paper, Commission 1, 12th Congress of International Society of Photogrammetry, Ottawa.

Methley, B.D.F.,(1970). Heights from Parallax Bar and Computer. Photogrammetric Record, 6 (35): 459-465.

Methley, B.D.F.,(1972). A Computer Program for Analytical Relative Orientation. Department of Geography Publication, University of Glasgow.

Mott, P.G.,(1975). Applications of Satellite Imagery to Small Scale Mapping. Presented Paper, ASP-ACSM Semi-Annual Convention, Phoenix, Arizona: 320-337.

Newhall, B.,(1969). Airborne Camera. The Focal Press Ltd., London and New York.

Nielsen, U.,(1975). More on Distortion by Focal Plane Shutters. Photogrammetric Engineering, 41 (2): 199-201.

Niels, J.,(1968). Optical and Photographic Reconnaissance Systems. John Wiley and Sons, Inc., New York.

Ockert, D.L.,(1960). Satellite Photography with Strip and Frame Cameras. Photogrammetric Engineering, 26 (4): 592-596.

Pestrecov, K.,(1947). Resolving Power of Photographic Lenses. Photogrammetric Engineering, 13 (1): 64-85.

Petrie, G.,(1970). Some Considerations regarding Mapping from Earth Satellites. Photogrammetric Record, 6 (36): 590-624.

Petrie, G.,(1974). Mapping from Earth Satellites. Road Design, 1. Planning and Transport Research and Computation Co. Ltd., London.

Quick, J.R.,(1964). Eye in the Sky. Archives, 10th Congress, International Society of Photogrammetry, Lisbon.

Richter, R.,(1956). Development and Perfection of the Topogon Lens. Photogrammetric Engineering, 22 (5): 868-873.

Rischmiller, D.W. and de Borde, A.H.,(1975). Graphical Output - a Users Guide. University of Glasgow Computing Service.

Rosenance, M.D.,(1961), Parabolic Image Motion. Photogrammetric Engineering, 27 (3); 421-427.

Schmid, E.,(1960). Transformation of Rectangular Space Coordinates. Coast and Geodetic Survey Technical Bulletin No. 15.

Schmid, H.H.,(1953). An Analytical Treatment of the Orientation of a Photogrammetric Camera. Aberdeen, Md., Ballistic Research Laboratories Report No. 880.

Schmid, H.H.,(1955). An Analytical Treatment of the Problem of Triangulation by Stereophotogrammetry. Ballistic Research Laboratories Report No. 961.

Schmid, H.H.,(1959). A General Analytical Solution to the Problem of Photogrammetry. Ballistic Research Laboratories Report No. 1065.

Schwidefsky, K.,(1956). On the Characteristics of the New Zeiss Aerial Lenses. Archives, 8th Congress of International Society of Photogrammetry, Stockholm.

Shershen, A.I.,(1958). Aerial Photography. Moscow.

Stark, E.,(1975). The Effect of Angular Field on Horizontal and Vertical Accuracy in Photogrammetric Plotting. Proceedings of the 35th Photogrammetric Week, Stuttgart.

Stuart, W.,(1945). Air Camera Design. The Photographic Journal, 85B, 50-56.

Stewart, R.A.,(1975). Mapping from Satellite Photography. Proceedings Commonwealth Survey Officers Conference, Paper No. K2: 1-25.

Tewinkel, G.C.,(1962). Analytic Absolute Orientation in Photogrammetry. Coast and Geodetic Survey Technical Bulletin No. 19.

Umbach, M.J.,(1967). Aerotriangulation: Transformation of Surveying and Mapping Coordinate Systems. Coast and Geodetic Survey Technical Bulletin No. 34.

Welch, R.,(1971). Modulation Transfer Functions. Photogrammetric Engineering, 37 (3): 247-259.

Welch, R.,(1974). Skylab-2 Photo Evaluation. Photogrammetric Engineering, 40 (10): 1221-1224.

Welch, R.,(1975). Photogrammetric Image Evaluation Techniques. Photogrammetria, 31: 161-190.

Welch, R.,(1976). Skylab S-190B ETC Photo Quality. Photogrammetric Engineering, 42 (8): 1057-1060.

Welch, R. and Lo, P.,(1977). Height Measurement from Satellite Images. Photogrammetric Engineering, 43 (10): 1233-1241.

Williamson, S.,(1957). The Cut Film Camera. Photogrammetric Record, 2 (11); 330-340.

Williamson Manufacturing Company Ltd.,(1954). A New High Altitude Panoramic Camera. Photogrammetric Record, 1 (3): 62-63.

Wiser, P., Liege, and Ackermann, F.,(1976). The OEEPE Test "Oberschwaben" Presented Paper, Commission III, 13th Congress of International Society of Photogrammetry, Helsinki.

Wolf, P.R.,(1974). Elements of Photogrammetry. McGraw-Hill Book Co. Inc., New York.

APPENDIX A

Coefficients of the Linearised Collinearity Equations

APPENDIX A

COEFFICIENTS OF THE LINEARISED COLLINEARITY EQUATIONS

$$\text{Rotation Matrix } A = \begin{bmatrix} A_1 \\ A_2 \\ A_3 \end{bmatrix} = \begin{bmatrix} a_{11} & a_{12} & a_{13} \\ a_{21} & a_{22} & a_{23} \\ a_{31} & a_{32} & a_{33} \end{bmatrix}$$

$$A_3B = a_{31} \quad a_{32} \quad a_{33} \begin{bmatrix} X - X_o \\ Y - Y_o \\ Z - Z_o \end{bmatrix}$$

$$P_{11} = \frac{1}{A_3B} \begin{vmatrix} x & z \\ \frac{\partial A_1}{\partial \omega} B & \frac{\partial A_3}{\partial \omega} B \end{vmatrix} \; ; \quad P_{21} = \frac{1}{A_3B} \begin{vmatrix} y & z \\ \frac{\partial A_2}{\partial \omega} B & \frac{\partial A_3}{\partial \omega} B \end{vmatrix}$$

$$P_{12} = \frac{1}{A_3B} \begin{vmatrix} x & z \\ \frac{\partial A_1}{\partial \phi} B & \frac{\partial A_3}{\partial \phi} B \end{vmatrix} \; ; \quad P_{22} = \frac{1}{A_3B} \begin{vmatrix} y & z \\ \frac{\partial A_2}{\partial \phi} B & \frac{\partial A_3}{\partial \phi} B \end{vmatrix}$$

$$P_{13} = \frac{1}{A_3B} \begin{vmatrix} x & z \\ \frac{A_1}{\partial \kappa} B & \frac{A_3}{\partial \kappa} B \end{vmatrix} \; ; \quad P_{23} = \frac{1}{A_3B} \begin{vmatrix} y & z \\ \frac{\partial A_2}{\partial \kappa} B & \frac{\partial A_3}{\partial \kappa} B \end{vmatrix}$$

$$P_{14} = \frac{1}{A_3B} \begin{vmatrix} x & z \\ a_{11} & a_{31} \end{vmatrix} \; ; \quad P_{24} = \frac{1}{A_3B} \begin{vmatrix} y & z \\ a_{21} & a_{31} \end{vmatrix}$$

$$P_{15} = \frac{1}{A_3B} \begin{vmatrix} x & z \\ a_{12} & a_{32} \end{vmatrix} \; ; \quad P_{25} = \frac{1}{A_3B} \begin{vmatrix} y & z \\ a_{22} & a_{32} \end{vmatrix}$$

$$P_{16} = \frac{1}{A_3B} \begin{vmatrix} x & z \\ a_{13} & a_{33} \end{vmatrix} \; ; \quad P_{26} = \frac{1}{A_3B} \begin{vmatrix} y & z \\ a_{23} & a_{33} \end{vmatrix}$$

APPENDIX B

Detailed Description of the Computer Programs

APPENDIX B

DETAILED DESCRIPTION OF THE COMPUTER PROGRAMS

1. Program (A) - Image Coordinates Refinement

1.1 General Information

Program Identification	-	IMCERT Image Coordinates Refinement
Type of Language	-	Complete Algol program
Computer	-	The program was first developed on the Nottingham ICL 1906A main University Computer. It was later transferred to the ICL 2980 in Edinburgh.

1.2 Definition of Variables

PH	-	Model Number
TAG	-	Tag to indicate type of correction to be applied.
FL	-	Focal length of the photography.
N	-	Number of image points to be corrected.
FH	-	Absolute flying height.
TH	-	Average terrain height above mean sea level.
AN	-	Number of points used in the data to represent the lens distortion curve.
XL, YL	-	Coordinates of the principal point of the left hand photograph.

XR, YR	-	Coordinates of the principal point of the right-hand photograph.
CAS	-	Tag indicating focal plane shutter direction of motion relative to the flight direction.
FK	-	Factor of correction for the focal plane shutter and IMC.

ARRAYS

B	-	Dynamic array containing the image coordinates, and used to determine the required corrections.
LD	-	Array containing the lens distortion correction data.
D, DT, V, T, DR	-	Working arrays to determine the polynomial parameters for the lens distortion curve.

1.3 Detailed account of the program

A step-by-step account of the program follows:

(i) Introduce the following matrix procedures to be used in calculating the polynomials for the lens distortion curve:

Procedure MATVEC - Matrix x Vector

Procedure MATMLT - Matrix x Matrix

Procedure MATRAN - Matrix transpose

Procedure INVERT - Matrix inversion

(ii) Input of Data

Declaration.

Read in the model number (PH). If the last model is corrected then PH = 0.

Read in the Tag (TAG) to indicate the type of correction required (1 to 7) as follows:

1 - earth curvature and atmospheric refraction

2 - lens distortion and atmospheric refraction

3 - lens distortion, earth curvature and atmospheric refraction

4 - lens distortion and earth curvature

5 - lens distortion

6 - earth curvature

7 - atmospheric refraction

Read in the camera focal length (FL), in the same unit as the image coordinates.

Read in the number of points to be corrected (N).

If either the atmospheric refraction or the earth curvature or both of them are to be corrected, then read the flying height (FH) and the terrain height (TH) in kilometres.

Declaration.

Read in the image coordinates of all the points into array B. These are read into columns 1, 2, 3, 4, 5 as follows:

a - the point number in column 1

b - x', y", dx, dy in columns 2, 3, 4 and 5, respectively.

Read the coordinates of the left-hand principal point (XL, YL).

Read the coordinates of the right-hand principal point (XR, YR).

Read the number of points whose radial lens distortion is given to determine the lens distortion curve (AN). If the lens distortion is not to be corrected, then AN = 0.

Read the tag (CAS) to indicate the direction of shutter motion. If the shutter moves in the same direction of flight for both exposures, then CAS = 11. If the shutter moves along the flight direction and opposite to it for the alternate exposure, then CAS = 12. If the shutter moves across the flight direction without changing direction then CAS = 22. If the shutter moves across the flight direction reversing its direction for the alternate exposure then CAS = 21. If no effect of focal plane shutter is to be corrected then CAS = 0.

Read the factor (FK) for correction of the effect of the focal plane shutter and IMC. If no correction is required then FK = 0.

(iii) Correction for the image coordinates

Reduce the image coordinates of each photograph to its principal point.

Compute the radial distances of the image points.

Compute the constant of atmospheric refraction if such a correction is to be applied.

Correct for lens distortion after computing the polynomial that fits the distortion curve.

Correct for earth curvature if required.

Correct for atmospheric refraction if required.

Correct for the focal plane shutter and IMC if required.

(iv) Output of the results

Write text.

Write text.

Print out the polynomial parameters for the lens distortion curve, if lens distortion is to be corrected.

Write text.

Print out the model number.

Write text.

Print out the corrected image coordiaates.

1.4 Flow Diagram for Program (A)

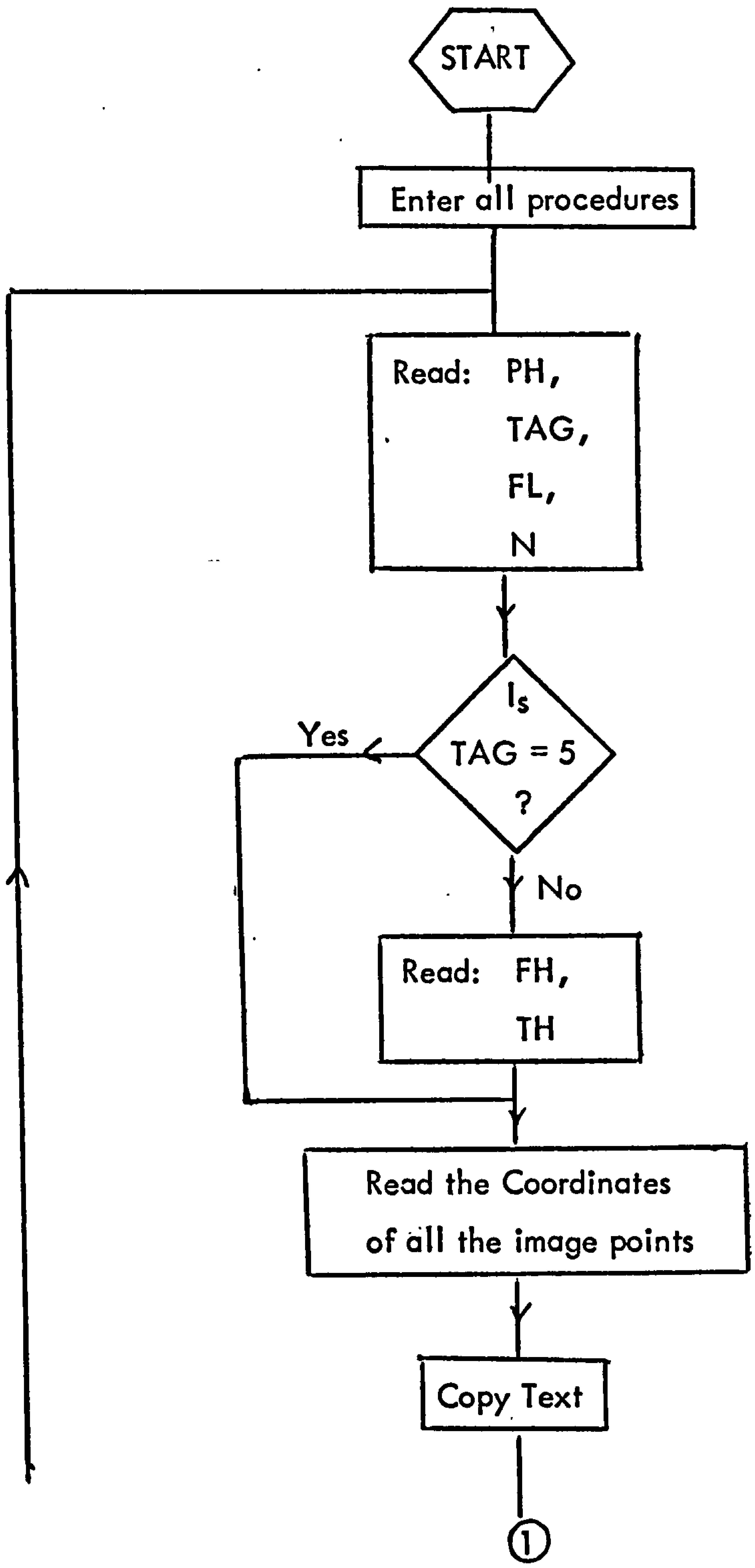

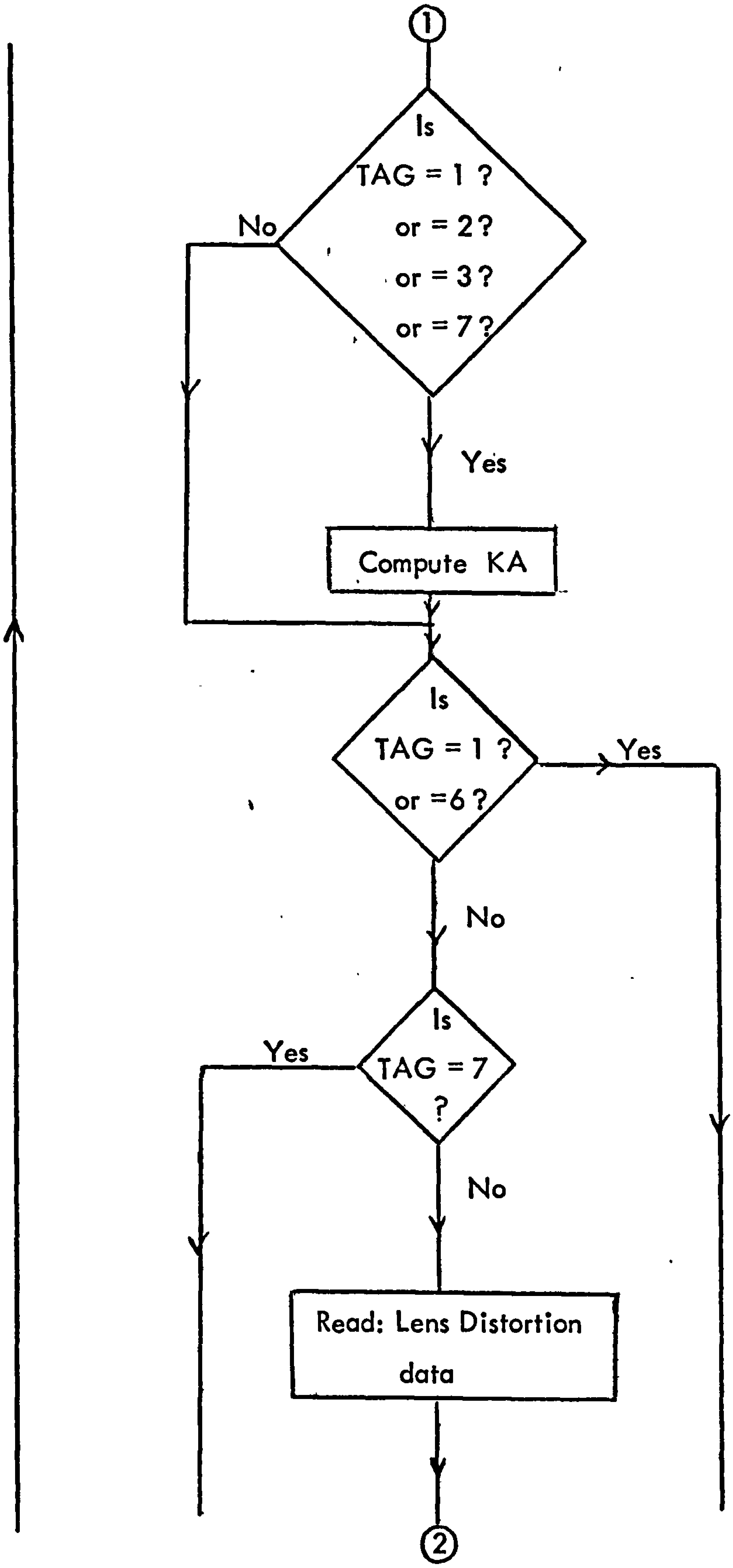
1
Is
TAG = 1 ?
or = 2?
or = 3?
or = 7?
No
Yes
Compute KA
Is
TAG = 1 ?
or =6 ?
Yes
No
Is
TAG = 7
?
Yes
No
Read: Lens Distortion
data
2

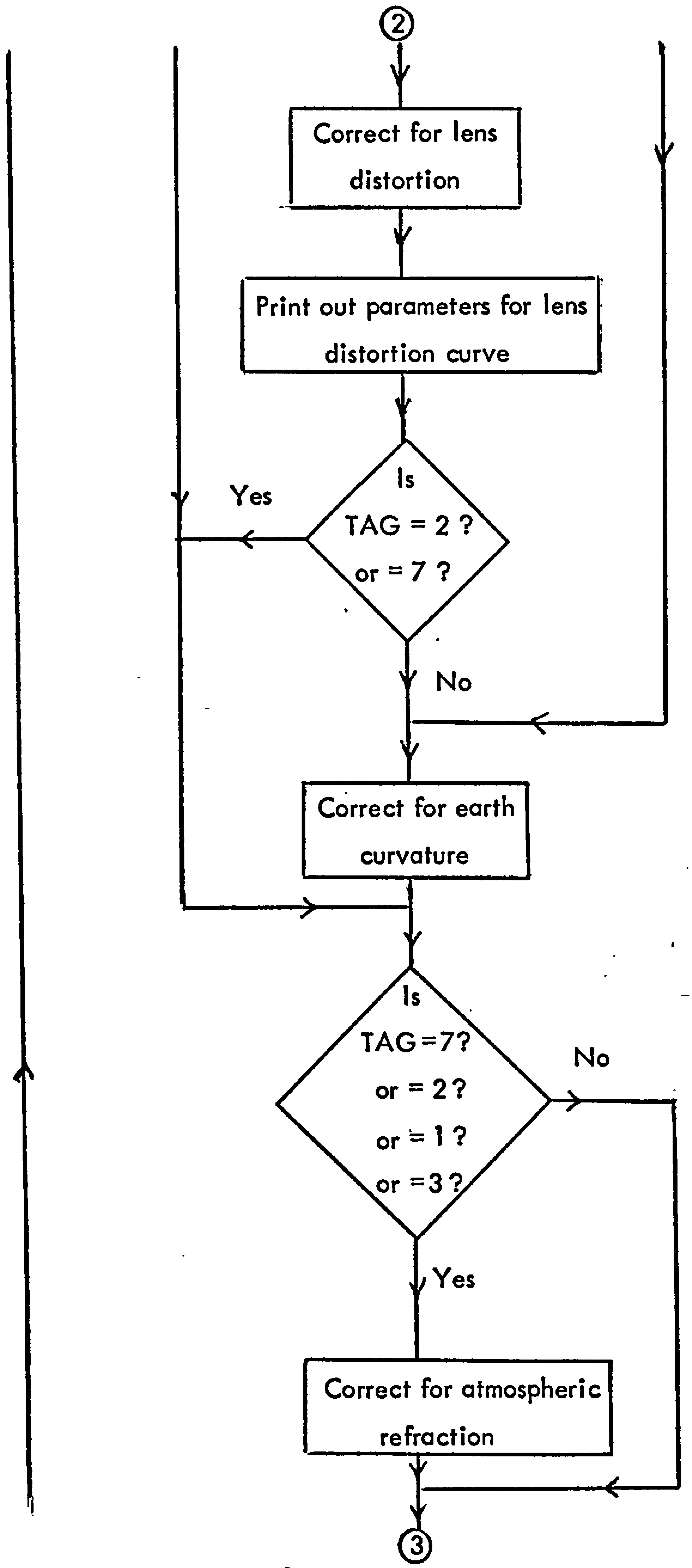
2
Correct for lens distortion
Print out parameters for lens distortion curve
Is TAG = 2 ? or = 7 ?
Yes
No
Correct for earth curvature
Is TAG = 7? or = 2? or = 1? or = 3?
No
Yes
Correct for atmospheric refraction
3

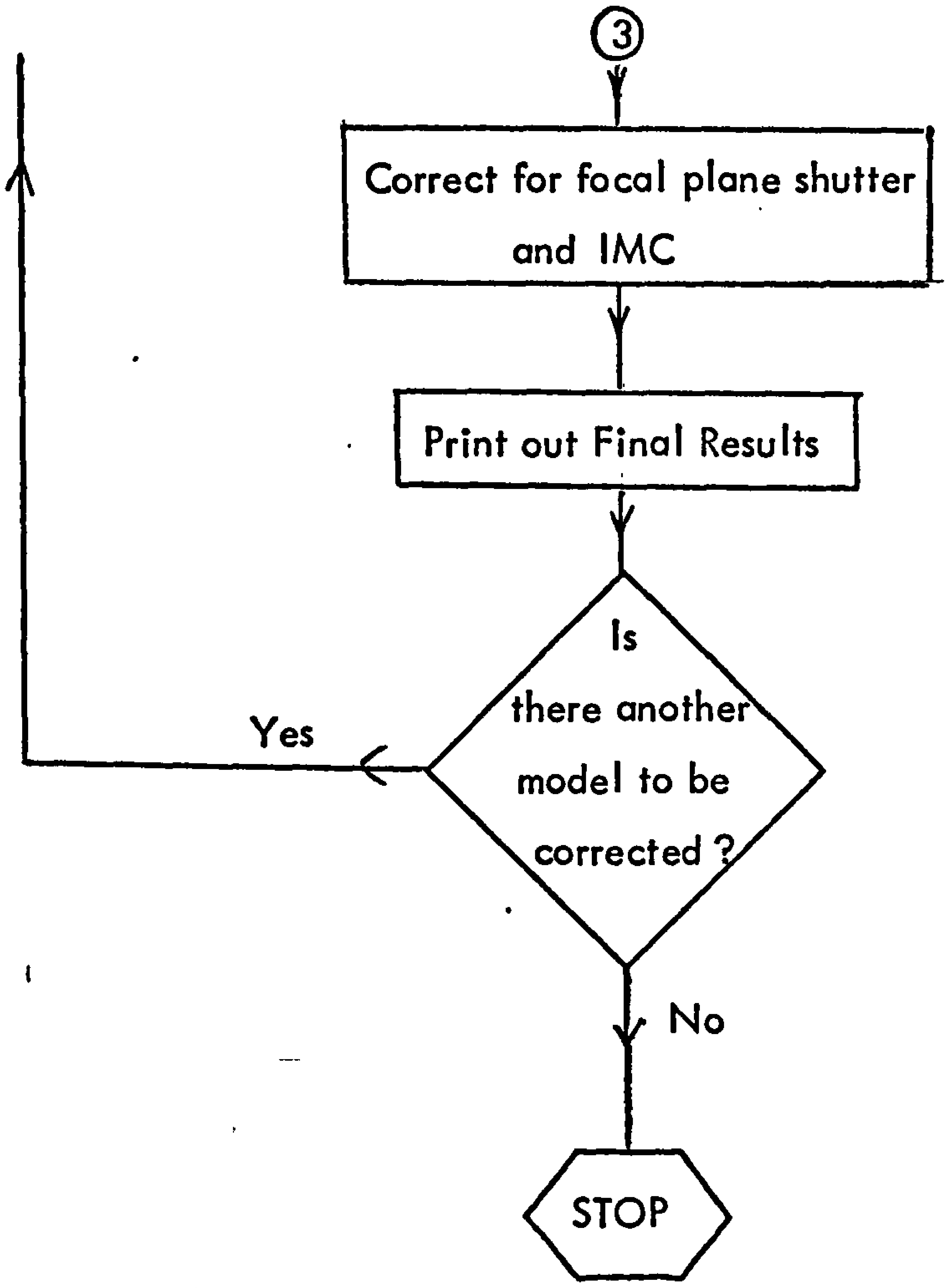
3
Correct for focal plane shutter and IMC
Print out Final Results
Is there another model to be corrected ?
Yes
No
STOP

1.5 The Program

```
STMNT
  1     'BEGIN'
  2     'COMMENT'  IMAGE COORDINATES
  2               REFINEMENT PROGRAM;
  3
  3
  3     'INTEGER'  M,  N,   AN;
  4     'PROCEDURE' MATVEC(A,X,Z,M,N);
  5     'VALUE' A,X,M,N;
  6     'INTEGER' M,N; 'ARRAY'A,X,Z;
  8     'BEGIN' 'INTEGER' I,J;
 10     'REAL' SUM;
 11     'FOR' I:=1 'STEP' 1 'UNTIL' N 'DO'
 11     'BEGIN' SUM:=0.0;
 13     'FOR' J:=1 'STEP' 1 'UNTIL' M 'DO'
 13     SUM:=SUM+A$I,J!*X$J!;
 14     Z$I!:=SUM;
 15     'END'; 'END' MATVEC;
 17     'PROCEDURE' MATMLT(A,U,T,M,N,P);
 18     'VALUE' A,U,M,N,P;
 19     'INTEGER' M,N,P;
 20     'REAL' 'ARRAY' A,U,T;
 21     'BEGIN' 'INTEGER' I,J,K;
 23     'FOR' I:=1 'STEP' 1 'UNTIL' N 'DO'
 23     'FOR' J:=1 'STEP' 1 'UNTIL' M 'DO'
 23     'BEGIN'
 24     T$I,J!:=0.0;
 25     'FOR' K:=1 'STEP' 1 'UNTIL' P 'DO'
 25     T$I,J!:=T$I,J!+A$I,K!*U$K,J!;
 26     'END';
 27     'END' MATMLT;
 28     'PROCEDURE' MATRAN(A,AT,M,N);
 29     'VALUE' A,M,N;
 30     'ARRAY'A,AT;
 31     'INTEGER' M,N;
 32     'BEGIN'
 33     'INTEGER'I,J;
 34     'FOR' I:=1 'STEP' 1 'UNTIL' M 'DO'
```

```
34      'FOR' J:=1 'STEP' 1 'UNTIL' N 'DO'
34      AT$I,J!:=A$J,I!
34      'END' MATRAN;
36      'PROCEDURE' INVERT(A,N,INVA);
37      'VALUE' N;
38      'ARRAY' A,INVA;
39      'INTEGER' N;
40      'BEGIN'
41      'REAL' 'ARRAY' B$1:N,1:2*N!, X$1:N,1:N!;
42      'INTEGER' M,I,J,K;
43      'REAL' PIVOT, TT;
44      M:=2*N;
45      'FOR' I:=1 'STEP' 1 'UNTIL' N 'DO'
45      'BEGIN'
46      'FOR' J:=1 'STEP' 1 'UNTIL' N 'DO'
46      B$I,J!:=A$I,J!;
47      'FOR' J:=N+1 'STEP' 1 'UNTIL' M 'DO'
47      B$I,J!:= 'IF' I+N 'EQ' J 'THEN' 1 'ELSE' 0;
48      'END';
49      'FOR' I:=1 'STEP' 1 'UNTIL' N 'DO'
49      'BEGIN'
50      PIVOT:=B$I,I!;
51      'FOR' J:=I+1 'STEP' 1 'UNTIL' N 'DO'
51      'IF' ABS(PIVOT) 'LT' ABS(B$J,I!) 'THEN'
51      'BEGIN'
52      'FOR' K:=1 'STEP' 1 'UNTIL' M 'DO'
52      'BEGIN'
53      TT:=B$I,K!;
54      B$I,K!:=B$J,K!;
55      B$J,K!:=TT;
56      'END';
57      PIVOT:=B$J,I!;
58      'END';
59      'FOR' K:=M 'STEP' -1 'UNTIL' I 'DO'
59      B$I,K!:=B$I,K!/B$I,I!;
60      'FOR' J:=I+1 'STEP' 1 'UNTIL' N 'DO'
60      'FOR' K:=M 'STEP' -1 'UNTIL' I 'DO'
60      B$J,K!:=B$J,K!-B$I,K!*B$J,I!;
61      'END';
62      'FOR' J:=1 'STEP' 1 'UNTIL' N 'DO'
62      'BEGIN'
63      K:=N+J;
64      X$N,J!:=B$N,K!;
65
65      'END';
66      'FOR' I:=N-1 'STEP' -1 'UNTIL' 1 'DO'
66      'BEGIN'
67      'FOR' J:=1 'STEP' 1 'UNTIL' N 'DO'
67      'BEGIN'
68      M:=N+J;
69      X$I,J!:=B$I,M!;
70      'END';
71      'FOR' K:=N 'STEP' -1 'UNTIL' I+1 'DO'
71      'FOR' J:=1 'STEP' 1 'UNTIL' N 'DO'
71      X$I,J!:=X$I,J!-B$I,K!*X$K,J!;
72      'END';
73      'FOR' I:=1 'STEP' 1 'UNTIL' N 'DO'
73      'FOR' J:=1 'STEP' 1 'UNTIL' N 'DO'
73      INVA$I,J!:=X$I,J!;
74      'END'INVERT;
75
75
75      'INTEGER' I, J, PH, TAG, CAS;
76      'REAL' FL, FH, KA, XL, YL,
76      XR, YR, TH, FK,       K1;
77
```

```
77    'COMMENT'  READ IN THE PHOTO NUMBER;
78    L1: PH:=READ;
79    'IF' PH=0 'THEN' 'GOTO' L9;
80
80    'COMMENT'   READ  IN :
80       TAG --- THE TYPE OF CORRECTION REQUIRED,
80       FL  --- THE CAMERA FOCAL LENGTH,
80        N  --- THE NUMBER OF POINTS TO BE CORRECTED;
81    TAG:=READ;
82    FL:=READ;
83    N:=READ;
84
84    'COMMENT'  FH AND TH ARE THE ABSOLUTE FLYING HEIGHT
84                                    AND
84                  THE AVERAGE TERRAIN HEIGHT  IN KMS
84                 THESE ARE NOT REQUIRED IF ONLY LENS
84                 DISTORTION IS TO BE CORRECTED;
85    'IF' TAG'LT' 5 'OR' TAG>5  'THEN'  'BEGIN'
86    FH:=READ;
87    TH:=READ;
88    'END';
89
89    'BEGIN'
90    'REAL' 'ARRAY'  B$1:N,1:22!;
91    'FOR' I:=1 'STEP' 1 'UNTIL' N 'DO'
91    'FOR' J:=1 'STEP' 1 'UNTIL' 22 'DO'
91    B$I,J!:=0.00;
92
92    'COMMENT'  READ IN THE IMAGE COORDINATES
92                OF ALL THE POINTS;
93    'FOR' I:=1 'STEP' 1 'UNTIL' N 'DO'
93    'FOR' J:=1,2,3,4,5 'DO'
93    B$I,J!:=READ;
94    XL:=READ;  YL:=READ;
96    XR:=READ;  YR:=READ;
98
98    'FOR' I:=1 'STEP' 1 'UNTIL' N 'DO'
98    'BEGIN'
99    B$I,6!:=B$I,2!-XL;
100   B$I,7!:=B$I,3!+B$I,5!-YL;
101   B$I,8!:=B$I,2!+B$I,4!-XR;
102   B$I,9!:=B$I,3!-YR;
103   'END';
104   'FOR' I:=1 'STEP' 1 'UNTIL' N 'DO'
104   'BEGIN'
105   B$I,10!:=SQRT(B$I,6!'**'2+B$I,7!'**'2);
106   B$I,11!:=SQRT(B$I,8!'**'2+B$I,9!'**'2);
107   'END';
108
108    WRITE TEXT('('''('P')'I.M. ELHASSAN ---
108
108    GEOGRAPHY**DEPARTMENT'('2C')'')');
109
109
109    'COMMENT'  READ IN THE NUMBER OF POINTS
109            WHOSE LENS DISTORTION IS GIVEN;
110    AN:=READ;
111
111    'COMMENT'  READ IN  :
111       CAS -- THE DIRECTION OF SHUTTER MOTION,
111        FK -- THE SHUTTER CORRECTION FACTOR;
112    CAS:=READ;
113    FK:=READ;
114
114    'BEGIN'
115    'REAL' 'ARRAY'  LD$1:AN,1:2!, DR$1:AN!,
```

```
115   D$1:AN,1:4!, DT$1:4,1:AN!, V$1:4,1:4!,
115   T$1:4,1:4!,   A$1:4!;
116
116   'COMMENT' COMPUTE THE CONSTANT OF
116      ATMOSPHERIC REFRACTION;
117   'IF' TAG=1 'OR' TAG=2 'OR' TAG=3 'OR'
117      TAG=7    'THEN'   'BEGIN'
118   KA:=(0.00241*FH)/(FH'**'2-6.00*FH+250.00)-
118   (TH/FH)*(0.00241*TH)/(TH'**'2-6.00*TH+250.00);
119   'END';
120
120   'IF' TAG=1 'OR' TAG=6 'THEN'
120   'GOTO' L3;
121   'IF' TAG=7 'THEN'
121   'GOTO' L4;
122
122   'COMMENT' CORRECTION FOR LENS DISTORTION;
123   'FOR' I:=1 'STEP' 1 'UNTIL' AN 'DO'
123   'FOR' J:=1,2 'DO'
123   LD$I,J!:=READ;
124   'FOR' I:=1 'STEP' 1 'UNTIL' AN 'DO'
124   'BEGIN'
125   D$I,1!:=LD$I,1!;
126   D$I,2!:=LD$I,1!'**'3;
127   D$I,3!:=LD$I,1!'**'5;
128   D$I,4!:=LD$I,1!'**'7;
129   DR$I!:=LD$I,2!;
130   'END';
131   'IF' AN=4 'THEN'
131   'BEGIN'
132   INVERT(D,4,V);
133   MATVEC(V,DR,A,4,4);
134   'GOTO' L2;
135   'END';
136   MATRAN(D,DT,4,AN);
137   MATMLT(DT,D,T,4,4,AN);
138   INVERT(T,4,V);
139   MATVEC(DT,DR,A,AN,4);
140   MATVEC(V,A,A,4,4);
141
141   L2: 'FOR' I:=1 'STEP' 1 'UNTIL' N 'DO'
141   'BEGIN'
142   'FOR' J:=10,11 'DO'
142   B$I,J+2!:=A$1!+A$2!*B$I,J!'**'2+A$3!*B$I,J!'**'4+
142   A$4!*B$I,J!'**'6;
143   'END';
144
144   WRITE TEXT('('('4C')'POLYN.%PARAMETERS%FOR%
144
144   LENS%DISTORTION%CURVE'('2C')')');
145
145   'FOR' I:=1 'STEP' 1 'UNTIL' 4 'DO'
145   'BEGIN'
146   PRINT(A$I!,0,6);
147   NEWLINES(2);
148   'END';
149
149   'IF' TAG=2 'OR' TAG=5 'THEN'   'BEGIN'
150   'FOR' I:=1 'STEP' 1 'UNTIL' N 'DO'
150   'BEGIN'
151   'FOR' J:=6,7 'DO'
151   B$I,J!:=B$I,J!*(1.0-B$I,12!);
152   'FOR' J:=8,9 'DO'
152   B$I,J!:=B$I,J!*(1.0-B$I,13!);
153   'END';
154   'END';
```

```
'IF' TAG=2 'THEN' 'GOTO' L4;
'IF' TAG=5 'THEN' 'GOTO' L5;

'COMMENT'  CORRECTION FOR EARTH CURVATURE;
L3: K1:=12740.0*FL'**'2;
'FOR' I:=1 'STEP' 1 'UNTIL' N 'DO'
'BEGIN'
'FOR' J:=10,11 'DO'
'BEGIN'    M:=J+4;
B$I,M!:=((FH-TH)*B$I,J!'**'2)/K1;
'END';
'END';
'FOR' I:=1 'STEP' 1 'UNTIL' N 'DO'
'BEGIN'
'FOR' J:=6,7 'DO'
B$I,J!:=B$I,J!*(1.0-B$I,12!+B$I,14!);
'FOR' J:=8,9 'DO'
B$I,J!:=B$I,J!*(1.0-B$I,13!+B$I,15!);
'END';

'IF' TAG=4 'THEN' 'GOTO' L5;
'IF' TAG=6 'THEN' 'GOTO' L5;

'COMMENT'  CORRECTION FOR ATM. REFRACTION;
L4: 'IF' TAG 'LT' 7 'THEN' 'BEGIN'
'FOR' I:=1 'STEP' 1 'UNTIL' N 'DO'
'BEGIN'
B$I,10!:=SQRT(B$I,6!'**'2+B$I,7!'**'2);
B$I,11!:=SQRT(B$I,8!'**'2+B$I,9!'**'2);
'END';
'END';
'FOR' I:=1 'STEP' 1 'UNTIL' N 'DO'
'BEGIN'
'FOR' J:=10,11 'DO'
B$I,J+6!:=KA*(1.0+B$I,J!'**'2/FL'**'2);
'END';
'FOR' I:=1 'STEP' 1 'UNTIL' N 'DO'
'BEGIN'
'FOR' J:=6,7 'DO'
B$I,J!:=B$I,J!*(1.0-B$I,16!);
'FOR' J:=8,9 'DO'
B$I,J!:=B$I,J!*(1.0-B$I,17!);
'END';


'COMMENT'  CORRECTION FOR THE DISTORTION DUE
     TO THE FOCAL PLANE SHUTTER;

L5: 'IF' CAS=11 'OR' CAS=21 'THEN' FK:=-FK;
'IF' CAS=11 'THEN'  'BEGIN'
'FOR' I:=1 'STEP' 1 'UNTIL' N 'DO'
'BEGIN'
B$I,6!:=B$I,6!+FK*B$I,6!;
B$I,8!:=B$I,8!+FK*B$I,8!;
'END';  'END';

'IF' CAS=12 'THEN'  'BEGIN'
'FOR' I:=1 'STEP' 1 'UNTIL' N 'DO'
'BEGIN'
B$I,6!:=B$I,6!-FK*B$I,6!;
B$I,8!:=B$I,8!+FK*B$I,8!;
'END';  'END';

'IF' CAS=21 'THEN'  'BEGIN'
'FOR' I:=1 'STEP' 1 'UNTIL' N 'DO'
```

```
'BEGIN'
B$I,6!:=B$I,6!+FK*B$I,7!;
B$I,8!:=B$I,8!+FK*B$I,9!;
'END';  'END';
'IF' CAS=22 'THEN'  'BEGIN'
'FOR' I:=1 'STEP' 1 'UNTIL' N 'DO'
'BEGIN'
B$I,6!:=B$I,6!-FK*B$I,7!;
B$I,8!:=B$I,8!+FK*B$I,9!;
'END';  'END';
'FOR' I:=1 'STEP' 1 'UNTIL' N 'DO'
'BEGIN'
B$I,18!:=B$I,6!-B$I,8!;
B$I,19!:=B$I,9!-B$I,7!;
'END';
WRITE TEXT('('('4C')''('20S')'REFINED%IMAGE%%
COORDINATES'('2C')'MODEL%NUMBER'('4S')'')');
PRINT(PH,4,0);
WRITE TEXT('('('2C')'POINT%NO.'('4S')'X1'('11S')'
Y1'('11S')'X2'('11S')'Y2'('11S')'DX'('11S')'
DY'('2C')'')');
'FOR' I:=1 'STEP' 1 'UNTIL' N 'DO'
'BEGIN'
PRINT(B$I,1!,4,0);
SPACES(4);
'FOR' J:=6,7,8,9,18,19 'DO'
'BEGIN'
PRINT(B$I,J!,1,6);
SPACES(4);
'END';
NEWLINES(2);
'END';
'END';  'END';
'GOTO' L1;
L9: 'END';
```

1.6 <u>Input</u>

47933 ———— Model number

3 ———— Tag indicating type of correction required.

0.156135 ———— Camera focal length (m)

3.040 ———— Flying height (km)

0.010 ———— Average terrain height (km)

Pt. No.	x	dx	y	dy (photo-coordinates)
3769	-0.019397	0.015074	-0.077504	0.000467
3767	-0.011480	0.043924	-0.077940	0.001204
3766	-0.008416	0.046833	-0.078065	0.001253
3770	0.025101	0.011851	-0.079200	0.000255
3771	0.031252	0.010841	-0.079382	0.000226
3762	0.047880	0.005944	-0.079796	0.000108
3703	0.046964	0.001196	-0.079755	0.000018
3702	0.055905	0.006497	-0.079930	0.000072
3775	0.081755	0.020440	-0.080497	0.000241
3774	0.087681	0.019834	-0.080591	0.000220
3710	0.082050	-0.025967	-0.080195	-0.000371
3735	0.079380	-0.040325	-0.080076	-0.000544
3729	0.093658	-0.052159	-0.080237	-0.000670
3751	0.102734	-0.032902	-0.080475	-0.000433
3750	0.098077	-0.025203	-0.080448	-0.000350
3728	0.093964	-0.027936	-0.080378	-0.000377
3761	0.043203	-0.028003	-0.079472	-0.000471
3760	0.041251	-0.045102	-0.079280	-0.000754
3768	-0.032599	-0.019773	-0.076803	-0.000452
3714	-0.015105	-0.026178	-0.077568	-0.000585
3713	-0.003688	-0.038515	-0.077943	-0.000823
3759	-0.014988	-0.069902	-0.077578	-0.001399
3758	-0.015161	-0.076646	-0.077484	-0.001522
3757	-0.016095	-0.092208	-0.077392	-0.001727
3772	0.014705	-0.067989	-0.078486	-0.001218
3755	0.031726	-0.093869	-0.078790	-0.001472
3754	0.041030	-0.095279	-0.079004	-0.001449
3752	0.083677	-0.084132	-0.080025	-0.001082
3753	0.108323	-0.082915	-0.080476	-0.000980
1709	0.115337	-0.070023	-0.080467	-0.000777
1706	0.112608	-0.055638	-0.080630	-0.000656
1707	0.110300	-0.051479	-0.080598	-0.000630
1726	0.104918	-0.026951	-0.080515	-0.000339
1727	0.107023	-0.025016	-0.080527	-0.000339
1728	0.104335	-0.025522	-0.080497	-0.000333
1725	0.082492	-0.049047	-0.080061	-0.000662
1703	0.084374	-0.072344	-0.080241	-0.000941
1710	0.075394	-0.092665	-0.080149	-0.001228
1701	0.029965	-0.075493	-0.078901	-0.001260
1702	0.035504	-0.071168	-0.079006	-0.001168
1705	-0.010923	-0.090624	-0.077876	-0.001698
1704	-0.015506	-0.092544	-0.077443	-0.001729
1732	-0.029828	-0.017361	-0.077074	-0.000369
1733	-0.030425	-0.018201	-0.077067	-0.000380
1734	-0.031018	-0.019012	-0.077055	-0.000396
1731	0.014495	-0.004666	-0.078808	-0.000087
1711	-0.011000	0.012553	-0.077912	0.000385

1724	0.038526	-0.029555	-0.079450	-0.000523
1722	0.047500	-0.037630	-0.079497	-0.000627
1723	0.045896	-0.039210	-0.079497	-0.000627
1720	0.074800	0.015295	-0.080393	0.000173
1721	0.081348	0.011975	-0.080434	0.000127
1719	0.087071	0.048138	-0.081448	0.000705
1718	0.086142	0.047730	-0.081414	0.000705
1716	0.046153	0.024258	-0.079887	0.000429
1713	-0.010159	0.096971	-0.079423	0.002543
1714	0.011847	0.094707	-0.079091	0.002283
1715	0.011638	0.094285	-0.079101	0.002283

0.000000 0.000000 — Comparator coordinates of L.H. principal point (XL, YL)

0.000000 0.000000 — Comparator coordinates of R.H. principal point (XR, YR)

17 — No. of points used to describe the lens distortion curve

Tag to indicate direction of slit motion

12 -0.000 — Focal plane shutter constant

radial distance	radial distortion
0.000000	0.000000
0.010000	0.000030
0.020000	0.000060
0.030000	0.000080
0.040000	0.000095
0.050000	0.000094
0.060000	0.000088
0.070000	0.000070
0.080000	0.000053
0.090000	0.000043
0.100000	0.000046
0.110000	0.000066
0.120000	0.000092
0.130000	0.000115
0.140000	0.000135
0.150000	0.000014
0.160000	-0.000134

Lens distortion data

0 — Tag indicating end of last model

1.7 Output

I.M.ELHASSAN---GEOGRAPHY**DEPARTMENT

POLYN. PARAMETERS FOR LENS DISTORTION CURVE

3.273081@ -3

-7.087432@ -1

5.721788@ 1

-1.402830@ 3

REFINED IMAGE COORDINATES

MODEL NUMBER 47933

POINT NO.	X1	Y1	X2	Y2	DX	DY
3769	-0.019351	0.015496	-0.096809	0.015067	0.077458	-0.000429
3767	-0.011463	0.045038	-0.089335	0.043904	0.077872	-0.001133
3766	-0.008404	0.047995	-0.086399	0.046812	0.077995	-0.001183
3770	0.025044	0.012072	-0.053985	0.011832	0.079029	-0.000240
3771	0.031187	0.011038	-0.048016	0.010821	0.079203	-0.000218
3762	0.047812	0.006040	-0.031817	0.005928	0.079629	-0.000112
3703	0.046894	0.001212	-0.032690	0.001193	0.079584	-0.000019
3702	0.055846	0.006559	-0.023944	0.006478	0.079789	-0.000080
3775	0.081747	0.020669	0.001254	0.020378	0.080494	-0.000290
3774	0.087681	0.020044	0.007065	0.019775	0.080616	-0.000269
3710	0.082045	-0.026323	0.001849	-0.025893	0.080196	0.000430
3735	0.079379	-0.040848	-0.000694	-0.040233	0.080073	0.000615
3729	0.093659	-0.052803	0.013392	-0.052072	0.080267	0.000731
3751	0.102734	-0.033318	0.022197	-0.032826	0.080538	0.000492
3750	0.098082	-0.025541	0.017573	-0.025136	0.080509	0.000406
3728	0.093969	-0.028300	0.013543	-0.027862	0.080426	0.000439
3761	0.043148	-0.028424	-0.036177	-0.027946	0.079325	0.000478
3760	0.041217	-0.045795	-0.037955	-0.045037	0.079172	0.000758
3768	-0.032538	-0.020177	-0.109289	-0.019763	0.076751	0.000415

3714	-0.015072	-0.026691	-0.092585	-0.026166	0.077513	0.000525
3713	-0.003681	-0.039247	-0.081549	-0.038496	0.077868	0.000751
3759	-0.014982	-0.071237	-0.092465	-0.069860	0.077483	0.001376
3758	-0.015158	-0.078113	-0.092538	-0.076596	0.077380	0.001518
3757	-0.016096	-0.093892	-0.093370	-0.092138	0.077274	0.001754
3772	0.014698	-0.069140	-0.063719	-0.067957	0.078417	0.001183
3755	0.031728	-0.095298	-0.047018	-0.093825	0.078746	0.001473
3754	0.041031	-0.096682	-0.037938	-0.095235	0.078969	0.001447
3752	0.083665	-0.085159	0.003648	-0.084082	0.080017	0.001077
3753	0.108299	-0.083834	0.027818	-0.082870	0.080481	0.000964
1709	0.115309	-0.070747	0.034827	-0.069971	0.080482	0.000776
1706	0.112583	-0.056253	0.031923	-0.055570	0.080660	0.000683
1707	0.110280	-0.052074	0.029645	-0.051406	0.080635	0.000668
1726	0.104918	-0.027276	0.024331	-0.026885	0.080587	0.000391
1727	0.107021	-0.025342	0.026418	-0.024955	0.080603	0.000387
1728	0.104336	-0.025842	0.023766	-0.025458	0.080570	0.000384
1725	0.082496	-0.049686	0.002425	-0.048954	0.080071	0.000732
1703	0.084371	-0.073246	0.004127	-0.072278	0.080244	0.000968
1710	0.075382	-0.093831	-0.004750	-0.092621	0.080133	0.001210
1701	0.029961	-0.076704	-0.048887	-0.075455	0.078848	0.001249
1702	0.035498	-0.072287	-0.043454	-0.071125	0.078951	0.001163
1705	-0.010923	-0.092278	-0.088690	-0.090558	0.077766	0.001721
1704	-0.015507	-0.094230	-0.092832	-0.092474	0.077326	0.001756
1732	-0.029768	-0.017685	-0.106795	-0.017352	0.077028	0.000333
1733	-0.030365	-0.018535	-0.107384	-0.018192	0.077019	0.000343
1734	-0.030958	-0.019361	-0.107963	-0.019002	0.077006	0.000358
1731	0.014457	-0.004738	-0.064203	-0.004660	0.078660	0.000078
1711	-0.010971	0.012898	-0.088823	0.012547	0.077851	-0.000351
1724	0.038472	-0.030021	-0.040829	-0.029501	0.079301	0.000520
1722	0.047459	-0.038205	-0.031921	-0.037559	0.079380	0.000646
1723	0.045856	-0.039783	-0.033525	-0.039141	0.079381	0.000642
1720	0.074778	0.015456	-0.005573	0.015247	0.080351	-0.000208
1721	0.081337	0.012094	0.000911	0.011937	0.080426	-0.000158

1719	0.087075	0.048821	0.005609	0.048046	0.081466	-0.000775
1718	0.086146	0.048413	0.004716	0.047637	0.081430	-0.000776
1716	0.046096	0.024644	-0.033642	0.024204	0.079738	-0.000440
1713	-0.010160	0.099469	-0.089469	0.096898	0.079310	-0.002572
1714	0.011848	0.096946	-0.067170	0.094651	0.079018	-0.002296
1715	0.011639	0.096524	-0.067389	0.094229	0.079028	-0.002295

2. Program (C) - Absolute Orientation and Polynomial Adjustment

2.1 General Information

Program identification	- ABTAN Absolute orientation and polynomial adjustment.
Type of Language	- Complete Algol program
Computer	- ICL 1906A of Nottingham and transferred to ICL 2980 Edinburgh.

2.2 Definition of Variables

MD	- Model number
BH	- Base to height ratio of the photography
IS	- Image scale number
BN	- Total number of points in the model
X	- Number of planimetric control points
Z	- Number of height control points
U	- Number of polynomial parameters for X or Y.
UH	- Number of polynomial parameters for Z.
TA	- Tag to indicate whether polynomial adjustment is to be applied or not.

ARRAYS

B	- Dynamic array containing the point number, the model coordinates and the ground coordinates.
PC, HC	- Arrays in which the plan and height data are stored.

R	-	Array containing the orthogonal rotation matrix.
A	-	Vector containing the absolute orientation elements.
P	-	Vector of the residuals of the transformed coordinates from the known values.
D	-	Array in which the observation equations are formed, in the absolute orientation phase.
D1	-	Working array to compute the approximate values for κ and λ.
T	-	Array containing the normal equations matrix.
DC, DH	-	Arrays including the observation equation matrices for the plan and height adjustments respectively.
TC, VC, V, DP, DR, P1, P2, P3	-	Working arrays
RS	-	Vector to determine the root mean square errors of the discrepancies.
PX, PY, PZ	-	Vectors to determine the polynomial parameters for X, Y and Z respectively.
C	-	Vector containing shifts Xo, Yo and Zo.

2.3 Detailed account of the program

A step-by-step account of the program is given as follows:

(i) Introduce the following matrix procedures to be used when computing the absolute orientation elements and the polynomial parameters:

Procedure MATVEC - Matrix x Vector

Procedure MATMLT - Matrix x Matrix

Procedure MATRAN - Matrix transpose

Procedure INVERT - Matrix inversion

(ii) Input of data

Declaration

Read in the model number (MD). If the last model is transformed, then MD = 0.

Read in the base to height ratio (BH) and the image scale number (IS) - these would be used when analysing the results.

Read in the number of points in the model (BN), the number of plan controls (X) and the number of height controls (Z).

Read in the number of polynomial parameters used in adjusting the X- or Y-coordinates (U).

Read in the number of polynomial parameters used in adjusting the Z-coordinates (UH).

Read in the tag (TA) to indicate whether polynomial adjustment is to be applied or not. If polynomial adjustment is to be applied then TA = 2; if not then TA, U and UH can be set to 1.

Declaration.

Read in the model coordinates and the ground coordinates of all the points in the model; these are read in array B as follows:-

Columns 1 and 2 - point number. The first column is composed of four digits. If the point is given in plan only the first digit should be 1. If it is given in plan and height then the first digit should be 2. And if it is given in height only the first digit should be 3. The three remaining digits are the point number which can be chosen from 0 to 999. The number in the second column should be 2 for any point used as control point. For check points, this will be 3.

Columns 3, 4 and 5 - x, y, z model coordinates.

Columns 6, 7 and 8 - X, Y, Z ground coordinates.

(N.B. If the point is given in plan only then column 8 will be read in as zero; if the point is given in height only, then columns 6 and 7 would be read in as zero.)

Store the plan control data in array PC and height control data in array HC.

(iii) Absolute orientation phase

Compute approximate scale factor (S) and approximate azimuth (KAP).

Compute approximate values for the translation elements - array C.

Compute approximate rotation matrix, IT = 0.

Form the observation equations in array D.

Form the vector of residuals of the transformed coordinates from the known values (P).

Solve the normal equations, deriving the corrections to the elements of transformation.

Compute the new elements of transformation.

Check whether corrections are significant; if any one of the corrections is greater than 0.00001 and the number of iterations is less than 7, the procedure is repeated; starting by forming new set of observation equations and adding one to IT.

Transform all the model coordinates using the computed elements of transformation.

Compute the residuals and the RMSE's.

(iv) Output of the results

Write text.

Print out the number of iterations.

Write text.

Print out the number of plan and height ground control used.

Print out the scale factor, the rotation matrix and the translation elements.

Write text.

Print out the transformed coordinates of all the points and their residuals.

Write text.

Print out the RMSE's of the discrepancies in the ground scale and in the image scale.

(v) Polynomial adjustment phase

Store the discrepancies of the plan controls in array PC.

Store the discrepancies of the height controls in array HC.

Form the observation equations for the plan corrections.

Compute the polynomial parameters for the plan adjustment.

Form the observation equations for the height corrections.

Compute the polynomial parameters for the height adjustment.

Apply the corrections to the transformed coordinates.

Determine the residuals of the adjusted coordinates and find the RMSE's.

(vi) Output of the results

Write text.

Print out the polynomial parameters for X, Y and Z.

Write text.

Print out the adjusted ground coordinates and their residuals from the known values.

Print out the RMSE's of the discrepancies.

2.4 Flow Diagram for Program (C)

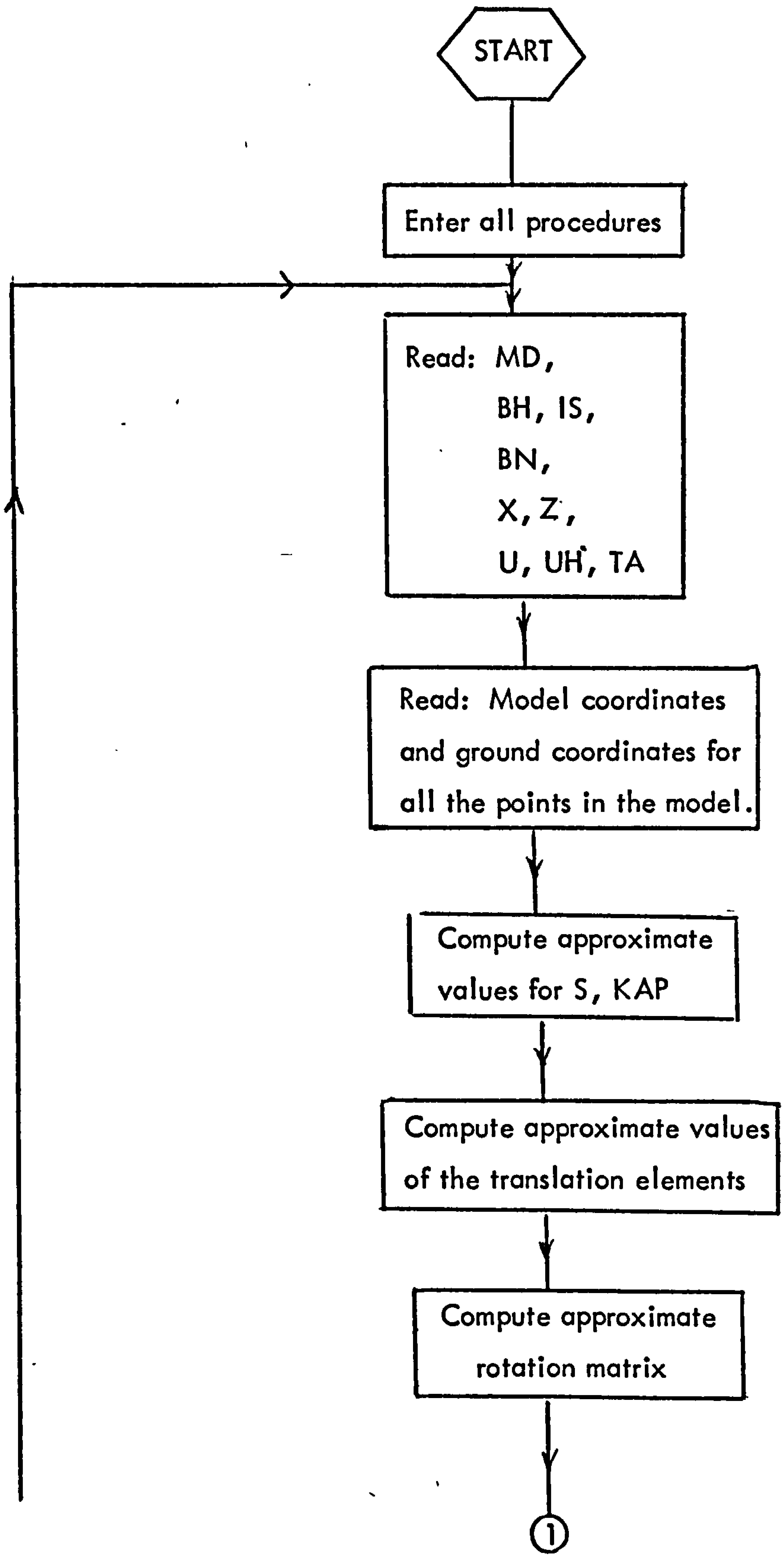

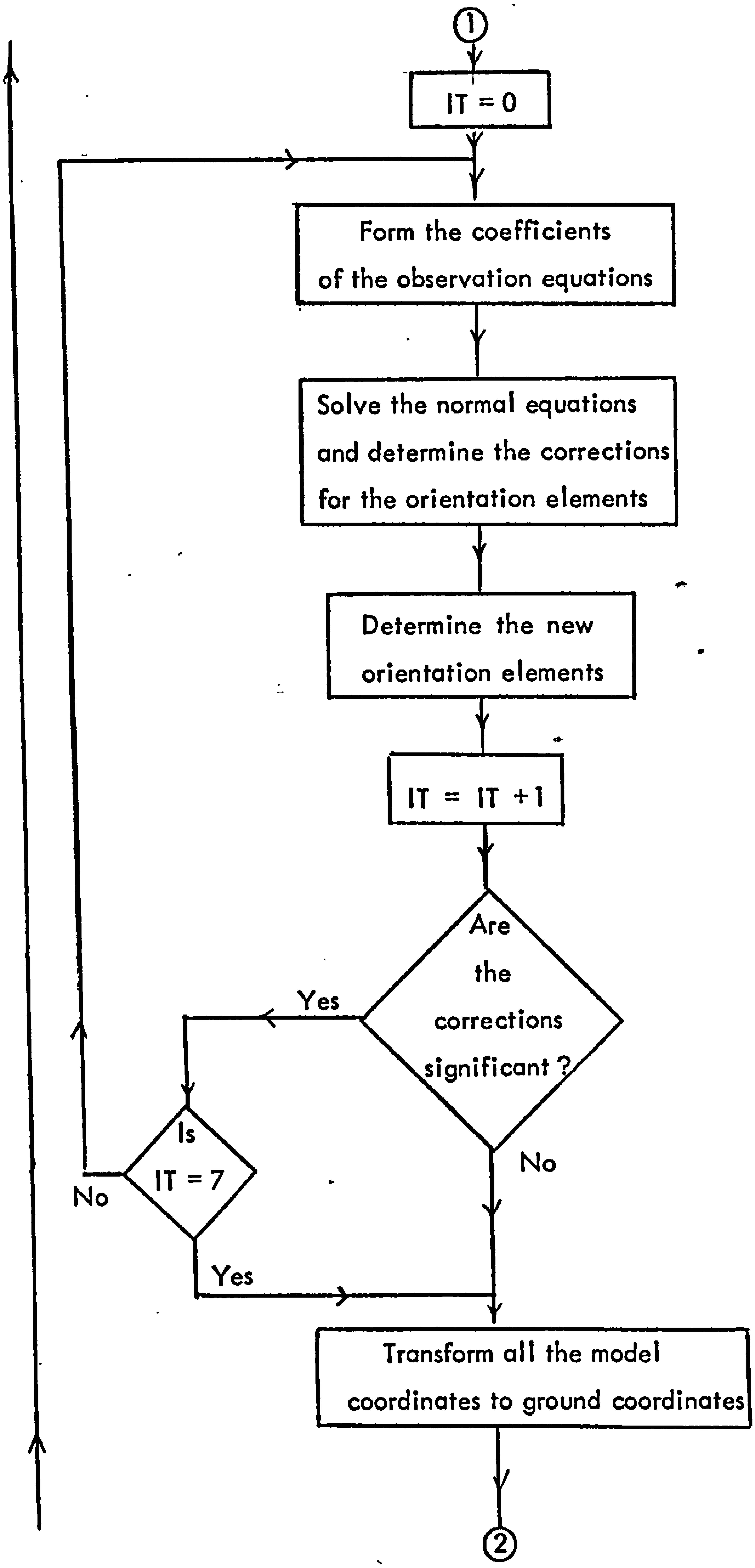
1
IT = 0
Form the coefficients of the observation equations
Solve the normal equations and determine the corrections for the orientation elements
Determine the new orientation elements
IT = IT + 1
Are the corrections significant ?
Yes
No
Is IT = 7
No
Yes
Transform all the model coordinates to ground coordinates
2

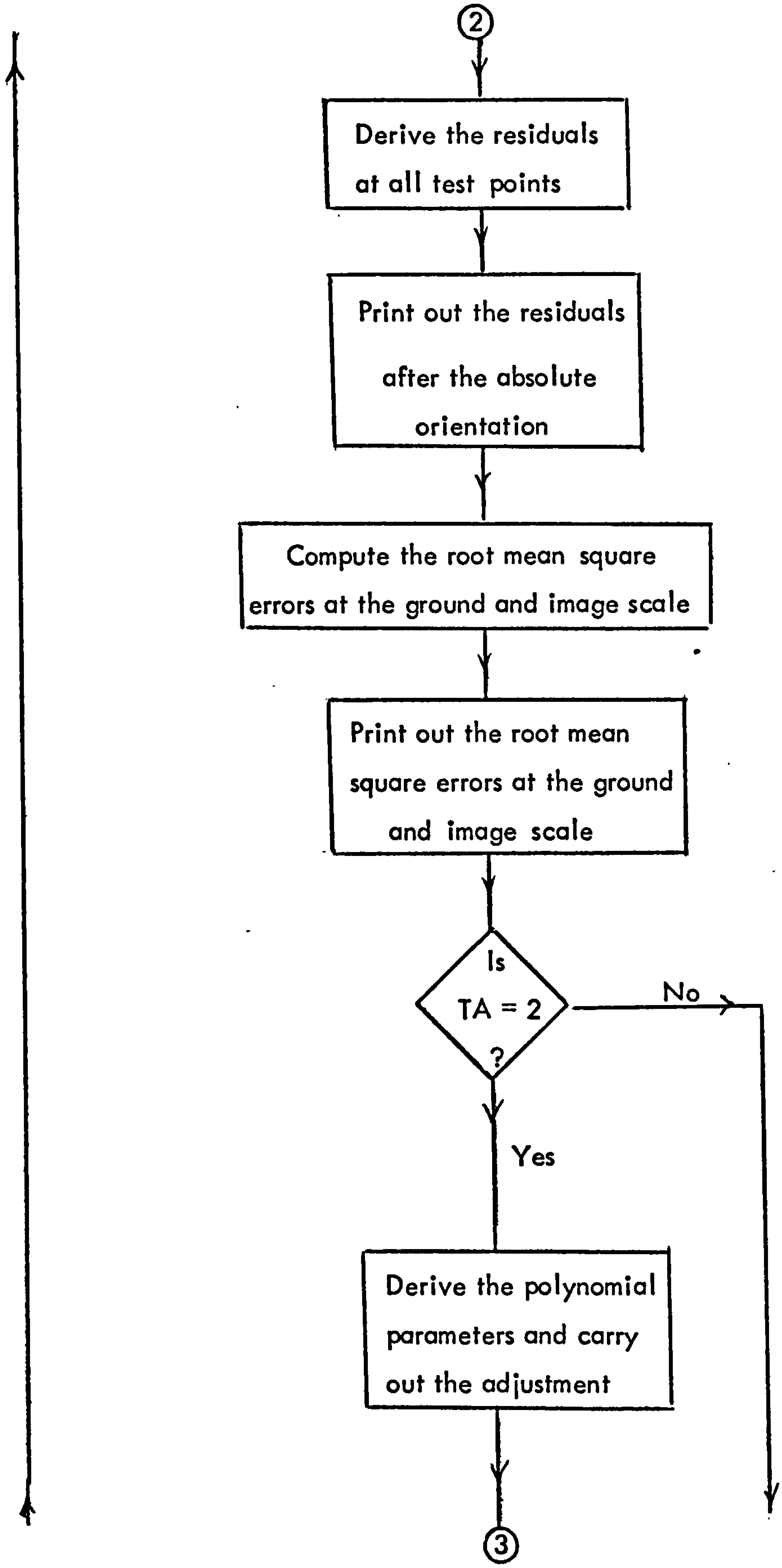
2
Derive the residuals at all test points
Print out the residuals after the absolute orientation
Compute the root mean square errors at the ground and image scale
Print out the root mean square errors at the ground and image scale
Is TA = 2 ?
No
Yes
Derive the polynomial parameters and carry out the adjustment
3

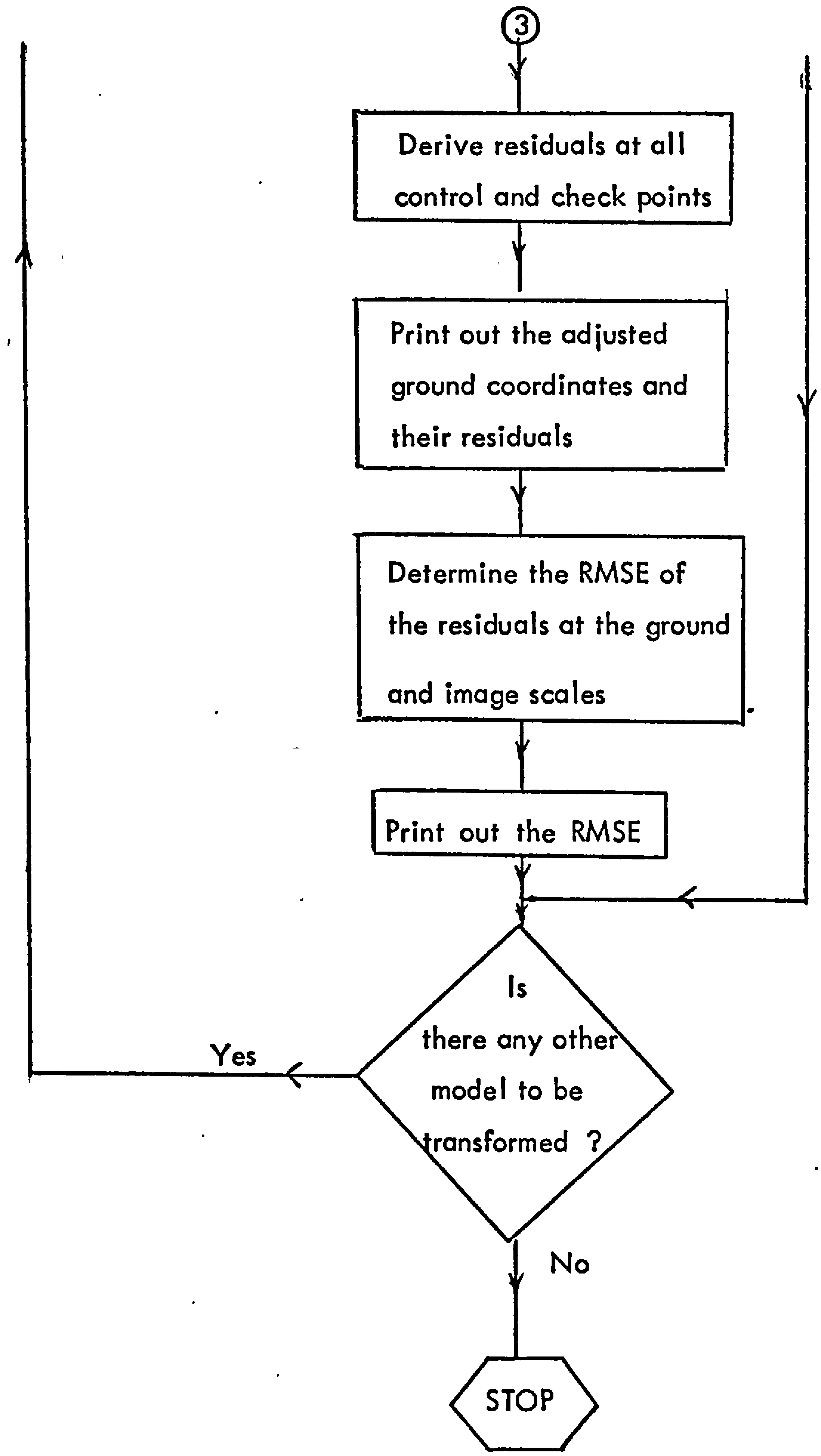
3
Derive residuals at all control and check points
Print out the adjusted ground coordinates and their residuals
Determine the RMSE of the residuals at the ground and image scales
Print out the RMSE
Is there any other model to be transformed ?
Yes
No
STOP

2.5 The Program

```
STMNT
  1      'BEGIN'
  2      'COMMENT' ABSOLUTE ORIENTATION PROGRAM;
  3
  3
  3      'INTEGER' Y,  G,  H;
  4      'PROCEDURE' MATVEC(A,X,Z,M,N);
  5      'VALUE' A,X,M,N;
  6      'INTEGER' M,N; 'ARRAY'A,X,Z;
  8      'BEGIN' 'INTEGER' I,J;
 10      'REAL' SUM;
 11      'FOR' I:=1 'STEP' 1 'UNTIL' N 'DO'
 11      'BEGIN' SUM:=0.0;
 13      'FOR' J:=1 'STEP' 1 'UNTIL' M 'DO'
 13      SUM:=SUM+A$I,J!*X$J!;
 14      Z$I!:=SUM;
 15      'END' 'END' MATVEC;
 17      'PROCEDURE' MATMLT(A,U,T,M,N,P);
 18      'VALUE' A,U,M,N,P;
 19      'INTEGER' M,N,P;
 20      'REAL' 'ARRAY' A,U,T;
 21      'BEGIN' 'INTEGER' I,J,K;
 23      'FOR' I:=1 'STEP' 1 'UNTIL' N 'DO'
 23      'FOR' J:=1 'STEP' 1 'UNTIL' M 'DO'
 23      'BEGIN'
 24      T$I,J!:=0.0;
 25      'FOR' K:=1 'STEP' 1 'UNTIL' P 'DO'
 25      T$I,J!:=T$I,J!+A$I,K!*U$K,J!;
 26      'END'
 26      'END' MATMLT;
 28      'PROCEDURE' MATRAN(A,AT,M,N);
 29      'VALUE' A,M,N;
 30      'ARRAY'A,AT;
 31      'INTEGER' M,N;
 32      'BEGIN'
 33      'INTEGER' I,J;
 34      'FOR' I:=1 'STEP' 1 'UNTIL' M 'DO'
 34      'FOR' J:=1 'STEP' 1 'UNTIL' N 'DO'
```

```
34   AT$I,J!:=A$J,I!;
35   'END' MATRAN;
36   'PROCEDURE' INVERT(A,N,INVA);
37   'VALUE' N;
38   'ARRAY' A,INVA;
39   'INTEGER' N;
40   'BEGIN'
41   'REAL' 'ARRAY' B$1:N,1:2*N!, X$1:N,1:N!;
42   'INTEGER' M,I,J,K;
43   'REAL' PIVOT, TT;
44   M:=2*N;
45   'FOR' I:=1 'STEP' 1 'UNTIL' N 'DO'
45   'BEGIN'
46   'FOR' J:=1 'STEP' 1 'UNTIL' N 'DO'
46   B$I,J!:=A$I,J!;
47   'FOR' J:=N+1 'STEP' 1 'UNTIL' M 'DO'
47   B$I,J!:= 'IF' I+N 'EQ' J 'THEN' 1 'ELSE' 0;
48   'END';
49   'FOR' I:=1 'STEP' 1 'UNTIL' N 'DO'
49   'BEGIN'
50   PIVOT:=B$I,I!;
51   'FOR' J:=I+1 'STEP' 1 'UNTIL' N 'DO'
51   'IF' ABS(PIVOT) 'LT' ABS(B$J,I!) 'THEN'
51   'BEGIN'
52   'FOR' K:=1 'STEP' 1 'UNTIL' M 'DO'
52   'BEGIN'
53   TT:=B$I,K!;
54   B$I,K!:=B$J,K!;
55   B$J,K!:=TT;
56   'END';
57   PIVOT:=B$J,I!;
58   'END';
59   'FOR' K:=M 'STEP' -1 'UNTIL' I 'DO'
59   B$I,K!:=B$I,K!/B$I,I!;
60   'FOR' J:=I+1 'STEP' 1 'UNTIL' N 'DO'
60   'FOR' K:=M 'STEP' -1 'UNTIL' I 'DO'
60   B$J,K!:=B$J,K!-B$I,K!*B$J,I!;
61   'END';
62   'FOR' J:=1 'STEP' 1 'UNTIL' N 'DO'
62   'BEGIN'
63   Y:=N+J;
64   X$N,J!:= B$N,Y!;
65   'END';
66   'FOR' I:=N-1 'STEP' -1 'UNTIL' 1 'DO'
66   'BEGIN'
67   'FOR' J:=1 'STEP' 1 'UNTIL' N 'DO'
67   'BEGIN'
68   G:=N+J;
69   X$I,J!:= B$I,G!;
70   'END';
71   'FOR' K:=N 'STEP' -1 'UNTIL' I+1 'DO'
71   'FOR' J:=1 'STEP' 1 'UNTIL' N 'DO'
71   X$I,J!:=X$I,J!-B$I,K!*X$K,J!;
72   'END';
73   'FOR' I:=1 'STEP' 1 'UNTIL' N 'DO'
73   'FOR' J:=1 'STEP' 1 'UNTIL' N 'DO'
73   INVA$I,J!:=X$I,J!;
74   'END'INVERT;
75
75
75   'REAL' KAP,  S,  IS,  BH,
75   K1,  K2,  K3,  K4;
76   'INTEGER' I, J, K, AN, MD,
76   X, Z, U, UH, BN, IT, TA;
77   'COMMENT'  READ MODEL NUMBER;
78   L1:MD:=READ;
```

```
 79   'IF' MD=0 'THEN' 'GOTO' L20;
 80   'COMMENT'  READ IN  :
 80     BH --- BASE TO HEIGHT RATIO
 80     IS --- THE IMAGE SCALE NUMBER,
 80     BN --- NUMBER OF POINTS IN THE MODEL,
 80     X  --- NUMBEP OF PLAN. CONTROLS,
 80     Z  --- NUMBER OF HEIGHT CONTROLS;
 81   BH:=READ;
 82   IS:=READ;
 83   BN:=READ;
 84   X:=READ;
 85   Z:=READ;
 86
 86   'COMMENT'  U  AND  UH  ARE THE NUMBER OF  UNKNOWN
 86          POLYN. PARAMETERS  FOR  PLAN. AND HEIGHT
 86         ADJUSTMENTS RESPECTIVELY.   THESE CAN BE  ANY
 86         INTEGERS IF NO ADJUSTMENT IS REQUIRED.  ;
 87   U:=READ;
 88   UH:=READ;
 89
 89   'COMMENT'   IF ABSOLUTE ORIENTATION ONLY IS REQUIRED
 89         THEN SET  TA  TO 1.  IF POLYN. ADJUSTMENT IS
 89          REQUIRED THEN SET TA  TO 2;
 90   TA:=READ;
 91   AN:=2*X+Z;
 92   'BEGIN'
 93   'REAL' 'ARRAY' B$1:BN,1:20!,  D1$1:2,1:4!,
 93   PC$1:X,1:14!,  HC$1:Z,1:14!,  A$1:7!,
 93   T$1:7,1:7!,  C$1:1,1:3!,
 93   D$1:AN,1:7!, DT$1:7,1:AN!,  V$1:7,1:7!,
 93   P$1:AN!, DP$1:AN!,R$1:3,1:3!, RS$1:9!,
 93   DR$1:3,1:3!;
 94   'FOR' I:=1 'STEP' 1 'UNTIL' BN 'DO'
 94   'FOR' J:=1 'STEP' 1 'UNTIL' 20 'DO'
 94    B$I,J!:=0.00;
 95   'FOR' I:=1 'STEP' 1 'UNTIL' X 'DO'
 95   'FOR' J:=1 'STEP' 1 'UNTIL' 14 'DO'
 95   PC$I,J!:=0.00;
 96   'FOR' I:=1 'STEP' 1 'UNTIL' Z 'DO'
 96   'FOR' J:=1 'STEP' 1 'UNTIL' 14 'DO'
 96   HC$I,J!:=0.00;
 97   'FOR' I:=1 'STEP' 1 'UNTIL' 3 'DO'
 97   'FOR' J:=1,2,3 'DO'
 97   R$I,J!:=0.00;
 98
 98
 98   'COMMENT' READ IN THE MODEL COORDINATES
 98   AND THE GROUND COORDINATES OF ALL THE POINTS;
 99   'FOR' I:=1 'STEP' 1 'UNTIL' BN 'DO'
 99   'FOR' J:=1,2,3,4,5,6,7,8 'DO'
 99   B$I,J!:=READ;
100
100   'COMMENT' STORE THE PLAN. CONTROLS IN ARRAY PC;
101   K:=0;
102     'FOR' I:=1 'STEP' 1 'UNTIL' BN 'DO'
102   'IF' B$I,1! 'LE' 2999 'AND' B$I,2!=2 'THEN'
102   'BEGIN'
103   K:=K+1;
104       'FOR' J:=1 'STEP' 1 'UNTIL' 8 'DO'
104   PC$K,J!:=B$I,J!;
105   'END';
106
106   'COMMENT' STORE THE HEIGHT CONTROLS IN ARRAY HC;
107   K:=0;
108      'FOR' I:=1 'STEP' 1 'UNTIL' BN 'DO'
108   'IF' B$I,1!>1999 'AND' B$I,2!=2 'THEN'
```

```
'BEGIN'
K:=K+1;
  'FOR' J:=1 'STEP' 1 'UNTIL' 8 'DO'
HC$K,J!:=B$I,J!;
'END';



'FOR' I:=1,2,3 'DO'
C$1,I!:=0.00;


'COMMENT' APPROXIMATE SCALE FACTOR;
'FOR' I:=1,2 'DO'
'FOR' J:=1,2,3,4 'DO'
D1$I,J!:=0.00;
'FOR' I:=1,2 'DO'
'BEGIN'
G:=I+2;   Y:=I+5;
D1$1,I!:=PC$1,G!-PC$2,G!;
D1$2,I!:=PC$1,Y!-PC$2,Y!;
 'END';
D1$2,3!:=D1$1,1!*D1$1,1!+D1$1,2!*D1$1,2!;
D1$2,4!:=D1$2,1!*D1$2,1!+D1$2,2!*D1$2,2!;
K1:=D1$1,2!;    K2:=D1$1,1!;
K1:=K1/K2;
K3:=D1$2,2!;   K4:=D1$2,1!;
K3:=K3/K4;
KAP:=ARCTAN(K1)-ARCTAN(K3);
K1:=D1$2,4!;   K2:=D1$2,3!;
K3:=K1/K2;
S:=ABS(SQRT(K3));


'COMMENT' APPRO. VALUES FOR THE TRANSLATION ELEMENTS;
C$1,1!:=PC$1,6!-S*(PC$1,3!*COS(KAP)+PC$1,4!*SIN(KAP));
C$1,2!:=PC$1,7!-S*(PC$1,3!*SIN(KAP)+PC$1,4!*COS(KAP));
C$1,3!:=HC$1,8!-S*HC$1,5!;


'COMMENT' APPROXIMATE ROTATION MATRIX;
R$1,1!:=COS(KAP);  R$1,2!:=SIN(KAP);
R$2,2!:=COS(KAP);  R$2,1!:=-SIN(KAP);
R$3,3!:=1.00;

IT:=0;
L2: 'FOR' I:=1 'STEP' 1 'UNTIL' AN 'DO'
'FOR' J:=1 'STEP' 1 'UNTIL' 7 'DO'
'BEGIN'
D$I,J!:=0.00;
DT$J,I!:=0.00;
'END';
DR$1,1!:=0.0;  DR$1,2!:=0.0;  DR$1,3!:=0.0;
DR$2,1!:=0.0;  DR$2,2!:=0.0;  DR$2,3!:=0.0;
DR$3,1!:=0.0;  DR$3,2!:=0.0;  DR$3,3!:=0.0;


'COMMENT'  OBSERVATION  EQUATIONS;
'FOR' I:=1 'STEP' 1 'UNTIL' X 'DO'
'BEGIN'
Y:=I+X;
D$I,2!:=-S*(R$3,1!*PC$I,3!+R$3,2!*PC$I,4!+
      R$3,3!*PC$I,5!)-C$1,3!;
D$I,3!:= S*(R$2,1!*PC$I,3!+R$2,2!*PC$I,4!+
     R$3,2!*PC$I,5!)+C$1,2!;
D$I,4!:=  R$1,1!*PC$I,3!+R$1,2!*PC$I,4!+R$1,3!*PC$I,5!;
```

```
164   D$I,5!:= 1.00;
165   P$I!:=PC$I,6!-S*(R$1,1!*PC$I,3!+R$1,2!*PC$I,4!+
165   R$1,3!*PC$I,5!)-C$1,1!;
166   D$Y,1!:=-D$I,2!;
167   D$Y,3!:=-S*(R$1,1!*PC$I,3!+R$1,2!*PC$I,4!+
167        R$1,3!*PC$I,5!)-C$1,1!;
168   D$Y,4!:=R$2,1!*PC$I,3!+R$2,2!*PC$I,4!+R$2,3!*PC$I,5!;
169   D$Y,6!:=1.00;
170   P$Y!:=PC$I,7!-S*(R$2,1!*PC$I,3!+R$2,2!*PC$I,4!+
170        R$2,3!*PC$I,5!)-C$1,2!;
171   'END';
172   'FOR' I:=1 'STEP' 1 'UNTIL' Z 'DO'
172   'BEGIN'
173   G:=I+2*X;
174   D$G,1!:=-S*(R$2,1!*HC$I,3!+R$2,2!*HC$I,4!+R$2,3!*
174   HC$I,5!)-C$1,2!;
175   D$G,2!:= S*(R$1,1!*HC$I,3!+R$1,2!*HC$I,4!+R$1,3!*
175   HC$I,5!)+C$1,1!;
176   D$G,4!:=R$3,1!*HC$I,3!+R$3,2!*HC$I,4!+R$3,3!*HC$I,5!;
177   D$G,7!:=1.00;
178   P$G!:=HC$I,8!-S*(R$3,1!*HC$I,3!+R$3,2!*HC$I,4!+
178   R$3,3!*HC$I,5!)-C$1,3!;
179   'END';
180   MATRAN(D,DT,7,AN);
181   MATMLT(DT,D,T,7,7,AN);
182   INVERT(T,7,V);
183   MATVEC(DT,P,DP,AN,7);
184   MATVEC(V,DP,A,7,7);
185   S:=S+A$4!;
186   'FOR' I:=1,2,3 'DO'
186   'BEGIN'
187   J:=I+4;
188   C$1,I!:= C$1,I!+A$J!;
189   'END';
190   DR$1,1!:=1.0;  DR$2,2!:=1.0;
192           DR$3,3!:=1.0;
193   DR$1,2!:=A$3!;  DR$1,3!:=-A$2!;
195   DR$2,1!:=-A$3!;  DR$2,3!:=A$1!;
197   DR$3,1!:=A$2!;  DR$3,2!:=-A$1!;
199
199
199   'COMMENT' COMPUTE NEW ROTATION MATRIX;
200   MATMLT(DR,R,R,3,3,3);
201
201
201   'COMMENT' CHECK WHETHER CORRECTIONS ARE SIGNIFICANT;
202   'IF' ABS(A$1!) 'LT' 0.00001 'AND' ABS(A$2!) 'LT' 0.00001
202   'AND' ABS(A$3!) 'LT' 0.00001 'AND' ABS(A$5!) 'LT' 0.00001
202   'AND' ABS(A$6!) 'LT' 0.00001 'AND' ABS(A$7!) 'LT' 0.00001
202   'AND' ABS(A$4!)  'LT'  0.00001
202   'THEN' 'GOTO' L3;
203   'IF' IT=7 'THEN'  'GOTO' L3;
204   IT:=IT+1;   'GOTO' L2;
206   L3: 'FOR' I:=1 'STEP' 1 'UNTIL' BN 'DO'
206   'BEGIN'
207   'FOR' J:=1,2,3 'DO'
207   'BEGIN'
208   Y:=J+8;
209   B$I,Y!:=S*(R$J,1!*B$I,3!+R$J,2!*B$I,4!+
209   R$J,3!*B$I,5!)+C$1,J!;
210   'END';
211   'END';
212   'COMMENT' COMPUTE THE DESCREPANCIES;
213   'FOR' I:=1 'STEP' 1 'UNTIL' BN 'DO'
213   'BEGIN'
214   'FOR' J:=1,2,3 'DO'
```

```
'BEGIN'
Y:=J+8;   G:=J+5;   H:=J+11;
B$I,H!:=B$I,Y!-B$I,G!;
'END';    'END';

WRITE TEXT('('('('P')'I.M.ELHASSAN%%%%

GEOGRAPHY %% DEPARTMENT'('4C')'

MODEL %% NUMBER '('2S')'!)');

PRINT(MD,5,0);


IT:=IT-1;
WRITE TEXT('('('('2C')'NUMBER%OF%ITERATIONS'('2S')'')');
PRINT(IT,1,0);
NEWLINES(2);
WRITE TEXT('('('('2C')'NUMBER%OF%PLAN.%CONTROLS'('2S')'
PRINT(X,2,0);
WRITE TEXT('('('('2C')'NUMBER%OF%HEIGHT%CONTROLS'('2S')
PRINT(Z,2,0);

WRITE TEXT('('('('2C')'SCALE %% FACTOR'('2S')'')');
PRINT(S,0,5);
WRITE TEXT('('('('4C')'ROTATION%MATRIX'('2C')'')');
'FOR' I:=1 'STEP' 1 'UNTIL' 3 'DO'
'BEGIN'
'FOR' J:=1,2,3 'DO'
'BEGIN'
PRINT(R$I,J!,0,5);
SPACES(4);
'END';
NEWLINES(2);
'END';
WRITE TEXT('('TRANSLATIONAL %% ELEMENTS'('2C')'')');
'FOR' I:=1,2,3 'DO'
'BEGIN'
PRINT(C$1,I!,0,6);
NEWLINE;
'END';
WRITE TEXT('('('('4C')''('20S')'GROUND %% COORDINATES

 %% AFTER %% ABSOLUTE %% ORIENTATION

'('2C')'PT.NO.'('15S')'E'('15S')'N'('15S')'

H'('11S')'DE'('10S')'DN'('10S')'DH'('2C')'')');

'FOR' I:=1 'STEP' 1 'UNTIL' BN 'DO'
'BEGIN'
PRINT(B$I,1!,4,0);
SPACES(2);
PRINT(B$I,2!,1,0);
SPACES(4);
'FOR' J:=9,10,11 'DO'
'BEGIN'
PRINT(B$I,J!,7,3);
SPACES(4);
'END';
'IF' B$I,1!'LT' 1999 'THEN'  'BEGIN'
'FOR' J:=12,13 'DO'
'BEGIN'
PRINT(B$I,J!,3,3);
SPACES(4);
'END';
```

```
261    SPACES(3);
262    WRITE TEXT('('--------')');
263    'GOTO' L10A;
264    'END';
265    'IF' B$I,1!'LT' 2999 'THEN'  'BEGIN'
266    'FOR' J:=12,13,14 'DO'
266    'BEGIN'
267    PRINT(B$I,J!,3,3);
268    SPACES(4);
269    'END';
270    'GOTO' L10A;
271    'END';
272    'IF' B$I,1!'LT' 3999 'THEN' 'BEGIN'
273    SPACES(3);
274    WRITE TEXT('('--------'('5S')'--------'('4S')'')');
275    PRINT(B$I,14!,3,3);
276    'GOTO' L10A;
277    'END';
278    L10A:NEWLINES(2);
279    'END';
280
280
280    'COMMENT'  PLAN. ACCURACY;
281    'FOR' J:=1 'STEP' 1 'UNTIL' 9 'DO'
281    RS$J!:=0.00;
282    K:=0;
283    'FOR' I:=1 'STEP' 1 'UNTIL' BN 'DO'
283    'IF' B$I,1! 'LT' 2999 'THEN'
283    'BEGIN'
284    K:=K+1;
285    'FOR' J:=1,2 'DO'
285    'BEGIN'
286    H:=J+11;
287    RS$J!:=RS$J!+B$I,H!'**'2;
288    'END';
289    'END';
290    'FOR' J:=1,2 'DO'
290    'BEGIN'
291    G:=J+3;
292    RS$G!:=SQRT(RS$J!/K);
293    'END';
294
294
294    'COMMENT' HEIGHT ACCRACY;
295    K:=0;
296    'FOR' I:=1 'STEP' 1 'UNTIL' BN 'DO'
296    'IF' B$I,1! > 1999 'THEN'  'BEGIN'
297    K:=K+1;
298    RS$3!:=RS$3!+B$I,14!'**'2;
299    'END';
300    RS$6!:=SQRT(RS$3!/K);
301    K4:=1/IS;
302    'FOR' J:=4,5 'DO'
302    'BEGIN'
303    Y:=J+3;
304    RS$Y!:=RS$J!*K4*10.0'**'6;
305    'END';
306    RS$9!:=RS$6!*BH*K4*10.0'**'6;
307    NEWLINES(2);
308    WRITE TEXT('('''('2C')'THE%ROOT%MEAN%SQUARE%ERRORS%
308
308    OF % THE % DESCREPANCIES '('C')'AT % THE %
308
308    GROUND % SCALE % IN % METERS'('2C')'
308
308    RMSE E'('10S')'RMSE N'('8S')'RMSE H'('2C')'')');
```

```
309   'FOR' I:=4,5,6 'DO'
309   'BEGIN'
310   PRINT(RS$I!,3,3);
311   SPACES(4);
312   'END';
313   WRITE TEXT('('('2C')'THE%ROOT%MEAN%SQUARE%ERRORS%

      OF % THE % DESCREPANCIES '('C')'AT % THE %

      IMAGE % SCALE % IN % MICRONS'('2C')'

      RMSE E'('10S')'RMSE N'('8S')'RMSE H'('2C')'')');
314   'FOR' I:=7,8,9 'DO'
314   'BEGIN'
315   PRINT(RS$I!,3,0);
316   SPACES(10);
317   'END';
318   NEWLINE;



319   'COMMENT' POLYNOMIAL CORRECTION;
320   'IF' TA=2 'THEN' 'BEGIN'
321   'REAL' 'ARRAY'   PZ$1:UH!,
      P1$1:X!, P2$1:X!, P3$1:Z!, PX$1:U!, PY$1:U!,
      DC$1:X,1:U!, DTC$1:U,1:X!,
      TC$1:U,1:U!, VC$1:U,1:U!, DH$1:Z,1:UH!, DHT$1:UH,1:Z!,
      TH$1:UH,1:UH!,  VH$1:UH,1:UH!;

322   'COMMENT' STORE THE DESCREPANCIES OF THE
      PLAN. CONTROLS IN ARRAY  PC;
323   K:=0;
324   'FOR' I:=1 'STEP' 1 'UNTIL' BN 'DO'
324   'IF' B$I,1! 'LE' 2999 'AND' B$I,2!=2 'THEN' 'BEGIN'
325   K:=K+1;
326   'FOR' J:=9 'STEP' 1 'UNTIL' 14 'DO'
326   PC$K,J!:=B$I,J!;
327   'END';
328   'FOR' I:=1 'STEP' 1 'UNTIL' X 'DO'
328   'BEGIN'
329   P1$I!:=PC$I,12!;
330   P2$I!:=PC$I,13!;
331   'END';

332   'COMMENT' STORE THE DESCREPANCIES OF THE
      HEIGHT CONTROLS IN ARRAY HC;
333   K:=0;
334   'FOR' I:=1 'STEP' 1 'UNTIL' BN 'DO'
334   'IF' B$I,1!>1999 'AND' B$I,2!=2 'THEN' 'BEGIN'
335   K:=K+1;
336   'FOR' J:=9 'STEP' 1 'UNTIL' 14 'DO'
336   HC$K,J!:=B$I,J!;
337   'END';
338   'FOR' I:=1 'STEP' 1 'UNTIL' Z 'DO'
338   P3$I!:=HC$I,14!;

339   'COMMENT' START THE ADJUSTMENT WITH 4 POLYN.
      PARAMETERS -- AND ADD THE REMAINING 5 ONE BY ONE;
340   'FOR' I:=1 'STEP' 1 'UNTIL' X 'DO'
340   'BEGIN'
341   DC$I,1!:=1.00;
342   DC$I,2!:=PC$I,9!;
343   DC$I,3!:=PC$I,10!;
344   DC$I,4!:=PC$I,9!*PC$I,10!;
345   'END';
346   'IF' U>4 'THEN'  'BEGIN'
```

```
347   'FOR' I:=1 'STEP' 1 'UNTIL' X 'DO'
347   DC$I,5!:=PC$I,9!'**'2;
348   'END';
349   'IF' U>5 'THEN'  'BEGIN'
350   'FOR' I:=1 'STEP' 1 'UNTIL' X 'DO'
350   DC$I,6!:=PC$I,10!'**'2;
351   'END';
352   'IF' U>6 'THEN'  'BEGIN'
353   'FOR' I:=1 'STEP' 1 'UNTIL' X 'DO'
353   DC$I,7!:=DC$I,5!*PC$I,10!;
354   'END';
355   'IF' U>7 'THEN'  'BEGIN'
356   'FOR' I:=1 'STEP' 1 'UNTIL' X 'DO'
356   DC$I,8!:=DC$I,6!*PC$I,9!;
357   'END';
358   'IF' U>8 'THEN' 'BEGIN'
359   'FOR' I:=1 'STEP' 1 'UNTIL' X 'DO'
359   DC$I,9!:=DC$I,5!*DC$I,6!;
360   'END';
361   'FOR' I:=1 'STEP' 1 'UNTIL' U 'DO'
361   'FOR' J:=1 'STEP' 1 'UNTIL' U 'DO'
361   'BEGIN'   TC$I,J!:=VC$I,J!:=0.000;  'END';
364   'FOR' I:=1 'STEP' 1 'UNTIL' U 'DO'
364   'BEGIN'
365   PX$I!:=0.00;   PY$I!:=0.00;
367   'END';
368   'FOR' I:=1 'STEP' 1 'UNTIL' UH 'DO'
368   PZ$I!:=0.00;
369   'IF' U=X 'THEN'  'BEGIN'
370   INVERT(DC,U,VC);
371   MATVEC(VC,P1,PX,U,U);
372   MATVEC(VC,P2,PY,U,U);
373   'GOTO' L9;
374   'END';
375
375   'COMMENT' SOLUTION BY LEAST SQ. METHOD;
376   MATRAN(DC,DTC,U,X);
377   MATMLT(DTC,DC,TC,U,U,X);
378   INVERT(TC,U,VC);
379   MATVEC(DTC,P1,P1,X,U);
380   MATVEC(DTC,P2,P2,X,U);
381   MATVEC(VC,P1,PX,U,U);
382   MATVEC(VC,P2,PY,U,U);
383   L9:'FOR' I:=1 'STEP' 1 'UNTIL' Z 'DO'
383   'BEGIN'
384   DH$I,1!:=1.00;
385   DH$I,2!:=HC$I,9!;
386   DH$I,3!:=HC$I,10!;
387   DH$I,4!:=HC$I,9!*HC$I,10!;
388   'END';
389   'IF' UH>4  'THEN'  'BEGIN'
390   'FOR' I:=1 'STEP' 1 'UNTIL' Z 'DO'
390   DH$I,5!:=HC$I,9!'**'2;
391   'END';
392   'IF' UH>5  'THEN'  'BEGIN'
393   'FOR' I:=1 'STEP' 1 'UNTIL' Z 'DO'
393   DH$I,6!:=HC$I,10!'**'2;
394   'END';
395   'IF' UH>6  'THEN'  'BEGIN'
396   'FOR' I:=1  'STEP' 1 'UNTIL' Z 'DO'
396   DH$I,7!:=DH$I,5!*HC$I,10!;
397   'END';
398   'IF' UH>7  'THEN'  'BEGIN'
399   'FOR' I:=1 'STEP' 1 'UNTIL' Z 'DO'
399   DH$I,8!:=DH$I,6!*HC$I,9!;
400   'END';
```

```
'IF' UH>8 'THEN' 'BEGIN'
'FOR' I:=1 'STEP' 1 'UNTIL' Z 'DO'
DH$I,9!:=DH$I,5!*DH$I,6!;
'END';
'FOR' I:=1 'STEP' 1 'UNTIL' UH 'DO'
'FOR' J:=1 'STEP' 1 'UNTIL' UH 'DO'
'BEGIN'  TH$I,J!:=VH$I,J!:=0.000;  'END';
'IF' UH=Z 'THEN'  'BEGIN'
INVERT(DH,UH,VH);
MATVEC(VH,P3,PZ,UH,UH);
'GOTO' L10;   'END';
MATRAN(DH,DHT,UH,Z);
MATMLT(DHT,DH,TH,UH,UH,Z);
INVERT(TH,UH,VH);
MATVEC(DHT,P3,P3,Z,UH);
MATVEC(VH,P3,PZ,UH,UH);
L10:WRITE TEXT('(''('P')'POLYNOM.%PARAMETERS%
FOR%%PLAN%CORRECTION'('2C')'')');
WRITE TEXT('('PARAMETERS%FOR%X'('2C')'')');
'FOR' I:=1 'STEP' 1 'UNTIL' U 'DO'
'BEGIN'
PRINT(PX$I!,0,5);
NEWLINE;
'END';
NEWLINES(2);
WRITE TEXT('('PARAMETERS%FOR%Y'('2C')'')');
'FOR' I:=1 'STEP' 1 'UNTIL' U 'DO'
'BEGIN'
PRINT(PY$I!,0,5);
NEWLINE;
'END';
WRITE TEXT('(''('4C')'POLYNOM.%PARAMETERS%FOR%HEIGHT%
CORRECTION'('2C')'')');
'FOR' I:=1 'STEP' 1 'UNTIL' UH 'DO'
'BEGIN'
PRINT(PZ$I!,0,5);
NEWLINE;
'END';
NEWLINES(2);
'COMMENT'  ADD THE CORRECTIONS TO THE
COMPUTED GROUND  COORDINATES;
'FOR' I:=1 'STEP' 1 'UNTIL' BN 'DO'
'BEGIN'
B$I,15!:=B$I,9!-(PX$1!+PX$2!*B$I,9!+PX$3!*B$I,10!+
     PX$4!*B$I,9!*B$I,10!);
B$I,16!:=B$I,10!-(PY$1!+PY$2!*B$I,9!+PY$3!*B$I,10!+
     PY$4!*B$I,9!*B$I,10!);
B$I,17!:=B$I,11!-(PZ$1!+PZ$2!*B$I,9!+PZ$3!*B$I,10!+
     PZ$4!*B$I,9!*B$I,10!);
'END';
'IF' U>4  'THEN'  'BEGIN'
'FOR' I:=1 'STEP' 1 'UNTIL' BN 'DO'
'BEGIN'
B$I,15!:=B$I,15!-PX$5!*B$I,9!'**'2;
B$I,16!:=B$I,16!-PY$5!*B$I,9!'**'2;
'END';      'END';
'IF' UH>4 'THEN'  'BEGIN'
'FOR' I:=1 'STEP' 1 'UNTIL' BN 'DO'
'BEGIN'
B$I,17!:=B$I,17!-PZ$5!*B$I,9!'**'2;
'END';      'END';
```

```
452   'IF' U>5 'THEN'   'BEGIN'
453   'FOR' I:=1 'STEP' 1 'UNTIL' BN 'DO'
453   'BEGIN'
454   B$I,15!:=B$I,15!-PX$6!*B$I,10!'**'2;
455   B$I,16!:=B$I,16!-PY$6!*B$I,10!'**'2;
456   'END';     'END';
458   'IF' UH>5  'THEN'   'BEGIN'
459   'FOR' I:=1 'STEP' 1 'UNTIL' BN 'DO'
459   B$I,17!:=B$I,17!-PZ$6!*B$I,10!'**'2;
460   'END';
461   'IF' U>6 'THEN'  'BEGIN'
462   'FOR' I:=1 'STEP' 1 'UNTIL' BN 'DO'
462   'BEGIN'
463   B$I,15!:=B$I,15!-PX$7!*B$I,10!*B$I,9!'**'2;
464   B$I,16!:=B$I,16!-PY$7!*B$I,10!*B$I,9!'**'2;
465   'END';    'END';
467   'IF' UH>6  'THEN'   'BEGIN'
468   'FOR' I:=1 'STEP' 1 'UNTIL' BN 'DO'
468   B$I,17!:=B$I,17!-PZ$7!*B$I,10!*B$I,9!'**'2;
469   'END';
470   'IF' U>7 'THEN' 'BEGIN'
471   'FOR' I:=1 'STEP' 1 'UNTIL' BN 'DO'
471   'BEGIN'
472   B$I,15!:=B$I,15!-PX$8!*B$I,9!*B$I,10!'**'2;
473   B$I,16!:=B$I,16!-PY$8!*B$I,9!*B$I,10!'**'2;
474   'END';    'END';
476   'IF' UH>7  'THEN'  'BEGIN'
477   'FOR' I:=1 'STEP' 1 'UNTIL' BN 'DO'
477   B$I,17!:=B$I,17!-PZ$8!*B$I,9!*B$I,10!'**'2;
478   'END';
479   'IF' U>8 'THEN' 'BEGIN'
480   'FOR' I:=1 'STEP' 1 'UNTIL' BN 'DO'
480   'BEGIN'
481   B$I,15!:=B$I,15!-PX$9!*B$I,9!*B$I,9!*B$I,10!'**'2;
482   B$I,16!:=B$I,16!-PY$9!*B$I,9!*B$I,9!*B$I,10!'**'2;
483   'END';    'END';
485   'IF' UH>8 'THEN'  'BEGIN'
486   'FOR' I:=1 'STEP' 1 'UNTIL' BN 'DO'
486   B$I,17!:=B$I,17!-PZ$9!*B$I,9!*B$I,9!*B$I,10!'**'2;
487   'END';
488   'FOR' I:=1 'STEP' 1 'UNTIL' BN 'DO'
488   'BEGIN'
489   'FOR' J:=6,7,8  'DO'
489   'BEGIN'
490   H:=J+9;  G:=J+12;
492   B$I,G!:=B$I,H!-B$I,J!;
493   'END';   'END';
495   WRITE TEXT('('('P')''('20S')'GROUND % COORDINATES %
495
495   AFTER % POLYN. % ADJUSTMENT'('2C')'
495
495   PT.NO.'('15S')' E'('15S')' N'('15S')'
495
495   H'('11S')'DE'('10S')'DN'('10S')'DH'('2C')'')');
496   'FOR' I:=1 'STEP' 1 'UNTIL' BN 'DO'
496   'BEGIN'
497   PRINT(B$I,1!,4,0);
498   SPACES(2);
499   PRINT(B$I,2!,1,0);
500   SPACES(4);
501   'FOR' J:=15,16,17 'DO'
501   'BEGIN'
502   PRINT(B$I,J!,7,3);
503   SPACES(4);
504   'END';
505   'IF' B$I,1!'LT' 1999'THEN'   'BEGIN'
```

```
506   'FOR' J:=18,19  'DO'
506   'BEGIN'
507   PRINT(B$I,J!,3,3);
508   SPACES(4);
509   'END';
510   SPACES(3);
511   WRITE TEXT('('--------')');
512   'GOTO' L11;
513   'END';
514   'IF' B$I,1!  'LT'  2999  'THEN'  'BEGIN'
515   'FOR' J:=18,19,20 'DO'
515   'BEGIN'
516   PRINT(B$I,J!,3,3);
517   SPACES(4);
518   'END';
519   'GOTO' L11;
520   'END';
521   'IF' B$I,1!  'LT' 3999  'THEN'  'BEGIN'
522   SPACES(3);
523   WRITE TEXT('('--------'('5S')'--------'('4S')'')');
524   PRINT(B$I,20!,3,3);
525   'GOTO' L11;
526   'END';
527   L11:NEWLINES(2);
528   'END';
529
529   'COMMENT' COMPUTE THE ROOT MEAN SQ. ERRORS;
530   'FOR' J:=1 'STEP' 1 'UNTIL' 9 'DO'
530   RS$J!:=0.00;
531   K:=0;
532   'FOR' I:=1 'STEP' 1 'UNTIL' BN 'DO'
532   'IF' B$I,1! 'LT' 2999 'THEN'
532   'BEGIN'
533   K:=K+1;
534   'FOR' J:=1,2 'DO'
534   'BEGIN'
535   Y:=J+17;
536   RS$J!:=RS$J!+B$I,Y!'**'2;
537   'END';
538   'END';
539   'FOR' J:=1,2 'DO'
539   'BEGIN'
540   H:=J+3;
541   RS$H!:=SQRT(RS$J!/K);
542   'END';
543   K:=0;
544   'FOR' I:=1 'STEP' 1 'UNTIL' BN 'DO'
544   'IF' B$I,1! > 1999 'THEN'
544   'BEGIN'
545   K:=K+1;
546   RS$3!:=RS$3!+B$I,20!'**'2;
547   'END';
548   RS$6!:=SQRT(RS$3!/K);
549   'FOR' J:=4,5 'DO'
549   'BEGIN'
550   G:=J+3;
551   RS$G!:=RS$J!*K4*10.0'**'6;
552   'END';
553   RS$9!:=RS$6!*BH*K4*10.0'**'6;
554   WRITE TEXT('(''('2C')'THE%ROOT%MEAN%SQUARE%ERRORS%
554
554   OF % THE % DESCREPANCIES '('C')' AT % THE %
554
554   GROUND % SCALE % IN % METERS'('2C')'
554
554   RMSE E'('10S')'RMSE N'('8S')'RMSE H'('2C')'')');
```

```
555   'FOR' I:=4,5,6 'DO'
555   'BEGIN'
556   PRINT(RS$I!,3,3);
557   SPACES(4);
558   'END';
559   WRITE TEXT('('('2C')'THE%ROOT%MEAN%SQUARE%ERRORS%
559
559   OF % THE % DESCREPANCIES '('C')' AT % THE%
559
559   IMAGE % SCALE % IN % MICRONS'('2C')'
559
559   RMSE E'('10S')'RMSE N'('8S')'RMSE H'('2C')'')');
560   'FOR' I:=7,8,9 'DO'
560   'BEGIN'
561   PRINT(RS$I!,3,0);
562   SPACES(10);
563   'END';
564   'END';
565   'END';
566   'GOTO' L1;
567   L20:'END';
```

2.6 Input

47933 —— Model number

—— B/H ratio

0.47   20000 —— Photo scale

—— Maximum number of points in any model

57

—— Number of planimetric control points

15   14 —— Number of height control points

—— Number of unknown polynomial parameters for X or Y

6   6 —— Number of unknown polynomial parameters for Z

2 —— Tag indicating that polynomial adjustment is to be applied

Pt. No.	Type of points	Model coordinates x_m	y_m	z_m	Ground coordinates X	Y	Z
3769	2	-0.017746	0.014214	0.856741	0.000	0.000	14.600
3767	2	-0.010481	0.041193	0.857160	0.000	0.000	18.600
3766	3	-0.007682	0.043885	0.857219	0.000	0.000	19.200
3770	2	0.022876	0.011040	0.857306	0.000	0.000	15.850
3771	3	0.028480	0.010087	0.857344	0.000	0.000	14.940
3762	2	0.043637	0.005511	0.857427	0.000	0.000	13.200
3703	3	0.042814	0.001106	0.857381	0.000	0.000	12.300
3702	3	0.050974	0.005999	0.857416	0.000	0.000	11.400
3775	3	0.074416	0.018824	0.857797	0.000	0.000	11.900
3774	2	0.079792	0.018247	0.857842	0.000	0.000	11.000
3710	3	0.074925	-0.024044	0.857343	0.000	0.000	6.600
3735	3	0.072552	-0.037351	0.857222	0.000	0.000	5.300
3729	2	0.085595	-0.048273	0.857236	0.000	0.000	3.960
3751	3	0.093738	-0.030409	0.857466	0.000	0.000	3.400
3750	2	0.089474	-0.023304	0.857496	0.000	0.000	4.600
3728	3	0.085749	-0.025833	0.857452	0.000	0.000	4.900
3761	2	0.039486	-0.026029	0.857048	0.000	0.000	9.100
3760	3	0.037773	-0.041993	0.856837	0.000	0.000	7.500
3714	3	-0.013852	-0.024538	0.856433	0.000	0.000	10.970
3713	2	-0.003383	-0.036083	0.856445	0.000	0.000	8.530
3759	2	-0.013792	-0.065605	0.856201	0.000	0.000	10.600
3758	3	-0.013973	-0.072030	0.855995	0.000	0.000	8.800
3757	2	-0.014860	-0.086725	0.855785	0.000	0.000	6.100
3772	2	0.013502	-0.063555	0.856507	0.000	0.000	9.750
3755	3	0.029171	-0.087670	0.856376	0.000	0.000	5.790
3754	2	0.037707	-0.088894	0.856445	0.000	0.000	6.100
3752	2	0.076541	-0.077950	0.857089	0.000	0.000	7.300
3753	3	0.098851	-0.076549	0.857415	0.000	0.000	7.000
1709	2	0.105361	-0.064689	0.857263	515824.750	103435.250	0.000
1713	2	-0.009114	0.089282	0.859861	512625.000	106222.125	0.000
1707	2	0.100565	-0.047506	0.857549	515640.750	103782.750	0.000
1706	3	0.102652	-0.051321	0.857567	515703.250	103710.250	0.000
1726	3	0.095715	-0.024902	0.857490	515428.875	104248.250	0.000
1727	2	0.097646	-0.023130	0.857471	515462.125	104295.000	0.000
1728	3	0.095198	-0.023592	0.857469	515411.000	104275.250	0.000
1725	2	0.075439	-0.045448	0.857150	515087.750	103709.812	0.000
1703	3	0.076992	-0.066874	0.857450	515221.750	103253.812	0.000
1710	2	0.068762	-0.085641	0.857504	515133.875	102809.500	0.000
1701	2	0.027494	-0.070427	0.856648	514170.625	102943.875	0.000
1702	3	0.032579	-0.066379	0.856630	514261.500	103055.375	0.000
1705	3	-0.010039	-0.084841	0.856440	513428.250	102455.688	0.000
1732	3	-0.027362	-0.016263	0.856413	512730.000	103854.000	0.000

1733	3	-0.027908	-0.017048	0.856429	512721.625	103834.750	0.000
1734	3	-0.028451	-0.017808	0.856435	512713.250	103815.500	0.000
1731	3	0.013225	-0.004332	0.857096	513550.000	104305.125	0.000
1711	2	-0.010045	0.011810	0.856977	512971.000	104542.875	0.000
1724	2	0.035173	-0.027461	0.857182	514134.375	103907.875	0.000
1722	2	0.043450	-0.034989	0.856986	514347.500	103785.625	0.000
1723	3	0.041964	-0.036435	0.857044	514323.313	103746.687	0.000
1720	2	0.068086	0.014084	0.857767	514648.125	104960.125	0.000
1721	3	0.074090	0.011018	0.857705	514792.250	104921.875	0.000
1719	3	0.078439	0.043993	0.859280	514730.375	105655.250	0.000
1718	2	0.077621	0.043634	0.859245	514714.625	105644.750	0.000
1716	2	0.041992	0.022468	0.857694	514044.875	105019.000	0.000
1714	2	0.010763	0.088117	0.858097	513061.125	106290.500	0.000
1704	2	-0.014309	-0.086998	0.855849	513346.000	102387.500	0.000
1715	3	0.010571	0.087712	0.858125	513058.750	106281.250	0.000

0 ——————————— Tag indicating end of last model

2.7 Output

MODEL NUMBER 47933

NUMBER OF ITERATIONS 3

NUMBER OF PLAN. CONTROLS 15

NUMBER OF HEIGHT CONTROLS 14

SCALE FACTOR 2.21136@ 4

ROTATION MATRIX

9.76947@ -1	-2.13482@ -1	1.12670@ -2
2.13482@ -1	9.76947@ -1	8.34946@ -3
-1.27886@ -2	-5.75424@ -3	1.00000@ 0

TRANSLATIONAL ELEMENTS

5.130302@ 5
1.041769@ 5
-1.893464@ 4

GROUND COORDINATES AFTER ABSOLUTE ORIENTATION

PT.NO.		E	N	H	DE	DN	DH
3769	2	512793.175	104558.388	14.220	-------	-------	-0.380
3767	2	512822.867	105175.612	17.998	-------	-------	-0.602
3766	3	512870.643	105246.995	18.168	-------	-------	-1.032
3770	2	513685.891	104681.693	15.630	-------	-------	-0.220
3771	3	513811.468	104687.567	15.007	-------	-------	0.067
3762	2	514160.541	104660.277	13.138	-------	-------	-0.062
3703	3	514163.545	104561.219	12.914	-------	-------	0.614
3702	3	514316.742	104705.455	10.758	-------	-------	-0.642
3775	3	514762.728	105093.261	10.922	-------	-------	-0.978
3774	2	514881.606	105106.183	10.470	-------	-------	-0.530
3710	3	514975.986	104169.467	6.193	-------	-------	-0.407
3735	3	514987.511	103870.759	5.881	-------	-------	0.581
3729	2	515320.854	103696.379	3.892	-------	-------	-0.068
3751	3	515412.498	104120.795	4.402	-------	-------	1.002

3750	2	515286.845	104254.166	5.368	-------	-------	0.768
3728	3	515218.299	104181.936	5.770	-------	-------	0.870
3761	2	514219.665	103959.226	9.944	-------	-------	0.844
3760	3	514257.969	103606.216	7.794	-------	-------	0.294
3714	3	513060.167	103739.522	11.239	-------	-------	0.269
3713	2	513340.843	103539.531	10.012	-------	-------	1.482
3759	2	513255.278	102852.557	11.317	-------	-------	0.717
3758	3	513281.648	102712.860	7.630	-------	-------	-1.170
3757	2	513331.806	102391.166	5.107	-------	-------	-0.993
3772	2	513835.331	103025.753	10.104	-------	-------	0.354
3755	3	514287.653	102578.724	5.845	-------	-------	0.055
3754	2	514477.859	102592.591	5.112	-------	-------	-0.988
3752	2	515265.318	103012.472	6.978	-------	-------	-0.322
3753	3	515740.767	103148.122	7.700	-------	-------	0.700
1709	2	515825.380	103435.048	0.988	0.630	-0.202	-------
1713	2	512626.051	106221.472	71.221	1.051	-0.653	-------
1707	2	515640.721	103783.678	6.483	-0.029	0.928	-------
1706	3	515703.823	103711.116	6.776	0.573	0.866	-------
1726	3	515429.217	104249.105	3.673	0.342	0.855	-------
1727	2	515462.564	104296.499	2.482	0.439	1.499	-------
1728	3	515411.858	104274.961	3.188	0.858	-0.289	-------
1725	2	515088.088	103709.449	4.503	0.338	-0.363	-------
1703	3	515222.863	103253.952	13.424	1.113	0.140	-------
1710	2	515133.673	102809.670	19.334	-0.202	0.170	-------
1701	2	514170.089	102943.372	10.140	-0.536	-0.503	-------
1702	3	514260.830	103054.827	7.788	-0.670	-0.548	-------
1705	3	513427.227	102454.747	17.988	-1.023	-0.941	-------
1732	3	512729.229	103854.511	13.564	-0.771	0.511	-------
1733	3	512721.143	103834.978	14.172	-0.482	0.228	-------
1734	3	512713.002	103815.996	14.555	-0.248	0.496	-------
1731	3	513549.910	104303.999	15.671	-0.090	-1.126	-------
1711	2	512970.954	104542.851	17.567	-0.046	-0.024	-------
1724	2	514133.281	103907.953	14.309	-1.094	0.078	-------

1722	2	514347.586	103784.357	8.592	0.086	-1.268	-------
1723	3	514322.324	103746.114	10.479	-0.989	-0.573	-------
1720	2	514648.346	104960.970	12.651	0.221	0.845	-------
1721	3	514792.514	104923.066	9.973	0.264	1.191	-------
1719	3	514731.191	105656.274	39.376	0.816	1.024	-------
1718	2	514715.205	105644.650	38.879	0.580	-0.100	-------
1716	2	514045.017	105018.897	17.350	0.142	-0.103	-------
1714	2	513060.531	106289.814	26.739	-0.594	-0.686	-------
1704	2	513345.014	102387.881	6.401	-0.986	0.381	-------
1715	3	513058.302	106280.163	27.464	-0.448	-1.087	-------

THE ROOT MEAN SQUARE ERRORS OF THE DESCREPANCIES
AT THE GROUND SCALE IN METERS

RMSEE	RMSEN	RMSEH
0.638	0.732	0.711

THE ROOT MEAN SQUARE ERRORS OF THE DESCREPANCIES
AT THE IMAGE SCALE IN MICRONS

RMSEE	RMSEN	RMSEH
32	37	17

```
POLYNOM. PARAMETERS FOR  PLAN CORRECTION

PARAMETERS FOR X

 6.23362@  4
-2.45015@ -1
 1.11837@ -2
-1.13361@ -9
 2.38587@ -7
-4.94479@ -8


PARAMETERS FOR Y

 1.37504@  5
-4.88304@ -1
-2.30783@ -1
 4.49463@ -7
 4.29489@ -7
-9.26812@-10


POLYNOM. PARAMETERS FOR HEIGHT CORRECTION

 6.43954@  3
-2.91397@ -2
 2.15405@ -2
 3.33140@ -7
-5.55635@ -9
-9.28400@ -7
```

GROUND COORDINATES AFTER POLYN. ADJUSTMENT

PT.NO.		E	N	H	DE	DN	DH
3769	2	512793.139	104558.264	13.910	-------	-------	-0.690
3767	2	512822.701	105175.811	19.130	-------	-------	0.530
3766	3	512870.483	105247.250	19.502	-------	-------	0.302
3770	2	513686.029	104681.980	15.526	-------	-------	-0.324
3771	3	513811.602	104687.849	14.909	-------	-------	-0.031
3762	2	514160.637	104660.475	12.990	-------	-------	-0.210
3703	3	514163.666	104561.427	12.626	-------	-------	0.326
3702	3	514316.788	104705.573	10.676	-------	-------	-0.724
3775	3	514762.513	105092.900	11.507	-------	-------	-0.393
3774	2	514881.326	105105.679	11.064	-------	-------	0.064
3710	3	514975.887	104169.300	5.657	-------	-------	-0.943
3735	3	514987.498	103870.730	5.335	-------	-------	0.035
3729	2	515320.672	103696.166	3.521	-------	-------	-0.439
3751	3	515412.107	104120.200	3.930	-------	-------	0.530
3750	2	515286.512	104253.634	4.907	-------	-------	0.307
3728	3	515218.037	104181.526	5.276	-------	-------	0.376
3761	2	514219.948	103959.502	9.211	-------	-------	0.111
3760	3	514258.362	103606.545	7.124	-------	-------	-0.376
3714	3	513060.480	103739.284	10.176	-------	-------	-0.794
3713	2	513341.296	103539.481	9.053	-------	-------	0.523
3759	2	513255.985	102852.239	10.954	-------	-------	0.354
3758	3	513282.422	102712.536	7.518	-------	-------	-1.282
3757	2	513332.738	102390.822	5.713	-------	-------	-0.387
3772	2	513836.013	103025.991	9.805	-------	-------	0.055
3755	3	514288.454	102579.237	6.673	-------	-------	0.883
3754	2	514478.593	102593.168	6.037	-------	-------	-0.063
3752	2	515265.436	103012.733	7.470	-------	-------	0.170
3753	3	515740.425	103147.889	8.188	-------	-------	1.188
1709	2	515824.845	103434.472	1.064	0.095	-0.778	-------
1713	2	512625.635	106222.148	76.517	0.635	0.023	-------
1707	2	515640.240	103783.048	6.154	-0.510	0.298	-------

1706	3	513703.308	103710.462	6.517	0.058	0.212	-------
1726	3	515428.774	104248.401	3.230	-0.101	0.151	-------
1727	2	515462.080	104295.718	2.059	-0.045	0.718	-------
1728	3	515411.422	104274.262	2.752	0.422	-0.988	-------
1725	2	515088.066	103709.427	4.050	0.316	-0.385	-------
1703	3	515222.915	103254.093	13.486	1.165	0.281	-------
1710	2	515133.970	102810.116	20.173	0.095	0.616	-------
1701	2	514170.759	102943.781	10.150	0.134	-0.094	-------
1702	3	514261.433	103055.248	7.670	-0.067	-0.127	-------
1705	3	513428.144	102454.541	18.511	-0.106	-1.147	-------
1732	3	512729.373	103853.965	12.452	-0.627	-0.035	-------
1733	3	512721.290	103834.411	13.049	-0.335	-0.339	-------
1734	3	512713.151	103815.410	13.422	-0.099	-0.090	-------
1731	3	513550.141	104304.219	15.043	0.141	-0.906	-------
1711	2	512970.994	104542.856	17.232	-0.006	-0.019	-------
1724	2	514133.600	103908.242	13.548	-0.775	0.367	-------
1722	2	514347.892	103784.646	7.891	0.392	-0.979	-------
1723	3	514322.650	103746.414	9.779	-0.663	-0.273	-------
1720	2	514648.213	104960.774	12.986	0.088	0.649	-------
1721	3	514792.320	104922.739	10.223	0.070	0.864	-------
1719	3	514730.890	105655.736	41.453	0.515	0.486	-------
1718	2	514714.914	105644.137	40.925	0.289	-0.613	-------
1716	2	514045.051	105019.110	17.877	0.176	0.110	-------
1714	2	513060.291	106290.533	32.128	-0.834	0.033	-------
1704	2	513345.950	102387.554	7.025	-0.050	0.054	-------
1715	3	513058.062	106280.879	32.807	-0.688	-0.371	-------

THE ROOT MEAN SQUARE ERRORS OF THE DESCREPANCIES
AT THE GROUND SCALE IN METERS

RMSEE	RMSEN	RMSEH
0.442	0.533	0.554

THE ROOT MEAN SQUARE ERRORS OF THE DESCREPANCIES
AT THE IMAGE SCALE IN MICRONS

RMSEE	RMSEN	RMSEH
22	27	13

3. Program (D) - Space Resection/Intersection

3.1 General Information

Program identification	— SRESI Space Resection/Intersection
Type of Language	- Complete Algol Program
Computer	- ICL 1906A Nottingham and transferred to ICL 2980 in Edinburgh.

3.2 Definition of Variables

N	-	Maximum number of points in any one photograph
MD	-	Model number
CH	-	Number of check points in the model
NI	-	Total number of control points in the photograph
BH	-	Base to height ratio
NH	-	Number of control points in the photograph and outside the model
PN	-	Photo number
TG	-	Tag to indicate the direction of the shutter motion
MAXIT	-	Maximum number of iterations to solve for the orientation elements
SOL	-	Tag to indicate type of resection solution
X	-	Number of unknowns in the normal equations.
FL	-	Camera focal length

OMG, PHY, KAP	-	Initial approximations for the camera rotation elements.
XO, YO, ZO	-	Initial approximations for the camera translation elements. (Exposure station coordinates in the ground coordinate system.)

ARRAYS

B	-	Array including the point number, the image coordinates and the ground coordinates of the test points. This array is also a working array used in computing the ground coordinates in the intersection phase.
GC	-	Array including the known ground coordinates of all the points, the computed ground coordinates and the residuals.
CN	-	Array containing the exterior orientation elements. It is also used to compute the scale factor.
C, AC	-	Working arrays to form the coefficients of the observation equations.
P1	-	Array containing the residuals of the computed image coordinates from the measured image coordinates, in the resection phase.
D	-	Working array including the normal equations matrix.

DT, V	-	Working arrays used in the solution of the normal equations in the least squares method.
CR	-	Array containing the corrections to the orientation elements.
A, DS, ST	-	Working arrays to compute the correlation matrix.
CS	-	Array containing the correlation matrix.
Q	-	Array containing the parameters correcting for the orientation elements.
AI, E	-	Working arrays to determine correction values to the orientation elements in the point-by-point resection case.
S	-	Array containing the root mean square errors of the discrepancies.

3.3 Detailed account of the program

The program is composed of six parts:-

(i) Entering matrix procedures.

(ii) Input of data .

(iii) Resection phase.

(iv) Output of resection results.

(v) Intersection phase.

(vi) Output of final results.

A step-by-step account of these parts follows.

(i) Enter the following matrix procedures to be used in solving the normal equations in the resection phase:

Procedure MATVEC - Matrix x Vector

Procedure MATMLT - Matrix x Matrix

Procedure MATRAN - Matrix transpose

Procedure INVERT - Matrix inversion

(ii) Input of data

Declaration

Read in the maximum number of points in any one photograph (N).

Declaration.

Write text.

Read in the model number (MD).

Read in the base to height ratio of the model (BH).

Read in the number of check points (CH).

Read in the number of control points (NI).

Read in the number of control points (NH) outside the model area.

Read in the photo serial number (PN).

Read in tag (TG) to show the direction of the slit motion relative to the flight direction as follows: TG = 1 for motion along the flight direction,

TG = 1 for motion across the flight direction,

TG = 3 for general case.

Read in the maximum number of iterations (MAXIT).

Read in tag (SOL) to indicate type of solution required, defined as follows:-

for conventional resection or additional parameters, SOL = 2;

for point-by-point resection, SOL = 1.

Read in the number of unknown parameters (X) as follows:-

for conventional resection X = 6 (the exterior orientation elements of the camera);

for point-by-point resection, X = 12;

for the additional parameters, X = 8, 14, 16 or 18.

Declaration of arrays.

Read in the camera focal length (FL).

Read in the image data in array (B) as follows:-

the point number in column 1 (starting with the control points);

the photo-coordinates (x, y) in columns 2 and 3 with the principal point as origin;

the ground coordinates (X, Y, Z) in columns 4, 5 and 6, respectively.

Store the ground coordinates in array (GC).

Read in the initial approximate values for the exterior orientation elements of the camera: ω_o, Φ_o, κ_o, X_o, Y_o, Z_o.

(iii) Resection phase:

Store the initial approximate values of the exterior orientation elements in array (CN).

Form the coefficients of the observation equations in array (AC).

Compute the correlation matrix if additional parameters are used.

Form the normal equations and solve for the corrections to the initial approximations of the camera orientation elements.

Compute the new orientation elements.

Check whether corrections are significant. (If the values of the corrections are greater than 0.00001 repeat the procedure using the new orientation elements as the new approximate values.)

(iv) Output of the results after resection phase:

Write text.

Print out the correlation matrix if additional parameters are used.

Write text.

Print out the corrections to the orientation elements.

Print out the number of iterations.

Print out the number of control points used in the resection phase.

Write text.

Print out the correction parameters if point-by-point resection is used.

Print out the self calibration parameters if additional parameters are used.

(v) Intersection phase:

Store the exterior orientation elements for each of the overlapping photographs in arrays (B) and(CN).

Compute the scale factor.

Compute the ground coordinates of all the test points.

Determine the residuals of the computed ground coordinates from the known values.

Compute the root mean square errors of the discrepancies.

(vi) Output of final results:

Write text.

Print out the computed ground coordinates of all the test points, together with their residuals from the known values.

Write text.

Print out the root mean square errors of the discrepancies at the ground scale and at the image scale.

Print out the x-parallax corresponding to the root mean square error in height.

3.4 Flow Diagram for Program (D)

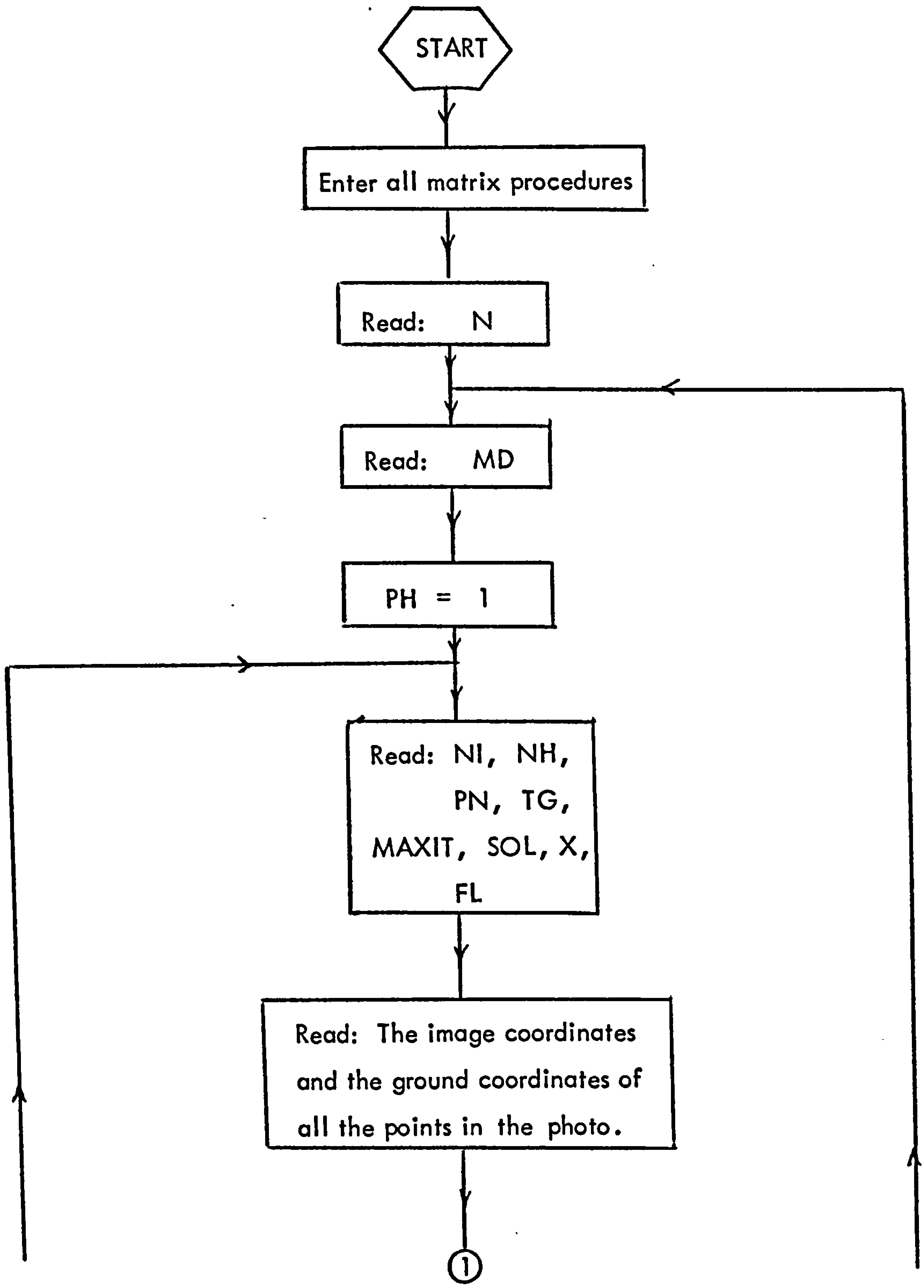

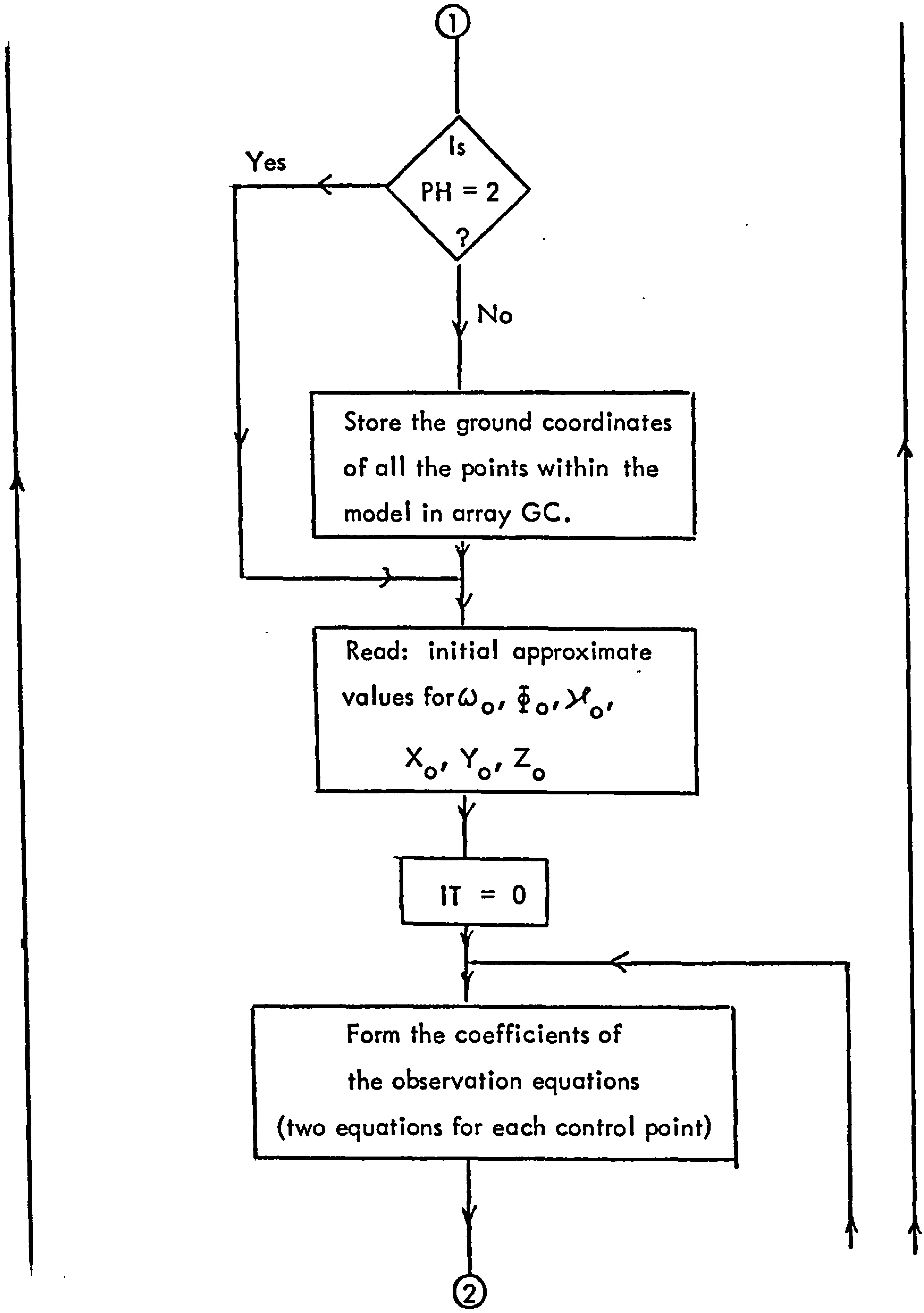
1
Is
PH = 2
?
Yes
No
Store the ground coordinates of all the points within the model in array GC.
Read: initial approximate values for ω_o, Φ_o, κ_o, X_o, Y_o, Z_o
IT = 0
Form the coefficients of the observation equations (two equations for each control point)
2

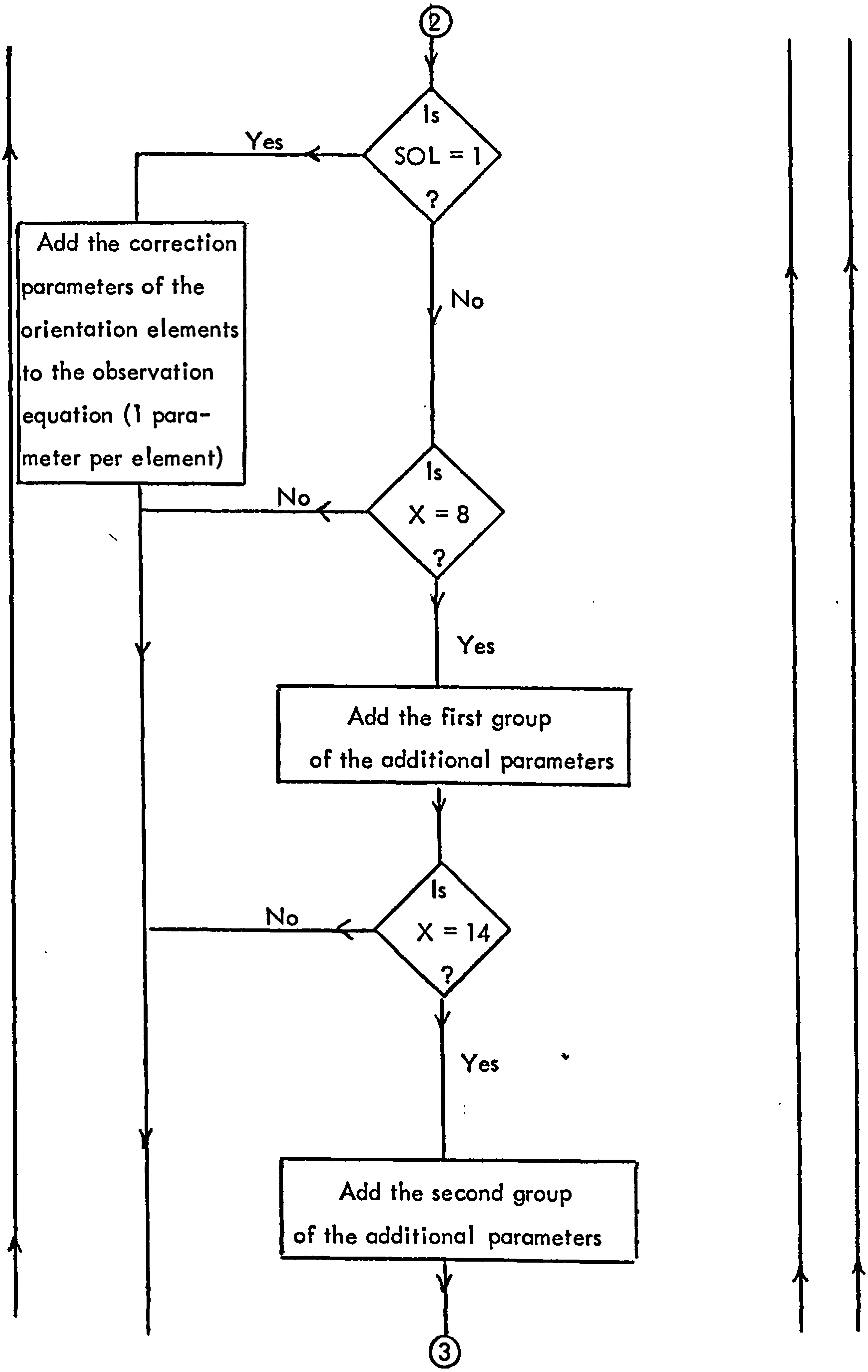
2
Is
SOL = 1
?
Yes
No
Add the correction parameters of the orientation elements to the observation equation (1 parameter per element)
Is
X = 8
?
No
Yes
Add the first group of the additional parameters
Is
X = 14
?
No
Yes
Add the second group of the additional parameters
3

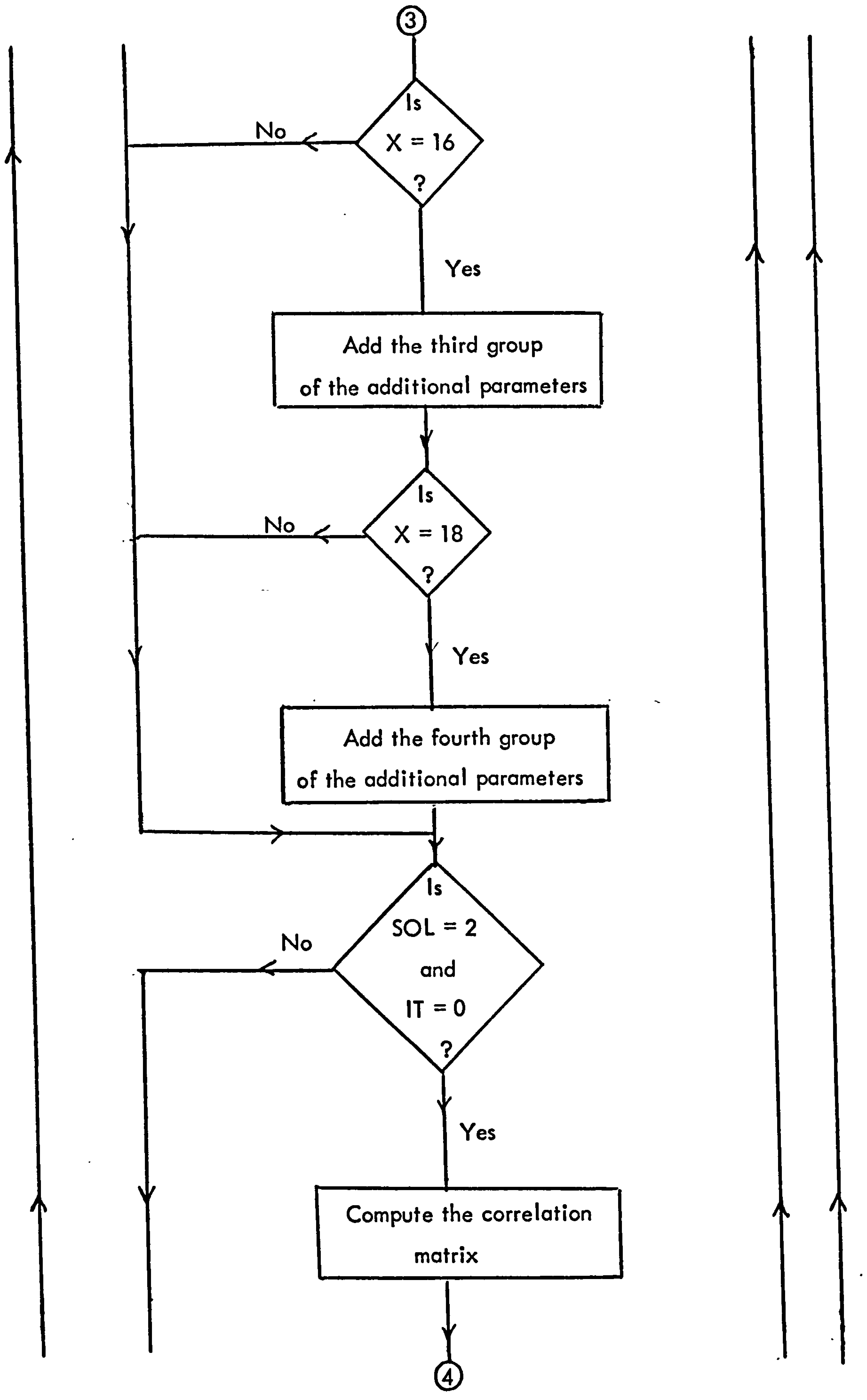
3
Is
X = 16
?
No
Yes
Add the third group
of the additional parameters
Is
X = 18
?
No
Yes
Add the fourth group
of the additional parameters
Is
SOL = 2
and
IT = 0
?
No
Yes
Compute the correlation
matrix
4

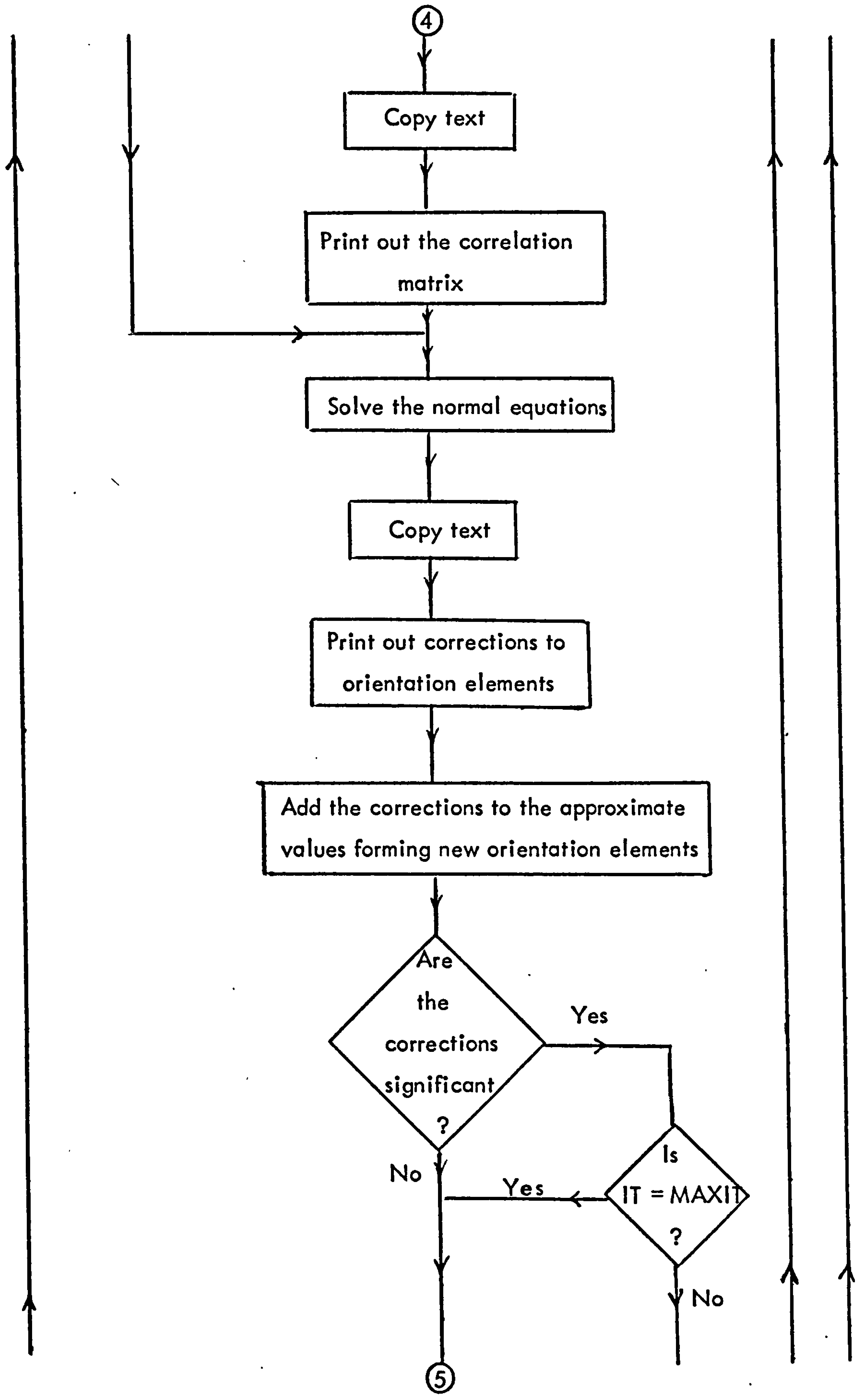
4
Copy text
Print out the correlation matrix
Solve the normal equations
Copy text
Print out corrections to orientation elements
Add the corrections to the approximate values forming new orientation elements
Are the corrections significant ?
Yes
No
Is IT = MAXIT ?
Yes
No
5

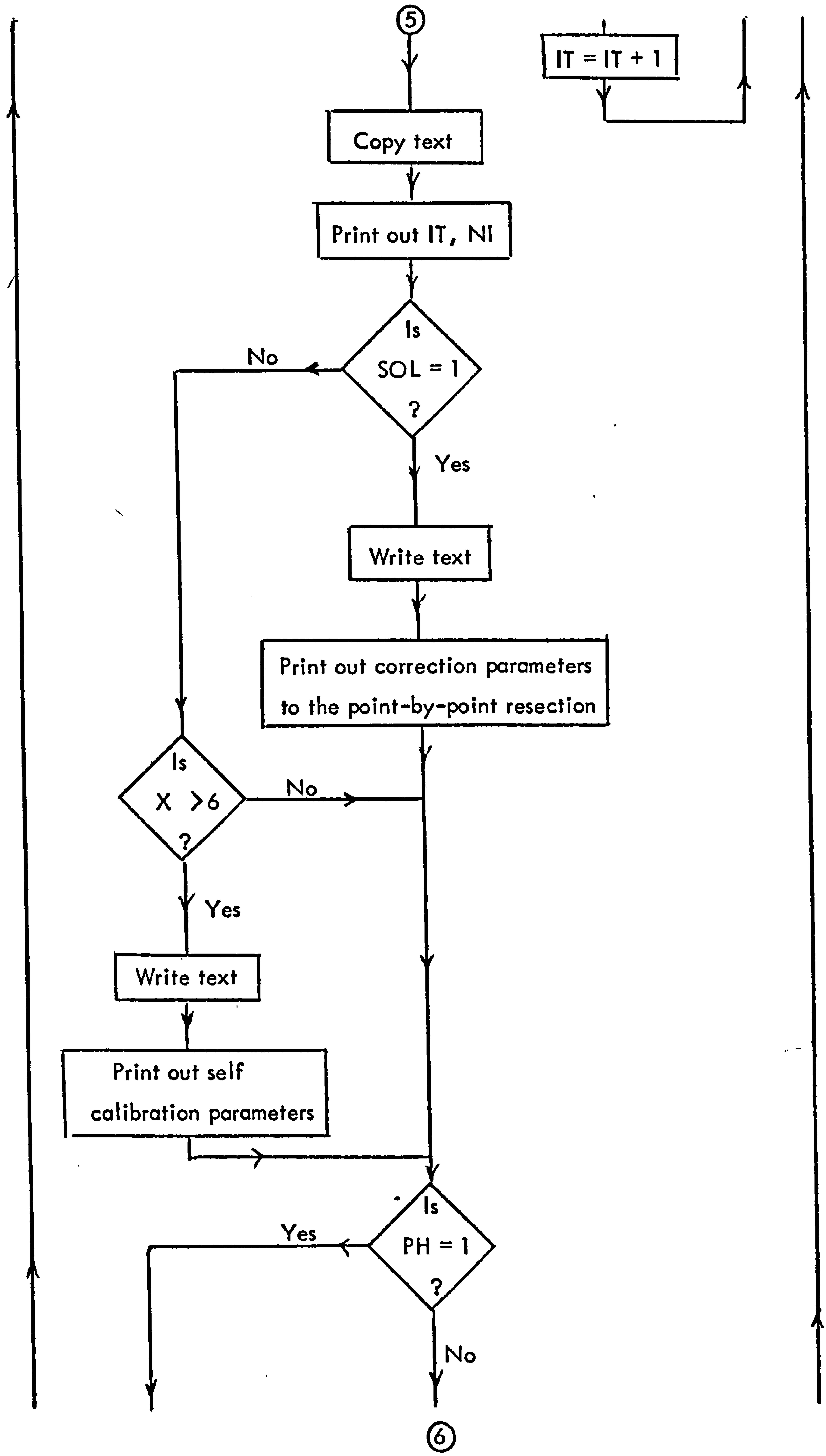
5
IT = IT + 1
Copy text
Print out IT, NI
Is SOL = 1 ?
No
Yes
Write text
Print out correction parameters to the point-by-point resection
Is X >6 ?
No
Yes
Write text
Print out self calibration parameters
Is PH = 1 ?
Yes
No
6

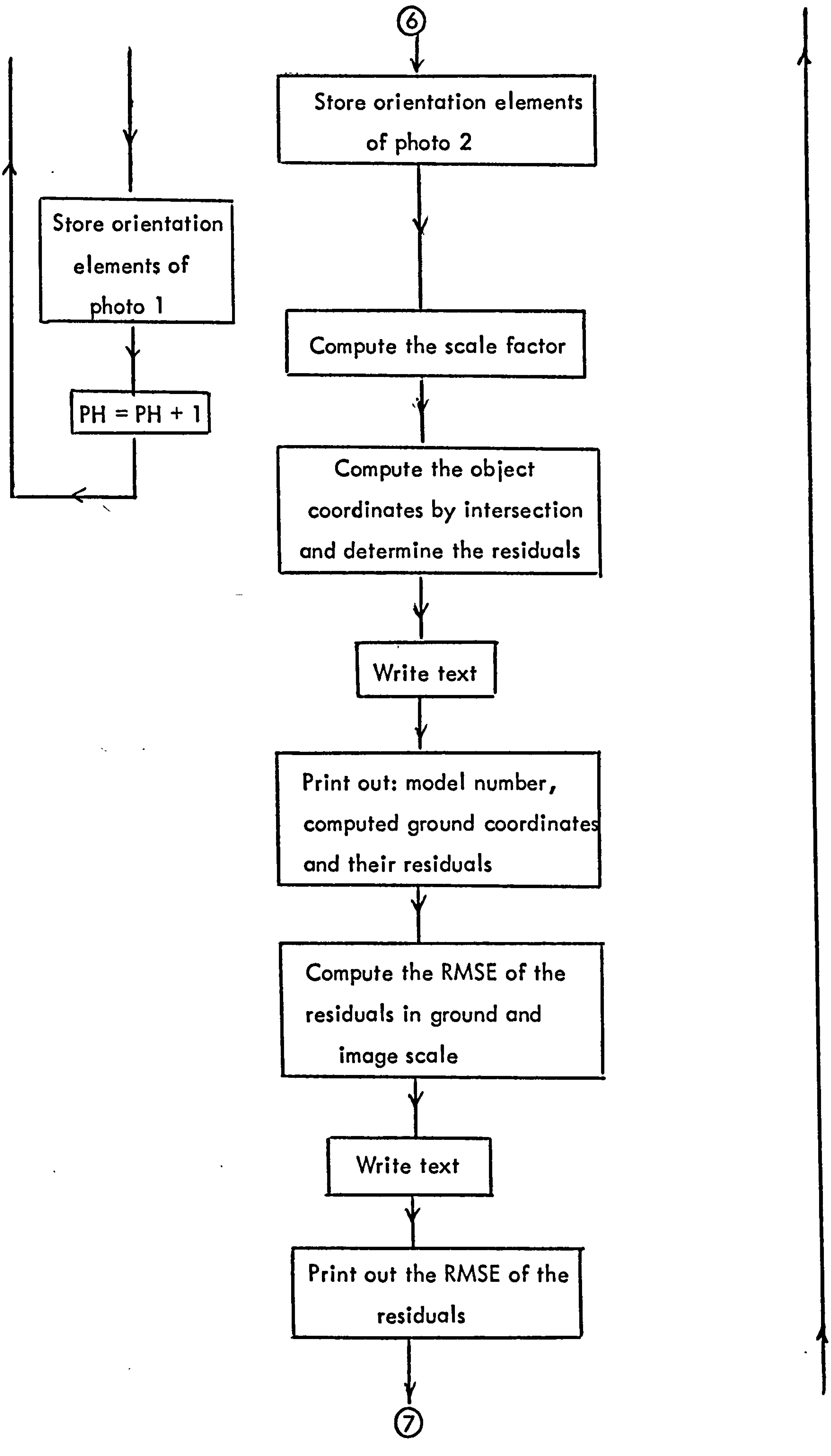
6
Store orientation elements of photo 2
Compute the scale factor
Compute the object coordinates by intersection and determine the residuals
Write text
Print out: model number, computed ground coordinates and their residuals
Compute the RMSE of the residuals in ground and image scale
Write text
Print out the RMSE of the residuals
7
Store orientation elements of photo 1
PH = PH + 1

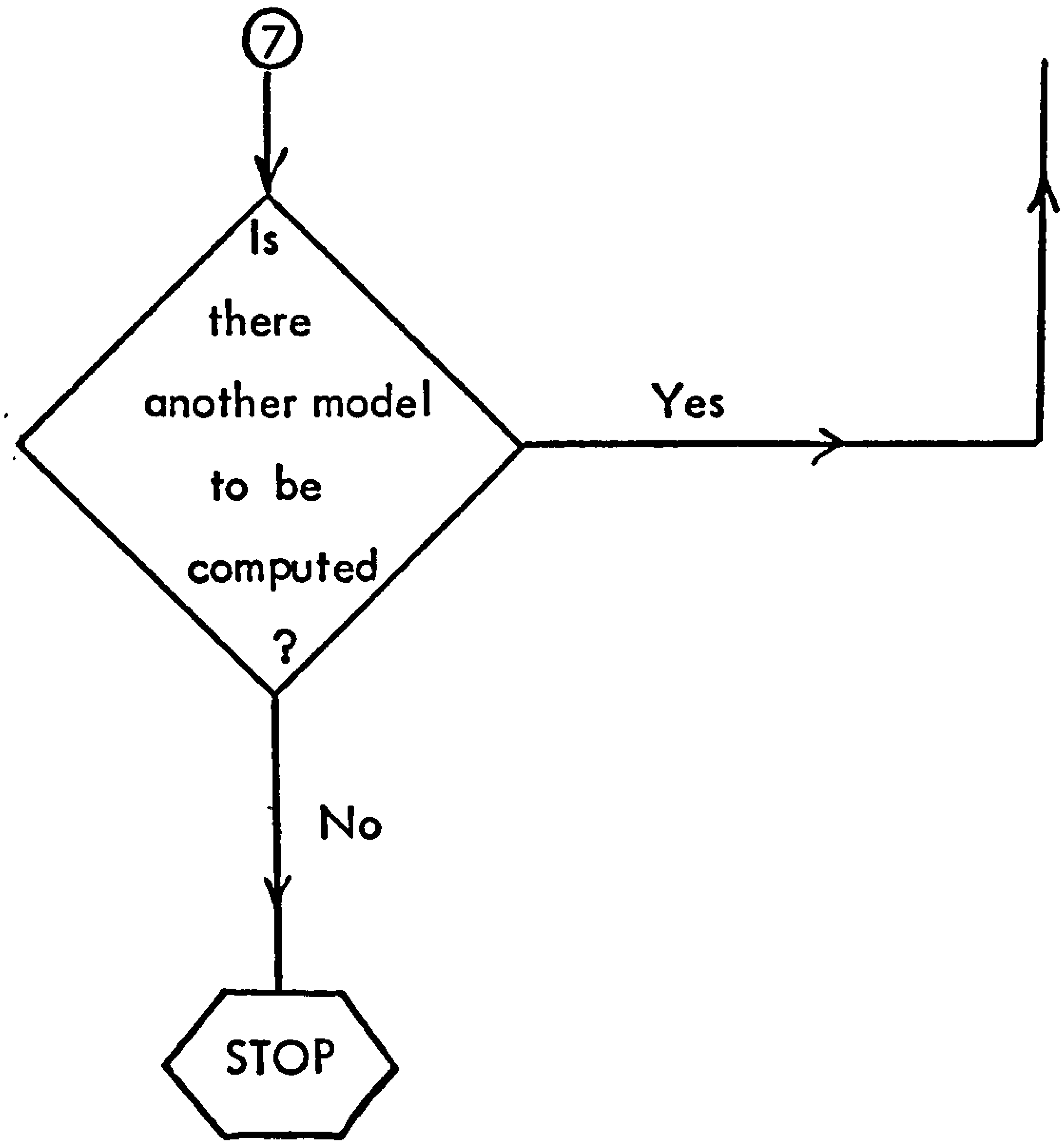
7
Is there another model to be computed ?
Yes
No
STOP

3.5 The Program

```
STMNT
  1      'BEGIN'
  2      'COMMENT'  SPACE RESECTION-INTERSECTION
  2                        PROGRAM;
  3      'INTEGER'  G,  W,  Y,  Z;
  4      'PROCEDURE' MATVEC(A,X,Z,M,N);
  5      'VALUE' A,X,M,N;
  6      'INTEGER' M,N; 'ARRAY'A,X,Z;
  8      'BEGIN' 'INTEGER' I,J;
 10      'REAL' SUM;
 11      'FOR'I:=1 'STEP'1 'UNTIL'N 'DO'
 11      'BEGIN' SUM:=0.0;
 13      'FOR'J:=1 'STEP'1 'UNTIL' M 'DO'
 13      SUM:=SUM+A$I,J!*X$J!;
 14      Z$I!:=SUM;
 15      'END' 'END' MATVEC;
 17      'PROCEDURE' MATMLT(A,U,T,M,N,P);
 18      'VALUE' A,U,M,N,P;
 19      'INTEGER' M,N,P;
 20      'REAL' 'ARRAY' A,U,T;
 21      'BEGIN' 'INTEGER' I,J,K;
 23      'FOR' I:=1 'STEP' 1 'UNTIL' N 'DO'
 23      'FOR' J:=1 'STEP' 1 'UNTIL' M 'DO'
 23      'BEGIN'
 24      T$I,J!:=0.0;
 25      'FOR' K:=1 'STEP' 1 'UNTIL' P 'DO'
 25      T$I,J!:=T$I,J!+A$I,K!*U$K,J!;
 26      'END'
 26      'END' MATMLT;
 28      'PROCEDURE' MATRAN(A,AT,M,N);
 29      'VALUE'A,M,N;
 30      'ARRAY'A,AT;
 31      'INTEGER'M,N;
 32      'BEGIN'
 33      'INTEGER'I,J;
 34      'FOR' I:=1 'STEP' 1 'UNTIL'M 'DO'
 34      'FOR' J:=1 'STEP' 1 'UNTIL' N 'DO'
 34      AT$I,J!:=A$J,I!
 34      'END' MATRAN;
 36      'PROCEDURE' INVERT(A,N,INVA);
 37      'VALUE' N;
```

```
'ARRAY' A,INVA;
'INTEGER' N;
'BEGIN'
'REAL' 'ARRAY' B$1:N,1:2*N!, X$1:N,1:N!;
'INTEGER' M,I,J,K;
'REAL' PIVOT, TT;
M:=2*N;
'FOR' I :=1 'STEP' 1 'UNTIL' N 'DO'
'BEGIN'
'FOR' J :=1 'STEP' 1 'UNTIL' N 'DO'
B$I,J!:=A$I,J!;
'FOR' J:=N+1 'STEP' 1 'UNTIL' M 'DO'
B$I,J!:= 'IF' I+N 'EQ' J 'THEN' 1 'ELSE' 0;
'END';
'FOR' I:=1 'STEP' 1 'UNTIL' N 'DO'
'BEGIN'
PIVOT:=B$I,I!;
'FOR' J:=I+1 'STEP' 1 'UNTIL' N 'DO'
'IF' ABS(PIVOT) 'LT' ABS(B$J,I!) 'THEN'
'BEGIN'
'FOR' K:=1 'STEP' 1 'UNTIL' M 'DO'
'BEGIN'
TT:=B$I,K!;
B$I,K!:=B$J,K!;
B$J,K!:=TT;
'END';
PIVOT:=B$J,I!;
'END';
'FOR' K:=M 'STEP' -1 'UNTIL' I 'DO'
B$I,K!:=B$I,K!/B$I,I!;
'FOR' J:=I+1 'STEP' 1 'UNTIL' N 'DO'
'FOR' K:=M 'STEP' -1 'UNTIL' I 'DO'
B$J,K!:=B$J,K!-B$I,K!*B$J,I!;
'END';
'FOR' J:=1 'STEP' 1 'UNTIL' N 'DO'
'BEGIN'
Y:=N+J;
X$N,J!:= B$N,Y!;
'END';
'FOR' I:=N-1 'STEP' -1 'UNTIL' 1 'DO'
'BEGIN'
'FOR' J:=1 'STEP' 1 'UNTIL' N 'DO'
'BEGIN'
G:=N+J;
X$I,J!:= B$I,G!;
'END';
'FOR' K:= N 'STEP' -1 'UNTIL' I+1 'DO'
'FOR' J:=1 'STEP' 1 'UNTIL' N 'DO'
X$I,J!:=X$I,J!-B$I,K!*X$K,J!;
'END';
'FOR' I:=1 'STEP' 1 'UNTIL' N 'DO'
'FOR' J:=1 'STEP' 1 'UNTIL' N 'DO'
INVA$I,J!:=X$I,J!;
'END'INVERT;


'REAL' FL, XO, YO, ZO,
OMG,  PHY,  KAP,    BH;
'INTEGER' I,J,K,L,M,N,PH,IT,MD,CH,
N1, PN, MAXIT, SN, NH,
H, TG, SOL,  X,  X1;
'COMMENT'  N  IS THE MAX. NUMBER OF POINTS
IN ANY ONE PHOTO,
   MD  IS MODEL NUMBER,
   BH  IS THE BASE TO HEIGHT  RATIO OF
THE MODEL;
```

```
78      N:=READ;
79      'BEGIN'
80      'REAL' 'ARRAY'  B$1:N,1:32!,   GC$1:N,1:16!,
80                      CN$1:N,1:25!,
80      C$1:N,1:6!,           S$1:9!,
80      AC$1:N,1:36!,  AB$1:N,1:15!;
81      WRITETEXT('(' '('P')' I. M. ELHASSAN  %%  %%
81
81          GEOGRAPHY    %%        DEPT.
81      '('4C')' SPACE % RESECTION % INTERSECTION %
81
81      PROGRAM                                    '('5C')'')');
82
82      L0:MD:=READ;
83      'IF' MD=0 'THEN' 'GOTO' L6;
84      BH:=READ;
85      'COMMENT' CH IS THE NUMBER OF CHECK POINTS;
86      CH:=READ;
87      'FOR' I:=1 'STEP' 1 'UNTIL' N 'DO'
87      'BEGIN'
88      'FOR' J:=1 'STEP' 1 'UNTIL' 25 'DO'
88      CN$I,J!:=0.00;
89      'FOR' J:=1 'STEP' 1 'UNTIL' 32 'DO'
89      B$I,J!:=0.00;
90      'END';
91      PH:=1;
92
92      'COMMENT' PN IS THE SERIAL PHOTO NUMBER
92             N1 IS THE NUMBER OF GROUND CONTROLS
92             NH IS THE NUMBER OF POINTS IN THE PHOTO AND
92             OUTSID THE MODEL AREA;
93      L1:N1:=READ;
94      M:=2*N1;
95      NH:=READ;
96      PN:=READ;
97      SN:=N1+CH;  H:=SN-NH;
99      'COMMENT' TG=1 FOR SHUTTER MOVING ALONG
99      FLIGHT DIRECTION,
99                TG=2 FOR SHUTTER MOVING ACROSS
99      FLIGHT DIRECTION,
99                TG=3 FOR GENERAL CASE;
100     TG:=READ;
101     'COMMENT' SPECIFY THE MAX. NO. OF ITERATIONS;
102     MAXIT:=READ;
103     'COMMENT' SOL=1 FOR POINT BY POINT RESECTION
103               SOL=2 FOR CONV. RESECTION AND
103               ADDITIONAL PARAMETERS,
103               X= NUMBER OF UNKNOWN PARAMETERS
103     INCLUDING THE SIX ORIENTATION ELEMENTS;
104     SOL:=READ;
105     X:=READ;
106     X1:=X-6;
107     'BEGIN'
108     'REAL' 'ARRAY' P1$1:M!, P$1:M,1:6!,
108     D$1:M,1:X!,DT$1:X,1:M!,A1$1:6,1:2!,E$1:2,1:SN!,
108     Q$1:X!,A$1:X!,V$1:X,1:X!,
108     CR$1:6,1:SN!;
109
109     'COMMENT'  READ IN  :
109               THE CAMERA FOCAL LENGTH,
109                THE  IMAGE COORDINATES AND  THE
109     GROUND COORDINATES FOR ALL THE POINTS IN METERS;
110     FL:=READ;
111     'FOR' I:=1 'STEP' 1 'UNTIL' SN 'DO'
111     'FOR' J:=1,2,3,4,5,6 'DO'
111     B$I,J!:=READ;
```

```
112   WRITE TEXT('('('2C')'PHOTO%NUMBER'('2S')')');
113   PRINT(PN,5,0);
114   NEWLINES(2);
115   'IF' PH=2 'THEN' 'GOTO' L0A;
116   'FOR' I:=1 'STEP' 1 'UNTIL' H 'DO'
116   'BEGIN'
117   Y:= I+NH;
118   GC$I,1!:= B$Y,1!;
119   'FOR' J:=2,3,4 'DO'
119   'BEGIN'
120   G:=J+2;
121   GC$I,J!:= B$Y,G!;
122   'END';
123   'END';
124
124
124   'COMMENT'  PHOTO  RESECTION PHASE;
125   L0A: 'FOR' I:=1 'STEP' 1 'UNTIL' N 'DO'
125   'FOR' J:=1,2,3,4,5,6 'DO'
125   CN$I,J!:=0.00;
126   'FOR' I:=1 'STEP' 1 'UNTIL' X 'DO'
126   A$I!:=0.00;
127
127   'COMMENT' READ IN THE INITIAL APPROX.  VALUES FOR THE
127         ROTATIONS    AND     TRANSLATIONS
127         OF THE PHOTO PERSPECTIVE CENTRE IN RADIANS AND
127         METERS RESPECTIVELY;
128   OMG:=READ;
129   PHY:=READ;
130   KAP:=READ;
131   XO:=READ;
132   YO:=READ;
133   ZO:=READ;
134   'FOR' I:=1 'STEP' 1 'UNTIL' SN 'DO'
134   'BEGIN'
135   CN$I,1!:=OMG;
136   CN$I,2!:=PHY;
137   CN$I,3!:=KAP;
138   CN$I,4!:=XO;
139   CN$I,5!:=YO;
140   CN$I,6!:=ZO;
141   'END';
142   L1A: 'FOR' I:=1 'STEP' 1 'UNTIL' X 'DO'
142   Q$I!:=0.00;
143   IT:=0;
144   L2: 'FOR' I:=1 'STEP' 1 'UNTIL' N 'DO'
144   'FOR' J:=1,2,3 'DO'
144   C$I,J!:=0.00;
145   'FOR' I:=1 'STEP' 1 'UNTIL' SN 'DO'
145   'BEGIN'
146    'FOR' J:=1,2,3 'DO'
146   'BEGIN'
147   Y:=J+3;
148    C$I,J!:=SIN(CN$I,J!);
149   C$I,Y!:=COS(CN$I,J!);
150    'END';
151   'END';
152   'FOR' I:=1 'STEP' 1 'UNTIL' N 'DO'
152   'FOR' J:=1 'STEP' 1 'UNTIL' 36 'DO'
152   AC$I,J!:=0.00;
153
153   'COMMENT' COMPUTE THE COEFFS. FOR THE
153             OBSERVATION  EQUATIONS;
154   'FOR' I:=1 'STEP' 1 'UNTIL' N1 'DO'
154   'BEGIN'
155   AC$I,1!:=C$I,5!*C$I,6!;
```

```
156   AC$I,2!:=C$I,4!*C$I,3!+C$I,1!*C$I,2!*C$I,6!;
157   AC$I,3!:=C$I,1!*C$I,3!-C$I,4!*C$I,2!*C$I,6!;
158   AC$I,4!:=-C$I,5!*C$I,3!;
159   AC$I,5!:=C$I,4!*C$I,6!-C$I,1!*C$I,2!*C$I,3!;
160   AC$I,6!:=C$I,1!*C$I,6!+C$I,4!*C$I,2!*C$I,3!;
161   AC$I,7!:=C$I,2!;
162   AC$I,8!:=-C$I,1!*C$I,5!;
163   AC$I,9!:=C$I,4!*C$I,5!;
164   AC$I,10!:=0.00;
165   AC$I,11!:=-AC$I,3!;
166   AC$I,12!:=AC$I,2!;
167   AC$I,13!:=0.00;
168   AC$I,14!:=-AC$I,6!;
169   AC$I,15!:=AC$I,5!;
170   AC$I,16!:=0.00;
171   AC$I,17!:=-AC$I,9!;
172   AC$I,18!:=AC$I,8!;
173   AC$I,19!:=-C$I,2!*C$I,6!;
174   AC$I,20!:=C$I,1!*AC$I,1!;
175   AC$I,21!:=-AC$I,9!*C$I,6!;
176   AC$I,22!:=C$I,2!*C$I,3!;
177   AC$I,23!:=AC$I,8!*C$I,3!;
178   AC$I,24!:=AC$I,9!*C$I,3!;
179   AC$I,25!:=C$I,5!;
180   AC$I,26!:=C$I,1!*C$I,2!;
181   AC$I,27!:=-C$I,4!*C$I,2!;
182   AC$I,28!:=AC$I,4!;
183   AC$I,29!:=AC$I,5!;
184   AC$I,30!:=AC$I.6!;
185   AC$I,31!:=-AC$I,1!;
186   AC$I,32!:=-AC$I,2!;
187   AC$I,33!:=-AC$I,3!;
188   AC$I,34!:=0.00;
189   AC$I,35!:=0.00;
190   AC$I,36!:=0.00;
191   'END';
192   'FOR' I:=1 'STEP' 1 'UNTIL' N1 'DO'
192   'FOR' J :=1 'STEP' 1 'UNTIL' 15 'DO'
192   AB$I,J!:=0.00;
193   'FOR' I:=1 'STEP' 1 'UNTIL' M 'DO'
193   'BEGIN'
194   P1$I!:=0.00;
195   'FOR' J:=1,2,3,4,5,6 'DO'
195   P$I,J!:=0.00;
196   'END';
197   'FOR' I:=1 'STEP' 1 'UNTIL' N1 'DO'
197   'BEGIN'
198   'FOR' J:=1,2,3 'DO'
198   'BEGIN'
199   Y:= J+3;
200   AB$I,J!:= B$I,Y!-CN$I,Y!;
201   'END';
202   'FOR' J:=1 'STEP' 1 'UNTIL' 12 'DO'
202   'BEGIN'
203   K:=2*(J-1)+J;
204   Y:= J+3;  G:=K+1;  W:=K+2;
207   AB$I,Y!:=AC$I,K!*AB$I,1!+AC$I,G!*AB$I,2!+
207                           AC$I,W!*AB$I,3!;
208   'END';
209   'END';
210
210
210   'COMMENT' COMPUTATION OF P-VALUES;
211   'FOR'I:=1 'STEP' 1 'UNTIL' N1 'DO'
211   'BEGIN'
212   Y:=I+N1;
```

```
213   P1$I!:=(-AB$I,6!*B$I,2!-FL*AB$I,4!)/AB$I,6!;
214   P1$Y!:=(-AB$I,6!*B$I,3!-FL*AB$I,5!)/AB$I,6!;
215   'FOR' J:=1,2,3 'DO'
215   'BEGIN'
216   L:=3*J+4;
217   G:=J+3;  W:=L+2;  K:=L+1;  Z:=J+6;
221   P$I,J!:=( AB$I,W!*B$I,2!+FL*AB$I,L!)/AB$I,6!;
222   P$I,G!:=(-AC$I,Z!*B$I,2!-FL*AC$I,J!)/AB$I,6!;
223   P$Y,J!:=(AB$I,W!*B$I,3!+FL*AB$I,K!)/AB$I,6!;
224   P$Y,G!:=(-AC$I,Z!*B$I,3!-FL*AC$I,G!)/AB$I,6!;
225   'END';
226   'END';
227
227   'FOR' I:=1 'STEP' 1 'UNTIL' M 'DO'
227   'FOR' J:=1 'STEP' 1 'UNTIL' X 'DO'
227   'BEGIN'
228   D$I,J!:=0.00;
229   DT$J,I!:=0.00;
230   'END';
231   'FOR' I:=1 'STEP' 1 'UNTIL' X 'DO'
231   'FOR' J:=1 'STEP' 1 'UNTIL' X 'DO'
231   V$I,J!:=0.00;
232   'IF' SOL>1 'THEN' 'GOTO' L1S;
233   'FOR' I:=1 'STEP' 1 'UNTIL' N1 'DO'
233   'BEGIN'
234   Y:= I+N1;
235   'FOR' J:=0 'STEP' 1 'UNTIL' 5 'DO'
235   'BEGIN'
236   K:=1+2*J;
237   W:= J+1;
238   D$I,K!:= P$I,W!;
239   D$Y,K!:= P$Y,W!;
240   'END';
241   'END';
242
242   'IF' TG=2 'OR' TG=3 'THEN' 'GOTO' L3D 'ELSE'
242   'BEGIN'
243   'FOR' I:=1 'STEP' 1 'UNTIL' N1 'DO'
243   'BEGIN'
244   Y:=I+N1;
245   'FOR' J:=0 'STEP' 1 'UNTIL' 5 'DO'
245   'BEGIN'
246   K:=1+2*J;
247   W:= J+1;    L:=K+1;
249   D$I,L!:= P$I,W!*B$I,2!;
250   D$Y,L!:= P$Y,W!*B$I,2!;
251   'END';
252   'END';
253   'GOTO' L2D;
254   'END';
255   L3D: 'FOR' I:=1 'STEP' 1 'UNTIL' N1 'DO'
255   'BEGIN'
256   Y:= I+N1;
257   'FOR' J:=0 'STEP' 1 'UNTIL' 5 'DO'
257   'BEGIN'
258   K:=1+2*J;
259   W:=J+1;   L:=K+1;
261   D$I,L!:= P$I,W!*B$I,3!;
262   D$Y,L!:= P$Y,W!*B$I,3!;
263   'END';
264   'END';
265
265   L2D: 'IF' N1=6 'THEN'
265   'BEGIN'
266   INVERT(D,12,V);
267   MATVEC(V,P1,A,12,12);
```

```
268   'GOTO' L3;
269   'END';
270
270   L1S: 'IF' SOL=2 'THEN'  'BEGIN'
271   'FOR' I:=1 'STEP' 1 'UNTIL' N1 'DO'
271   'BEGIN'
272   Y:= I+N1;
273   'FOR' J:=1,2,3,4,5,6 'DO'
273   'BEGIN'
274   D$I,J!:=P$I,J!;
275   D$Y,J!:=P$Y,J!;
276   'END';
277   'END';
278   'END';
279   'IF' X=6 'THEN'  'GOTO' L1C;
280
280   'COMMENT'  ADDITIONAL  PARAMETERS;
281   'IF' SOL=2 'AND' IT=0 'THEN'  'BEGIN'
282   'FOR' I:=1 'STEP' 1 'UNTIL' SN 'DO'
282   'BEGIN'
283   B$I,24!:=B$I,2!;
284   B$I,25!:=B$I,3!;
285   B$I,21!:=B$I,2!*B$I,3!;
286   B$I,22!:=B$I,3!*B$I,2!'**'2;
287   B$I,23!:=B$I,2!*B$I,3!'**'2;
288   B$I,31!:=B$I,2!'**'2;
289   B$I,32!:=B$I,3!'**'2;
290   B$I,26!:=B$I,31!*B$I,32!;
291   B$I,27!:=SQRT(B$I,31!+B$I,32!);
292   'END';
293   'END';
294   'IF' SOL=2 'THEN'  'BEGIN'
295   'FOR' I:=1 'STEP' 1 'UNTIL' N1 'DO'
295   'BEGIN'
296   Y:=I+N1;
297   D$I,7!:=B$I,2!;
298   D$I,8!:=B$I,3!;
299   D$Y,7!:=-B$I,3!;
300   D$Y,8!:=B$I,2!;
301   'END';
302   'IF' X>8 'THEN'  'BEGIN'
303   'FOR' I:=1 'STEP' 1 'UNTIL' N1 'DO'
303   'BEGIN'
304   Y:=I+N1;
305   D$I,9!:=B$I,21!;
306   D$I,10!:=B$I,23!;
307   D$I,11!:=B$I,22!;
308   D$Y,12!:=B$I,21!;
309   D$Y,13!:=B$I,23!;
310   D$Y,14!:=B$I,22!;
311   'END';
312   'END';
313   'IF' X>14 'THEN'  'BEGIN'
314   'FOR' I:=1 'STEP' 1 'UNTIL' N1 'DO'
314   'BEGIN'
315   Y:=I+N1;
316   D$I,15!:=B$I,2!*B$I,27!'**'2;
317   D$I,16!:=B$I,2!*B$I,27!'**'5;
318   D$Y,15!:=B$I,3!*B$I,27!'**'2;
319   D$Y,16!:=B$I,3!*B$I,27!'**'5;
320   'END';
321   'END';
322   'IF' X>16 'THEN'  'BEGIN'
323   'FOR' I:=1 'STEP' 1 'UNTIL' N1 'DO'
323   'BEGIN'
324   Y:=I+N1;
```

```
D$I,17!:=1.0;
D$Y,18!:=1.0;
'END';
'END';
'FOR' I:=1 'STEP' 1 'UNTIL' N1 'DO'
'BEGIN'
Y:=I+N1;
P1$I!:=P1$I!-(Q$7!*D$I,7!+Q$8!*D$I,8!);
P1$Y!:=P1$Y!-(Q$7!*D$Y,7!+Q$8!*D$Y,8!);
'END';
'IF' X>8 'THEN'  'BEGIN'
'FOR' I:=1 'STEP' 1 'UNTIL' N1 'DO'
'BEGIN'
Y:=I+N1;
P1$I!:=P1$I!-(Q$9!*D$I,9!+Q$10!*D$I,10!+Q$11!*D$I,11!);
P1$Y!:=P1$Y!-(Q$12!*D$Y,12!+Q$13!*D$Y,13!+
      Q$14!*D$Y,14!);
'END';
'END';
'IF' X>14 'THEN'  'BEGIN'
'FOR' I:=1 'STEP' 1 'UNTIL' N1 'DO'
'BEGIN'
Y:= I+N1;
P1$I!:=P1$I!-(Q$15!*D$I,15!+Q$16!*D$I,16!);
P1$Y!:=P1$Y!-(Q$15!*D$Y,15!+Q$16!*D$Y,16!);
'END';
'END';
'IF' X>16 'THEN'  'BEGIN'
'FOR' I:=1 'STEP' 1 'UNTIL' N1 'DO'
'BEGIN'
Y:=I+N1;
P1$I!:=P1$I!-Q$17!;
P1$Y!:=P1$Y!-Q$18!;
'END';
'END';
'END';


'COMMENT' COMPUTE THE CORRELATION MATRIX;
'IF' SOL=2  'AND' IT=0  'THEN'  'BEGIN'
'REAL' 'ARRAY' DS$1:M,1:X1!, ST$1:X1,1:M!, VS$1:X1,1:X1!,
CS$1:X1,1:X1!;
'FOR' I:=1 'STEP' 1 'UNTIL' M 'DO'
'FOR' J:=1 'STEP' 1 'UNTIL' X1 'DO'
'BEGIN'
K := J+6;
DS$I,J!:= D$I,K!;
'END';
MATRAN(DS,ST,X1,M);
MATMLT(ST,DS,VS,X1,X1,M);
INVERT(VS,X1,VS);
'FOR' I:=1 'STEP' 1 'UNTIL' X1 'DO'
'BEGIN'
'FOR' J:=1 'STEP' 1 'UNTIL' X1 'DO'
CS$I,J!:=SQRT(VS$I,J!'**'2/(VS$I,I!*VS$J,J!));
'END';
WRITE TEXT('('''('2C')'CORRELATION%%MATRIX%

%OF%%THE%%CALIBRATION%%PARAMETERS'('2C')'')');

'FOR' I:=1 'STEP' 1 'UNTIL' X1 'DO'
'BEGIN'
'FOR' J:=1 'STEP' 1 'UNTIL' X1 'DO'
PRINT(CS$I,J!,1,2);
NEWLINES(2);
'END';
```

```
'END';
L1C: 'FOR' I:=1 'STEP' 1 'UNTIL' X 'DO'
A$I!:=0.00;
'COMMENT' COMPUTATION USING LEAST SQUARE METHOD;
MATRAN(D,DT,X,M);
MATMLT(DT,D,V,X,X,M);
MATVEC(DT,P1,A,M,X);
INVERT(V,X,V);
MATVEC(V,A,A,X,X);
'IF' SOL=2 'THEN'  'BEGIN'
'FOR' I:=1 'STEP' 1 'UNTIL' SN 'DO'
'FOR' J:=1,2,3,4,5,6 'DO'
CR$J,I!:=A$J!;
'GOTO' L2S;
'END';
L3: 'FOR' J:=1,2 'DO'
'BEGIN'
G:=J+2;    W:=J+4;    K:=J+6;
L:=J+8;               Y:=J+10;
A1$1,J!:=A$J!;
A1$2,J!:=A$G!;
A1$3,J!:=A$W!;
A1$4,J!:=A$K!;
A1$5,J!:=A$L!;
A1$6,J!:=A$Y!;
'END';
'COMMENT' CORRECTION VALUES;
'FOR' I:=1,2 'DO'
'FOR' J:=1 'STEP' 1 'UNTIL' SN 'DO'
E$I,J!:=0.00;
'FOR' I:=1 'STEP' 1 'UNTIL' SN 'DO'
E$1,I!:=1.00;
'IF' TG=2 'OR' TG=3 'THEN'  'BEGIN'
'FOR' I:=1 'STEP' 1 'UNTIL' SN 'DO'
E$2,I!:=B$I,3!;
'GOTO' L3C;
'END';
'FOR' I:=1 'STEP' 1 'UNTIL' SN 'DO'
E$2,I!:=B$I,2!;
L3C:MATMLT(A1,E,CR,SN,6,2);
L2S: 'IF' IT=0 'THEN'
'BEGIN'
WRITE TEXT('('''('2C')'CORRECTIONS%TO%ORIENTATION%
ELEMENTS%DURING%SUCCESSIVE%ITERATIONS'('2C')'
ROTATIONS%ARE%GIVEN%IN%RADIANS%WHILE%TRANSLATIONS%
ARE%GIVEN%IN%METERS'('2C')'
PT.NO.'('6S')'D-OMEGA'('10S')'D-PHI'('12S')'
D-KAPA'('10S')'D-XO'('12S')'D-YO'('12S')'D-ZO
                          '('C')'   ')' );
'END';
SPACES(2);
PRINT(B$1,1!,5,0);
SPACES(4);
'FOR' J:=1 'STEP' 1 'UNTIL' 6 'DO'
'BEGIN'
PRINT(CR$J,1!,0,5);
```

```
SPACES(4);
'END';
NEWLINE;


'COMMENT' NEW ORIENTATION ELEMENTS;
 'FOR' I:=1 'STEP' 1 'UNTIL' X 'DO'
Q$I!:=Q$I!+A$I!;
'FOR' I:=1 'STEP' 1 'UNTIL' SN 'DO'
'BEGIN'
'FOR' J:=1,2,3,4,5,6 'DO'
CN$I,J!:=CN$I,J!+CR$J,I!;
'END';

'COMMENT' CHECK WHETHER CORRECTIONS ARE SIGNIFICANT;
'IF' IT=MAXIT 'THEN' 'GOTO' L2A;
'IF' ABS(CR$1,1!) <0.00001 'AND' ABS(CR$2,1!) <
0.00001  'AND' ABS(CP$3,1!) < 0.00001 'AND'
ABS(CR$4,1!) < 0.00001  'AND' ABS(CR$5,1!)<
0.00001  'AND' ABS(CR$6,1!) < 0.00001
'THEN'  'GOTO' L2A;
IT:=IT+1;
'GOTO' L2;

L2A:
WRITETEXT('('''('2C')'NUMBER % OF % ITERATIONS'('2S')'
                                                  ')')');
PRINT(IT,2,0);
NEWLINES(2);
WRITE TEXT('('NUMBER%%OF %% CONTROLS '('2S')'
                                    ')')');
PRINT(N1,2,0);
NEWLINES(2);
'IF' SOL=1 'THEN'  'BEGIN'
WRITE TEXT('('''('2C')'CORRECTION%PARAMETERS%FOR%THE%

POINT%BY%POINT%RESECTION'('2C')'')')');
'FOR' I:=1,2 'DO'
'BEGIN'
G:=I+2;  W:=I+4;  K:=I+6;
L:=I+8;            Y:=I+10;
PRINT(Q$I!,0,8);
SPACES(2);
PRINT(Q$G!,0,8);
SPACES(2);
PRINT(Q$W!,0,8);
SPACES(2);
PRINT(Q$K!,0,8);
SPACES(2);
PRINT(Q$L!,0,8);
SPACES(2);
PRINT(Q$Y!,0,8);
NEWLINE;
'END';
'END';
'IF' SOL=1 'AND' TG=3  'THEN'  'BEGIN'
TG:=1;
'GOTO' L1A;
'END';
'IF' SOL=2 'AND' X>6 'THEN'  'BEGIN'
WRITE TEXT('('''('2C')'SELF % CALIBRATION %

PARAMETERS'('2C')'')')');
'FOR' I:=7 'STEP' 1 'UNTIL' X 'DO'
'BEGIN'
PRINT(Q$I!,0,5);
```

```
465     NEWLINE;
466     'END';
467     'FOR' I:=1 'STEP' 1 'UNTIL' SN 'DO'
467     'BEGIN'
468     B$I,2!:=B$I,2!+(Q$7!*B$I,24!+Q$8!*B$I,25!);
469     B$I,3!:=B$I,3!+(-Q$7!*B$I,25!+Q$8!*B$I,24!);
470     'END';
471     'IF' X>8 'THEN'  'BEGIN'
472     'FOR' I:=1 'STEP' 1 'UNTIL' SN 'DO'
472     'BEGIN'
473     B$I,2!:=B$I,2!+Q$9!*B$I,21!+Q$10!*B$I,23!+Q$11!*B$I,22!;
474     B$I,3!:=B$I,3!+Q$12!*B$I,21!+Q$13!*B$I,23!+Q$14!*B$I,22!;
475     'END';
476     'END';
477     'IF' X>14 'THEN'  'BEGIN'
478     'FOR' I:=1 'STEP' 1 'UNTIL' SN 'DO'
478     'BEGIN'
479     B$I,2!:=B$I,2!+Q$15!*B$I,24!*B$I,27!'**'2+
479           Q$16!*B$I,24!*B$I,27!'**'5;
480     B$I,3!:=B$I,3!+Q$15!*B$I,25!*B$I,27!'**'2+
480            Q$16!*B$I,25!*B$I,27!'**'5;
481     'END';
482     'END';
483     'IF' X>16 'THEN'  'BEGIN'
484     'FOR' I:=1 'STEP' 1 'UNTIL' SN 'DO'
484     'BEGIN'
485     B$I,2!:=B$I,2!+Q$17!;
486     B$I,3!:=B$I,3!+Q$18!;
487     'END';
488     'END';
489     'END';
490     'FOR' I:=1 'STEP' 1 'UNTIL' N 'DO'
490     'FOR' J:=1,2,3,4,5,6 'DO'
490     C$I,J!:=0.00;
491     'FOR' I:=1 'STEP' 1 'UNTIL' N 'DO'
491     'FOR' J:=1 'STEP' 1 'UNTIL' 36 'DO'
491     AC$I,J!:=0.00;
492     'FOR' I:=1 'STEP' 1 'UNTIL' H 'DO'
492     'FOR' J:=1,2,3 'DO'
492     'BEGIN'
493     Y:= I+NH;    G:=J+3;
495     C$I,J!:=SIN(CN$Y,J!);
496     C$I,G!:=COS(CN$Y,J!);
497     'END';
498
498
498     'COMMENT' COMPUTE THE ORIENTATION FACTORS
498               FOR THE  INTERSECTION  PHASE;
499     'FOR' I:=1 'STEP' 1 'UNTIL' H 'DO'
499     'BEGIN'
500     AC$I,1!:=C$I,5!*C$I,6!;
501     AC$I,2!:=C$I,4!*C$I,3!+C$I,1!*C$I,2!*C$I,6!;
502     AC$I,3!:=C$I,1!*C$I,3!-C$I,4!*C$I,2!*C$I,6!;
503     AC$I,4!:=-C$I,5!*C$I,3!;
504     AC$I,5!:=C$I,4!*C$I,6!-C$I,1!*C$I,2!*C$I,3!;
505     AC$I,6!:=C$I,1!*C$I,6!+C$I,4!*C$I,2!*C$I,3!;
506     AC$I,7!:=C$I,2!;
507     AC$I,8!:=-C$I,1!*C$I,5!;
508     AC$I,9!:=C$I,4!*C$I,5!;
509     'END';
510     'FOR' I:=1 'STEP' 1 'UNTIL' N 'DO'
510     'FOR' J:=7,8,9 'DO'
510     B$I,J!:=0.00;
511     'FOR' I:=1 'STEP' 1 'UNTIL' H 'DO'
511     'FOR' J:=1,2,3 'DO'
511     'BEGIN'
```

```
512   Y:= I+NH;  G:=J+3;  K:=J+6;
515   B$I,K!:=AC$I,J!*B$Y,2!+AC$I,G!*B$Y,3!-
515                   FL*AC$I,K!;
516   'END';
517   'IF' PH=1 'THEN' 'GOTO' L4 'ELSE' 'GOTO' L5;
518   L4: 'FOR' I:=1 'STEP' 1 'UNTIL' H 'DO'
518   'BEGIN'
519   'FOR' J:=4,5,6 'DO'
519   'BEGIN'
520   Y:= I+NH;     G:=J+3;    K:=J+6;
523   B$I,K!:=B$I,G!;
524   CN$I,K!:=CN$Y,J!;
525   'END';
526   'END';
527   PH:=2;  'GOTO' L1;
529
529   'COMMENT'  INTERSECTION  PHASE;
530   L5: 'FOR' I:=1 'STEP' 1 'UNTIL' H 'DO'
530   'BEGIN'
531   'FOR' J:=4,5,6 'DO'
531   'BEGIN'
532   Y:= I+NH;    G:=J+3;    K:=J+9;
535   B$I,K!:= B$I,G!;
536   CN$I,K!:=CN$Y,J!;
537   'END';
538   'END';
539
539   'COMMENT' SCALE FACTOR;
540   'FOR' I:=1 'STEP' 1 'UNTIL' H 'DO'
540   'BEGIN'
541   CN$I,16!:=B$I,10!*B$I,15!-B$I,13!*B$I,12!;
542   CN$I,17!:=CN$I,13!-CN$I,10!;
543   CN$I,18!:=CN$I,15!-CN$I,12!;
544   'END';
545   'FOR' I:=1 'STEP' 1 'UNTIL' H 'DO'
545   'BEGIN'
546   CN$I,19!:=(CN$I,17!*B$I,15!-CN$I,18!*B$I,13!)/CN$I,16!;
547   CN$I,20!:=(CN$I,18!*B$I,10!-CN$I,17!*B$I,12!)/CN$I,16!;
548   'END';
549
549
549   'COMMENT' GROUND COORDINATES;
550   'FOR' I:=1 'STEP' 1 'UNTIL' H 'DO'
550   'FOR' J:=1,2,3 'DO'
550   'BEGIN'
551   K:=J+4;  G:=J+7;   Y:=J+9;  W:=J+12;
555   GC$I,K!:=CN$I,Y!+B$I,Y!*ABS(CN$I,19!);
556   GC$I,G!:=CN$I,W!+B$I,W!*ABS(CN$I,20!);
557   'END';
558   'FOR' I:=1 'STEP' 1 'UNTIL' H 'DO'
558   'FOR' J:=5,6,7 'DO'
558   'BEGIN'
559   K:= J+6;    L:=J+3;
561   GC$I,K!:=(GC$I,J!+GC$I,L!)/2.00;
562   'END';
563   'FOR' I:=1 'STEP' 1 'UNTIL' H 'DO'
563   'FOR' J:=2,3,4 'DO'
563   'BEGIN'
564   K:=J+12;     L:=J+9;
566   GC$I,K!:=GC$I,L!-GC$I,J!;
567   'END';
568   NEWLINES(5);
569   WRITE TEXT('(''('P')'MODEL%%NUMBER'('4S')'')');
570   PRINT(MD,6,0);
571   NEWLINES(3);
572   WRITE TEXT('(''('2C')'FINAL%%RESULTS'('2C')'
```

```
572
572    THE % COMPUTED % GROUND % COORDINATES %
572
572    X, % Y, % AND % Z , % AND  '('C')'
572
572    THEIR % DEVIATIONS % DX, % DY , % AND % DZ %
572
572    % ARE % GIVEN % IN % METERS '('2C')'
572
572                            ')')';
573
573    WRITE TEXT('('POINT % NUMBER'('6S')' X
573
573    '('14S')'  Y                     '('18S')'
573
573    Z'('11S')' DX'('11S')' DY'('11S')' DZ
573
573                               '('2C')'')')';
574    'FOR' I:=1 'STEP' 1 'UNTIL' H 'DO'
574    'BEGIN'
575    SPACES(2);
576    PRINT(GC$I,1!,5,0);
577    SPACES(3);
578    'FOR' J:=11,12,13 'DO'
578    'BEGIN'
579    PRINT(GC$I,J!,8,3);
580    SPACES(3);
581    'END';
582    'FOR' J:=14,15,16 'DO'
582    'BEGIN'
583    PRINT(GC$I,J!,5,3);
584    SPACES(3);
585    'END';
586    NEWLINES(2);
587    'END';
588
588    'COMMENT'  ACCURACY OF THE RESULTS;
589    'FOR' J:=1 'STEP' 1 'UNTIL' 9 'DO'
589    S$J!:=0.00;
590    'FOR' J:=1,2,3 'DO'
590    'BEGIN'
591    K:= J+13;
592    'FOR' I:=1 'STEP' 1 'UNTIL' H 'DO'
592    S$J!:=S$J!+GC$I,K!'**'2;
593    'END';
594    'FOR' J:=1,2,3 'DO'
594    'BEGIN'
595    Y:= J+3;
596    S$Y!:=SQRT(S$J!/H);
597    'END';
598    'FOR' J:=4,5 'DO'
598    'BEGIN'
599    Y:=J+3;
600    S$Y!:=(S$J!*10.0'**'6)/ABS(CN$1,19!);
601    'END';
602    S$9!:=(S$6!*BH*10.0'**'6)/ABS(CN$1,19!);
603    WRITE TEXT('('''('2C')'THE%ROOT%MEAN%SQUAR%ERRORS%
603
603    OF  %%  THE % DISCREPANCIES '('C')' AT % THE %
603
603    GROUND % SCALE % IN% METERS '('2C')'
603
603    RMSE X'('10S')'RMSE Y'('8S')'RMSE Z'('2C')'')')';
604
```

```
605     PRINT(S$I!,3,3);
606     SPACES(4);
607     'END';
608     WRITE TEXT('('('2C')'THE%ROOT%MEAN%SQUARE%ERRORS%
608
608     OF  %%  THE % DISCREPANCIES '('C')' AT % THE %
608
608     IMAGE % SCALE % IN% MICRONS '('2C')'
608
608     RMSE X'('10S')'RMSE Y'('8S')'RMSE Z'('2C')'')');
609
609     'FOR' I:=7,8,9 'DO'
609     'BEGIN'
610     PRINT(S$I!,3,0);
611     SPACES(10);
612     'END';
613     'END';
614     'GOTO' L0;
615     L6: 'END';
616     'END';
```

3.6 Input

56 — No. of test points

47933 — Model number

0.47 — B/H ratio

27 — No. of check points
29 — No. of control points

0 — No. of control points outside model area

47933 No. of first photo.

1 — Tag to indicate direction of shutter motion
6 — Maximum number of iterations

2 — Type of solution
18 — No. of unknown parameters

0.156135 — Principal distance

	Photo-coordinates		Ground coordinates		
Pt.No.	x	y	X	Y	Z
1709	0.115251	-0.070747	515824.750	103435.250	0.988
1713	-0.010154	0.099469	512625.000	106222.125	71.221
1707	0.110225	-0.052074	515640.750	103782.750	6.483
1706	0.112527	-0.056253	515703.250	103710.250	6.776
1726	0.104866	-0.027276	515428.875	104248.250	3.673
1727	0.106968	-0.025342	515462.125	104295.000	2.483
1728	0.104284	-0.025842	515411.000	104275.250	3.188
1725	0.082455	-0.049686	515087.750	103709.812	4.503
1703	0.084329	-0.073246	515221.750	103253.812	13.424
1710	0.075344	-0.093831	515133.875	102809.500	19.334
1701	0.029946	-0.076704	514170.625	102943.875	10.140
1702	0.035480	-0.072287	514261.500	103055.375	7.788
1705	-0.010918	-0.092278	513428.250	102455.688	17.988
1732	-0.029753	-0.017685	512730.000	103854.000	13.564
1733	-0.030350	-0.018535	512721.625	103834.750	14.172
1734	-0.030942	-0.019361	512713.250	103815.500	14.555
1731	0.014449	-0.004738	513551.500	104305.125	15.671
1711	-0.010966	0.012898	512971.000	104542.875	17.567
1724	0.038453	-0.030021	514134.375	103907.875	14.309
1722	0.047436	-0.038205	514349.000	103785.625	8.592
1723	0.045833	-0.039783	514323.313	103746.687	10.479
1720	0.074741	0.015456	514648.125	104960.125	12.651
1721	0.081296	0.012094	514792.250	104921.875	9.973
1719	0.087032	0.048821	514730.375	105655.250	39.376
1718	0.086103	0.048413	514714.625	105644.750	38.879
1716	0.046073	0.024644	514044.875	105019.000	17.350
1714	0.011842	0.096946	513061.125	106290.500	26.739
1704	-0.015499	-0.094230	513346.000	102387.500	6.401
1715	0.011633	0.096524	513058.750	106281.250	27.464
3769	-0.019341	0.015496	512793.139	104558.264	14.600

3767	-0.011457	0.045038	512822.701	105175.811	18.600
3766	-0.008400	0.047995	512870.483	105247.250	19.200
3770	0.025031	0.012072	513686.029	104681.980	15.850
3771	0.031171	0.011038	513811.602	104687.849	14.940
3762	0.047788	0.006040	514160.637	104660.475	13.200
3702	0.055818	0.006559	514316.788	104705.573	11.400
3775	0.081707	0.020669	514762.513	105092.900	11.900
3774	0.087637	0.020044	514881.326	105105.679	11.000
3710	0.082004	-0.026323	514975.887	104169.300	6.600
3735	0.079339	-0.040848	514987.498	103870.730	5.300
3729	0.093612	-0.052803	515320.672	103696.166	3.960
3751	0.102683	-0.033318	515412.107	104120.200	3.400
3750	0.098033	-0.025541	515286.512	104253.634	4.600
3728	0.093922	-0.028300	515218.037	104181.526	4.900
3761	0.043127	-0.028424	514219.948	103959.502	9.100
3760	0.041196	-0.045795	514258.362	103606.545	7.500
3714	-0.015065	-0.026691	513060.480	103739.284	10.970
3713	-0.003679	-0.039247	513341.296	103539.481	8.530
3759	-0.014975	-0.071237	513255.985	102852.239	10.600
3758	-0.015150	-0.078113	513282.422	102712.536	8.800
3757	-0.016088	-0.093892	513332.738	102390.822	6.100
3772	0.014691	-0.069140	513836.013	103025.991	9.750
3755	0.031712	-0.095298	514288.454	102579.237	5.790
3754	0.041011	-0.096682	514478.593	102593.168	6.100
3752	0.083623	-0.085159	515265.436	103012.733	7.300
3753	0.108245	-0.083834	515740.425	103147.889	7.000

0.00 0.00 0.00 Approximate rotation elements (ω, Φ, χ)

513250.000 104300.000 3100.000 Approximate translational element X_o, Y_o, Z_o

(second photo)

29 — No. of control points (second photo)

0 — No. of control points outside model area

47934 — No. of second photo

— Tag indicating direction of shutter motion

1 6 — Maximum no. of iterations

— Tag indicating type of solution

2 18 — No. of unknown parameters

0.156135 — Principal distance

Pt. No.	Photo-coordinates		Ground coordinates		
1709	0.034844	-0.069971	515824.750	103435.250	0.988
1713	-0.089514	0.096898	512625.000	106222.125	71.221
1707	0.029660	-0.051406	515640.750	103782.750	6.483
1706	0.031939	-0.055570	515703.250	103710.250	6.776
1726	0.024343	-0.026885	515428.875	104248.250	3.673
1727	0.026431	-0.024955	515462.125	104295.000	2.483
1728	0.023778	-0.025458	515411.000	104275.250	3.188
1725	0.002426	-0.048954	515087.750	103709.812	4.503
1703	0.004129	-0.072278	515221.750	103253.812	13.424
1710	-0.004753	-0.092621	515133.875	102809.500	19.334

1701	-0.048911	-0.075455	514170.625	102943.875	10.140
1702	-0.043475	-0.071125	514261.500	103055.375	7.788
1705	-0.088734	-0.090558	513428.250	102455.688	17.988
1732	-0.106849	-0.017352	512730.000	103854.000	13.564
1733	-0.107438	-0.018192	512721.625	103834.750	14.172
1734	-0.108017	-0.019002	512713.250	103815.500	14.555
1731	-0.064235	-0.004660	513551.500	104305.125	15.671
1711	-0.088867	0.012547	512971.000	104542.875	17.567
1724	-0.040849	-0.029501	514134.375	103907.875	14.309
1722	-0.031937	-0.037559	514349.000	103785.625	8.592
1723	-0.033541	-0.039141	514323.313	103746.687	10.479
1720	-0.005576	0.015247	514648.125	104960.125	12.651
1721	0.000911	0.011937	514792.250	104921.875	9.973
1719	0.005612	0.048046	514730.375	105655.250	39.376
1718	0.004719	0.047637	514714.625	105644.750	38.879
1716	-0.033659	0.024204	514044.875	105019.000	17.350
1714	-0.067204	0.094651	513061.125	106290.500	26.739
1704	-0.092879	-0.092474	513346.000	102387.500	6.401
1715	-0.067423	0.094229	513058.750	106281.250	27.464
3769	-0.096857	0.015067	512793.139	104558.264	14.600
3767	-0.089380	0.043904	512822.701	105175.811	18.600
3766	-0.086442	0.046812	512870.483	105247.250	19.200
3770	-0.054012	0.011832	513686.029	104681.980	15.850
3771	-0.048040	0.010821	513811.602	104687.849	14.940
3762	-0.031833	0.005928	514160.637	104660.475	13.200
3702	-0.023956	0.006478	514316.788	104705.573	11.400
3775	0.001254	0.020378	514762.513	105092.900	11.900
3774	0.007069	0.019775	514881.326	105105.679	11.000
3710	0.001850	-0.025893	514975.887	104169.300	6.600
3735	-0.000694	-0.040233	514987.498	103870.730	5.300
3729	0.013399	-0.052072	515320.672	103696.166	3.960
3751	0.022208	-0.032826	515412.107	104120.200	3.400
3750	0.017582	-0.025136	515286.512	104253.634	4.600
3728	0.013550	-0.027862	515218.037	104181.526	4.900
3761	-0.036195	-0.027946	514219.948	103959.502	9.100
3760	-0.037974	-0.045037	514258.362	103606.545	7.500
3714	-0.092631	-0.026166	513060.480	103739.284	10.970
3713	-0.081590	-0.038496	513341.296	103539.481	8.530
3759	-0.092511	-0.069860	513255.985	102852.239	10.600
3758	-0.092584	-0.076596	513282.422	102712.536	8.800
3757	-0.093416	-0.092138	513332.738	102390.822	6.100
3772	-0.063751	-0.067957	513836.013	103025.991	9.750
3755	-0.047042	-0.093825	514288.454	102579.237	5.790
3754	-0.037957	-0.095235	514478.593	102593.168	6.100
3752	0.003650	-0.084082	515265.436	103012.733	7.300
3753	0.027832	-0.082870	515740.425	103147.889	7.000

0.00 0.00 0.00 ——— Approximate rotation elements (second photo)

514980.000 104600.000 3100.000 ——— Approximate translational elements

0 ——————— Tag indicating that last model is tested.

3.7 Output

I.M.ELHASSAN GEOGRAPHY DEPT.

SPACE RESECTION INTERSECTION PROGRAM

PHOTO NUMBER 47933

CORRELATION MATRIX OF THE CALIBRATION PARAMETERS

1.00	0.00	0.03	0.25	0.02	0.11	0.03	0.05	0.21	0.14	0.40	0.06
0.00	1.00	0.04	0.01	0.13	0.08	0.33	0.14	0.06	0.14	0.08	0.30
0.03	0.04	1.00	0.50	0.93	0.23	0.28	0.33	0.41	0.59	0.26	0.19
0.25	0.01	0.50	1.00	0.39	0.18	0.22	0.26	0.13	0.38	0.22	0.14
0.02	0.13	0.93	0.39	1.00	0.29	0.39	0.43	0.50	0.74	0.25	0.17
0.11	0.08	0.23	0.18	0.29	1.00	0.43	0.89	0.36	0.40	0.08	0.25
0.03	0.33	0.28	0.22	0.39	0.43	1.00	0.28	0.39	0.50	0.09	0.35
0.05	0.14	0.33	0.26	0.43	0.89	0.28	1.00	0.38	0.53	0.12	0.24
0.21	0.06	0.41	0.13	0.50	0.36	0.39	0.38	1.00	0.86	0.45	0.19
0.14	0.14	0.59	0.38	0.74	0.40	0.50	0.53	0.86	1.00	0.34	0.23
0.40	0.08	0.26	0.22	0.25	0.08	0.09	0.12	0.45	0.34	1.00	0.07
0.06	0.30	0.19	0.14	0.17	0.25	0.35	0.24	0.19	0.23	0.07	1.00

CORRECTIONS TO ORIENTATION ELEMENTS DURING SUCCESSIVE ITERATIONS

ROTATIONS ARE GIVEN IN RADIANS WHILE TRANSLATIONS ARE GIVEN IN METERS

PT.NO.	D-OMEGA	D-PHI	D-KAPA	D-XO	D-YO	D-ZO
1709	-8.57061@ -3	1.44663@ -2	2.18438@ -1	-3.55252@ 1	3.40563@ 0	1.55026@ 2
1709	2.36979@ -4	-1.44556@ -4	-3.29350@ -3	-3.97960@ -2	2.29583@ 1	-7.36271@ 1
1709	2.01174@ -7	-5.37333@ -7	2.04752@ -6	1.80302@ 0	8.03427@ -1	-5.33979@ -2
1709	1.51605@-11	3.57321@-10	-5.34338@-10	4.85199@ -4	2.44342@ -4	-3.11609@ -5
1709	7.88288@-14	-5.40446@-13	2.11598@-12	5.19404@ -7	2.21132@ -7	3.62596@ -9

NUMBER OF ITERATIONS 4

NUMBER OF CONTROLS 29

SELF CALIBRATION PARAMETERS

```
 5.53742@ -4
 1.85473@ -6
-1.18578@ -3
-6.67737@ -2
-1.91417@ -2
 1.07938@ -2
 2.07090@ -2
 3.39444@ -2
 2.75294@ -2
 1.66679@  1
 3.91567@ -3
 8.77834@ -4
```

PHOTO NUMBER 47934

CORRFLATION MATRIX OF THE CALIBRATION PARAMETERS

1.00	0.13	0.32	0.08	0.32	0.07	0.18	0.38	0.01	0.27	0.24	0.27
0.13	1.00	0.02	0.09	0.26	0.27	0.40	0.01	0.20	0.04	0.35	0.39
0.32	0.02	1.00	0.32	0.93	0.02	0.02	0.28	0.26	0.41	0.37	0.03
0.08	0.09	0.32	1.00	0.39	0.00	0.03	0.46	0.22	0.66	0.15	0.13
0.32	0.26	0.93	0.39	1.00	0.05	0.08	0.30	0.20	0.44	0.27	0.05
0.07	0.27	0.02	0.00	0.05	1.00	0.04	0.70	0.20	0.09	0.13	0.42
0.18	0.40	0.02	0.03	0.08	0.04	1.00	0.02	0.12	0.09	0.14	0.28
0.38	0.01	0.28	0.46	0.30	0.70	0.02	1.00	0.22	0.53	0.11	0.26
0.01	0.20	0.26	0.22	0.20	0.20	0.12	0.22	1.00	0.77	0.37	0.41
0.27	0.04	0.41	0.66	0.44	0.09	0.09	0.53	0.77	1.00	0.22	0.26
0.24	0.35	0.37	0.15	0.27	0.13	0.14	0.11	0.37	0.22	1.00	0.16
0.27	0.39	0.03	0.13	0.05	0.42	0.28	0.26	0.41	0.26	0.16	1.00

CORRFCTIONS TO ORIENTATION ELEMENTS DURING SUCCESSIVE ITERATIONS

ROTATIONS ARE GIVEN IN RADIANS WHILE TRANSLATIONS ARE GIVEN IN METERS

PT.NO.	D-OMEGA	D-PHI	D-KAPA	D-XO	D-YO	D-ZO
1709	-4.71294@ -3	2.56859@ -2	2.17400@ -1	-1.11297@ 2	1.08124@ 2	1.75432@ 2
1709	-1.33744@ -4	-4.85661@ -4	-3.32922@ -3	-2.59359@ 1	-6.95727@ 0	-7.01839@ 1
1709	1.69379@ -7	-3.44890@ -7	-9.34645@ -7	1.37872@ 0	-5.31750@ -2	-7.79551@ -2
1709	8.19581@-12	-2.72654@-10	1.97622@ -9	8.44953@ -4	-8.17053@ -5	-3.05637@ -5
1709	-8.76081@-14	1.93854@-13	3.06483@-13	1.82009@ -7	-1.18610@ -8	-1.31020@ -8

NUMBER OF ITERATIONS 4

NUMBER OF CONTROLS 29

SELF CALIBRATION PARAMETERS

-3.50404@ -4
-1.47399@ -4
-1.41930@ -2
-5.56061@ -2
-8.43119@ -2
1.48468@ -2
6.97188@ -2
3.01939@ -2
1.05997@ -1
-1.23479@ 1
2.92603@ -3
-9.33055@ -4

MODEL NUMBER 47933

FINAL RESULTS

THE COMPUTED GROUND COORDINATES X, Y, AND Z, AND
THEIR DEVIATIONS DX, DY, AND DZ ARE GIVEN IN METERS

POINT NUMBER	X	Y	Z	DX	DY	DZ
1709	515824.981	103434.482	1.144	0.231	-0.768	0.156
1713	512625.163	106222.214	71.266	0.163	0.089	0.045
1707	515640.071	103783.167	6.490	-0.679	0.417	0.007
1706	515703.224	103710.556	6.721	-0.026	0.306	-0.055
1726	515428.628	104248.546	3.577	-0.247	0.296	-0.096
1727	515461.881	104295.911	2.583	-0.244	0.911	0.100
1728	515411.276	104274.403	3.138	0.276	-0.847	-0.050
1725	515087.973	103709.509	4.539	0.223	-0.303	0.036
1703	515222.624	103253.999	13.215	0.874	0.187	-0.209
1710	515133.542	102809.806	19.243	-0.333	0.306	-0.091
1701	514170.890	102944.125	10.358	0.265	0.250	0.218
1702	514261.609	103055.546	7.958	0.109	0.171	0.170
1705	513428.240	102455.020	18.164	-0.010	-0.668	0.176
1732	512729.591	103854.496	13.559	-0.409	0.496	-0.005
1733	512721.439	103834.955	14.072	-0.186	0.205	-0.100
1734	512713.261	103815.959	14.430	0.011	0.459	-0.125
1731	513550.969	104304.009	15.567	-0.531	-1.116	-0.104
1711	512971.602	104542.794	17.434	0.602	-0.081	-0.133
1724	514134.109	103908.179	14.321	-0.266	0.304	0.012
1722	514348.293	103784.685	8.730	-0.707	-0.940	0.138
1723	514323.069	103746.406	10.307	-0.244	-0.281	-0.172
1720	514648.453	104960.403	12.716	0.328	0.278	0.065
1721	514792.468	104922.497	9.945	0.218	0.622	-0.028
1719	514730.334	105655.746	39.372	-0.041	0.496	-0.004
1718	514714.404	105644.141	38.816	-0.221	-0.609	-0.063
1716	514045.801	105018.525	17.272	0.926	-0.475	-0.078

1714	513060.922	106290.606	26.894	-0.203	0.106	0.155
1704	513346.216	102387.968	6.362	0.216	0.468	-0.039
1715	513058.658	106280.978	27.535	-0.092	-0.272	0.071
3769	512793.677	104558.327	14.179	0.538	0.063	-0.421
3767	512823.349	105175.588	17.925	0.648	-0.223	-0.675
3766	512871.230	105246.975	18.168	0.747	-0.275	-1.032
3770	513686.964	104681.528	15.498	0.935	-0.452	-0.352
3771	513812.488	104687.399	14.869	0.886	-0.450	-0.071
3762	514161.363	104660.016	12.937	0.726	-0.459	-0.263
3702	514317.407	104705.114	10.832	0.619	-0.459	-0.568
3775	514762.628	105092.623	10.994	0.115	-0.277	-0.906
3774	514881.321	105105.525	10.523	-0.005	-0.154	-0.477
3710	514975.909	104169.253	6.251	0.022	-0.047	-0.349
3735	514987.529	103870.736	5.757	0.031	0.006	0.457
3729	515320.551	103696.239	3.812	-0.121	0.073	-0.148
3751	515411.907	104120.341	4.448	-0.200	0.141	1.048
3750	515286.345	104253.698	5.425	-0.167	0.064	0.825
3728	515217.919	104181.558	5.741	-0.118	0.032	0.841
3761	514220.490	103959.419	9.895	0.542	-0.083	0.795
3760	514258.803	103606.665	7.800	0.441	0.120	0.300
3714	513061.023	103739.697	11.345	0.543	0.413	0.375
3713	513341.914	103539.885	10.158	0.618	0.404	1.628
3759	513256.289	102852.921	11.527	0.304	0.682	0.927
3758	513282.805	102713.304	8.002	0.383	0.768	-0.798
3757	513333.039	102391.250	5.018	0.301	0.428	-1.082
3772	513836.317	103026.366	10.160	0.304	0.375	0.410
3755	514288.468	102579.465	6.063	0.014	0.228	0.273
3754	514478.492	102593.386	5.435	-0.101	0.218	-0.665
3752	515265.265	103012.536	6.806	-0.171	-0.197	-0.494
3753	515740.183	103147.842	8.318	-0.242	-0.047	1.318

THE ROOT MEAN SQUAR ERRORS OF THE DISCREPANCIES
AT THE GROUND SCALE IN METERS

RMSEX	RMSEY	RMSEZ
0.423	0.436	0.523

THE ROOT MEAN SQUARE ERRORS OF THE DISCREPANCIES
AT THE IMAGE SCALE IN MICRONS

RMSEX	RMSEY	RMSEZ
21	22	12

4. Program (E) - Plot discrepancies

4.1 Definition of variables

N	-	Number of points to be plotted.
ARRAY		
B	-	Array containing the point number, the ground coordinates and the discrepancies.

4.2 Point numbering

As in the case of the absolute orientation program (Program C), each point has a system of two numbers. The first number is to be read in column 1 of array (B). This indicates the serial number of the point. This second number which classifies the point, is read in column 2 of array (B). A control point is classified by the number 2 and the check point is classified by the number 3.

4.3 Flow diagram

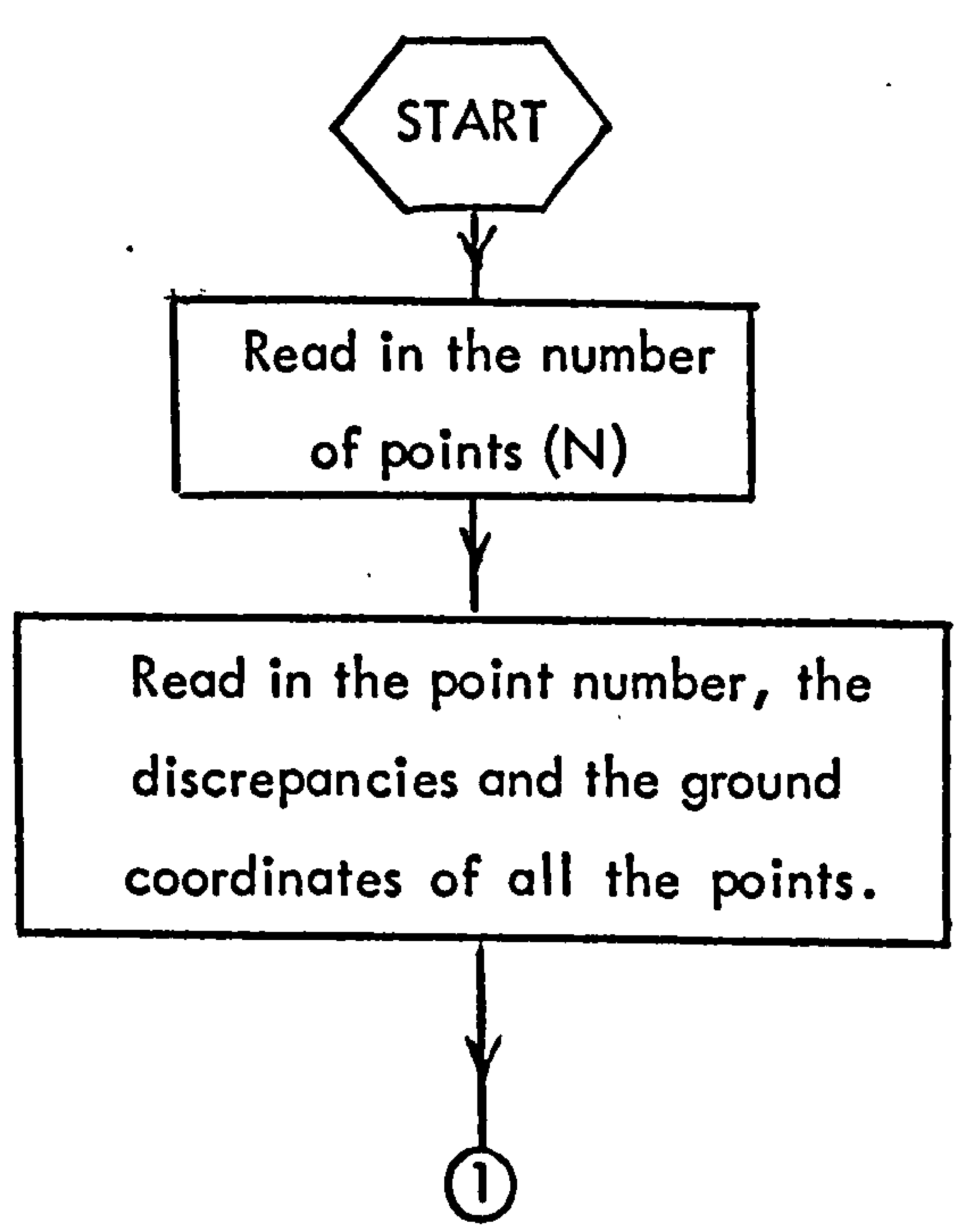

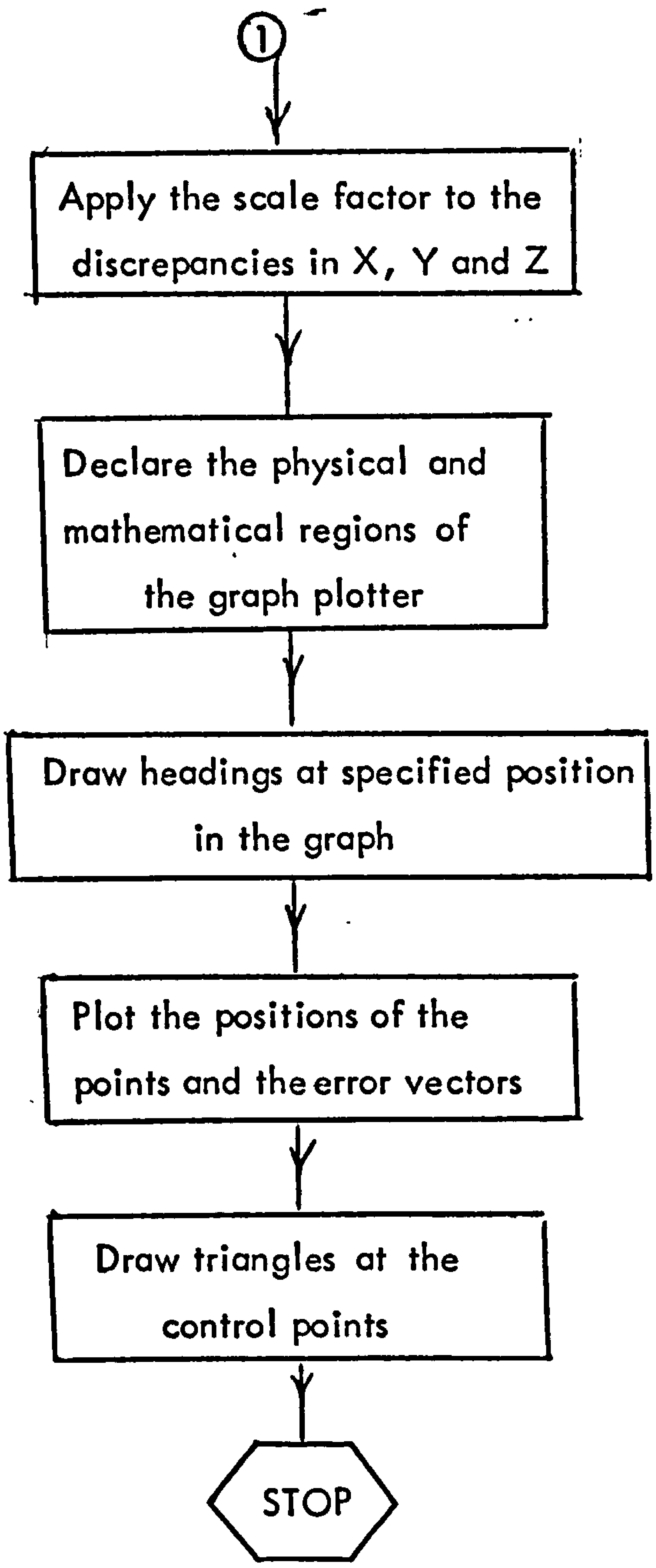

4.4 <u>Detailed account of the program</u>

A step-by-step account of the program follows:

Declarations.

Read in the number of points to be plotted.

Declarations.

Read in the point number, the discrepancies and the ground coordinates.

Multiply the discrepancies by an appropriate scale factor.

Call Algol subroutine to switch on the plotter.

Declarations of the physical regions, the border limits and the mathematical limits of the plotter output.

Call Algol subroutines to draw the heading in specified size, and in specified position in the graph.

Call Algol subroutine to draw the point number in specified size.

Plot all test points and their error vectors (control points are plotted in red pen).

Draw small triangles at the control points.

Call Algol subroutine to terminate the current plot.

```
'BEGIN'
'INTEGER' I,J,N,K;
N:=READ;
'BEGIN'
'REAL' 'ARRAY' B 1:N,1:6?, X 1:N?,
         Y 1:N?,    DY 1:N?;
'FOR' I:=1 'STEP' 1 'UNTIL' N 'DO'
'FOR' J:=1 'STEP' 1 'UNTIL' 6 'DO'
B I,J?:=READ;
'FOR' I:=1 'STEP' 1 'UNTIL' N 'DO'
'BEGIN'
X I?:=B I,4?;
Y I?:=B I,5?;
DY I?:=B I,3?*131,50;
'END';
PAPER(1);
PSPACE(0,10,0,75,0,10,0,75);
MAP(512000,0,516500,0,102000,0,106500,0);
SCALES;                BORDER;
ITALIC(1);     PLACE(12,3);
TYPECS('('VECTOR MAP OF HEIGHT ERRORS')',29);
CTRMAG(10);    ITALIC(0);     PLACE(30,9);
TYPECS('('MODEL NUMBER 7 ** PHOTO SCALE  1/20000')',38);
PLACE(28,11);
TYPECS('('MAP SCALE 1/26300  ** VECTOR SCALE 1/200')',40);
PLACE(40,13);
TYPECS('('SOLUTION NUMBER A1')',18);
CTRMAG(5);
'FOR' I:=1 'STEP' 1 'UNTIL' N 'DO'
'BEGIN'    J:=B I,1?;
PLOTNI(X I?,Y I?,J);
'END';
K:=1;
L1: 'FOR' I:=1 'STEP' 1 'UNTIL' N 'DO'
'BEGIN'
'IF' B I,2?=3 'THEN'  'BEGIN'
POINT(X I?,Y I?);
LINE(0,00,DY I?);
'END';              'END';
K:=K+1;      'IF' K=2 'THEN' 'GOTO' L1;
CTRSET(4);    REDPEN;
K:=1;
L2: 'FOR' I:=1 'STEP' 1 'UNTIL' N 'DO'
'BEGIN'
'IF' B I,2?=2 'THEN'  'BEGIN'
POINT(X I?,Y I?);
PLOTNC(X I?,Y I?,50);
LINE(0,00,DY I?);
'END';    'END';
K:=K+1;    'IF' K=2  'THEN'  'GOTO' L2;
GREND;
'END';     'END'
```

4.6 Input

28 ———————————No. of points to be plotted

Pt.No.		dZ	X	Y
69	2	-0.776	512793.359	104558.283
67	2	0.427	512822.997	105175.547
66	3	0.217	512870.799	105246.926
2	3	-0.584	514316.769	104705.388
28	3	0.180	515218.269	104181.888
53	2	0.461	515740.616	103148.150
58	3	-1.258	513281.838	102712.815
70	2	-0.181	513685.980	104681.625
71	3	0.122	513811.539	104687.519
62	2	-0.059	514160.594	104660.220
3	3	0.470	514163.575	104561.162
75	3	-0.297	514762.742	105093.197
74	2	0.130	514881.601	105106.141
10	3	-1.035	514975.991	104169.396
35	3	-0.107	514987.486	103870.704
29	2	-0.774	515320.805	103696.336
51	3	0.224	515412.437	104120.751
50	2	0.090	515286.803	104254.103
61	2	0.198	514219.697	103959.175
60	3	-0.330	514258.030	103606.151
14	3	-0.779	513060.335	103739.438
13	2	0.588	513341.002	103539.462
59	2	0.382	513255.453	102852.531
57	2	-0.378	513331.996	102391.147
72	2	0.101	513835.412	103025.720
55	3	0.797	514287.724	102578.675
54	2	-0.207	514477.899	102592.539
52	3	-0.269	515265.257	103012.478

4.7 Output

See Vector maps in Appendix C.

5. Program (F) - Transformation of Geographic Coordinates to Secant Plane Coordinate System

5.1 General Information

Type of Language	- Basic
Computer	- This is a small program, therefore the Wang 2200 in the Department of Geography, University of Glasgow is used.

5.2 Definition of Variables

A	-	Ellipsoid major semidiameter.
B	-	Ellipsoid minor semidiameter.
C	-	Square of the ellipsoid eccentricity.
N	-	Length of the normal of the ellipsoid, through the point to be transformed.
M	-	Length of the normal of the ellipsoid through the origin.
H	-	Height of point above ellipsoid.

ARRAY

F	-	Dynamic array including the coordinates of the point in the Geographic and Secant Plane systems.

5.3 Flow Diagram for Program (F)

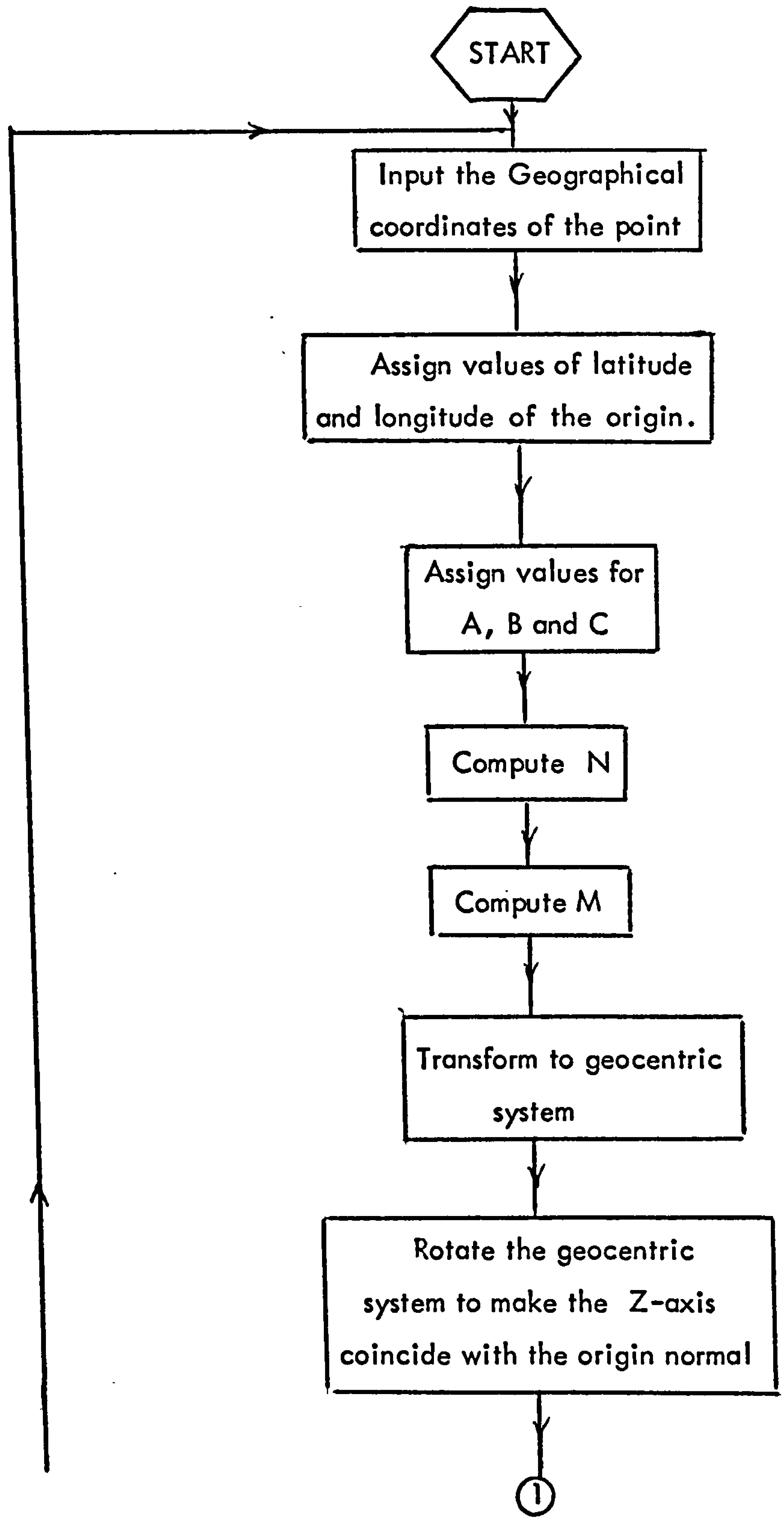

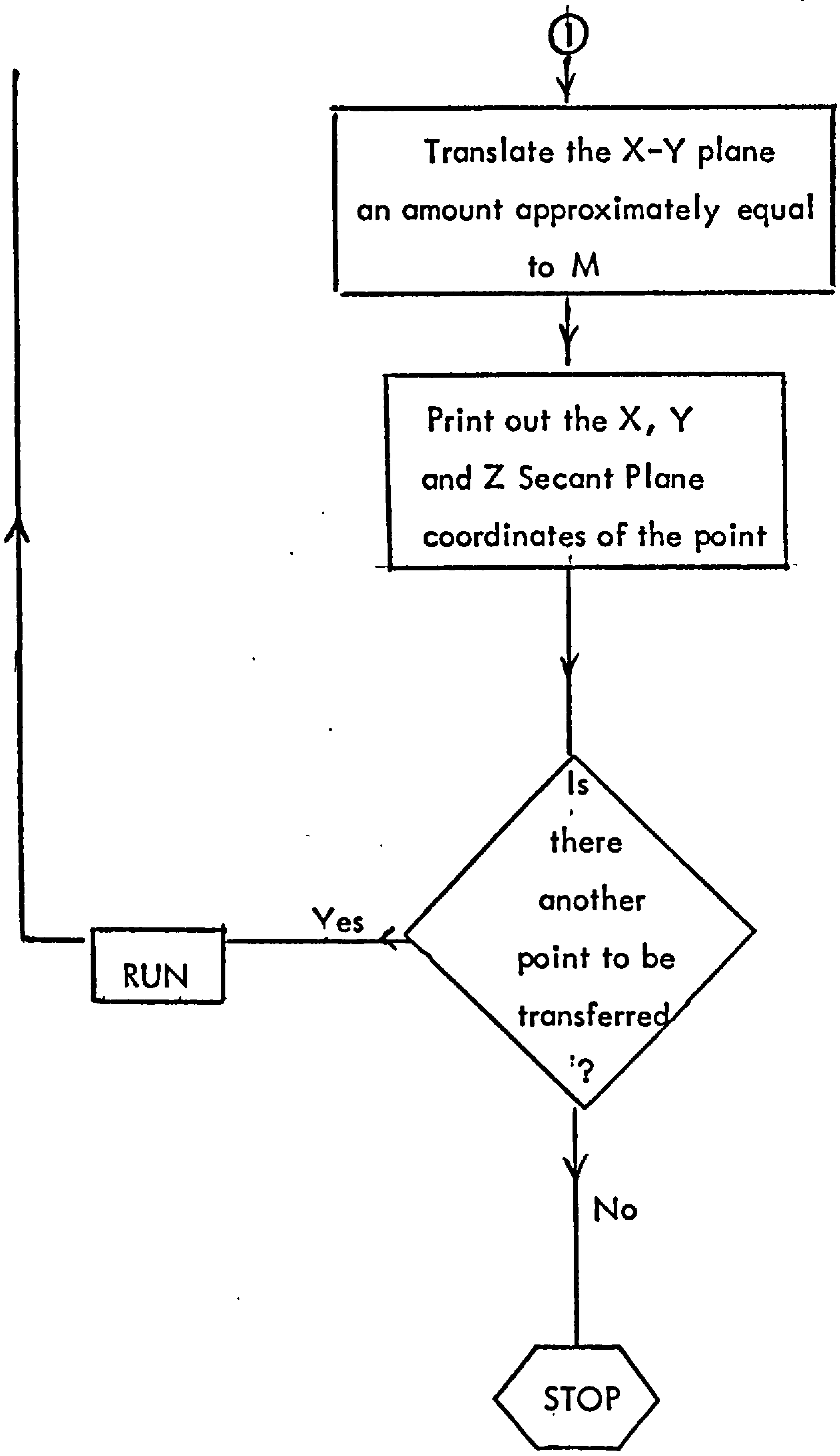
1
Translate the X-Y plane an amount approximately equal to M
Print out the X, Y and Z Secant Plane coordinates of the point
Is there another point to be transferred ?
Yes
RUN
No
STOP

5.4 The Program

TRANSFORMATION OF GEOGRAPHIC COORDINATES TO

SECANT PLANE RECTANGULAR COORDINATE SYSTEM

```
10 SELECT D
20 DIM F(10)
30 PRINT "PT,LAT,LONG,HT"
40 INPUT F(10),F(1),F(2),F(3)
50 INPUT F(4),F(5),F(6)
60 INPUT H
70 T=F(1)+F(2)/60+F(3)/3600
80 G=F(4)+F(5)/60+F(6)/3600
90 K=40+1.0/60
100 L=-88-50/60-30/3600
110 A=6378206.4
120 B=6356583.8
130 C=6768657997291E-15
140 S=SIN(T)
150 Q=COS(T)
160 N=A^2/((A^2*Q^2+B^2*S^2)^0.5)
170 V=SIN(K)
180 W=COS(K)
190 M=A^2/((A^2*W^2+B^2*V^2)^0.5)
200 H=H/3.28084
210 X=(N+H)*Q*SIN(G)
220 Y=(N+H)*Q*COS(G)
230 Z=(N*(1.0-C)+H)*S+M*C*V
240 F(7)=X*COS(L)-Y*SIN(L)
250 F(8)=-X*V*SIN(L)-Y*V*COS(L)+Z*W
260 F(9)=X*W*SIN(L)+Y*W*COS(L)+Z*V
270 F(9)=F(9)-6387000
280 SELECT PRINT 01D(100)
290 PRINT F(10),F(7),F(8),F(9)
300 SELECT PRINT 005(64)
```

5.5 Input

Pt.No.	Latitude °	'	"	Longitude °	'	"	Height (feet)
2404	39	42	48.706	89	11	47.874	616.0
2405	39	41	3.062	89	11	46.220	616.0
2406	39	40	10.746	89	11	45.380	617.0
2407	39	39	18.137	89	11	44.855	614.0
2408	39	40	11.760	89	7	13.931	624.0
2460	39	40	10.746	89	6	6.113	627.0
2426	40	9	52.894	89	17	31.542	604.0
2427	40	9	52.996	89	16	23.091	609.0
2428	40	9	26.195	89	16	56.644	610.0
2433	40	1	12.739	89	26	32.713	577.0
2458	40	0	20.623	89	26	32.581	594.0
2431	40	0	17.276	89	18	39.350	614.0
2432	40	0	17.683	89	20	4.978	605.0
2430	40	5	31.065	89	17	31.780	607.0
2429	40	6	23.654	89	17	31.911	608.0
2459	40	4	38.978	89	17	31.252	627.0
2420	40	20	0.810	89	10	6.880	685.0
2421	40	19	34.089	89	10	6.748	695.0
2422	40	19	7.166	89	11	15.416	689.0
2423	40	19	34.393	89	8	14.320	700.0
2424	40	17	47.611	89	10	5.424	704.0
2401	39	58	6.168	89	10	52.236	615.0
2402	39	56	46.729	89	10	50.921	610.0
2403	39	56	32.931	89	11	57.894	608.0
2436	40	5	35.675	89	4	0.370	671.0
2437	40	5	30.608	89	9	51.161	611.0
2434	40	10	52.789	89	5	7.856	776.0
2435	40	10	0.253	89	5	8.095	766.0
2450	39	43	35.733	88	49	51.988	704.0
2451	39	43	35.632	88	51	0.867	708.0
2452	39	43	34.691	88	52	8.439	710.0
2453	39	42	42.412	88	50	59.289	710.0
2455	39	37	30.304	88	59	45.302	643.0
2438	39	58	30.082	89	15	48.771	616.0
2439	39	58	31.502	89	18	38.887	607.0
2440	39	58	31.908	89	19	46.985	599.0
2441	39	56	51.001	89	26	33.963	624.0
2447	40	11	32.901	88	35	32.247	726.0
2448	40	7	37.607	88	33	32.775	708.0
2449	40	6	48.317	88	43	33.039	707.0
2409	39	56	7.601	88	56	13.027	686.0
2410	39	54	48.928	88	56	11.734	681.0
2411	39	56	3.435	88	59	34.418	674.0
2412	39	54	44.032	88	59	34.418	676.0
2413	39	57	54.377	88	55	6.073	694.0
2414	39	57	5.000	88	53	55.454	687.0
2418	40	20	29.068	88	52	51.050	793.0
2419	40	15	12.458	88	52	49.329	804.0
2442	40	22	9.743	88	40	10.723	770.0
2443	40	21	17.076	88	40	10.458	780.0
2444	40	21	15.962	88	36	44.986	767.0
2445	40	21	15.557	88	35	35.746	769.0
2462	40	23	27.326	88	35	35.746	786.0
2456	39	50	31.323	88	51	35.244	680.0
2415	39	58	53.182	88	50	29.677	687.0

2416	39	57	21.653	88	50	47.422	685.0
2417	39	57	8.733	88	50	30.712	689.0
2446	40	17	43.894	88	31	3.283	786.0
2425	40	12	3.254	89	18	41.303	601.0
2461	40	12	4.068	89	16	23.979	603.0
2465	40	10	44.542	89	18	40.775	603.0
2630	39	43	35.733	88	49	51.988	704.0
2631	39	43	35.632	88	51	0.867	708.0
2632	39	43	34.691	88	52	8.439	710.0
2633	39	42	42.412	88	50	59.289	710.0
2634	39	41	48.080	88	50	57.449	711.0
2635	39	58	53.182	88	50	29.677	687.0
2636	39	50	31.323	88	51	35.244	680.0
2637	39	49	39.060	88	51	34.034	675.0
2662	40	23	27.326	88	35	35.746	786.0
2647	40	11	32.901	88	35	32.247	726.0
2649	40	6	48.317	88	43	33.039	707.0
2641	39	57	21.653	88	50	47.422	685.0
2642	39	57	8.733	88	50	30.712	689.0
2639	39	56	7.601	88	56	13.027	686.0
2640	39	54	48.928	88	56	11.734	681.0
2643	39	57	54.377	88	55	6.073	694.0
2644	39	57	5.000	88	53	55.545	687.0
2645	40	21	15.557	88	35	35.746	769.0
2601	40	0	39.584	88	19	55.335	690.0
2602	40	0	38.883	88	18	48.296	691.0
2603	40	1	31.324	88	19	48.702	690.0
2604	40	1	32.338	88	19	56.045	690.0
2605	40	1	5.766	88	19	22.373	692.0
2606	40	3	18.349	88	19	57.515	693.0
2665	40	1	30.608	88	17	40.040	727.0
2618	39	51	52.347	88	36	11.316	684.0
2619	39	50	8.322	88	36	11.316	677.0
2620	39	50	7.916	88	35	37.368	676.0
2621	39	49	15.852	88	35	37.631	672.0
2622	39	48	23.785	88	35	38.947	669.0
2616	39	49	13.417	88	18	40.140	674.0
2617	39	48	21.939	88	18	40.403	665.0
2611	39	59	46.226	88	18	47.069	686.0
2615	39	54	55.608	88	17	35.344	693.0
2614	39	54	54.733	88	15	19.579	705.0
2613	39	55	21.269	88	15	19.185	704.0
2612	39	58	53.964	88	19	54.087	693.0
2666	39	54	29.828	88	18	42.733	694.0
2628	39	36	30.893	88	44	28.421	650.0
2629	39	36	31.824	88	45	19.422	655.0
2609	40	7	39.501	88	24	26.633	708.0
2607	40	7	39.355	88	22	10.730	721.0
2610	40	8	31.902	88	22	11.136	737.0
2608	40	11	8.961	88	17	46.463	783.0
2623	39	44	21.306	88	31	45.388	678.0
2624	39	43	29.105	88	31	44.993	674.0
2625	39	42	36.625	88	32	52.667	675.0
2626	39	42	37.031	88	34	0.902	688.0
2627	39	40	50.338	88	31	43.168	670.0
2667	39	42	36.880	88	30	36.736	681.0
2646	40	17	43.894	88	31	3.283	786.0
2668	40	4	10.494	88	18	49.716	701.0
2669	40	4	10.650	88	19	57.972	699.0
2681	39	56	3.435	88	59	34.418	674.0
2682	39	54	44.032	88	59	34.418	676.0

5.6 Output

GROUND COORDINATES IN RECTANGULAR SECANT PLANE SYSTEM

Pt.No.	X	Y	Z
2404	-30439.612	-33597.545	176.660
2405	-30413.090	-36855.866	158.743
2406	-30399.444	-38469.414	149.560
2407	-30393.327	-40091.955	138.656
2408	-23929.264	-38461.141	179.262
2460	-22312.889	-38497.307	185.809
2426	-38372.969	+16533.440	197.504
2427	-36753.136	+16528.574	208.567
2428	-37551.238	+15705.819	206.314
2433	-51287.365	+565.806	120.089
2458	-51295.112	-1041.610	125.148
2431	-40071.227	-1212.237	211.491
2432	-42102.179	-1188.715	195.688
2430	-38419.530	+8457.737	214.000
2429	-38414.420	+10079.778	211.972
2459	-38415.190	+6851.143	222.055
2420	-27781.386	+35238.342	200.936
2421	-27781.327	+34414.151	208.496
2422	-29405.697	+33589.835	203.801
2423	-25127.063	+34414.264	221.012
2424	-27762.190	+31129.789	228.241
2401	-29006.879	-5306.286	269.529
2402	-28984.978	-7756.528	265.589
2403	-30576.618	-8175.878	257.033
2436	-19197.294	+8527.082	320.112
2437	-27507.785	+8396.310	271.614
2434	-20769.267	+18312.430	326.558
2435	-20779.362	+16692.003	327.935
2450	+905.304	-32207.879	283.140
2451	-735.137	-32211.019	284.365
2452	-2344.460	-32239.719	284.442
2453	-697.704	-33852.411	276.457
2454	-654.013	-35500.335	267.784
2438	-36040.834	-4538.644	234.611
2439	-40077.398	-4474.662	207.860
2440	-41693.245	-4453.459	195.093
2441	-51371.542	-7506.656	129.334
2447	+21236.483	+19550.912	306.096
2448	+24085.652	+12301.908	308.648
2449	+9874.733	+10749.833	348.933
2409	-8144.911	-9014.190	347.668
2410	-8116.788	-11440.727	342.279
2411	-12926.986	-9136.062	335.949
2412	-12931.135	-11585.082	332.562
2413	-6552.313	-5722.421	355.752
2414	-4877.216	-7246.620	353.563
2463	-7353.145	-7374.358	350.436
2418	-3329.270	+36059.910	288.800
2419	-3292.917	+26294.131	340.028
2442	+14611.016	+39178.554	247.505
2443	+14620.435	+37554.077	260.328
2444	+19469.378	+37530.611	243.564

2445	+21103.389	+37522.501	239.032
2462	+21091.992	+41586.928	218.982
2456	-1551.273	-19390.116	327.681
2457	-1522.823	-21002.031	321.047
2415	+7.664	-3911.500	358.350
2416	-413.548	-6734.539	355.365
2417	-16.902	-7133.045	356.163
2446	+27557.070	+31014.511	254.686
2425	-40002.513	+20562.749	174.845
2461	-36754.487	+20571.429	194.942
2465	-40002.872	+18134.912	182.836
2455	-13244.540	-43466.592	183.915
2601	+43514.221	-505.263	212.224
2602	+45104.325	-517.624	201.497
2603	+43662.377	+1091.456	211.139
2604	+43488.079	+1121.734	212.323
2605	+44290.080	+306.773	207.513
2606	+43434.541	+4391.247	212.185
2665	+46713.445	+1087.499	200.832
2618	+20409.760	-16863.977	303.678
2619	+20418.311	-20072.348	292.203
2620	+21225.576	-20082.665	289.234
2621	+21223.768	-21688.447	282.749
2622	+21196.908	-23294.385	276.246
2616	+45423.333	-21657.849	157.207
2617	+45426.470	-23245.543	148.838
2611	+45143.047	-2141.545	199.359
2615	+46899.644	-11094.673	179.521
2614	+50124.268	-11101.135	158.676
2612	+43562.463	-3762.721	211.716
2613	+50128.248	-10282.641	159.716
2666	+45303.868	-11899.474	189.890
2628	+8626.098	-45305.477	181.126
2629	+7409.356	-45278.050	184.372
2609	+37016.604	+12412.341	246.584
2607	+40234.424	+12424.210	231.064
2610	+40216.238	+14044.914	232.684
2608	+46451.872	+18925.003	191.755
2623	+26778.999	-30755.407	226.330
2624	+26794.012	-32365.319	217.061
2625	+25187.555	-33989.355	215.433
2626	+23562.065	-33982.039	225.638
2627	+26854.560	-37261.716	188.792
2667	+28425.618	-33970.141	203.774
2646	+27557.070	+31014.511	254.686
2668	+45032.033	+6008.919	202.239
2669	+43414.500	+6004.320	212.833

6. Program (G) - Transformation of Geographic coordinates to UTM system

6.1 General Information

Type of Language	- Complete Algol program
Computer	- ICL 2980 in Edinburgh.

6.2 Definition of Variables

M	-	Number of points to be transformed.
PT	-	Point number.
H	-	Height of point above the ellipsoid.

ARRAYS

F	-	Array including the geographic positions of the points.
K	-	Dynamic array to compute the transformation parameters.
G	-	Dynamic array containing the transformed UTM coordinates of the point.

6.3 Flow Diagram of Program (G)

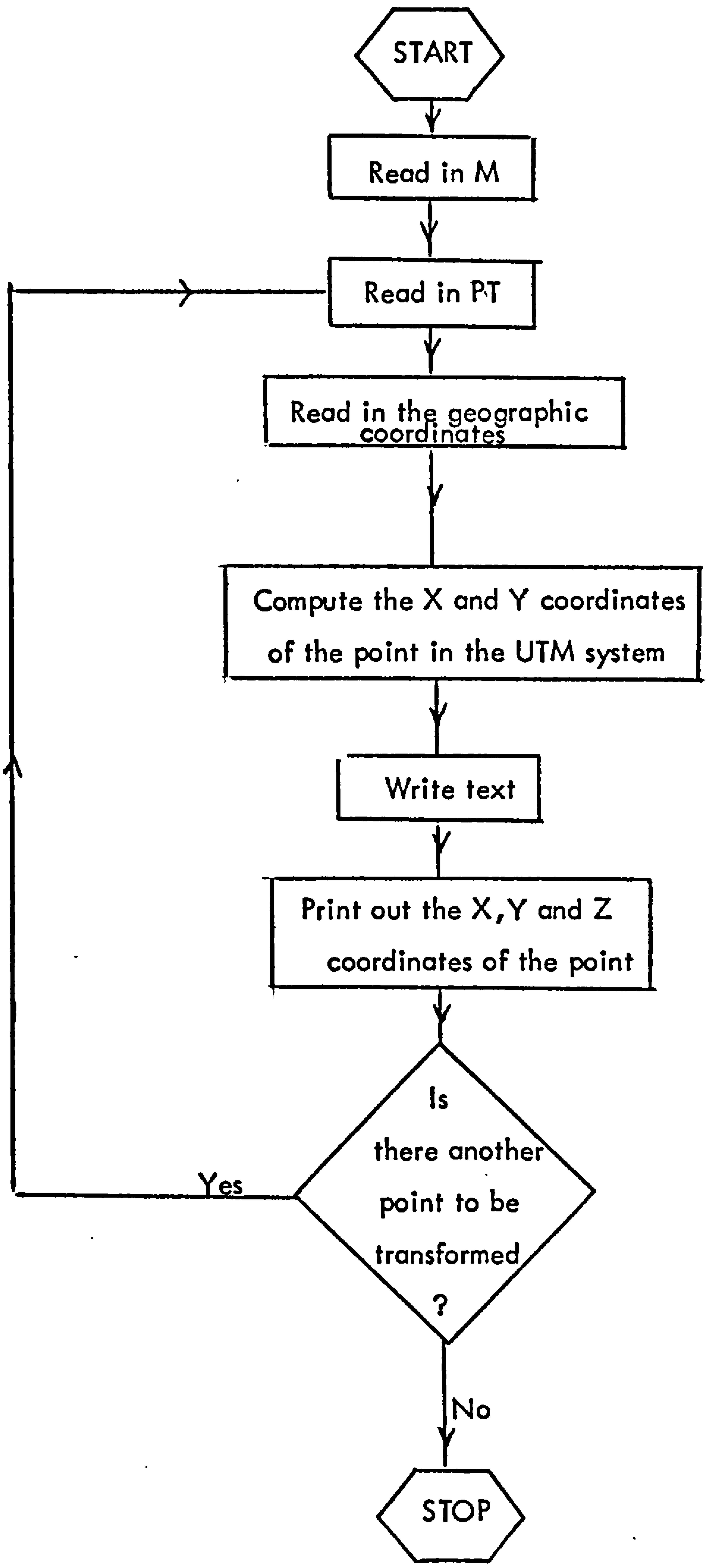

6.4 The Program

```
STMNT
  1    'BEGIN'
  2    'COMMENT'  TRANSFORMATION OF GEOGRAPHIC
  2    COORDINATES  TO  UTM  RECTANGULAR SYSTEM;
  3    'INTEGER' I,PT,CT;
  4    'REAL' A,B,C,L,P,Q,R,S,T,
  4    H,M,N,W,V;
  5    'REAL' 'ARRAY' K$1:15!, F$1:10!, G$1:8!;
  6    CT:=1;
  7    A:=6378206.4;  B:=6356583.8;
  9    C:=((A'**'2)-(B'**'2))/(A'**'2);
 10    C:=SQRT(C);
 11    R:=((A'**'2)-(B'**'2))/(B'**'2);
 12    'COMMENT'  READ IN CENTRAL MEREDIAN OF
 12    THE   AREA            ;
 13    L:=0.9996;      M:=READ;
 15    L1: PT:=READ;    'IF' PT=0  'THEN'  'GOTO' L2;
 17    'FOR' I:=1 'STEP' 1 'UNTIL' 8 'DO'
 17    G$I!:=0.00;
 18    'FOR' I:=1 'STEP' 1 'UNTIL' 10 'DO'
 18    F$I!:=0.00;
 19    'FOR' I:=1 'STEP' 1 'UNTIL' 15 'DO'
 19    K$I!:=0.00;
 20    'COMMENT'  READ IN THE GEOGRAPHIC  COORDINATES;
 21    'FOR' I:=1 'STEP' 1 'UNTIL' 6 'DO'
 21    F$I!:=READ;
 22    H:=READ;
 23    H:=H/3.28084;
 24    T:=F$1!+F$2!/60.0+F$3!/3600.0;
 25    T:=T*3.14159264/180.0;
 26    F$9!:=F$6!+F$5!*60.0+F$4!*3600.0;
 27    F$10!:=M*3600.0-F$9!;
 28    P:=(1.0&-4)*F$10!;
 29    S:=SIN(T);      Q:=COS(T);
 31    W:=S/Q;     W:=W'**'2;
 33    N:=SIN(3.14159264/(180.0*3600.0));
 34    V:=C*S*C*S;
 35    V:=A/((1.0-V)'**'0.5);
 36    K$9!:=6367399.689*L;
 37    K$10!:=21.73607-0.11422*Q'**'2;
 38    K$11!:=5104.57388-K$10!*Q'**'2;
```

```
39    K$12!:=T-S*Q*K$11!*1.0&-6;
40    K$1!:=K$9!*K$12!;
41    K$2!:=V*S*Q*L*((N'**'2)*(1.0&8))/2.0;
42    K$13!:=((N'**'4)*(1.0&6))*V*S*(Q'**'3)/24.0;
43    K$14!:=9.0*R*(Q'**'2)+4.0*(R'**'2)*Q'**'4;
44    K$3!:=K$13!*(5.0-W+K$14!)*L;
45    K$4!:=V*Q*N*L*(1.0&4);
46    K$15!:=(1.0-W+R*Q'**'2)*L;
47    K$5!:=((N'**'3)*(1.0&12))*V*(Q'**'3)*K$15!/6.0;
48    G$3!:=((N'**'6)*(1.0&24))*V*S*(Q'**'5)/720.0;
49    G$4!:=(W'**'2)+270.0*R*(Q'**'2)-330.0*R*S'**'2;
50    G$8!:=(P'**'6)*G$3!*L;
51    K$6!:=G$8!*(61.0-58.0*W+G$4!);
52    G$5!:=((N'**'5)*(1.0&20))*V*Q'**'5;
53    G$6!:=5.0-18.0*W+(W'**'2)+14.0*R*Q'**'2;
54    G$7!:=G$6!-58.0*R*S'**'2;
55    K$7!:=(P'**'5)*G$5!*G$7!*L/120.0;
56    G$1!:=K$1!+K$2!*(P'**'2)+K$3!*(P'**'4)+K$6!;
57    G$2!:=P*K$4!+(P'**'3)*K$5!+K$7!+500000.0;
58    'IF' CT=1 'THEN'  'BEGIN'
59    WRITE TEXT('('('P')''('6S')' GROUND %%
59    COORDINATES                    %%
59    IN%%UNIVERSAL%%TRANSVERSE%%MERCATOR%%
59          SYSTEM '('3C')'
59    '('10S')'PT.NO.'('12S')'E'('15S')'N'('15S')'
59    H  '('C')'  ')' );
60    'END';
61    CT:=CT+1;
62    NEWLINE;
63    SPACES(10);
64    PRINT(PT,4,0);
65    SPACES(5);
66    PRINT(G$2!,7,3);
67    SPACES(6);
68    PRINT(G$1!,7,3);
69    SPACES(6);
70    PRINT(H,3,3);
71    'GOTO' L1;
72    L2: 'END';
```

6.5 Input

87.00 ———————— Central meridian

Pt.No.	Latitude °	'	"	Longitude °	'	"	Height (feet)
2404	39	42	48.706	89	11	47.874	616.0
2405	39	41	3.062	89	11	46.220	616.0
2406	39	40	10.746	89	11	45.380	617.0
2407	39	39	18.137	89	11	44.855	614.0
2408	39	40	11.760	89	7	13.931	624.0
2460	39	40	10.746	89	6	6.113	627.0
2426	40	9	52.894	89	17	31.542	604.0
2427	40	9	52.996	89	16	23.091	609.0
2428	40	9	26.195	89	16	56.644	610.0
2433	40	1	12.739	89	26	32.713	577.0
2458	40	0	20.623	89	26	32.581	594.0
2431	40	0	17.276	89	18	39.350	614.0
2432	40	0	17.683	89	20	4.978	605.0
2430	40	5	31.065	89	17	31.780	607.0
2429	40	6	23.654	89	17	31.911	608.0
2459	40	4	38.978	89	17	31.252	627.0
2420	40	20	0.810	89	10	6.880	685.0
2421	40	19	34.089	89	10	6.748	695.0
2422	40	19	7.166	89	11	15.416	689.0
2423	40	19	34.393	89	8	14.320	700.0
2424	40	17	47.611	89	10	5.424	704.0
2401	39	58	6.168	89	10	52.236	615.0
2402	39	56	46.729	89	10	50.921	610.0
2403	39	56	32.931	89	11	57.894	608.0
2436	40	5	35.675	89	4	0.370	671.0
2437	40	5	30.608	89	9	51.161	611.0
2434	40	10	52.789	89	5	7.856	776.0
2435	40	10	0.253	89	5	8.095	766.0
2450	39	43	35.733	88	49	51.988	704.0
2451	39	43	35.632	88	51	0.867	708.0
2452	39	43	34.691	88	52	8.439	710.0
2453	39	42	42.412	88	50	59.289	710.0
2455	39	37	30.304	88	59	45.302	643.0
2438	39	58	30.082	89	15	48.771	616.0
2439	39	58	31.502	89	18	38.887	607.0
2440	39	58	31.908	89	19	46.985	599.0
2441	39	56	51.001	89	26	33.963	624.0
2447	40	11	32.901	88	35	32.247	726.0
2448	40	7	37.607	88	33	32.775	708.0
2449	40	6	48.317	88	43	33.039	707.0
2409	39	56	7.601	88	56	13.027	686.0
2410	39	54	48.928	88	56	11.734	681.0
2411	39	56	3.435	88	59	34.418	674.0
2412	39	54	44.032	88	59	34.418	676.0
2413	39	57	54.377	88	55	6.073	694.0
2414	39	57	5.000	88	53	55.454	687.0
2418	40	20	29.068	88	52	51.050	793.0
2419	40	15	12.458	88	52	49.329	804.0
2442	40	22	9.743	88	40	10.723	770.0
2443	40	21	17.076	88	40	10.458	780.0
2444	40	21	15.962	88	36	44.986	767.0
2445	40	21	15.557	88	35	35.746	769.0
2462	40	23	27.326	88	35	35.746	786.0
2456	39	50	31.323	88	51	35.244	680.0
2415	39	58	53.182	88	50	29.677	687.0

2416	39	57	21.653	88	50	47.422	685.0
2417	39	57	8.733	88	50	30.712	689.0
2446	40	17	43.894	88	31	3.283	786.0
2425	40	12	3.254	89	18	41.303	601.0
2461	40	12	4.068	89	16	23.979	603.0
2465	40	10	44.542	89	18	40.775	603.0
2630	39	43	35.733	88	49	51.988	704.0
2631	39	43	35.632	88	51	0.867	708.0
2632	39	43	34.691	88	52	8.439	710.0
2633	39	42	42.412	88	50	59.289	710.0
2634	39	41	48.080	88	50	57.449	711.0
2635	39	58	53.182	88	50	29.677	687.0
2636	39	50	31.323	88	51	35.244	680.0
2637	39	49	39.060	88	51	34.034	675.0
2662	40	23	27.326	88	35	35.746	786.0
2647	40	11	32.901	88	35	32.247	726.0
2649	40	6	48.317	88	43	33.039	707.0
2641	39	57	21.653	88	50	47.422	685.0
2642	39	57	8.733	88	50	30.712	689.0
2639	39	56	7.601	88	56	13.027	686.0
2640	39	54	48.928	88	56	11.734	681.0
2643	39	57	54.377	88	55	6.073	694.0
2644	39	57	5.000	88	53	55.545	687.0
2645	40	21	15.557	88	35	35.746	769.0
2601	40	0	39.584	88	19	55.335	690.0
2602	40	0	38.883	88	18	48.296	691.0
2603	40	1	31.324	88	19	48.702	690.0
2604	40	1	32.338	88	19	56.045	690.0
2605	40	1	5.766	88	19	22.373	692.0
2606	40	3	18.349	88	19	57.515	693.0
2665	40	1	30.608	88	17	40.040	727.0
2618	39	51	52.347	88	36	11.316	684.0
2619	39	50	8.322	88	36	11.316	677.0
2620	39	50	7.916	88	35	37.368	676.0
2621	39	49	15.852	88	35	37.631	672.0
2622	39	48	23.785	88	35	38.947	669.0
2616	39	49	13.417	88	18	40.140	674.0
2617	39	48	21.939	88	18	40.403	665.0
2611	39	59	46.226	88	18	47.069	686.0
2615	39	54	55.608	88	17	35.344	693.0
2614	39	54	54.733	88	15	19.579	705.0
2613	39	55	21.269	88	15	19.185	704.0
2612	39	58	53.964	88	19	54.087	693.0
2666	39	54	29.828	88	18	42.733	694.0
2628	39	36	30.893	88	44	28.421	650.0
2629	39	36	31.824	88	45	19.422	655.0
2609	40	7	39.501	88	24	26.633	708.0
2607	40	7	39.355	88	22	10.730	721.0
2610	40	8	31.902	88	22	11.136	737.0
2608	40	11	8.961	88	17	46.463	783.0
2623	39	44	21.306	88	31	45.388	678.0
2624	39	43	29.105	88	31	44.993	674.0
2625	39	42	36.625	88	32	52.667	675.0
2626	39	42	37.031	88	34	0.902	688.0
2627	39	40	50.338	88	31	43.168	670.0
2667	39	42	36.880	88	30	36.736	681.0
2646	40	17	43.894	88	31	3.283	786.0
2668	40	4	10.494	88	18	49.716	701.0
2669	40	4	10.650	88	19	57.972	699.0
2681	39	56	3.435	88	59	34.418	674.0
2682	39	54	44.032	88	59	34.418	676.0

0 ———————— Tag indicating that last point is transformed.

6.6 Output

GROUND COORDINATES IN UNIVERSAL TRANSVERSE MERCATOR SYSTEM

PT.NO.	E	N	H
2404	311701.512	4398059.299	187.757
2405	311661.110	4394801.048	187.757
2406	311641.632	4393187.522	188.062
2407	311614.446	4391565.149	187.147
2408	318110.641	4393063.270	190.195
2460	319725.906	4392994.001	191.110
2426	304804.309	4448344.537	184.099
2427	306423.789	4448306.076	185.623
2428	305608.757	4447500.015	185.928
2433	291560.673	4432646.478	175.870
2458	291519.731	4431039.392	181.051
2431	302738.898	4430636.989	187.147
2432	300708.695	4430702.450	184.404
2430	304590.402	4440271.186	185.014
2429	304629.108	4441892.841	185.318
2459	304561.513	4438664.772	191.110
2420	315782.587	4466825.609	208.788
2421	315765.509	4466001.578	211.836
2422	314124.337	4465211.257	210.007
2423	318419.172	4465946.436	213.360
2424	315716.339	4462717.521	214.579
2401	313716.717	4426315.311	187.452
2402	313688.013	4423865.142	185.928
2403	312088.033	4423478.702	185.318
2436	323810.142	4439942.632	204.521
2437	315498.854	4439983.917	186.233
2434	322441.465	4449757.916	236.525
2435	322397.756	4448138.129	233.477
2450	343066.554	4398805.554	214.579
2451	341426.604	4398836.108	215.798
2452	339817.226	4398840.464	216.408
2453	341430.309	4397194.478	216.408
2455	328690.014	4387840.196	195.986
2438	306699.929	4427227.951	187.757
2439	302665.296	4427375.222	185.014
2440	301050.095	4427429.766	182.575
2441	291309.801	4424576.617	190.195
2447	364458.384	4450125.146	221.285
2448	367156.125	4442820.218	215.798
2449	352918.791	4441562.928	215.494
2409	334496.819	4422178.056	209.093
2410	334474.871	4419751.681	207.569
2411	329713.643	4422154.830	205.435
2412	329658.971	4419706.599	206.045
2413	336156.870	4425435.948	211.531
2414	337799.965	4423877.669	209.398
2418	340244.936	4467137.912	241.706
2419	340078.254	4457374.562	245.059
2442	358243.446	4469882.344	234.696
2443	358219.041	4468258.283	237.744
2444	363065.516	4468134.046	233.782
2445	364698.671	4468091.972	234.391
2462	364771.875	4472154.941	239.573
2456	340874.450	4411669.579	207.264
2415	342752.086	4427110.872	209.398
2416	342272.727	4424297.486	208.788
2417	342661.013	4423890.933	210.007
2446	371014.203	4461452.663	239.573
2425	303258.606	4452406.986	183.185
2461	306506.304	4452348.242	183.794
2465	303207.873	4449979.550	183.794

2630	343066.554	4398805.554	214.579
2631	341426.604	4398836.108	215.798
2632	339817.226	4398840.464	216.408
2633	341430.309	4397194.478	216.408
2634	341439.574	4395518.439	216.713
2635	342752.086	4427110.872	209.398
2636	340874.450	4411669.579	207.264
2637	340869.700	4410057.602	205.740
2662	364771.875	4472154.941	239.573
2647	364458.384	4450125.146	221.285
2649	352918.791	4441562.928	215.494
2641	342272.727	4424297.486	208.788
2642	342661.013	4423890.933	210.007
2639	334496.819	4422178.056	209.093
2640	334474.871	4419751.681	207.569
2643	336156.870	4425435.948	211.531
2644	337797.806	4423877.715	209.398
2645	364698.671	4468091.972	234.391
2601	386311.134	4429617.193	210.312
2602	387900.240	4429571.990	210.617
2603	386492.215	4431210.072	210.312
2604	386318.624	4431243.936	210.312
2605	387104.615	4430412.785	210.922
2606	386332.695	4434512.961	211.226
2665	389541.693	4431143.074	221.590
2618	362879.329	4413742.534	208.483
2619	362821.811	4410535.292	206.350
2620	363628.534	4410508.355	206.045
2621	363593.676	4408903.265	204.826
2622	363533.782	4407298.532	203.911
2616	387783.238	4408435.500	205.435
2617	387753.725	4406848.497	202.692
2611	387905.409	4427948.066	209.093
2615	389476.408	4418963.094	211.226
2614	392699.350	4418890.120	214.884
2613	392720.209	4419708.119	214.579
2612	386292.067	4426360.326	211.226
2666	387864.782	4418191.607	211.531
2628	350515.894	4385553.861	198.120
2629	349300.154	4385606.224	199.644
2609	380083.678	4442662.957	215.798
2607	383300.247	4442608.218	219.761
2610	383315.609	4444228.511	224.638
2608	389649.369	4448977.067	238.658
2623	368960.136	4399725.784	206.654
2624	368942.076	4398116.232	205.435
2625	367302.942	4396525.890	205.740
2626	365678.266	4396566.624	209.702
2627	368902.081	4393220.624	204.216
2667	370540.022	4396478.563	207.569
2646	371014.203	4461452.663	239.573
2668	387962.835	4436096.813	213.665
2669	386346.014	4436125.660	213.055
2681	329713.643	4422154.830	205.435
2682	329658.971	4419706.599	206.045

APPENDIX C

Vector Maps of the height and planimetric Residuals for the tested photography

1 - S-190B Photography

VECTOR MAP OF HEIGHT ERRORS

MODEL NUMBER 4 ++ PHOTO SCALE 1/945600

MAP SCALE 1/580000 ++ VECTOR SCALE 1/29000

SOLUTION NUMBER 1b

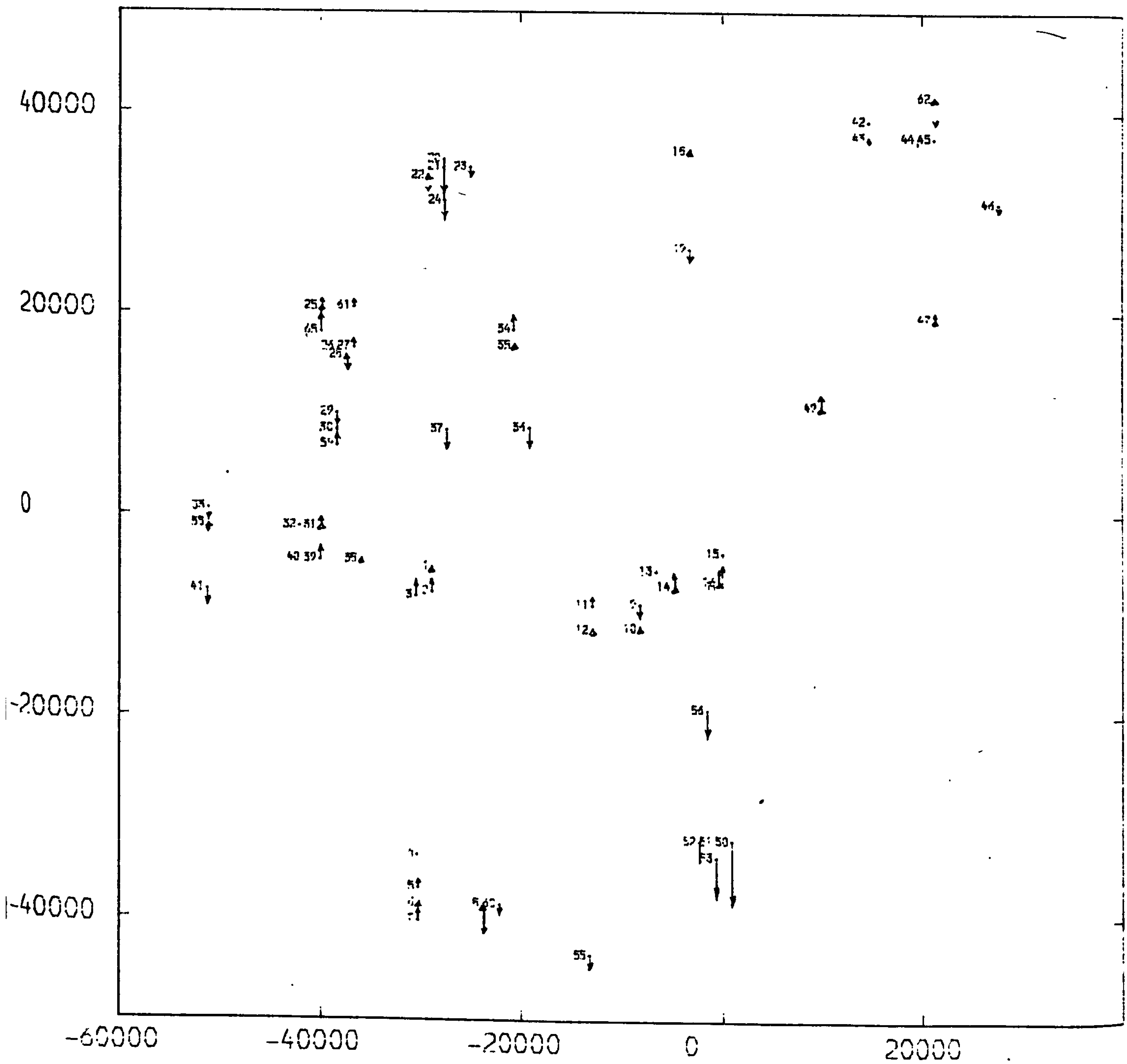

VECTOR MAP OF HEIGHT ERRORS

MODEL NUMBER 6 ** PHOTO SCALE 1/945600

MAP SCALE 1/580000 ** VECTOR SCALE 1/29000

SOLUTION NUMBER 1b

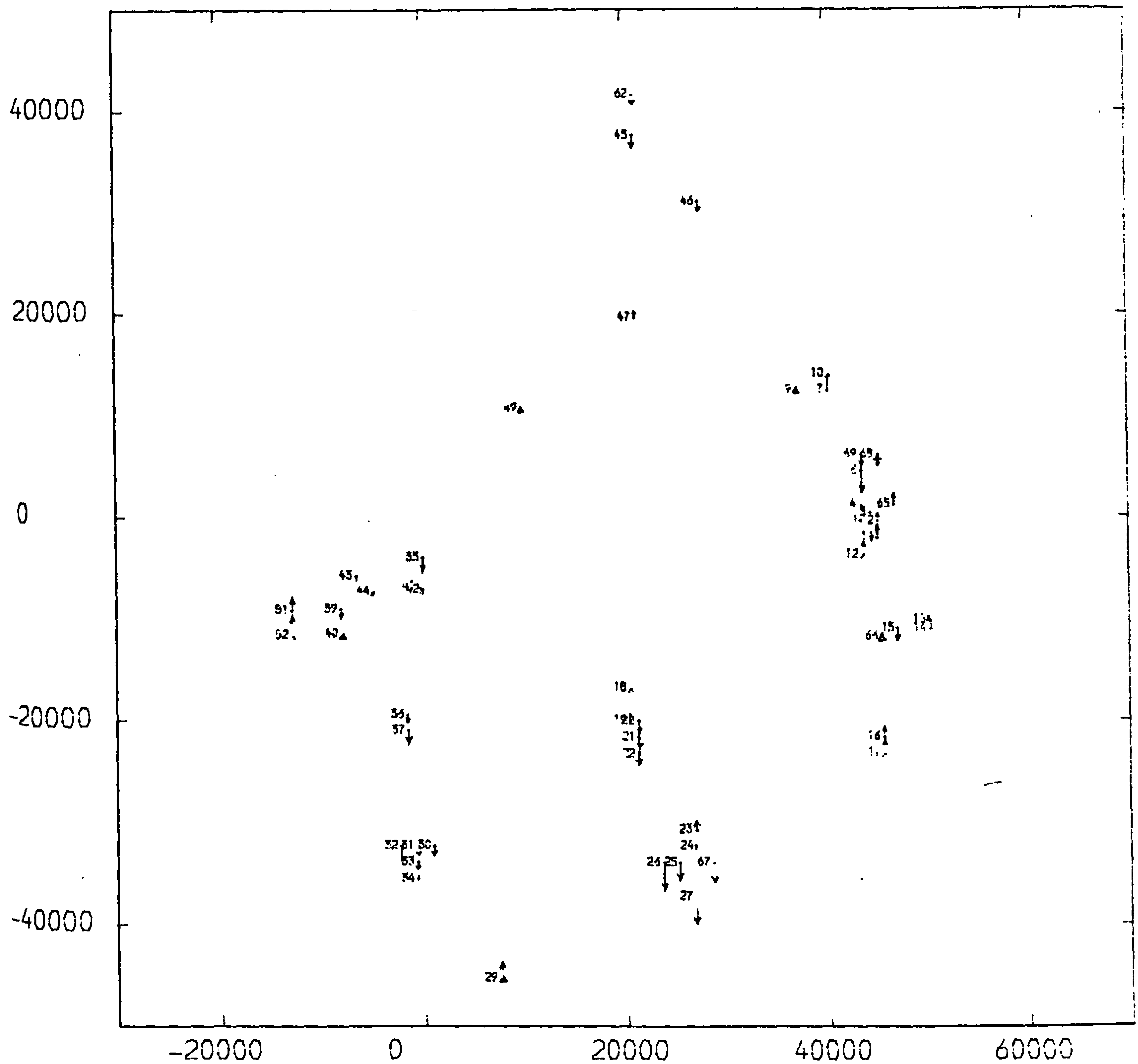

VECTOR MAP OF HEIGHT ERRORS

MODEL NUMBER 4 ++ PHOTO SCALE 1/945600

MAP SCALE 1/580000 ++ VECTOR SCALE 1/29000

SOLUTION NUMBER 19

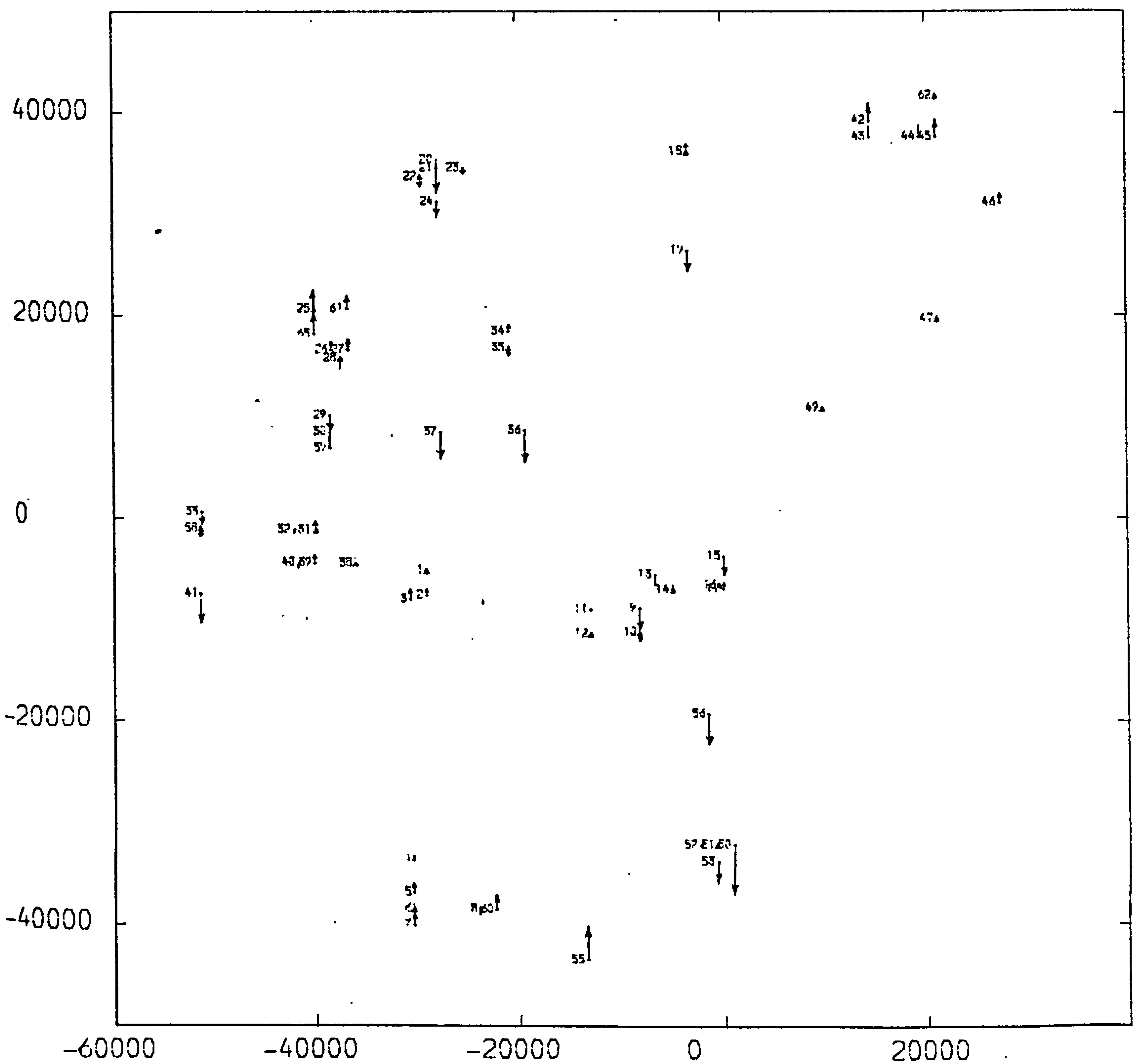

VECTOR MAP OF HEIGHT ERRORS

MODEL NUMBER 6 ** PHOTO SCALE 1/945600

MAP SCALE 1/580000 ** VECTOR SCALE 1/29000

SOLUTION NUMBER 19

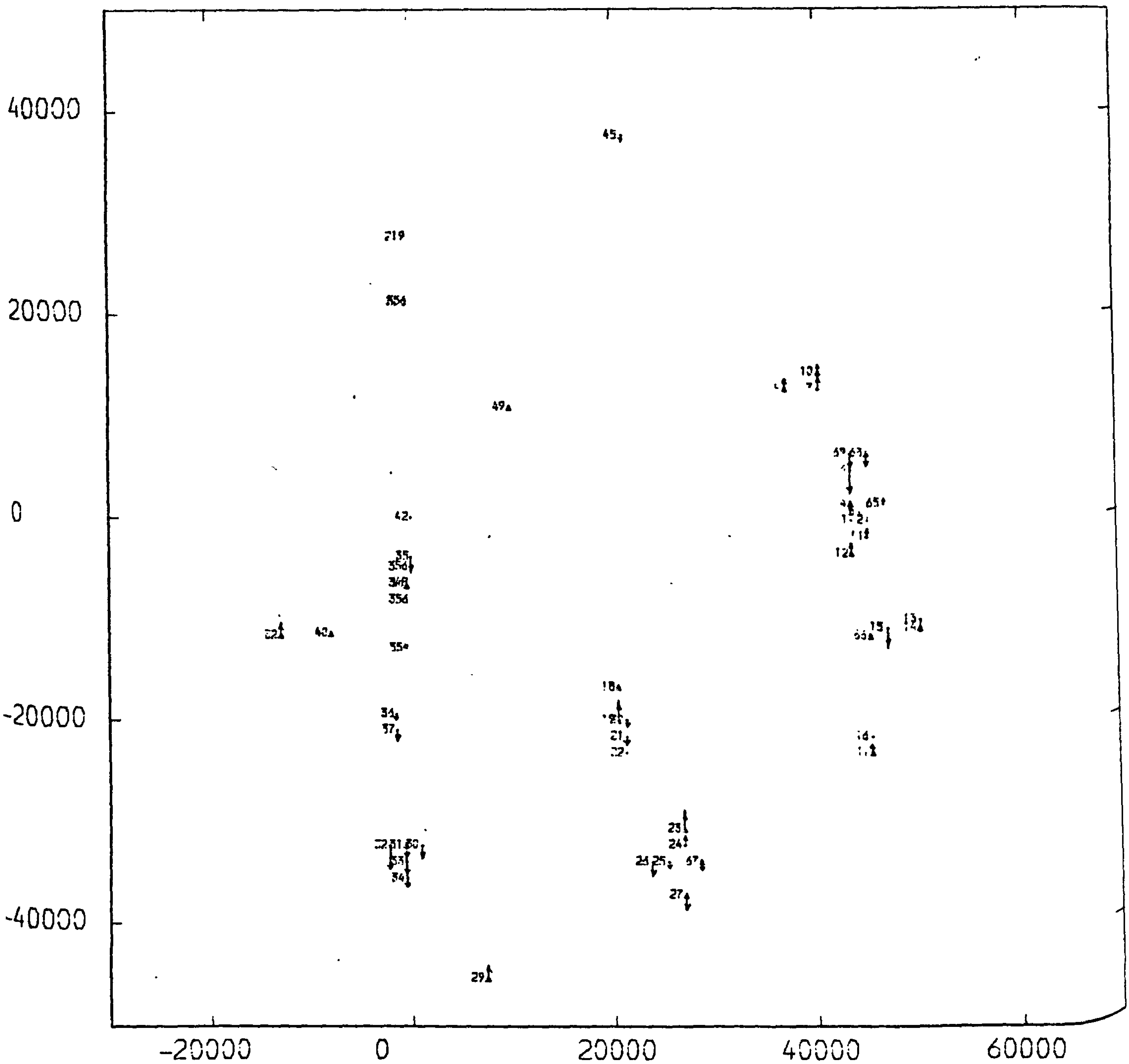

VECTOR MAP OF HEIGHT ERRORS

MODEL NUMBER 4 ++ PHOTO SCALE 1/945600

MAP SCALE 1/560000 ++ VECTOR SCALE 1/29000

SOLUTION NUMBER II10

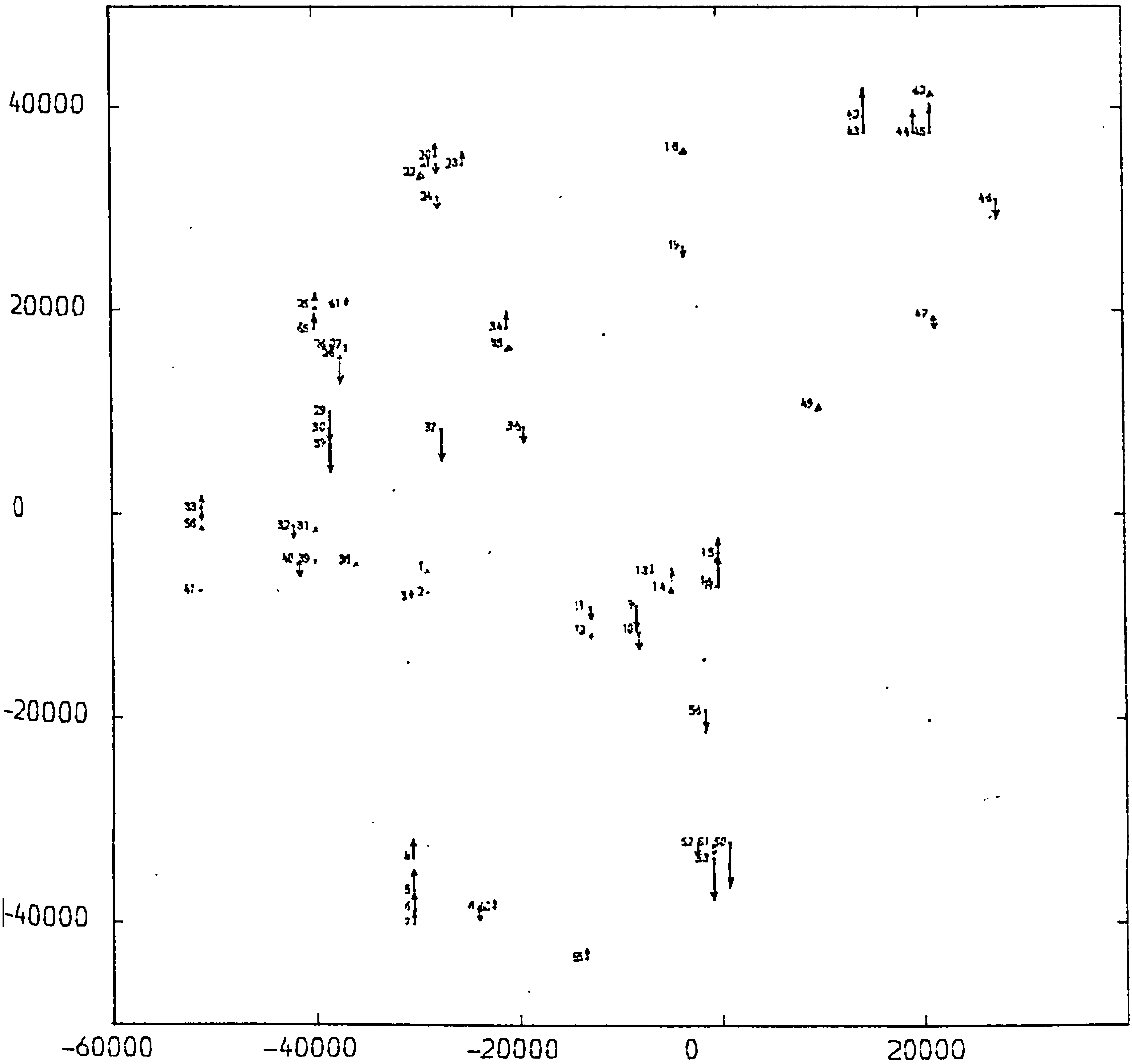

VECTOR MAP OF HEIGHT ERRORS

MODEL NUMBER 6 ++ PHOTO SCALE 1/945600

MAP SCALE 1/560000 ++ VECTOR SCALE 1/29000

SOLUTION NUMBER 1110

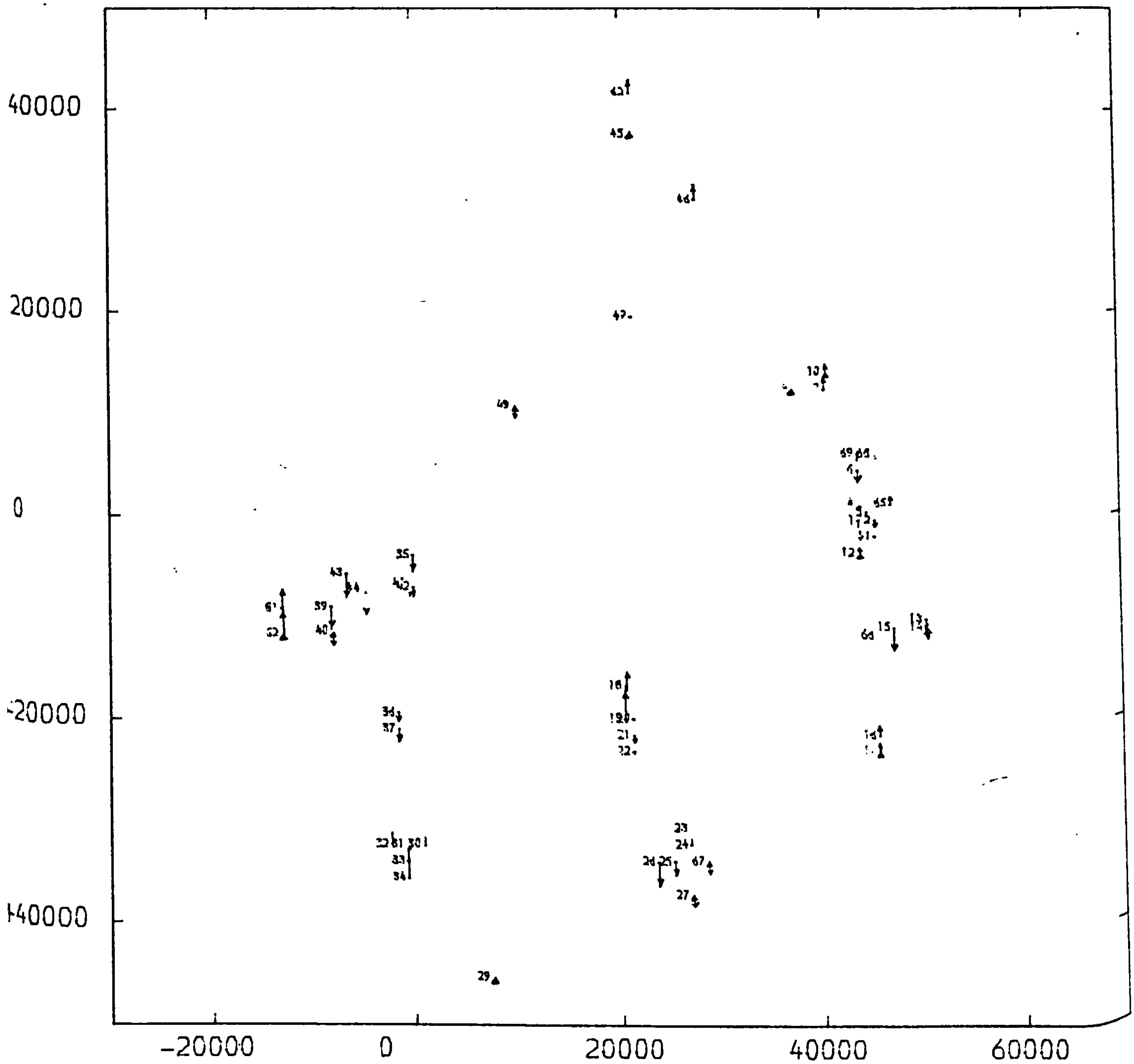

VECTOR MAP OF HEIGHT ERRORS

MODEL NUMBER 4 ++ PHOTO SCALE 1/245600

MAP SCALE 1/560000 ++ VECTOR SCALE 1/29000

SOLUTION NUMBER IIiii

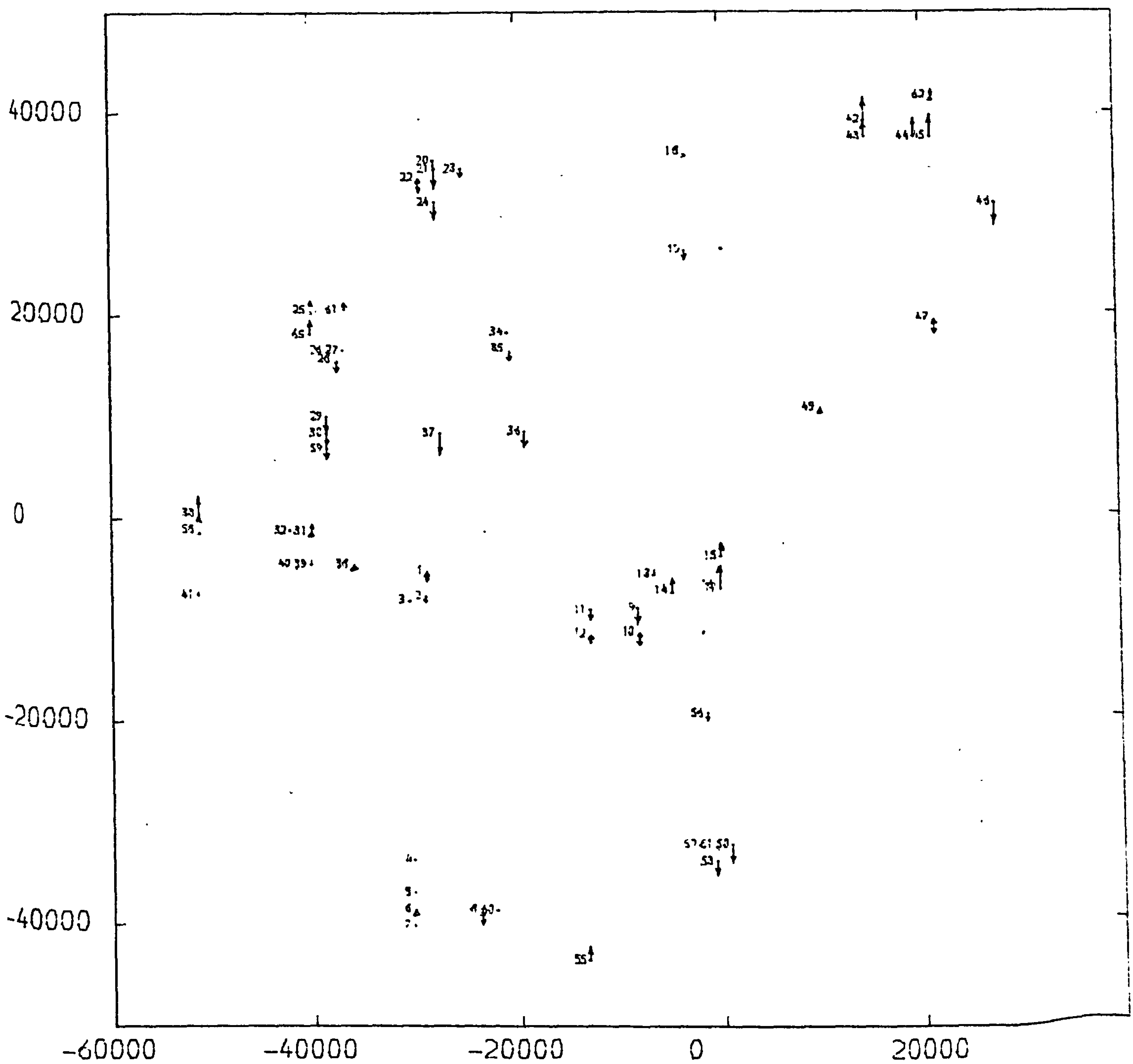

VECTOR MAP OF HEIGHT ERRORS

MODEL NUMBER 6 ++ PHOTO SCALE 1/945600

MAP SCALE 1/580000 ++ VECTOR SCALE 1/29000

SOLUTION NUMBER IIiii

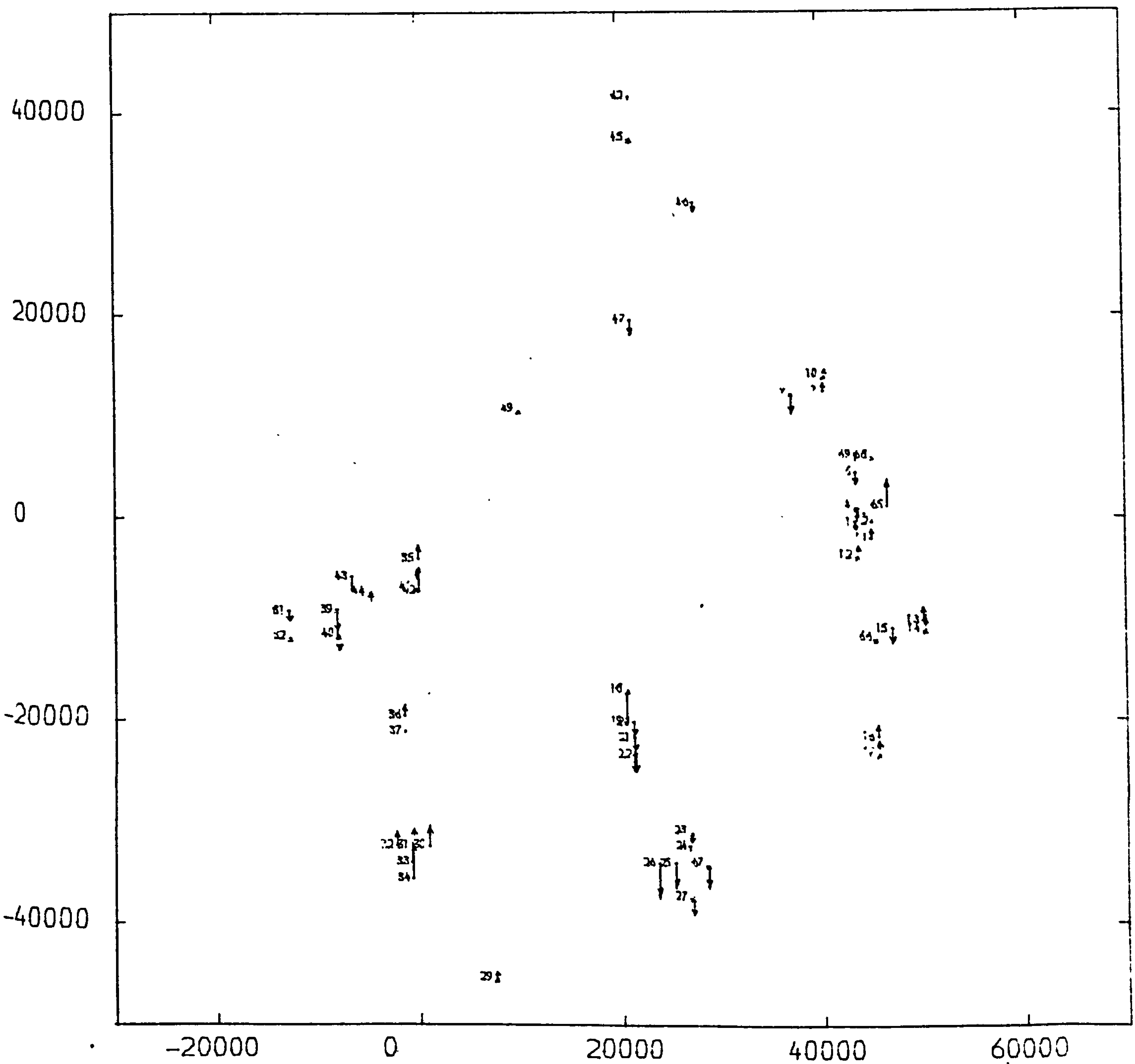

VECTOR MAP OF POSITION ERRORS

MODEL NUMBER 4 ++ PHOTO SCALE=1/945600

MAP SCALE 1/580000 +++ VECTOR SCALE 1/4000

SOLUTION NUMBER 1b

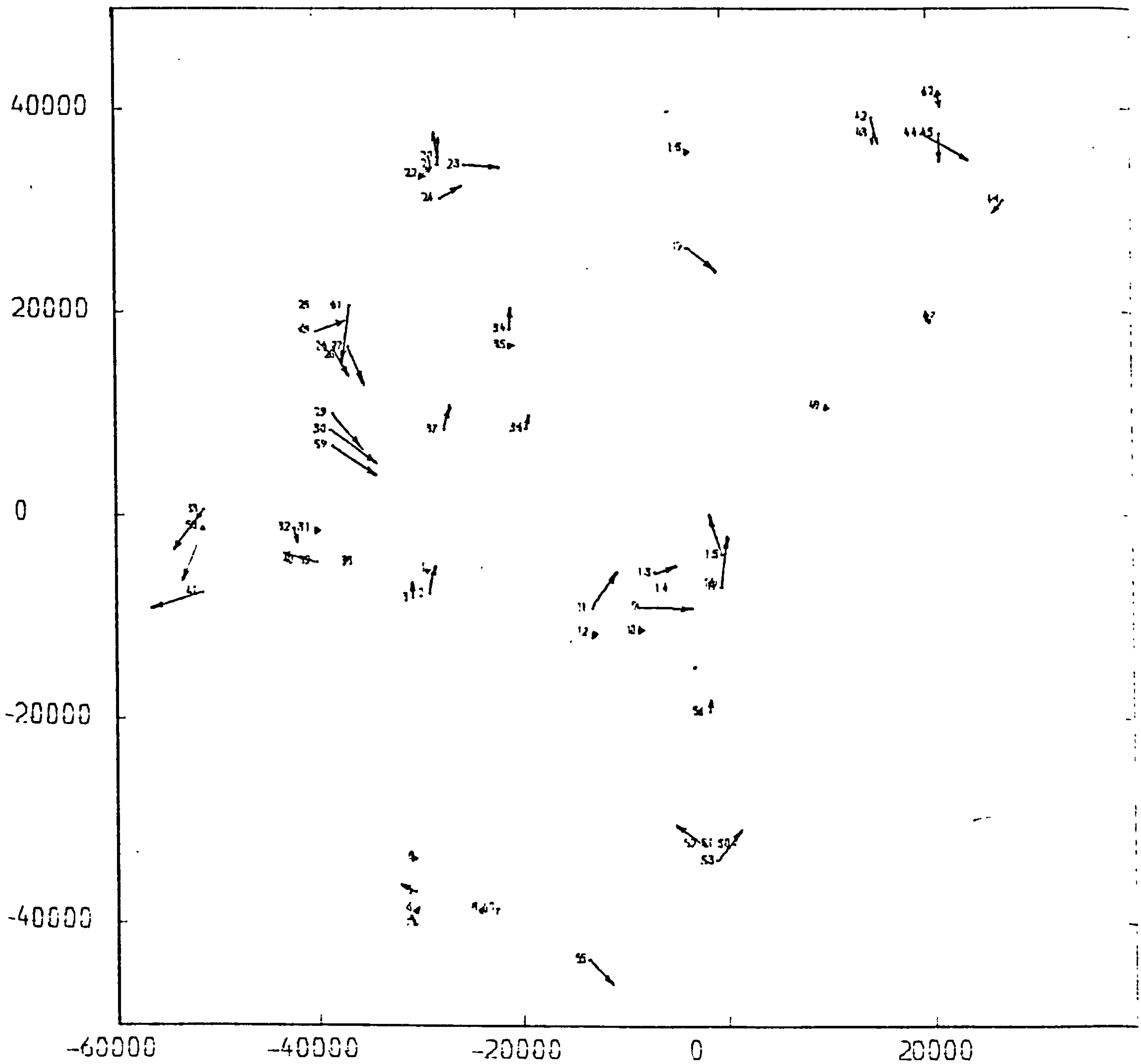

VECTOR MAP OF POSITION ERRORS

MODEL NUMBER 6 ++ PHOTO SCALE 1/945600

MAP SCALE 1/580000 +++ VECTOR SCALE 1/4000

SOLUTION NUMBER 16

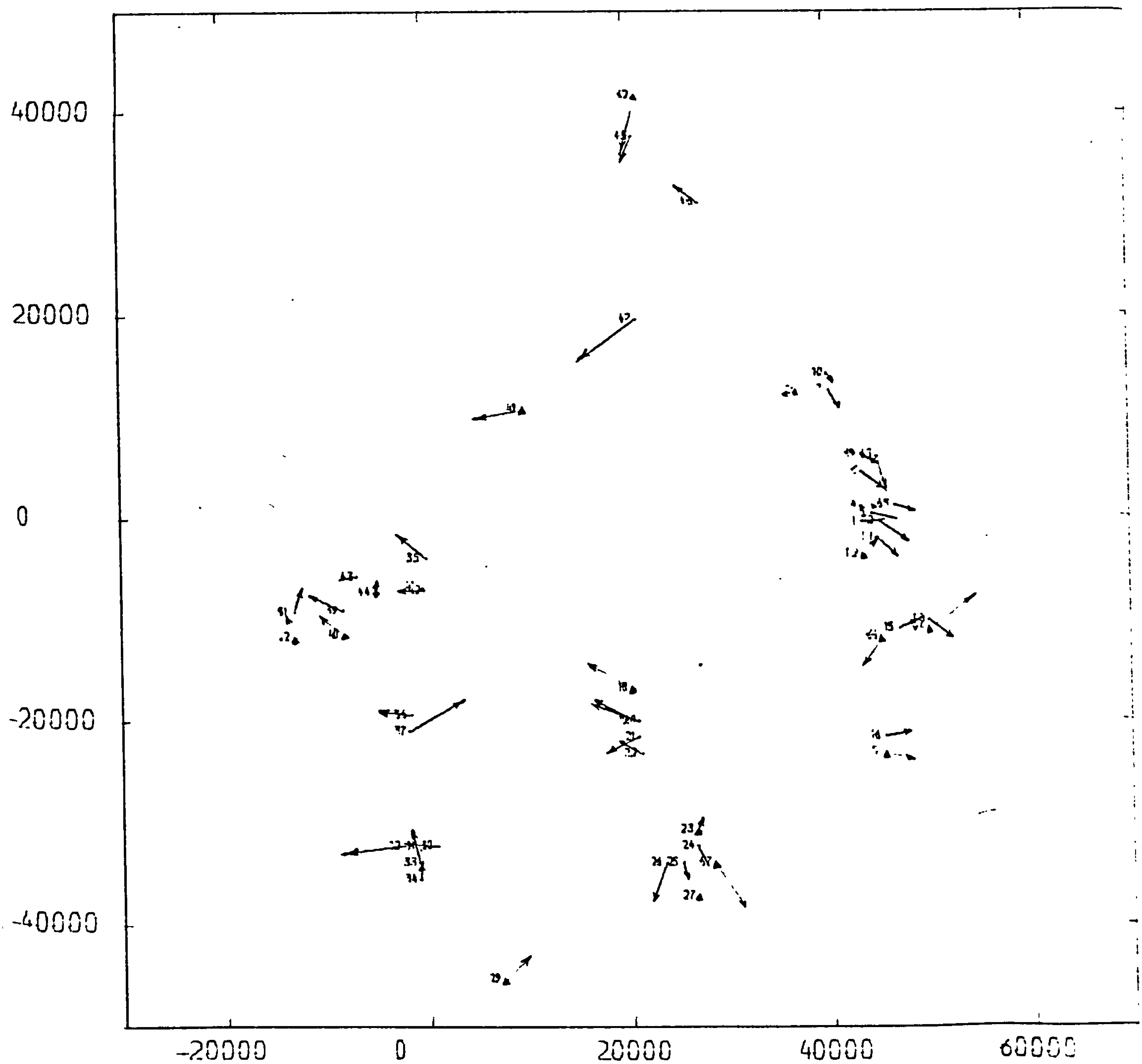

VECTOR MAP OF POSITION ERRORS

MODEL NUMBER 4 ** PHOTO SCALE 1/945600

MAP SCALE 1/580000 *** VECTOR SCALE 1/4000

SOLUTION NUMBER I9

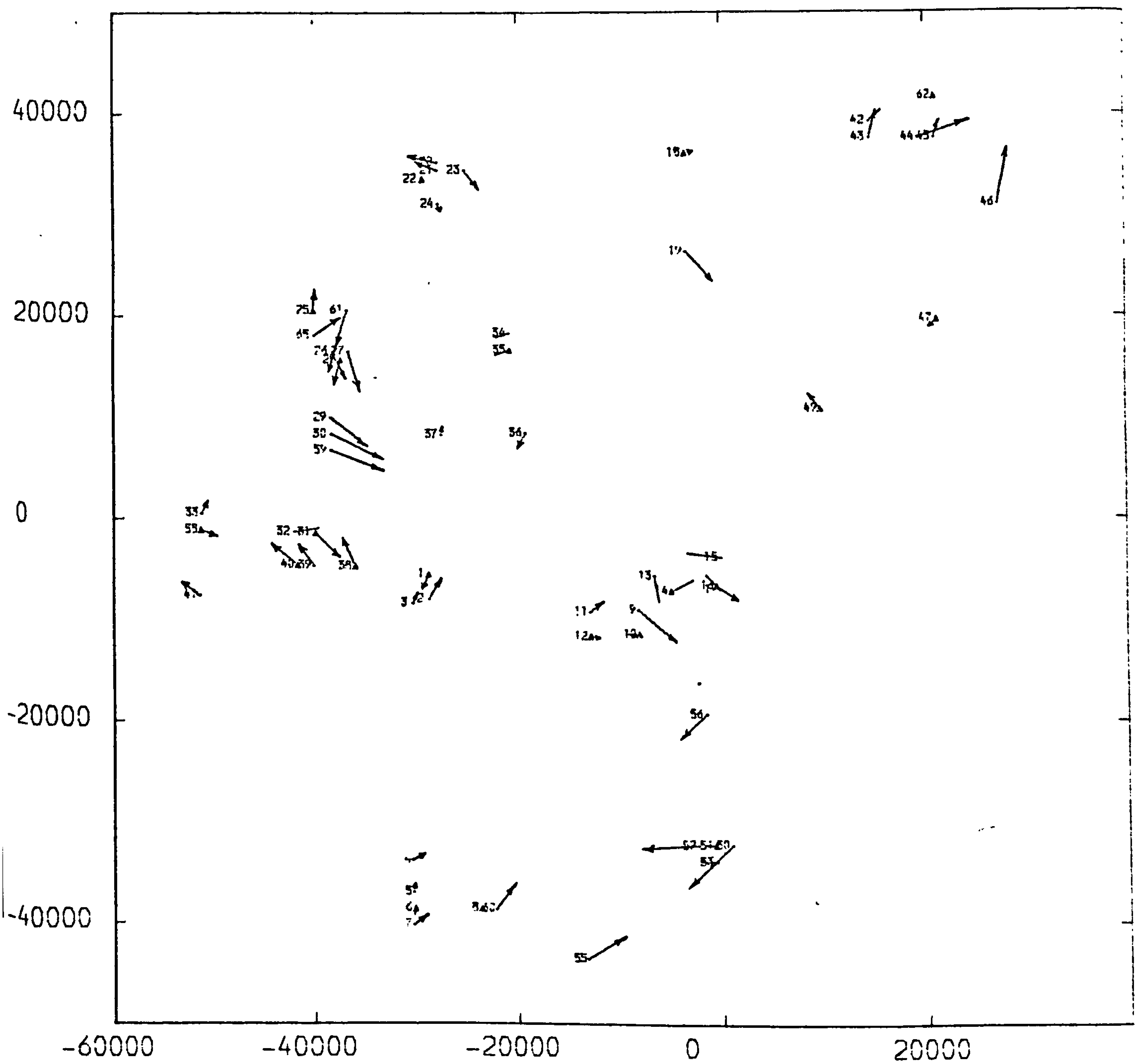

VECTOR MAP OF POSITION ERRORS

MODEL NUMBER 6 ++ PHOTO SCALE 1/945600

MAP SCALE 1/580000 +++ VECTOR SCALE 1/4000

SOLUTION NUMBER I9

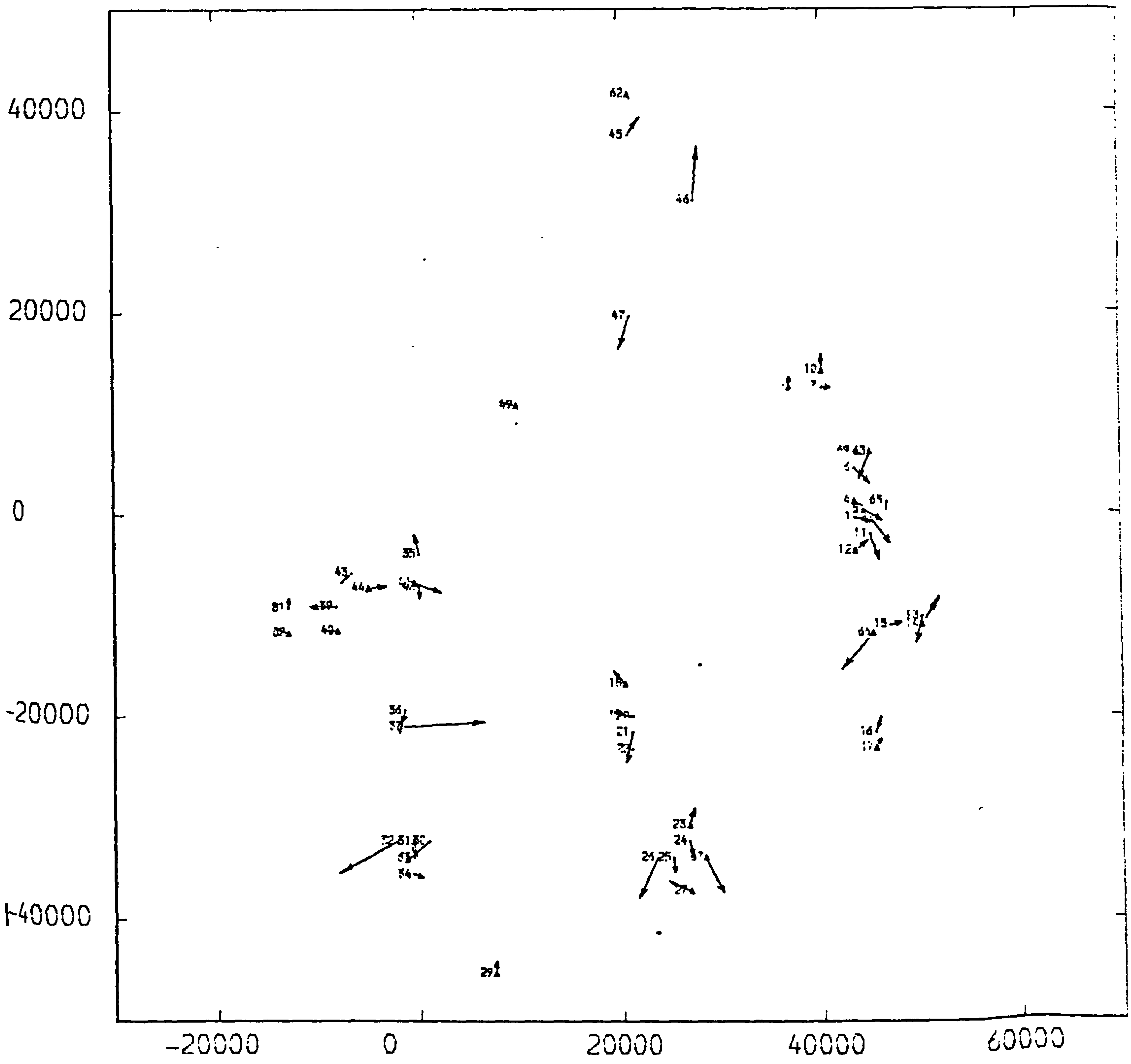

VECTOR MAP OF POSITION ERRORS

MODEL NUMBER 4 ++ PHOTO SCALE 1/945600

MAP SCALE 1/580000 +++ VECTOR SCALE 1/4000

SOLUTION NUMBER 1110

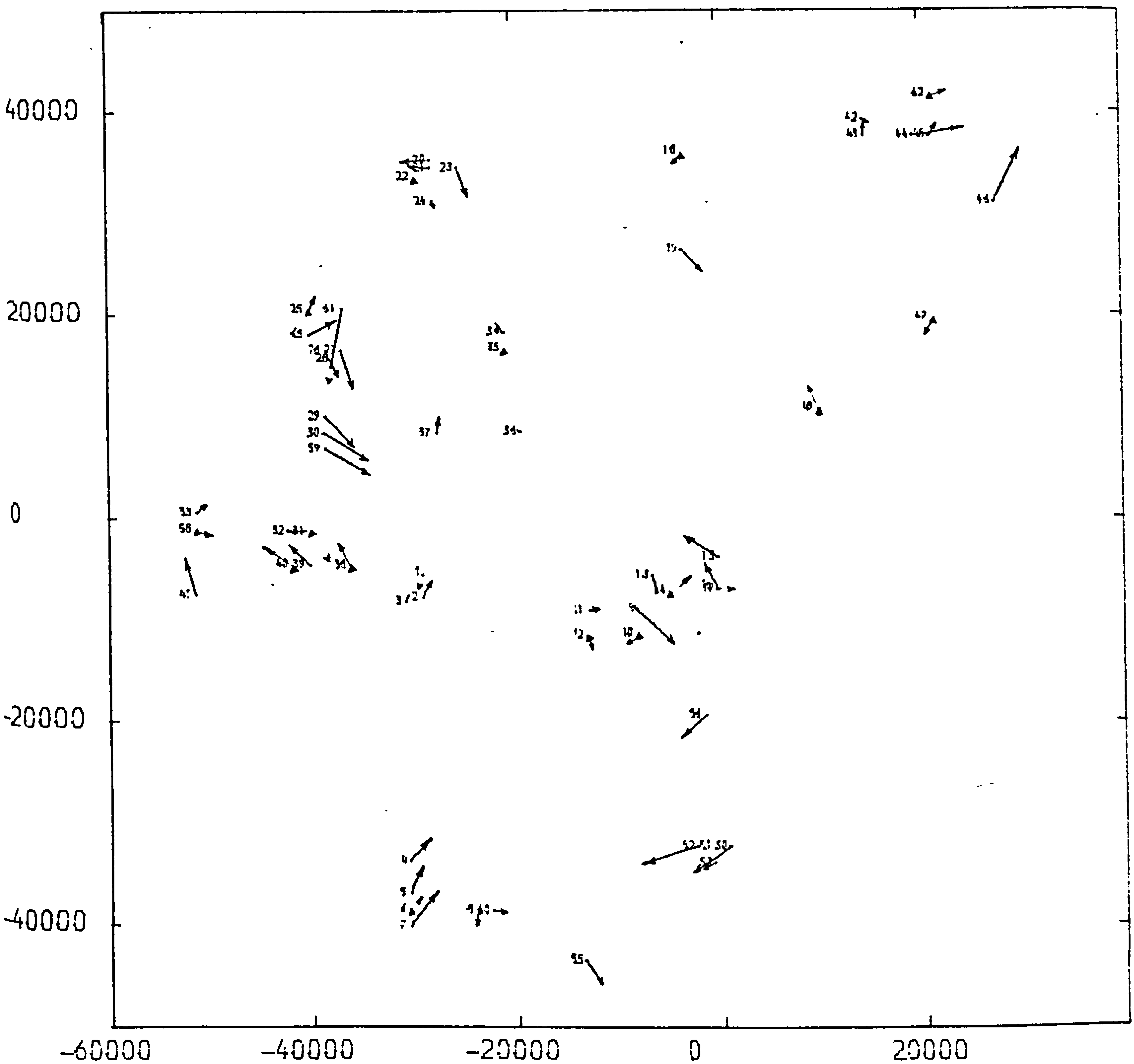

VECTOR MAP OF POSITION ERRORS

MODEL NUMBER 6 ++ PHOTO SCALE 1/945600

MAP SCALE 1/580000 +++ VECTOR SCALE 1/4000

SOLUTION NUMBER 1110

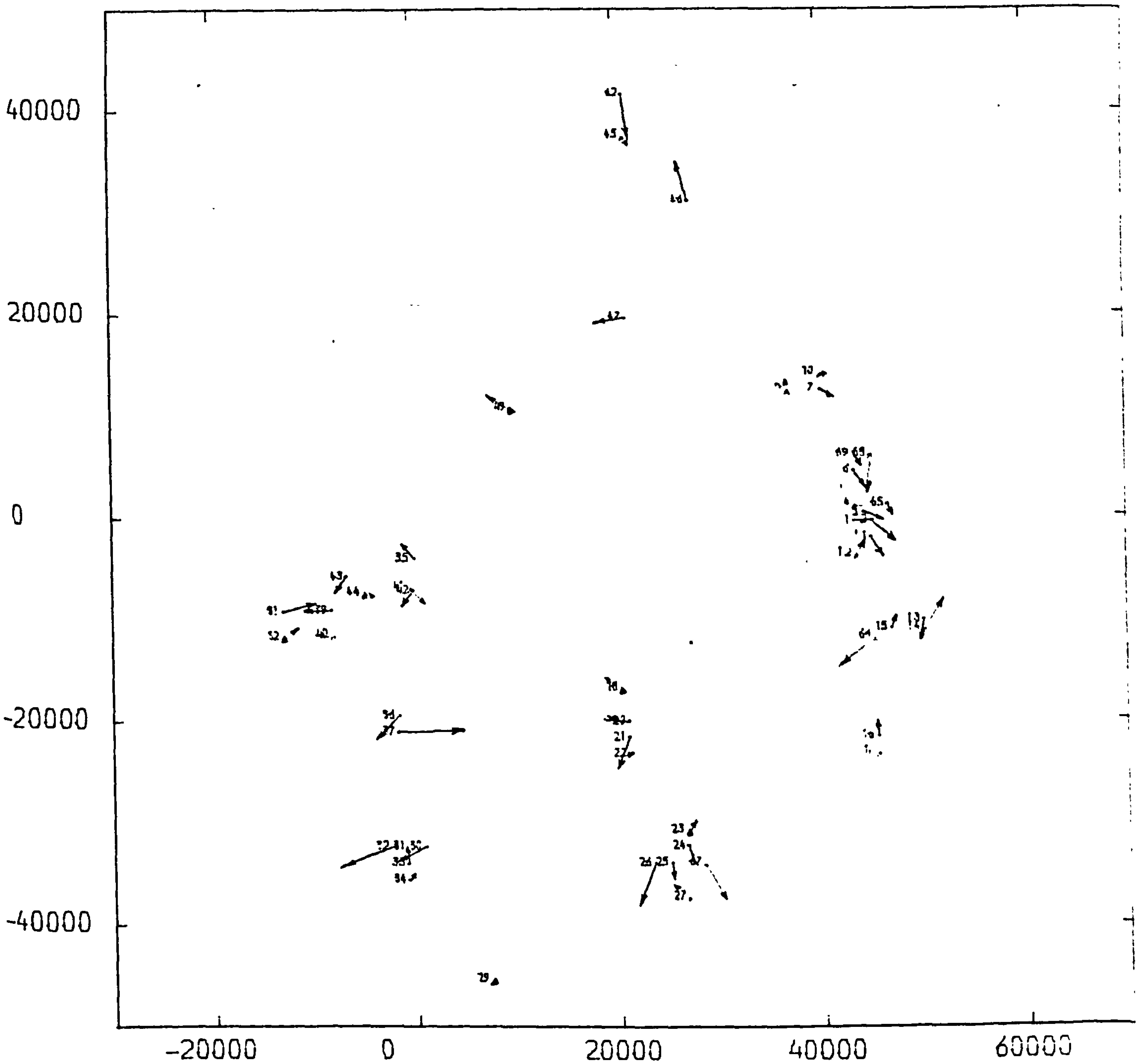

VECTOR MAP OF POSITION ERRORS

MODEL NUMBER 4 ++ PHOTO SCALE 1/945600

MAP SCALE 1/580000 +++ VECTOR SCALE 1/4000

SOLUTION NUMBER IIiii

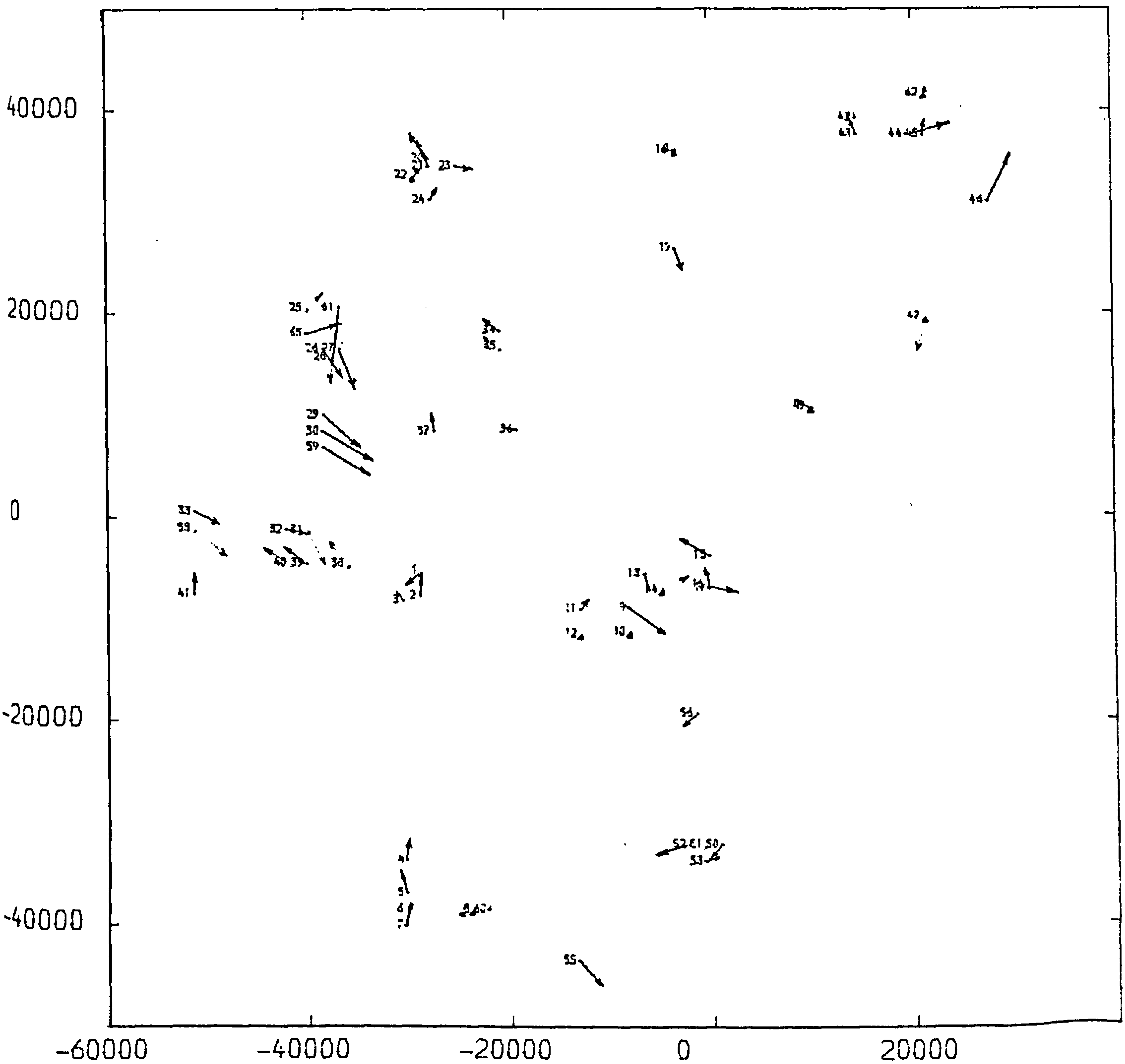

VECTOR MAP OF POSITION ERRORS

MODEL NUMBER 6 ++ PHOTO SCALE 1/945600

MAP SCALE 1/580000 +++ VECTOR SCALE 1/4000

SOLUTION NUMBER IIiii

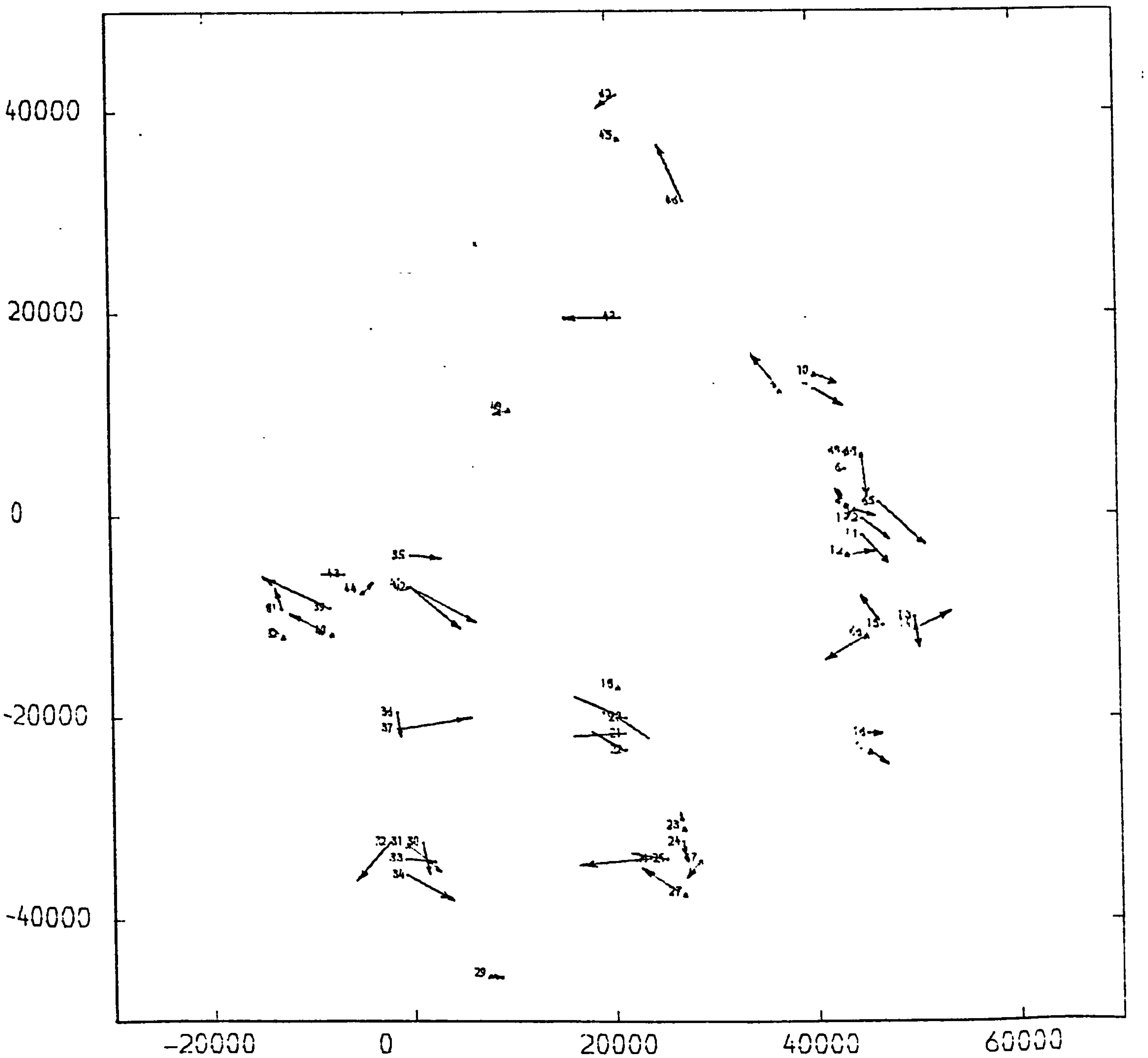

2 - F-126 Photography

VECTOR MAP OF HEIGHT ERRORS

MODEL NUMBER 5 ** PHOTO SCALE 1/40000

MAP SCALE 1/52600 ** VECTOR SCALE 1/400

SOLUTION NUMBER 1b

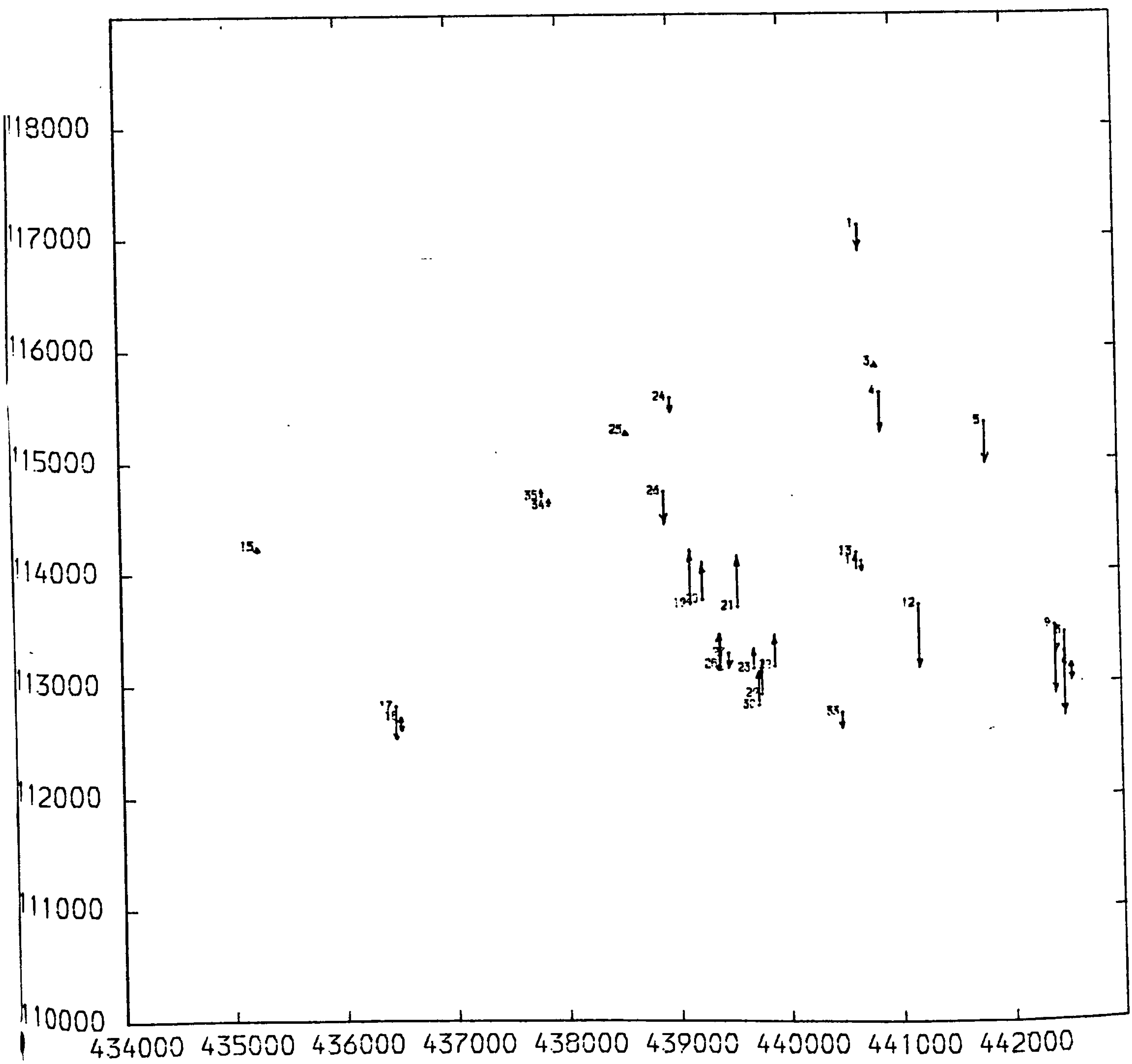

VECTOR MAP OF HEIGHT ERRORS

MODEL NUMBER 7 ** PHOTO SCALE 1/20000

MAP SCALE 1/26300 ** VECTOR SCALE 1/200

SOLUTION NUMBER Id

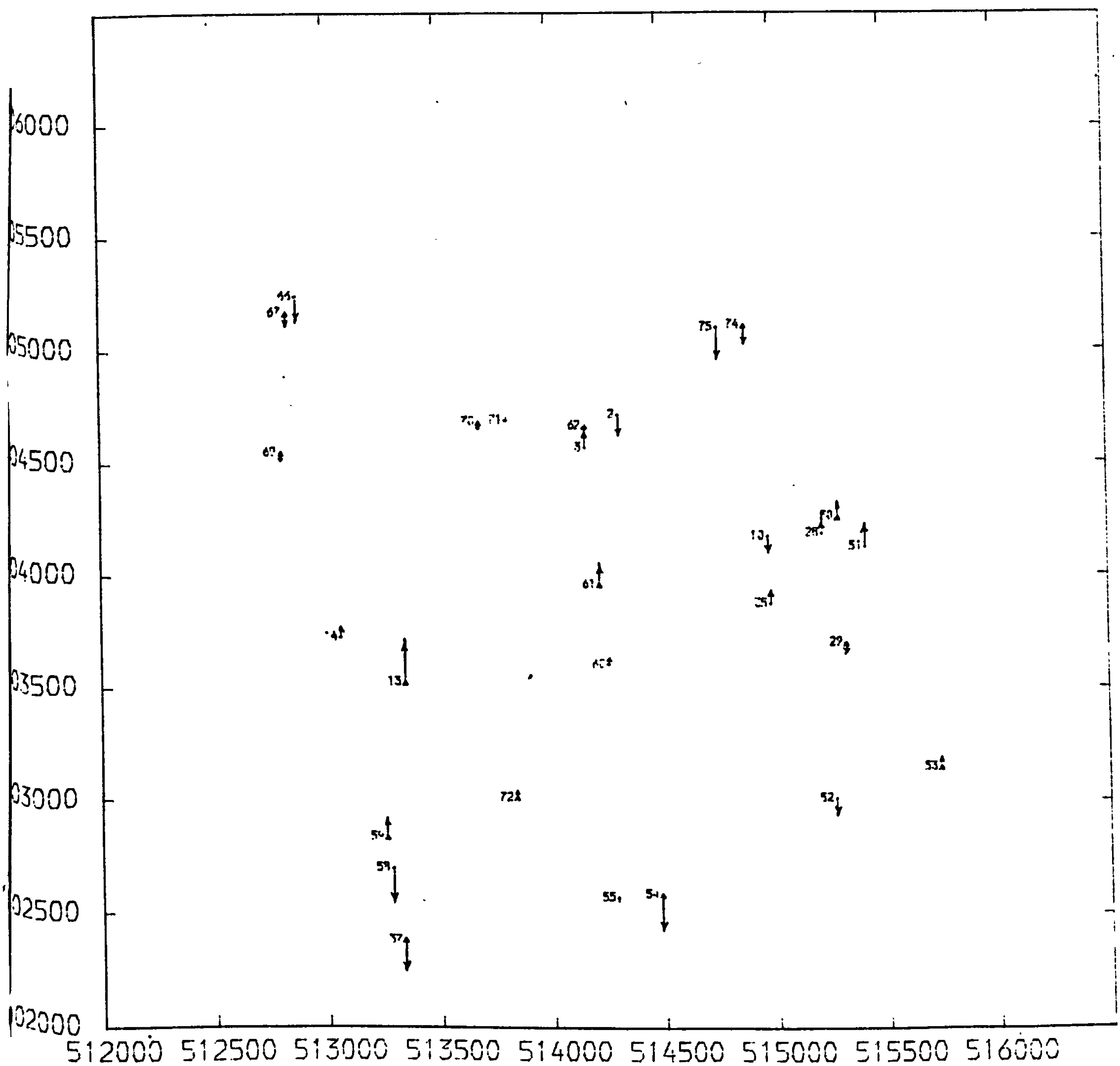

VECTOR MAP OF HEIGHT ERRORS

MODEL NUMBER 5 ** PHOTO SCALE 1/40000

MAP SCALE 1/52600 ** VECTOR SCALE 1/400

SOLUTION NUMBER 19

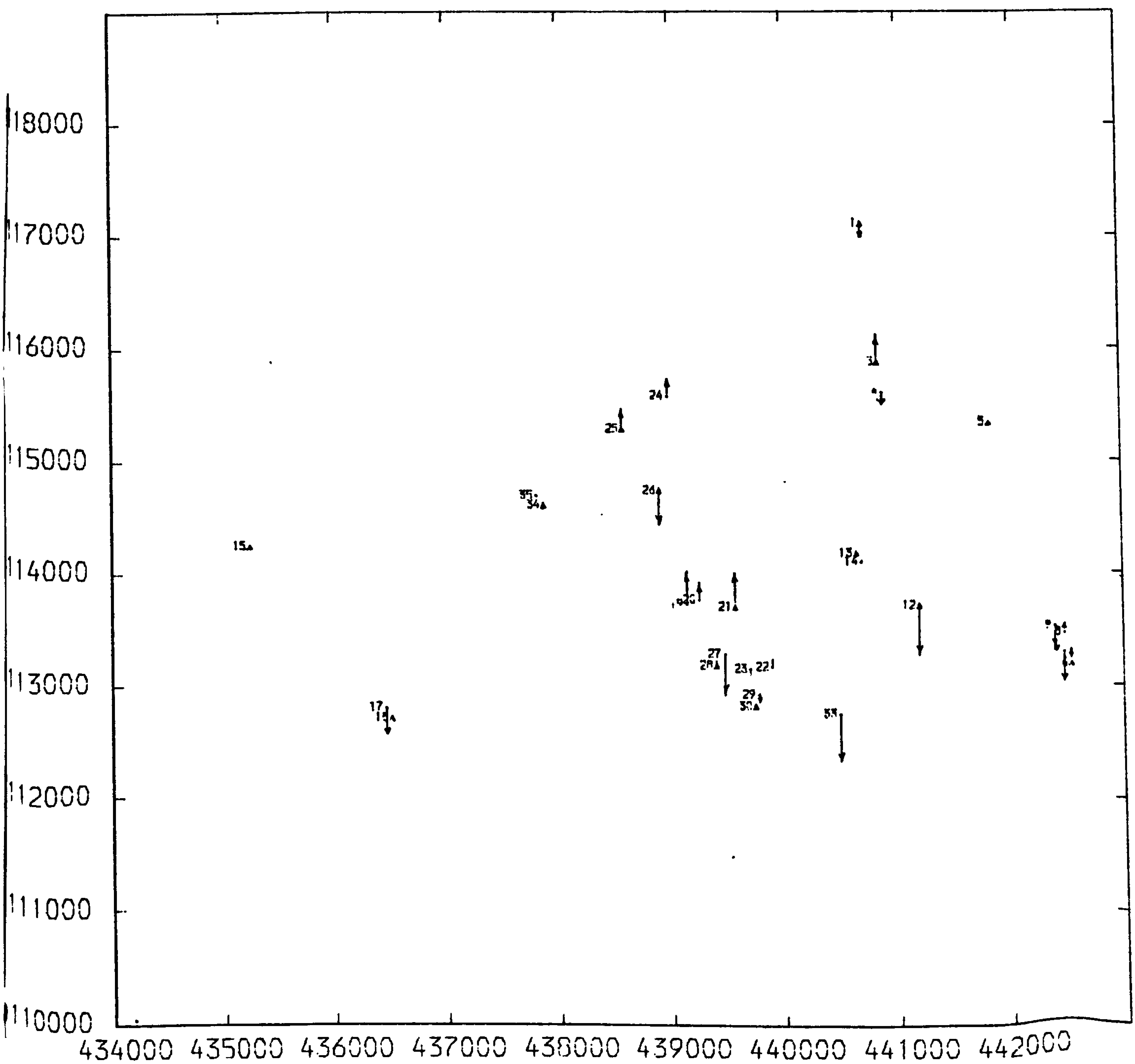

VECTOR MAP OF HEIGHT ERRORS

MODEL NUMBER 7 ** PHOTO SCALE 1/20000

MAP SCALE 1/26300 ** VECTOR SCALE 1/200

SOLUTION NUMBER 19

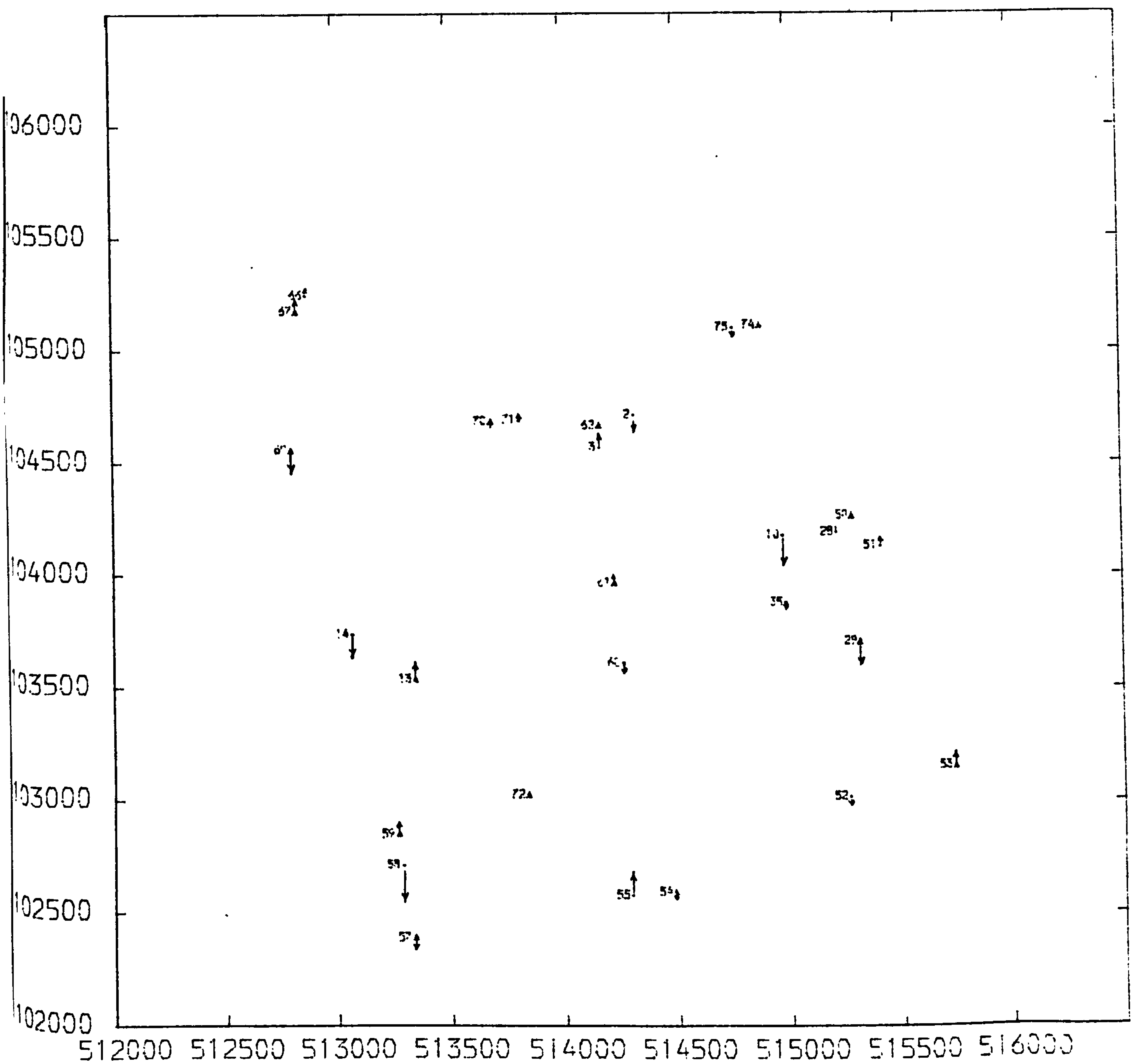

VECTOR MAP OF POSITION ERRORS

MODEL NUMBER 5 ** PHOTO SCALE 1/40000

MAP SCALE 1/52600 ** VECTOR SCALE 1/400

SOLUTION NUMBER 1b

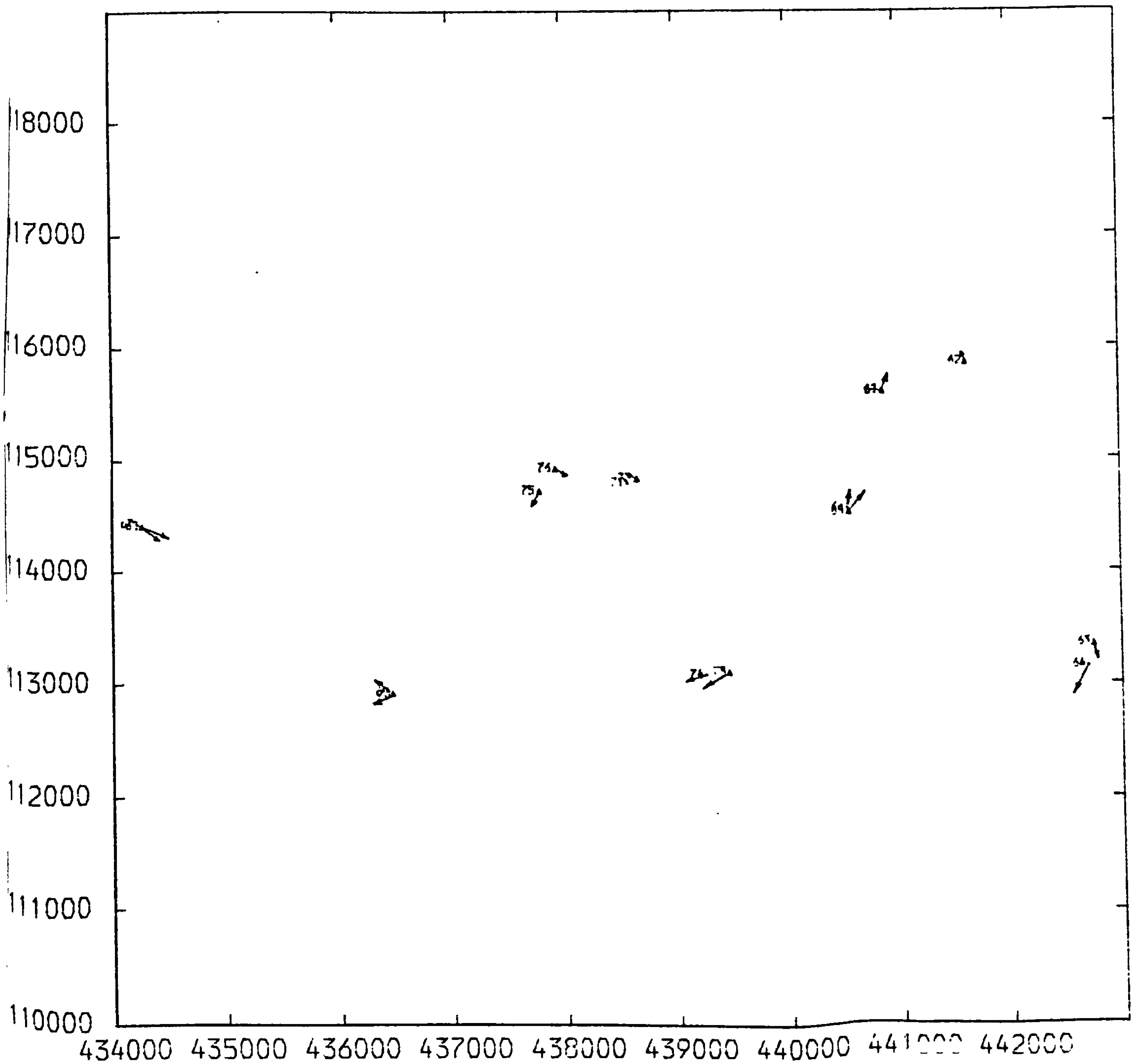

VECTOR MAP OF POSITION ERRORS

MODEL NUMBER 7 ** PHOTO SCALE 1/20000

MAP SCALE 1/26300 ** VECTOR SCALE 1/200

SOLUTION NUMBER 1d

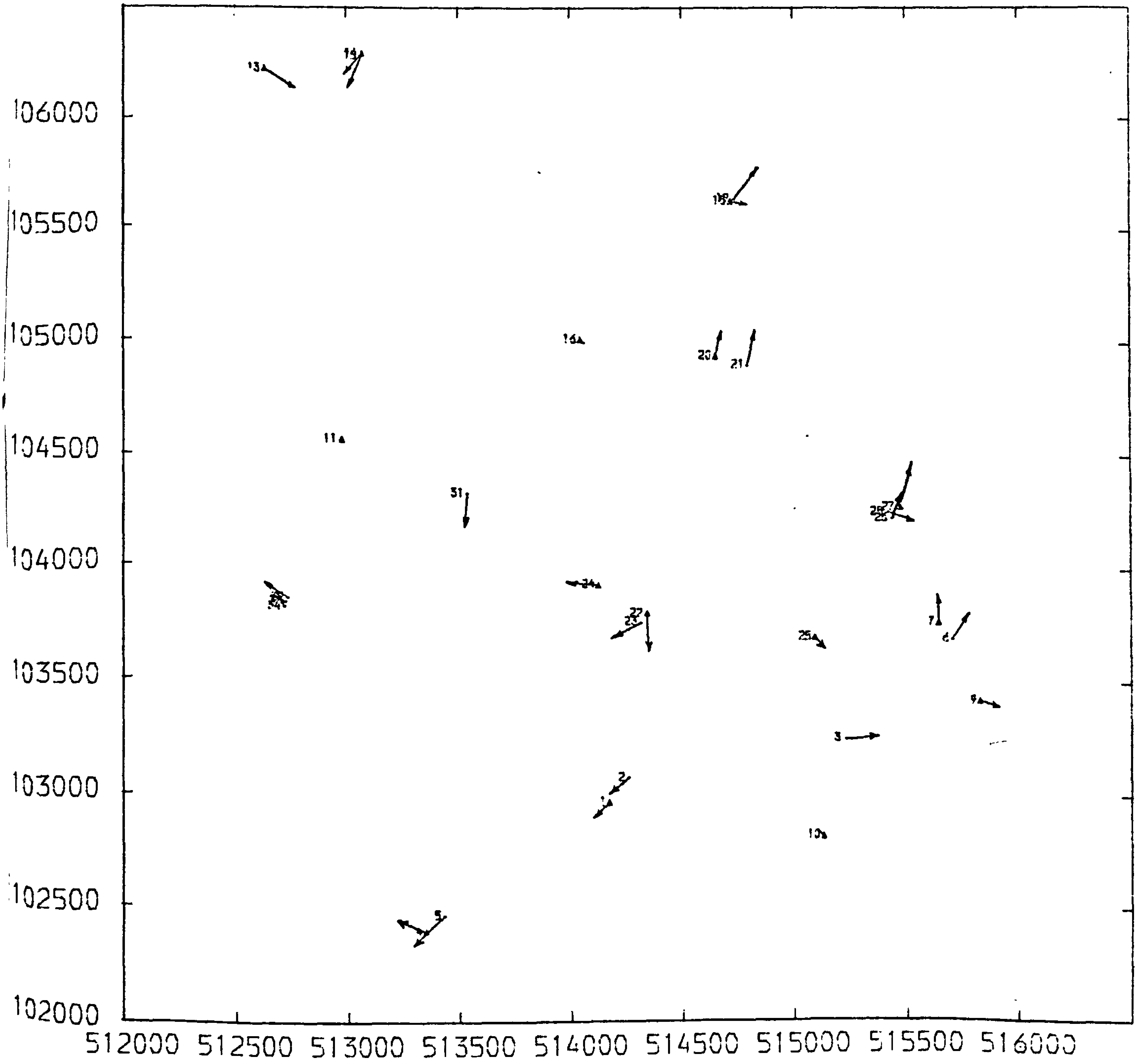

VECTOR MAP OF POSITION ERRORS

MODEL NUMBER 5 ** PHOTO SCALE 1/40000

MAP SCALE 1/52600 ** VECTOR SCALE 1/400

SOLUTION NUMBER 19

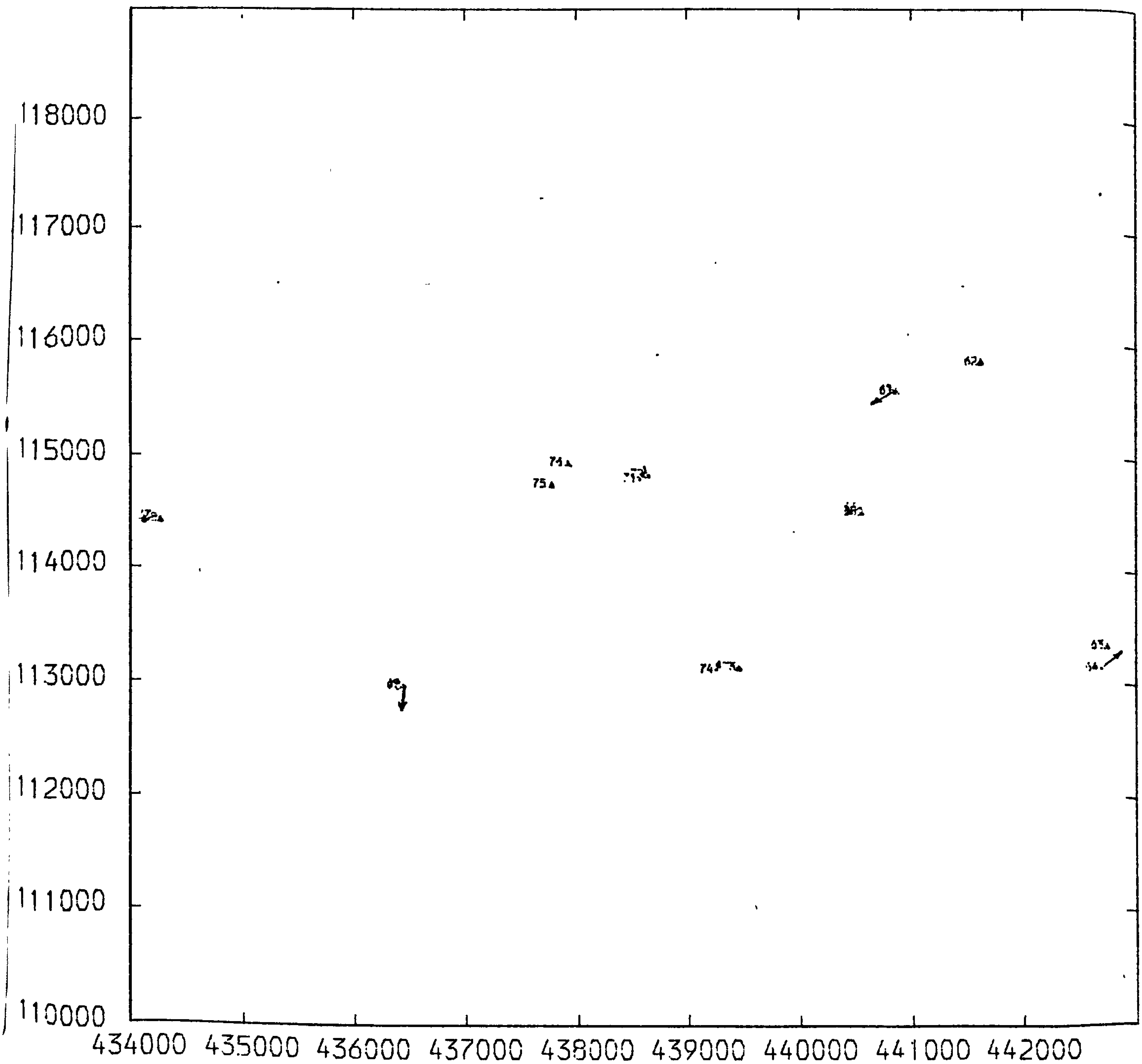

VECTOR MAP OF POSITION ERRORS

MODEL NUMBER 7 ** PHOTO SCALE 1/20000

MAP SCALE 1/26300 ** VECTOR SCALE 1/200

SOLUTION NUMBER 19